

**EFFECT OF BIOREACTOR MODE OF OPERATION ON
MIXED-ACID FERMENTATIONS**

A Dissertation

by

KRISTINA WARNOCK GOLUB

Submitted to the Office of Graduate Studies of
Texas A&M University
in partial fulfillment of the requirements for the degree of

DOCTOR OF PHILOSOPHY

August 2012

Major Subject: Chemical Engineering

Effect of Bioreactor Mode of Operation on Mixed-Acid Fermentations

Copyright 2012 Kristina Warnock Golub

**EFFECT OF BIOREACTOR MODE OF OPERATION
ON MIXED-ACID FERMENTATIONS**

A Dissertation

by

KRISTINA WARNOCK GOLUB

Submitted to the Office of Graduate Studies of
Texas A&M University
in partial fulfillment of the requirements for the degree of

DOCTOR OF PHILOSOPHY

Approved by:

Chair of Committee,	Mark T. Holtzapple
Committee Members,	Mahamoud El-Halwagi
	Cady R. Engler
	Charles J. Glover
Head of Department,	Charles J. Glover

August 2012

Major Subject: Chemical Engineering

ABSTRACT

Effect of Bioreactor Mode of Operation on Mixed-Acid Fermentations. (August 2012)

Kristina Warnock Golub, B.S., Georgia Institute of Technology

Chair of Advisory Committee: Dr. Mark T. Holtzapple

Using mixed-culture fermentation, the carboxylate platform produces carboxylic acids, which are chemically converted into chemicals and fuels. To optimize the mixed-acid fermentation, different bioreactor configurations and operating modes were investigated.

Intermittent air exposure did not affect fermentation performance and bacterial profiles, but reduced the high-molecular-weight carboxylic acids. The microbial flora contained strict and facultative microbes, suggesting the presence of a facultative anaerobic community existing in a biofilm.

Compared to countercurrent trains, propagated fixed-bed fermentations have similar selectivity and acid distribution, but lower yield, conversion, productivity, and acid concentration.

One- to six-stage countercurrent fermentations were operated with similar conditions. Fewer stages increased conversion, whereas more stages increased acid concentration and selectivity. One to four stages achieved similar yield, and four to six stages achieved similar maximum acid concentration. Maximum conversion was achieved with a single stage.

Recycling residual biomass retained microorganisms and nutrients and increased yield and productivity. Relative to lower biomass reflux, higher reflux increased conversion, decreased selectivity, and did not affect yield. The recommended carbon-nitrogen ratio is ~24 g carbon/g nitrogen. In four-stage fermentations, recycle to the second fermentor and in parallel to the first three fermentors was optimal.

Fermentations with excess or insufficient nitrogen had higher selectivity, but decreased yield and conversion.

The glucose-utilization assay is a rapid and repeatable method for determining the amount of microbial activity in a sample. This method determined ~25% efficiency of a new cell separation method.

In continuous fermentation, compared to no cell recycle, recycling cellular biomass increased selectivity and yield, but decreased conversion. Compared to lower cell reflux, higher reflux increased productivity, yield, and conversion, but decreased selectivity. Compared to residual biomass recycle, cell recycle had increased selectivity and yield, but decreased conversion.

A new method to screen and rank inoculum sources from natural environments was successfully developed and tested.

To my parents, for always believing in me and whom this would not be possible without. Thank you for the words of encouragement throughout my life, and your enduring support during my undergraduate and graduate school years. I wish you both many blessings, and let your names live on in this dedication as you both do in my heart.

ACKNOWLEDGEMENTS

I am forever grateful to my parents, Alexander J. Golub and Ruth A. Warnock, and my siblings, Scott A. Golub and Stacey R. Golub, for their everlasting encouragement and love.

My extreme gratitude goes to my academic advisor, Professor Mark Holtzapple, for his guidance and encouragement, which has greatly helped in developing my research skills. My appreciation goes out to my committee members, Prof. Mahamoud El-Halwagi, Prof. Charles Glover, and Prof. Cady Engler, for their time in reading this dissertation and their valuable feedback. Tremendous thanks to Dr. Melinda Wales and Dr. John Dunkleman for their continuous advice, support in the lab, and guidance in writing and presentation skills.

I express my appreciation for fellow graduate students Andrea Forrest, Aaron Smith, Michael Landoll, Daniel Meysing, Matt Falls, Austin Bond, Sebastian Vasquez, Tyler Mann, Pratik Darvekar, and Nick Zentay for their assistance and friendship. I extend my gratitude to Emily Hollister and Terry Gentry for running DNA extractions and sequence comparisons, all their advice, and reviewing my manuscripts. I would also like to thank Cesar Granda, Katherine Taconi, Kyle Ross, Amy Jo Hammett, Zhihong Fu, and Gary Luce for their help and feedback. I also want to extend my gratitude to each and every one of the 20+ student workers who I have had the honor of working with in the laboratory over these years.

I would like to thank Jim Wild for encouraging me during my transition from pursuing a genetics PhD to a chemical engineering PhD. As you stated so bluntly, “What’s four years when you’re eighty?” Thanks to all the scientists who have invited me to do research in their labs: Prof. Jim Wild and Dr. Melinda Wales (TAMU), Prof. Christie Sayes (TAMU), Dr. Chris Rhodes (Lynntech, Inc.), Prof. Stephen Safe (TAMU), Prof. Brian Perkins (TAMU), Prof. Thomas Spencer (TAMU), Prof. David Stelly (TAMU), Prof. Mariah Hahn (TAMU), Prof. Rachel Chen (Georgia Tech), and

Dr. Laura Bittle (Air Products and Chemicals, Inc.). The experiences I have gained in your labs have helped direct my graduate studies.

Thanks also to the friends I have made over these past years in College Station, my colleagues, and the department faculty, staff, and members in the Artie McFerrin Department of Chemical Engineering for making my time at Texas A&M University a tremendous experience. I would like to express my gratitude for Louis Muniz and Towanna Arnold, and I would also like to thank Randy Marek for fixing laboratory equipment when we were in need.

TABLE OF CONTENTS

	Page
ABSTRACT	iii
DEDICATION	v
ACKNOWLEDGEMENTS	vi
TABLE OF CONTENTS	viii
LIST OF FIGURES.....	xiii
LIST OF TABLES	xxvi
1. INTRODUCTION.....	1
2. INVESTIGATION OF INTERMITTENT AIR EXPOSURE ON FOUR-STAGE AND ONE-STAGE ANAEROBIC SEMI-CONTINUOUS MIXED-ACID FERMENTATION.....	7
2.1 Introduction.....	7
2.2 Methods.....	11
2.3 Results and discussion	22
2.4 Conclusion	36
3. PROPAGATED FIXED-BED MIXED-ACID FERMENTATION: EFFECT OF VOLATILE SOLID LOADING RATE AND AGITATION AT HIGH PH	37
3.1 Introduction.....	37
3.2 Materials and methods	41
3.3 Results and discussion	50
3.4 Conclusion	61
4. PROPAGATED FIXED-BED MIXED-ACID FERMENTATION: EFFECT OF VOLATILE SOLID LOADING RATE AND AGITATION AT NEAR-NEUTRAL PH.....	62
4.1 Introduction.....	62
4.2 Materials and methods	64
4.3 Results and discussion	73
4.4 Conclusion	91

	Page
5. EFFECT OF ONE-TO-SIX STAGES IN COUNTERCURRENT MIXED-ACID FERMENTATION	92
5.1 Introduction.....	92
5.2 Materials and methods	96
5.3 Results and discussion	106
5.4 Conclusions.....	116
6. RESIDUAL BIOMASS RECYCLE IN COUNTERCURRENT MIXED-ACID FERMENTATION: EFFECT OF DIFFERENT RECYCLE POINTS AND REFLUX RATIOS	117
6.1 Introduction.....	117
6.2 Materials and methods	120
6.3 Results and discussion	128
6.4 Conclusion	145
7. RESIDUAL BIOMASS RECYCLE IN COUNTERCURRENT MIXED-ACID FERMENTATION: COMPARISON OF THREE CARBON-NITROGEN RATIOS AT DIFFERENT RECYCLE POINTS	148
7.1 Introduction.....	148
7.2 Materials and methods	151
7.3 Results and discussion	160
7.4 Conclusions.....	186
8. RESIDUAL BIOMASS RECYCLE IN COUNTERCURRENT MIXED-ACID FERMENTATION: DECOUPLING CARBON-NITROGEN RATIO AND PH.....	187
8.1 Introduction.....	187
8.2 Materials and methods	191
8.3 Results and discussion	201
8.4 Conclusions.....	215
9. RAPID METHOD TO QUANTIFY TOTAL MICROBIAL ACTIVITY IN BIOMASS, BIOPROCESSES, SOIL, AND SEDIMENT	216
9.1 Introduction.....	216
9.2 Materials and methods	221
9.3 Results and discussion	225
9.4 Conclusion	229

	Page
10. GLUCOSE-UTILIZATION ASSAY ON CELL SEPARATION PROCEDURE	228
10.1 Introduction.....	231
10.2 Materials and methods	235
10.3 Results and discussion	239
10.4 Conclusions.....	252
11. CELLULAR BIOMASS RECYCLE IN COUNTERCURRENT MIXED- ACID FERMENTATION: EFFECT OF TWO REFLUX RATIOS AND THREE CARBON-NITROGEN RATIOS	255
11.1 Introduction.....	255
11.2 Materials and methods	258
11.3 Results and discussion	266
11.4 Conclusion	278
12. COMPARISON OF THREE SCREENING METHODS TO SELECT MIXED-MICROBIAL INOCULUM FOR MIXED-ACID FERMENTATION.....	279
12.1 Introduction.....	279
12.2 Materials and methods	282
12.3 Results and discussion	296
12.4 Conclusion	307
13. BIOSCREENING.....	308
13.1 Introduction.....	308
13.2 Initial site screening	311
13.3 CPDM for inoculum selection in carboxylate fermentation	323
13.4 Continuous fermentations screenings	350
13.5 Conclusions.....	357
14. INVESTIGATION OF MULTIPLE SUBSTRATES FOR VIABILITY IN THE MIXALCO™ PROCESS	358
14.1 Introduction.....	358
14.2 Materials and methods	360
14.3 Batch anaerobic fermentation of municipal solid waste-derived pulp.....	361
14.4 Batch anaerobic fermentation of SunChips® compostable bag	365
14.5 Batch anaerobic fermentation of oregano-supplemented shredded paper ...	374
14.6 Batch anaerobic fermentation of raw corn stover	384

	Page
15. NUTRIENT MICROBIAL LOAD EFFECTS ON BATCH FERMENTATIONS.....	387
15.1 Introduction.....	387
15.2 Materials and methods	387
15.3 Results and discussion	391
15.4 Conclusion	401
16. SUGAR-UTILIZATION ASSAY DEVELOPMENT	402
16.1 Introduction.....	402
16.2 Materials and methods	406
16.3 Experiment 1	412
16.4 Experiments 2 and 3.....	415
16.5 Experiment 4.....	416
16.6 Experiment 5.....	422
16.7 Experiment 6.....	426
16.8 Experiment 7: Glucose oxidase calibration curve (Method B).....	433
16.9 Experiment 8: Glucose oxidase calibration curve at different incubation times with potassium phosphate buffer using Method B	436
16.10 Experiment 9: The effect of buffer on sugar digestion using Method B	437
16.11 Experiment 10: The effect of bacteria type and cell concentration inoculated with cells not at log growth using Method B.....	439
16.12 Experiment 11: Sugar-utilization assay inoculated with <i>E. coli</i> , <i>Pseudomonas</i> , and mixed culture from log growth grown in the presence and absence of glucose using Method B	442
16.13 Experiment 12: Reproducibility of sugar digestion using Method B	445
16.14 Experiment 13: Sugar-utilization assay of <i>E. coli</i> and mixed culture from log growth with and without glucose with different inocula-to-media loadings using Method B.....	448
16.15 Experiment 15: Sugar-utilization assay of fermentation broth and waste solids using Method B.....	452
16.16 Summary of Experiments 9, 10, 13: Glucose digestion rate with cell concentration	455
16.17 Conclusion	457
17. CONCLUSIONS AND RECOMMENDATIONS.....	459
17.1 Conclusions.....	459
17.2 Future work.....	464
REFERENCES.....	466

	Page
APPENDIX A. DEOXYDIZED LIQUID MEDIA PREPARATION.....	480
APPENDIX B. COUNTERCURRENT TRANSFER PROCEDURE.....	481
APPENDIX C. PROPAGATED FIXED-BED TRANSFER PROCEDURE.....	483
APPENDIX D. MULTISTAGE COUNTERCURRENT TRANSFER PROCEDURE.....	486
APPENDIX E. CARBOXYLIC ACID ANALYSIS.....	493
APPENDIX F. MOISTURE AND ASH CONTENT ANALYSIS.....	495
APPENDIX G. CELL SEPARATION PROCEDURE.....	496
APPENDIX H. GLUCOSE ASSAY PROCEDURE.....	497
APPENDIX I. GLUCOSE OXIDASE ENZYME ASSAY FOR GLUCOSE DETERMINATION.....	498
APPENDIX J. TYE MEDIA PREPARATION.....	499
APPENDIX K. BRIEF TUTORIAL ON DIRECT CELL PLATING.....	500
APPENDIX L. HOT-LIME-WATER PRETREATMENT PROCEDURE.....	503
APPENDIX M. EXAMPLE OF EXPERIMENTAL DESIGN FOR THE OREGANO SUPPLEMENTED PAPER BATCH FERMENTATION.....	504
APPENDIX N. CPDM MATLAB PROGRAM FOR SIMULATION OF A FOUR-STAGE COUNTERCURRENT FERMENTATION.....	506
VITA.....	515

LIST OF FIGURES

	Page
Figure 1-1. Diagram of the carboxylate platform.....	3
Figure 1-2. Diagram of the four-stage continuous countercurrent fermentation.	4
Figure 2-1. Diagram of four- and one-stage fermentations.....	9
Figure 2-2. Plastic fermentation reactor.	11
Figure 2-3. Photo of biomass during a 90-minute air exposure. A – filter solids in weigh boat; B – filter liquid in beaker; C – 1-L fermentation bottle.....	14
Figure 2-4. Total and acetic acid equivalent carboxylic acid concentrations for Fermentations 4S, 4R, 1S, and 1R. The vertical lines mark the onset of steady state (Days 128–218). Error bars represent the 95% confidence interval of acid concentrations during the steady-state period.	25
Figure 2-5. Summation of non-acid dry solids (NADS) exiting and fed and total acids exiting for Fermentations 4S, 4R, 1S, and 1R. The vertical lines mark the onset of steady state (Days 128–218).	26
Figure 2-6. Carboxylic acid composition profile. Error bars are the 95% confidence intervals for each carboxylic acid composition during the steady-state period.	28
Figure 2-7. Yield values for Trains 4S, 4R, 1S, and 1R.....	30
Figure 2-8. Conversion, selectivity, productivity, and acetic acid equivalent selectivity for Trains 4S, 4R, 1S, and 1R.	31
Figure 2-9. Relative abundances of bacterial phyla across oxygen exposure treatments and fermentation train configurations.	34
Figure 2-10. Neighbor-joining phylogenetic tree of the seven most abundant OTUs found within the bioreactor communities, collectively, and three nearest neighbor isolates from the Greengenes chimera-checked database.....	35

Figure 3-1. Illustration of laboratory operating procedure for four-stage propagated fixed-bed fermentation system.	40
Figure 3-2. Total and acetic acid equivalent carboxylic acid concentrations for propagated fixed-bed fermentation Trains 1, 2, 3, 4, and 5 at high C-N ratio. The vertical lines mark the onset of quasi-steady state. Error bars represent the 95% confidence interval of acid concentrations during the quasi-steady-state period.	53
Figure 3-3. Summation of non-acid dry solids (NADS) exiting and fed and total acids exiting for propagated fixed-bed fermentation Trains 1, 2, 3, 4, and 5 at high C-N ratio. The vertical lines mark the onset of quasi-steady state.	54
Figure 3-4. Carboxylic acid composition profile for propagated fixed-bed fermentation trains at high C-N ratio. Error bars are the 95% confidence intervals for each carboxylic acid composition during the quasi-steady-state period.	55
Figure 4-1. Total and acetic acid equivalent carboxylic acid concentrations for fermentation propagated fixed-bed Trains 1 to 5 at near-neutral pH. The solid vertical lines mark the onset of quasi-steady state.	77
Figure 4-2. Summation of non-acid dry solids (NADS) (exiting and fed) and total acids exiting for fermentation propagated fixed-bed fermentation Trains 1 to 5 at near-neutral pH. The vertical solid lines mark the onset of quasi-steady state.	78
Figure 4-3. Carboxylic acid composition profile for propagated fixed-bed fermentations at near-neutral pH. Error bars are the 95% confidence intervals for each carboxylic acid composition during the quasi-steady-state period.	79
Figure 4-4. Total acid concentration versus VSLR at high pH and low C-N ratio for propagated fixed-bed fermentations.	87
Figure 4-5. Yield versus VSLR at high pH and low C-N ratio for propagated fixed-bed fermentations.	88

	Page
Figure 4-6. Total acid concentration versus VSLR at near-neutral pH and optimal C-N ratio for propagated fixed-bed fermentations.	88
Figure 4-7. Yield versus VSLR at near-neutral pH and optimal C-N ratio for propagated fixed-bed fermentations.	89
Figure 5-1. Diagram of the multi-stage experiment, depicting the one- to six-stage trains (Trains 1, 2, 3, 4, 5, and 6).....	95
Figure 5-2. Acid concentration in each stage of the fermentation trains. Error bars are the 95% confidence intervals during the steady-state period.	110
Figure 5-3. Carboxylic acid composition profile. Error bars are the 95% confidence intervals for each carboxylic acid composition during the steady-state period.	111
Figure 5-4. Exit, process, culture, and feed yield for Trains 1, 2, 3, 4, 5, and 6. Error bars are the 95% confidence intervals during the steady-state period.	113
Figure 5-5. Selectivity and conversion for Trains 1, 2, 3, 4, 5, and 6. Error bars are the 95% confidence intervals during the steady-state period.	114
Figure 5-6. Conversion in each stage of the fermentation trains. Error bars are the 95% confidence intervals during the steady-state period.	115
Figure 6-1. Diagram of the biomass recycle experiment, depicting the control (Train C) with no biomass recycle, and the four different residual biomass recycle trains (Trains R1, R2, R3, P).....	119
Figure 6-2. Conversion and selectivity for residual biomass recycle at different recycle points with 14% reflux ratio and optimal C-N ratio.	141
Figure 6-3. Conversion and selectivity for residual biomass recycle at different recycle points with 35% reflux ratio and optimal C-N ratio.	141
Figure 6-4. Carboxylic acid composition profile at 14% residual biomass reflux. Error bars are the 95% confidence intervals for each carboxylic acid composition during the steady-state period.	146
Figure 6-5. Carboxylic acid composition profile at 35% residual biomass reflux. Error bars are the 95% confidence intervals for each carboxylic acid composition during the steady-state period.	147

Figure 7-1. Diagram of the residual biomass recycle experiment, depicting the control (Train C) with no residual biomass recycle, and the four different residual biomass recycle trains (Trains R1, R2, R3, P).	151
Figure 7-2. Carboxylic acid composition profile at C-N ratio ~14 g OC _{NA} /g N. Error bars are the 95% confidence intervals for each carboxylic acid composition during the steady-state period.	176
Figure 7-3. Carboxylic acid composition profile at C-N ratio ~24 g OC _{NA} /g N. Error bars are the 95% confidence intervals for each carboxylic acid composition during the steady-state period.	177
Figure 7-4. Carboxylic acid composition profile at C-N ratio ~74 g OC _{NA} /g N. Error bars are the 95% confidence intervals for each carboxylic acid composition during the steady-state period.	178
Figure 8-1. Diagram of the residual biomass recycle experiment, depicting the control (Train C) with no recycle and residual biomass recycle to the Fermentor 2 (Train R2).	190
Figure 8-2. Carboxylic acid composition profile at (a) low C-N ratio and high pH, (b) low C-N ratio and near-neutral pH, and (c) medium C-N ratio and low pH. Error bars are the 95% confidence intervals for each carboxylic acid composition during the steady-state period.	209
Figure 9-1. Glucose calibration curve without biomass in triplicates. Error bars represent the SE.	225
Figure 9-2. Glucose digestion with time inoculated with <i>E. coli</i> at an OD of (a) 0.6, (b) 0.8, (c) 1.0, and (d) 1.2. Error bars represent the SE from triplicate experiments.	226
Figure 9-3. Standard curve for CFU corresponding to OD for <i>E. coli</i> . Error bars represent the standard error from triplicate plates.	227
Figure 9-4. Glucose digestion rate inoculated with <i>E. coli</i> . Error bars represent the standard error from triplicate experiments. (<i>Note</i> : It is assumed that 1 g <i>E. coli</i> = 10 ¹² CFU, (Neidhardt et al., 1990))	228
Figure 9-5. Fermentation broth glucose digestion rate. Error bars represent the standard error from triplicate experiments.	230

	Page
Figure 9-6. Marine sediment glucose digestion rate. Error bars represent the standard error from triplicate experiments.	230
Figure 10-1. Outline of cell-recycle research ideas.....	234
Figure 10-2. Diagram of cell recycle procedure.	236
Figure 10-3. Example of glucose calibration curves for (a) biomass solids and (b) “cells” at 0.10, 0.08, 0.06, and 0.04 g biomass/mL.	242
Figure 10-4. Residual biomass glucose digestion with time for 0.10 g biomass/mL loading. Error bars represent the standard error in triplicate experiments.....	243
Figure 10-5. Cake glucose digestion with time for 0.10 g biomass/mL loading. Error bars represent the standard error in triplicate experiments.	243
Figure 10-6. Filtrate glucose digestion with time for 0.10 g biomass/mL loading. Error bars represent the standard error in triplicate experiments.	244
Figure 10-7. Sediment glucose digestion with time for 0.10 g biomass/mL loading. Error bars represent the standard error in triplicate experiments.	244
Figure 10-8. Liquid phase glucose digestion with time for 0.10 g biomass/mL loading. Error bars represent the standard error in triplicate experiments.....	245
Figure 10-9. “Cells” glucose digestion with time for 0.10 g biomass/mL loading. Error bars represent the standard error in triplicate experiments.	245
Figure 10-10. Glucose digestion using residual biomass. Error bars represent the standard error in triplicate experiments.	246
Figure 10-11. Glucose digestion using cake. Error bars represent the standard error in triplicate experiments.	246
Figure 10-12. Glucose digestion using filtrate. Error bars represent the standard error in triplicate experiments.....	247
Figure 10-13. Glucose digestion using sediment. Error bars represent the standard error in triplicate experiments.....	247
Figure 10-14. Glucose digestion using liquid phase. Error bars represent the standard error in triplicate experiments.	248

	Page
Figure 10-15. Glucose digestion using “cells.” Error bars represent the standard error in triplicate experiments.....	248
Figure 10-16. Diagram of cell balance on cell recycle procedure using the glucose-utilization assay.	250
Figure 10-17. Diagram of cell balance on cell recycle procedure using real-time PCR assay.	252
Figure 11-1. Diagram of the cellular recycle experiment, depicting the control (Train C) with no biomass recycle and the cell recycle train (Train CR).....	257
Figure 11-2. Carboxylic acid composition profile for the control (Train C) with no cellular recycle and the cell recycle train (Train CR). For each Train CR, cells were recovered from the recycle stream with the indicated reflux ratio (g wet residual biomass recycled/100 g wet residual biomass exiting Fermentor 4). Error bars are the 95% confidence intervals for each carboxylic acid composition during the steady-state period.	273
Figure 12-1. Diagram of the batch screen, CPDM, and countercurrent fermentations.	282
Figure 12-2. Carboxylic acid composition profile for batch Fermentations 1, 2, 3, 4, and 5.....	297
Figure 12-3. Data fit of acetic acid equivalent (Aceq) concentrations to 20, 40, 70, 100 and 100+ g/L batch fermentations for CPDM 1.	298
Figure 12-4. The experimental value and the CPDM prediction value for the specific reaction rates in 20, 40, 70, 100 and 100+ g/L batch fermentations for CPDM 1.	299
Figure 12-5. Maps for (a) CPDM 1, (b) CPDM 2, (c) CPDM 3, (d) CPDM 4, and (e) CPDM 5.....	301
Figure 12-6. Carboxylic acid composition profile for countercurrent Trains 1, 2, 3, 4, and 5. Error bars are the confidence intervals for each carboxylic acid composition during the steady-state period.	306
Figure 13-1. Overview of the microbial community screening using carboxylate platform fermentations.....	310

	Page
Figure 13-2. Diagram of the (a) initial screen, (b) CPDM, and (c) countercurrent fermentations for the bioscreening experiment.	311
Figure 13-3. Aceq concentrations of A21 inoculated paper/yeast extract fermentation at 20, 40, 70, 100, and 100+ g substrate/L liquid with calcium carbonate buffer.	332
Figure 13-4. The experimental value and the CPDM prediction value for the specific reaction rate in five batch paper/yeast extract fermentation with A21 inoculum.	333
Figure 13-5. The CPDM “map” for 90 wt% paper/10 wt% yeast extract with A21 inoculum.	334
Figure 13-6. Aceq concentrations of A23 inoculated paper/yeast extract fermentation at 20, 40, 70, 100, and 100+ g substrate/L liquid with calcium carbonate buffer.	335
Figure 13-7. The experimental value and the CPDM prediction value for the specific reaction rate in five batch paper/yeast extract fermentation with A23 inoculum.	336
Figure 13-8. The CPDM “map” for 90 wt% paper/10 wt% yeast extract with A23 inoculum.	338
Figure 13-9. Aceq concentrations of A25 inoculated paper/yeast extract fermentation at 20, 40, 70, 100, and 100+ g substrate/L liquid with calcium carbonate buffer.	339
Figure 13-10. The experimental value and the CPDM prediction value for the specific reaction rate in five batch paper/yeast extract fermentation with A25 inoculum.	340
Figure 13-11. The CPDM “map” for 90 wt% paper/10 wt% yeast extract with A25 inoculum.	341
Figure 13-12. Aceq concentrations of G21 inoculated paper/yeast extract fermentation at 20, 40, 70, 100, and 100+ g substrate/L liquid with calcium carbonate buffer.	343
Figure 13-13. The experimental value and the CPDM prediction value for the specific reaction rate in five batch paper/yeast extract fermentation with G21 inoculum.	344

Figure 13-14. The CPDM “map” for 90 wt% paper/10 wt% yeast extract with G21 inoculum.	345
Figure 13-15. Aceq concentrations of G38 inoculated paper/yeast extract fermentation at 20, 40, 70, 100, and 100+ g substrate/L liquid with calcium carbonate buffer.	346
Figure 13-16. The experimental value and the CPDM prediction value for the specific reaction rate in five batch paper/yeast extract fermentation with G38 inoculum.	347
Figure 13-17. The CPDM “map” for 90 wt% paper/10 wt% yeast extract with G38 inoculum.	349
Figure 13-18. Total and Aceq acid concentrations of Trains G08, H20, and K49. Values represent the mean of the steady-state values \pm CI (95% CI).	356
Figure 13-19. Conversion and selectivity comparisons of Trains G08, H20, and K49. Values represent the mean of the steady-state values \pm CI (95% CI).	356
Figure 14-1. Total carboxylic acid concentrations for the MSW-derived pulp and control fermentations. Error bars represent standard errors.	363
Figure 14-2. Total carboxylic acid concentrations for the SunChips® compostable bag fermentations. Error bars represent standard deviations of triplicate fermentations.	368
Figure 14-3. Acetic acid concentrations for the SunChips® compostable bag fermentations. Error bars represent the standard deviation of triplicate fermentations.	369
Figure 14-4. Picture comparing the pre- and post-reactor fermentation biomass for non-pretreated compostable bags at 55 °C after 28 days.	371
Figure 14-5. Picture comparing the pre- and post-reactor fermentation biomass for pretreated compostable bags at 55 °C after 28 days.	372
Figure 14-6. Picture comparing the pre- and post-reactor fermentation biomass for non-pretreated compostable bags at 40 °C after 28 days.	372
Figure 14-7. Picture comparing the pre- and post-reactor fermentation biomass for pretreated compostable bags at 40 °C after 28 days.	373

	Page
Figure 14-8. Total carboxylic acid concentrations for the oregano supplemented paper fermentations. Error bars were removed for clarity.....	377
Figure 14-9. Volume of gas produced during the 28-d oregano supplemented paper fermentations. Error bars are standard error.	378
Figure 14-10. Total carboxylic acid concentrations for the paper fermentations without oregano supplementation comparing iodoform addition (I) and without iodoform at 40 and 55 °C. Error bars represent standard error of triplicate fermentations.	380
Figure 14-11. Total carboxylic acid concentrations for fermentations without iodoform fed with 80% paper and 0% oregano (P80) and 50% paper and 30% oregano on a dry mass basis, at 40 and 55 °C. Error bars represent the standard error of triplicate fermentations.	381
Figure 14-12. Total carboxylic acid concentrations for fermentations without iodoform fed with 80% paper and 0% oregano (P80), 75% paper and 5% oregano (P75), 65% paper and 15% oregano (P65), and 50% paper and 30% oregano on a dry mass basis, at 55 °C. Error bars are standard error.	382
Figure 14-13. Total acid concentration of raw corn stover during a 28-d batch fermentation. Error bars represent the standard error of quadruplet fermentations.	385
Figure 15-1. Total carboxylic acid concentration during the 28-d batch fermentation for the eight different chicken manure conditions. Error bars were removed for clarity.	392
Figure 15-2. Total carboxylic acid concentration produced during the 28-d batch fermentation for the eight different chicken manure conditions. Error bars were removed for clarity.	393
Figure 15-3. Cumulative gas produced during the 28-d batch fermentation for the eight different chicken manure conditions. Error bars are the standard errors of the triplicate fermentations.....	394
Figure 15-4. Total carboxylic acid produced during the 28-d batch fermentation for the nonfrozen wet unsterilized chicken manure (NWU). Error bars are the standard error of the triplicate fermentations.....	397

Figure 15-5. Total carboxylic acid produced during the 28-d batch fermentation for the frozen wet unsterilized chicken manure (FWU). Error bars are the standard error of the triplicate fermentations.....	398
Figure 15-6. Total carboxylic acid produced during the 28-d batch fermentation for the nonfrozen dry unsterilized chicken manure (NDU). Error bars are the standard error of the triplicate fermentations.....	398
Figure 15-7. Total carboxylic acid produced during the 28-d batch fermentation for the frozen dry unsterilized chicken manure (FDU). Error bars are the standard error of the triplicate fermentations.....	399
Figure 15-8. Total carboxylic acid produced during the 28-d batch fermentation for the nonfrozen wet sterilized chicken manure (NWS). Error bars are the standard error of the triplicate fermentations.....	399
Figure 15-9. Total carboxylic acid produced during the 28-d batch fermentation for the frozen wet sterilized chicken manure (FWS). Error bars are the standard error of the triplicate fermentations.....	400
Figure 15-10. Total carboxylic acid produced during the 28-d batch fermentation for the nonfrozen dry sterilized chicken manure (NDS). Error bars are the standard error of the triplicate fermentations.....	400
Figure 15-11. Total carboxylic acid produced during the 28-d batch fermentation for the frozen dry sterilized chicken manure (FDS). Error bars are the standard error of the triplicate fermentations.....	401
Figure 16-1. Diagram of the overall sugar-utilization assay procedure and experimental setup for Method A.....	407
Figure 16-2. Diagram of the overall sugar-utilization assay procedure and general experimental setup for Method B.	410
Figure 16-3. Representation of the chemistry of the glucose oxidase enzyme assay. ...	411
Figure 16-4. Spectrophotometric analysis.....	411
Figure 16-5. Pictures of spectrophotometers.....	412
Figure 16-6. Sugar digestion of liquid fermentation broth for (a) cellobiose, glucose, and xylose, (b) glucose, (c) xylose, (d) cellobiose over 30 min in the vertical vial orientation.....	413

Figure 16-7. HPLC calibrations of cellobiose, glucose, and xylose.	414
Figure 16-8. Sugar digestion inoculated with (a) liquid broth and (b) solid fermentation waste biomass for cellobiose, glucose, and xylose during 24 h.	416
Figure 16-9. Sugar digestion control measuring cellobiose, glucose, and xylose during 12 days.	418
Figure 16-10. Sugar digestion inoculated with liquid broth and solid fermentation waste biomass for cellobiose, glucose, and xylose during 12 h with (a) same tube, and (b) separate tube sampling procedures.	419
Figure 16-11. Sugar digestion of (a) glucose, (b) cellobiose, and (c) glucose, xylose, and cellobiose inoculated with separated cells (Appendix G) during 12 days.	420
Figure 16-12. Sugar digestion of (a) glucose, and (b) glucose, xylose, and cellobiose inoculated with frozen pure <i>Clostridia</i> culture during 12 days.	421
Figure 16-13. Experiment 5 sugar digestion of soil inoculum with vials in (a) horizontal position with glucose, (b) horizontal position with xylose, (c) horizontal position with cellobiose, and (d) vertical position with cellobiose.	423
Figure 16-14. Experiment 5 sugar digestion inoculated with fermentation solid waste with vials in (a) horizontal position with glucose, (b) horizontal position with xylose, (c) horizontal position with cellobiose, and (d) vertical position with cellobiose.	424
Figure 16-15. Experiment 5 sugar digestion inoculated with cells from bioreactor waste with vials in (a) horizontal position with glucose, (b) horizontal position with xylose, (c) horizontal position with cellobiose, and (d) vertical position with cellobiose.	425
Figure 16-16. Experiment 6 sugar-utilization assay inoculated with unsterilized yeast extract with (a) glucose and (b) cellobiose digestion.	427
Figure 16-17. Experiment 6 sugar-utilization assay inoculated with unsterilized shredded office paper with (a) glucose and (b) cellobiose digestion.	428

Figure 16-18. Experiment 6 sugar-utilization assay inoculated with unsterilized wet chicken manure with (a) glucose and (b) cellobiose digestion.	429
Figure 16-19. Experiment 6 sugar-utilization assay inoculated with autoclaved wet chicken manure with (a) glucose and (b) cellobiose digestion.	430
Figure 16-20. Experiment 6 sugar-utilization assay inoculated with unsterilized dry chicken manure with (a) glucose and (b) cellobiose digestion.	431
Figure 16-21. Experiment 6 sugar-utilization assay inoculated with autoclaved dry chicken manure with (a) glucose and (b) cellobiose digestion.	432
Figure 16-22. Calibration curves for glucose oxidase assay. (a) Glucose concentrations were analyzed with glucose oxidase in 1-mL cuvettes in the spectrophotometer. Glucose concentrations were analyzed with glucose oxidase in a 96-well plate with a volume of (b) 250 μ L per well and (c) 100 μ L per well in the spectrophotometer.	435
Figure 16-23. Glucose concentration versus absorbance calibration curves for glucose oxidase assay at three different incubation times: 10, 20, and 30 min.	437
Figure 16-24. Glucose concentration with time for <i>E. coli</i> inoculated sugar-utilization assay with and without potassium phosphate buffer.	439
Figure 16-25. Glucose digestion with time inoculated with (a) <i>E. coli</i> , (b) <i>Pseudomonas</i> , and (c) mixed-culture of bacteria from fermentation solids waste.	441
Figure 16-26. Growth curves in the presence and absence of glucose for glucose oxidase assay. The left-hand axis reflects the optical density (OD) of the bacteria with time, and the right-hand axis reflects the pH of the growth media with time for (a) <i>E. coli</i> , (b) mixed culture, and (c) <i>Pseudomonas</i>	443
Figure 16-27. Reproducibility of glucose-utilization assay. (a) Three glucose-utilization assays inoculated with <i>E. coli</i> from three different cell stock tubes and three different cell growth tubes (E1, E2, E3A), (b) averaged glucose-utilization assay with error bars.	446

Figure 16-28. Reproducibility of glucose-utilization assay. (a) Three glucose-utilization assays inoculated with <i>E. coli</i> from from the same cell stock and cell growth tube (E3A, E3B, E3C), and (b) averaged glucose-utilization assay with error bars.	447
Figure 16-29. Growth curves in the presence and absence of glucose, grown with different ratios of cell stock-to-TYE media. The left hand axis reflects the optical density (OD) of the bacteria with time for (a) <i>E. coli</i> and (b) Mixed culture.	450
Figure 16-30. Glucose-utilization curves inoculated with cells in the log growth phase grown in the presence (+) and absence (–) of glucose at cell concentrations of 0.75 OD and 1.5 OD. The left hand axis reflects the optical density (OD) of the bacteria with time for (a) <i>E. coli</i> and (b) Mixed culture.....	451
Figure 16-31. Glass sealed reaction vessels for glucose-utilization assay.....	453
Figure 16-32. Glucose digestion curves inoculated with fermentation mixed-culture cells in the log growth phase grown in the absence of glucose at cell concentrations of 0.75 OD. The left-hand axis reflects the glucose concentration.	454
Figure 16-33. Glucose-utilization rate versus optical density (OD) for (a) <i>E. coli</i> and (b) fermentation mixed culture.	456

LIST OF TABLES

	Page
Table 2-1. Operating parameters for the air exposure fermentations.....	17
Table 2-2. Performance measures for fermentations 4S, 4R, 1S, and 1R. Values represent the mean of the steady-state values \pm CI (95% CI).....	27
Table 2-3. Summary of sequence library sized, operational taxonomic units (OTUs, 97% similarity) and diversity and richness estimates for each of the reactor bacterial communities. The number of OTUs listed as “overall” is not equivalent to the sum of OTUs across all samples, because many OTUs were found within multiple fermentor communities.....	33
Table 2-4. Overlap of OTUs among the reactor communities, as θ_{YC} , the Yue-Clayton similarity estimator. θ_{YC} considers the number of OTUs shared between two communities, as well as their relative abundances. θ_{YC} is scored on a scale of 0 to 1, where 0 represents complete dissimilarity and a score of 1 represents identity.....	33
Table 3-1. Operating parameters for propagated fixed-bed fermentations at high pH.	46
Table 3-2. Performance measures for fermentation propagated fixed-bed Trains 1, 2, 3, 4, and 5 at high C-N ratio. Values represent the mean of the quasi-steady-state values \pm CI (95% CI).	51
Table 3-3. <i>p</i> values for performance measures for propagated fixed-bed fermentation Trains 1, 2, 3, 4, and 5 ($\alpha = 0.05$) at high C-N ratio.....	52
Table 4-1. Operating parameters for propagated fixed-bed fermentations at near-neutral pH. Normalized parameters represent the mean of the quasi-steady-state values \pm CI (95% CI).	70
Table 4-2. Performance measures for propagated fixed-bed fermentation Trains 1 to 5 at near-neutral pH. Values represent the mean of the quasi-steady-state values \pm CI (95% CI).	75
Table 4-3. <i>p</i> values for performance measures for propagated fixed-bed fermentation Trains 1 to 5 at near-neutral pH($\alpha = 0.05$).	76

Table 4-4. Operating parameters for four-stage countercurrent fermentations with comparable operating parameters (e.g., VSLR, LRT, pH) as the propagated fixed-bed fermentations. All fermentations were run continuously at 40 °C, had a transfer frequency of 2 or 3 days, were fed 80% substrate and 20% nutrient on a dry basis, and had an original inoculum size of 50 to 60 mL. Dashes indicate unknown.	85
Table 4-5. Performance data for four-stage countercurrent fermentations with comparable operating parameters (e.g., VSLR, LRT, pH) as the propagated fixed-bed fermentations. All fermentations were run continuously at 40 °C, had a transfer frequency of 2 or 3 days, were fed 80% substrate and 20% nutrient on a dry basis, and had an original inoculum size of 50 to 60 mL. Dashes indicate unknown.	86
Table 4-6. Performance variable percent difference in non-mixed versus mixed propagated fixed-bed fermentations at near-neutral and high pH.	89
Table 5-1. Operating parameters. Normalized parameters represent the mean of the steady-state values \pm CI (95% CI).	102
Table 5-2. Fermentation performance measures for Trains 1, 2, 3, 4, 5, and 6. Values represent the mean of the steady-state values \pm CI (95% CI).	108
Table 5-3. <i>p</i> values for fermentation performance measures ($\alpha = 0.05$).	109
Table 6-1. Operating parameters at ~14% residual biomass reflux ratio. Normalized parameters represent the mean of the steady-state values \pm CI (95% CI).	130
Table 6-2. Operating parameters at ~35% residual biomass reflux ratio. Normalized parameters represent the mean of the steady-state values \pm CI (95% CI).	131
Table 6-3. Performance measures for 14% residual biomass reflux. Values represent the mean of the steady-state values \pm CI (95% CI).	132
Table 6-4. Performance measures for 35% residual biomass reflux. Values represent the mean of the steady-state values \pm CI (95% CI).	133
Table 6-5. <i>p</i> values for performance measures at 14% residual biomass reflux ($\alpha = 0.05$).	134

	Page
Table 6-6. p values for performance measures at 35% residual biomass reflux ($\alpha = 0.05$).....	135
Table 6-7. p values for performance measures to compare 14% and 35% residual biomass reflux ($\alpha = 0.05$).....	136
Table 6-8. Qualitative comparison of performance variables for different recycle points at 14% and 35% residual biomass reflux.....	143
Table 7-1. Operating parameters at C-N ratio ~ 14 g OC _{NA} /g N. Normalized parameters represent the mean of the steady-state values \pm CI (95% CI).....	162
Table 7-2. Operating parameters at C-N ratio ~ 24 g OC _{NA} /g N. Normalized parameters represent the mean of the steady-state values \pm CI (95% CI).....	163
Table 7-3. Operating parameters at C-N ratio ~ 74 g OC _{NA} /g N. Normalized parameters represent the mean of the steady-state values \pm CI (95% CI).....	164
Table 7-4. Performance measures at C-N ratio ~ 14 g OC _{NA} /g N. Values represent the mean of the steady-state values \pm CI (95% CI).	165
Table 7-5. Performance measures at C-N ratio ~ 24 g OC _{NA} /g N. Values represent the mean of the steady-state values \pm CI (95% CI).	166
Table 7-6. Performance measures at C-N ratio ~ 74 g OC _{NA} /g N. Values represent the mean of the steady-state values \pm CI (95% CI).	167
Table 7-7. p values for performance measures at C-N ratio ~ 14 g OC _{NA} /g N ($\alpha = 0.05$).....	168
Table 7-8. p values for performance measures at C-N ratio ~ 24 g OC _{NA} /g N ($\alpha = 0.05$).....	169
Table 7-9. p values for performance measures at C-N ratio ~ 74 g OC _{NA} /g N ($\alpha = 0.05$).....	170
Table 7-10. p values for performance measures to compare fermentations with C-N of 14, 24, and 74 g OC _{NA} /g N ($\alpha = 0.05$).....	171

Table 8-1. Operating parameters at (a) low C-N ratio and low pH, (b) low C-N ratio and near-neutral pH, and (c) medium C-N and low pH. Normalized parameters represent the mean of the steady-state values \pm CI (95% CI).	194
Table 8-2. Performance measures at (a) low C-N ratio and low pH, (b) low C-N ratio and near-neutral pH, and (c) medium C-N and low pH. Values represent the mean of the steady-state values \pm CI (95% CI).....	203
Table 8-3. <i>p</i> values for fermentation performance measures to compare Train C and R2 at (a) low C-N ratio and low pH, (b) low C-N ratio and near-neutral pH, and (c) medium C-N and low pH ($\alpha = 0.05$).	204
Table 9-1. Specific digestion rates for <i>E. coli</i> in log growth, fermentation broth from carboxylate fermentation, and marine sediment.	229
Table 10-1. Mineral analysis of dry chicken manure, solid biomass, and cells.....	240
Table 10-2. From the glucose-utilization assay, specific digestion rate of the different separated phases in the cell separation procedure.....	249
Table 10-3. Cell balances using real-time PCR.	251
Table 11-1. Operating parameters for the control (Train C) and cell recycle train (Train CR) with various C-N ratios and amount of wet biomass used for cell recycle. Normalized values represent the mean of the steady-state values \pm CI (95% CI).....	260
Table 11-2. Performance measures for control (Train C) and cellular recycle (Train CR) at various C-N ratios and reflux ratios. Values represent the mean of the steady-state values \pm CI (95% CI).	268
Table 11-3. <i>p</i> values for performance measures to compare control (Train C) to cellular recycle (Train CR) at various recycle ratios (RR) and C-N ratios ($\alpha = 0.05$).	269
Table 12-1. Soil sample locations for mixed-cultured fermentations.	283
Table 12-2. Operating parameters for batch fermentations.....	290
Table 12-3. Operating parameters for CPDM fermentations.	293

	Page
Table 12-4. Operating parameters for countercurrent fermentations. Normalized parameters represent the mean of the steady-state values \pm CI (95% CI).....	295
Table 12-5. Performance for batch fermentations.....	297
Table 12-6. Sample data matrix for the rate equation fit for CPDM 1.	299
Table 12-7. Constant values used to simulate the fermentations and generate the performance maps in CPDM 1, 2, 3, 4, and 5 and resulting conversion and total acid concentration.	300
Table 12-8. Performance measures of countercurrent fermentation Trains 1, 2, 3, 4, and 5. Values represent the mean of the steady-state values \pm CI (95% CI).	304
Table 12-9. p values for performance measures for countercurrent fermentation Trains 1, 2, 3, 4, and 5 ($\alpha = 0.05$).	305
Table 13-1. Initial batch fermentation ingredients.	316
Table 13-2. Initial batch fermentation sample IDs and location.	317
Table 13-3. Initial batch fermentation results at 55 °C for Site V. Yellow highlight indicates highest performers for that variable.	318
Table 13-4. Initial batch fermentation results at 40 °C for Site V. Yellow highlight indicates highest performers for that variable. Red highlight indicates erroneous results*.	320
Table 13-5. Initial batch fermentation rankings at 40 °C and 55 °C for Site V.	322
Table 13-6. The carboxylate salts used in 100+ fermentations.....	324
Table 13-7. Samples selected for CPDM modeling.....	331
Table 13-8. Values of the parameters a , b , and c fitted by least squares analysis for La Sal del Rey inoculum A21.....	331
Table 13-9. Values of the parameters a , b , and c fitted by least squares analysis for La Sal del Rey inoculum A21.....	333
Table 13-10. Values of the parameters a , b , and c fitted by least squares analysis for La Sal del Rey inoculum A23.....	335

	Page
Table 13-11. Values of the parameters <i>a</i> , <i>b</i> , and <i>c</i> fitted by least squares analysis for La Sal del Rey inoculum A23.....	337
Table 13-12. Values of the parameters <i>a</i> , <i>b</i> , and <i>c</i> fitted by least squares analysis for La Sal del Rey inoculum A25.....	339
Table 13-13. Values of the parameters <i>a</i> , <i>b</i> , and <i>c</i> fitted by least squares analysis for La Sal del Rey inoculum A25.....	340
Table 13-14. Values of the parameters <i>a</i> , <i>b</i> , and <i>c</i> fitted by least squares analysis for Roswell-Carlsbad, NM inoculum G21.....	342
Table 13-15. Values of the parameters <i>a</i> , <i>b</i> , and <i>c</i> fitted by least squares analysis for Roswell-Carlsbad, NM inoculum G21.....	344
Table 13-16. Values of the parameters <i>a</i> , <i>b</i> , and <i>c</i> fitted by least squares analysis for Roswell-Carlsbad, NM inoculum G38.....	346
Table 13-17. Values of the parameters <i>a</i> , <i>b</i> , and <i>c</i> fitted by least squares analysis for Roswell-Carlsbad, NM inoculum G38.....	348
Table 13-18. Operating parameters for countercurrent continuous Trains G08, H20, and K49.....	354
Table 13-19. Performance measures for fermentation Trains G08, H20, and K49. Values represent the mean of the steady-state values \pm CI (95% CI).	355
Table 14-1. Performance results for MSW-derived pulp and control fermentations. Values represent averaged values of triplicates \pm standard deviation. ...	364
Table 14-2. Substrate-to-control final acid concentration ratio of MSW-derived pulp and other substrates (Forrest et al., 2010b).....	364
Table 14-3. Performance results for SunChips® compostable bag fermentations. Values represent averages of triplicate fermentations \pm standard deviation.	370
Table 14-4. Performance comparison of SunChips® compostable bag and other substrates.....	370
Table 14-5. Performance results of oregano supplemented paper \pm standard error.....	379
Table 14-6. Performance data of raw corn stover for a 28-d batch fermentation. Values represent the average of quadruplets \pm standard deviation.....	386

Table 15-1. Chicken manure conditions that were used as the nutrient source in batch carboxylate fermentations.	389
Table 15-2. Performance of different conditioned chicken manure batch fermentations. Values represent the mean of the triplicate fermentations \pm standard deviation.	395
Table 16-1. Original sugar concentration of liquid fermentation broth and “cells” for cellobiose, glucose, and xylose.	414
Table 16-2. Acid product concentrations and percent composition of mixed-culture (F) and <i>E. coli</i> (E) after incubation in TYE media in the presence (+glu) and absence (–glu) of glucose after a digestion time of 480 min and 1200 min.	444
Table 16-3. Glucose-utilization assay summary of experiments for <i>E. coli</i> and fermentation mixed culture.	455
Table 16-4. Glucose-utilization assay summary of experiments for <i>E. coli</i> and fermentation mixed culture.	457
Table 17-1. Qualitative comparison of performance measures for fermentations operating with different configurations and modes of operation.	459

1. INTRODUCTION

Fossil fuels (e.g., natural gas, petroleum, and coal) currently meet most of the world's energy needs. The consumption of liquid transportation fuels (e.g., gasoline, diesel, and aviation fuel) is continuing to increase with economic expansion and population growth (Nigam and Singh, 2011). Transportation fuels are predominately supplied by petroleum. Their combustion causes pollution and acid rain (Armaroli and Balzani, 2011; Demirbas, 2007) and accounts for 57% of global anthropogenic greenhouse gas emissions (WWI, 2009). It is projected that the share of non-hydro renewables in power generation will increase from 3% in 2009 to 15% in 2035 (IEA, 2011b). Also, petroleum is a finite resource that has volatile and increasing prices (Alekkett et al., 2010). To meet growing energy needs, sustainable and nonpolluting energy sources are needed to supply growing transportation fuel needs and increase national security by replacing foreign oil with domestic fuels.

On an energy basis, lignocellulose is the fourth largest energy source in the world, behind oil, coal, and natural gas, respectively. The oldest and most versatile renewable fuel, biomass is commonly used to produce steam and electricity. About 50% of the world's population burns biomass fuels (BMFs) (e.g., wood, litter, and crop residues) as the primary source of energy for household cooking (Ezzati and Kammen, 2002; WHO, 2005). Because non-food lignocellulosic biomass is inexpensive and abundant, it is an important energy source (Zhang, 2008). Biomass is already a large contributor to global energy supply, and will continue to grow in both developed and developing countries (Demirbas, 2008). Converting biomass into a liquid fuel does not cause net increase in atmospheric carbon dioxide (Hileman, 1999; Ragauskas et al., 2006) because biomass growth removes the same amount of carbon dioxide from the atmosphere that was released during the combustion of the biomass (Sterzinger, 1995).

This dissertation follows the style and format of Bioresource Technology.

An alternative method for creating energy from BMFs is to produce liquid and gaseous biofuels. Currently, biofuels are the only renewable means of displacing liquid fossil fuels, and represent 3.5% of transport fossil fuels on a volumetric basis (IEA, 2011c). Bioethanol and biodiesel are the main liquid biofuel contributors, which are made from starchy grains and oil seeds, respectively (Demirbas, 2008). However, these fuels are inconvenient to handle and use in the existing petroleum infrastructure (Savage, 2011). Both bioethanol and biodiesel have not been commercially viable without significant government support, even with the two top biofuels markets (e.g., United States, Brazil) being the most efficient producers of the feedstock (e.g., maize, sugarcane). For both of these biofuels, feedstock costs comprise more than half the total production cost, and trade policies create market distortions (Kojima et al., 2007).

The most common method to convert biomass to bioethanol is simultaneous saccharification and fermentation (SSF), a process that enzymatically hydrolyzes lignocellulose to sugars that are simultaneously fermented to alcohol. The primary drawbacks of this process are the need for expensive enzymes and sterile operating conditions, both of which contribute to high production costs. To unlock the potential of lignocellulose, which is much more abundant and less costly than starchy grains and oil seeds, new conversion technologies are required. The carboxylate platform, which converts lignocellulose to liquid fuels and chemicals, is a promising alternative (Agler et al., 2011).

The carboxylate platform (Figure 1-1) is a biomass-to-energy technology that biologically converts biomass (e.g., lignocellulose, lipids, proteins, carbohydrates) into carboxylate salts that are then chemically converted into chemicals and hydrocarbon fuels (Holtzaple et al., 1999; Holtzaple and Granda, 2009). In the fermentation step, biomass is fermented by a mixed-culture of microorganisms to produce carboxylic acids, which are buffered to form carboxylate salts. These salts can be precipitated and thermally converted to ketones (e.g., acetone), hydrogenated to produce mixed alcohols (e.g., isopropanol), and catalytically converted to hydrocarbons (e.g., gasoline, jet fuel, synthetic hydrocarbons). This continuous and versatile process produces liquid fuels

that can be fully used by existing engines, uses nearly any biomass feedstock (which minimizes market distortions and food scarcity), has low capital and operating costs, does not require sterile operating conditions or added enzymes, and has already reached the demonstration level of development.

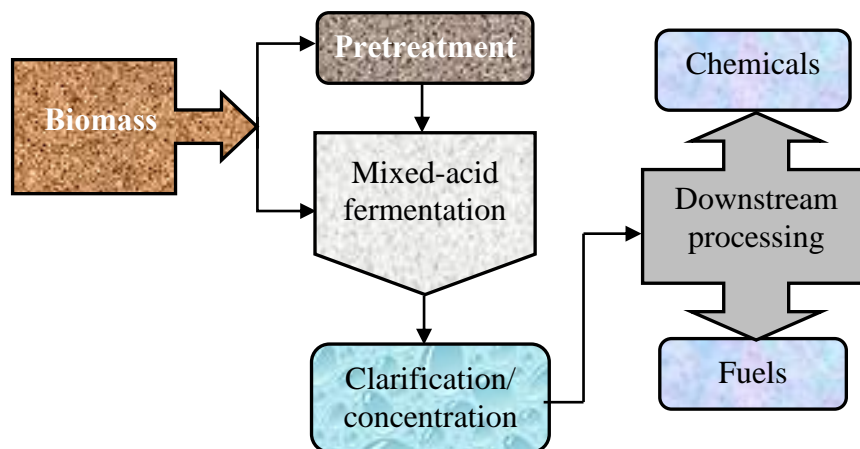


Figure 1-1. Diagram of the carboxylate platform.

Multi-staged fermentations have been used for many years in anaerobic digestors. In the anaerobic digestors, anaerobic conversion of biomass occurs in four phases:

- (1) *Hydrolysis* (or “liquefaction”) – complex molecules of organic matter (e.g., polysaccharides, lipids, and proteins) are hydrolyzed into simple sugars, fatty acids, and amino acids.
- (2) *Acidogenesis* – acidogenic bacteria produce new cells, short-chain organic acids, alcohols, hydrogen, carbon dioxide, and ammonia (Koster, 1984).
- (3) *Acetogenesis* – the products from acidogenesis are converted into more biomass, hydrogen, acetic acid, and carbon dioxide (Gujer and Zehnder, 1983).
- (4) *Methanogenesis* – these products are converted to carbon dioxide, methane, and other reduced metabolites.

In carboxylate fermentations, methanogenesis is inhibited to preserve the carboxylic acids. Each step in anaerobic digestion is performed by a specific group of microorganisms, each having an optimal temperature, pH, and substrate source for optimal growth. A single stage can be used; however, having different conditions in multiple stages allows each step in anaerobic digestion to be optimized (Ward et al., 2008).

In carboxylate fermentations, multi-staged countercurrent fermentations (Figure 1-2), such as the four-stage train studied in this dissertation, have filtered liquid and solid phases flowing countercurrently. As biomass digests, it becomes less reactive, decreasing production of carboxylic acids. The fermentation product (carboxylic acids) further inhibits biomass digestion. Countercurrent fermentation minimizes inhibition by allowing the most digested biomass to contact the lowest concentration of carboxylate salts and the least digested biomass to contact the highest concentration (Aiello-Mazzarri et al., 2006). This fermentation design allows for high conversions and product concentrations, making it preferred over batch or single-stage fermentation. A single-staged fermentation is a semi-continuous continuously stirred tank reactor (CSTR), where liquids and solids are added and removed in a single fermentor.

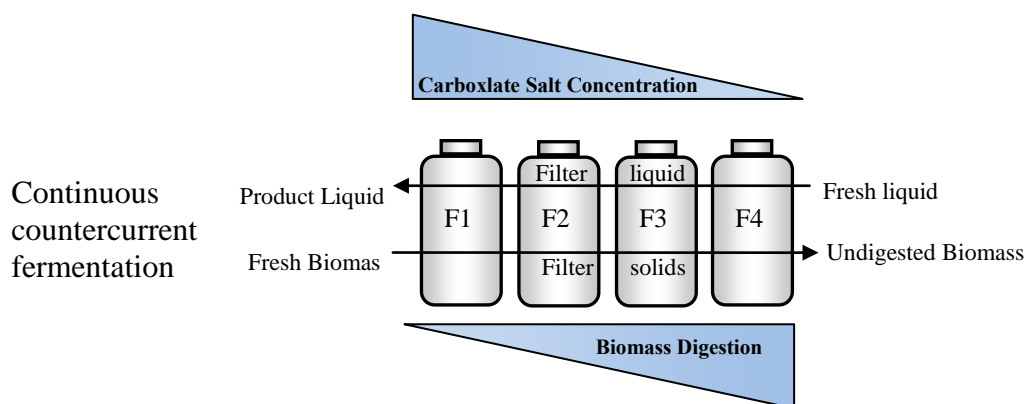


Figure 1-2. Diagram of the four-stage continuous countercurrent fermentation.

Fermentation performance and product spectra depend on the types and proportions of microorganisms present in the inoculum. To study different inocula in the carboxylate platform, biodiversity prospecting (a.k.a. bioprospecting) can be used (Leary et al., 2009), where microorganisms, plants, and fungi in nature are evaluated for their usefulness in specific products, applications, or processes. For the carboxylate platform, mixed cultures of microorganisms already existing in unique environments can be harvested for specific biological reactions. This mixed culture survives and thrives in nature and is far more stable and robust than pure cultures (Hawkes et al., 2007).

A mixed culture is extremely well suited to a non-sterile, fluctuating environment with multiple feedstocks, offering advantages over a pure culture (Angenent et al., 2004; Das and Veziroglu, 2001). A pure culture of one bacterial species might produce significant amounts of a single desired product, but only in batch mode in a sterile system protected from outside microorganisms. The mixed culture may establish a robust, synergistic community that grows faster than a pure culture and will also maintain itself better against microbial contamination (Rokem et al., 1980). The stability of the mixed-culture system has been linked to increased diversity of the microbial community and to an increased ability to adapt to changes in the system environment (Angenent et al., 2004). Additionally, because of their high diversity, these cultures can metabolize mixtures of substrates and the variable composition observed in waste streams (Kleerebezem and van Loosdrecht, 2007; Reis et al., 2003; Rodriguez et al., 2006).

The main purpose of this research is to understand the effects of different fermentation modes (e.g., propagated fixed-bed, multiple stages, biomass and cell recycle, and air exposure), inoculum source (e.g., bioscreening), and feedstocks (e.g., recycled municipal solid waste, biodegradable polylactic acid (PLA) plastic bags, and shredded paper) on fermentation performance at varying fermentation conditions.

This dissertation focuses on improving the fermentation performance of the carboxylate platform by investigating the effects of several different bioreactor modes of operation, inoculum sources and loadings, and substrates.

The following is a list of detailed objectives performed to meet the main goal:

- Determine the effects of air exposure on anaerobic mixed-acid fermentation.
- Determine the effects of propagated fixed-bed configuration on fermentation performance.
- Determine effects of cell recycle and biomass recycle on fermentation performance.
- Experimentally determine the effects of stage number on fermentation performance variables.
- Validate a three-part bioscreening technique to screen for optimal fermentation performance in natural bacterial communities, and employ these bioscreens on a series of inoculum sites.
- Develop a method to quantify microbial load in biomass and soil samples using a glucose-utilization assay.
- Ferment multiple substrates with Galveston inoculum to determine potential yield and conversion in the carboxylate platform.
- Determine the effects of different conditions of chicken manure on batch fermentation performance.

2. INVESTIGATION OF INTERMITTENT AIR EXPOSURE ON FOUR-STAGE AND ONE-STAGE ANAEROBIC SEMI- CONTINUOUS MIXED-ACID FERMENTATIONS

This study evaluated anaerobic mixed-acid countercurrent fermentations in both *strict*, S (minimal oxygen), and *relaxed*, R (high oxygen), conditions. In relaxed fermentations, filter solids and liquids were exposed to air for 90 min every 56 h. The total acid concentrations for four-stage trains were 23.0 (4S) and 22.1 (4R) g/L_{Liq}, and for one-stage trains were 17.2 (1S) and 18.4 (1R) g/L_{Liq}. The strict and relaxed trains had statistically similar exit yields. The strict trains had significantly more high-molecular-weight carboxylic acids. Air exposure had no significant effect on the bacterial profiles of the strict and relaxed fermentations. For all fermentations, the most abundant bacterial genus was *Prevotella*, a strict anaerobe. This study shows that the mixed-culture community is oxygen tolerant because it maintains fermentation performance during oxygen-induced stress.

2.1 Introduction

On an energy basis, lignocellulose is the fourth largest energy source in the world, behind oil, coal, and natural gas, respectively (Rosillo-Calle and Hall, 1992). The oldest and most versatile renewable fuel, biomass is commonly used to produce steam and electricity. As an alternative, biomass can be converted to liquid transportation fuels and industrial chemicals using the MixAlco™ process, an example of the carboxylate platform (Holtzapfle and Granda, 2009). It reduces dependence on imported fossil fuels, provides an alternative to more expensive renewable energy resources, and is more easily scaled down than thermochemical techniques.

The MixAlco™ process is a biomass-to-energy technology that biologically converts biomass (e.g., lignocellulose, fats, proteins, carbohydrates) into carboxylate salts that are then chemically converted into chemicals and hydrocarbon fuel (Holtzapfle

et al., 1999). In the fermentation step, biomass is fermented by a mixed-culture of microorganisms to produce carboxylic acids, which are buffered to form carboxylate salts. These salts are precipitated and thermally converted to ketones (e.g., acetone), hydrogenated to mixed alcohols (e.g., isopropanol), and catalytically converted to hydrocarbons (e.g., gasoline, jet fuel).

Multi-staged countercurrent fermentations (Figure 2-1), such as the four-stage train in this study, have filtered liquid and solid phases flowing countercurrently. As biomass digests, it becomes less reactive, decreasing production of carboxylic acids. The fermentation product (carboxylic acids) further inhibits biomass digestion. Countercurrent fermentation minimizes inhibition by allowing the most digested biomass to contact the lowest concentration of carboxylate salts and the least digested biomass to contact the highest concentration (Aiello-Mazzarri et al., 2006). This fermentation design allows for high conversions and product concentrations, making it preferred over batch or single-stage fermentation. A single-staged fermentation (Figure 2-1) is a semi-continuous continuously stirred tank reactor (CSTR), where liquids and solids are added and removed in a single fermentor.

Fermentations have been conducted successfully on a pilot plant scale (Moody, 2006); however, because solids and liquids were exposed to the open air, the pilot plant operations were not completely anaerobic. Air exposure occurred particularly during the filtration operations that were performed to transfer mass countercurrently. During mass transfers, biomass would be stored in open buckets for 60–120 min while waiting to be processed. Further, air would enter the headspace when the fermentors were open for manual mixing. Previous pilot plant data suggests that air exposure allowed for significant aerobic degradation of the biomass (Smith, 2011). Understanding the aerotolerance of the mixed-culture fermentations is necessary to determine the effect of air exposure on pilot plant performance, and conclude the necessity of a more quantitative oxygen study. Also, determining the oxygen tolerance of the MixAlco™ fermentations helps guide equipment selection in industrial fermentations.

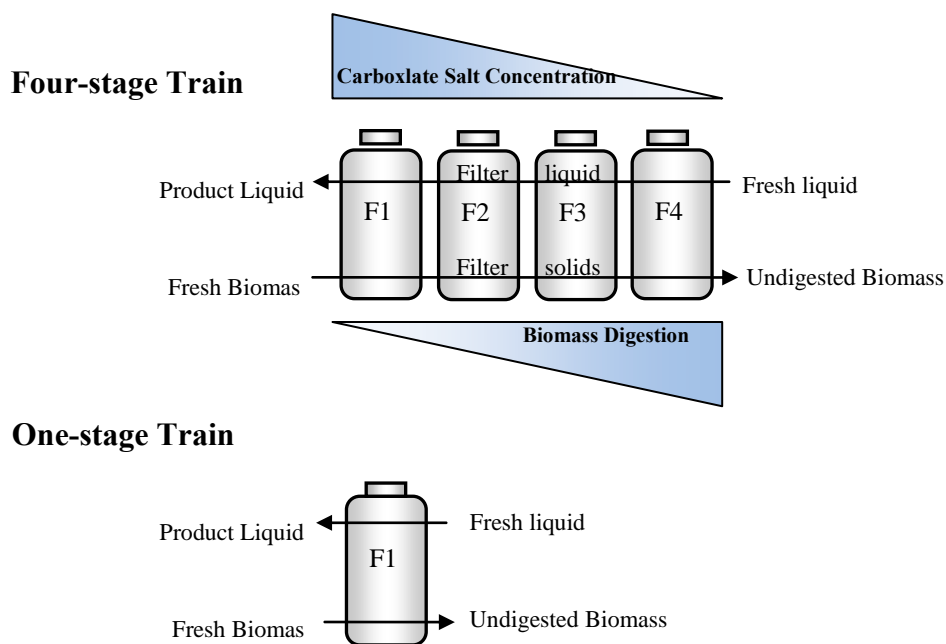


Figure 2-1. Diagram of four- and one-stage fermentations.

For oxygen to affect the fermentation, oxygen must transport through three phases: gas, liquid (culture medium), and solid (microbial cells). The following mass transfer steps must occur during aerobiosis: (1) dissolution of oxygen from bulk gas phase into liquid phase (assumed to be at equilibrium at the interface), (2) diffusion of oxygen through liquid film into the bulk liquid phase, (3) transport of oxygen through the liquid film that adheres to solids at the liquid-solid interface, (4) transport of oxygen across the cell envelope, and (5) transport through the cytoplasm to the intracellular reaction sites. The solubility of oxygen in water depends on temperature, oxygen partial pressure, and the amount of dissolved solids (salts, organics) present in the liquid. The solubility of gas in liquid is inversely proportional to the salt and organics content. Step 1 is the rate-limiting step because oxygen is sparingly soluble in water, around 8.10 mg/L (ppm) for pure water. With 20 g/L salt, oxygen solubility in water was calculated as 6.7 ppm using the Bunsen coefficient (Blanch and Clark, 1996).

Even for strict anaerobes, exposure to atmospheric oxygen does not guarantee death. Anaerobes have different aerotolerances depending on the oxygen concentration, exposure time, and growth phase. For example, in the stationary growth phase, some communities are more tolerant of oxygen (Fournier et al., 2006). Some obligate anaerobes die upon exposure to nanomolar concentrations of oxygen, whereas microaerotolerant or aerotolerant anaerobes can survive with varying degrees of oxygen consumption and cell viability (Loesche, 1969). Some strict anaerobes tolerate aerobic environments by growing in a mixed-culture biofilm where they are protected by oxygen-consuming facultative anaerobes or aerobes. For example, the strict anaerobe *Prevotella nigresces* can grow in the mouth cavity even though it is an aerobic environment (Bradshaw et al., 1997). In a mixed culture, strict anaerobes can be protected from aerobiosis by facultative anaerobic and aerobic microorganisms that consume dissolved oxygen, diffusional resistances of oxygen in water, antioxidative enzymes, physical barriers such as extracellular polymeric substance (EPS) matrix if a biofilm is present, and other cellular debris (Morris, 1976).

Traditionally, inocula for MixAlco™ fermentations are collected from saline, anaerobic environments (Fu and Holtzapple, 2010a) that are exploited to digest biomass to produce mixed volatile carboxylic acids (C₂–C₇). This naturally occurring mixed culture offers a robust community that is well suited to the non-sterile environment and multiple feedstocks found in the MixAlco™ process (Forrest et al., 2010b). At the laboratory scale, it is fairly easy to maintain strict anaerobic conditions. For example, when fermentors are open during solid/liquid mass transfers, the fermentor head space is purged with an inert gas (e.g., N₂). Also, the culture medium has oxygen-depleting chemicals, such as cysteine hydrochloride and sodium sulfide. However, at the industrial scale, it can be difficult and expensive to maintain strict anaerobic conditions. It requires sealing the fermentors, pipelines, pumps, heat exchangers, and filtration equipment, and purging the headspace with an inert and oxygen-free gas. To determine the impact of air exposure on anaerobic fermentations, this study compared air-depleted (*strict*) fermentations to air-exposed (*relaxed*) fermentations.

2.2 Methods

2.2.1 Fermentor configuration

The fermentation reactors are 1-L polypropylene centrifuge bottles capped by a rubber stopper inserted with a glass tube (Figure 2-2) (Ross, 1998). Two segments of 1/4-in stainless steel pipe were inserted through the rubber stopper into the vessel which mixed the contents of the fermentor as it rotated in the rolling incubator. A rubber septum sealed the glass tube and allowed for gas sampling and release. A rubber septum sealed the glass tube and allowed for gas sampling and release.

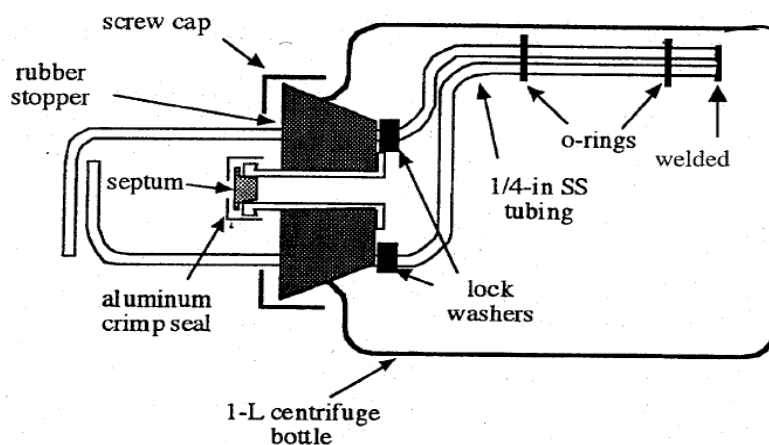


Figure 2-2. Plastic fermentation reactor.

2.2.2 Substrate

Shredded office copier paper was obtained from local recycling center and fermented in continuous mode, and because it is free of lignin, did not undergo pretreatment. Chicken manure was the nutrient source for the microorganisms and was obtained from Feathercrest Farms, Inc., (Bryan, TX).

2.2.3 *Fermentation medium*

For strict operation, the deoxygenated medium was prepared by boiling distilled water to liberate dissolved oxygen. After cooling to room temperature in a covered vessel, to further reduce the oxygen content, 0.275 g/L cysteine hydrochloride and 0.275 g/L sodium sulfide were added. For relaxed operation, distilled water was used.

2.2.4 *Inoculum*

Mixed-microbial inoculum was collected from the MixAlco™ pilot plant, located at Texas A&M in College Station, TX, which was initially inoculated with a mixed-culture of marine microorganisms found in beach sediment collected on Galveston Island, TX. Sediment was removed from the bottom of multiple shoreline pits 0.5 m deep. Samples were immediately placed in airtight plastic bottles filled with deoxygenated water, capped, and frozen at $-20\text{ }^{\circ}\text{C}$ until use. Before inoculation, samples were thawed, shaken vigorously, and allowed to settle by gravity. Equal parts of the resulting supernatant were homogenized, and aliquots were used to inoculate each fermentation reactor to 12.5% of the working volume.

2.2.5 *Methanogen inhibition*

Iodoform (CHI_3) was used to inhibit methane production. Iodoform solution (80 μL , 20 g CHI_3/L 190-proof ethanol) was added to each fermentor, relaxed and strict, every 56 hr (Ross, 1998). Because iodoform is light, air, and temperature sensitive, to prevent degradation the solution was kept in amber-colored glass bottles wrapped in foil, stored at $-20\text{ }^{\circ}\text{C}$, and special care was taken to replace the cap immediately after use (Agbogbo and Holtzapple, 2007).

2.2.6 *Countercurrent strict and relaxed fermentation procedure*

Two oxygen exposure conditions (strict and relaxed) were studied for two fermentation configurations (one-stage and four-stage fermentation train). By purging fermentor headspace with nitrogen gas during transfers and sample collection and using deoxygenated water, the strict trains had minimal oxygen contact. The relaxed train was designed to mimic oxygen exposure exhibited during pilot-plant operations.

Because this chapter compares oxygen exposure effects and not fermentor configuration, comparisons will be limited to the strict and relaxed trains of their respective one- or four-stage trains. The one- and four-stage trains were tested to observe oxygen effects on different reactor configurations. The one-stage fermentation (Figure 2-1) is a semi-continuous flow continuously stirred tank reactor (CSTR). In this reactor configuration, liquids and solids were added and removed in a single fermentor. The one-stage train has a single carboxylate salt concentration whereas the four-stage train has a different concentration in each stage. In the one-stage train, the reactor volume is significantly less than the four-stage train. To achieve the same volatile solid loading rate (VSLR) and liquid residence times (LRT) in all trains, the fed non-acid volatile solid (NAVS) and fermentation liquid were scaled down in the one-stage train.

The four- and one-stage fermentations were initiated as batch cultures under anaerobic conditions with a concentration of 100 g NADS/L deoxygenated water, which was achieved by adding substrate, nutrient source (manure), inoculum, calcium carbonate (buffer), and liquid medium to each fermentor. The feed consisted of 80% shredded office copier paper and 20% wet homogenized chicken manure on a dry mass basis. Each fermentor was incubated in a roller incubator at mesophilic conditions (40 °C) for 8 months. The initial pH for all fermentations was approximately 6.6. During the fermentations, the pH varied from 5.3 to 6.6.

Every 56 h, the strict and relaxed fermentors were removed from the incubator, the gas volume was collected, liquid samples were taken, the pH was measured, and the mass transfers were performed. After completing the solid/liquid mass transfer, iodoform was added, and 1.0 g calcium carbonate was added to each fermentor to neutralize carboxylic acids and buffer the system. When they were open to the atmosphere during the mass transfers, anaerobic conditions were maintained in the strict fermentors by flushing the fermentors with nitrogen gas (Praxair, Bryan, TX). The fermentors were then resealed and placed back in the incubator.



Figure 2-3. Photo of biomass during a 90-minute air exposure. A – filter solids in weigh boat; B – filter liquid in beaker; C – 1-L fermentation bottle

In the relaxed train, a nitrogen purge and deoxygenated water were not used during solid/liquid mass transfers. The liquid and solid biomass from each fermentor was separated via centrifuge and underwent air exposure for 90 min (Figure 2-3). To facilitate aeration, the solid biomass was broken up into approximately 1.25-cm homogeneous pieces and dispersed on a weigh boat. The solid biomass and liquid were weighed before and after air exposure to measure volatile evaporation. This exposure time was chosen because it corresponds to the maximum biomass air exposure during pilot-plant operations.

2.2.7 Dissolved oxygen in fermentation liquid

The dissolved oxygen (DO) was measured with a dissolved oxygen meter (Cole-palmer, EW53026-00). Atmospheric air was the calibration standard, accounting for elevation and salt content. To find the DO in the fermentation liquid of the relaxed train for the duration of the 90-min air exposure, the probe was placed at the specified liquid depth and measured with time. The fermentation liquid was not agitated at the pilot plant for the majority of the air-exposure period; therefore the air-exposed fermentation liquid for this experiment was not agitated, making diffusion, not convection, the main mode of oxygen transport. To minimize agitation, the probe was placed in the fermentation liquid at a height of 3 cm from the liquid bottom, at an average depth of 7

cm below the liquid surface, for the entire 90-min air exposure. The DO for the fermentation liquid was measured for both strict and relaxed fermentors before and after incubation, and monitored throughout the air exposure period of the relaxed train. During the incubation time, all fermentors were sealed and not exposed to the atmosphere.

2.2.8 *Analytical methods*

2.2.8.1 *Carboxylic acid concentration determination*

Fermentation product liquid was collected on a time interval basis for acid analysis. Centrifuged (4,000 rpm, 3300×g, 25 min) fermentation liquid was mixed with equal parts of internal standard (1.162 g/L 4-methyl-*n*-valeric acid) and 3-M phosphoric acid (H₃PO₄), and then ultra-centrifuged (15,000 rpm, 18,360×g, 8 min). The H₃PO₄ ensures that the carboxylate salts are converted into carboxylic acid prior to analysis. The carboxylic acid concentration was measured using an Agilent 6890 Series gas chromatograph (GC) system equipped with a flame ionization detector (FID) and an Agilent 7683 automatic liquid sampler. A 30-m fused-silica capillary column (J&W Scientific Model # 123-3232) was used. The column head pressure was maintained at 2 atm abs. After each sample injection, the GC temperature program raised the temperature from 40 °C to 200 °C at 20 °C/min. The temperature was subsequently held at 200 °C for 2 min. The total run time per sample was 11 min. Helium was the carrier gas. The external standard was volatile acid mix (Matreya, LLC, Cat No. 1075), used to calibrate the samples against the IC-6 internal standard.

2.2.8.2 *Biogas analysis*

Biogas is a product of fermentation and needs to be removed from the fermentation reactors to relieve pressure buildup and prevent fermentor rupture. For the first two weeks, each fermentor was vented daily due to the high initial digestion rate, and then each fermentor was vented three times a week. The biogas was removed by puncturing a needle through the fermentor septum and controlled with a valve on the needle. A polypropylene tube connected the needle to a well-sealed inverted cylinder.

The biogas volume was measured by liquid displacement using an inverted graduated glass cylinder filled with an aqueous solution of 300 g CaCl₂/L to prevent microbial growth and carbon dioxide adsorption (Domke, 1999). Average maximum pressure in the reactors was found by dividing the headspace area by the total volume of biogas released every 56 h.

Biogas composition was measured and methane was monitored by manual injection of a 5-mL gas sample into an Agilent 6890 Series chromatograph with a thermal conductivity detector (TCD). A 4.6-m stainless steel packed column with 2.1-mm ID (60/80 Carboxen 100, Supelco 1-2390) was used. The inlet temperature was 230 °C, the detector temperature was 200 °C, and the oven temperature was 200 °C. The total run time was 10 min, and helium was the carrier gas.

2.2.8.3 *Moisture and ash contents*

Moisture and ash contents were determined as previously described (NREL, 2004). The ash content was calculated on a dry basis. To accurately account for the produced volatile acids, 30 mg Ca(OH)₂/(g sample) was added to the sample before drying to ensure all volatile acids were in the salt form. The consumption of non-acid volatile solids (NAVS) was determined using the inert-ash approach as described previously (Smith et al., 2011).

2.2.9 *Operating parameters*

The liquid residence time (LRT) and volatile solid loading rate (VSLR) (Table 2-1) were regulated by controlling the transfer frequency (T), the non-acid volatile solids (NAVS) feed rate, the liquid feed rate, and the amount of cake retained in each fermentation reactor per transfer.

Volatile solids (VS) are defined as the mass of dry solid material that is combusted at 575 °C after 12 h, and NAVS are defined as VS less the amount of carboxylate salt residue that remains in the ash:

$$\text{NAVS} = (\text{g total biomass})(1 - \text{MC})(1 - \text{AC}) - (\text{g acid in biomass}) \quad (2-1)$$

where MC is the fraction of moisture in the biomass (g water/g wet biomass), and AC is the fraction of dry ash left after 12 h of combustion at 575 °C (g inert biomass/g dry biomass). Because the desired fermentation product is carboxylic acids, NAVS is used instead of VS to achieve a more accurate measure of performance. The nutrient source (fresh chicken manure) typically has indigenous carboxylic acids. Because fermentation performance is measured by the carboxylic acids produced in the fermentation system, the amount of acid fed to the system is subtracted from the amount of exiting acid.

The volatile solid loading rate (VSLR) and the liquid residence time (LRT) are calculated as follows:

$$\text{VSLR} = \frac{\text{NAVS feed}}{\text{total liquid volume in all fermentors} \cdot \text{time}} \quad (2-2)$$

$$\text{LRT} = \frac{\text{total liquid volume in all fermentors}}{\text{flow rate out of fermentation train}} \quad (2-3)$$

Table 2-1. Operating parameters for the air exposure fermentations.

		4S	4R	1S	1R
Fermentation Train					
Transfer frequency (T)		3 per week; every 56 h			
Controlled	NAVS feed rate (g NAVS/T)	16.7	16.7	4.0	4.0
	Liquid feed rate (mL/T)	300	300	44	44
	Wet filter cake and bottle setpoint (g)	300	300	300	300
	Filter liquid retained in F1–F4 (mL)	0	0	131	131
	Methane inhibitor ($\mu\text{L}/(\text{T} \cdot \text{bottle})$)	80	80	80	80
Normalized	Volatile solid loading rate, VSLR (g NAVS/(L _{liq} ·d))	5.1	5.2	5.1	5.1
	Liquid residence time, LRT (d)	32.6	29.6	32.0	29.0
	Volatile solid, VS, concentration (g NAVS/L _{liq})	101	102	107	116
	Dry solid, DS, concentration (g NADS/L _{liq})	161	163	184	195
	Total liquid volume, TLV (L)	1.40	1.37	0.34	0.34

T = transfer = 56 h

2.2.10 Definition of terms

Cellulose is a polysaccharide composed of individual glucan units (MW = 162 g) which, during digestion, are enzymatically hydrolyzed to glucose. The water of hydrolysis was calculated as previously described (Aiello-Mazzarri et al., 2006). The mixed-acid concentration can be expressed as acetic acid equivalents (Aceq), which is the reducing potential of an equivalent amount of acetic acid (Holtzapple et al., 1999). Aceq proportionally weighs the higher-chained carboxylic acids (C₃ to C₇); the higher acids have higher Aceq than lower acids.

2.2.11 Measuring performance

The inlet and outlet rate of acid, ash, NAVS, water, and gas were determined during the steady-state period. The average rate of each component was calculated using the *slope method*, which is described as follows (Smith and Holtzapple, 2011b). The moving cumulative sum of each component is plotted with respect to time. The slope of the steady-state portion of this line is the rate. All performance variables (e.g., conversion, selectivity, and yield) were calculated from the averaged component rates determined by the slope method, as described below:

$$\begin{aligned}
 \text{Conversion } (x) &\equiv \frac{\text{NADS}_{\text{feed}} - \text{NADS}_{\text{exit}}}{\text{NAVS}_{\text{feed}}} \\
 &= \frac{\text{NAVS}_{\text{feed}} + \text{Ash}_{\text{feed}} - \text{NAVS}_{\text{exit}} - \text{Ash}_{\text{exit}}}{\text{NAVS}_{\text{feed}}} \quad (2-4) \\
 &= \frac{\text{NAVS}_{\text{consumed}}}{\text{NAVS}_{\text{feed}}}
 \end{aligned}$$

$$\text{Exit yield } (Y_E) \equiv \frac{\text{g total acid output from solid and liquid streams}}{\text{g NAVS}_{\text{feed}}} \quad (2-5)$$

$$\text{Process yield } (Y_P) \equiv \frac{\text{g total acid output in liquid stream}}{\text{g NAVS}_{\text{feed}}} \quad (2-6)$$

Culture yield (Y_C)

$$\equiv \frac{\text{g total acid produced in solid and liquid streams}}{\text{g NAVS}_{\text{feed}}} \quad (2-7)$$

$$\equiv Y_E - Y_F$$

$$\text{Feed yield } (Y_F) \equiv \frac{\text{g total acid entering with feed}}{\text{g NAVS}_{\text{feed}}} \quad (2-8)$$

$$\text{Selectivity } (\sigma) \equiv \frac{\text{g total acid produced}}{\text{g NAVS}_{\text{feed}} - \text{g NAVS}_{\text{exit}}} \equiv \frac{\text{g total acid produced}}{\text{g NAVS digested}} \quad (2-9)$$

$$= \frac{Y_E}{x}$$

$$\text{Acid productivity } (P) \equiv \frac{\text{g total acids produced}}{\text{TLV} \cdot \text{d}} \quad (2-10)$$

where $\text{NADS}_{\text{feed}}$ is the non-acid dry solids fed, $\text{NADS}_{\text{exit}}$ is the non-acid dry solids removed from the fermentation, $\text{NAVS}_{\text{feed}}$ is the non-acid volatile solids fed, $\text{NAVS}_{\text{exit}}$ is the non-acid volatile solids removed from the fermentation, Ash_{feed} is the inert solids fed in biomass feed and buffer, Ash_{exit} is the inert solids exiting in all solid and liquid streams, and TLV is the total liquid volume in the fermentation train including free and interstitial liquid. NADS includes the ash and volatile solid component of biomass. Ash is assumed to be conserved in the fermentation (Ash_{feed} equals Ash_{exit}), canceling Ash from Equation 2-4.

Per g NAVS fed, the exit yield (Y_E) represents the sum of acid in the product transfer liquid, waste transfer solids, and liquid samples removed from sampling. The process yield (Y_P) represents all the acid in the product transfer liquid per g of NAVS fed. The feed yield (Y_F) is the total g acid entering with the feed per g NAVS fed, and the culture yield (Y_C) is the exit yield less the feed yield.

2.2.12 *DNA isolation and sequencing to obtain bacterial profile*

To evaluate the effect of air exposure on the microbial community, DNA analysis was performed on the strict four-stage (4S), relaxed four-stage (4R), strict one-stage train (1S), and relaxed one-stage (1R) fermentation trains. For each train, homogenized solid biomass was collected from each reactor, combined in equal portions, homogenized again, and then frozen until DNA extraction.

2.2.12.1 *DNA extraction and purification*

Emily Hollister in Soil and Crop Sciences extracted community DNA from each sample using a DNeasy blood and tissue kit (Qiagen, Valencia, CA). Prior to extraction, 5 mL of fermentor fluid and an equal volume of fermentor solids were placed in a 15-mL centrifuge tube and vortexed at high speed for 2 min. The samples were centrifuged at 1000×g for 1 min, the supernatants collected, and 1.5 mL of each was extracted according to the kit manufacturer's protocol for Gram-positive bacteria. Following elution, the DNA samples were purified using illustra MicroSpin S-400 HR columns (GE Healthcare Bio-Sciences Corp, Piscataway, NJ, USA), and then quantified with a NanoDrop ND-1000 spectrophotometer (NanoDrop Technologies, Wilmington, DE, USA).

2.2.12.2 *Bacterial tag-encoded amplicon pyrosequencing*

The purified bioreactor DNA samples were submitted to the Research and Testing Laboratory (Lubbock, TX, USA) for tag-pyrosequencing. Samples were amplified with modified versions of the primers 27F and 519R (Hollister et al., 2011), and the amplicons were sequenced using Roche 454 Titanium chemistry, producing reads in the forward direction from 27F. Sequences were quality checked and trimmed according to Acosta-Martínez *et al.* (Acosta-Martínez et al., 2008).

2.2.12.3 *Sequence analysis and community comparisons*

The Ribosomal Database Project (RDP) pyrosequencing pipeline and Classifier function were used to align and assign identities to the 454 sequence data (Cole et al., 2007) (accessed November 9, 2009). Those sequences that were shorter than 400 bp

length, contained any ambiguous base-pair reads, or did not align with the 16S rRNA region were considered to be sequencing errors and were excluded from further analysis.

Distance matrices were constructed for 454 sequence libraries using the `dist.seqs` function in MOTHUR, version 1.7.0 (Schloss et al., 2009). MOTHUR was also used to assign sequences to operational taxonomic units (OTU, 97% similarity) and calculate Shannon's diversity index values (H'), Chao I richness estimates, and θ_{YC} similarity values.

To illustrate the relationships shared among them and aid in their classification, the most abundant OTUs encountered within the fermentors were identified and subjected to additional phylogenetic analysis. Three nearest-neighbor sequences for each OTU were obtained from the Greengenes chimera-checked database (DeSantis et al., 2006). Sequences were aligned using the Infernal model-based alignment feature at the Ribosomal Database Project (Cole et al., 2009; Nawrocki et al., 2009), they were bootstrapped with 100 replicates using Phylip's Seqboot function, and then the corresponding distance matrices were calculated using DNAdist with the Jukes-Cantor evolutionary model (Felsenstein, 2005). Phylip's Neighbor function was used to construct neighbor-joining phylogenetic trees, and the Consense function was used to identify a consensus tree (Felsenstein, 2005).

Sequence reads were submitted to the NCBI Short Read Archive under accession number SRA021000.

2.2.13 *Statistical analysis*

The statistical analysis in this study was performed using Excel 2007 (Microsoft, USA). The mean and standard deviations of the total acid concentrations, acetic acid equivalent (Aceq), non-acid volatile solids (NAVS) in and out were determined from steady-state operating data (Days 128 to 216). These averaged values were then used to calculate the acid productivity (P), selectivity (σ), yield (Y), and conversion (x) with a 95% confidence interval (CI). The steady-state region was determined to be when the product acid concentration varied by 2.2 standard deviations or less away from the average for a period of at least two liquid residence times. Student's two sample t -test

(two-tailed, type 3) was used to compute p values. Results were considered statistically significant at the 5% level. All error bars are reported at 95% CI.

2.3 Results and discussion

With regard to oxygen utilization, bacteria may be classified into three groups: (1) obligate aerobic microorganisms, which need oxygen to support microbial activity; (2) strict anaerobes, which cannot obtain energy from oxygen respiration and, in general, cannot survive in atmospheric oxygen for extended time; and (3) facultative microorganisms, which can grow either with or without oxygen using different metabolic processes (Brioukhanov and Netrusov, 2007). During aerobic growth, microorganisms utilize organic matter along with gaseous oxygen to create more biomass and oxidized metabolites. In contrast, strict anaerobes – including bacteria of genera *Bacteroides*, *Clostridium*, *Desulfovibrio* (sulfate-reducing bacteria), and *Methanosarcina* (methanogenic archae) – must metabolize oxygen in organic molecules to obtain energy.

Anaerobic conversion of biomass occurs in four phases: (1) Via hydrolysis (or “liquefaction”), complex molecules of organic matter (e.g., polysaccharides, lipids, and proteins) are hydrolyzed into simple sugars, fatty acids, and amino acids. (2) Via acidogenesis, acidogenic bacteria produce new cells, short-chain organic acids, alcohols, hydrogen, carbon dioxide, and ammonia (Koster, 1984). (3) Via acetogenesis, the products from acidogenesis are converted into more biomass, hydrogen, acetic acid, and carbon dioxide (Gujer and Zehnder, 1983). (4) Via methanogenesis, these products are converted to carbon dioxide, methane, and other reduced metabolites. In the MixAlco™ process, methanogenesis is inhibited to preserve the carboxylic acids. To allow strict anaerobes to be maintained in the culture, oxygen must be restricted below a threshold of 0.4% O₂ (Tally et al., 1975).

At the laboratory scale, the fermentors have a higher surface-to-volume ratio than the pilot plant; thus, it is expected that air exposure will have less of a detrimental effect with increasing scale.

2.3.1 *Dissolved oxygen in fermentation broth and oxygen toxicity of microbes*

In the relaxed trains, the dissolved oxygen (DO) in the fermentation liquid was measured during the 90-min air exposure at an average depth of 6 mm from the surface at 24°C. After the 90-min air exposure, the average DO in the liquid broth of the one- and four-stage relaxed trains was experimentally found to be 6.7 ppm (0.21 $\mu\text{mol O}_2/\text{mL}$) which is equivalent to air-saturated water with a salt content of 20 g/L. Before incubating, the strict fermentors had 2.2 ppm DO in the filtered liquid whereas the relaxed fermentors had an average of 6.7 ppm DO. After being incubated for 56 hours, DO decreased in all fermentors. In all relaxed fermentors, the filtered liquid reached an average DO of 0.6 ± 0.2 ppm. In all strict fermentors, the filtered liquid reached an average DO of 0.2 ± 0.1 ppm. One study suggests that strict anaerobes are defined as being able to divide below 0.4% O_2 in the gas headspace (0.16 ppm DO) and aerotolerant anaerobes can divide from 0.4% to 10% O_2 (3.25 ppm DO) (Tally et al., 1975). Based on these criteria, strict anaerobes may exist in the strict fermentors whereas aerotolerant anaerobes may exist in the relaxed fermentors.

2.3.2 *Evaporation of water during air exposure*

Under normal atmospheric conditions, the pilot plant experiences evaporative loss of the fermentation liquid. At the laboratory scale, to determine mass lost to evaporation, the filter solid and filter liquid were weighed before and after the 90-min air exposure. For the relaxed fermentors, the average change in mass was 0.71 ± 0.06 and 0.68 ± 0.08 g per fermentor for the liquid and solids, respectively. This resulted in a total loss of 1.39 g, or 0.3% of total fermentation mass per fermentor, which is not significant.

2.3.3 *Biogas*

During a 56-h batch period, the four-stage fermentors produced 2.01 ± 0.16 (4S) and 1.31 ± 0.10 (4R) g gas, whereas the one-stage fermentors produced 0.44 ± 0.05 (1S) and 0.30 ± 0.04 (1R) g gas. The strict fermentations produced significantly more gas

than their relaxed counterparts ($p \ll 0.001$). No methane was detected in any fermentor. After 56 h, the average pressure in the fermentors was 1.7 atm abs.

2.3.4 Acid concentration, productivities, and daily acid production

For all four experimental conditions, Figure 2-4 shows the total carboxylic and Aceq concentrations. Figure 2-5 shows the accumulated amount of total carboxylic acids exiting and the accumulated amounts of NADS added and removed from their respective trains. After Day 128, the slopes of the lines provide the data needed to calculate the productivity and exiting daily amounts presented in Table 2-2. The four-stage fermentors had average steady-state total carboxylic acid concentrations of 23.0 ± 0.7 (4S) and 22.1 ± 0.6 (4R) g/L_{liq}, acetic acid equivalent concentrations of 32.4 ± 0.9 (4S) and 28.9 ± 0.8 (4R) g/L_{liq}, and productivities of 0.81 (4S) and 0.80 (4R) g/(L_{liq}·d). The one-stage fermentors had average steady-state total carboxylic acid concentrations of 17.2 ± 0.4 (1S) and 18.3 ± 0.4 (1R) g/L_{liq}, acetic acid equivalent concentration of 23.9 ± 0.6 (1S) and 24.0 ± 0.5 (1R) g/L_{liq}, and productivities of 0.81 (1S) and 0.82 (1R) g/(L_{liq}·d).

However, because the relaxed trains had slightly higher conversions, and evaporation occurred during the 90-min air exposure, the relaxed trains had decreased LRT and TLV. To minimize the effects of liquid volume changes, the amount of acid exiting the fermentors per day is calculated on a mass basis from the product liquid and waste streams. The total carboxylic acid exiting the four-stage fermentors was 1.07 ± 0.07 (4S) and 1.04 ± 0.07 (4R) g total acid/d ($p = 0.94$), and exiting the one-stage fermentors was 0.26 ± 0.02 (1S) and 0.26 ± 0.02 (1R) g total acid/d ($p = 0.80$). The amount of total Aceq exiting per day for the four-stage fermentors was 1.50 ± 0.10 (4S) and 1.36 ± 0.10 (4R) g Aceq acid/d ($p = 0.14$), and exiting the one-stage fermentors was 0.36 ± 0.03 (1S) and 0.34 ± 0.02 (1R) g Aceq acid/d ($p = 0.36$). These data indicate that the daily amounts of total acid and Aceq exiting the 4S and 4R, and 1S and 1R fermentors are not statistically different. It is interesting that the strict trains had slightly higher daily amounts of exiting Aceq.

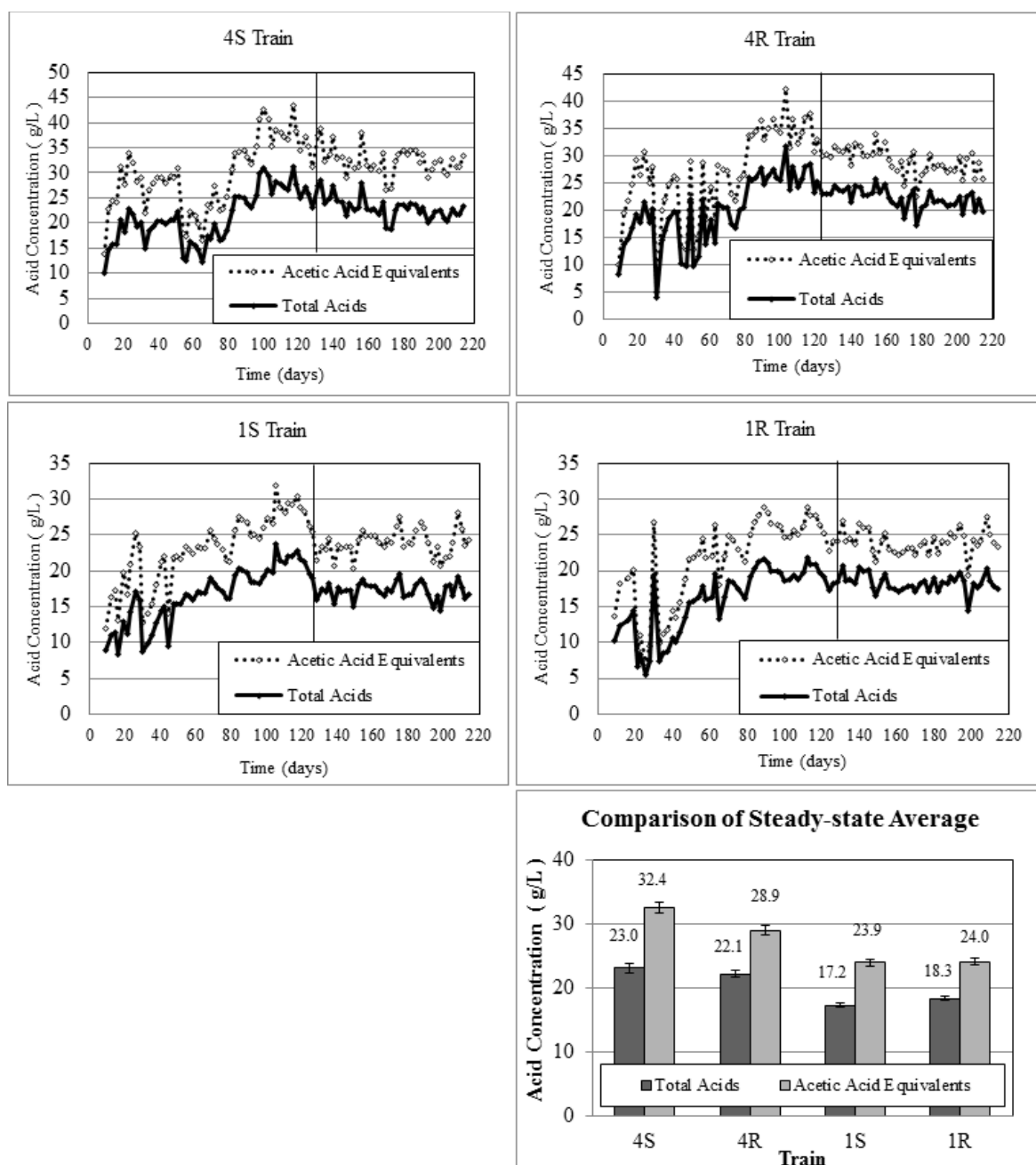


Figure 2-4. Total and acetic acid equivalent carboxylic acid concentrations for Fermentations 4S, 4R, 1S, and 1R. The vertical lines mark the onset of steady state (Days 128–218). Error bars represent the 95% confidence interval of acid concentrations during the steady-state period.

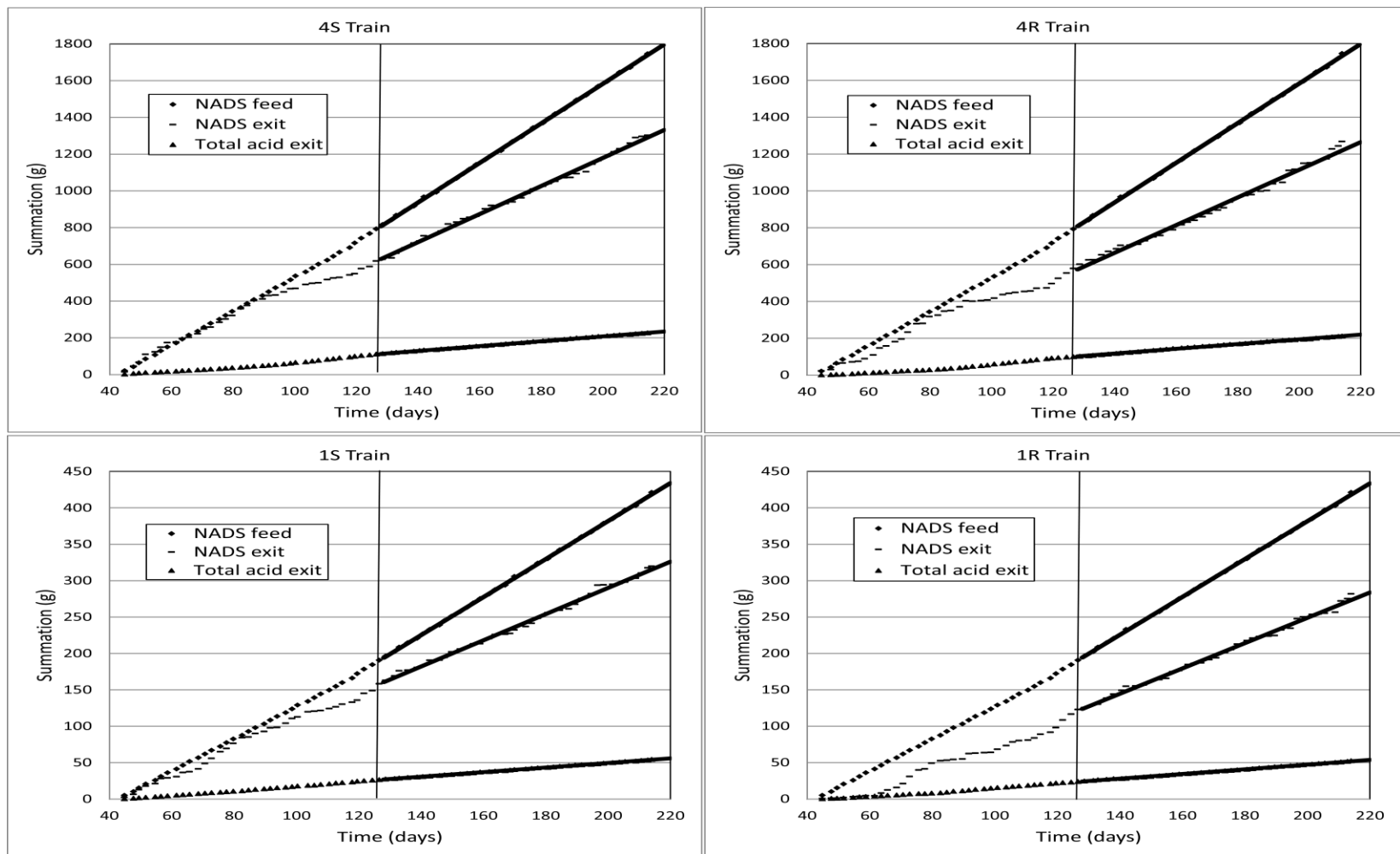


Figure 2-5. Summation of non-acid dry solids (NADS) exiting and fed and total acids exiting for Fermentations 4S, 4R, 1S, and 1R. The vertical lines mark the onset of steady state (Days 128–218).

Table 2-2. Performance measures for fermentations 4S, 4R, 1S, and 1R. Values represent the mean of the steady-state values \pm CI (95% CI).

	4S	4R	1S	1R
Total carboxylic acid concentration (g/L)	23.0 \pm 0.7	22.1 \pm 0.6	17.2 \pm 0.4	18.3 \pm 0.4
Aceq concentration (g/L)	32.4 \pm 0.8	28.9 \pm 0.8	23.9 \pm 0.6	24.0 \pm 0.5
Acetic acid (wt %)	35.62 \pm 0.88	41.85 \pm 0.66	33.01 \pm 1.12	39.88 \pm 0.68
Propionic acid (wt %)	36.74 \pm 1.44	43.71 \pm 1.56	43.06 \pm 0.50	46.64 \pm 0.35
Butyric acid (wt %)	7.00 \pm 0.48	5.70 \pm 0.47	5.78 \pm 0.30	5.21 \pm 0.08
Valeric acid (wt %)	13.85 \pm 0.72	7.25 \pm 0.34	13.14 \pm 0.81	7.16 \pm 0.50
Caproic acid (wt %)	2.28 \pm 0.27	0.75 \pm 0.12	1.53 \pm 0.11	0.54 \pm 0.04
Heptanoic acid (wt %)	4.52 \pm 0.56	0.66 \pm 0.09	3.47 \pm 0.29	0.57 \pm 0.09
Aceq/Acid ratio	1.41 \pm 0.01	1.31 \pm 0.00	1.39 \pm 0.02	1.31 \pm 0.01
Conversion, x (g VS digested/g VS fed)	0.437 \pm 0.015	0.454 \pm 0.023	0.470 \pm 0.018	0.502 \pm 0.019
Selectivity, σ (g acid produced/g NAVS consumed)	0.422 \pm 0.015	0.394 \pm 0.021	0.389 \pm 0.015	0.374 \pm 0.015
Aceq selectivity, σ_a (g Aceq produced/g NAVS consumed)	0.595 \pm 0.022	0.514 \pm 0.027	0.541 \pm 0.021	0.488 \pm 0.020
Exit yield, Y_E (g acid/g NAVS fed)	0.184 \pm 0.003	0.179 \pm 0.004	0.183 \pm 0.003	0.188 \pm 0.003
Exit Aceq yield, Y_{aE} (g Aceq/g NAVS fed)	0.260 \pm 0.003	0.233 \pm 0.003	0.254 \pm 0.002	0.245 \pm 0.003
Culture yield, Y_C (g acid/g NAVS fed)	0.159 \pm 0.003	0.153 \pm 0.004	0.157 \pm 0.003	0.162 \pm 0.003
Process yield, Y_P (g acid/g NAVS fed)	0.166 \pm 0.002	0.170 \pm 0.002	0.128 \pm 0.002	0.147 \pm 0.003
Productivity, P (g total acid/(L _{liq} ·d))	0.808 \pm 0.010	0.799 \pm 0.014	0.805 \pm 0.006	0.824 \pm 0.011
Total carboxylic acid exiting (g/d)	1.07 \pm 0.07	1.04 \pm 0.07	0.26 \pm 0.02	0.26 \pm 0.02
Aceq exiting (g/d)	1.50 \pm 0.10	1.36 \pm 0.10	0.36 \pm 0.03	0.34 \pm 0.02

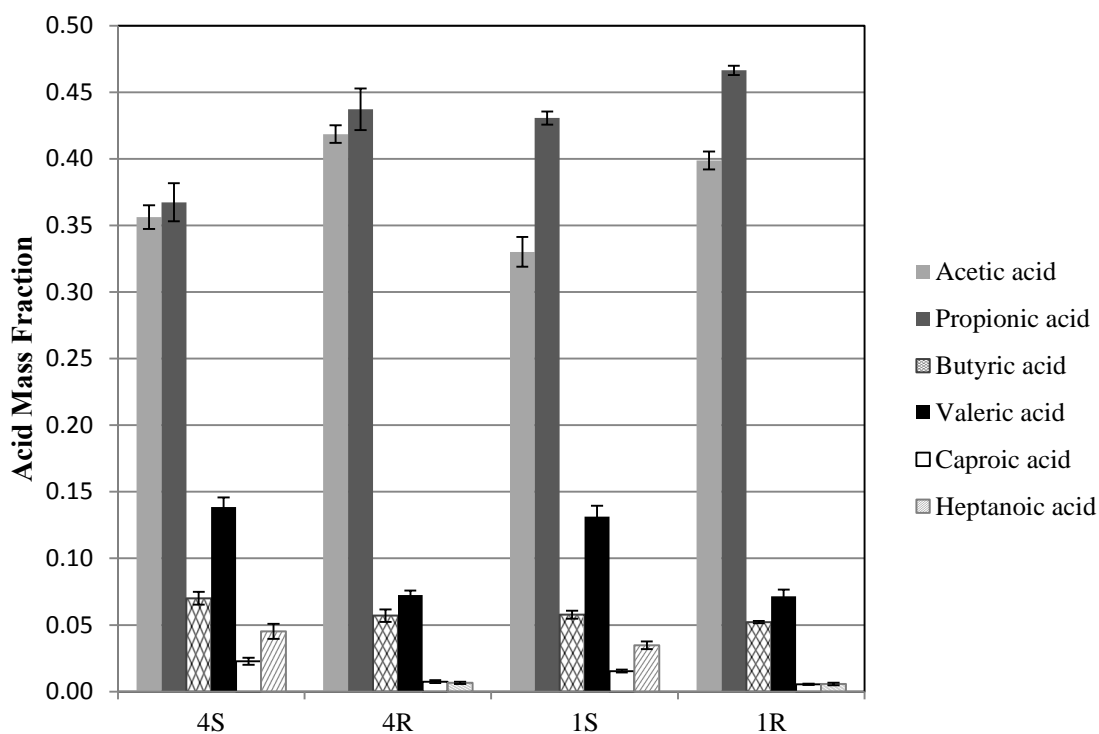


Figure 2-6. Carboxylic acid composition profile. Error bars are the 95% confidence intervals for each carboxylic acid composition during the steady-state period.

Compared to the relaxed trains, the strict fermentors tended to have a greater proportion of high-molecular-weight carboxylic acids (e.g., valeric, caproic, and heptanoic acid). The Aceq-to-total-acid ratio for the four-stage fermentors was 1.41 ± 0.01 (4S) and 1.31 ± 0.00 (4R) ($p \ll 0$), and for the one-stage fermentors was 1.39 ± 0.02 (1S) and 1.31 ± 0.01 (1R) ($p \ll 0$) (Table 2-2, Figure 2-4).

2.3.5 Yield

The exit (Y_E) and culture yields (Y_C) were not significantly influenced by air exposure (Table 2-2, Figure 2-7). The exit yield Y_E (Equation 2-5) quantifies the sum of acid *exiting* the fermentation in the product transfer liquid, waste transfer solids, and liquid samples per g NAVS feed. The exit yield for the four-stage fermentors was 0.184 (4S) and 0.179 (4R) g acid/g NAVS_{feed} ($p = 0.27$) and for the one-stage fermentors was 0.183 (1S) and 0.188 (1R) g acid/g NAVS_{feed} ($p = 0.28$). In each case, the differences

were *not* statistically significantly. However, the exit Aceq yield for the four-stage fermentors was 0.260 (4S) and 0.233 (4R) g Aceq/g NAVS_{feed} ($p \ll 0$) and for the one-stage fermentors was 0.254 (1S) and 0.245 (1R) g Aceq/g NAVS_{feed} ($p = 0.02$). In these cases, the differences were statistically significantly because the strict trains produced more high-molecular-weight acids (Table 2-2, Figure 2-4).

The process yield Y_P (Equation 2-6) quantifies only the acid in the product transfer liquid per g NAVS_{feed}, which is sent downstream to be clarified, concentrated, and processed into chemicals and fuel; thus, Y_P represents the net acid yield. The process yields tended to be higher for the relaxed trains than the strict trains, but only significantly so for the one-stage trains (0.166 (4S) vs. 0.170 (4R) ($p = 0.22$) and 0.128 (1S) vs. 0.147 (1R) g acid produced/g NAVS_{feed}) ($p \ll 0$). This is most likely caused by the relaxed trains having a slightly higher conversion.

The culture yield Y_C (Equation 2-7) represents the acid *produced* by the mixed-culture per g NAVS_{feed} and is equal to the exit yield less the feed yield. The culture yields were not significantly different for the four-stage trains (0.159 (4S) vs. 0.153 (4R) g acid produced/g NAVS_{feed}) ($p = 0.52$) nor between the one-stage trains (0.157 (1S) vs. 0.162 (1R) g acid produced/g NAVS_{feed}) ($p = 0.54$), indicating insignificant reduction in bacterial performance from air exposure.

Similar trends in the yield, total carboxylic acid, and Aceq concentrations between the 4S and 4R trains and the 1S and 1R trains supports the conclusion that 90-min air exposure will not reduce fermentation performance on an industrial scale.

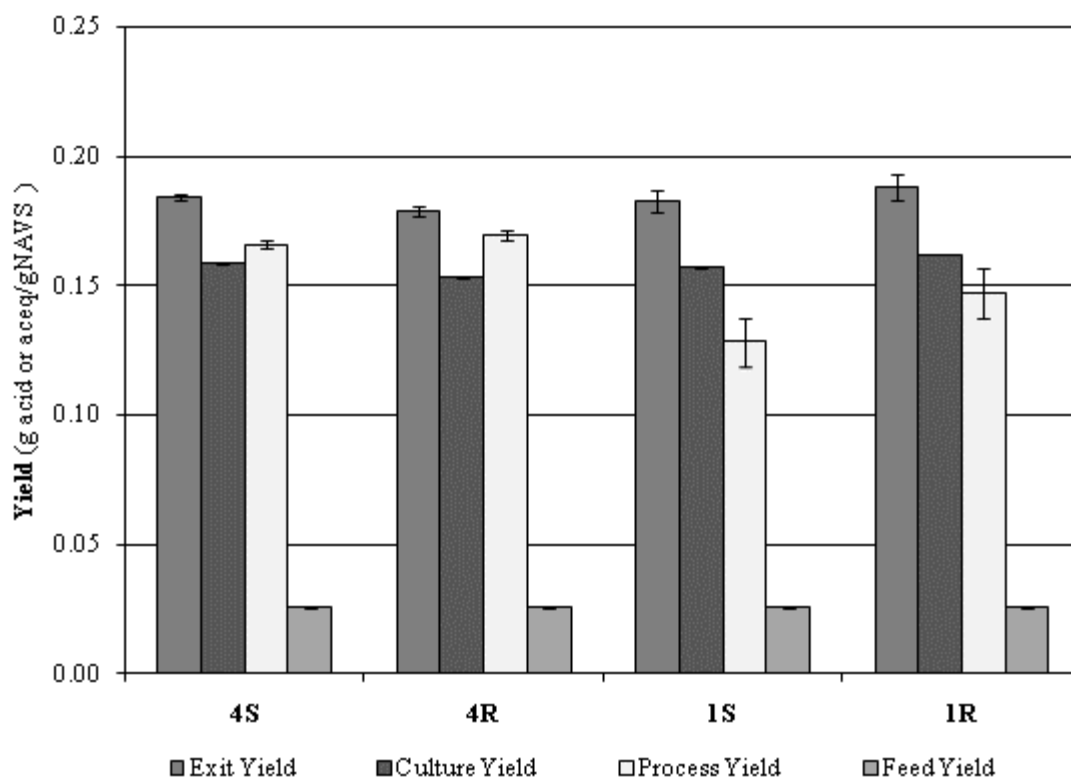


Figure 2-7. Yield values for Trains 4S, 4R, 1S, and 1R.

2.3.6 Conversion and selectivity

Conversion and selectivity (Equations 2-4 and 2-9) are shown in Table 2-2 and Figure 2-8. The strict trains did not have significantly higher conversions than the relaxed trains train (0.437 (4S) vs 0.454 (4R)) ($p = 0.54$) and 0.023 (1S) vs. 0.018 (1R)) ($p = 0.23$) g NAVS consumed /g NAVS fed). Although the difference is not significant, the relaxed fermentors tended to have a higher conversion than the strict fermentors, which could have resulted from aerobic degradation of the biomass during the air-exposure period. The 4S train did not have significantly higher selectivity than the 4R train (0.422 vs 0.394 g acid produced/g NAVS consumed) ($p = 0.30$), nor did the 1S and 1R trains (0.389 vs 0.374 g acid produced/g NAVS consumed) ($p = 0.50$). However, because the strict trains produced more high-molecular-weight acids (e.g., valeric,

caproic, and heptanoic acid) (Figure 2-6, Table 2-2), the 4S train had a significantly higher acetic acid equivalent selectivity than 4R (0.595 vs 0.514 g Aceq produced/g NAVS consumed) ($p < 0$); and 1S was higher than 1R (0.541 vs 0.488 g Aceq produced/g NAVS consumed) ($p = 0.02$).

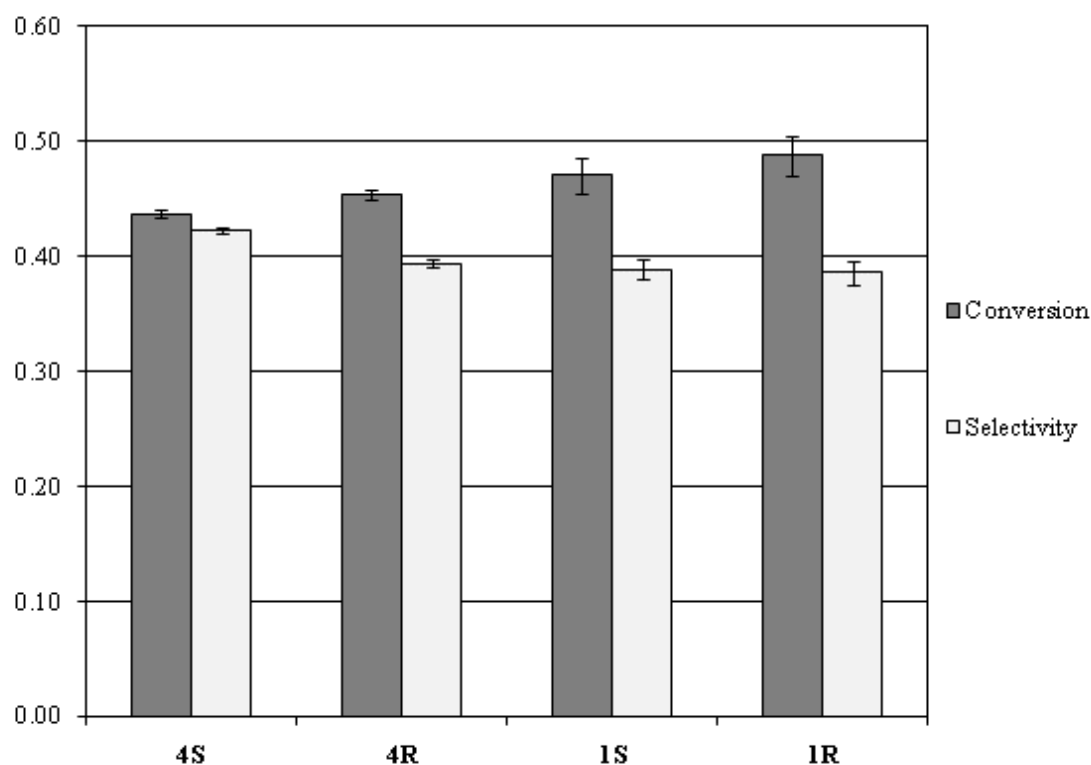


Figure 2-8. Conversion, selectivity, productivity, and acetic acid equivalent selectivity for Trains 4S, 4R, 1S, and 1R.

2.3.7 Bacterial profile

To characterize the bacterial communities across the two oxygen exposure treatments and fermentation train configurations (Table 2-3), a total of 25,228 partial 16S rRNA sequences were generated. The size, diversity, and estimated richness of the reactor communities were relatively similar to one another (Table 2-4). Likewise, the

communities were similar to each other (Figure 2-9). Bacteria from the phyla *Bacteroidetes* and the genus *Prevotella* (phylum: *Bacteroidetes*) were the most commonly encountered taxa accounting for 56–78% of each fermentor's bacterial community. Members of the *Actinobacteria* (closest genus-level matches including *Arcanobacterium* and *Actinobaculum*) accounted for an additional 14–27% of each community. Figure 2-10 illustrates the relationships of the most abundant operational taxonomic units (OTU) encountered within the reactor systems and their positions within the phylogeny of the *Bacteroidetes* and *Actinobacteria*.

Bacteria belonging to the genus *Prevotella* are characterized as starch- and xylose-degrading anaerobes, and are commonly found in cattle rumen (Stevenson and Weimer, 2007), other mammalian gut systems (Avgustin et al., 1997), and the human oral cavity. *Prevotella* spp have also been isolated from environmental sources, including plant roots and residues in rice paddy soils (Ueki et al., 2007). Similarly, members of the *Arcanobacterium* and *Actinobaculum* are commonly characterized as anaerobic or facultatively anaerobic species, many of which are able to ferment starch, xylose, and simple sugars (Schaal et al., 2006). Given this, it is likely that both the *Prevotella* and *Actinobaculum*- and *Arcanobacterium*-like bacteria identified here play important roles in degrading the non-cellulose portion of biomass feedstocks in the MixAlco™ system, whereas *Firmicutes* and *Actinobacteria* helped degrade the cellulose portion.

Table 2-3. Summary of sequence library sized, operational taxonomic units (OTUs, 97% similarity) and diversity and richness estimates for each of the reactor bacterial communities. The number of OTUs listed as “overall” is not equivalent to the sum of OTUs across all samples, because many OTUs were found within multiple fermentor communities.

Reactor	Sequence library size	Number of OTUs detected	Shannon (H')	Chao I richness
Overall	25,228	464	---	---
4S	5,681	190	2.47	307
4R	6,081	203	2.66	385
1S	7,292	261	2.84	468
1R	6,174	206	2.71	338

Table 2-4. Overlap of OTUs among the reactor communities, as θ_{YC} , the Yue-Clayton similarity estimator. θ_{YC} considers the number of OTUs shared between two communities, as well as their relative abundances. θ_{YC} is scored on a scale of 0 to 1, where 0 represents complete dissimilarity and a score of 1 represents identity.

	Reactor community		
	4S	4R	1S
4R	0.950	--	
1S	0.776	0.913	--
1R	0.904	0.977	0.946

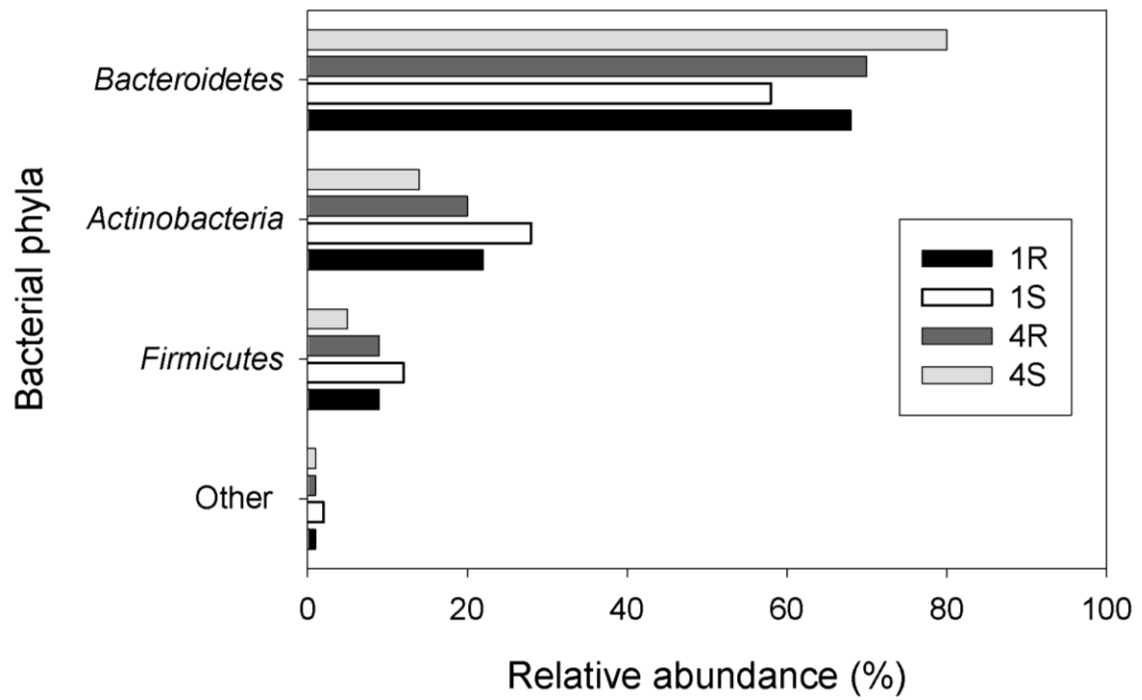


Figure 2-9. Relative abundances of bacterial phyla across oxygen exposure treatments and fermentation train configurations.

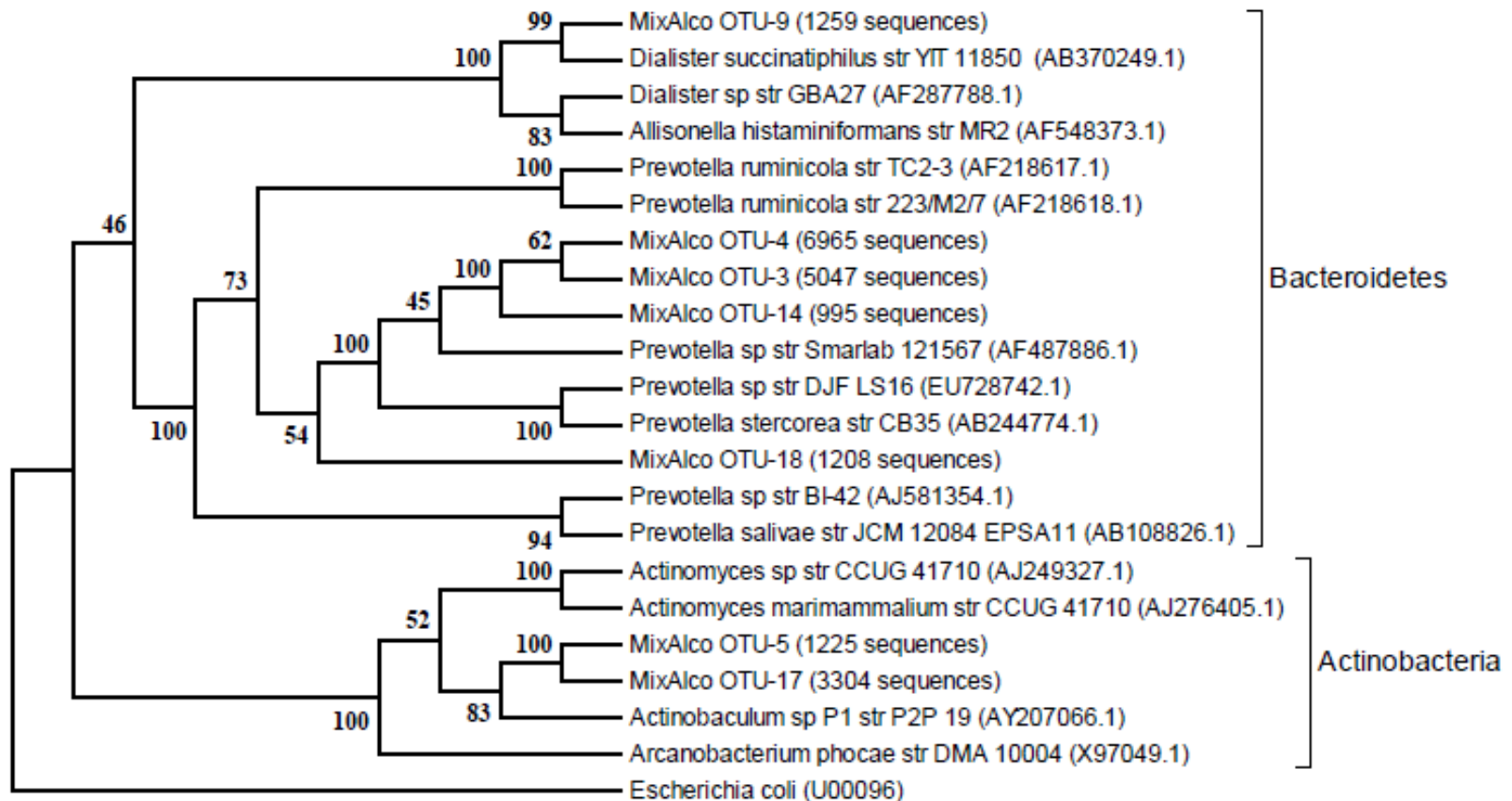


Figure 2-10. Neighbor-joining phylogenetic tree of the seven most abundant OTUs found within the bioreactor communities, collectively, and three nearest neighbor isolates from the Greengenes chimera-checked database. Bootstrap values (out of a possible 100) are provided at each branch point, but values < 50 are not presented. GenBank accession numbers are provided following each of the database-derived entries, and the number of sequences affiliated with each OTU is provided in parentheses.

2.3.8 *Biofilms*

No attempt was made to identify or quantify biofilms in this experiment. Their presence, however, could be suggested by the following reasons: (1) all bacterial profiles identified predominantly strict microorganisms; (2) similar trends in fermentation performance variables between the strict and relaxed fermentations; (3) substrate particles form spherical aggregates when rotating and digesting; (4) studies showing that strict anaerobes can live in aerated environments within a mixed-culture biofilm (Bradshaw et al., 1997). Reasons 1–3 could also be explained by the presence of facultative microorganisms, but the predominantly strict bacterial profiles found from DNA sequencing challenges this. Future work includes investigating the importance of biofilms and facultative anaerobes in these anaerobic mixed-acid fermentations.

2.4 **Conclusion**

Based on total carboxylic acid concentration, strict and relaxed fermentations had similar yields, conversions, and selectivities. However, based on acetic-acid-equivalent concentration, strict trains had significantly higher yields and selectivities than relaxed trains because strict trains produced more high-molecular-weight carboxylic acids. After intermittent oxygen exposure, the microbial flora contained both strict and facultative microbes, and all four fermentor configurations had similar bacterial profiles. Because the quantity and duration of oxygen exposure did not strongly affect fermentor performance or bacterial community composition, an industrial MixAlco™ fermentation could be intermittently exposed to air and maintain efficiency.

The effects of intermittent oxygen exposure on the bacterial profile showed no statistical differences in the bacterial profiles of all four fermentor configurations, and the amount of oxygen transport was less than the bacterial tolerance. These results suggest the presence of a facultative anaerobic *community* existing in a biofilm. The facultative anaerobes utilize the majority of oxygen before the oxygen exposure becomes toxic to strict anaerobes; additionally, biofilms may offer strict anaerobes protection from oxygen stresses in the environment.

3. PROPAGATED FIXED-BED MIXED-ACID FERMENTATION: EFFECT OF VOLATILE SOLID LOADING RATE AND AGITATION AT HIGH PH

Countercurrent fermentation is a high performing process design for mixed-acid fermentation. However, there are high operating costs associated with moving solids, which is an integral component of this configuration. This study investigated the effect of volatile solid loading rate (VSLR) and agitation in propagated fixed-bed fermentation, a configuration which may be more commercially viable. To evaluate the role of agitation on fixed-bed configuration performance, continuous mixing was compared with periodic mixing. VSLR was also varied and not found to affect acid yields. However, increased VSLR and liquid residence time did result in higher conversions, productivity, acid concentrations, but lower selectivities. Agitation was demonstrated to be important for this fermentor configuration; the periodically-mixed fermentation had the lowest conversion and yields. Operating at a high pH (~9) contributed to the high selectivity to acetic acid, which might be industrially desirable but at the cost of lower yield compared to a neutral pH.

3.1 Introduction

Fossil fuels (e.g., natural gas, petroleum, and coal) currently meet most of the world's energy needs. However, growing demand for these depleting resources (Jefferson, 2006) causes price instability and shortages; and fossil fuel combustion contributes to global warming, acid rain, and pollution (Demirbas, 2007). Sustainable and non-polluting energy sources are becoming increasingly important to meet our growing energy needs and help replace foreign oil with domestic fuels. The carboxylate platform, which converts lignocellulose to liquid fuels, is a promising alternative (Agler et al., 2011).

Lignocellulosic biomass is an important energy source (Carroll and Somerville, 2009). The oldest and most versatile renewable fuel, biomass is most commonly used to produce steam and electricity. As an alternative, using the carboxylate platform, biomass can be converted to liquid transportation fuels and industrial chemicals (Holtzaple and Granda, 2009). Converting biomass into liquid fuel does not cause a net increase in atmospheric carbon dioxide (Ragauskas et al., 2006) because biomass growth removes the same amount of carbon dioxide from the atmosphere that is released during combustion (Sterzinger, 1995). The carboxylate platform has attractive economics and is readily scaled down (Granda et al., 2009; Pham et al., 2010).

The carboxylate platform is being commercialized as the MixAlco™ process, a biomass-to-energy technology that biologically converts biomass (e.g., lignocellulose, fats, proteins, carbohydrates) into carboxylate salts that are then chemically converted into chemicals and hydrocarbon fuels (Holtzaple et al., 1999; Holtzaple and Granda, 2009). In the fermentation step, biomass is fermented by a mixed-culture of microorganisms to produce carboxylic acids (e.g., acetic acid), which are buffered to form carboxylate salts (e.g., calcium acetate). These salts are precipitated and thermally converted to ketones (e.g., acetone), hydrogenated to mixed alcohols (e.g., isopropanol), and catalytically converted to hydrocarbons (e.g., gasoline, jet fuel). This versatile continuous process uses nearly any biomass feedstock, which minimizes market distortions and food scarcity. It has low capital and operating costs, does not require sterile operating conditions or added enzymes, and has reached the demonstration level of development.

In a countercurrent fermentation, solids and liquids are transported through a series of fermentors (a *train*) in opposite directions, allowing the least reactive (most digested) biomass to contact the lowest acid concentration, thereby reducing product inhibition. This countercurrent strategy achieves both high product concentration and high conversion (Fu and Holtzaple, 2010b). However, at pilot-plant and industrial scales, the high solids content makes filtering and moving biomass difficult and time-consuming (Domke et al., 2004; Smith, 2011). The equipment used to filter and

transport solids is expensive and prone to fouling; however, transporting liquids or slurries is easily accomplished using pumps and piping.

Fixed-bed fermentation, a process in which only the liquid phase is transferred between fermentors in series, provides an alternative to the countercurrent configuration. The benefits of a fixed-bed fermentation include minimal solids handling and the potential for high product concentrations and productivities (Agbogbo and Holtzapple, 2007). Both pile fermentation, a configuration in which liquid flows by gravity through a fixed-bed or *pile*, and a submerged fixed-bed configuration minimize solids handling. However, previous studies demonstrated that fixed-bed fermentation without propagation can result in unsteady product concentrations with time because as the biomass digests, it becomes less reactive and produces less acid (Agbogbo and Holtzapple, 2007).

To address this unsteady-state issue, a propagated fixed-bed fermentation system (Figure 3-1) was implemented. In this system, fresh liquid is added to the most-digested fermentor, cascades through four fermentor stages, and exits as product liquid from the least-digested fermentor, while the solid phase remains stationary. The oldest fermentor with the most recalcitrant (digested) biomass is systematically replaced by a fermentor with fresh biomass. This “round robin” propagation of fermentors allows the system to have fresh substrate and so should achieve quasi-steady state and near-constant product concentrations, and still simulate a desirable commercial scenario. Understanding the performance of propagated fixed-bed fermentations helps evaluate the potential benefits of countercurrent flow in carboxylate fermentations, and can guide equipment selection in industrial fermentations.

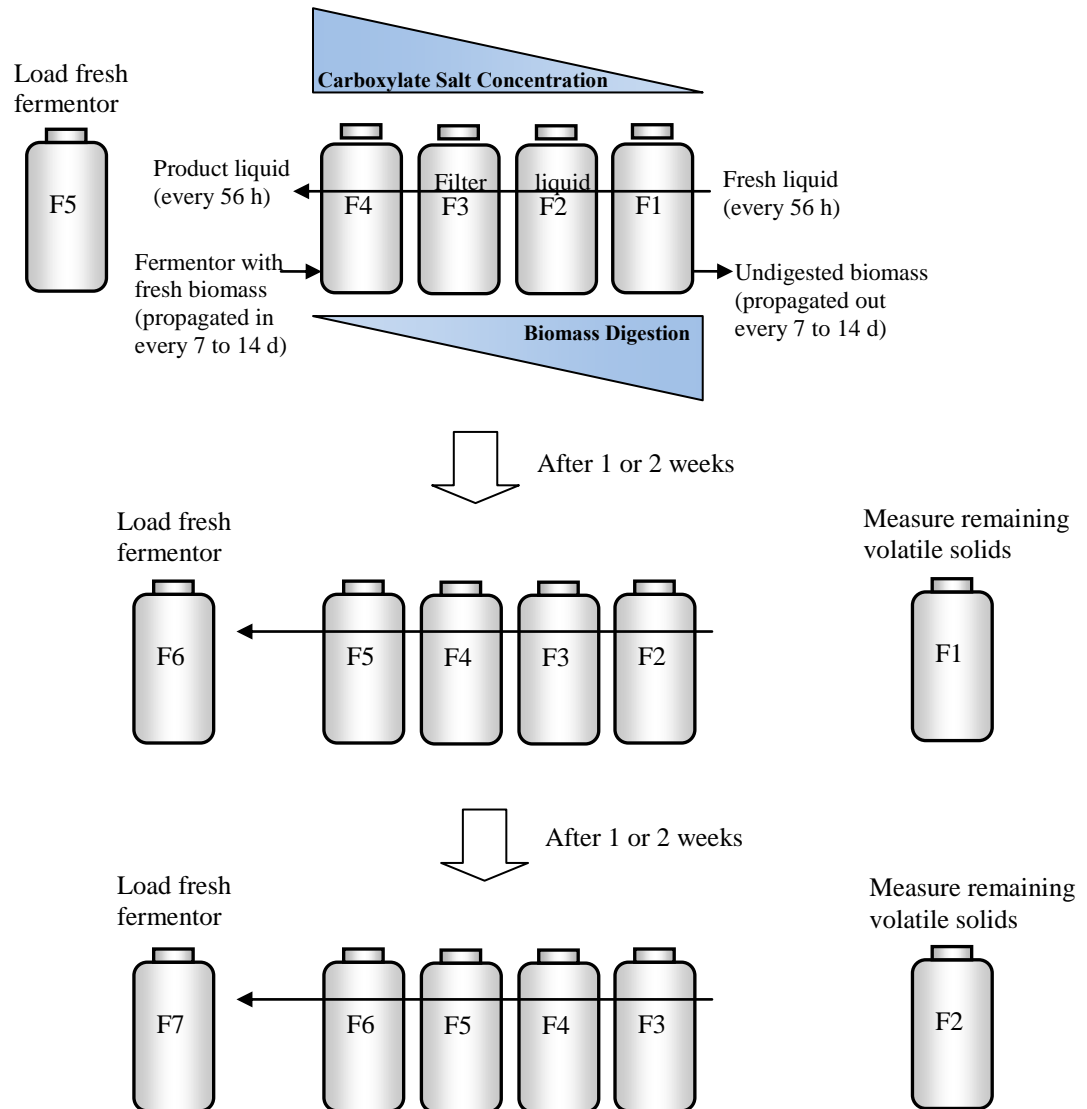


Figure 3-1. Illustration of laboratory operating procedure for four-stage propagated fixed-bed fermentation system.

In certain industrial processes, it is desirable to have high acetic acid concentrations. For example, the market for acetic acid is much larger than the market for higher acids. Additionally, if one is targeting ethylene from ethanol (Granda et al., 2009) or propylene from isopropanol (Pham et al., 2010), it would be desirable to increase selectivity to acetate. One way to accomplish this is by adjusting the fermentation pH. Generally, carboxylate fermentations are conducted at a pH between 5.5 to 6.5, an acceptable pH for acidogens (Khanal, 2008). However, numerous studies have shown that marine microorganisms tolerate alkalinity (Maeda and Taga, 1980). In batch studies, subjecting fermentation bacteria to a pH of >8 has been demonstrated to produce >92% acetic acid (Fu, 2007), compared to 40–60% acetic acid from similar studies at an average pH of 6 (Fu, 2007; Smith, 2011).

In this study, a novel propagated fixed-bed fermentation system was employed to evaluate high pH fermentation under continuous conditions. In addition, the effect of volatile solids loading rate (VSLR) is quantified, and a minimal mixing configuration was used to assess the potential impact on performance that might be expected in a fixed-bed system such as a pile fermentation.

3.2 Materials and methods

3.2.1 Fermentor configuration

The fermentors were 1-L polypropylene centrifuge bottles capped by a rubber stopper inserted with a glass tube (Ross, 1998). Two segments of ¼-in stainless steel pipe were inserted through the rubber stopper into the vessel to mix the contents of the fermentor as it rotated in the rolling incubator. A rubber septum sealed the glass tube and allowed for gas sampling and release.

3.2.2 Substrate

Shredded office paper, which served as the energy source, was obtained from a local recycling center. No pretreatment was required. Chicken manure, which served as an undefined nutrient source, was obtained from Feather Crest Farms, Inc. (Bryan, TX) and dried at 105 °C for 48 h. The substrate concentration is expressed as non-acid

volatile solids (NAVS), which is the combustible portion of the substrate minus carboxylic acids present in the feed.

3.2.3 *Fermentation medium*

The deoxygenated medium was prepared by boiling distilled water to liberate dissolved oxygen. After cooling to room temperature in a covered vessel, to further reduce the oxygen content, 0.275 g/L cysteine hydrochloride and 0.275 g/L sodium sulfide were added.

3.2.4 *Inoculum*

The inoculum was a mixed-culture of marine microorganisms found in beach sediment collected in Galveston Island, TX. Sediment was removed from the bottom of multiple 0.5-m-deep shoreline pits. Samples were immediately placed in airtight plastic bottles filled with deoxygenated water, capped, and frozen at $-20\text{ }^{\circ}\text{C}$ until use. Before inoculation, samples were thawed, shaken vigorously, and allowed to settle by gravity. Equal parts of the resulting supernatant were homogenized, and aliquots were used to standardize the fermentation inoculum to 12.5% of the initial working volume (Forrest et al., 2010a; Thanakoses, 2002). Bacterial community composition of mixed-acid fermentation has been reported elsewhere (Hollister et al., 2010; Hollister et al., 2011).

3.2.5 *Methanogen inhibition*

Iodoform (CHI_3) was used to inhibit methane production. Iodoform solution (80 μL , 20 g CHI_3/L 190-proof ethanol) was added to each fermentor every 56 h. Iodoform is sensitive to light, air, and temperature, and so the solution was kept in amber-colored glass bottles wrapped in foil and stored at $-20\text{ }^{\circ}\text{C}$ (Agbogbo and Holtzaple, 2007).

3.2.6 *Propagated fixed-bed fermentation procedure*

Four-stage propagated fixed-bed fermentation trains were used to investigate the effects of volatile solids loading rate (VSLR) and mixing. Five fermentation trains were initiated as batch cultures under anaerobic conditions with a concentration of 100, 200, or 300 g non-acid dry solids (NADS)/L deoxygenated water, which was achieved by

adding substrate, nutrient source (manure and urea), inoculum, buffer (calcium carbonate), and liquid medium to each fermentor. The feed consisted of 80% shredded office copier paper and 20% dry homogenized chicken manure on a dry mass basis. Each fermentor was incubated at 40 °C as a submerged fermentation. On an industrial scale, mixing a high-solids fermentor is difficult and expensive. Common problems include liquid channeling, which leads to unconverted biomass and methane generation. Therefore, the quantitative effect of agitation on round-robin fermentation performance was studied. Trains 1, 2, 4, and 5 were constantly mixed in a roller incubator and were shaken before incubation to homogenize all of the material components. Train 3 was “periodically mixed” meaning it was unmixed during the incubation; however, to disperse all of the components after centrifugation, Train 3 fermentors were shaken before they were put back into the incubator.

Every 56 h, fermentors were removed from the incubator, the gas volume was collected, liquid samples were taken, the pH was measured, and the liquid mass transfers were performed. The fermentors were centrifuged (3300×g, 25 min) then the supernatant was transferred. Fresh deoxygenated water was added to Fermentor 1 (F1), and filtered liquid from F1 was transferred to F2, F2 to F3, F3 to F4, and exited from F4 as product liquid. In addition to the liquid transfer, every 7 (Trains 2, 3, 4, 5) or 14 days (Train 1) a fermentor with fresh substrate was propagated into the train as Fermentor 5 (F5), and F1 was removed for performance measurements. In each fermentor, the solids were resuspended, iodoform was added, and 1.0 g calcium carbonate was added to neutralize carboxylic acids and buffer the system. Urea was added to adjust the carbon-nitrogen (C-N) ratio. Anaerobic conditions were maintained by flushing the fermentors with nitrogen gas (Praxair, Bryan, TX) when they were open to the atmosphere during the transfers. The fermentors were then resealed and placed back in the incubator. These anaerobic fermentations have been shown to resist intermittent air exposure (Golub et al., 2011b).

3.2.7 *Carbon-nitrogen ratio*

The carbon-nitrogen (C-N) ratio was quantified as previously described (Smith and Holtzapple, 2010). The C-N ratio was affected by the ratio of nutrients and substrate. Urea was added to supplement nitrogen in the manure.

3.2.8 *Analytical methods*

3.2.8.1 *Carboxylic acid concentration determination*

Fermentation product liquid was collected every 56 h for acid analysis. Centrifuged (3300×g, 5 min) fermentation liquid was mixed with equal parts of IC-6 internal standard (1.162 g/L 4-methyl-*n*-valeric acid) and 3-M phosphoric acid (H₃PO₄), and then ultra-centrifuged (12,000 rpm, 18,360×g, 5 min). The internal standard concentration was verified by titration with a sodium hydroxide standard (0.03 N). The H₃PO₄ ensures that the carboxylate salts are converted into carboxylic acid prior to analysis. The carboxylic acid concentration was measured using an Agilent 6890 Series gas chromatograph (GC) system equipped with a flame ionization detector (FID), an Agilent 7683 automatic liquid sampler and injector, and a 30-m fused-silica capillary column (J&W Scientific Model # 123-3232). Helium was the carrier gas, and the column head pressure was maintained at 2 atm abs. After each sample injection, the temperature ramped from 40 °C to 200 °C at 20 °C per min. The temperature was subsequently held at 200 °C for 2 min. The total run time per sample was 11 min. The external standard, a volatile acid mix (Matreya, LLC, Cat No. 1075), was used to calibrate the samples against the IC-6 internal standard.

3.2.8.2 *Biogas analysis*

For the first two weeks, each fermentor was vented daily because of the high initial digestion rate. Thereafter, it was vented every 56 h. Biogas was removed through the fermentor septum, and the volume was measured by displacing liquid in an inverted graduated glass cylinder filled with a 300 g/L CaCl₂ solution, which prevented microbial growth and carbon dioxide adsorption (Domke, 1999).

Biogas composition was determined (i.e., carbon dioxide, nitrogen, oxygen, and methane) by manually injecting 5-mL gas samples into an Agilent 6890 Series chromatograph with a thermal conductivity detector (TCD). A 4.6-m-long, 2.1-mm-ID stainless steel packed column (60/80 Carboxen 100, Supelco 1-2390) was used. The inlet temperature was 230 °C, the detector temperature was 200 °C, and the oven temperature was 200 °C. The total run time was 10 min, and helium was the carrier gas.

3.2.8.3 Moisture and ash contents

Moisture and ash content were determined by drying in a 105 °C forced-convection oven for over 24 h, and subsequent combustion in a 575 °C furnace for over 12 hours by NREL procedures No. 001 and 005, respectively (NREL, 2004). The ash content was calculated on a dry basis. The consumption of NAVS was determined using the inert-ash approach as described previously (Smith et al., 2011).

3.2.9 Operating parameters

Previous investigations using countercurrent fermentations have shown that adequate performance of conversion and exit yield was achieved with volatile solid loading rate (VSLR) between 1.5–6.5 g NAVS/L·d (Agbogbo, 2005; Aiello-Mazzarri, 2002; Chan and Holtzapple, 2003; Thanakoses, 2002). Therefore, this range was used to investigate how increasing VSLR affects the performance of propagated fixed-bed fermentations. The liquid residence time (LRT) and volatile solid loading rate (VSLR) (Table 3-1) were regulated by controlling the liquid transfer frequency (T_L), the non-acid volatile solids (NAVS) feed rate, the fermentor retention time (FRT), and the liquid feed rate per transfer. FRT is defined as the length of time a fermentor is on-stream. Volatile solids (VS) are defined as the mass of dry solid material that is combusted at 575 °C after 12 h, and NAVS are defined as VS less the amount of carboxylate salt residue that remains in the ash:

$$\text{NAVS} = (\text{g total biomass})(1 - \text{MC})(1 - \text{AC}) - (\text{g acid in biomass}) \quad (3-1)$$

where MC (g water/g wet biomass) is the fraction of moisture in the biomass, and AC (g inert biomass/g dry biomass) is the fraction of dry ash left after 12 h of combustion at

575 °C. In performance calculations, NAVS is preferred because it removes the product from being quantified with the reactant. Also, the nutrient source (dried chicken manure) contains carboxylic acids. To achieve a more accurate measure of fermentor performance, the amount of acid in the manure that is fed to the system is subtracted from the amount of exiting acid.

Table 3-1. Operating parameters for propagated fixed-bed fermentations at high pH.

Fermentation Train		1	2	3	4	5
Controlled	Liquid transfer frequency, T_L (h)	56	56	56	56	56
	Solid transfer frequency, T_S (wk)	2	1	1	1	1
	NAVS feed rate (g NAVS/ T_S)	28.2	28.2	28.2	56.8	85.5
	Fermentor retention time, FRT (d)	56	28	28	28	28
	Agitation	Y	Y	N	Y	Y
	Liquid feed rate (mL/ T_L)	300	300	300	300	300
	Dry solids added (g/ T_S)	32	32	32	64	96
	Manure added (g/ T_S)	8	8	8	16	24
	Urea added (g/ T_L)	0.5	0.5	0.5	1	1.5
	Calcium carbonate added (g/ T_S)	6	6	6	12	12
Methane inhibitor (μ L/(T_L ·fermentor))	80	80	80	80	80	
Normalized	Volatile solid loading rate, VSLR (g NAVS/(L_{liq} ·d))	1.5	2.8	2.9	4.9	6.5
	Liquid residence time, LRT (d)	20.5	19.9	19.9	26.0	37.3
	Total liquid volume, TLV (L)	1.36	1.45	1.38	1.65	1.89
	Volatile solid, VS, concentration (g NAVS/ L_{liq})	122	91	74	124	147
	Dry solid, DS, concentration (g NADS/ L_{liq})	238	158	138	203	231
	Average carbon-nitrogen ratio, C-N (g OC_{NA} /g N)	31.38	13.53	17.62	9.19	17.61
	Average pH (F1–F4)	9.0	9.1	9.2	9.0	8.7

The volatile solid loading rate (VSLR) and liquid residence time (LRT) are calculated as follows:

$$\text{VSLR} = \frac{\text{NAVS fed}}{\text{total liquid volume in all fermentors} \cdot \text{time}} \quad (3-2)$$

$$\text{LRT} = \frac{\text{total liquid volume in all fermentors}}{\text{liquid flow rate out of fermentation train}} \quad (3-3)$$

3.2.10 Definition of terms

To account for the total mass in the system, mass balance closure was calculated with Equation 3-4,

$$\text{mass balance closure} = \frac{\text{mass out}}{\text{mass in} + \text{water of hydrolysis}} \quad (3-4)$$

Cellulose is a polysaccharide composed of individual units of glucan (MW = 162 g/mol) and, during digestion, is enzymatically hydrolyzed to glucose by reacting with a water molecule. The water of hydrolysis was calculated as previously described (Chan and Holtzaple, 2003).

The mixed-acid concentration can be expressed as molar acetic acid equivalents (α), which is the reducing potential of an equivalent amount of acetic acid (Datta, 1981):

$$\begin{aligned} \alpha = & 1.00 \times \text{acetic (mol/L)} + 1.75 \times \text{propionic (mol/L)} \\ & + 2.50 \times \text{butyric (mol/L)} + 3.25 \times \text{valeric (mol/L)} \\ & + 4.00 \times \text{caproic (mol/L)} + 4.75 \times \text{heptanoic (mol/L)} \end{aligned} \quad (3-5)$$

The acetic acid equivalent (Aceq) can be expressed on a mass basis as

$$\text{Aceq (g/L)} = 60.05 \text{ (g/mol)} \times \alpha \text{ (mol/L)} \quad (3-6)$$

Aceq proportionally weighs longer-chained carboxylic acids (C₃ to C₇); high-molecular-weight acids have a higher Aceq than low-molecular-weight acids.

3.2.11 Measuring performance

The inlet and outlet rate of acid, ash, NAVS, water, and gas were determined during the quasi-steady-state period. As previously described (Smith and Holtzapple, 2011b), the average rate of each component was calculated using the *slope method*. In this method, the moving cumulative sum of each component is plotted with respect to time. The slope of the quasi-steady-state portion of this line is the rate. All performance variables (e.g., conversion, selectivity, and yield) were calculated from the averaged component rates determined by the slope method, as described below:

$$\begin{aligned} \text{Conversion } (x) &\equiv \frac{\text{NADS}_{\text{feed}} - \text{NADS}_{\text{exit}}}{\text{NAVS}_{\text{feed}}} \\ &= \frac{\text{NAVS}_{\text{feed}} + \text{Ash}_{\text{feed}} - \text{NAVS}_{\text{exit}} - \text{Ash}_{\text{exit}}}{\text{NAVS}_{\text{feed}}} \\ &= \frac{\text{NAVS}_{\text{consumed}}}{\text{NAVS}_{\text{feed}}} \end{aligned} \quad (3-7)$$

$$\text{Exit yield } (Y_E) \equiv \frac{\text{g total acid output from solid and liquid stream}}{\text{g NAVS}_{\text{feed}}} \quad (3-8)$$

$$\text{Process yield } (Y_P) \equiv \frac{\text{g total acid output in liquid stream}}{\text{g NAVS}_{\text{feed}}} \quad (3-9)$$

$$\begin{aligned} \text{Culture yield } (Y_C) &\equiv \frac{\text{g total acid produced in solid and liquid stream}}{\text{g NAVS}_{\text{feed}}} \\ &\equiv Y_E - Y_F \end{aligned} \quad (3-10)$$

$$\text{Feed yield } (Y_F) \equiv \frac{\text{g total acid entering with feed}}{\text{g NAVS}_{\text{feed}}} \quad (3-11)$$

$$\begin{aligned} \text{Selectivity } (\sigma) &\equiv \frac{\text{g total acid produced}}{\text{g NAVS}_{\text{feed}} - \text{g NAVS}_{\text{exit}}} \equiv \frac{\text{g total acid produced}}{\text{g NAVS digested}} \\ &= \frac{Y_E}{x} \end{aligned} \quad (3-12)$$

$$\text{Acid productivity } (P) \equiv \frac{\text{g total acids produced}}{\text{TLV} \cdot \text{d}} \quad (3-13)$$

where $\text{NADS}_{\text{feed}}$ is the non-acid dry solids fed, $\text{NADS}_{\text{exit}}$ is the non-acid dry solids removed from the fermentation, $\text{NAVS}_{\text{feed}}$ is the non-acid volatile solids fed, $\text{NAVS}_{\text{exit}}$ is the non-acid volatile solids removed from the fermentation, Ash_{feed} is the inert solids fed in biomass feed and buffer, Ash_{exit} is the inert solids exiting in all solid and liquid streams, and TLV is the total liquid volume in the fermentation train including free and interstitial liquid. NADS includes the ash and volatile solid component of biomass. Ash is assumed to be unaffected by the fermentation (Ash_{feed} equals Ash_{exit}), canceling Ash from Equation 3-7.

Per g NAVS fed, the exit yield (Y_E) represents the sum of acid in the product transfer liquid, waste transfer solids, and liquid samples removed from sampling. The process yield (Y_P) represents all the acid in the product transfer liquid per g of NAVS fed. The feed yield (Y_F) is the total g acid entering with the feed per g NAVS fed, and the culture yield (Y_C) is the exit yield less the feed yield.

3.2.12 Statistical analysis

Statistical analysis was performed using Excel 2007 (Microsoft, USA). The mean and standard deviations of the total acid concentrations, acetic acid equivalent (Aceq), non-acid volatile solids (NAVS) in and out were determined from quasi-steady-state operating data. Quasi-steady state was determined to be 89–125 (Train 1), 72–110 (Train 2), 80–100 (Train 3), 37–65 (Train 4), 40–65 (Train 5) days. These averaged values were then used to calculate the acid productivity (P), selectivity (σ), yield (Y), and conversion (x) with a 95% confidence interval (CI). The quasi-steady-state region was the period during which the product total acid and Aceq concentration, dry solids exiting, liquid volume and solid weight of each fermentor, pH, and mass of acid exiting did not vary by more than 20% from the average for a period of at least one-half liquid residence time. An analysis of variance (ANOVA) test was used to compare the means of the groups, followed by a Student's two sample t -test (two-tailed, Type 3) to compute

the p values between the performance variables of the trains. Results were considered statistically significant at the 5% level. All error bars are reported at 95% CI.

3.3 Results and discussion

Fermentation performance in five fermentor trains compared the effects of varying volatile solid loading rates (VSLRs) (Trains 1, 2, 4, and 5) and agitation (Train 3) in a propagated fixed-bed fermentation system (Table 3-1, 3-2). Trains 1, 2, 4, and 5 were continuously mixed whereas Train 3 was periodically mixed to understand the quantitative effects of agitation on performance and to imitate a pile fermentation instead of a submerged bed. The relative VSLRs were Train 1 < Train 2 = Train 3 < Train 4 < Train 5 (Table 3-1). All trains had a similar LRT except for Trains 4 and 5 which had an elevated LRT. Trains 4 and 5 had a higher liquid holdup – they were fed the same amount of liquid as Trains 1, 2, and 3 – but their higher solids concentration resulted in more liquid retained.

3.3.1 Biogas

Biogas production significantly increased with increased VSLR and with mixing. During a 56-h batch period between liquid transfers, Trains 1, 2, 3, 4, and 5 produced 1.50 ± 0.03 , 0.77 ± 0.03 , 1.02 ± 0.06 , 3.12 ± 0.17 , and 4.28 ± 0.24 g gas, respectively, which were all significantly different (Table 3-3). The average biogas composition was $88.9 \pm 7.1\%$ N₂, $11.1 \pm 1.3\%$ CO₂ (Train 1), $91.6 \pm 7.3\%$ N₂, $8.3 \pm 0.9\%$ CO₂ (Train 2), $83.2 \pm 6.9\%$ N₂, $16.8 \pm 1.7\%$ CO₂ (Train 3), $82.5 \pm 6.5\%$ N₂, $17.5 \pm 1.4\%$ CO₂ (Train 4), $60.0 \pm 5.1\%$ N₂, $40.0 \pm 3.3\%$ CO₂ (Train 5). No methane was detected in any fermentor.

Table 3-2. Performance measures for fermentation propagated fixed-bed Trains 1, 2, 3, 4, and 5 at high C-N ratio. Values represent the mean of the quasi-steady-state values \pm CI (95% CI).

	1	2	3	4	5
Total carboxylic acid concentration (g/L)	3.2 \pm 0.2	6.1 \pm 0.8	4.6 \pm 0.8	12.9 \pm 2.1	14.6 \pm 2.6
Total carboxylic acid exiting (g/d)	0.25 \pm 0.01	0.50 \pm 0.01	0.33 \pm 0.02	1.07 \pm 0.09	1.41 \pm 0.12
Aceq exiting (g/d)	0.26 \pm 0.01	0.53 \pm 0.01	0.37 \pm 0.03	1.24 \pm 0.11	1.79 \pm 0.16
Aceq concentration (g/L)	3.3 \pm 0.3	6.5 \pm 0.9	5.1 \pm 1.0	14.9 \pm 2.6	18.6 \pm 3.3
Aceq/Acid ratio	1.03 \pm 0.02	1.06 \pm 0.01	1.11 \pm 0.03	1.15 \pm 0.02	1.27 \pm 0.02
Conversion, x (g VS digested/g VS fed)	0.215 \pm 0.019	0.166 \pm 0.006	0.121 \pm 0.005	0.317 \pm 0.011	0.455 \pm 0.014
Selectivity, σ (g acid produced/g NAVS consumed)	0.615 \pm 0.025	0.745 \pm 0.019	0.658 \pm 0.050	0.398 \pm 0.035	0.248 \pm 0.022
Aceq selectivity, σ_a (g Aceq produced/g NAVS consumed)	0.608 \pm 0.089	0.676 \pm 0.047	0.593 \pm 0.057	0.345 \pm 0.033	0.192 \pm 0.018
Exit yield, Y_E (g acid/g NAVS fed)	0.132 \pm 0.006	0.124 \pm 0.003	0.079 \pm 0.006	0.126 \pm 0.011	0.113 \pm 0.010
Exit Aceq yield, Y_{aE} (g Aceq/g NAVS fed)	0.137 \pm 0.006	0.130 \pm 0.004	0.087 \pm 0.007	0.147 \pm 0.013	0.143 \pm 0.013
Culture yield, Y_C (g acid/g NAVS fed)	0.118 \pm 0.006	0.110 \pm 0.003	0.066 \pm 0.006	0.113 \pm 0.011	0.099 \pm 0.010
Process yield, Y_P (g acid/g NAVS fed)	0.131 \pm 0.006	0.112 \pm 0.003	0.071 \pm 0.005	0.109 \pm 0.008	0.087 \pm 0.006
Productivity, P (g total acid/(L _{liq} ·d))	0.176 \pm 0.025	0.318 \pm 0.038	0.201 \pm 0.027	0.596 \pm 0.104	0.677 \pm 0.119
Mass balance closure (g mass in/g mass out)	0.99 \pm 0.01	0.99 \pm 0.01	0.97 \pm 0.03	0.94 \pm 0.02	0.92 \pm 0.02

Table 3-3. *p* values for performance measures for propagated fixed-bed fermentation Trains 1, 2, 3, 4, and 5 ($\alpha = 0.05$) at high C-N ratio.

Trains	Conv.	Selectivity	Exit yield	Exit yield Aceq	Culture yield	Feed yield	Process yield	TLV	Productivity	Biogas produced (g)	Total acid conc. (g/L)	Aceq conc. (g/L)	Total acid exit (g/d)	Total Aceq exit (g/d)	Aceq/Total acid (g/g)
1 and 2	0.021	0.000	0.205	0.328	0.256	0.527	0.006	0.444	0.003	0.000	0.00	0.00	0.000	0.000	0.100
1 and 3	0.000	0.447	0.000	0.000	0.000	0.286	0.000	0.477	0.520	0.002	0.12	0.09	0.002	0.011	0.028
1 and 4	0.000	0.000	0.639	0.536	0.717	0.235	0.043	0.119	0.001	0.000	0.00	0.00	0.000	0.000	0.000
1 and 5	0.000	0.000	0.106	0.677	0.129	0.302	0.000	0.019	0.000	0.000	0.00	0.00	0.000	0.000	0.000
2 and 3	0.000	0.119	0.000	0.000	0.000	0.470	0.000	0.955	0.015	0.000	0.19	0.32	0.000	0.000	0.143
2 and 4	0.000	0.000	0.828	0.257	0.791	0.328	0.750	0.318	0.016	0.000	0.01	0.01	0.000	0.000	0.000
2 and 5	0.000	0.000	0.318	0.344	0.336	0.494	0.001	0.061	0.007	0.000	0.00	0.00	0.000	0.000	0.000
3 and 4	0.000	0.000	0.001	0.001	0.001	0.928	0.001	0.296	0.001	0.000	0.00	0.00	0.000	0.000	0.303
3 and 5	0.000	0.000	0.008	0.001	0.008	0.792	0.064	0.055	0.001	0.000	0.00	0.00	0.000	0.000	0.000
4 and 5	0.000	0.001	0.381	0.863	0.374	0.573	0.038	0.374	0.611	0.001	0.61	0.39	0.000	0.000	0.000

p value < 0.05 statistically different

p value > 0.05 not statistically different

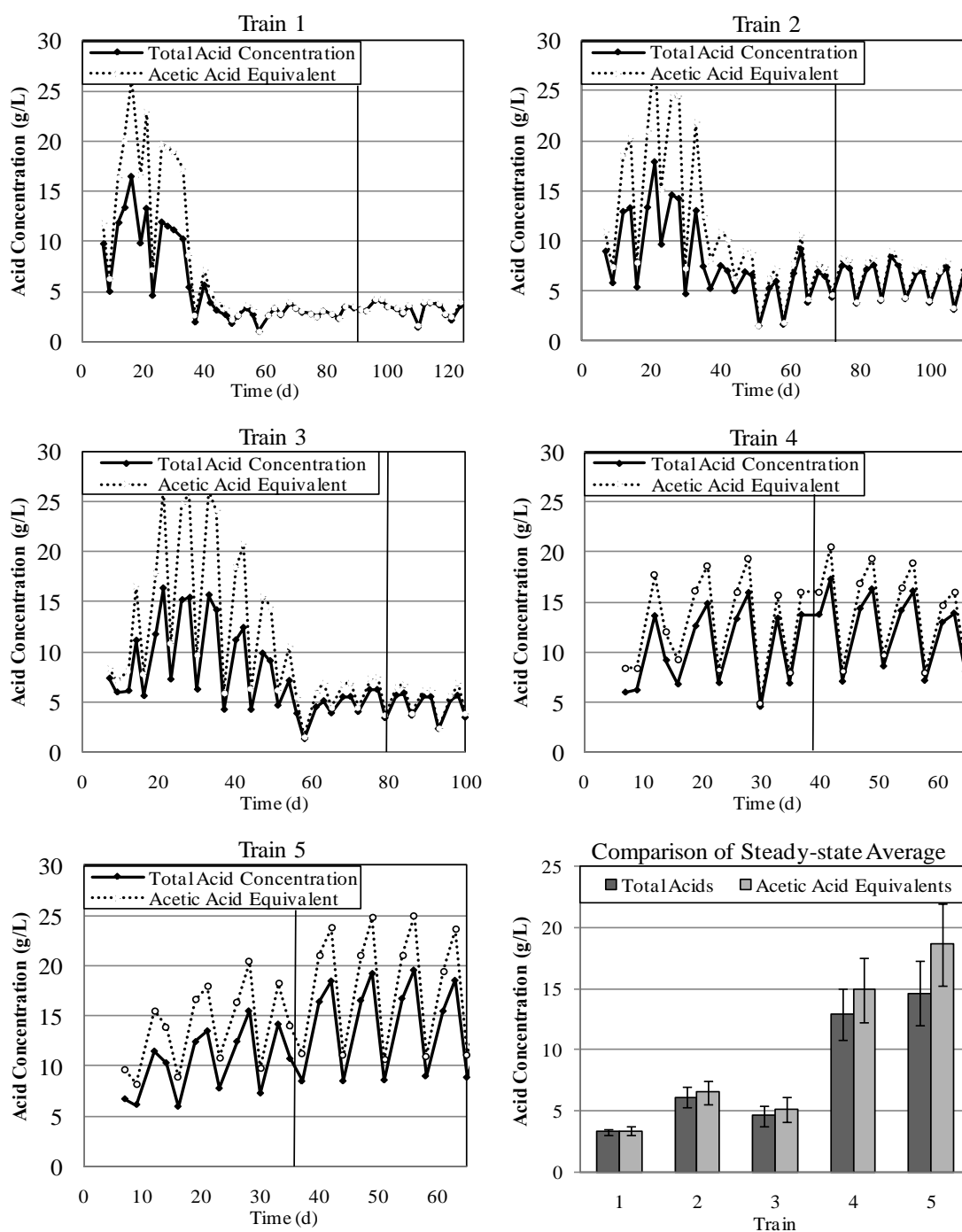


Figure 3-2. Total and acetic acid equivalent carboxylic acid concentrations for propagated fixed-bed fermentation Trains 1, 2, 3, 4, and 5 at high C-N ratio. The vertical lines mark the onset of quasi-steady state. Error bars represent the 95% confidence interval of acid concentrations during the quasi-steady-state period.

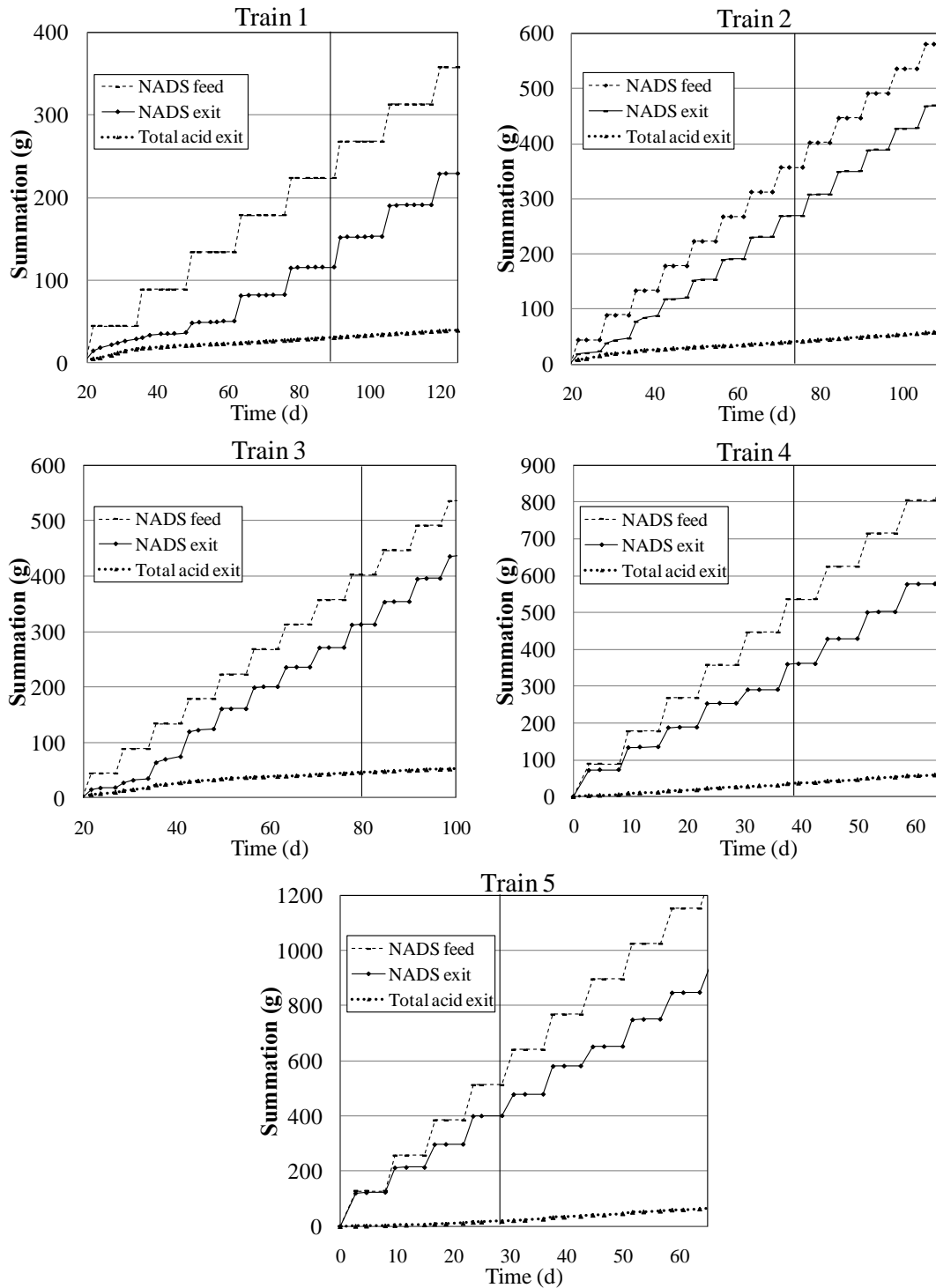


Figure 3-3. Summation of non-acid dry solids (NADS) exiting and fed and total acids exiting for propagated fixed-bed fermentation Trains 1, 2, 3, 4, and 5 at high C-N ratio. The vertical lines mark the onset of quasi-steady state.

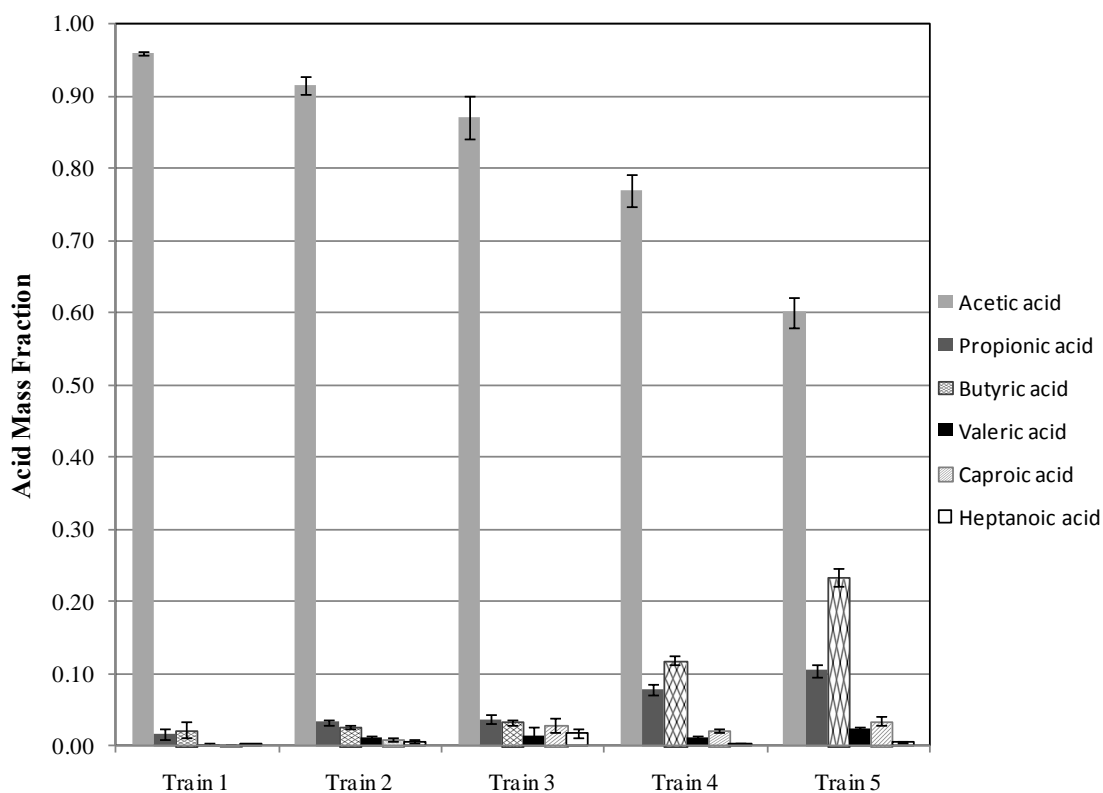


Figure 3-4. Carboxylic acid composition profile for propagated fixed-bed fermentation trains at high C-N ratio. Error bars are the 95% confidence intervals for each carboxylic acid composition during the quasi-steady-state period.

3.3.2 Acid concentration, productivities, and daily acid production

For all five experimental conditions, the total carboxylic and Aceq concentrations (Figure 3-2) were summed to find the accumulated amount of total carboxylic acids exiting, NADS added, and NADS removed from their respective trains (Figure 3-3). The slopes of the quasi-steady-state regression lines provided the productivity and total acids and Aceq exiting daily amounts (Table 3-2).

Trains 4 and 5 did not significantly differ in their total acid and Aceq concentration (Table 3-3), but were significantly higher than Trains 1, 2, and 3, most likely from their higher volatile solid loading rate (VSLR) (Table 3-1). Fermentor propagation was performed every two weeks on Train 1 as opposed to every week for all

other trains, resulting in Train 1 having a VSLR of 1.5 g NAVS/ L_{liq} – the lowest VSLR of all the trains. Consequently, Train 1 had the lowest total acid and Aceq concentrations, but was not significantly different from the periodically mixed Train 3. This result showed that with a stirred fermentation, similar acid concentrations could be achieved with half the VSLR of a non-stirred propagated fixed-bed fermentation.

Trains 4 and 5 did not have significantly different productivities (Table 3-3) and had the highest VSLR of all trains. The diminishing return on productivity between Trains 4 and 5 indicates that fixed-bed fermentations might be nearing peak acid productivity at a VSLR slightly above 6.5 g NAVS/ $(L_{\text{liq}} \cdot d)$. Train 4 had the maximum productivity-to-VSLR ratio, making the VSLR of Train 4 more desirable in large-scale fixed-bed fermentors. Train 1 (stirred and half the VSLR as Train 2) and Train 3 (unstirred but the same VSLR as Train 2) did not have significantly different productivities (Table 3-3). Train 1 had a higher productivity-to-VSLR ratio than Train 3, demonstrating the importance of stirring in large-scale propagated fixed-bed fermentation.

Total liquid volume (TLV) quantifies the total volume of liquid in the solid and liquid phases in each fermentor of a train. Only Trains 1 and 5 had statistically different TLVs. This discrepancy may be because Train 5 had the highest solids concentration (which retains more liquid in the solid phase) and Train 1 had the lowest solid concentration (which retains the least amount of liquid).

To minimize the effects of liquid volume changes and standardize the analyses, the amount of acid exiting the fermentors per day was calculated on a mass basis from the product liquid and waste streams (Table 3-2). The total carboxylic acid and the amount of Aceq exiting per day were significantly different for all fermentation trains (Table 3-3). VSLR and mixing greatly impacted daily exiting acid. Train 5 (highest VSLR) had the highest daily amounts of total acid and Aceq exiting, followed by Train 4 (second highest VSLR). Train 3 (periodically mixed) had a lower daily concentration of total acid and Aceq exiting, again signifying that fermentations must be stirred and

homogeneous for the bacteria to access enough nutrients and substrate for optimal acid production.

Train 5, with an Aceq-to-total-acid ratio of 1.27, had a greater proportion of high-molecular-weight carboxylic acids (e.g., valeric, caproic, and heptanoic acid) than all other trains, possibly because it had the lowest pH (Table 3-1). Across all the trains, there were three instances in which the Aceq-to-total-acid ratios were not statistically different: Trains 1 and 2, Trains 2 and 3, and Trains 3 and 4. The Aceq-to-total-acid ratios for Trains 1 and 3 were significantly different, suggesting that having a VSLR ≤ 1.5 g NAVS/(L_{liq}·d) or being periodically mixed did not significantly affect the production of high-molecular-weight acids.

3.3.3 Yield

The exit (Y_E), exit acetic acid equivalent (Y_{aE}), and culture yields (Y_C) were significantly influenced by agitation, but not VSLR (Table 3-2). The Y_E and Y_{aE} for Trains 1, 2, 4, and 5 were *not* significantly different (Table 3-3), indicating that VSLRs ranging from 1.5 to 6.5 g NAVS/(L_{liq}·d) had no significant impact on the yield of propagated fixed-bed fermentations.

For Train 3, the Y_E and Y_{aE} were significantly lower than Train 2, which had the same VSLR. The lack of mixing in Train 3 significantly reduced the exit yield, implying that a periodically mixed fermentation at a specific VSLR would have much lower yield than a stirred fermentation at the same or even lower VSLR. Trains 1, 2, 4, and 5 had similar Y_C even though they had different VSLRs. As expected, Y_F for all fermentations was not statistically different (Table 3-3).

Compared to all other trains, Train 1 (lowest VSLR) had a significantly higher process yield (Y_P). Because of the lower VSLR, Train 1 produced a lower concentration of acids than the other trains, minimizing the inhibitory effects of acids. In most cases, minimizing acid inhibition is essential to obtain high yields. This same tendency was shown in Trains 4 and 5; Train 5 had a higher VSLR and acid concentration than Train 4, but also a significantly lower Y_P . However, Y_P for Train 2 and Train 4 were not significantly different, even though Train 4 had a higher VSLR and acid concentration

than Train 2. For Trains 3 and 5, Y_P was not significantly different; showing that nonmixing was just as devastating to Y_P as having inhibition from high acid concentrations. Reduced mixing allows acids to accumulate within the biomass particles, so perhaps the reduced Y_P results from the inhibitory effect of the acids.

3.3.4 *Conversion and selectivity*

The high VSLR of Trains 4 and 5 resulted in a significantly higher conversion but a lower selectivity than Train 2. In Train 1, a doubled FRT resulted in half the VSLR (1.5 g NAVS/(L_{liq}·d)) of Train 2, resulting in a lower conversion but higher selectivity. No agitation in Train 3 resulted in a lower conversion than Train 2. All conversions were statistically different, and all selectivities were statistically different (except Train 3 and 1 or 2).

3.3.5 *C-N ratio and pH*

To properly compare fermentation trains, it is necessary to control C-N ratio and pH, which affect ammonia emissions and fermentation performance. Using computer modeling and urea addition, efforts were made to control the C-N ratio to 20 g C/g N, which is desired for carboxylate fermentations (Smith et al., 2011). There were several difficulties in obtaining tight C-N ratio control: 1) lack of real-time measurements produces lags, 2) difficult to predict amount of urea needed to adjust C-N ratio because some was lost as ammonia in vapor, and 3) difficult to obtain a representative sample of inherently non-homogenous fermentation mass. Because of these difficulties, the C-N ratio varied from 9.2 to 31.4 OC_{NA}/g N (Table 3-1). Although C-N ratio could not be tightly regulated, sufficient nitrogen was present to meet microbial needs. Further, it was not present in excessive amounts that could potentially lead to toxicity. Additional discussion is provided below.

In this study, the total ammonia nitrogen was typically 2,435 mg nitrogen (N)/L. At neutral pH, free ammonia accounts for 0.5% of the total ammonia nitrogen (free ammonia (NH₃) + ammonium ion (NH₄⁺)). When the pH reaches 8.0 to 9.0, toxic amounts of aqueous nitrogen might be present as free ammonia (Ekinici et al., 2000). In

this study, at pH 9, the free ammonia was about $36 \pm 7.7\%$ of total ammonia nitrogen, or 877 mg N/L of free ammonia. In the case of anaerobic microorganisms that perform the acidogenic step – the dominant microorganisms in this study – they highly resist ammonia nitrogen concentrations up to 16,000 mg N/L at a neutral pH (Lü et al., 2008).

Ammonia is a source of nitrogen for the synthesis of amino acids in microbial cells (Hungate, 1966). In this study, most of the fermentations operated with an abundance of nitrogen (C-N ratio < 20 g C/g N). Excess nitrogen is thought to be lost as ammonia gas at C-N ratio < 25 g C/g N (Cheremisinoff and Ouellette, 1985). Train 1 had the lowest amount of nitrogen (31.4 g OC_{NA} /g N), which is still sufficient to meet microbial needs (Smith et al., 2011).

An additional advantage of increased ammonia nitrogen is the inhibitory nature of ammonia to methanogenesis, making it unnecessary to add methanogen inhibitors to fermentations (e.g., iodoform). If not acclimated, methanogens are very susceptible to ammonia toxicity because the unionized molecule can readily penetrate the cell membrane.

Fermentations are generally conducted at a pH between 5.5 to 6.5, a preferable pH for acidogens (Khanal, 2008). However, earlier studies have shown that marine microorganisms can tolerate greater alkalinity (Maeda and Taga, 1980). In the fermentation trains in this study, the pH was ~ 9 , which occurred when added urea was hydrolyzed to ammonia and reacted with water to form ammonium hydroxide. In Trains 1 to 5, the pH was high (8.7 to 9.2), and all trains produced a remarkably high proportion of acetic acid (Figure 3-4). For example, Train 2 produced 91% acetic acid, compared to 40% acetic acid from studies with similar LRT, VSLR, and TLV, but at an average pH of 6 (Aiello-Mazzarri, 2002). Acetic acid is a primary fermentation product (Agler et al., 2011). On a mass basis, of all carboxylic acids, acetic acid has the highest number of carboxylic groups (i.e., most protonating power), and therefore, can counteract the high pH (~ 9). At a lower pH (~ 6), the conversion of acetic acid to high-molecular-weight carboxylic acids reduces acidity and helps mitigate the effect of low pH.

Compared to trains at pH 6 (Aiello-Mazzarri, 2002), the fermentation trains reported here (pH ~9) had a higher proportion of acetic acid, but lower yields and acid concentrations. Literature studies at an average pH of 6 with similar LRT, VSLR, and TLV as Train 2 had acid concentrations of 16.9 g/L and a yield of 0.276 g acid/g NAVS fed, whereas Train 2 had an acid concentration of 6.1 g/L and a yield of 0.124 g/L (Aiello-Mazzarri, 2002). If a high selectivity to acetic acid is desired, operating fermentations at a high pH could be an option, although at the cost of lower yields and product concentrations.

3.3.6 Overview

Constant mixing allows the propagated fixed-bed fermentations to achieve homogeneity, which improves the performance in acid production, conversion, selectivity, and yield. A homogeneous fermentation allows the bacteria increased access to dispersed nutrients and substrates. Varying the VSLR between 1.5 and 6.5 g NAVS/(L_{liq}·d) impacts fermentation performance by affecting the concentration of the acid products, which are inhibitory. In carboxylate fermentations, when LRT remains constant and VSLR increases, both conversion and selectivity decrease. This trend holds true for Trains 1, 2, and 3, which had similar LRTs. In our system, LRT increased for Trains 4 and 5, giving them a higher conversion and lower selectivity. At constant LRT, decreased VSLR allows higher process yields by minimizing the inhibitory effects of acids but it lowers selectivities and increases conversions, as shown when comparing Trains 1 and 2. Increased VSLR and LRT resulted in higher acid productivity and acid concentrations, but led to lower selectivities and higher conversions, as shown when comparing Trains 1, 4, and 5. Therefore, the optimal operating conditions for commercial-scale propagated fixed-bed fermentation depend on the available downstream processing technology. Lower VSLR and LRT is advantageous with economical dewatering technology but more expensive feedstock, whereas higher VSLR and LRT is beneficial with more expensive dewatering technology but fairly inexpensive feedstock. The high pH contributed to low yields but high selectivity to acetic acid, which could be desirable for select chemical markets.

3.4 Conclusion

In this propagated fixed-bed fermentation system, the periodically mixed Train 3 had the lowest yield and conversion, showing the importance of agitation. Varying VSLR between 1.5 and 6.5 g NAVS/(L_{liq}·d) did not affect exit and culture yields. Lower VSLR allowed higher process yields by minimizing acid inhibition (Train 1). Increased VSLR and LRT resulted in higher acid productivity and acid concentrations, but caused lower selectivities and higher conversions (Trains 4 and 5). Operating at a high pH contributed to the high selectivity to acetic acid, which might be industrially desirable, but at the cost of lower yields and product concentrations.

4. PROPAGATED FIXED-BED MIXED-ACID FERMENTATION: EFFECT OF VOLATILE SOLID LOADING RATE AND AGITATION AT NEAR-NEUTRAL PH

To increase conversion and product concentration, mixed-acid fermentation can use a countercurrent strategy where solids and liquids pass in opposite directions through a series of fermentors. To limit the requirement for moving solids, this study employed a propagated fixed-bed fermentation, where solids were stationary and only liquid was transferred. To evaluate the role of agitation, continuous mixing was compared with periodic mixing. The periodically mixed fermentation had similar conversion, but lower yield and selectivity. Increasing volatile solid loading rate from 1.5 to 5.1 g non-acid volatile solids/(L_{liq}·d) and increasing liquid residence time decreased yield, conversion, and selectivity but increased product concentrations. Compared to a previous study at high pH (~9), this study achieved better results at near neutral pH (~6.5) and optimal C-N ratios. Compared to countercurrent trains, propagated fixed-bed fermentations have similar selectivities and produce similar proportions of acetic acid, but have lower yields, conversion, productivities, and acid concentrations.

4.1 Introduction

High volatile fuel prices, harmful environmental effects from combusting fossil fuels, and rising food prices from converting starch and sugar crops to biofuels emphasize the need for a clean, economically viable energy source (Davis et al., 2011). Rather than converting food crops to biofuels, processes should employ lignocellulose, the most plentiful form of biomass (Schubert, 2006). One promising technology that converts lignocellulose into liquid fuels is the carboxylate platform. Using versatile fermentation configurations, this process ferments any biodegradable feedstock into carboxylic acids (Forrest et al., 2010b; Holtzaple et al., 1999). Through chemical

transformations, these acids can be converted to hydrocarbon fuel, offering a potential viable solution to global fuel problems (Agler et al., 2011).

The carboxylate platform is a biomass-to-energy technology that biologically converts biomass (e.g., lignocellulose, fats, proteins, carbohydrates) into carboxylate salts that can be chemically converted into chemicals and hydrocarbon fuels (Holtzapple et al., 1999; Holtzapple and Granda, 2009). In the fermentation step, a mixed culture of microorganisms is employed in a series of fermentors that digest substrate to produce carboxylic acids that are neutralized with a buffer (e.g., calcium carbonate) to form the corresponding salts. The salts can be concentrated and further processed into industrial chemicals and hydrocarbon fuels (Landoll and Holtzapple, 2011). The carboxylate platform has attractive economics, does not require sterile operating conditions or added enzymes, and has reached the demonstration level of development (Granda et al., 2009; Pham et al., 2010).

Because the carboxylate salts are inhibitory and the biomass becomes less reactive as it digests, high product concentrations and high conversions are achieved using a countercurrent configuration, in which the solid and liquid phases are transferred in opposite directions through a series of fermentors, to form a *train* (Ross and Holtzapple, 2001). To limit the need to move solids, fixed-bed fermentation is a fermentor configuration where only the liquid phase is transferred from fermentor to fermentor in the fermentation train while the solid phase remains stationary (Agbogbo and Holtzapple, 2007). Both a pile fermentation – a configuration in which liquid flows by gravity through a fixed-bed or *pile* – and a submerged fixed-bed configuration minimize solids handling. A propagated fixed-bed fermentation system is when the solid phase remains stationary in each stage, and fresh liquid is added to the most-digested fermentor and cascaded through a series of four fermentor stages (Golub et al., 2011a). The product liquid exits from the least-digested fermentor. The oldest fermentor has the most recalcitrant (digested) biomass and is systematically replaced by a fermentor containing fresh biomass (Figure 3-1). This propagated fixed-bed fermentation modification is advantageous because the system achieves quasi-steady product

concentrations and higher acid production compared to the unpropagated design (Agbogbo and Holtzapfle, 2007), and it reduces solids handling compared to the countercurrent configuration.

A previous propagated fixed-bed fermentation systems was operated at high pH (~9) (Golub et al., 2011a). In contrast, this study operated at near-neutral pH (~6.5) and optimal carbon-nitrogen ratio (~25 g C/g N), a desirable commercial scenario. In addition, the effect of volatile solids loading rate (VSLR) was assessed. On an industrial scale, mixing a high-solids fermentor is difficult. Common problems include liquid channeling, which leads to unconverted biomass and methane generation. Therefore, a minimal mixing configuration was used to assess the potential impact of mixing on the performance of a fixed-bed system (Agbogbo and Holtzapfle, 2007). This study will evaluate potential performance benefits of propagated fixed-bed fermentation.

4.2 Materials and methods

4.2.1 Fermentor configuration

The fermentors were 1-L polypropylene centrifuge bottles capped by a rubber stopper inserted with a glass tube (Ross, 1998). Two segments of ¼-in stainless steel pipe were inserted through the rubber stopper into the vessel to mix the contents of the fermentor as it rotated in the rolling incubator. A rubber septum sealed the glass tube and allowed for gas sampling and release.

4.2.2 Substrate

Shredded office paper, which served as the energy source, was obtained from a local recycling center. No pretreatment was required. Chicken manure, which served as an undefined nutrient source, was obtained from Feather Crest Farms, Inc. (Bryan, TX) and dried at 105 °C for 48 h. Wet chicken manure will degrade over time, so to maintain consistency in the nutrient source over the course of the entire experiment, dried and homogenized chicken manure was used. Dried chicken manure was found to have a C-N ratio of 12.9 ± 3.4 g non-acid organic carbon (OC_{NA})/g nitrogen (N) and an acid concentration of 0.05 ± 0.01 g acid/g dry chicken manure. Studies have found the C-N

ratio of shredded office paper is 138.3 ± 43 g OC_{NA}/g N (Smith and Holtzapple, 2010). The substrate concentration is expressed as non-acid volatile solids (NAVS), which is the combustible portion of the substrate minus carboxylic acids present in the feed.

4.2.3 *Fermentation medium*

The deoxygenated medium was prepared by boiling distilled water to liberate dissolved oxygen. After cooling to room temperature in a covered vessel, to further reduce the oxygen content, 0.275 g/L cysteine hydrochloride and 0.275 g/L sodium sulfide were added.

4.2.4 *Inoculum*

The inoculum was a mixed-culture of marine microorganisms found in beach sediment collected in Galveston Island, TX. Sediment was removed from the bottom of multiple 0.5-m-deep shoreline pits. Samples were immediately placed in airtight plastic bottles filled with deoxygenated water, capped, and frozen at -20 °C until use. Before inoculation, samples were thawed, shaken vigorously, and allowed to settle by gravity. Equal parts of the resulting supernatant were homogenized, and aliquots were used to standardize the fermentation inoculum to 12.5% of the initial working volume (Forrest et al., 2010a; Thanakoses, 2002). Bacterial community composition of mixed-acid fermentation has been reported elsewhere (Hollister et al., 2010; Hollister et al., 2011).

4.2.5 *Methanogen inhibition*

Iodoform (CHI₃) was used to inhibit methane production. Iodoform solution (80 μL, 20 g CHI₃/L 190-proof ethanol) was added to each fermentor every 56 h. Iodoform is sensitive to light, air, and temperature, and so the solution was kept in amber-colored glass bottles wrapped in foil and stored at -20 °C (Agbogbo and Holtzapple, 2007).

4.2.6 *Propagated fixed-bed (round-robin) fermentation procedure*

Four-stage propagated fixed-bed fermentation trains were used to investigate the effects of volatile solids loading rate (VSLR) and mixing. Five fermentation trains were initiated as batch cultures under anaerobic conditions with a concentration of 100, 200,

or 300 g non-acid dry solid (NADS)/L deoxygenated water, which was achieved by adding substrate, nutrient source (manure and urea), inoculum, buffer (calcium carbonate), and liquid medium to each fermentor. The feed consisted of 80% shredded office copier paper and 20% dry homogenized chicken manure on a dry mass basis. Each fermentor was incubated at 40 °C as a submerged fermentation. The effect of agitation on propagated fixed-bed fermentation performance was studied. Trains 1, 2, 4, and 5 were constantly mixed in a roller incubator and were shaken before incubation to homogenize all of the material components. Train 3 was “periodically mixed” meaning it was unmixed during the incubation; however, to disperse all of the components after liquid transfers, Train 3 fermentors were shaken before they were put back into the incubator. Because of the periodic mixing, Train 3 may be anticipated to perform better than a true unmixed process.

Every 56 h, fermentors were removed from the incubator, the gas volume was collected, liquid samples were taken, the pH was measured, and the liquid mass transfers were performed. (*Note:* This specific time interval is not critical as long as the controlled variables are adjusted to achieve the appropriate normalized variables.) The fermentors were centrifuged (3300×g, 25 min) then all of the supernatant was transferred from one fermentor to the adjacent fermentor. For example, fresh deoxygenated water was added to Fermentor 1 (F1), and all of the filtered liquid from F1 was transferred to F2, F2 to F3, F3 to F4, and exited from F4 as product liquid (Figure 3-1). In addition to the liquid transfer, every 7 (Trains 2, 3, 4, 5) or 14 days (Train 1) a fermentor with fresh substrate was propagated into the train as Fermentor 5 (F5), and F1 was removed for performance measurements. In each fermentor, the solids were resuspended by shaking, iodoform was added, and 1.0 g calcium carbonate was added to neutralize carboxylic acids and buffer the system. Urea was added to adjust the carbon-nitrogen (C-N) ratio. Anaerobic conditions were maintained by flushing the fermentor headspace with nitrogen gas (Praxair, Bryan, TX) when they were open to the atmosphere during the transfers. The fermentors were then resealed and placed back in the incubator. These

anaerobic fermentations have been shown to resist intermittent air exposure (Golub et al., 2011b).

4.2.7 *Carbon-nitrogen ratio*

The carbon-nitrogen (C-N) ratio was quantified as previously described (Smith et al., 2011). The C-N ratio was affected by the ratio of nutrients and substrate. Urea was added to supplement nitrogen in the manure (Table 4-1).

4.2.8 *Analytical methods*

4.2.8.1 *Carboxylic acid concentration determination*

Fermentation product liquid was collected every 56 h for acid analysis. Centrifuged (3300×g, 5 min) fermentation liquid was mixed with equal parts of IC-6 internal standard (1.162 g/L 4-methyl-*n*-valeric acid) and 3-M phosphoric acid (H₃PO₄), and then ultra-centrifuged (12,000 rpm, 18,360×g, 5 min). The internal standard concentration was verified by titration with a 0.03-N sodium hydroxide standard. The H₃PO₄ ensured that the carboxylate salts are converted into carboxylic acid prior to analysis. The carboxylic acid concentration was measured using an Agilent 6890 Series gas chromatograph (GC) system equipped with a flame ionization detector (FID), an Agilent 7683 automatic liquid sampler and injector, and a 30-m fused-silica capillary column (J&W Scientific Model # 123-3232). Helium was the carrier gas, and the column head pressure was maintained at 2 atm abs. After each sample injection, the temperature ramped from 40 to 200 °C at 20 °C per min. The temperature was subsequently held at 200 °C for 2 min. The total run time per sample was 11 min. The external standard, a volatile acid mix (Matreya, LLC, Cat No. 1075), was used to calibrate the samples against the IC-6 internal standard.

4.2.8.2 *Biogas analysis*

For the first two weeks, each fermentor was vented daily because of the high initial digestion rate. Thereafter, it was vented every 56 h. Biogas was removed through the fermentor septum, and the volume was measured by displacing liquid in an inverted

graduated glass cylinder filled with a 300 g/L CaCl₂ solution, which prevented microbial growth and carbon dioxide adsorption (Domke, 1999).

Biogas composition was determined (i.e., carbon dioxide, nitrogen, oxygen, and methane) by manually injecting 5-mL gas samples into an Agilent 6890 Series chromatograph with a thermal conductivity detector (TCD). A 4.6-m-long, 2.1-mm-ID stainless steel packed column (60/80 Carboxen 100, Supelco 1-2390) was used. The inlet temperature was 230 °C, the detector temperature was 200 °C, and the oven temperature was 200 °C. The total run time was 10 min, and helium was the carrier gas.

4.2.8.3 *Moisture and ash contents*

Moisture and ash content were determined by drying in a 105 °C forced-convection oven for over 24 h, and subsequent combustion in a 575 °C furnace for over 12 h by NREL procedures No. 001 and 005, respectively (NREL, 2004). The ash content was calculated on a dry basis. The consumption of NAVS was determined using the inert-ash approach as described previously (Smith et al., 2011).

4.2.9 *Operating parameters*

Previous investigations using countercurrent fermentations have shown that adequate performance of conversion and exit yield was achieved with volatile solid loading rate (VSLR) between 1.5–5.1 g NAVS/(L·d) (Agbogbo, 2005; Aiello-Mazzarri, 2002; Chan and Holtzapfel, 2003; Thanakoses, 2002). Therefore, this range was used to investigate how increasing VSLR affects the performance of propagated fixed-bed fermentations. The liquid residence time (LRT) and volatile solid loading rate (VSLR) (Table 4-1) were regulated by controlling the liquid transfer frequency (T_L), non-acid volatile solids (NAVS) feed rate, fermentor retention time (FRT), solid transfer frequency (T_S), and liquid feed rate per transfer. The solid transfer frequency is the length of time (wks) between fermentor propagation. FRT is defined as the length of time a fermentor is on-stream. Volatile solids (VS) are defined as the mass of dry solid material that is combusted at 575 °C after 12 h, and NAVS are defined as VS less the amount of carboxylate acid:

$$\text{NAVS} = (\text{g total wet biomass})(1 - \text{MC})(1 - \text{AC}) - (\text{g acid in biomass}) \quad (4-1)$$

where MC (g water/g wet biomass) is the fraction of moisture in the biomass, and AC (g ash/g dry biomass) is the fraction of dry ash left after 12 h of combustion at 575 °C. In performance calculations, NAVS is preferred because it removes the product from being quantified with the reactant. Also, the nutrient source (dried chicken manure) contains carboxylic acids. To achieve a more accurate measure of fermentor performance, the amount of acid in the manure that is fed to the system is subtracted from the amount of exiting acid. To determine the amount of acid in the manure, the dry manure was resuspended in distilled water at different concentrations. The acid in the supernatant was analyzed by GC.

The volatile solid loading rate (VSLR) and liquid residence time (LRT) are calculated as follows:

$$\text{VSLR} = \frac{\text{NAVS fed (g)}}{\text{total liquid volume in all fermentors (L)} \cdot \text{time (d)}} \quad (4-2)$$

$$\text{LRT} = \frac{\text{total liquid volume in all fermentors (L)}}{\text{liquid flow rate out of fermentation train (L/d)}} \quad (4-3)$$

The total liquid volume includes both free and interstitial liquid. Liquid flow rate out of fermentation train includes product liquid exiting and liquid in cake exiting.

Table 4-1. Operating parameters for propagated fixed-bed fermentations at near-neutral pH. Normalized parameters represent the mean of the quasi-steady-state values \pm CI (95% CI).

Fermentation Train	1	2	3	4	5
Liquid transfer frequency, T_L (h)	56	56	56	56	56
Solid transfer frequency, T_S (wk)	2	1	1	1	1
NAVS feed rate (g NAVS/ T_S)	28.7	28.7	28.7	57.9	87.1
Fermentor retention time, FRT (d)	56	28	28	28	28
Continuous agitation	Y	Y	N	Y	Y
Liquid feed rate (mL/ T_L)	300	300	300	300	300
Dry solids added (g/ T_S)	32	32	32	64	96
Manure added (g/ T_S)	8	8	8	16	24
Urea added to F4 (g/ T_S)	0.2	0.2	0.2	0.3	0.4
Urea added to F1 (g/ T_L)	0.4	0.4	0.4	0.6	0.8
Calcium carbonate added (g/ T_S)	6	6	6	12	12
Methane inhibitor (μ L/(T_L ·fermentor))	80	80	80	80	80
Controlled					
Volatile solid loading rate, VSLR (g NAVS/(L_{liq} ·d))	1.50 \pm 0.03	2.68 \pm 0.03	2.52 \pm 0.02	4.01 \pm 0.04	5.11 \pm 0.07
Liquid residence time, LRT (d)	17.3 \pm 2.0	18.1 \pm 2.6	19.3 \pm 2.7	24.6 \pm 3.8	29.1 \pm 4.4
Total liquid volume, TLV (L)	1.37 \pm 0.03	1.53 \pm 0.02	1.63 \pm 0.01	2.06 \pm 0.02	2.43 \pm 0.03
Normalized					
Volatile solid, VS, concentration (g NAVS/ L_{liq})	47 \pm 3	54 \pm 3	62 \pm 3	88 \pm 4	115 \pm 6
Dry solid, DS, concentration (g NADS/ L_{liq})	73 \pm 3	87 \pm 3	96 \pm 2	140 \pm 4	176 \pm 5
Average carbon-nitrogen ratio, C-N ratio (g OC_{NA} /g N)	19.5 \pm 0.6	22.2 \pm 2.0	20.3 \pm 0.7	25.7 \pm 0.4	24.7 \pm 0.6
Average pH (F1–F4)	7.84 \pm 0.38	6.75 \pm 0.39	6.37 \pm 0.35	6.07 \pm 0.36	5.96 \pm 0.49
Urea addition rate (g urea/(L_{liq} ·d))	1.19 \pm 0.03	1.52 \pm 0.02	1.44 \pm 0.01	1.70 \pm 0.02	1.92 \pm 0.03

NAVS = Non-acid volatile solids

NADS = Non-acid dry solids

4.2.10 Definition of terms

To account for the total mass in the system, mass balance closure was calculated with Equation 4-4

$$\text{mass balance closure} = \frac{\text{mass out (g)}}{\text{mass in (g)} + \text{water of hydrolysis (g)}} \quad (4-4)$$

Cellulose is a polysaccharide composed of individual units of glucan (MW = 162 g/mol). During digestion, it is enzymatically hydrolyzed to glucose by reacting with a water molecule. The water of hydrolysis was calculated as previously described (Chan and Holtzapple, 2003).

The mixed-acid concentration can be expressed as molar acetic acid equivalents (α), which is the reducing potential of an equivalent amount of acetic acid (Datta, 1981):

$$\begin{aligned} \alpha = & 1.00 \times \text{acetic (mol/L)} + 1.75 \times \text{propionic (mol/L)} \\ & + 2.50 \times \text{butyric (mol/L)} + 3.25 \times \text{valeric (mol/L)} \\ & + 4.00 \times \text{caproic (mol/L)} + 4.75 \times \text{heptanoic (mol/L)} \end{aligned} \quad (4-5)$$

The acetic acid equivalent (Aceq) can be expressed on a mass basis as

$$\text{Aceq (g/L)} = 60.05 \text{ (g/mol)} \times \alpha \text{ (mol/L)} \quad (4-6)$$

Aceq proportionally weighs longer-chained carboxylic acids (C₃ to C₇); high-molecular-weight acids have a higher Aceq than low-molecular-weight acids.

4.2.11 Measuring performance

The feed and exit rate of acid, ash, NAVS, water, and gas were determined during the quasi-steady-state period. As previously described (Smith and Holtzapple, 2011b), the average rate of each component was calculated using the *slope method*. In this method, the moving cumulative sum of each component is plotted with respect to time. The slope of the quasi-steady-state portion of this line is the rate. All performance variables (e.g., conversion, selectivity, and yield) were calculated from the averaged component rates determined by the slope method, as described below:

$$\begin{aligned} \text{Conversion } (x) &\equiv \frac{\text{NADS}_{\text{feed}} - \text{NADS}_{\text{exit}}}{\text{NAVS}_{\text{feed}}} \\ &= \frac{\text{NAVS}_{\text{feed}} + \text{Ash}_{\text{feed}} - \text{NAVS}_{\text{exit}} - \text{Ash}_{\text{exit}}}{\text{NAVS}_{\text{feed}}} \end{aligned} \quad (4-7)$$

$$= \frac{\text{NAVS}_{\text{consumed}}}{\text{NAVS}_{\text{feed}}}$$

$$\text{Exit yield } (Y_E) \equiv \frac{\text{g total acid output from solid and liquid stream}}{\text{g NAVS}_{\text{feed}}} \quad (4-8)$$

$$\text{Process yield } (Y_P) \equiv \frac{\text{g total acid output in liquid stream}}{\text{g NAVS}_{\text{feed}}} \quad (4-9)$$

$$\text{Culture yield } (Y_C) \equiv \frac{\text{g total acid produced in solid and liquid stream}}{\text{g NAVS}_{\text{feed}}} \quad (4-10)$$

$$\equiv Y_E - Y_F$$

$$\text{Feed yield } (Y_F) \equiv \frac{\text{g total acid entering with feed}}{\text{g NAVS}_{\text{feed}}} \quad (4-11)$$

$$\text{Selectivity } (\sigma) \equiv \frac{\text{g total acid produced}}{\text{g NAVS}_{\text{feed}} - \text{g NAVS}_{\text{exit}}} \quad (4-12)$$

$$\equiv \frac{\text{g total acid produced}}{\text{g NAVS digested}} = \frac{Y_E}{x}$$

$$\text{Acid productivity } (P) \equiv \frac{\text{g total acids produced}}{\text{TLV} \cdot \text{d}} \quad (4-13)$$

where $\text{NADS}_{\text{feed}}$ is the non-acid dry solids fed, $\text{NADS}_{\text{exit}}$ is the non-acid dry solids removed from the fermentation, $\text{NAVS}_{\text{feed}}$ is the non-acid volatile solids fed, $\text{NAVS}_{\text{exit}}$ is the non-acid volatile solids removed from the fermentation, Ash_{feed} is the ash fed in biomass feed and buffer, Ash_{exit} is the ash exiting in all solid and liquid streams, and TLV is the total liquid volume in the fermentation train including free and interstitial

liquid. NADS includes the ash, calcium carbonate, and volatile solid component of biomass. Ash is assumed to be unaffected by the fermentation (Ash_{feed} equals Ash_{exit}), canceling Ash from Equation 4-7.

Per g NAVS fed, the exit yield (Y_E) represents the sum of acid in the product transfer liquid, waste transfer solids, and liquid samples removed from sampling. The process yield (Y_P) represents all the acid in the product transfer liquid per g of NAVS fed. The feed yield (Y_F) is the total g acid entering with the feed per g NAVS fed, and the culture yield (Y_C) is the exit yield less the feed yield.

4.2.12 *Statistical analysis*

Statistical analysis was performed using Excel 2007 (Microsoft, USA). The mean and standard deviations of the total acid concentrations, acetic acid equivalent (Aceq), non-acid volatile solids (NAVS) in and out were determined from quasi-steady-state operating data (Smith and Holtzapfle, 2011b). Quasi-steady state was determined to be 64–134 (Train 1), 81–154 (Train 2), 80–154 (Train 3), 79–138 (Train 4), 79–138 (Train 5) days. These averaged values were then used to calculate the acid productivity (P), selectivity (σ), yield (Y), and conversion (x) with a 95% confidence interval (CI). Unless specified otherwise, all comparisons in the Results and Discussion section are statistically significant. The quasi-steady-state region was the period during which the product total acid and Aceq concentration, dry solids exiting, liquid volume and solid weight of each fermentor, pH, and mass of acid exiting did not vary by more than 20% from the average for a period of at least one-half liquid residence time. For each train, the slope of the summed data (Figure 4-1) was used to calculate the means of the performance variables which were compared using a Student's two sample t -test (two-tailed, Type 3). The p values had a familywise error rate of 0.05 using the Bonferroni correction. All error bars are reported at 95% CI.

4.3 **Results and discussion**

The fermentation performance of the propagated fixed-bed fermentation system was studied in five fermentation trains employing varying volatile solid loading rates

(VSLRs) (Trains 1, 2, 4, and 5) and agitation (Train 3) (Table 4-1, 4-2). To understand the effects of agitation on performance, Trains 1, 2, 4, and 5 were continuously mixed whereas Train 3 was periodically mixed. The relative VSLRs ($\text{g NAVS}/(\text{L}_{\text{liq}}\cdot\text{d})$) were Train 1 (1.50) < Train 2 (2.68) = Train 3 (2.52) < Train 4 (4.01) < Train 5 (5.11) (Table 4-1). All trains had a similar liquid residence time (LRT) except for Trains 4 and 5, which had an elevated LRT (Table 4-1). Although Trains 4 and 5 were fed the same amount of liquid as Trains 1, 2, and 3, they had a higher liquid holdup because their higher solids concentration retained more liquid.

4.3.1 *Biogas*

VSLR and mixing did affect biogas production, but not biogas compositions (Table 4-2). The daily amount of biogas produced increased with increasing VSLR, except between Trains 4 and 5 which had similar biogas production (Tables 4-2, 4-3). The volatile and dry solids concentrations increased as the daily amount of feed increased but the solids setpoint was not controlled. The microorganisms were exposed to higher concentrations of available feedstock, produced more energy and higher amounts carboxylic acid product, resulting in higher biogas production. Also, the continuously mixed train produced more biogas than the periodically mixed train, indicating the importance of mixing on gas production. No methane was detected in any fermentor.

Table 4-2. Performance measures for propagated fixed-bed fermentation Trains 1 to 5 at near-neutral pH. Values represent the mean of the quasi-steady-state values \pm CI (95% CI).

	1	2	3	4	5
Total carboxylic acid concentration (g/L)	7.88 \pm 0.90	10.64 \pm 1.26	10.29 \pm 1.13	13.39 \pm 2.03	14.47 \pm 2.07
Total carboxylic acid exiting (g/d)	0.73 \pm 0.00	1.03 \pm 0.00	0.95 \pm 0.00	1.35 \pm 0.00	1.48 \pm 0.00
Aceq exiting (g/d)	1.02 \pm 0.01	1.37 \pm 0.00	1.29 \pm 0.00	1.77 \pm 0.01	1.98 \pm 0.01
Aceq concentration (g/L)	10.94 \pm 1.40	13.85 \pm 1.69	13.95 \pm 1.61	17.60 \pm 2.82	19.09 \pm 2.89
Aceq/Acid ratio	1.38 \pm 0.03	1.30 \pm 0.02	1.35 \pm 0.01	1.30 \pm 0.02	1.31 \pm 0.03
Conversion, x (g VS digested/g VS fed)	0.457 \pm 0.011	0.386 \pm 0.005	0.395 \pm 0.005	0.299 \pm 0.005	0.309 \pm 0.006
Selectivity, σ (g acid produced/g NAVS consumed)	0.745 \pm 0.007	0.639 \pm 0.003	0.581 \pm 0.003	0.544 \pm 0.004	0.385 \pm 0.003
Aceq selectivity, σ_a (g Aceq produced/g NAVS consumed)	1.051 \pm 0.011	0.854 \pm 0.005	0.784 \pm 0.004	0.714 \pm 0.004	0.515 \pm 0.003
Exit yield, Y_E (g acid/g NAVS fed)	0.341 \pm 0.012	0.247 \pm 0.005	0.230 \pm 0.004	0.162 \pm 0.004	0.119 \pm 0.003
Exit Aceq yield, Y_{aE} (g Aceq/g NAVS fed)	0.481 \pm 0.007	0.330 \pm 0.002	0.310 \pm 0.002	0.213 \pm 0.002	0.159 \pm 0.002
Culture yield, Y_C (g acid/g NAVS fed)	0.328 \pm 0.004	0.234 \pm 0.002	0.216 \pm 0.002	0.149 \pm 0.002	0.106 \pm 0.001
Process yield, Y_P (g acid/g NAVS fed)	0.340 \pm 0.004	0.242 \pm 0.007	0.207 \pm 0.002	0.140 \pm 0.001	0.097 \pm 0.001
Feed yield, Y_F (g acid fed/g NAVS fed)	0.013 \pm 0.000	0.013 \pm 0.000	0.013 \pm 0.000	0.013 \pm 0.000	0.013 \pm 0.000
Productivity, P (g total acid/(L _{liq} ·d))	0.510 \pm 0.011	0.633 \pm 0.007	0.553 \pm 0.004	0.599 \pm 0.006	0.541 \pm 0.007
Mass balance closure (g mass in/g mass out)	0.97 \pm 0.01	0.96 \pm 0.01	0.96 \pm 0.01	0.93 \pm 0.01	0.93 \pm 0.01
Biogas produced (g/d)	0.60 \pm 0.00	0.74 \pm 0.00	0.64 \pm 0.00	0.79 \pm 0.01	0.79 \pm 0.00
N ₂ (%)	62.9 \pm 3.7	64.2 \pm 3.7	58.9 \pm 3.3	59.7 \pm 3.9	61.2 \pm 3.8
CO ₂ produced (%)	37.1 \pm 3.2	41.1 \pm 3.1	35.8 \pm 2.8	40.3 \pm 3.0	38.8 \pm 3.1

Table 4-3. *p* values for performance measures for propagated fixed-bed fermentation Trains 1 to 5 at near-neutral pH ($\alpha = 0.05$).

Trains	Conv.	Selectivity	Exit yield	Exit yield Aceq	Culture yield	Feed yield	Process yield	TLV	Productivity	Biogas produced	Total acid conc.	Aceq conc.	Total acid exit	Total Aceq exit	Aceq/T total acid (g/g)
1 and 2	0.000	0.000	0.000	0.000	0.000	0.011	0.000	0.000	0.000	0.000	0.000	0.000	0.000	0.000	0.001
1 and 3	0.000	0.000	0.000	0.000	0.000	0.011	0.000	0.000	0.000	0.000	0.001	0.000	0.000	0.000	0.259
1 and 4	0.000	0.000	0.000	0.000	0.000	0.007	0.000	0.000	0.000	0.000	0.000	0.000	0.000	0.000	0.003
1 and 5	0.000	0.000	0.000	0.000	0.000	0.007	0.000	0.000	0.000	0.000	0.000	0.000	0.000	0.000	0.004
2 and 3	0.012	0.000	0.000	0.000	0.000	0.997	0.000	0.000	0.000	0.000	0.666	0.813	0.000	0.000	0.000
2 and 4	0.000	0.000	0.000	0.000	0.000	0.748	0.000	0.000	0.000	0.000	0.021	0.000	0.000	0.000	0.441
2 and 5	0.000	0.000	0.000	0.000	0.000	0.752	0.000	0.000	0.000	0.000	0.002	0.000	0.000	0.000	0.121
3 and 4	0.000	0.000	0.000	0.000	0.000	0.751	0.000	0.000	0.000	0.000	0.008	0.000	0.000	0.000	0.000
3 and 5	0.000	0.000	0.000	0.000	0.000	0.754	0.000	0.000	0.000	0.000	0.001	0.000	0.000	0.000	0.000
4 and 5	0.009	0.000	0.000	0.000	0.000	0.992	0.000	0.000	0.000	0.832	0.437	0.066	0.000	0.000	0.621

p value < 0.005 statistically different, with a familywise error rate of 0.05 using the Bonferroni correction

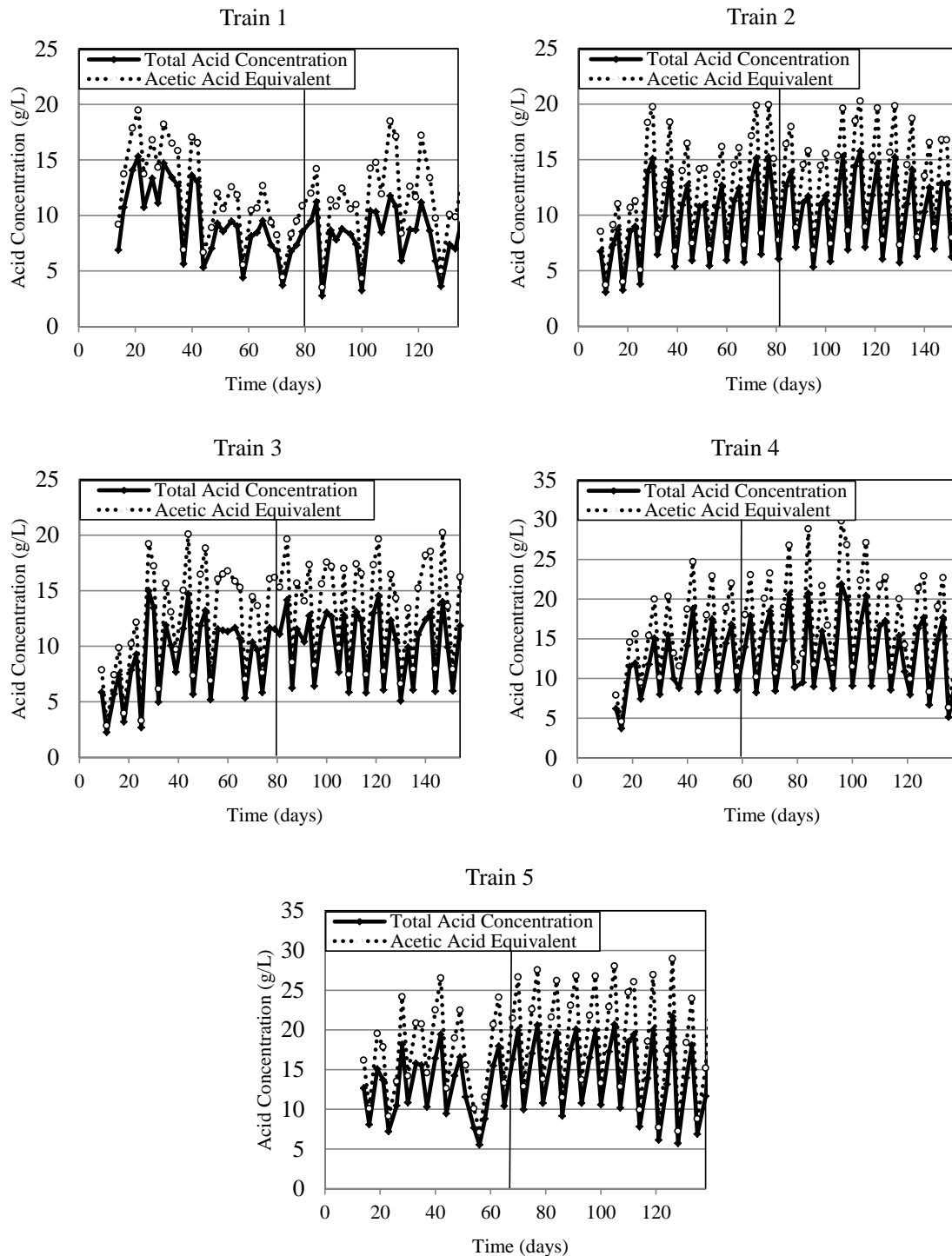


Figure 4-1. Total and acetic acid equivalent carboxylic acid concentrations for fermentation propagated fixed-bed Trains 1 to 5 at near-neutral pH. The solid vertical lines mark the onset of quasi-steady state.

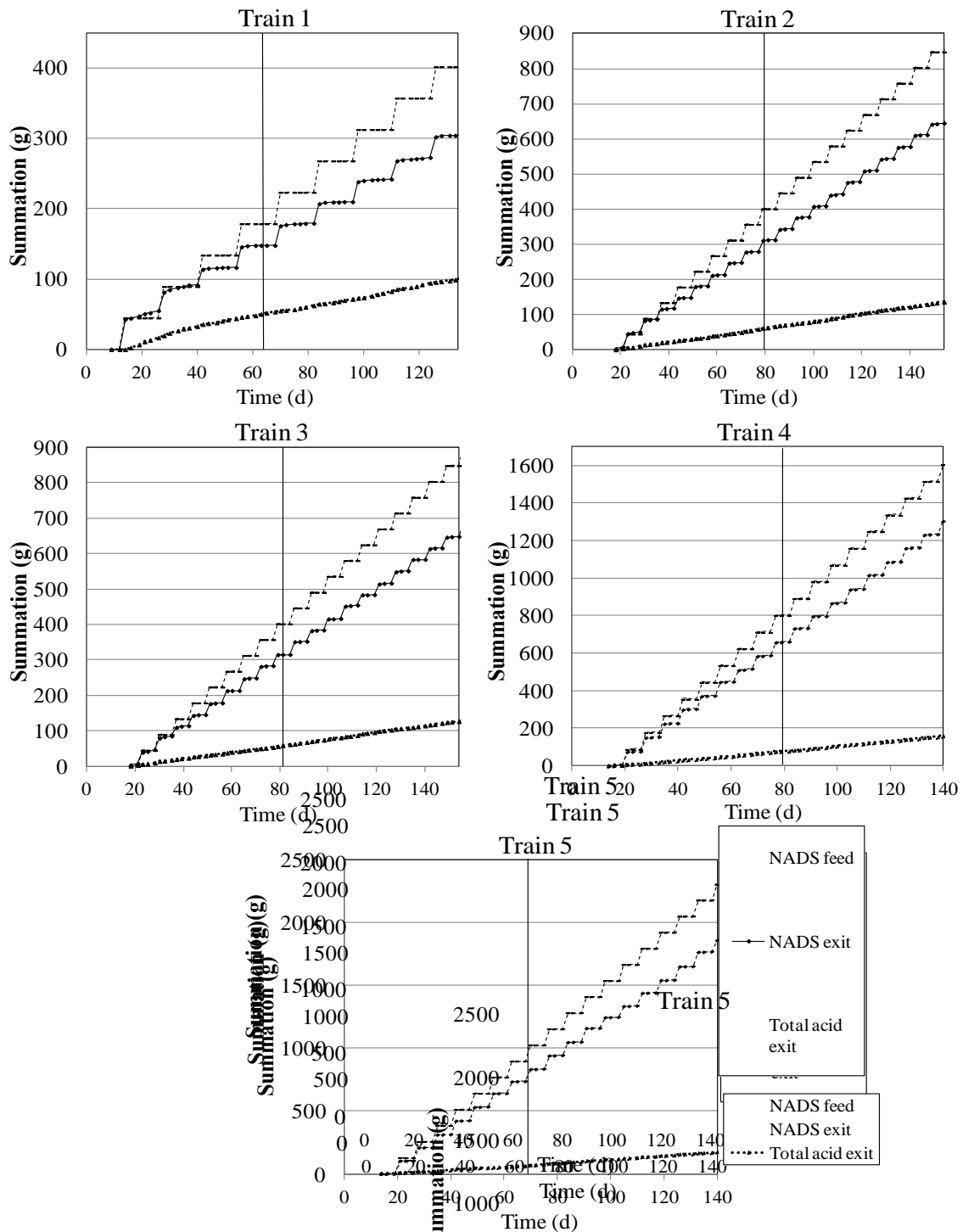


Figure 4-2. Summation of non-acid dry solids (NADS) (exiting and fed) and total acids exiting for fermentation propagated fixed-bed fermentation Trains 1 to 5 at near-neutral pH. The vertical solid lines mark the onset of quasi-steady state.

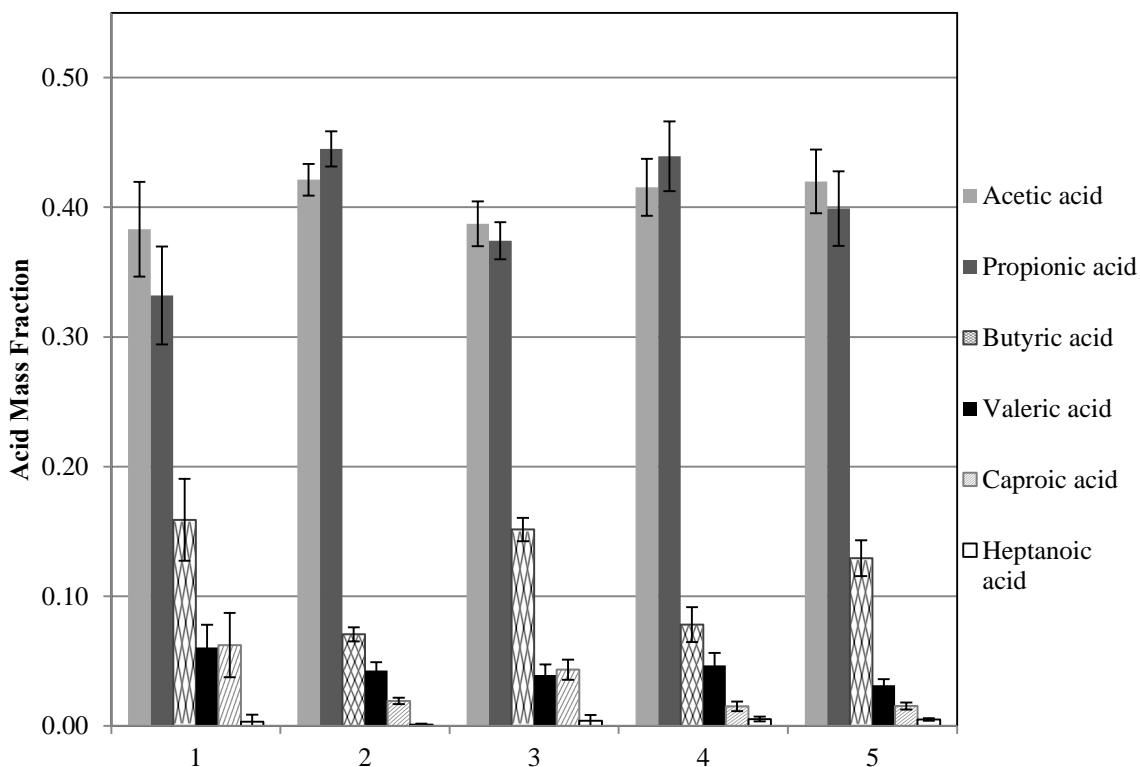


Figure 4-3. Carboxylic acid composition profile for propagated fixed-bed fermentations at near-neutral pH. Error bars are the 95% confidence intervals for each carboxylic acid composition during the quasi-steady-state period.

4.3.2 Acid concentration, productivities, and daily acid production

For all five experimental conditions, the accumulated mass of total carboxylic acids and Aceq exiting, NADS added, and NADS removed from their respective trains was found. The slopes of the quasi-steady-state regression lines provided the daily total acid and Aceq exiting, NADS exiting, and NADS removed on a mass basis (Table 4-2). Productivity was calculated as the mass rate of acid produced per total fermentor volume.

Overall, the trains did differ in the concentrations of total acid and Aceq (Tables 4-2, 4-3), except between Train 2 versus 3 and Train 4 versus 5. Most likely, the differences resulted from different volatile solid loading rates (VSLR) (Table 4-1). In

Train 1, fermentors were propagated every two weeks whereas all other trains were propagated every week. As a result, Train 1 had a VSLR of only 1.5 g NAVS/ L_{liq} , the lowest VSLR of all the trains. Consequently, Train 1 had the lowest total acid and Aceq concentrations, 7.88 and 10.94 g acid/L, respectively. The next highest total acid and Aceq concentration was Train 2 (next highest VSLR) which was not different from Train 3 (periodically mixed). Because propagated fixed-bed fermentations do not control cake setpoint, higher VSLR corresponded to higher solids concentrations in the fermentors and a longer liquid retention. This phenomenon occurs because larger amounts of solids will absorb more liquid, retaining the liquid for a longer time period. Microorganisms exposed to higher solids concentration produced more energy and higher amounts carboxylic acid product. This result shows that a periodically mixed fermentation can achieve similar acid concentrations as a continuously stirred fermentation operating with similar conditions. Also, continuously stirred propagated fixed-bed fermentations with a VSLR from 2.7 to 4.0 g NAVS/ $(L_{\text{liq}} \cdot d)$ have increasing acid concentrations.

For propagated fixed-bed fermentations, the total acid and Aceq concentrations undergo oscillations that are not found in countercurrent fermentations (Figure 4-2). These oscillations occur when the fermentors are propagated, which is referred to as a solid transfer (T_S). When the fermentors are propagated, the acid concentrations decrease because the product liquid is diluted from the fresh feed. The acid concentrations increase during the liquid transfers, where the substrate is digested into carboxylic acids and the liquids remain undiluted from fresh solid movement.

Train 2 had the highest productivity (Tables 4-2, 4-3). The increased productivity of Train 2 compared with Train 1 and minor decrease in productivity in Trains 4 and 5 indicates that fixed-bed fermentations might be nearing peak acid productivity at a VSLR ~ 2.7 g NAVS/ $(L_{\text{liq}} \cdot d)$, the VSLR of Train 2. (*Note: the peak acid productivity is a relative assessment for the operating parameters studied and is not intended to imply a theoretical maximum.*) Although they have similar VSLR, Train 2 (continuous mixing) had higher productivity than Train 3 (periodically mixed) (Tables 4-2, 4-3),

demonstrating the importance of mixing in large-scale propagated fixed-bed fermentation.

In each fermentor of a train, total liquid volume (TLV) quantifies the total volume of liquid in the solid and liquid phases. All trains had different TLVs because of the different solids concentrations (i.e., higher solids concentrations retain more liquid, whereas lower solids concentrations retain less liquid).

To minimize the effects of liquid volume changes and standardize the analyses, the daily amount of acid exiting the fermentors was calculated on a mass basis from the product liquid and waste streams (Table 4-2). The waste stream is the undigested solids that exit from the most digested fermentor. For all fermentation trains, the daily amount of total carboxylic acid and Aceq exiting per day were different (Tables 4-2, 4-3). VSLR and mixing greatly impacted daily exiting acid. Train 5 (highest VSLR) had the highest daily amounts of total acid and Aceq exiting, followed by Train 4 (second highest VSLR). Train 3 (periodically mixed) had a lower daily concentration of total acid and Aceq exiting, again signifying that fermentations must be stirred and homogeneous for the bacteria to access enough nutrients and substrate for optimal acid production.

Trains 1 and 3 had the highest Aceq-to-total-acid ratios, showing that VSLR and mixing did affect the production of high-molecular-weight acids (e.g., valeric, caproic, and heptanoic acid) (Tables 4-2, 4-3). Train 1 had the lowest VSLR, allowing a more diluted acid environment. The lower concentration of acid in the fermentation provides a more optimal environment for the microorganisms, corresponding to production of more high-molecular weight acids. Surprisingly, the periodically mixed train produced more high-molecular weight acids than the continuously mixed train, which is not yet fully understood.

4.3.3 Yield

The exit yield of total acid (Y_E) and exit yield of acetic acid equivalents (Y_{aE}) were influenced by agitation and VSLR (Table 4-2). For Trains 1, 2, 4, and 5, Y_E and Y_{aE} increased in order from high to low VSLR (5.1 to 1.5 g NAVS/(L_{liq}·d)) (Tables 4-2, 4-3), indicating that, as expected, lower VSLRs increased the yield of propagated fixed-

bed fermentations at near-neutral pH. When LRT is constant, decreasing VSLR increases yield in countercurrent fermentations (Aiello-Mazzarri, 2002). For Train 3, Y_E and Y_{aE} were lower than Train 2, which had the same VSLR. The periodic mixing in Train 3 reduced the exit yield, implying that a periodically mixed fermentation has a much lower yield than a continuously mixed fermentation at the same VSLR.

All trains had similar Y_F (Tables 4-2, 4-3). Although Trains 1, 2/3, 4, and 5 had increasing VSLR, the trains had the same proportion of fed external acids from the nutrient source (manure) to NAVS fed, because the manure-to-substrate feed ratios were kept constant for all fermentations.

Y_C was influenced by agitation and VSLR (Tables 4-2, 4-3). In the continuously mixed trains (Trains 1, 2, 4, and 5), the Y_C decreased, indicating that decreased VSLR increased Y_C (Tables 4-1, 4-2, 4-3). Compared to Train 2, Train 3 had decreased Y_C , indicating the importance of agitation.

For the continuously mixed fermentations (Trains 1, 2, 4, and 5), the process yield (Y_P) decreased with increasing VSLR. Because propagated fixed-bed fermentations do not control cake setpoint, higher VSLR corresponded to higher solids concentrations in the fermentors and a longer liquid retention. The higher solids concentration correlates with increased concentrations of acid, which are inhibitory, and so could suppress yield. Reduced mixing allows acids to accumulate within the biomass particles causing pH variations that affect bacterial metabolism, which could explain why Y_P was lower for Train 3 than Train 2 (Tables 4-2, 4-3). Mixing is anticipated to influence other variables, such as nutrient and buffer dispersion.

4.3.4 *Conversion and selectivity*

For the continuously mixed fermentations (Trains 1, 2, 4, and 5), the conversion and selectivity decreased with increasing VSLR, except between Trains 4 and 5. Train 1, with the lowest VSLR of 1.5 g NAVS/(L_{liq}·d), had the highest conversion and selectivity. Because of the lack of solid cake setpoint, higher VSLR corresponded to higher solids concentrations in the fermentors. This higher solids concentration led to higher acid concentrations, which most likely inhibited the microorganisms responsible

for digesting the volatile solids, decreasing the conversion. Train 1 also had the highest pH. As a stress response to higher pH, the microorganisms might have converted a majority of the substrate into acids.

Compared to the continuously mixed fermentation, the periodically mixed fermentation (Train 3) resulted in decreased selectivity but similar conversion (Train 2). This suggests that a minimally stirred fermentation could achieve conversions comparable to a stirred fermentor (Tables 4-2, 4-3).

4.3.5 C-N ratio and pH

To properly compare fermentation trains, it is necessary to control C-N ratio and pH, which affect ammonia emissions and fermentation performance. For the synthesis of amino acids in microbial cells, ammonia is a source of nitrogen (Hungate, 1966). Excess nitrogen is thought to be lost as ammonia gas when C-N ratio < 25 g C/g N (Cheremisinoff and Ouellette, 1985). In this study, using computer modeling and urea addition, efforts were made to control the C-N ratio to 20–25 g OC_{NA}/g N (Table 4-1), which is desired for carboxylate fermentations (Smith et al., 2011). (*Note*: OC_{NA} refers to non-acid organic carbon). In Table 4-1, the different urea loading rates were found with the computer model described above, and correspond to the VSLR and LRT. Trains 4 and 5 were anticipated to have higher acid concentrations and TLV. Therefore, to ensure adequate buffering capacity, the amount of calcium carbonate was doubled for these trains.

At neutral pH, free ammonia accounts for 0.5% of the total ammonia nitrogen (free ammonia (NH₃) + ammonium ion (NH₄⁺)), a nontoxic amount of free ammonia (Ekinici et al., 2000). Carboxylate fermentations are generally conducted at a pH between 5.5 to 6.5, a preferred pH for acidogens (Khanal, 2008). In this study, fermentations operated at a pH between 6.0 and 7.8 (Table 4-1). All fermentation trains had similar pH except Train 1, which had a higher pH (Table 4-1).

4.3.6 *Comparison of fermentation configuration: propagated fixed-bed versus countercurrent trains at near-neutral pH*

The operating conditions in the propagated fixed-bed fermentations are different from what is typically found in countercurrent trains. Previous countercurrent studies employing a countercurrent flow of solids and liquids have comparable LRT, VSLR, temperature, substrate-to-nutrient ratio, transfer frequency, inoculum size, and pH (Tables 4-4 and 4-5) (Agbogbo, 2005; Aiello-Mazzarri, 2002; Domke, 1999; Ross, 1998; Thanakoses, 2002) as the propagated fixed-bed fermentation in this study. However, not all conditions were identical (i.e., pretreatment method, substrate, nutrient). Forrest (2010) showed that many pretreated substrates have similar performance to shredded paper (the substrate used here), so to a first approximation, differences in performance between countercurrent and propagated fixed-bed fermentation can be attributed to the fermentation configuration and not the substrate.

With the given data, propagated fixed-bed fermentations have similar selectivities and produce similar proportions of acetic acid as countercurrent fermentation, but have lower yields, conversion, productivities, and acid concentrations. These general trends are observed for the continuously mixed trains (Trains 1, 4, and 5) (Table 4-5). A previous countercurrent fermentation with similar substrate, nutrient (except wet not dry), VSLR, LRT, and buffer, was comparable to Train 5, and showed that Train 5 had a lower yield, conversion, productivity, and acid concentration than the countercurrent train (Golub et al., 2011b).

Also, when comparing countercurrent and propagated fixed-bed fermentations that have similar operating parameters (e.g., LRT, VSLR, and pH), the propagated fixed-bed fermentations had higher TLV and lower solids concentration than the countercurrent fermentations (Table 4-5). This resulted because, unlike the countercurrent trains, the propagated fixed-bed fermentations have no cake set point control, which increased the LRT.

Table 4-4. Operating parameters for four-stage countercurrent fermentations with comparable operating parameters (e.g., VSLR, LRT, pH) as the propagated fixed-bed fermentations. All fermentations were run continuously at 40 °C, had a transfer frequency of 2 or 3 days, were fed 80% substrate and 20% nutrient on a dry basis, and had an original inoculum size of 50 to 60 mL. Dashes indicate unknown.

Code	Operating Parameters									
	Substrate		Pretreatment Method	Inoculum source	Buffer	Substrate Conc.	TLV	LRT	VSLR	pH
	Carbohydrate	Nutrient				g VS/L _{liq.}	L _{liq.}	Days	g VS/(L·d)	–
Train 1	Office Paper	Dry Chicken Manure	Untreated	Marine	CaCO₃	47	1.37	17.3	1.5	7.8
A	Corn Stover	Dry Pig Manure	Hammermill/Ca(OH) ₂	80:20 Rumen:Compost	CaCO ₃	20	1.24	15.9	1.6	6.0
Train 2	Office Paper	Dry Chicken Manure	Untreated	Marine	CaCO₃	54	1.53	18.1	2.7	6.8
B	Corn Stover	Dry Pig Manure	Hammermill/Ca(OH) ₂	80:20 Rumen:Compost	CaCO ₃	39	0.88	20.5	2.2	6.0
C	Bagasse	Dry Chicken Manure	Hammermill/Ca(OH) ₂ and Intermediate	Marine and Terrestrial	–	39	0.92	20.5	2.1	6.2
D	Bagasse	Dry Chicken Manure	Hammermill/Ca(OH) ₂	Marine	–	39	0.92	20.5	2.1	6.3
E	Bagasse	Dry Chicken Manure	Hammermill/Ca(OH) ₂	40:40:10:10 Rumen:Marine: Biomass:Compost	–	39	0.92	20.5	2.1	6.3
F	MSW	Sewage Sludge	Hammermill	Rumen Fluid	CaCO ₃	117	–	19.3	3.3	6.1
Train 3	Office Paper	Dry Chicken Manure	Untreated	Marine	CaCO₃	62	1.63	19.3	2.5	6.4
	no unmixed data available		–	–	–	–	–	–	–	–
Train 4	Office Paper	Dry Chicken Manure	Untreated	Marine	CaCO₃	88	2.06	24.6	4.0	6.1
G	Rice Straw	Dry Chicken Manure	Mill	Adapted Marine	CaCO ₃	70	1.01	23.7	3.5	6.4
H	Paper fines	Dry biosludge	Ca(OH) ₂	Adapted Rumen Fluid	CaCO ₃	12	1.40	20.0	3.9	5.9
Train 5	Office Paper	Dry Chicken Manure	Untreated	Marine	CaCO₃	115	2.43	29.1	5.1	6.0
I	MSW	Dry Sewage Sludge	Untreated	Rumen Fluid	CaCO ₃	80	0.91	25.8	5.8	5.8
J	Office Paper	Wet Chicken Manure	Untreated	Marine	CaCO ₃	101	1.40	32.6	5.1	6.0

- A. Thanakoses (2002) Chapter 5.1 J. Golub et al., 2011b
- B. Thanakoses (2002) Chapter 5.1
- C. Thanakoses (2002) Chapter 4.2
- D. Thanakoses (2002) Chapter 4.6
- E. Thanakoses (2002) Chapter 4.6
- F. Ross (1998) Chapter 4
- G. Agbogbo (2005) Chapter 3
- H. Domke (1999) Chapter 4
- I. Aiello-Mazzarri (2002) Chapter 6

Table 4-5. Performance data for four-stage countercurrent fermentations with comparable operating parameters (e.g., VSLR, LRT, pH) as the propagated fixed-bed fermentations. All fermentations were run continuously at 40 °C, had a transfer frequency of 2 or 3 days, were fed 80% substrate and 20% nutrient on a dry basis, and had an original inoculum size of 50 to 60 mL. Dashes indicate unknown.

Code	Performance					
	Acetic Acid	Final Acid Conc.	Exit yield	Conversion	Selectivity	Acid Productivity
	%	g acid/L _{liq}	g acid _{exit} / g NAVS _{feed}	g VS _{consumed} / g VS _{feed}	g Acid/ g VS _{consumed}	g/L _{liq} ·d
Train 1	38%	7.9	0.341	0.457	0.745	0.51
A	40%	16.0	0.550	0.770	0.714	0.89
Train 2	42%	10.6	0.247	0.386	0.639	0.63
B	38%	21.4	0.450	0.765	0.588	1.02
C	33%	18.6	0.345	0.630	0.548	0.75
D	45%	19.7	0.425	0.760	0.559	0.93
E	45%	18.8	0.385	0.695	0.554	0.84
F	54%	21.7	0.340	0.470	0.730	1.13
Train 3	39%	10.3	0.230	0.395	0.581	0.55
no unmixed data available	—	—	—	—	—	—
Train 4	42%	13.4	0.162	0.299	0.544	0.60
G	36%	25.0	0.290	0.692	0.419	1.00
H	39%	16.8	0.210	0.490	0.430	0.90
Train 5	42%	14.5	0.119	0.309	0.385	0.54
I	44%	19.6	0.122	0.385	0.317	0.71
J	36%	23.0	0.184	0.437	0.422	0.81

4.3.7 Comparison of propagated fixed-bed fermentations at high pH and low C-N ratio with near-neutral pH and optimal C-N ratio

Previous propagated fixed-bed studies were performed with similar LRT, VSLR, and TLV, but at a high pH (~ 9) and low C-N ratio (~ 14 g OC_{NA}/g N) (Golub et al., 2011a). In contrast, the fermentation trains reported here were performed with near-neutral pH (~ 6.5) and a more optimal C-N ratio (~ 25 g OC_{NA}/g N) (Table 4-1). As a result, the fermentations here had a higher proportion of high-molecular-weight acids, higher yields, and higher acid concentrations (Figure 4-3), indicating the importance of operating mixed-acid fermentations in the preferred range of pH and C-N ratio.

The importance of mixing is observed in Figures 4-4 to 4-7 and Table 4-6. For optimal fermentation performance, fermentations must be stirred and homogenous so the bacteria can access sufficient nutrients and substrate. Also, at near-neutral pH, non-mixed fermentations are less negatively affected. In contrast, at high pH, non-mixed fermentations have significantly worse performance than the mixed-fermentations. Perhaps this is because stirring helps to minimize local pH gradients in the fermenting solids, thus preventing inhibition and allowing for high performance.

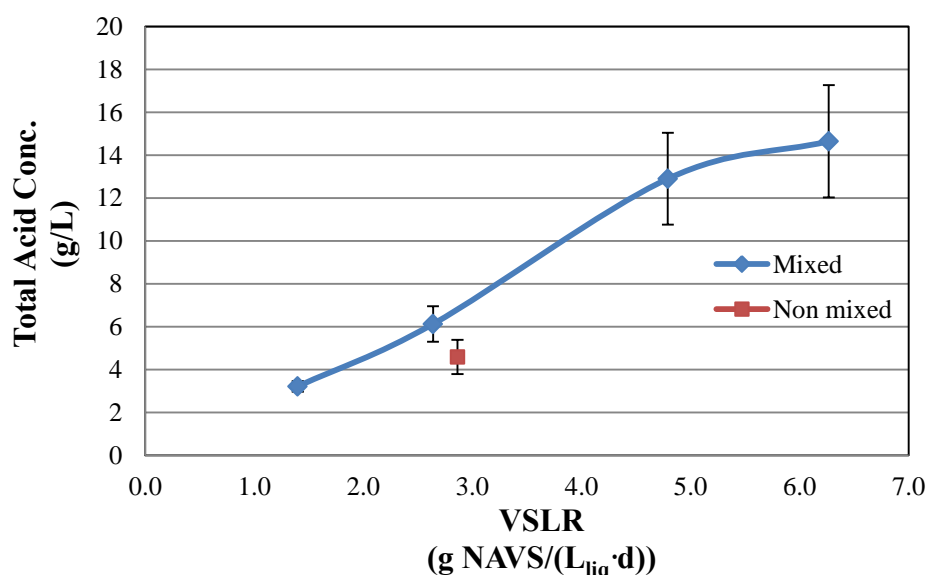


Figure 4-4. Total acid concentration versus VSLR at high pH and low C-N ratio for propagated fixed-bed fermentations.

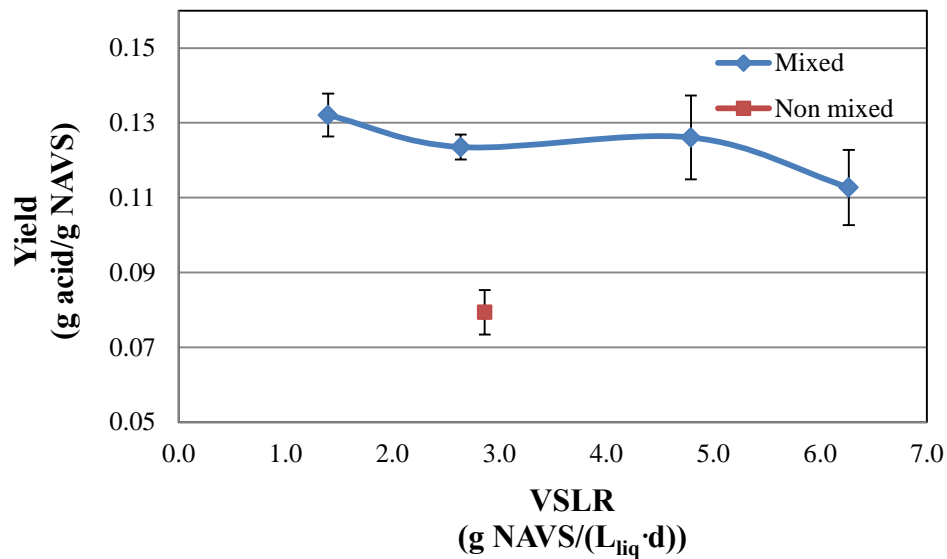


Figure 4-5. Yield versus VSLR at high pH and low C-N ratio for propagated fixed-bed fermentations.

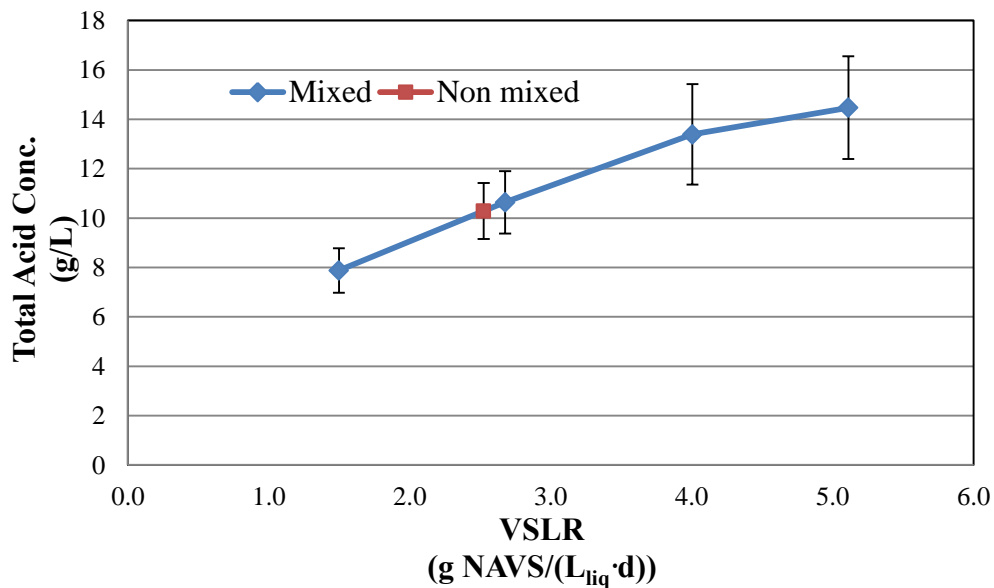


Figure 4-6. Total acid concentration versus VSLR at near-neutral pH and optimal C-N ratio for propagated fixed-bed fermentations.

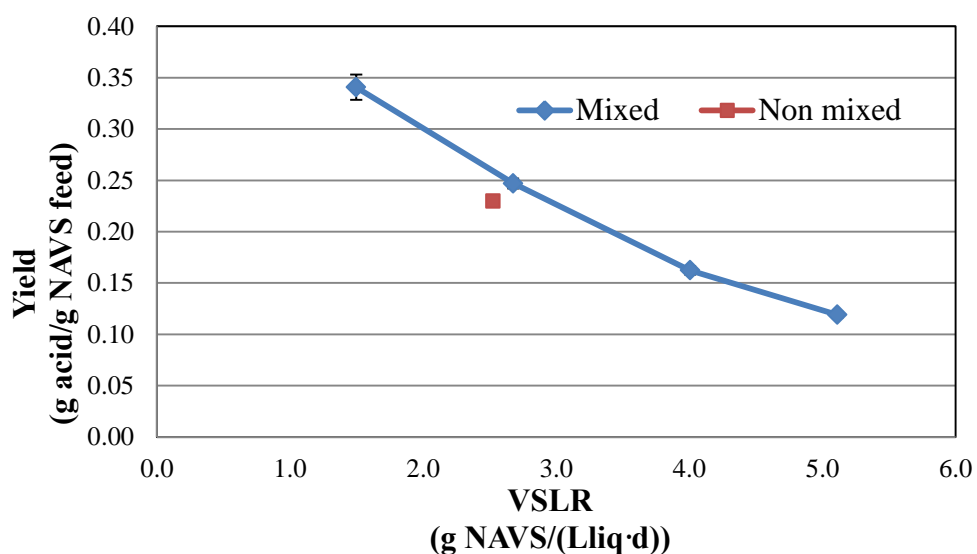


Figure 4-7. Yield versus VSLR at near-neutral pH and optimal C-N ratio for propagated fixed-bed fermentations.

Table 4-6. Performance variable percent difference in non-mixed versus mixed propagated fixed-bed fermentations at near-neutral and high pH.

	% Difference Non-mixed vs. Mixed	
	Near-neutral pH	High pH
Acid Conc. (g/L)	-3%	-25%
Conversion (g NAVS dig./g NAVS feed)	+2%	-27%
Yield (exit) (g acid exit/g NAVS feed)	-7%	-36%
Selectivity (g acid exit/g NAVS dig.)	-9%	-12%

4.3.8 Overview

Mixing – Compared to periodic mixing, constant mixing allows the propagated fixed-bed fermentations to achieve homogeneity, which improves the acid production, selectivity, and yield, but not conversion. A homogeneous fermentation allows the bacteria increased access to dispersed nutrients and substrates. Mixing is difficult to scale up. Although studying mixing at lab scale is important, it does not necessarily reflect what can be achieved at large scale.

VSLR – Because the cake setpoint is not controlled in propagated fixed-bed fermentations, studies done with constant mixing indicate that increasing VSLR, but not increasing the liquid feed rate, increased the substrate concentration. This impacted fermentation performance by increasing the LRT, which increased the concentration of inhibitory acid products. In carboxylate fermentations, when LRT remains constant and VSLR increases, conversion, yield, and selectivity decrease (Aiello-Mazzarri, 2002). In the studies reported here, this trend holds true for all trains, even though Trains 4 and 5 had higher LRTs. Increasing both VSLR and LRT resulted in higher acid productivity and acid concentrations which inhibited the metabolism of the microorganisms, lowering yields, selectivities, and conversions. Based on these observations, the recommended operating conditions for propagated fixed-bed fermentation are at lower VSLR ($\sim 1.5 \text{ g NAVS}/(L_{\text{liq}} \cdot \text{d})$) and LRT ($\sim 18 \text{ d}$). This recommendation is based on performance and not economics.

Fermentation configuration – Compared to countercurrent fermentations, propagated fixed-bed fermentations have similar selectivities and produce similar proportions of acetic acid, but have lower yields, conversion, productivities, and acid concentrations. However, compared to countercurrent fermentation, the propagated fixed-bed potentially reduces solids handling, which could lower costs.

pH and C-N ratio – A previous propagated fixed-bed fermentation had high pH (~ 9) and low C-N ratio ($\sim 14 \text{ g OC}_{\text{NA}}/\text{g N}$) (Golub et al., 2011a). In contrast, the fermentation trains reported here had near-neutral pH (~ 6.5) and a more optimal C-N ratio ($\sim 25 \text{ g OC}_{\text{NA}}/\text{g N}$) (Table 4-1), which resulted in a higher proportion of high-molecular-weight acids, higher yields, and higher acid concentrations (Figure 4-3). Attempts were made to control pH and C-N ratios, which resulted in all trains having similar pH except Train 1, which had a higher pH. Controlling the pH precisely is a challenge in high-solids fermentations, and the effects of pH on performance variables are difficult to uncouple from other operating parameters. pH is an important variable in any type of fermentation and so deserves further investigation.

4.4 Conclusion

This propagated fixed-bed fermentation system operated at near-neutral pH (~6.5) and optimal C-N ratios (~25 g OC_{NA}/g N). Compared to a previous study at high pH (~9) and suboptimal C-N ratio, this study achieved better results. Compared to continuously mixed fermentations, periodic mixing had a similar conversion, but lower yield, selectivity, and acid concentrations. Increasing volatile solid loading rate (VSLR) and increasing liquid residence time decreased yield, conversion, selectivity, but increased product concentrations. Compared to countercurrent trains, propagated fixed-bed fermentations have similar selectivities and proportions of acetic acid, but have lower yields, conversion, productivities, and acid concentrations.

5. EFFECT OF ONE-TO-SIX STAGES IN COUNTERCURRENT MIXED-ACID FERMENTATION

To improve performance, mixed-acid fermentations employ a countercurrent strategy where solids and liquids pass in opposite directions through a series of fermentors. Traditionally, four fermentation stages have been employed. This study investigates how one to six stages affects fermentation performance. All fermentation trains employed a similar liquid residence time (LRT, ~20 d), volatile solid loading rate (VSLR, ~6.4 g NAVS/L·d), optimal carbon-nitrogen ratio (~40 g organic C_{NA}/g N), and pH (~5.8). Fewer stages increased yield and conversion, whereas more stages increased acid concentration and selectivity. Four to six stages achieved the same maximum acid concentrations, suggesting that ~30 g/L is the maximum acid concentration tolerated by the microorganisms with the selected LRT and VSLR. The higher acid concentration that occurs with more stages could inhibit the microorganisms, and therefore decrease yield and conversion. A single stage maximizes yield and conversion, but four stages maximize acid concentration.

5.1 Introduction

Worldwide energy demand is predominately supplied by fossil fuels (e.g., natural gas, petroleum, and coal); however, they cannot be used indefinitely because they are a finite resource and their combustion causes global warming and pollution (Alekkett et al., 2010; Demirbas, 2007). It is projected that the share of non-hydro renewables in power generation will increase from 3% in 2009 to 15% in 2035 (IEA, 2011b). To meet growing energy needs, inexhaustible and nonpolluting energy sources are becoming increasingly important.

Liquid biofuels, primarily bioethanol and biodiesel, provide about 3% of global transportation fuel (REN21, 2011). Both bioethanol and biodiesel require significant government support, even though the two top biofuels markets (e.g., United States, Brazil) are the most efficient producers of the feedstock (e.g., maize, sugarcane). For

both these biofuels, feedstock costs comprise more than half the total production cost. In both cases, food is used as feedstock, which affects trade policies and creates market distortions (Kojima et al., 2007). A promising alternative is the carboxylate platform, which converts inexpensive and abundant lignocellulose to liquid transportation fuels (Agler et al., 2011; Holtzapple et al., 1999; Holtzapple and Granda, 2009; Pham et al., 2010) and chemicals (Granda and Holtzapple, 2008).

The carboxylate platform is a cost-effective, versatile, and continuous biomass-to-energy technology that converts a variety of lignocellulosic feedstocks into chemicals and liquid fuels (Forrest et al., 2010b; Granda et al., 2009). It has low capital and operating costs, does not require sterile operating conditions or added enzymes, and has reached the demonstration level of development. A mixed culture of naturally occurring microorganisms ferments the biomass into carboxylic salts, which are converted into a wide array of chemicals (e.g., alcohols) and hydrocarbons (e.g., jet fuel, gasoline) (Aiello-Mazzarri et al., 2006; Landoll and Holtzapple, 2011).

For many years, multi-stage fermentations have been used in anaerobic digestors (AD) that produce methane. In AD systems, anaerobic conversion of biomass to methane occurs in four phases: (1) *Hydrolysis*, complex molecules of organic matter (e.g., polysaccharides, lipids, and proteins) are hydrolyzed into simple sugars, fatty acids, and amino acids. (2) *Acidogenesis*, acidogenic bacteria produce new cells, short-chain organic acids, alcohols, hydrogen, carbon dioxide, and ammonia (Koster, 1984). (3) *Acetogenesis*, the products from acidogenesis are converted into more biomass, hydrogen, acetic acid, and carbon dioxide (Gujer and Zehnder, 1983). (4) *Methanogenesis*, these products are converted to carbon dioxide, methane, and other reduced metabolites. In anaerobic digestion, each step is performed by a specific group of microorganisms, each having an optimal temperature, pH, and substrate for optimal growth. A single stage can be used; however, employing different conditions in multiple stages allows each step to be optimized (Ward et al., 2008).

In carboxylate fermentations, the final methanogenesis step is inhibited, which preserves product acids. In carboxylate fermentations, all three steps (hydrolysis,

acidogenesis, acetogenesis) occur in each stage. Instead, multiple stages are used to manage the effect of the inhibiting carboxylate salts that accumulate.

A single-stage fermentation (Figure 5-1) is a semi-continuous continuously stirred tank reactor (CSTR), where liquids and solids are added and removed in a single fermentor. In multi-stage countercurrent fermentations (Figure 5-1), such as the two- to six-stage trains in this study, solids and liquids are transported through a series of fermentors (a *train*) in opposite directions, allowing the least-reactive (most-digested) biomass to contact the lowest acid concentration, thereby minimizing inhibition from accumulated carboxylate salts (Aiello-Mazzarri et al., 2006). Because biomass is a heterogeneous mixture, it is hypothesized that the easily fermentable components can digest, even in the presence of high product concentrations. In a countercurrent train, biomass waste exits the last fermentor, while product liquid exits the first fermentor (Figure 5-1). This fermentor arrangement is designed to allow both high conversions and product concentrations, making it preferred over batch or single-stage fermentation (Fu and Holtzapfle, 2010b).

Traditionally, four-stage fermentations have been employed based on earlier modeling efforts (Loescher, 1996; Ross, 1998). However, Ross (1998) modeled only two-, four-, and six-stage fermentations, and did not verify with experiments. Other researchers have had success with continuous fermentations other than the traditional countercurrent four-stage fermentations. For example, pilot plant fermentations have been conducted in three stages (Smith, 2011), and continuous fermentations have been demonstrated in single-stage fermentors (Golub et al., 2011b). Systematic experimental investigation of multiple stages is necessary to understand the effect on performance measures (e.g., product concentration, yield, conversion, selectivity) and to guide equipment selection in industrial fermentations.

The purpose of this study is to employ one- to six-stage fermentations with similar liquid residence times (LRT) and volatile solid loading rates (VSLR) to evaluate the effect of stage-number on countercurrent fermentation performance.

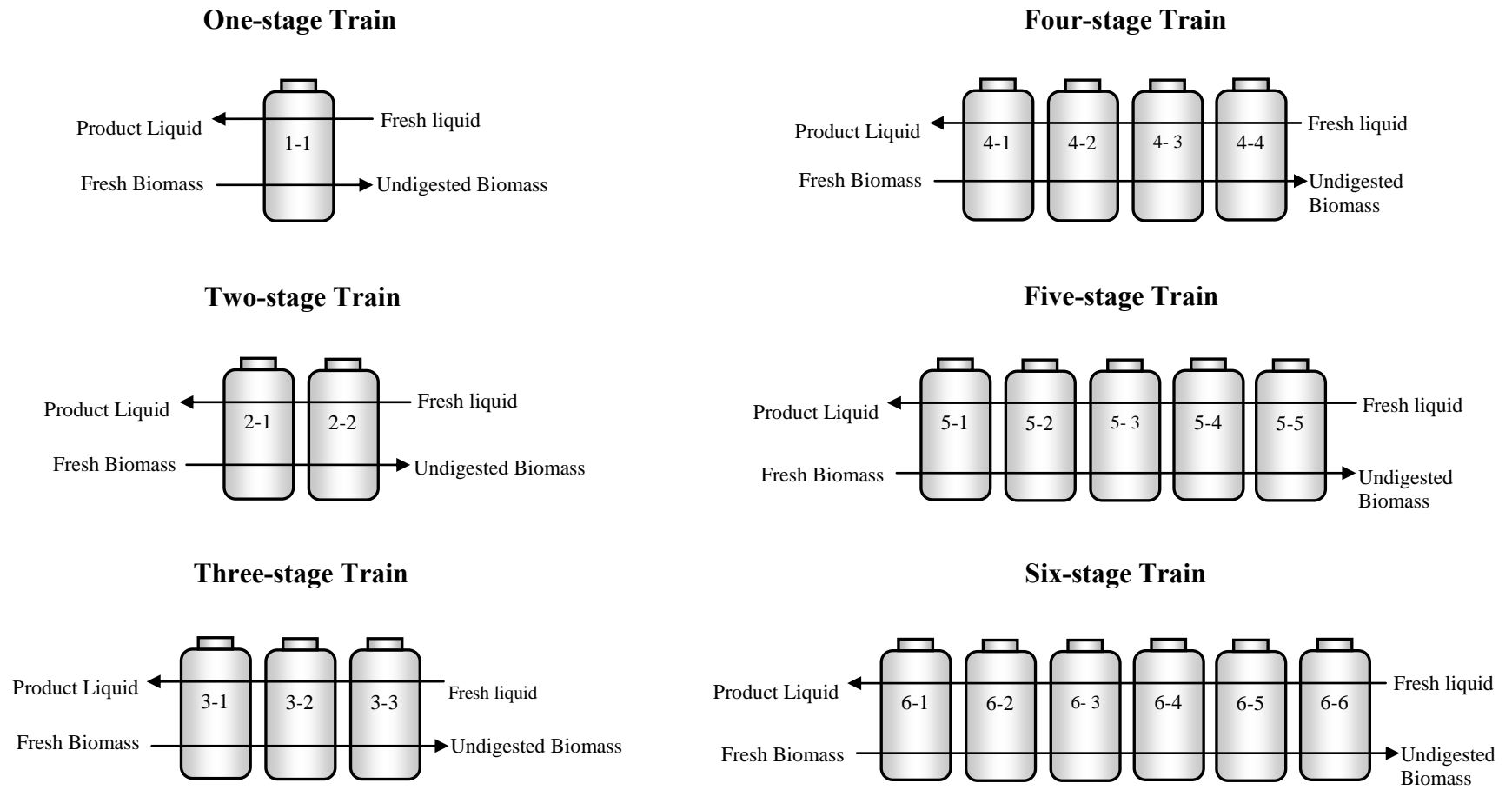


Figure 5-1. Diagram of the multi-stage experiment, depicting the one- to six-stage trains (Trains 1, 2, 3, 4, 5, and 6).

5.2 Materials and methods

5.2.1 *Fermentor configuration*

The fermentors were 1-L polypropylene centrifuge bottles capped by a rubber stopper inserted with a glass tube (Domke et al., 2004; Thanakoses et al., 2003). Two segments of ¼-in stainless steel pipe were inserted through the rubber stopper into the vessel to mix the fermentor contents as it rotated in the rolling incubator. A rubber septum sealed the glass tube and allowed for gas sampling and release.

5.2.2 *Substrate*

Shredded office paper, which served as the energy source, was obtained from a local recycling center. No pretreatment was required. Chicken manure, which served as an undefined nutrient source, was obtained from Feather Crest Farms, Inc. (Bryan, TX) and was dried at 105 °C for 48 h. (*Note:* Wet chicken manure degrades over time, so to maintain consistency during the entire experiment, dried and homogenized chicken manure was used.) Dried chicken manure had a C-N ratio of 12.9 ± 3.4 g non-acid organic carbon (OC_{NA})/g nitrogen (N) and an acid concentration of 0.05 ± 0.01 g acid/g dry chicken manure. Previous studies found that the C-N ratio of shredded office paper is 138.3 ± 43 g OC_{NA} /g N (Smith and Holtzapple, 2010). The substrate concentration is expressed as non-acid volatile solids (NAVS), which is the combustible portion of the substrate minus carboxylic acids present in the feed. Urea was used as supplemental nitrogen source.

5.2.3 *Fermentation medium*

The deoxygenated medium was prepared by boiling distilled water to liberate dissolved oxygen. After cooling to room temperature in a covered vessel, to further reduce the oxygen content, 0.275 g/L cysteine hydrochloride and 0.275 g/L sodium sulfide were added.

5.2.4 *Inoculum*

The inoculum was a mixed-culture of marine microorganisms from beach sediment collected in Galveston Island, TX. Sediment was removed from the bottom of multiple 0.5-m-deep shoreline pits. Samples were immediately placed in airtight plastic bottles filled with deoxygenated water, capped, and frozen at $-20\text{ }^{\circ}\text{C}$ until use. Before inoculation, samples were thawed, shaken vigorously, and allowed to settle by gravity. Equal parts of the resulting supernatant were homogenized, and aliquots were used to standardize the fermentation inoculum to 12.5% of the initial working volume (Forrest et al., 2010a; Thanakoses, 2002). Bacterial community composition of mixed-acid fermentation has been reported elsewhere (Hollister et al., 2010; Hollister et al., 2011).

5.2.5 *Methanogen inhibition*

Iodoform (CHI_3) was used to inhibit methane production. Iodoform solution (80 μL , 20 g CHI_3/L 190-proof ethanol) was added to each fermentor every 48 h (Domke et al., 2004). Iodoform is sensitive to light, air, and temperature, and so the solution was kept in amber-colored glass bottles wrapped in foil and stored at $-20\text{ }^{\circ}\text{C}$ (Agbogbo and Holtzapfle, 2007).

5.2.6 *Multiple-stage fermentation procedure*

Six continuous fermentation trains (Figure 5-1) were run: a one-stage fermentor (Train 1), a two-stage train (Train 2), a three-stage train (Train 3), a four-stage train (Train 4), a five-stage train (Train 5), and a six-stage train (Train 6).

The feed consisted of 80% shredded office copier paper and 20% dry homogenized chicken manure on a dry mass basis. Each fermentor was incubated at $40\text{ }^{\circ}\text{C}$ as a submerged fermentation. The six fermentations were initiated as batch cultures under anaerobic conditions with a concentration of 100 g non-acid dry solid (NADS)/L deoxygenated water, which was achieved by adding substrate, nutrient source (manure and urea), inoculum, buffer (calcium carbonate), and liquid medium to each fermentor.

After the first two weeks of batch growth, solid/liquid transfers began and occurred every 48 h to reach steady state. The transfer frequency (48 h) was chosen to

help normalize the solid and liquid residence times. To achieve the same volatile solid loading rate (VSLR) and liquid residence times (LRT) in all trains, the mass of solids was held constant in each fermentor, but the fed non-acid volatile solid (NAVS), fed fermentation liquid, and liquid retained were scaled accordingly (Figure 5-1).

Every 48 h, fermentors were removed from the incubator, the gas volume was collected, liquid samples were taken, the pH was measured, and fermentors were centrifuged ($3300\times g$, 25 min) to separate the liquid and solid phases as *transfer liquid* and *transfer solids*. For each fermentor, the liquid phase was decanted into a separate graduated cylinder and measured. The remaining solid phase was weighed. The first fermentor was fed a constant amount of fresh substrate. The remaining fermentors in the train were fed the transfer solids from the previous fermentor. The transfer solids retained in each fermentor was controlled by a solid-weight setpoint. The mass of transfer solids removed was determined by a simple material balance, which equaled the initial solid weight + transfer solids added from previous fermentor – solid-weight setpoint. Once the solid transfers were performed, all or a portion of the transfer liquid from one fermentor was added to the fermentor upstream of it. More description about solid/liquid mass transfers follows and can also be found in Table 5-1.

In Train 1, liquids and solids were added and removed in a single fermentor. To achieve a similar LRT, a portion of the fermentation liquid was retained. The one-stage train has a single carboxylate salt concentration whereas the multi-stage trains have different concentrations in each stage.

For Train 2, after centrifugation, the liquid and solid phases were separated. Fresh substrate was fed to 2-1 and a portion of the homogenized solids was transferred from 2-1 to 2-2, and exited 2-2 as biomass waste. In a countercurrent manner, fresh deoxygenated water was added to the second fermentor (2-2), and a portion of the filtered liquid was transferred from 2-2 to the first fermentor (2-1), and a portion of filtered liquid was transferred out of 2-1 as the product liquid. During transfers, the solid wet weight retained in 2-1 and 2-2 equaled 225 g.

For Train 3, after centrifugation, the liquid and solid phases were separated. Fresh substrate was fed to 3-1 and a portion of the homogenized solids was transferred from 3-1 to 3-2, 3-2 to 3-3, and exited 3-3 as biomass waste. In a countercurrent manner, fresh deoxygenated water was added to the third fermentor (3-3), and a portion of the filtered liquid was transferred from 3-3 to the second fermentor (3-2), from 3-2 to the first fermentor (3-1), and a portion of filtered liquid was transferred out of 3-1 as the product liquid. During transfers, the solid wet weight retained in 3-1, 3-2, and 3-3 equaled 225 g.

For Trains 4 to 6, after centrifugation, the liquid and solid phases were separated. Fresh substrate was fed to the first fermentor and a portion of the homogenized solids was transferred to the adjacent fermentor. Finally, in the last fermentor, solids were withdrawn as biomass waste. In a countercurrent manner, fresh deoxygenated water was added to the last fermentor. *All* of the filtered liquid was transferred to the adjacent fermentor. This process was repeated until liquid was harvested from the first fermentor. During transfers, the solid wet weight retained in each fermentor equaled 225 g.

In each fermentor, after a transfer, the solids were resuspended, iodoform was added (120 μ L of 20 g/L ethanol solution), and calcium carbonate was added to neutralize carboxylic acids and buffer the system (Table 5-1). Urea was added to adjust the carbon-nitrogen (C-N) ratio. During solid and liquid transfers, when the fermentors were open to the atmosphere, anaerobic conditions were maintained by flushing the fermentors with nitrogen gas (Praxair, Bryan, TX). (*Note:* Nitrogen flushing was a precautionary step; these anaerobic fermentations have been shown to resist intermittent air exposure (Golub et al., 2011b).) The fermentors were then resealed and placed back in the incubator.

5.2.7 Carbon-nitrogen ratio

The C-N ratio is defined as the mass of non-acid organic carbon (g OC_{NA}) per total mass of nitrogen (g N) (Smith et al., 2011). Total C and N contents (g/100 g wet sample) were determined by Texas A&M University Soil, Water, and Forage Testing Laboratory (College Station, TX) using an Elementar Variomax CN. Based on the

carbon and nitrogen contents of the paper, chicken manure, and urea (ACS grade), the amount of each was calculated to achieve the desired C-N ratio and volatile solids (VS) concentration (Table 5-1).

5.2.8 Analytical methods

5.2.8.1 Carboxylic acid concentration determination

Fermentation product liquid was collected every 48 h and analyzed for C2–C7 carboxylic acids (a.k.a. volatile fatty acids) as previously described (Golub et al., 2011a).

5.2.8.2 Biogas analysis

For the first two weeks, because of the high initial digestion rate, each fermentor was vented daily; thereafter, it was vented every 48 h. Biogas was removed through the fermentor septum, and the volume was measured by displacing liquid in an inverted graduated glass cylinder filled with a 300 g/L CaCl₂ solution, which prevented microbial growth and carbon dioxide adsorption (Domke, 1999).

Biogas composition (i.e., carbon dioxide, nitrogen, oxygen, and methane) was determined by manually injecting 5-mL gas samples into an Agilent 6890 Series chromatograph with a thermal conductivity detector (TCD). A 4.6-m-long, 2.1-mm-ID stainless steel packed column (60/80 Carboxen 100, Supelco 1-2390) was used. The inlet temperature was 230 °C, the detector temperature was 200 °C, and the oven temperature was 200 °C. The total run time was 10 min, and helium was the carrier gas.

5.2.8.3 Moisture and ash contents

Moisture and ash contents were determined by drying in a 105 °C forced-convection oven for at least 24 h, and subsequent combustion in a 575 °C furnace for at least 12 h by NREL procedures No. 001 and 005, respectively (NREL, 2004). The ash content was calculated on a dry basis. The consumption of non-acid volatile solids (NAVS) was determined using the inert-ash approach as described previously (Smith et al., 2011).

5.2.9 Operating parameters

Previous investigations using continuous countercurrent fermentations have shown that adequate conversion and exit yield were achieved with VSLR of ~6.4 g NAVS/L·d and LRT of ~20 d (Agbogbo, 2005; Chan and Holtzapple, 2003; Thanakoses, 2002); therefore, this VSLR and LRT were chosen to investigate the performance of this multi-stage fermentation system. The LRT and VSLR (Table 5-1) were regulated by controlling the liquid and solid transfer frequency (T), NAVS feed rate, and the liquid feed rate per transfer. VS is defined as the mass of dry solid material that is combusted at 575 °C after 12 h, and NAVS is defined as VS less the amount of carboxylate acid:

$$\text{NAVS} = (\text{g total wet biomass})(1 - \text{MC})(1 - \text{AC}) - (\text{g acid in biomass}) \quad (5-1)$$

where MC (g water/g wet biomass) is the fraction of moisture in the biomass, and AC (g ash in biomass/g dry biomass) is the fraction of dry ash remaining after 12 h of combustion at 575 °C. In performance calculations, NAVS is preferred because it ensures the product is not quantified with the reactant.

The nutrient source (dried chicken manure) contains carboxylic acids. To more accurately quantify fermentor productivity, the amount of acid entering the system in the manure is subtracted from the amount of acid exiting the system in the product liquid and discarded solids. To determine the amount of acid in the manure, the dry manure was resuspended in distilled water at different concentrations. The acid in the supernatant was analyzed by GC.

Table 5-1. Operating parameters. Normalized parameters represent the mean of the steady-state values \pm CI (95% CI).

Fermentation Train	1	2	3	4	5	6
Controlled						
Solid and liquid transfer frequency, T (h)	48	48	48	48	48	48
NAVS feed rate (g NAVS/ T)	3.5	7.0	10.6	14.1	21.1	32.0
Dry solids added (g/ T)	4	8	12	16	24	36.4
Manure added (g/ T)	1.0	2.0	3.0	4.0	6.0	9.0
Urea added (g/ T)	0.03	0.10	0.20	0.30	0.40	0.50
Calcium carbonate added (g/ T)	1.0	2.0	3.0	4.0	5.0	6.0
Liquid feed rate (mL/ T)	30	60	90	121	183	277
Solid cake retained in each fermentor (g wet)	225	225	225	225	225	225
Centrifuged liquid retained in each fermentor (mL)	90	60	30	0	0	0
Methane inhibitor (μ L/(T ·fermentor))	80	80	80	80	80	80
Normalized						
Volatile solid loading rate, VSLR (g NAVS/(L_{liq} ·d))	6.4 \pm 0.06	6.5 \pm 0.08	6.4 \pm 0.06	6.4 \pm 0.04	6.2 \pm 0.05	6.4 \pm 0.04
Liquid residence time, LRT (d)	20.2 \pm 1.4	21.2 \pm 1.2	22.3 \pm 3.0	20.8 \pm 1.6	21.2 \pm 1.6	19.2 \pm 1.0
Total liquid volume, TLV (L)	0.27 \pm 0.00	0.54 \pm 0.01	0.83 \pm 0.01	1.11 \pm 0.01	1.70 \pm 0.01	2.48 \pm 0.02
Volatile solid, VS, concentration (g NAVS/ L_{liq})	138 \pm 6	135 \pm 4	123 \pm 3	114 \pm 2	98 \pm 2	95 \pm 2
Dry solid, DS, concentration (g NADS/ L_{liq})	230 \pm 9	219 \pm 6	200 \pm 4	193 \pm 3	152 \pm 2	151 \pm 2
Average carbon-nitrogen ratio, C-N ratio (g OC_{NA} /g N)	40.0 \pm 13.0	40.5 \pm 3.1	37.3 \pm 7.7	39.9 \pm 2.1	42.8 \pm 6.1	43.7 \pm 6.4
Average pH (F1–F4)	5.76 \pm 0.06	5.78 \pm 0.14	5.83 \pm 0.15	5.81 \pm 0.14	5.66 \pm 0.13	5.77 \pm 0.09
Urea addition rate (g urea/(L_{liq} ·d))	0.05 \pm 0.00	0.09 \pm 0.00	0.12 \pm 0.00	0.14 \pm 0.00	0.12 \pm 0.00	0.10 \pm 0.00

NAVS = Non-acid volatile solids; NADS = Non-acid dry solids

The VSLR and LRT are calculated as follows:

$$\text{VSLR} = \frac{\text{NAVS feed (g)}}{\text{TLV(L)} \cdot \text{time (d)}} \quad (5-2)$$

$$\text{LRT} = \frac{\text{TLV (L)}}{\text{liquid flow rate out of fermentation train (L/d)}} \quad (5-3)$$

The total liquid volume (TLV) quantifies the total volume of liquid in the solid and liquid phases, and includes both free and interstitial liquid. Liquid flow rate out of fermentation train includes exiting liquid product from the first fermentor and interstitial liquid in cake exiting from the last fermentor.

5.2.10 *Definition of terms*

To account for the total mass in the system, a mass balance closure was calculated with Equation 5-4,

$$\text{mass balance closure} = \frac{\text{mass out (g)}}{\text{mass in (g)} + \text{water of hydrolysis (g)}} \quad (5-4)$$

Cellulose is a polysaccharide composed of individual anhydroglucose units (glucan, MW = 162 g/mol). During digestion, cellulose is enzymatically hydrolyzed to glucose by adding water. The water of hydrolysis was calculated as previously described (Chan and Holtzapple, 2003).

The mixed-acid concentration can be expressed as molar acetic acid equivalents (α), which is the reducing potential of an equivalent amount of acetic acid (Datta, 1981).

$$\begin{aligned}
 \alpha &= 1.00 \times \text{acetic (mol/L)} + 1.75 \times \text{propionic (mol/L)} \\
 &+ 2.50 \times \text{butyric (mol/L)} + 3.25 \times \text{valeric (mol/L)} \\
 &+ 4.00 \times \text{caproic (mol/L)} + 4.75 \times \text{heptanoic (mol/L)}
 \end{aligned}
 \tag{5-5}$$

Acetic acid equivalents (Aceq) can be expressed on a mass basis as

$$\text{Aceq (g/L)} = 60.05 \text{ (g/mol)} \times \alpha \text{ (mol/L)} \tag{5-6}$$

Aceq proportionally weighs the higher-chained carboxylic acids (C₃ to C₇); the higher acids have higher Aceq than lower acids.

5.2.11 *Measuring performance*

The feed and exit rate of acid, ash, NAVS, water, and gas were determined during the steady-state period. As previously described (Smith and Holtzapple, 2011b), the average rate of each component was calculated using the *slope method*. In this method, the moving cumulative sum of each component is plotted with respect to time. The slope of the steady-state portion of this line is the rate. All performance variables (e.g., conversion, selectivity, and yield) were calculated from the averaged component rates determined by the slope method, as described below:

$$\begin{aligned}
 \text{Conversion } x &\equiv \frac{\text{NADS}_{\text{feed}} \text{ (g)} - \text{NADS}_{\text{exit}} \text{ (g)}}{\text{NAVS}_{\text{feed}} \text{ (g)}} \\
 &= \frac{\text{NAVS}_{\text{feed}} \text{ (g)} + \text{Ash}_{\text{feed}} \text{ (g)} - \text{NAVS}_{\text{exit}} \text{ (g)} - \text{Ash}_{\text{exit}} \text{ (g)}}{\text{NAVS}_{\text{feed}} \text{ (g)}} \\
 &= \frac{\text{NAVS}_{\text{consumed}} \text{ (g)}}{\text{NAVS}_{\text{feed}} \text{ (g)}}
 \end{aligned}
 \tag{5-7}$$

$$\text{Exit yield } (Y_E) \equiv \frac{\text{total acid output from solid and liquid streams (g)}}{\text{NAVS}_{\text{feed}} \text{ (g)}} \tag{5-8}$$

$$\text{Process yield } (Y_P) \equiv \frac{\text{total acid output in product liquid stream (g)}}{\text{NAVS}_{\text{feed}}(\text{g})} \quad (5-9)$$

$$\text{Culture yield } (Y_C) \equiv \frac{\text{total acid produced (g)}}{\text{NAVS}_{\text{feed}}(\text{g})} \equiv Y_E - Y_F \quad (5-10)$$

$$\text{Feed yield } (Y_F) \equiv \frac{\text{total acid entering with feed (g)}}{\text{NAVS}_{\text{feed}}(\text{g})} \quad (5-11)$$

$$\begin{aligned} \text{Selectivity } (\sigma) &\equiv \frac{\text{total acid produced (g)}}{\text{NAVS}_{\text{feed}}(\text{g}) - \text{NAVS}_{\text{exit}}(\text{g})} \quad (5-12) \\ &\equiv \frac{\text{total acid produced (g)}}{\text{NAVS digested (g)}} = \frac{Y_E}{x} \end{aligned}$$

$$\text{Acid productivity } (P) \equiv \frac{\text{total acids produced (g)}}{\text{TLV (L)} \cdot \text{d}} \quad (5-13)$$

where $\text{NADS}_{\text{feed}}$ is the non-acid dry solids fed, $\text{NADS}_{\text{exit}}$ is the non-acid dry solids removed from the fermentation, $\text{NAVS}_{\text{feed}}$ is the non-acid volatile solids fed, $\text{NAVS}_{\text{exit}}$ is the non-acid volatile solids removed from the fermentation, Ash_{feed} is the inert solids fed in biomass feed and buffer, and Ash_{exit} is the inert solids exiting in all solid and liquid streams. NADS includes the ash and volatile solid component of biomass. Ash is assumed to be conserved in the fermentation (Ash_{feed} equals Ash_{exit}), canceling Ash from Equation 5-7.

Per g NAVS fed, the exit yield (Y_E) represents the sum of acid in the product transfer liquid, waste transfer solids, and liquid samples removed from sampling. The process yield (Y_P) represents all the acid in the product transfer liquid per g of NAVS fed. The feed yield (Y_F) is the total g acid entering with the feed per g NAVS fed, and the culture yield (Y_C) is the exit yield less the feed yield.

5.2.12 Statistical analysis

Statistical analysis was performed using Excel 2007 (Microsoft, USA). The mean and standard deviations of the total acid concentrations, acetic acid equivalent

(Aceq), non-acid volatile solids (NAVS) in and out were determined from steady-state operating data. For all countercurrent trains, the average time required to reach steady state was ~120 d. These averaged values were then used to calculate the acid productivity (P), selectivity (σ), yield (Y), and conversion (x) with a 95% confidence interval (CI). Unless specified otherwise, all comparisons in the Results and Discussion section are statistically significant. The steady-state region was the period during which the product total acid and Aceq concentration, dry solids exiting, liquid volume and solid weight of each fermentor, pH, and mass of acid exiting did not vary by more than 2.2 standard deviations from the average for a period of at least one liquid residence time. From the slope of the summed data, to compare the means of the groups, a Student's two sample t -test (two-tailed, Type 3) was used to compute the p values between the performance variables of the trains. The p values had a familywise error rate of 0.05 using the Bonferroni correction. Results were considered statistically significant at the 5% level. All error bars are reported at 95% CI.

5.3 Results and discussion

Each fermentation train consisted of a staged countercurrent semi-continuous submerged fermentation system. Six fermentation trains were operated, each having a different number of stages: a one-stage CSTR (Train 1), a two-stage train (Train 2), a three-stage train (Train 3), a four-stage train (Train 4), a five-stage train (Train 5), and a six-stage train (Train 6). To compare the results of all trains, the LRT and VSLR operating parameters were normalized by explicitly controlling the liquid/solid mass transfer frequency (T), NAVS feed rate, the liquid feed rate, and the mass of solids and liquid retained in each fermentor per transfer (Table 5-1).

5.3.1 Biogas

At steady state, Trains 1, 2, 3, 4, 5, and 6 produced 0.14 ± 0.00 , 0.27 ± 0.00 , 0.42 ± 0.00 , 0.55 ± 0.00 , 0.84 ± 0.00 , and 1.24 ± 0.00 g gas/day, respectively. This increase in gas production with increasing stage number results from increased NAVS feed. After normalizing by the rate of NAVS feed (g/day), the biogas yield for Trains 1 to 6 was

found. The biogas yield decreased with increasing stage number (Tables 5-2, 5-3). The amount of biogas produced loosely correlates with conversion. Other studies of ethanol and ruminal fermentations show gas production is related to substrate digestibility (Contreras-Govea et al., 2011; Weimer et al., 2005). For all trains, the average biogas compositions were similar ($45.2 \pm 18.3\%$ N₂, $54.8 \pm 19.7\%$ CO₂). No methane was detected in any fermentor.

5.3.2 *Acid concentration, productivities, and daily acid production*

For all six trains at steady state, the accumulated mass of total carboxylic acids and Aceq exiting, NADS added, and NADS removed from their respective trains was found. The slopes of the steady-state regression lines provided the daily total acid and Aceq exiting, NADS exiting, and NADS removed on a mass basis (Table 5-2). Productivity was calculated as the mass rate of acid produced per total fermentor volume.

Increased number of stages, proceeding from Train 1 to 4, increased acid concentration (Tables 5-2, 5-3). However, the mixed-acid fermentation reached a maximum acid concentration of ~30 g/L with four stages (Train 4, Figure 5-2), indicating that the fifth and sixth countercurrent stages in Trains 5 and 6, respectively, were redundant and provided diminished product returns. During the unsteady-state start-up period, higher acid concentrations were observed initially in the fermentation, up to ~45 g/L in Train 6. However, these high acid concentrations were unsustainable as evidenced by the lower (~30 g/L) steady-state acid concentrations for Trains 4–6.

Table 5-2. Fermentation performance measures for Trains 1, 2, 3, 4, 5, and 6. Values represent the mean of the steady-state values \pm CI (95% CI).

	1	2	3	4	5	6
Total carboxylic acid concentration (g/L)	17.53 \pm 0.95	26.06 \pm 0.99	27.19 \pm 0.76	30.81 \pm 0.33	29.48 \pm 0.34	30.55 \pm 0.34
Aceq concentration (g/L)	22.17 \pm 1.13	32.32 \pm 1.25	33.99 \pm 0.97	39.86 \pm 0.40	36.13 \pm 0.44	39.12 \pm 0.57
Aceq/Acid ratio	1.27 \pm 0.01	1.24 \pm 0.00	1.25 \pm 0.00	1.29 \pm 0.00	1.23 \pm 0.01	1.28 \pm 0.01
Conversion, x (g VS digested/g VS fed)	0.372 \pm 0.018	0.323 \pm 0.005	0.273 \pm 0.003	0.241 \pm 0.002	0.192 \pm 0.002	0.130 \pm 0.002
Selectivity, σ (g acid produced/g NAVS consumed)	0.390 \pm 0.003	0.453 \pm 0.001	0.538 \pm 0.001	0.608 \pm 0.001	0.709 \pm 0.001	0.799 \pm 0.002
Aceq selectivity, σ_a (g Aceq produced/g NAVS consumed)	0.334 \pm 0.004	0.378 \pm 0.002	0.383 \pm 0.001	0.468 \pm 0.001	0.516 \pm 0.001	0.596 \pm 0.002
Exit yield, Y_E (g acid/g NAVS fed)	0.145 \pm 0.000	0.147 \pm 0.000	0.147 \pm 0.000	0.146 \pm 0.000	0.136 \pm 0.000	0.104 \pm 0.000
Exit Aceq yield, Y_{aE} (g Aceq/g NAVS fed)	0.124 \pm 0.001	0.122 \pm 0.001	0.105 \pm 0.000	0.113 \pm 0.000	0.099 \pm 0.000	0.078 \pm 0.000
Culture yield, Y_C (g acid/g NAVS fed)	0.132 \pm 0.000	0.133 \pm 0.000	0.134 \pm 0.000	0.133 \pm 0.000	0.123 \pm 0.000	0.091 \pm 0.000
Process yield, Y_P (g acid/g NAVS fed)	0.083 \pm 0.001	0.083 \pm 0.001	0.067 \pm 0.000	0.073 \pm 0.000	0.067 \pm 0.000	0.051 \pm 0.000
Productivity, P (g total acid/(L _{liq} ·d))	0.884 \pm 0.008	0.890 \pm 0.007	0.882 \pm 0.006	0.885 \pm 0.005	0.805 \pm 0.007	0.614 \pm 0.004
Biogas yield (g gas/g NAVS fed)	0.120 \pm 0.001	0.111 \pm 0.000	0.102 \pm 0.000	0.097 \pm 0.000	0.107 \pm 0.000	0.079 \pm 0.000
Mass balance closure (g mass in/g mass out)	0.91 \pm 0.01	0.90 \pm 0.00	0.88 \pm 0.00	0.94 \pm 0.00	0.94 \pm 0.00	0.94 \pm 0.00

Table 5-3. *p* values for fermentation performance measures ($\alpha = 0.05$).

Trains	Conv.	Selectivity	Exit yield	Exit yield Aceq	Culture yield	Feed yield	Process yield	TLV	Productivity	Biogas yield	Total acid conc.	Aceq conc.	Aceq/Total acid
1 and 2	0.000	0.000	0.000	0.004	0.000	0.741	0.333	0.000	0.234	0.000	0.000	0.000	0.000
1 and 3	0.000	0.000	0.000	0.000	0.000	0.942	0.000	0.000	0.739	0.000	0.000	0.000	0.000
1 and 4	0.000	0.000	0.000	0.000	0.000	0.641	0.000	0.000	0.762	0.000	0.000	0.000	0.000
1 and 5	0.000	0.000	0.000	0.000	0.000	0.627	0.000	0.000	0.000	0.000	0.000	0.000	0.000
1 and 6	0.000	0.000	0.000	0.000	0.000	0.671	0.000	0.000	0.000	0.000	0.000	0.000	0.000
2 and 3	0.000	0.000	0.122	0.000	0.105	0.614	0.000	0.000	0.084	0.000	0.069	0.037	0.000
2 and 4	0.000	0.000	0.283	0.000	0.276	0.833	0.000	0.000	0.271	0.000	0.000	0.000	0.000
2 and 5	0.000	0.000	0.000	0.000	0.000	0.089	0.000	0.000	0.000	0.000	0.000	0.000	0.000
2 and 6	0.000	0.000	0.000	0.000	0.000	0.107	0.000	0.000	0.000	0.000	0.000	0.000	0.000
3 and 4	0.000	0.000	0.001	0.000	0.001	0.296	0.000	0.000	0.437	0.000	0.000	0.000	0.000
3 and 5	0.000	0.000	0.000	0.000	0.000	0.113	0.808	0.000	0.000	0.000	0.000	0.000	0.000
3 and 6	0.000	0.000	0.000	0.000	0.000	0.143	0.000	0.000	0.000	0.000	0.000	0.000	0.000
4 and 5	0.000	0.000	0.000	0.000	0.000	0.000	0.000	0.000	0.000	0.000	0.000	0.000	0.000
4 and 6	0.000	0.000	0.000	0.000	0.000	0.000	0.000	0.000	0.000	0.000	0.000	0.000	0.000
5 and 6	0.000	0.000	0.000	0.000	0.000	0.730	0.000	0.000	0.000	0.000	0.000	0.000	0.000

p value < 0.003 statistically different, with a familywise error rate of 0.05 using the Bonferroni correction

To normalize the rate of acid exiting the fermentation train on a TLV basis, the productivity was obtained for each train. Trains 1, 2, 3, and 4 had similar productivities; however, trains with over four stages had decreased productivity (Tables 5-2, 5-3). As the number of stages increased, the carboxylic acid concentration increased, which inhibited the mixed-culture of microorganisms, making Stages 5 and 6 ineffective.

A measure of the production of higher molecular weight carboxylic acids (e.g., valeric, caproic, and heptanoic acid) is the Aceq-to-total-acid ratio. When comparing fermentation trains with different numbers of stages, the Aceq-to-total-acid ratios were different; however, there was no consistent trend (Tables 5-2, 5-3).

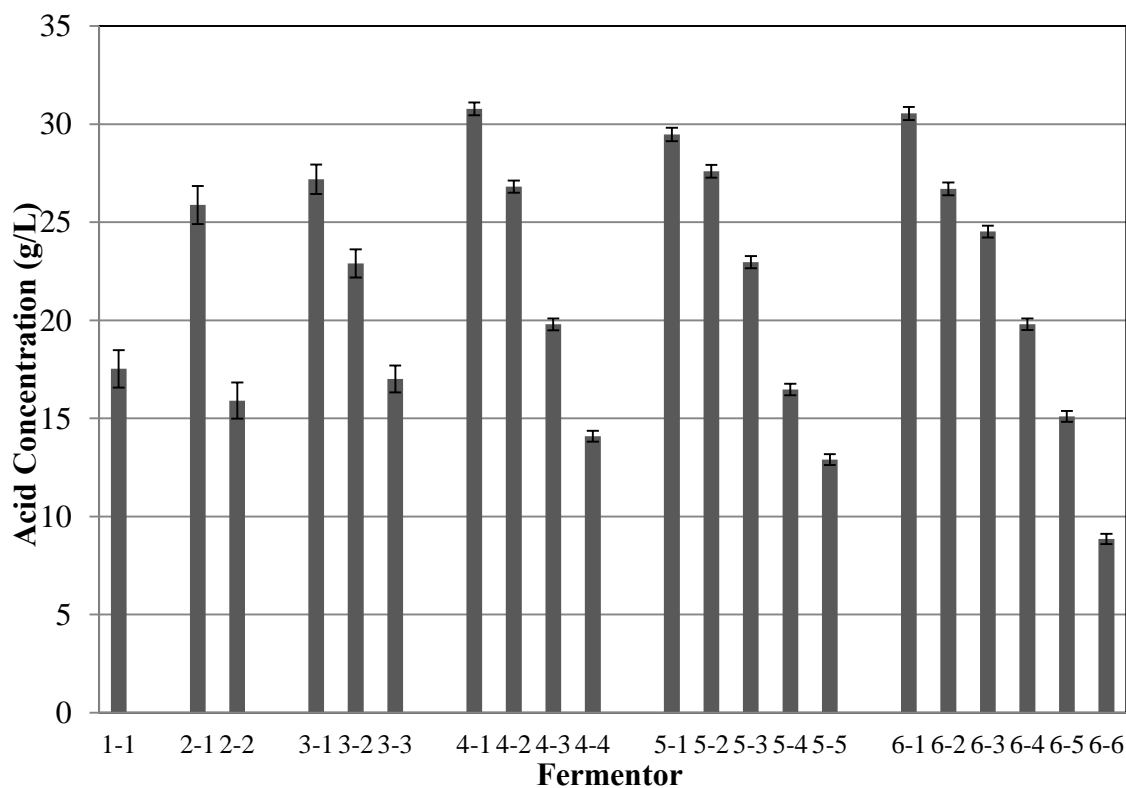


Figure 5-2. Acid concentration in each stage of the fermentation trains. Error bars are the 95% confidence intervals during the steady-state period.

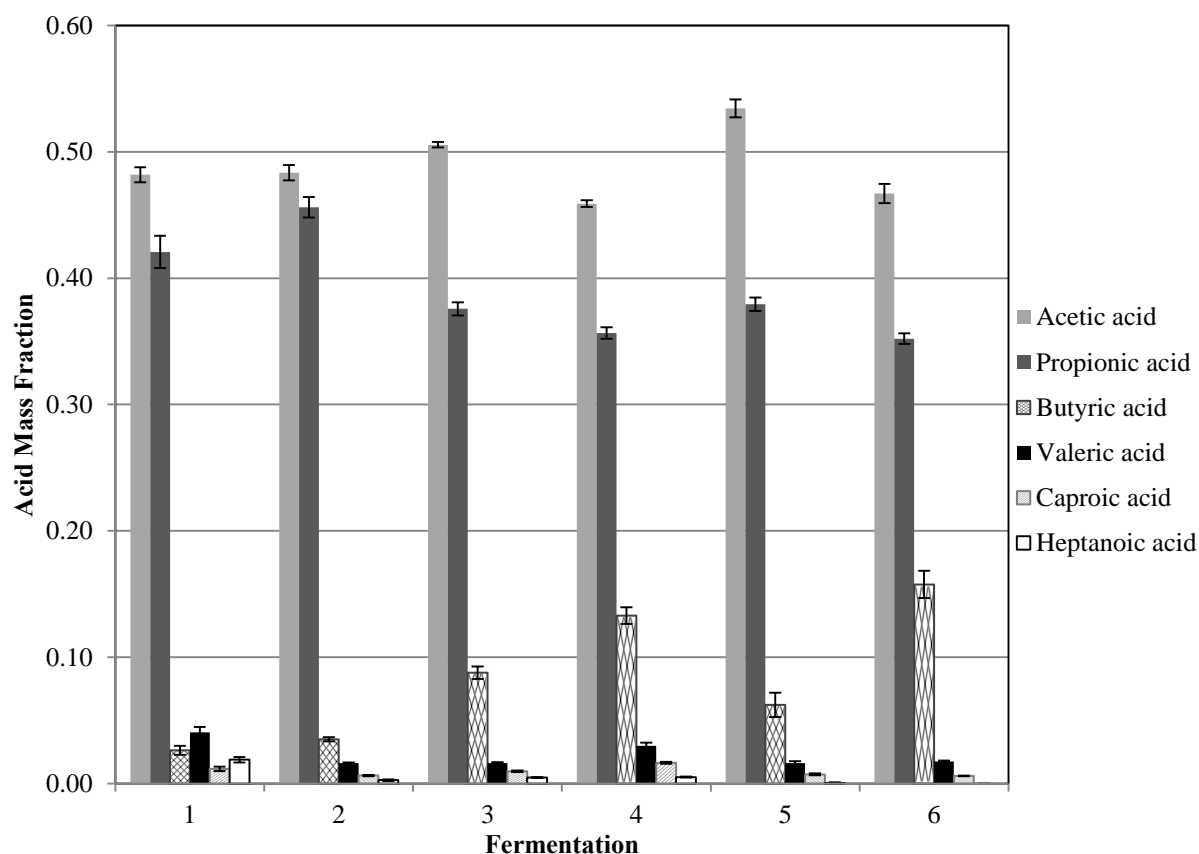


Figure 5-3. Carboxylic acid composition profile. Error bars are the 95% confidence intervals for each carboxylic acid composition during the steady-state period.

5.3.3 Yield

The exit acetic acid equivalent yield Y_{aE} quantifies the sum of acetic acid equivalents *exiting* the fermentation in the product transfer liquid, waste transfer solids, and liquid samples per g NAVS feed. Generally, Y_{aE} significantly improved with fewer stages, because the trains with fewer stages (Trains 1 and 2) produced more acids from the fed NAVS. Although the trains with more stages produced slightly more high-molecular-weight acids (Figure 5-3), Y_{aE} decreased with more stages (Tables 5-2, 5-3). Increasing the number of stages most likely inhibited the overall metabolism of the microorganisms, which suppressed the overall production rates of acids but allowed for the production of higher-chained carboxylic acids. The production of higher acids from

lower acids reduced the osmotic stress on the microorganisms. This was not expected because previous studies showed that inhibitory stress caused by high pH or low C-N ratio makes higher-molecular-weight acids unfavored (Golub et al., 2011a; Rodriguez et al., 2006).

The exit yield Y_E (Equation 5-8) quantifies the sum of acid *exiting* the fermentation in the product transfer liquid, waste transfer solids, and liquid samples per g NAVS feed. The culture yield Y_C (Equation 5-11) represents the acid *produced* by the mixed culture per g NAVS_{feed} and is equal to the exit yield less the feed yield Y_F (Equation 5-10). The Y_E and Y_C for Trains 1, 2, 3, and 4 did not vary by more than 1.5%; however, not all were statistically similar (95% CI). The Y_E and Y_C decreased with more fermentation stages in Train 5 and 6, -7% and -30%, respectively (Figure 5-4, Tables 5-2, 5-3). With more stages, the higher carboxylate concentration inhibits the microorganisms and decreases the amount of acid produced compared to the mass of NAVS fed.

The process yield Y_P (Equation 5-9) quantifies only the acid in the product transfer liquid per g NAVS_{feed}, which is sent downstream to be clarified, concentrated, and processed into chemicals and fuel; thus, Y_P represents a commercially relevant acid yield. In general, fewer stages increased Y_P ; thus, the fermentations with the least number of stages produced more acid in the product liquor (Figure 5-4, Table 5-2). Again, increasing the number of stages most likely inhibited the overall metabolism of the microorganisms, suppressing the acid production rate in the product liquor.

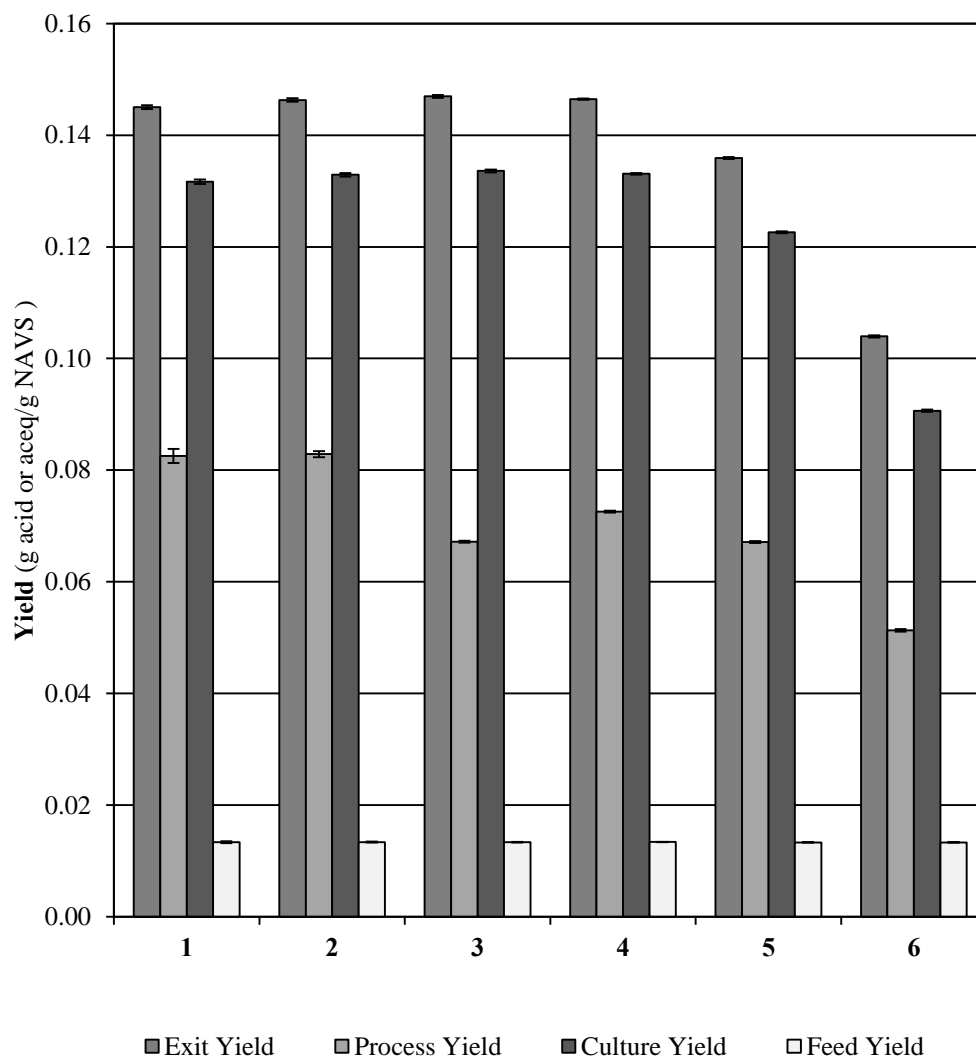


Figure 5-4. Exit, process, culture, and feed yield for Trains 1, 2, 3, 4, 5, and 6. Error bars are the 95% confidence intervals during the steady-state period.

5.3.4 Conversion and selectivity

Conversion significantly improved with fewer stages (Tables 5-3, 5-4). Fermentations with fewer stages are not inhibited by high acid concentrations found in the trains with more stages (i.e., Trains 5 and 6), allowing the trains with fewer stages to digest more of fed NAVS. Figure 5-6 shows the conversion in individual stages of the

trains. Here, the first fermentors of the trains had the lowest conversion, which corresponded with the highest acid concentration (Figure 5-2). The acid concentration was lower in fermentors closer to the fresh inlet liquid feed, which was where the majority of conversion occurs. In Trains 5 and 6, the conversion decreased in the last fermentor. Although this fermentor had the lowest acid concentration, the large amount of recalcitrant biomass might have overwhelmed the advantage of a lower acid concentration.

With regards to selectivity, increased fermentation stage number increased selectivity (Tables 5-2 and 5-3, Figure 5-5). This suggests that in fermentations with increased stages, the microorganisms become stressed from a longer exposure to higher concentrations of product acids, causing the microorganisms to make less alternative products besides acids, such as cells. Because the cells are stressed, less of the metabolic energy goes into growth and more goes into maintenance.

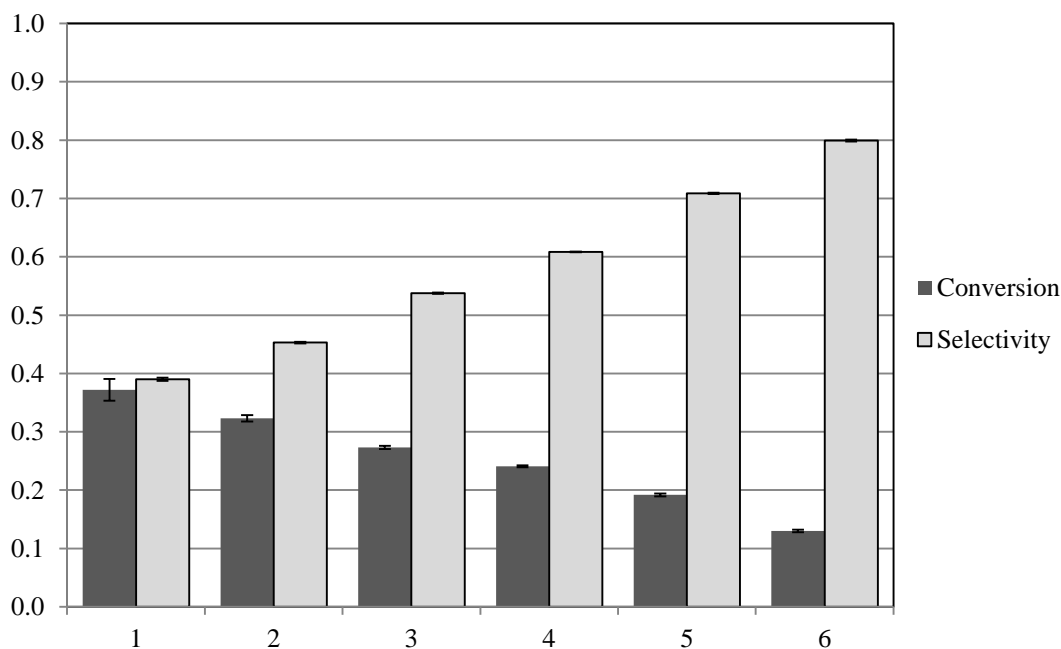


Figure 5-5. Selectivity and conversion for Trains 1, 2, 3, 4, 5, and 6. Error bars are the 95% confidence intervals during the steady-state period.

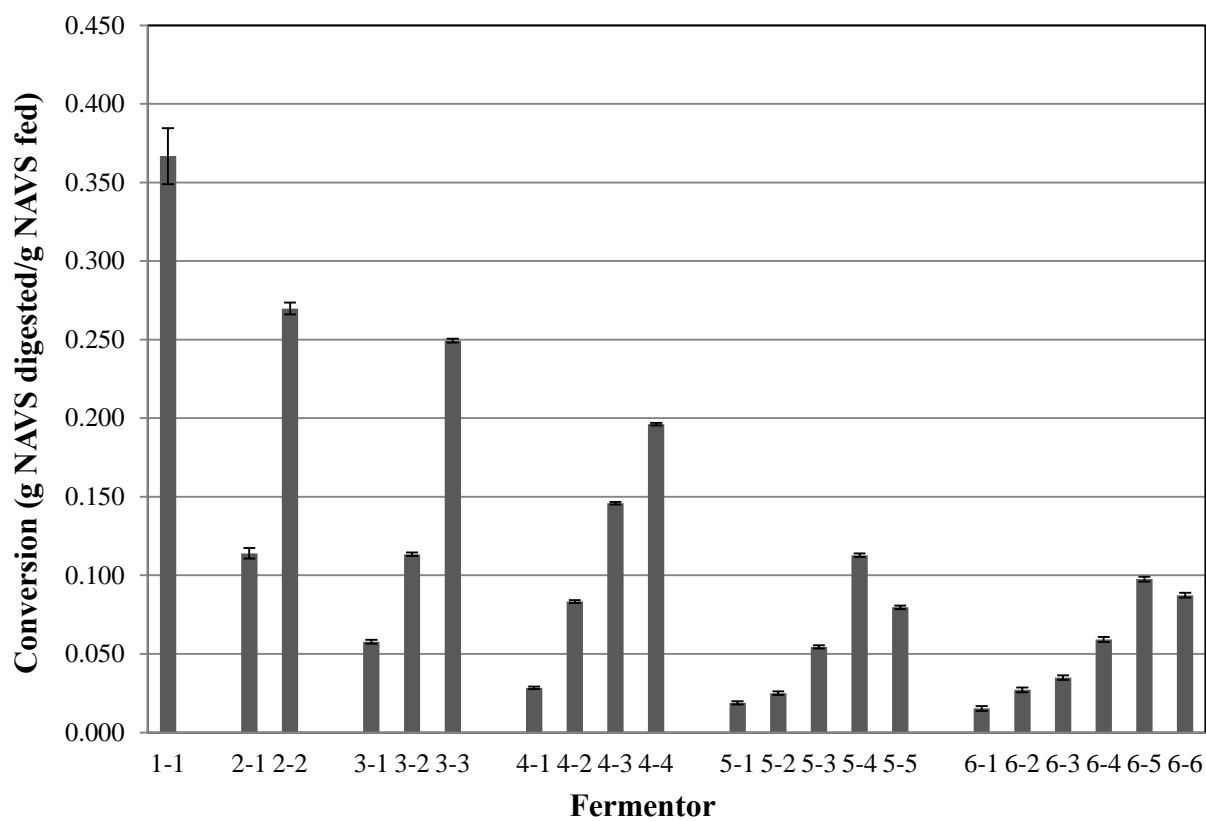


Figure 5-6. Conversion in each stage of the fermentation trains. Error bars are the 95% confidence intervals during the steady-state period.

5.3.5 *Carbon-nitrogen ratio*

Because the carbon-nitrogen (C-N) ratio and pH affect fermentation performance, they must be controlled for accurate conclusions to be drawn. To compare fermentation trains, the carbon-nitrogen (C-N) ratio was used to control the nutrients and substrate and was quantified as previously described (Smith et al., 2011). A computer model developed in Excel 2007 (Microsoft, USA) was used to predict the amount of nitrogen (as urea) that needed to be added to the system (Smith et al., 2011). This study controlled the C-N ratio to 41 ± 6 g non-acid organic carbon (C_{NA}) /g total nitrogen (N), and pH to 5.8 ± 0.1 , which is in the desired range for carboxylate fermentations (Smith et al., 2011).)

5.4 **Conclusions**

To investigate the effect of additional fermentors, one- to six-stage countercurrent fermentations were operated with similar LRT and VSLR. Fewer stages increased conversion, whereas more stages increased acid concentration and selectivity. One- to four-stage fermentations had similar yields, but yield decreased in five- and six-stage fermentations. Four- to six-stage fermentations achieved similar maximum acid concentrations (~30 g/L), suggesting that this is the maximum acid concentration that the microorganisms can produce at this LRT and VSLR. Higher acid concentrations that occur with more stages inhibit the microorganisms, which decreases yield and conversion. Carboxylate fermentations achieve maximum yield and conversion with a single stage, but achieve maximum acid concentration with a minimum of four stages.

6. RESIDUAL BIOMASS RECYCLE IN COUNTERCURRENT MIXED-ACID FERMENTATION: EFFECT OF DIFFERENT RECYCLE POINTS AND REFLUX RATIOS

In carboxylate fermentations, microorganisms are the biocatalysts, but are typically discarded in exit streams. To improve fermentation performance, this study investigated the effect of residual biomass recycle, which includes cell biomass. A countercurrent four-stage fermentation was implemented with four different biomass recycle entry points at reflux ratios of 14 and 35 g recycle/100 g total exit biomass. An optimal carbon-nitrogen ratio (~22 g organic C_{NA}/g N) and near-neutral pH (~5.6) was maintained. Compared to the control (i.e., no biomass recycle), biomass recycle increased yield and productivity. The recycle point affected the conversion and selectivity. Relative to the lower reflux, the higher biomass reflux increased conversion, decreased selectivity, but did not affect yield.

6.1 Introduction

Global energy demand is predominately supplied by fossil fuels (e.g., natural gas, petroleum, and coal). However, fossil fuels cannot be used indefinitely because (1) the resources are finite, (2) costs are rising and more volatile, (3) shortages disrupt economies, and (4) their combustion causes global warming, acid rain, and pollution (Alekkett et al., 2010; Demirbas, 2007). To meet growing energy needs and increase national security, inexhaustible environmentally friendly energy sources are becoming increasingly important. The carboxylate platform, which converts lignocellulose to conventional liquid fuels, is a promising alternative (Agler et al., 2011).

Because lignocellulosic biomass is inexpensive and abundant, it is an important energy source (Carroll and Somerville, 2009). The oldest and most versatile renewable fuel, biomass is most commonly used to produce steam and electricity. As an alternative, using the carboxylate platform, biomass can be converted to liquid transportation fuels

and industrial chemicals (Holtzaple and Granda, 2009). Converting biomass into liquid fuels does not cause a net increase in atmospheric carbon dioxide because biomass growth sequesters the same amount of carbon dioxide that was released during combustion (Ragauskas et al., 2006; Sahin, 2011). The carboxylate platform has attractive economics and is readily scaled down (Granda et al., 2009; Pham et al., 2010).

The carboxylate platform is a biomass-to-energy technology that biologically converts biomass (e.g., lignocellulose, fats, proteins, carbohydrates) into carboxylate salts that can be chemically converted into chemicals and hydrocarbon fuels (Holtzaple et al., 1999; Holtzaple and Granda, 2009). In the fermentation, biomass is fermented by a mixed-culture of microorganisms to produce carboxylic acids, which are buffered to form carboxylate salts. These salts can be precipitated and thermally converted to ketones (e.g., acetone), hydrogenated to mixed alcohols (e.g., isopropanol), and catalytically converted to hydrocarbons (e.g., gasoline, jet fuel). This versatile and continuous process uses nearly any biomass feedstock, which minimizes market distortions and food scarcity. It has low capital and operating costs, does not require sterile operating conditions or added enzymes, and has reached the demonstration level of development.

In multi-staged countercurrent fermentations (Figure 6-1), such as the four-stage train in this study, solids and liquids are transported through a series of fermentors (a *train*) in opposite directions, allowing the least reactive (most digested) biomass to contact the lowest acid concentration, thereby minimizing product inhibition (Aiello-Mazzarri et al., 2006). This countercurrent strategy achieves both high product concentration and high conversion (Fu and Holtzaple, 2010b). As the biomass decomposes, it becomes less reactive. Because biomass is a heterogeneous mixture, the easily fermentable solids quickly convert into acids in the first fermentor, with the remaining solid residue undergoing conversion in subsequent fermentors to achieve greater substrate conversion. Residual biomass exits from Fermentor 4, while product liquid exits from Fermentor 1 (Figure 6-1).

Microorganisms (e.g., bacteria, archae, fungi) are the biocatalysts that convert lignocellulose to mixed acids. Recovering and recycling the microorganisms from the waste streams may improve fermentation performance; however, separating microorganisms from biomass may be difficult and costly. Separating microorganisms from the waste stream might be an unnecessary step if there are no negative impacts from other contents of the recycle stream (i.e., acids, ash, recalcitrant volatile solids, etc.).

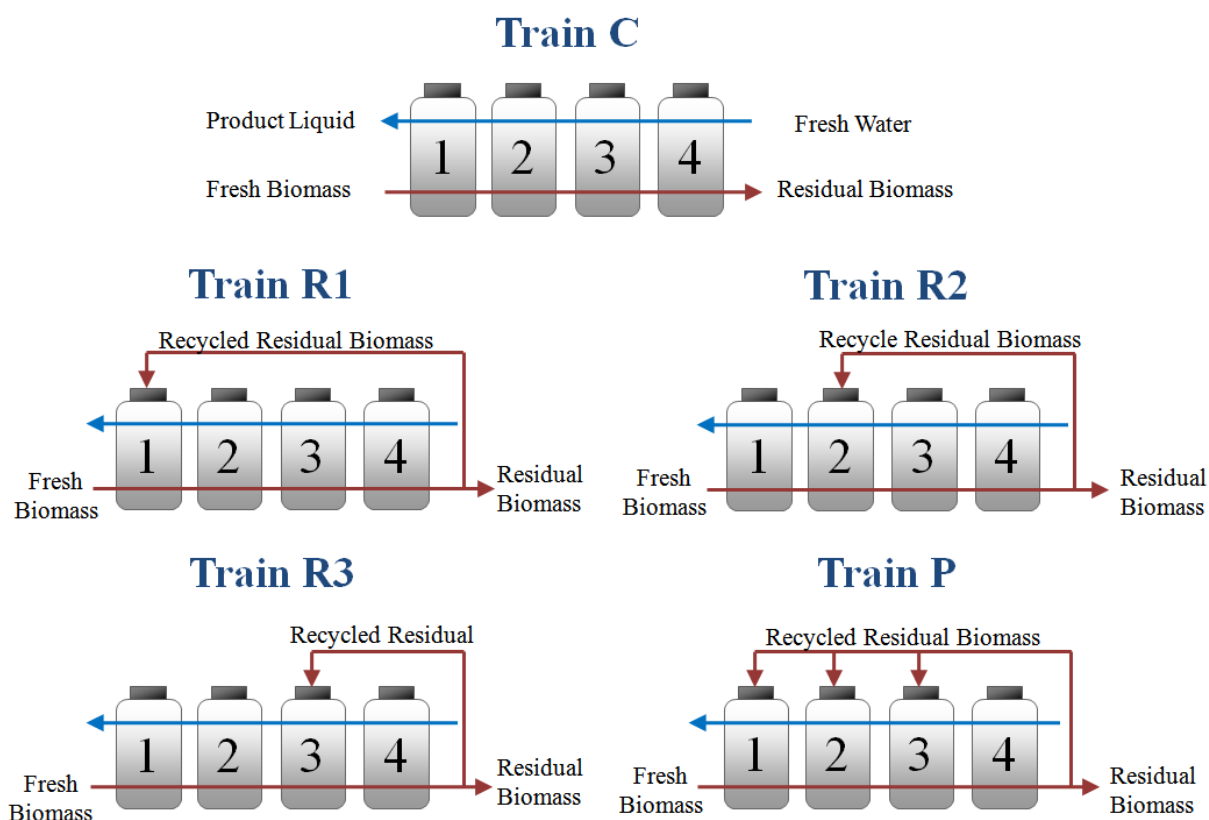


Figure 6-1. Diagram of the biomass recycle experiment, depicting the control (Train C) with no biomass recycle, and the four different residual biomass recycle trains (Trains R1, R2, R3, P).

Compared to cell recycle, recycling unprocessed residual biomass back into the fermentation system (Figure 6-1) is potentially less expensive and perhaps more commercially viable. Recycling will allow adapted microorganisms to be retained, and possibly enhance fermentor performance. The purpose of this study is to employ biomass recycle to evaluate its effects on continuous fermentation performance at four recycle entry points and two reflux ratios at near-neutral pH and optimal carbon-nitrogen ratio.

6.2 Materials and methods

6.2.1 Fermentor configuration

The fermentors were 1-L polypropylene centrifuge bottles capped by a rubber stopper inserted with a glass tube (Ross, 1998). Two segments of ¼-in stainless steel pipe were inserted through the rubber stopper into the vessel to mix the fermentor contents as it rotated in the rolling incubator. A rubber septum sealed the glass tube and allowed for gas sampling and release.

6.2.2 Substrate

Shredded office paper, which served as the energy source, was obtained from a local recycling center. No pretreatment was required. Chicken manure, which served as an undefined nutrient source, was obtained from Feather Crest Farms, Inc. (Bryan, TX) and was dried at 105 °C for 48 h. Wet chicken manure will degrade over time, so to maintain consistency in the nutrient source over the course of the entire experiment, dried and homogenized chicken manure was used. Dried chicken manure was found to have a C-N ratio of 12.9 ± 3.4 g non-acid organic carbon (OC_{NA})/g nitrogen (N) and an acid concentration of 0.05 ± 0.01 g acid/g dry chicken manure. Studies have found the C-N ratio of shredded office paper is 138.3 ± 43 g OC_{NA} /g N (Smith and Holtzapple, 2010). The substrate concentration is expressed as non-acid volatile solids (NAVS), which is the combustible portion of the substrate minus carboxylic acids present in the feed. Urea was used as an additional nitrogen source.

6.2.3 *Fermentation medium*

The deoxygenated medium was prepared by boiling distilled water to liberate dissolved oxygen. After cooling to room temperature in a covered vessel, to further reduce the oxygen content, 0.275 g/L cysteine hydrochloride and 0.275 g/L sodium sulfide were added.

6.2.4 *Inoculum*

The inoculum was a mixed-culture of marine microorganisms from beach sediment collected in Galveston Island, TX. Sediment was removed from the bottom of multiple 0.5-m-deep shoreline pits. Samples were immediately placed in airtight plastic bottles filled with deoxygenated water, capped, and frozen at $-20\text{ }^{\circ}\text{C}$ until use. Before inoculation, samples were thawed, shaken vigorously, and allowed to settle by gravity. Equal parts of the resulting supernatant were homogenized, and aliquots were used to standardize the fermentation inoculum to 12.5% of the initial working volume (Forrest et al., 2010a; Thanakoses, 2002). Bacterial community composition of mixed-acid fermentation has been reported elsewhere (Hollister et al., 2010; Hollister et al., 2011).

6.2.5 *Methanogen inhibition*

Iodoform (CHI_3) was used to inhibit methane production. Iodoform solution (80 μL , 20 g CHI_3/L 190-proof ethanol) was added to each fermentor every 48 h (Ross, 1998). Iodoform is sensitive to light, air, and temperature, and so the solution was kept in amber-colored glass bottles wrapped in foil and stored at $-20\text{ }^{\circ}\text{C}$ (Agbogbo and Holtzapple, 2007).

6.2.6 *Residual biomass recycle fermentation procedure*

Five four-stage countercurrent fermentation trains (Figure 6-1) were run: a control train with no recycle (Train C), a train that recycled residual biomass to the first fermentor (Train R1), a train that recycled residual biomass to the second fermentor (Train R2), a train that recycled residual biomass to the third fermentor (Train R3), and a train that recycled residual biomass in parallel to the first three fermentors (Train P). These five countercurrent trains were run at 14% and 35% residual biomass reflux, i.e.,

14 and 35 g wet residual recycled biomass/100 g residual biomass exiting the process from Fermentor 4. (*Note:* The moisture content of the recycle stream is the same as the moisture content of the exit stream; therefore, this can be either a wet or dry basis.)

The feed consisted of 80% shredded office copier paper and 20% dry homogenized chicken manure on a dry mass basis. Each fermentor was incubated at 40 °C as a submerged fermentation. The five fermentation trains were initiated as batch cultures under anaerobic conditions with a concentration of 100 g non-acid dry solid (NADS)/L deoxygenated water, which was achieved by adding substrate, nutrient source (manure and urea), inoculum, buffer (calcium carbonate), and liquid medium to each fermentor.

After the first week of batch growth, solid/liquid transfers began and occurred every 48 hours to reach steady state. Every 48 h, fermentors were removed from the incubator, the gas volume was collected, liquid samples were taken, the pH was measured, fermentors were centrifuged (3300×g, 25 min), and the solid/liquid mass transfers were performed. (*Note:* This specific time interval is not critical as long as the controlled variables are adjusted to achieve the appropriate normalized variables.) Fresh deoxygenated water was added to Fermentor 4 (F4), and all of the filtered liquid was transferred from Fermentor 3 (F3) to Fermentor 2 (F2), F2 to Fermentor 1 (F1), and out of F1 as the product liquid. In a countercurrent manner, fresh substrate was fed to F1 and a portion of the homogenized solids was transferred from F1 to F2, F2 to F3, F3 to F4, and exited F4 as residual biomass. During transfers, the solid wet weight retained (including the fed recycled residual biomass) equaled 225 g in F2, F3, and F4, and 125 g in F1. A preset amount of residual biomass (Tables 6-1, 6-2) was homogenized and recycled back into F1 (Train R1), F2 (Train R2), F3 (Train R3), and parallel to F1, F2, and F3 (Train P). In each fermentor, the solids were resuspended by shaking, iodoform was added, and calcium carbonate was added to neutralize carboxylic acids and buffer the system (Tables 6-1, 6-2). Urea was added to adjust the carbon-nitrogen (C-N) ratio. During solid and liquid transfers, when the fermentors were open to the atmosphere, anaerobic conditions were maintained by flushing the fermentor headspace with nitrogen

gas (Praxair, Bryan, TX). (Note: Nitrogen flushing was a precautionary step; these anaerobic fermentations have been shown to resist intermittent air exposure (Golub et al., 2011b).) The fermentors were then resealed and placed back in the incubator.

6.2.7 *Biomass recycle mass balance*

All performance variables were calculated based on a mass balance outside of the four fermentations and biomass recycle loop system.

6.2.8 *Carbon-nitrogen ratio*

The carbon-nitrogen (C-N) ratio was quantified as previously described (Smith et al., 2011). Urea was added to supplement nitrogen in the manure.

6.2.9 *Analytical methods*

6.2.9.1 *Carboxylic acid concentration determination*

Fermentation product liquid was collected every 48 h and analyzed for C2–C7 fatty acids as previously described (Golub et al., 2011a).

6.2.9.2 *Biogas analysis*

For the first two weeks, because of the high initial digestion rate, each fermentor was vented daily; thereafter, it was vented every 48 h. Biogas was removed through the fermentor septum, and the volume was measured by displacing liquid in an inverted graduated glass cylinder filled with a 300 g/L CaCl₂ solution, which prevented microbial growth and carbon dioxide adsorption (Domke, 1999).

Biogas composition (i.e., carbon dioxide, nitrogen, oxygen, and methane) was determined by manually injecting 5-mL gas samples into an Agilent 6890 Series chromatograph with a thermal conductivity detector (TCD). A 4.6-m-long, 2.1-mm-ID stainless steel packed column (60/80 Carboxen 100, Supelco 1-2390) was used. The inlet temperature was 230 °C, the detector temperature was 200 °C, and the oven temperature was 200 °C. The total run time was 10 min, and helium was the carrier gas.

6.2.9.3 Moisture and ash contents

Moisture and ash contents were determined by drying in a 105°C forced-convection oven for at least 24 h, and subsequent combustion in a 575 °C furnace for at least 12 h by NREL procedures No. 001 and 005, respectively (NREL, 2004). The ash content was calculated on a dry basis. The consumption of NAVS was determined using the inert-ash approach as described previously (Smith et al., 2011).

6.2.10 Operating parameters

Previous investigations using continuous countercurrent fermentations have shown that adequate conversion and exit yield were achieved with volatile solid loading rate (VSLR) of ~6.3 g NAVS/(L·d) and liquid residence time (LRT) of ~13 d (Chan and Holtzapfle, 2003; Ross, 1998; Smith et al., 2011); therefore, this VSLR and LRT were chosen to investigate the performance of a biomass recycle fermentation system. The LRT and VSLR (Tables 6-1, 6-2) were regulated by controlling the liquid and solid transfer frequency (T), non-acid volatile solids (NAVS) feed rate, and the liquid feed rate per transfer. Volatile solids (VS) are defined as the mass of dry solid material that is combusted at 575 °C after 12 h, and NAVS are defined as VS less the amount of carboxylate acid:

$$\text{NAVS} = (\text{g total biomass})(1 - \text{MC})(1 - \text{AC}) - (\text{g acid in biomass}) \quad (6-1)$$

where MC (g water/g wet biomass) is the fraction of moisture in the biomass, and AC (g inert biomass/g dry biomass) is the fraction of dry ash remaining after 12 h of combustion at 575 °C. In performance calculations, NAVS is preferred because it ensures the product is not quantified with the reactant.

The nutrient source (dried chicken manure) contains carboxylic acids. To more accurately quantify fermentor productivity, the amount of acid entering the system in the manure is subtracted from the amount of acid exiting the system in the product liquid and discarded solids. To determine the amount of acid in the manure, the dry manure

was resuspended in distilled water at different concentrations. The acid in the supernatant was analyzed by GC.

The volatile solid loading rate (VSLR) and the liquid residence time (LRT) are calculated as follows:

$$\text{VSLR} = \frac{\text{NAVS feed (g)}}{\text{total liquid volume in all fermentors (L) \cdot \text{time (d)}}} \quad (6-2)$$

$$\text{LRT} = \frac{\text{total liquid volume in all fermentors (L)}}{\text{liquid flow rate out of fermentation train (L/d)}} \quad (6-3)$$

The total liquid volume (TLV) includes both free and interstitial liquid. Liquid flow rate out of fermentation train includes product liquid exiting and liquid in cake exiting.

6.2.11 *Definition of terms*

To account for the total mass in the system, a mass balance closure was calculated as follows:

$$\text{mass balance closure} = \frac{\text{mass out (g)}}{\text{mass in (g) + water of hydrolysis (g)}} \quad (6-4)$$

Cellulose is a polysaccharide composed of individual anhydroglucose units (glucan, MW = 162 g/mol). During digestion, cellulose is enzymatically hydrolyzed to glucose by adding water. The water of hydrolysis was calculated as previously described (Chan and Holtzapple, 2003).

The mixed-acid concentration can be expressed as molar acetic acid equivalents (α), which is the reducing potential of an equivalent amount of acetic acid (Datta, 1981).

$$\begin{aligned}
 \alpha &= 1.00 \times \text{acetic (mol/L)} + 1.75 \times \text{propionic (mol/L)} \\
 &+ 2.50 \times \text{butyric (mol/L)} + 3.25 \times \text{valeric (mol/L)} \\
 &+ 4.00 \times \text{caproic (mol/L)} + 4.75 \times \text{heptanoic (mol/L)}
 \end{aligned}
 \tag{6-5}$$

The acetic acid equivalent (Aceq) can be expressed on a mass basis as

$$\text{Aceq (g/L)} = 60.05 \text{ (g/mol)} \times \alpha \text{ (mol/L)}
 \tag{6-6}$$

Aceq proportionally weighs the higher-chained carboxylic acids (C3 to C7); the higher acids have higher Aceq than lower acids.

6.2.12 *Measuring performance*

The feed and exit rate of acid, ash, NAVS, water, and gas were determined during the steady-state period. As previously described (Smith and Holtzapple, 2011b), the average rate of each component was calculated using the slope method. In this method, the moving cumulative sum of each component is plotted with respect to time. The slope of the steady-state portion of this line is the rate. All performance variables (e.g., conversion, selectivity, and yield) were calculated from the averaged component rates determined by the slope method, as described below:

$$\begin{aligned}
 \text{Conversion } x &\equiv \frac{\text{NADS}_{\text{feed}} \text{ g} - \text{NADS}_{\text{exit}} \text{ (g)}}{\text{NAVS}_{\text{feed}} \text{ (g)}} \\
 &= \frac{\text{NAVS}_{\text{feed}} \text{ g} + \text{Ash}_{\text{feed}} \text{ g} - \text{NAVS}_{\text{exit}} \text{ g} - \text{Ash}_{\text{exit}} \text{ (g)}}{\text{NAVS}_{\text{feed}} \text{ (g)}} \\
 &= \frac{\text{NAVS}_{\text{consumed}} \text{ (g)}}{\text{NAVS}_{\text{feed}} \text{ (g)}}
 \end{aligned}
 \tag{6-7}$$

$$\text{Exit yield } (Y_E) \equiv \frac{\text{total acid output from solid and liquid streams (g)}}{\text{NAVS}_{\text{feed}}(\text{g})} \quad (6-8)$$

$$\text{Process yield } (Y_P) \equiv \frac{\text{total acid output in product liquid stream (g)}}{\text{NAVS}_{\text{feed}}(\text{g})} \quad (6-9)$$

$$\text{Culture yield } (Y_C) \equiv \frac{\text{total acid produced (g)}}{\text{NAVS}_{\text{feed}}(\text{g})} \equiv Y_E - Y_F \quad (6-10)$$

$$\text{Feed yield } (Y_F) \equiv \frac{\text{total acid entering with feed (g)}}{\text{NAVS}_{\text{feed}}(\text{g})} \quad (6-11)$$

$$\begin{aligned} \text{Selectivity } (\sigma) &\equiv \frac{\text{total acid produced (g)}}{\text{NAVS}_{\text{feed}}(\text{g}) - \text{NAVS}_{\text{exit}}(\text{g})} \quad (6-12) \\ &\equiv \frac{\text{total acid produced (g)}}{\text{NAVS digested (g)}} = \frac{Y_E}{x} \end{aligned}$$

$$\text{Acid productivity } (P) \equiv \frac{\text{total acids produced (g)}}{\text{TLV (L)} \cdot \text{d}} \quad (6-13)$$

where $\text{NADS}_{\text{feed}}$ is the non-acid dry solids fed, $\text{NADS}_{\text{exit}}$ is the non-acid dry solids removed from the fermentation, $\text{NAVS}_{\text{feed}}$ is the non-acid volatile solids fed, $\text{NAVS}_{\text{exit}}$ is the non-acid volatile solids removed from the fermentation, Ash_{feed} is the ash fed in biomass feed and buffer, and Ash_{exit} is the ash exiting in all solid and liquid streams. NADS includes the ash, CaCO_3 , and volatile solid component of biomass. Ash is assumed to be conserved in the fermentation (Ash_{feed} equals Ash_{exit}), canceling Ash from Equation 6-7.

Per g NAVS fed, the exit yield (Y_E) represents the sum of acid in the product transfer liquid, waste transfer solids, and liquid removed from sampling. The process yield (Y_P) represents all the acid in the product transfer liquid per g of NAVS fed. The feed yield (Y_F) is the total g acid entering with the feed per g NAVS fed, and the culture yield (Y_C) is the exit yield less the feed yield.

6.2.13 Statistical analysis

Statistical analysis was performed using Excel 2007 (Microsoft, USA). The mean and standard deviations of the total acid concentrations, acetic acid equivalent (Aceq), non-acid volatile solids (NAVS) in and out were determined from steady-state operating data. At the 14% reflux ratio, steady state was determined to be Days 60–92 (Train R1), 94–120 (Train R2), 68–92 (Train R3), and 106–124 (Train P). At the 35% reflux ratio, steady state was determined to be Days 36–64 (Train R1), 32–62 (Train R2), 38–98 (Train R3), and 58–95 (Train P). The control (Train C) operated at steady state during Days 52–82. These averaged values were then used to calculate the acid productivity (P), selectivity (σ), yield (Y), and conversion (x) with a 95% confidence interval (CI). Unless specified otherwise, all comparisons in the Results and Discussion section are statistically significant. The steady-state region was the period during which the product total acid and Aceq concentration, dry solids exiting, liquid volume and solid weight of each fermentor, pH, and mass of acid exiting did not vary by more than 2.2 standard deviations from the average for a period of at least one liquid residence time. For each train, the slope of the summed data was used to calculate the means of the performance variables which were compared using a Student's two sample t -test (two-tailed, Type 3). The p values had a familywise error rate of 0.05 using the Bonferroni correction. All error bars are reported at 95% CI.

6.3 Results and discussion

Each fermentation train consisted of a four-stage countercurrent semi-continuous submerged-bed fermentation system. Five fermentation trains were operated, each with different residual biomass recycle points: a control train with no recycle (Train C), a train that recycled biomass to the first fermentor (Train R1), a train that recycled biomass to the second fermentor (Train R2), a train that recycled biomass to the third fermentor (Train R3), and a train that recycled biomass in parallel to the first three fermentors (Train P). Each fermentation train was operated with two residue reflux ratios: 14% and 35%. For all countercurrent trains, the average time required to reach steady state was ~59 d, and the average days at steady state was 32 d. To compare the

results of all trains, the liquid residence time (LRT) and volatile solid loading rate (VSLR) operating parameters were normalized by explicitly controlling the liquid/solid mass transfer frequency (T), the volatile solids (VS) feed rate, the liquid feed rate, and the amount of cake retained in each fermentation reactor per transfer (Tables 6-1, 6-2). Overall, the performance trends that occurred with biomass recycle could be the result of any of the multiple components in the residual biomass (e.g., cells, volatile solids, ash, acid, nutrients) that are transported in the solid or liquid streams.

6.3.1 *Biogas*

At 14% reflux, the amount of biogas produced in each train is ranked as follows: Train P>R1>C>R2>R3 (Tables 6-3, 6-5). At 35% reflux, the amount of biogas produced in each train is ranked as follows: Train R1>R2>C>P>R3 (Tables 6-4, 6-6). When comparing 14% and 35% reflux, the amount of biogas produced in each respective train in both reflux ratios were all different (Table 6-7). For both reflux ratios, the average biogas compositions were found to be similar. The biogas compositions were $54.3 \pm 13.8\%$ N₂, $43.8 \pm 11.1\%$ CO₂ (Train C), $54.6 \pm 21.0\%$ N₂, $44.0 \pm 18.3\%$ CO₂ (Train R1), $58.3 \pm 11.0\%$ N₂, $41.7 \pm 11.0\%$ CO₂ (Train R2), $53.3 \pm 15.3\%$ N₂, $45.2 \pm 12.7\%$ CO₂ (Train R3), $59.4 \pm 7.2\%$ N₂, and $42.3 \pm 7.1\%$ CO₂ (Train P). No methane was detected in any fermentor.

Table 6-1. Operating parameters at ~14% residual biomass reflux ratio. Normalized parameters represent the mean of the steady-state values \pm CI (95% CI).

	C	R1	R2	R3	P
Fermentation Train					
Solid and liquid transfer frequency, T (h)	48	48	48	48	48
NAVS feed rate (g NAVS/ T)	24.3	24.3	24.3	24.3	24.3
Dry solids added (g/ T)	32	32	32	32	32
Manure added (g/ T)	7.6	7.6	7.6	7.6	7.6
Urea added (g/ T)	1.0	1.0	1.0	1.0	1.0
Calcium carbonate added (g/ T)	4.0	4.0	4.0	4.0	4.0
Fermentor recycle point	–	F1	F2	F3	F1,2,3
Residual biomass recycled (g)	0	18	18	18	18
Liquid feed rate (mL/ T)	300	300	300	300	300
Solid cake retained in F1 (g, wet)	125	125	125	125	125
Solid cake retained in F2–F4 (g, wet)	225	225	225	225	225
Centrifuged liquid retained in F1–F4 (mL)	0	0	0	0	0.0
Methane inhibitor (μ L/(T ·fermentor))	80	80	80	80	80
Fermentor reflux ratio (g recycled biomass/g exiting biomass)	–	0.14 \pm 0.02	0.15 \pm 0.02	0.12 \pm 0.01	0.15 \pm 0.03
Volatile solid loading rate, VSLR (g NAVS/(L_{liq} ·d))	6.1 \pm 0.06	6.2 \pm 0.10	6.4 \pm 0.05	6.1 \pm 0.07	6.3 \pm 0.15
Liquid residence time, LRT (d)	13.6 \pm 0.6	13.8 \pm 1.3	13.7 \pm 0.7	13.6 \pm 1.2	13.6 \pm 1.1
Total liquid volume, TLV (L)	1.98 \pm 0.02	1.95 \pm 0.03	1.90 \pm 0.02	1.98 \pm 0.02	1.92 \pm 0.05
Volatile solid, VS, concentration (g NAVS/ L_{liq})	55 \pm 1	69 \pm 2	54 \pm 2	58 \pm 2	57 \pm 3
Dry solid, DS, concentration (g NADS/ L_{liq})	91 \pm 2	107 \pm 3	81 \pm 2	94 \pm 2	88 \pm 3
Average carbon-nitrogen ratio, C-N ratio (g OC_{NA} /g N)	21.4 \pm 2.2	21.8 \pm 2.3	27.2 \pm 6.5	25.5 \pm 2.6	26.6 \pm 6.3
Average pH (F1–F4)	5.67 \pm 0.12	5.47 \pm 0.09	5.31 \pm 0.13	5.48 \pm 0.12	5.51 \pm 0.13
Total urea added (g urea/(L_{liq} ·d))	0.25 \pm 0.00	0.26 \pm 0.00	0.26 \pm 0.00	0.25 \pm 0.01	0.26 \pm 0.00

NAVS = Non-acid volatile solids

NADS = Non-acid dry solids

Table 6-2. Operating parameters at ~35% residual biomass reflux ratio. Normalized parameters represent the mean of the steady-state values \pm CI (95% CI).

Fermentation Train		C	R1	R2	R3	P
Controlled	Solid and liquid transfer frequency, T (h)	48	48	48	48	48
	NAVS feed rate (g NAVS/ T)	24.3	24.3	24.3	24.3	24.3
	Dry solids added (g/ T)	32	32	32	32	32
	Manure added (g/ T)	7.6	7.6	7.6	7.6	7.6
	Urea added (g/ T)	1.0	1.0	1.0	1.0	1.0
	Calcium carbonate added (g/ T)	4.0	4.0	4.0	4.0	4.0
	Fermentor recycle point	–	F1	F2	F3	F1,2,3
	Residual biomass recycled (g)	0	45	45	45	45
	Liquid feed rate (mL/ T)	300	300	300	300	300
	Solid cake retained in F1 (g, wet)	125	125	125	125	125
	Solid cake retained in F2–F4 (g, wet)	225	225	225	225	225
	Centrifuged liquid retained in F1–F4 (mL)	0	0	0	0	0.0
	Methane inhibitor (μ L/(T ·fermentor))	80	80	80	80	80
	Normalized	Fermentor reflux ratio (g recycled biomass/g exiting biomass)	–	0.38 \pm 0.02	0.36 \pm 0.02	0.33 \pm 0.01
Volatile solid loading rate, VSLR (g NAVS/(L_{liq} ·d))		6.2 \pm 0.05	6.2 \pm 0.10	6.2 \pm 0.05	6.1 \pm 0.07	6.3 \pm 0.15
Liquid residence time, LRT (d)		14.1 \pm 1.0	12.1 \pm 1.3	12.2 \pm 0.7	12.6 \pm 1.2	12.2 \pm 1.1
Total liquid volume, TLV (L)		1.97 \pm 0.02	1.95 \pm 0.03	1.95 \pm 0.02	1.99 \pm 0.02	1.94 \pm 0.05
Volatile solid, VS, concentration (g NAVS/ L_{liq})		67 \pm 2	68 \pm 2	65 \pm 2	64 \pm 2	63 \pm 2
Dry solid, DS, concentration (g NADS/ L_{liq})		95 \pm 2	107 \pm 2	102 \pm 2	95 \pm 2	96 \pm 2
Average carbon-nitrogen ratio, C-N ratio (g OC_{NA} /g N)		18.1 \pm 5.0	18.1 \pm 2.9	20.7 \pm 5.3	22.2 \pm 8.6	20.1 \pm 0.6
Average pH (F1–F4)		5.68 \pm 0.13	5.88 \pm 0.10	5.82 \pm 0.12	5.72 \pm 0.07	5.73 \pm 0.09
Total urea added (g urea/(L_{liq} ·d))	0.25 \pm 0.01	0.26 \pm 0.00	0.26 \pm 0.00	0.25 \pm 0.00	0.26 \pm 0.01	

NAVS = Non-acid volatile solids

NADS = Non-acid dry solids

Table 6-3. Performance measures for 14% residual biomass reflux. Values represent the mean of the steady-state values \pm CI (95% CI).

	C	R1	R2	R3	P
Total carboxylic acid concentration (g/L)	16.69 \pm 0.52	17.24 \pm 0.65	18.46 \pm 0.75	17.99 \pm 0.56	18.55 \pm 0.89
Aceq concentration (g/L)	26.10 \pm 0.88	27.10 \pm 0.97	29.06 \pm 1.33	28.33 \pm 0.91	29.21 \pm 1.48
Total carboxylic acid exiting (g/d)	2.01 \pm 0.01	2.05 \pm 0.01	2.16 \pm 0.01	2.14 \pm 0.02	2.22 \pm 0.03
Aceq exiting (g/d)	3.15 \pm 0.01	3.24 \pm 0.01	3.52 \pm 0.01	3.40 \pm 0.02	3.52 \pm 0.04
Aceq/Acid ratio	1.57 \pm 0.01	1.57 \pm 0.00	1.57 \pm 0.01	1.57 \pm 0.01	1.57 \pm 0.01
Conversion, x (g VS digested/g VS fed)	0.405 \pm 0.002	0.427 \pm 0.004	0.364 \pm 0.003	0.334 \pm 0.003	0.465 \pm 0.008
Selectivity, σ (g acid produced/g NAVS consumed)	0.403 \pm 0.002	0.388 \pm 0.002	0.482 \pm 0.002	0.522 \pm 0.004	0.387 \pm 0.005
Aceq selectivity, σ_a (g Aceq produced/g NAVS consumed)	0.632 \pm 0.003	0.616 \pm 0.003	0.785 \pm 0.004	0.829 \pm 0.007	0.613 \pm 0.008
Exit yield, Y_E (g acid/g NAVS fed)	0.163 \pm 0.001	0.166 \pm 0.001	0.176 \pm 0.001	0.174 \pm 0.001	0.180 \pm 0.002
Exit Aceq yield, Y_{aE} (g Aceq/g NAVS fed)	0.256 \pm 0.001	0.263 \pm 0.001	0.286 \pm 0.001	0.277 \pm 0.002	0.285 \pm 0.003
Culture yield, Y_C (g acid/g NAVS fed)	0.148 \pm 0.001	0.151 \pm 0.001	0.160 \pm 0.001	0.159 \pm 0.001	0.164 \pm 0.002
Process yield, Y_P (g acid/g NAVS fed)	0.143 \pm 0.001	0.138 \pm 0.001	0.145 \pm 0.001	0.140 \pm 0.001	0.149 \pm 0.003
Productivity, P (g total acid/(L _{liq} ·d))	0.921 \pm 0.010	0.953 \pm 0.015	1.038 \pm 0.009	0.983 \pm 0.012	1.055 \pm 0.027
Biogas produced (g/d)	2.53 \pm 0.01	2.70 \pm 0.01	2.51 \pm 0.01	2.20 \pm 0.01	2.93 \pm 0.02
Mass balance closure (g mass in/g mass out)	0.95 \pm 0.00	0.93 \pm 0.00	0.91 \pm 0.00	0.96 \pm 0.00	0.89 \pm 0.00

Table 6-4. Performance measures for 35% residual biomass reflux. Values represent the mean of the steady-state values \pm CI (95% CI).

	C	R1	R2	R3	P
Total carboxylic acid concentration (g/L)	16.69 \pm 0.52	18.02 \pm 0.35	17.50 \pm 0.68	17.43 \pm 0.24	17.80 \pm 0.51
Aceq concentration (g/L)	26.10 \pm 0.88	29.10 \pm 0.54	28.40 \pm 1.09	27.75 \pm 0.44	28.56 \pm 0.87
Total carboxylic acid exiting (g/d)	2.01 \pm 0.01	2.26 \pm 0.01	2.19 \pm 0.01	2.15 \pm 0.00	2.21 \pm 0.01
Aceq exiting (g/d)	3.15 \pm 0.01	3.65 \pm 0.01	3.56 \pm 0.01	3.44 \pm 0.01	3.56 \pm 0.01
Aceq/Acid ratio	1.57 \pm 0.01	1.62 \pm 0.01	1.62 \pm 0.01	1.59 \pm 0.01	1.59 \pm 0.01
Conversion, x (g VS digested/g VS fed)	0.405 \pm 0.002	0.491 \pm 0.005	0.435 \pm 0.005	0.392 \pm 0.001	0.441 \pm 0.003
Selectivity, σ (g acid produced/g NAVS consumed)	0.403 \pm 0.002	0.370 \pm 0.002	0.410 \pm 0.002	0.444 \pm 0.001	0.407 \pm 0.002
Aceq selectivity, σ_a (g Aceq produced/g NAVS consumed)	0.632 \pm 0.003	0.598 \pm 0.003	0.666 \pm 0.004	0.712 \pm 0.002	0.655 \pm 0.003
Exit yield, Y_E (g acid/g NAVS fed)	0.163 \pm 0.001	0.182 \pm 0.001	0.178 \pm 0.001	0.174 \pm 0.000	0.180 \pm 0.001
Exit Aceq yield, Y_{aE} (g Aceq/g NAVS fed)	0.256 \pm 0.001	0.294 \pm 0.001	0.289 \pm 0.001	0.279 \pm 0.001	0.289 \pm 0.001
Culture yield, Y_C (g acid/g NAVS fed)	0.148 \pm 0.001	0.167 \pm 0.001	0.163 \pm 0.001	0.159 \pm 0.000	0.164 \pm 0.001
Process yield, Y_P (g acid/g NAVS fed)	0.143 \pm 0.001	0.165 \pm 0.000	0.159 \pm 0.001	0.150 \pm 0.000	0.154 \pm 0.001
Productivity, P (g total acid/(L _{liq} ·d))	0.921 \pm 0.010	1.063 \pm 0.007	1.027 \pm 0.010	0.983 \pm 0.007	1.040 \pm 0.009
Biogas produced (g/d)	2.53 \pm 0.01	3.14 \pm 0.01	2.79 \pm 0.01	2.51 \pm 0.01	2.59 \pm 0.02
Mass balance closure (g mass in/g mass out)	0.95 \pm 0.00	0.96 \pm 0.00	0.96 \pm 0.00	0.95 \pm 0.00	0.96 \pm 0.00

Table 6-5. *p* values for performance measures at 14% residual biomass reflux ($\alpha = 0.05$).

Trains	Conv.	Selectivity	Exit yield	Exit yield Aceq	Culture yield	Process yield	TLV	Productivity	Biogas produced	Total acid conc.	Aceq conc.	Total acid exit	Total Aceq exit	Aceq/ Total acid
C and R1	0.000	0.000	0.000	0.000	0.000	0.000	0.068	0.001	0.000	0.187	0.125	0.000	0.000	0.135
C and R2	0.000	0.000	0.000	0.000	0.000	0.004	0.000	0.000	0.027	0.000	0.001	0.000	0.000	0.865
C and R3	0.000	0.000	0.000	0.000	0.000	0.000	0.856	0.000	0.000	0.002	0.001	0.000	0.000	0.598
C and P	0.000	0.000	0.000	0.000	0.000	0.000	0.028	0.000	0.000	0.001	0.001	0.000	0.000	0.255
R1 and R2	0.000	0.000	0.000	0.000	0.000	0.000	0.005	0.000	0.000	0.015	0.019	0.000	0.000	0.370
R1 and R3	0.000	0.000	0.000	0.000	0.000	0.001	0.050	0.003	0.000	0.078	0.066	0.000	0.000	0.606
R1 and P	0.000	0.563	0.000	0.000	0.000	0.000	0.396	0.000	0.000	0.018	0.019	0.000	0.000	0.798
R2 and R3	0.000	0.000	0.131	0.000	0.117	0.000	0.000	0.000	0.000	0.313	0.355	0.025	0.000	0.762
R2 and P	0.000	0.000	0.001	0.000	0.001	0.002	0.250	0.229	0.000	0.872	0.879	0.000	0.885	0.463
R3 and P	0.000	0.000	0.000	0.000	0.000	0.000	0.020	0.000	0.000	0.281	0.299	0.000	0.000	0.717

p value < 0.005 statistically different, results in family-wise error rate of 0.05

Table 6-6. *p* values for performance measures at 35% residual biomass reflux ($\alpha = 0.05$).

Trains	Conv.	Selectivity	Exit yield	Exit yield Aceq	Culture yield	Process yield	TLV	Productivity	Biogas produced	Total acid conc.	Aceq conc.	Total acid exit	Total Aceq exit	Aceq/ Total acid
C and R1	0.000	0.000	0.000	0.000	0.000	0.000	0.010	0.000	0.000	0.000	0.000	0.000	0.000	0.000
C and R2	0.000	0.000	0.000	0.000	0.000	0.000	0.036	0.000	0.000	0.064	0.002	0.000	0.000	0.000
C and R3	0.000	0.000	0.000	0.000	0.000	0.000	0.379	0.000	0.003	0.011	0.001	0.000	0.000	0.000
C and P	0.000	0.007	0.000	0.000	0.000	0.000	0.005	0.000	0.000	0.003	0.000	0.000	0.000	0.003
R1 and R2	0.000	0.000	0.000	0.000	0.000	0.000	0.847	0.000	0.000	0.176	0.246	0.000	0.000	0.798
R1 and R3	0.000	0.000	0.000	0.000	0.000	0.000	0.000	0.000	0.000	0.007	0.000	0.000	0.000	0.000
R1 and P	0.000	0.000	0.000	0.000	0.000	0.000	0.565	0.000	0.000	0.476	0.290	0.000	0.000	0.001
R2 and R3	0.000	0.000	0.000	0.000	0.000	0.000	0.001	0.000	0.000	0.841	0.267	0.000	0.000	0.000
R2 and P	0.011	0.050	0.001	0.000	0.001	0.000	0.516	0.046	0.000	0.480	0.818	0.001	0.642	0.001
R3 and P	0.000	0.000	0.000	0.000	0.000	0.000	0.000	0.000	0.000	0.190	0.102	0.000	0.000	0.682

p value < 0.005 statistically different, results in family-wise error rate of 0.05

Table 6-7. *p* values for performance measures to compare 14% and 35% residual biomass reflux ($\alpha = 0.05$).

Trains	Conversion	Selectivity	Exit yield	Exit yield Aceq	Culture yield	Process yield	TLV	Productivity	Biogas produced	Total acid conc.	Aceq conc.	Total acid exit	Total Aceq exit	Aceq/ Total acid
R1 (14%) and R1 (35%)	0.0000	0.0000	0.0000	0.0000	0.0000	0.0000	0.8873	0.0000	0.0000	0.0000	0.0006	0.0000	0.0000	0.0000
R2 (14%) and R2 (35%)	0.0000	0.0000	0.0000	0.0002	0.0000	0.0000	0.0000	0.0865	0.0000	0.0000	0.4344	0.0000	0.0000	0.0000
R3 (14%) and R3 (35%)	0.0000	0.0000	0.5237	0.0982	0.6111	0.0000	0.5122	0.9516	0.0000	0.0000	0.2505	0.3954	0.0022	0.0188
P (14%) and P (35%)	0.0000	0.0000	0.8002	0.0318	0.7728	0.0009	0.4099	0.2829	0.0000	0.0000	0.4381	0.4921	0.0686	0.0169

p value < 0.0125 statistically different, results in family-wise error rate of 0.05

6.3.2 *Acid concentration, productivities, and daily acid production*

For all five experimental conditions, the accumulated mass of total carboxylic acids and Aceq exiting, NADS added, and NADS removed from their respective trains was found. The slopes of the steady-state regression lines provided the daily total acid and Aceq exiting, NADS exiting, and NADS removed on a mass basis (Tables 6-3, 6-4). Productivity was calculated as the mass rate of acid produced per total fermentor volume.

For the 14% reflux, Trains P, R2, and R3 had higher total acid and Aceq concentration than Train C. For the 35% reflux, Trains R1 and P had higher total acid and Aceq concentration than Train C. This shows that recycling residual biomass had an overall positive effect on the total acid and Aceq concentrations (Tables 6-3 to 6-6). Except for Train P, increasing the reflux ratio from 14% to 35% did increase the total acid and Aceq concentrations (Table 6-7). This result demonstrates that increasing the reflux ratios from 14% to 35% did not increase acid concentrations at different recycle points.

At both 14% and 35% reflux ratios, all biomass recycle trains had higher productivity than the control (Tables 6-3 to 6-6). Increasing the residual biomass reflux from 14% to 35% did not have much effect on productivity, except for fermentation Train R1, which had higher productivity at the higher reflux ratio (Tables 6-3, 6-4, 6-7). This result indicates that, when comparing Train R1 operating at two different reflux ratios (e.g., Train R1 at 14% and 35% reflux), there was an increase in productivity with the higher reflux ratio (Table 6-7). For the other trains, productivity might not have increased with increased reflux due to a buildup of inhibiting materials, or because a key water-insoluble nutrient that was recycled back into the system was not retained for a significant length of time. These results indicate that biomass recycle to any of the first three fermentors at 14% reflux is optimal for increased productivity.

In each fermentor of a train, total liquid volume (TLV) quantifies the total volume of liquid in the solid and liquid phases. Most fermentation trains had similar TLVs, indicating that most trains had similar amounts of liquids. Because some trains

had different TLVs, to further standardize the analyses, the amount of acid exiting the fermentors per day was calculated on a mass basis from the product liquid and waste streams (Tables 6-3, 6-4). At 14% reflux, the total carboxylic acid exiting (g/d) is ranked as follows: Train $P > R3 = R2 > R1 > C$. For Aceq exiting (g/d), the corresponding ranks are $R1 > R2 > P > R3 > C$ (Tables 6-3, 6-5). At 35% reflux, the total carboxylic acid exiting (g/d) and Aceq exiting (g/d) ranking was as follows: Train $R1 > R2 = P > R3 > C$ (Tables 6-4, 6-6). At both 14% and 35% reflux, compared to no recycle, these results show that recycling biomass to any entry point improved the amount of daily total acid and Aceq exiting the fermentation train. Increasing the biomass reflux from 14% to 35% increased the daily total acid exiting (g/d) and Aceq exiting (g/d) in Trains R1 and R2 (Tables 6-3, 6-4, 6-7).

Another measure of the production of higher molecular weight carboxylic acids (e.g., valeric, caproic, and heptanoic acid) is the Aceq-to-total-acid ratio. When comparing recycle points at 14% reflux ratio, the Aceq-to-total-acid ratios were not different; thus, at a lower residual biomass reflux, the recycle point did not affect the production of higher-molecular-weight carboxylic acids (Tables 6-3 to 6-6). However, at the 35% reflux ratio, the Aceq-to-total-acid ratio ranking was as follows: Train $R1 = R2 > R3 = P > C$. At the higher biomass reflux, recycling biomass to any recycle point, but especially to Fermentors 1 and 2, increased production of higher molecular weight acids. For Trains R1 and R2, increased reflux ratio increased the Aceq-to-total-acid ratios (Tables 6-3, 6-4, 6-7), suggesting that increased biomass recycle increased the proportion of higher molecular weight acids. Compared to 14% reflux, at 35% reflux, perhaps the amount of recycled cells, nutrients, and/or substrate reached an optimal and significant concentration and retention time for the cellular metabolism to produce more high-molecular-weight acids. For example, if the key material was retained longer in the system because it is not water soluble then it remains in system longer by flowing with the solid stream as opposed to being washed out in the liquid stream from Fermentor 1 (Train 1). At 35% reflux, to maximize production of high-molecular-weight acids, Fermentors 1 and 2 are the optimal recycle points.

6.3.3 Yield

The exit yield Y_E quantifies the sum of acid *exiting* the fermentation in the product transfer liquid, waste transfer solids, and liquid samples per g NAVS feed. The culture yield Y_C represents the acid *produced* by the mixed culture per g NAVS_{feed} and is equal to the exit yield less the feed yield Y_F . At 14% reflux, the Y_E and Y_C ranking was as follows: Train P>R2=R3>R1>C (Tables 6-3, 6-5). At 35% reflux, the Y_E and Y_C ranking was as follows: Train R1>P>R2>R3>C (Tables 6-4, 6-6). At 14% and 35% reflux, Y_E and Y_C were improved by biomass recycle to Fermentors 1, 2, 3, and parallel to the first three fermentors. With increased reflux, Trains R1 and R2 experienced significant improvement in Y_E and Y_C (Table 6-7).

The exit acetic acid equivalent yield Y_{aE} quantifies the sum of acetic acid equivalents *exiting* the fermentation in the product transfer liquid, waste transfer solids, and liquid samples per g NAVS feed. At 14% and 35% reflux, Y_{aE} was improved in all residue recycle trains because they produced more acids than the control, and at 35% reflux, the trains produced more high-molecular weight acids. At 14% reflux, the Y_{aE} ranking was as follows: Train R2=P>R3>R1>C (Tables 6-3, 6-5). At 35% reflux, the Y_{aE} ranking was as follows: Train R1>R2=P>R3>C (Tables 6-4, 6-6). With increased reflux, Trains R1 and R2 had significant improvement in Y_{aE} (Table 6-7).

The process yield Y_P quantifies only the acid in the product transfer liquid per g NAVS_{feed}, which is sent downstream to be clarified, concentrated, and processed into chemicals and fuel; thus, Y_P represents a commercially relevant acid yield. At 14% reflux, Y_P was improved by biomass recycle in parallel to the first three fermentors and to the second fermentor. At 14% reflux, it is not clear why Y_P decreased with recycle to the first and last fermentor. At 35% reflux, Y_P was improved by all biomass recycle trains; thus, compared to the respective control, the biomass recycle trains (Trains R1, R2, R3, P) produced more acid in the product liquor. At 14% reflux, the Y_P ranking was as follows: Train P>R2>C>R3>R1 (Tables 6-3, 6-5). At 35% reflux, the Y_P ranking was as follows: Train R1>R2>P>R3>C (Tables 6-4, 6-6). For each recycle point, Y_P improved with increased reflux (Table 6-7).

6.3.4 *Conversion and selectivity*

At both 14% and 35% reflux, biomass recycle to the first fermentor and in parallel to the first three fermentors improved conversion because the biomass recycle trains (Trains R1, R2, R3) retained nutrients and cells. Recycling residual biomass to the third fermentor decreased conversion because, since the solid stream exits from the fourth fermentor, the recycled residue had less time in the fermentation. At 14% reflux, the conversion ranking was as follows: Train P>R1>C>R2>R3 (Tables 6-3, 6-5). At 35% reflux, the conversion ranking was as follows: Train R1>P=R2>C>R3 (Tables 6-4, 6-6). Except for Train P, conversion improved with increased reflux (Table 6-7), suggesting that fermentations with a higher residual biomass reflux tend to digest more of the original NAVS (Figures 6-2, 6-3).

At both 14% and 35% reflux, compared to the control, biomass recycle to Fermentor 1 had the lowest selectivity and biomass recycle to Fermentor 3 had the highest selectivity. At 14% reflux, the selectivity ranking was as follows: Train R3>R2>C>R1=P (Tables 6-3, 6-5). At 35% reflux, the selectivity ranking was as follows: Train R3>R2=P=C>R1 (Tables 6-4, 6-6). Except for Train P, there was a significant decline in selectivity with increased reflux (Table 6-7), suggesting that with increased reflux, the fermentations begin to make alternative products besides the C2–C7 acids measured in this study (Figures 6-3, 6-4).

6.3.5 *Carbon-nitrogen ratio*

Because the carbon-nitrogen (C-N) ratio and pH affect fermentation performance, they must be controlled for accurate analysis. To compare fermentation trains, the carbon-nitrogen (C-N) ratio was used to control the nutrients and substrate and was quantified as previously described (Smith et al., 2011). A computer model developed in Excel 2007 (Microsoft, USA) was used to predict the amount of nitrogen (as urea) that needed to be added to the system. This study evaluated these fermentations at 22 ± 5 non-acid organic carbon (C_{NA}) /g total nitrogen (N), and pH 5.6 ± 0.2 (Tables 6-1, 6-2), which is in the optimal range for carboxylate fermentations (Smith et al.,

2011). In Tables 6-1 and 6-2, the different urea loading rates were found with the computer model described above, and correspond to the VSLR and LRT.

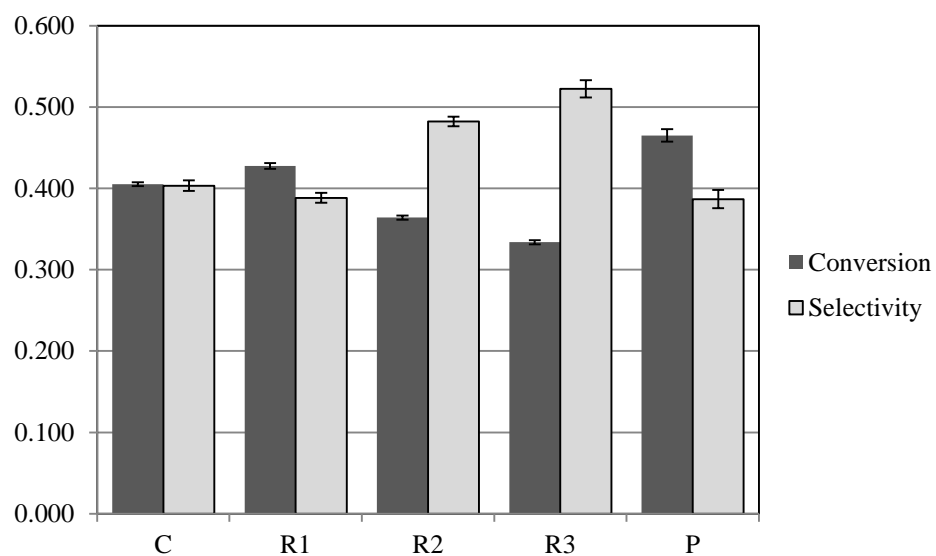


Figure 6-2. Conversion and selectivity for residual biomass recycle at different recycle points with 14% reflux ratio and optimal C-N ratio.

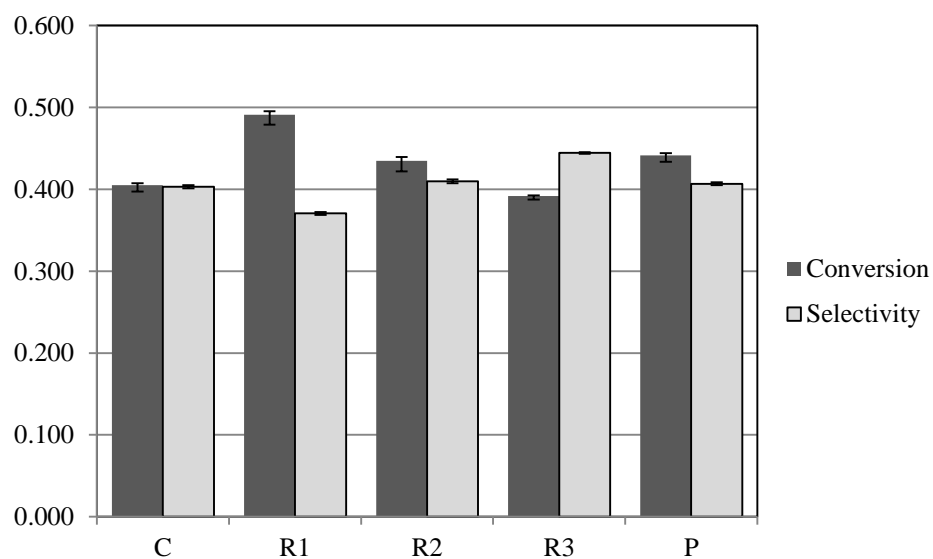


Figure 6-3. Conversion and selectivity for residual biomass recycle at different recycle points with 35% reflux ratio and optimal C-N ratio.

6.3.6 Overview

Using solid residual biomass recycle, many fermentation performance variables are improved; Table 6-8 summarizes the improvements in a qualitative manner. Recycling residual biomass affects many coupled variables. Uncoupling the variables responsible for the positive or negative effects is difficult. The following discussion describes the separate effects of biomass recycle point and reflux ratio.

6.3.6.1 Effect of biomass recycle point

At both reflux ratios, compared to the control with no recycle, the biomass recycle trains either had a positive or neutral effect on total acid and Aceq concentrations. This indicates that the recycling biomass does not negatively affect the concentration of product carboxylic acids (Tables 6-3 to 6-6).

At both 14% and 35% reflux ratios, compared to no residue recycle, recycling biomass to any entry point improved productivity, the amount of daily total acid and Aceq exiting, Y_E , Y_C , and Y_{aE} (Tables 6-3 to 6-6). At 35% reflux, compared to no recycle, Trains R1 and R2 had increased Aceq-to-total-acid ratios (Tables 6-3, 6-4, 6-7). This indicates that biomass recycle improved the yield of carboxylate fermentations with an increase in microbial performance, production of more acid, and production of high-molecular-weight acids (Tables 6-2 and 6-3, Figures 6-3 and 6-4). Perhaps residual biomass recycle altered the amount of recycled cells, nutrients, and/or substrate to reach an optimal and significant concentration for the cellular metabolism to produce more and higher molecular weight acids.

At 14% reflux, compared to the control with no recycle, it is not clear why Y_P decreased with recycle to the first and third fermentor. At 35% reflux, Y_P was improved by all biomass recycle trains; thus, compared to the respective control, the biomass recycle trains (Trains R1, R2, R3, and P) produced more acid in the product liquor.

Table 6-8. Qualitative comparison of performance variables for different recycle points at 14% and 35% residual biomass reflux.

	14% Reflux				35% Reflux			
	R1	R2	R3	P	R1	R2	R3	P
Total carboxylic acid concentration (g/L)	—	↑	↑	↑	↑	—	—	↑
Aceq concentration (g/L)	—	↑	↑	↑	↑	—	—	↑
Total carboxylic acid exiting (g/d)	↑	↑↑	↑↑	↑↑↑	↑↑↑	↑↑	↑	↑↑
Aceq exiting (g/d)	↑↑↑↑	↑↑↑	↑	↑↑	↑↑↑	↑↑	↑	↑↑
Aceq/Acid ratio	—	—	—	—	↑↑	↑↑	↑	↑
Conversion, x (g VS digested/g VS fed)	↑	↓	↓↓	↑↑	↑↑	↑	↓	↑
Selectivity, σ (g acid produced/g NAVS consumed)	↓	↑	↑↑	↓	↓	—	↑	—
Exit yield, Y_E (g acid/g NAVS fed)	↑	↑↑	↑↑	↑↑↑	↑↑↑	↑↑	↑	↑↑
Exit Aceq yield, Y_{aE} (g Aceq/g NAVS fed)	↑	↑↑↑	↑↑	↑↑↑	↑↑↑	↑↑	↑	↑↑
Culture yield, Y_C (g acid/g NAVS fed)	↑	↑↑	↑↑	↑↑↑	↑↑↑	↑↑	↑	↑↑
Process yield, Y_P (g acid/g NAVS fed)	↓↓	↑	↓	↑↑	↑↑↑↑	↑↑↑	↑	↑↑
Productivity, P (g total acid/(L _{liq} ·d))	↑	↑↑↑	↑↑	↑↑↑	↑↑↑	↑↑	↑	↑↑↑

Arrows indicate the qualitative increase or decrease relative to the control; more arrows indicate a greater change between trains with the same reflux ratio. Dashes indicate no difference from the control.

At both reflux ratios, R1 and P tended to have higher conversions but lower selectivities than the control with no recycle, while Train R2 and R3 had lower conversion but higher selectivity. When comparing Trains R1, R2, and R3, recycling biomass solids to the fermentor that allowed for the longest retention of the biomass in the fermentation system (F1) greatly increased conversion but decreased selectivity. Recycling solids to the fermentor that allowed for the shortest retention of biomass (F3) increased selectivity but decreased conversion.

When recycling residual biomass to F1 (Train R1), both the adapted cells (which are largely present in the solid phase) and concentrated recalcitrant solids are retained in the fermentation system for a longer period of time than if the residual biomass is recycled to F2, F3 or in parallel to F1, F2, F3. This longer residence time allows the microorganisms a maximum amount of time to digest the easily digestible fermentor solids and recalcitrant recycled solids, giving Train R1 a higher conversion than Train R3.

When comparing the recycle entry points of Trains R1, R2, and R3, selectivity and LRT increase as follows: $R1 > R2 > R3$ (Figures 6-2 and 6-3). When the residual biomass stream enters further from the liquid exit stream, LRT increases because the liquid entering with the solid waste stream is retained in the system for a longer time. Nitrogen – a major nutrient in the fermentation – was supplemented with urea, which is liquid soluble. Therefore, this trend in selectivity might exist because recycling to the first fermentor (Train R1) allows the soluble nitrogen in the liquid portion of the residual biomass to exit in the fermentation broth more quickly than recycling to the second (Train R2), or third fermentors (Train R3). Thus, Trains R2, R3, and P might have a longer nitrogen retention time because the nitrogen from the residual biomass is fed to a fermentor farther from the exiting product liquid stream.

6.3.6.2 *Effect of biomass reflux ratio*

Each of the five four-stage countercurrent fermentation trains (Figure 6-1) was run at 14% and 35% residual biomass reflux. To conservatively summarize, with increased reflux, some performance variables increased (Y_p , conversion), some were not

affected (total acid and Aceq concentrations, productivity) and one decreased (selectivity). This suggests that fermentations with high residual biomass reflux tended to digest more solids but made alternate products besides C2–C7 carboxylic acids (e.g., CO₂, H₂, lactic acid, formic acid) (Kim et al., 2003). However, for Trains R1 and R2, with increased reflux, Y_E , Y_C , Y_{aE} , Y_P , conversion, Aceq-to-total-acid ratios, daily Aceq exiting, daily total acid exiting all increased (Tables 6-3, 6-4, 6-5, 6-6, and 6-7). Therefore, at 35% reflux, recycling residual biomass to Fermentors 1 and 2 increased the overall exiting amount of Aceq and the proportion of high-molecular-weight acids (Tables 6-2 and 6-3, Figures 6-3 and 6-4).

Based on this study, except for Trains R1 and R2, both reflux ratios achieve similar yields at the same recycle points. To reduce the costs associated with recycling larger amounts of biomass, 14% residual biomass reflux is recommended over 35% reflux. However, if a higher conversion is desired to reduce costs associated with disposing of solid effluents or to produce more byproducts (i.e., H₂, lactic acid, formic acid), then the higher biomass reflux can be used.

6.4 Conclusion

Recycling residual biomass retained microorganisms and nutrients and increased selected fermentation performance measures. In general, compared to no recycle, recycling residual biomass into Fermentors 1, 2, 3, or in parallel increased yield and productivity. The recycle point affected the conversion and selectivity. Relative to lower biomass reflux, higher reflux increased conversion, decreased selectivity, and did not affect acid yield. Because of its simplicity and positive benefit on fermentation performance, industrial carboxylate fermentation systems could employ residual biomass recycle. Based on this study, 14% residual biomass reflux is recommended. However, if it's desirable to produce other byproducts (e.g., H₂) or reduce solid effluent, then 35% residual biomass reflux is recommended.

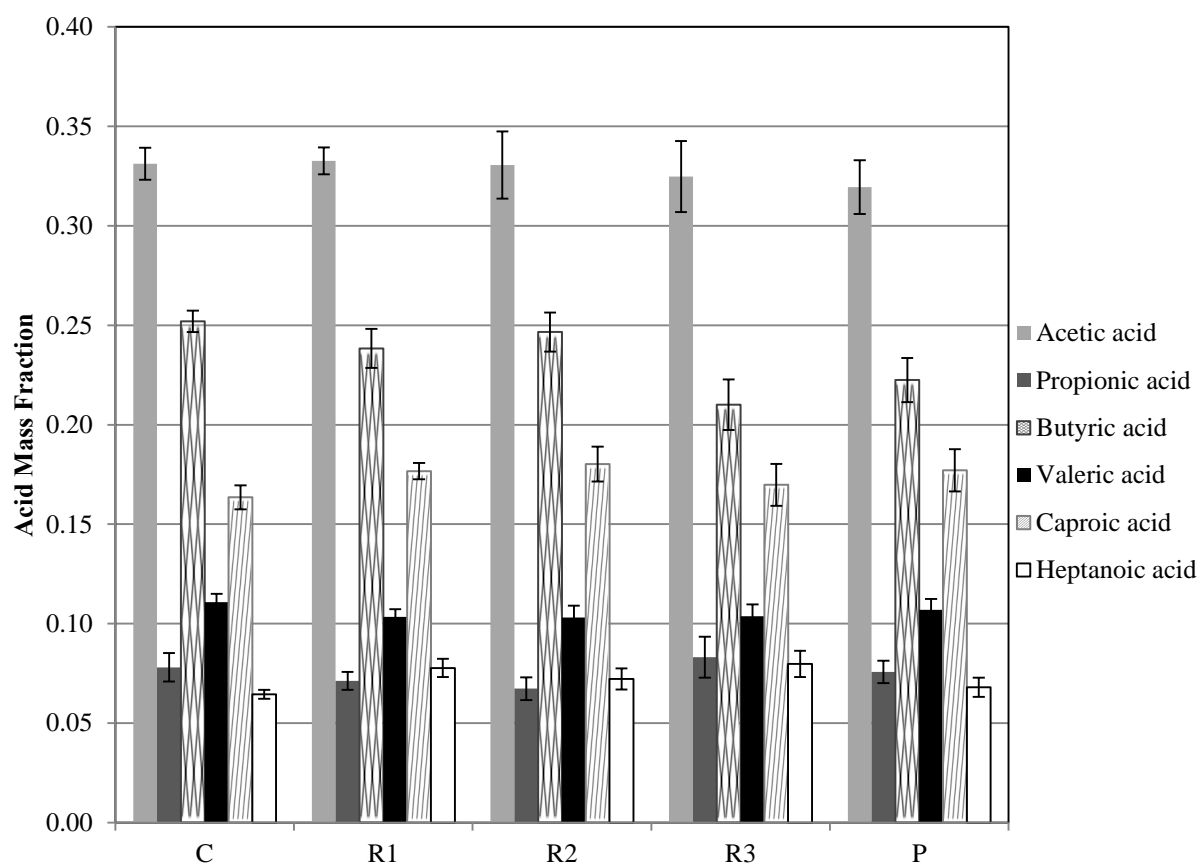


Figure 6-4. Carboxylic acid composition profile at 14% residual biomass reflux. Error bars are the 95% confidence intervals for each carboxylic acid composition during the steady-state period.

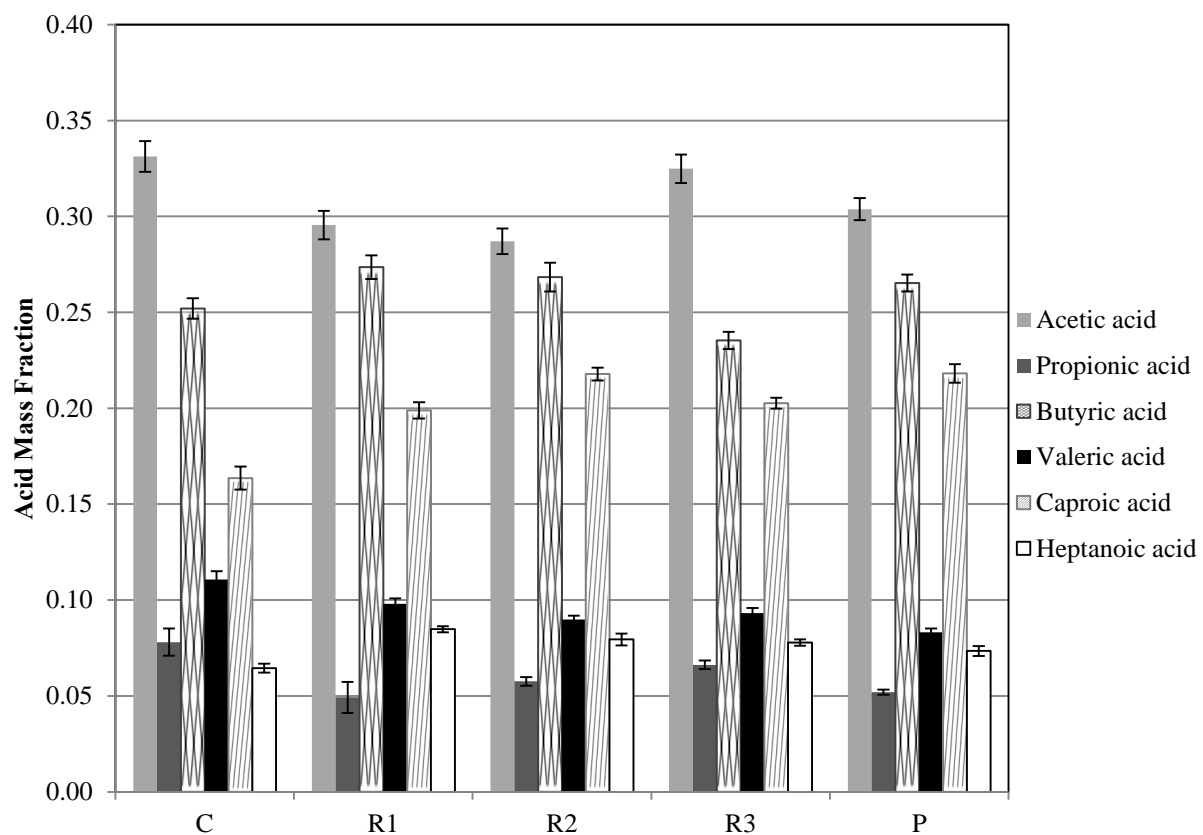


Figure 6-5. Carboxylic acid composition profile at 35% residual biomass reflux. Error bars are the 95% confidence intervals for each carboxylic acid composition during the steady-state period.

7. RESIDUAL BIOMASS RECYCLE IN COUNTERCURRENT MIXED-ACID FERMENTATION: COMPARISON OF THREE CARBON-NITROGEN RATIOS AT DIFFERENT RECYCLE POINTS

In carboxylate fermentations, microorganisms are self-generating biocatalysts, but are typically discarded in exit streams. To improve fermentation performance, a portion of the residual waste biomass was recycled to various fermentors in a countercurrent four-staged fermentation train. Three carbon-nitrogen (C-N) ratios were employed: ~14 (low), 24 (medium), and 74 g C/g N (high). Overall, compared to the control (i.e., no residual biomass recycle), recycling residual biomass to Fermentor 2 was the optimal recycle point and boosted nearly all fermentation performance measures. In general, compared to the high and low C-N ratio, fermentations running at a medium C-N ratio had increased yield, conversion, and amounts of high-molecular-weight acid, but decreased selectivity. Based on this study, the recommendation for industrial carboxylate fermentations is recycle to Fermentor 2 and C-N ratio of ~24 g C/g N.

7.1 Introduction

The demand for liquid transportation fuels (e.g., gasoline, diesel, and aviation fuels) is predominately supplied by fossil fuels; however, fossil fuels are not an ideal energy source. Fossil fuels are a finite resource, prices are rising, and their combustion contributes to global warming and pollution (Alekklett et al., 2010; Bose, 2010). To supply growing energy needs, inexhaustible, environmentally friendly energy sources must be commercialized. Currently, biofuels are the only means to displace liquid fossil fuels, and currently represent 3.5% vol. of global transportation fuels (IEA, 2011c). Biofuels do not cause a net increase in atmospheric carbon dioxide because biomass growth sequesters the same amount of carbon dioxide that is released during combustion

(Ragauskas et al., 2006; Sahin, 2011). Lignocellulosic biomass is inexpensive, abundant, and does not compete with food production (Carroll and Somerville, 2009; Sierra et al., 2008). The carboxylate platform is a promising approach for converting lignocellulose to conventional liquid hydrocarbon fuels (Agler et al., 2011; Holtzapple and Granda, 2009). The carboxylate platform is versatile and has attractive economics (Granda et al., 2009; Pham et al., 2010).

The carboxylate platform is a biomass-to-energy technology that biologically converts all biodegradable biomass components (e.g., cellulose, hemicellulose, starch, free sugar, pectin, fat, protein) into carboxylate salts (Holtzapple et al., 1999; Holtzapple and Granda, 2009). The fermentation employs a mixed-culture of microorganisms that produce carboxylic acids (e.g., acetic acid), which are buffered to form carboxylate salts (e.g., calcium acetate). These salts are precipitated and thermally converted to ketones (e.g., acetone), hydrogenated to mixed alcohols (e.g., isopropanol), and catalytically converted to hydrocarbons (e.g., gasoline, jet fuel). This versatile and continuous process uses nearly any biomass feedstock, which minimizes market distortions and food scarcity. It has low capital and operating costs, does not require sterile operating conditions or added enzymes, and has reached the demonstration level of development.

Biomass is a heterogeneous mixture. The easily fermentable solids digest first; therefore, as biomass decomposes, the remaining biomass becomes less reactive. In multi-staged countercurrent fermentations, solids and liquids are transported through a series of fermentors (a *train*) in opposite directions. Biomass waste exits from Fermentor 4, while product liquid exits from Fermentor 1 (Figure 7-1). This strategy allows the least reactive (most digested) biomass to contact the lowest acid concentration, thereby minimizing the effect of product inhibition (Aiello-Mazzarri et al., 2006). This countercurrent strategy achieves both high product concentration and high conversion (Fu and Holtzapple, 2010b).

Microorganisms (e.g., bacteria, archae, fungi) are the biocatalysts that convert lignocellulose to mixed acids. Achieving high performance in carboxylate fermentations requires a high concentration of cells that are adapted to the environment. One way to

achieve this is to recover and recycle the microorganisms that would be discarded in the residual biomass streams. There are several fermentation studies that show increased productivity with cell recycle because of increased cell retention (Nishiwaki and Dunn, 1999; Wee and Ryu, 2009). Most cell recycle techniques employ membranes; however, these are prone to fouling. Separating a mixed-culture of microorganisms from residual undigested biomass is difficult and costly, and may be impossible industrially. If there are no negative impacts from other contents of the recycle stream (e.g., acids, ash, recalcitrant volatile solids), separating microorganisms from the residual waste stream might be an unnecessary step.

Nitrogen is an essential nutrient needed for cell reproduction, maintenance, and metabolism, and therefore has a pronounced impact on fermentation performance. The C-N ratio quantifies the relative proportion of energy (organic carbon) to nutrient (total nitrogen). Studies have shown that carboxylic acid productivity increases as the C-N ratio approached 30 g C/g N in continuous fermentations (Smith and Holtzapple, 2010), and that the optimal acid production is 20–40 g C/g N in batch fermentations (Smith and Holtzapple, 2011a). However, no studies have investigated C-N ratio in continuous fermentations with residue recycle for optimal carboxylic acid production.

Compared to cell recycle, recycling residual biomass back into the fermentation system will allow adapted microorganisms to be retained, yet is potentially less expensive and so perhaps more commercially viable. The primary objective of this study was to evaluate the effect of recycling residual biomass on continuous fermentation performance. In addition, because nitrogen is an essential nutrient for cell growth and reproduction, it was important to address the effect of C-N ratio on countercurrent fermentations. To achieve these objectives, three different carbon-nitrogen (C-N) ratios at four recycle entry points were evaluated.

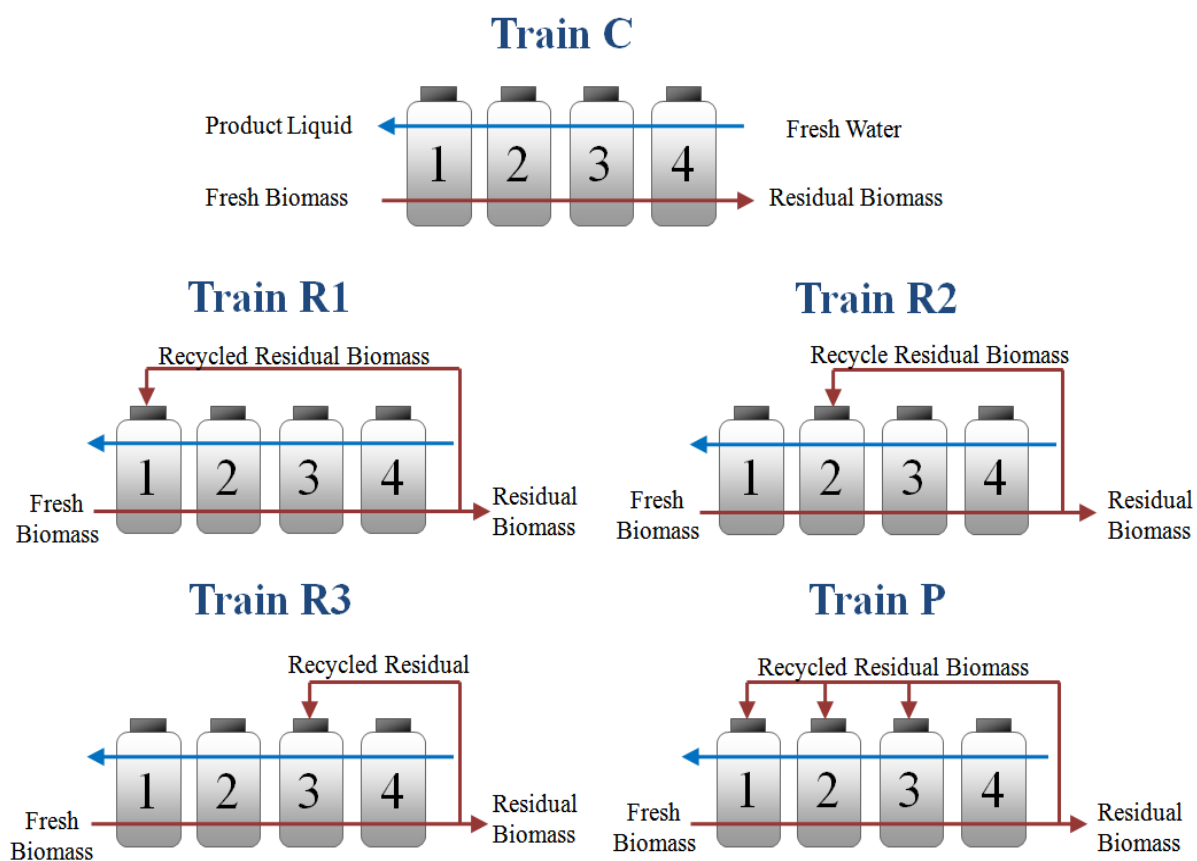


Figure 7-1. Diagram of the residual biomass recycle experiment, depicting the control (Train C) with no residual biomass recycle, and the four different residual biomass recycle trains (Trains R1, R2, R3, P).

7.2 Materials and methods

7.2.1 *Fermentor configuration*

The fermentors were 1-L polypropylene centrifuge bottles capped by a rubber stopper inserted with a glass tube (Domke et al., 2004; Thanakoses et al., 2003). Two segments of ¼-in stainless steel pipe were inserted through the rubber stopper into the vessel to mix the fermentor contents as it rotated in the rolling incubator. A rubber septum sealed the glass tube and allowed for gas sampling and release.

7.2.2 *Fermentation medium*

Deoxygenated medium was prepared by boiling distilled water to liberate dissolved oxygen. After cooling to room temperature in a covered vessel, to further reduce the oxygen content, 0.275 g/L cysteine hydrochloride and 0.275 g/L sodium sulfide were added.

7.2.3 *Inoculum*

The inoculum was a mixed-culture of marine microorganisms from beach sediment collected from Galveston Island, TX. Sediment was removed from the bottom of multiple 0.5-m-deep shoreline pits. Samples were immediately placed in airtight plastic bottles filled with deoxygenated water, capped, and frozen at $-20\text{ }^{\circ}\text{C}$ until use. Before inoculation, samples were thawed, shaken vigorously, and allowed to settle by gravity. Equal parts of the resulting supernatant were homogenized, and aliquots were used to standardize the fermentation inoculum to 12.5% of the initial working volume (Forrest et al., 2010a; Thanakoses, 2002). The bacterial community composition of mixed-acid fermentation has been reported elsewhere (Hollister et al., 2010; Hollister et al., 2011).

7.2.4 *Methanogen inhibition*

Iodoform (CHI_3) was used to inhibit methane production. Iodoform solution (80 μL , 20 g CHI_3/L 190-proof ethanol) was added to each fermentor every 48 h (Domke et al., 2004). Iodoform is sensitive to light, air, and temperature, and so the solution was kept in amber-colored glass bottles wrapped in foil and stored at $-20\text{ }^{\circ}\text{C}$ (Agbogbo and Holtzapple, 2007).

7.2.5 *Carbon-nitrogen ratio*

The C-N ratio is defined as the mass of non-acid organic carbon (g C_{NA}) per total mass of nitrogen (g N), on a wet sample basis (Smith et al., 2011). Total C and N contents (g/100 g wet sample) were determined by Texas A&M University Soil, Water, and Forage Testing Laboratory (College Station, TX) using an Elementar Variomax CN. Based on the carbon and nitrogen contents of the paper, chicken manure, and urea (ACS

grade), the amount of each was calculated to achieve the desired C-N ratio and VS concentration (Tables 7-1 to 7-3).

7.2.6 *Substrate*

Shredded office paper, which served as the energy source, was obtained from a local recycling center. No pretreatment was required. Chicken manure, which served as an undefined nutrient source, was obtained from Feather Crest Farms, Inc. (Bryan, TX) and was dried at 105 °C for 48 h. Wet chicken manure will degrade over time, so to maintain consistency during the entire experiment, dried and homogenized chicken manure was used. Dried chicken manure had a C-N ratio of 12.9 ± 3.4 g non-acid organic carbon (OC_{NA})/g nitrogen (N) and an acid concentration of 0.05 ± 0.01 g acid/g dry chicken manure. Previous studies determined that the C-N ratio of shredded office paper is 138.3 ± 43 g OC_{NA} /g N (Smith and Holtzapple, 2010). The substrate concentration is expressed as non-acid volatile solids (NAVS), which is the combustible portion of the substrate minus carboxylic acids present in the feed. Urea was used as the supplemental nitrogen source.

7.2.7 *Residual biomass recycle fermentation procedure*

In four-stage countercurrent fermentation trains, fresh biomass is fed to Fermentor 1 (F1) and liquid product is harvested from Fermentor 4 (F4) (Figure 7-1). The following five trains were operated: (1) a control train with no recycle (Train C), (2) a train that recycled residue to F1 (Train R1), (3) a train that recycled residue to F2 (Train R2), (4) a train that recycled residue to F3 (Train R3), and (5) a train that recycled residue in parallel to F1, F2, and F3 (Train P). (*Note: Residue* is defined as the centrifuge solids exiting F4, which consists of ~15% dry mass for the low and high C-N ratio fermentations and ~25% for the medium C-N ratio fermentations.) To understand the effect of C-N ratio on countercurrent fermentations with residual biomass recycle, each fermentation train was operated at three C-N ratios: low (~14 g OC_{NA} /g N), medium (~24 g OC_{NA} /g N), and high (~74 g OC_{NA} /g N). For Trains R1, R2, R3, and P,

to normalize the residual biomass recycle ratio, the amount of residual biomass recycled from F4 to the chosen fermentor was controlled (18 g wet, Tables 7-1 to 7-3).

The feed consisted of 80% shredded office copier paper and 20% dry homogenized chicken manure on a dry mass basis. Each fermentor was incubated at 40 °C and operated as a submerged fermentation. The five fermentation trains were initiated as batch cultures under anaerobic conditions with a concentration of 100 g non-acid dry solids (NADS)/L deoxygenated water, which was achieved by adding substrate, nutrient source (manure and urea), inoculum, buffer (calcium carbonate), and liquid medium to each fermentor.

After the first week of batch growth, solid/liquid transfers began with the objective to reach steady state. Every 48 h, fermentors were removed from the incubator, the gas volume was collected, liquid samples were taken, the pH was measured, fermentors were centrifuged (3300×g, 25 min), and the solid/liquid mass transfers were performed. Fresh deoxygenated water was added to F4, and all of the filtered liquid was transferred from F3 to F2, F2 to F1, and out of F1 as the product liquid. In a countercurrent manner, fresh substrate was fed to F1 and a portion of the homogenized solids was transferred from F1 to F2, F2 to F3, F3 to F4, and exited F4 as residual biomass waste. During transfers, the solid wet weight retained, including the fed residual biomass, equaled 225 g in F2, F3, and F4, and 125 g for F1. A preset amount of residual biomass (Tables 7-1 to 7-3) was homogenized and recycled back into F1 (Train R1), F2 (Train R2), F3 (Train R3), and parallel to F1, F2, and F3 (Train P). In each fermentor, the solids were resuspended, iodoform was added, and calcium carbonate was added to neutralize carboxylic acids and buffer the system. Urea was added to adjust the carbon-nitrogen (C-N) ratio to a high (~74 g non-acid organic carbon/g nitrogen, $OC_{NA}/g\ N$), medium (~24 g $OC_{NA}/g\ N$), and low (~14 g $OC_{NA}/g\ N$) value (Tables 7-1 to 7-3). During solid and liquid transfers, when the fermentors were open to the atmosphere, anaerobic conditions were maintained by flushing the fermentors with nitrogen gas (Praxair, Bryan, TX). (*Note*: Nitrogen flushing was a precautionary step; these anaerobic

fermentations have been shown to resist intermittent air exposure (Golub et al., 2011b.) The fermentors were then resealed and placed back in the incubator.

7.2.8 *Residual biomass recycle mass balance*

All performance variables were calculated based on a mass balance outside of the four fermentations and residual biomass recycle loop system.

7.2.9 *Analytical methods*

The following analytical methods were employed.

7.2.9.1 *Carboxylic acid concentration determination*

Fermentation product liquid was collected every 48 h and analyzed for C2–C7 fatty acids as previously described (Golub et al., 2011a).

7.2.9.2 *Biogas analysis*

For the first two weeks, because of the high initial digestion rate, each fermentor was vented daily; thereafter, it was vented every 48 h. Biogas was removed through the fermentor septum, and the volume was measured by displacing liquid in an inverted graduated glass cylinder filled with a 300 g/L CaCl₂ solution, which prevented microbial growth and carbon dioxide adsorption (Domke, 1999).

Biogas composition (i.e., carbon dioxide, nitrogen, oxygen, and methane) was determined by manually injecting 5-mL gas samples into an Agilent 6890 Series chromatograph with a thermal conductivity detector (TCD). A 4.6-m-long, 2.1-mm-ID stainless steel packed column (60/80 Carboxen 100, Supelco 1-2390) was used. The inlet temperature was 230 °C, the detector temperature was 200 °C, and the oven temperature was 200 °C. The total run time was 10 min, and helium was the carrier gas.

7.2.9.3 *Moisture and ash contents*

Moisture and ash contents were determined by drying in a 105°C forced-convection oven for at least 24 h, and subsequent combustion in a 575 °C furnace for at least 12 h by NREL procedures No. 001 and 005, respectively (NREL, 2004). The ash content was calculated on a dry basis. The consumption of non-acid volatile solids

(NAVS) was determined using the inert-ash approach as described previously (Smith et al., 2011).

7.2.10 *Operating parameters*

Previous investigations using continuous countercurrent fermentations have shown that adequate conversion and exit yield were achieved with volatile solid loading rate (VSLR) of ~6.3 g NAVS/(L·d) and liquid residence time (LRT) of ~13 d (Chan and Holtzaple, 2003; Ross, 1998; Smith et al., 2011); therefore, this VSLR and LRT were chosen to investigate the performance of a residual biomass recycle fermentation system. The LRT and VSLR (Tables 7-1 to 7-3) were regulated by controlling the liquid and solid transfer frequency (T), the non-acid volatile solids (NAVS) feed rate, and the liquid feed rate per transfer. Volatile solids (VS) are defined as the mass of dry solid material that is combusted at 575 °C after 12 h, and NAVS are defined as VS less the amount of carboxylic acid:

$$\text{NAVS} = (\text{g total wet biomass})(1 - \text{MC})(1 - \text{AC}) - (\text{g acid in biomass}) \quad (7-1)$$

where MC (g water/g wet biomass) is the fraction of moisture in the biomass, and AC (g ash in biomass/g dry biomass) is the fraction of dry ash remaining after 12 h of combustion at 575 °C. In performance calculations, NAVS is preferred to ensure that the product acids are not quantified with the reactant.

The nutrient source (dried chicken manure) contains carboxylic acids. To more accurately quantify fermentor productivity, the amount of acid entering the system in the manure is subtracted from the amount of acid exiting the system in the product liquid and discarded solids. To determine the amount of acid in the manure, the dry manure was resuspended in distilled water at different concentrations. The acid in the supernatant was analyzed by GC.

The volatile solid loading rate (VSLR) and the liquid residence time (LRT) are calculated as follows:

$$\text{VSLR} = \frac{\text{NAVS feed (g)}}{\text{TLV(L)} \cdot \text{time (d)}} \quad (7-2)$$

$$\text{LRT} = \frac{\text{TLV (L)}}{\text{liquid flow rate out of fermentation train (L/d)}} \quad (7-3)$$

The total liquid volume (TLV) includes both free and interstitial liquid. Liquid flow rate out of fermentation train includes both product liquid and liquid in cake in the exiting streams.

7.2.11 Definition of terms

To account for the total mass in the system, a mass balance closure was calculated with Equation 7-4.

$$\text{mass balance closure} = \frac{\text{mass out (g)}}{\text{mass in (g)} + \text{water of hydrolysis (g)}} \quad (7-4)$$

Cellulose is a polysaccharide composed of individual anhydroglucose units (glucan, MW = 162 g/mol). During digestion, cellulose is enzymatically hydrolyzed to glucose by adding a water molecule. The water of hydrolysis was calculated as previously described (Chan and Holtzapfle, 2003).

The mixed-acid concentration can be expressed as molar acetic acid equivalents (α), which is the reducing potential of an equivalent amount of acetic acid (Datta, 1981).

$$\begin{aligned} \alpha = & 1.00 \times \text{acetic (mol/L)} + 1.75 \times \text{propionic (mol/L)} \\ & + 2.50 \times \text{butyric (mol/L)} + 3.25 \times \text{valeric (mol/L)} \\ & + 4.00 \times \text{caproic (mol/L)} + 4.75 \times \text{heptanoic (mol/L)} \end{aligned} \quad (7-5)$$

The acetic acid equivalent (Aceq) can be expressed on a mass basis as

$$\text{Aceq (g/L)} = 60.05 \text{ (g/mol)} \times \alpha \text{ (mol/L)} \quad (7-6)$$

Aceq proportionally weighs the higher-chained carboxylic acids (C₃ to C₇); the higher acids have higher Aceq than lower acids.

7.2.12 Measuring performance

The feed and exit rate of acid, ash, NAVS, water, and gas were determined during the steady-state period. The average rate of each component was calculated using the *slope method* (Smith and Holtzapfle, 2011b). In this method, the moving cumulative sum of each component is plotted with respect to time. The slope of the steady-state portion of this line is the rate. All performance variables (e.g., conversion, selectivity, and yield) were calculated from the averaged component rates determined by the slope method, as described below:

$$\begin{aligned} \text{Conversion } x &\equiv \frac{\text{NADS}_{\text{feed}} \text{ (g)} - \text{NADS}_{\text{exit}} \text{ (g)}}{\text{NAVS}_{\text{feed}} \text{ (g)}} \\ &= \frac{\text{NAVS}_{\text{feed}} \text{ (g)} + \text{Ash}_{\text{feed}} \text{ (g)} - \text{NAVS}_{\text{exit}} \text{ (g)} - \text{Ash}_{\text{exit}} \text{ (g)}}{\text{NAVS}_{\text{feed}} \text{ (g)}} \quad (7-7) \\ &= \frac{\text{NAVS}_{\text{consumed}} \text{ (g)}}{\text{NAVS}_{\text{feed}} \text{ (g)}} \end{aligned}$$

Exit yield (Y_E)

$$\equiv \frac{\text{total acid output from solid and liquid streams (g)}}{\text{NAVS}_{\text{feed}} \text{ (g)}} \quad (7-8)$$

$$\text{Process yield } (Y_P) \equiv \frac{\text{total acid output in product liquid stream (g)}}{\text{NAVS}_{\text{feed}} \text{ (g)}} \quad (7-9)$$

$$\text{Culture yield } (Y_C) \equiv \frac{\text{total acid produced (g)}}{\text{NAVS}_{\text{feed}}(\text{g})} \equiv Y_E - Y_F \quad (7-10)$$

$$\text{Feed yield } (Y_F) \equiv \frac{\text{total acid entering with feed (g)}}{\text{NAVS}_{\text{feed}}(\text{g})} \quad (7-11)$$

$$\begin{aligned} \text{Selectivity } (\sigma) &\equiv \frac{\text{total acid produced (g)}}{\text{NAVS}_{\text{feed}}(\text{g}) - \text{NAVS}_{\text{exit}}(\text{g})} \quad (7-12) \\ &\equiv \frac{\text{total acid produced (g)}}{\text{NAVS digested (g)}} = \frac{Y_E}{x} \end{aligned}$$

$$\text{Acid productivity } (P) \equiv \frac{\text{total acids produced (g)}}{\text{TLV (L)} \cdot \text{d}} \quad (7-13)$$

where $\text{NADS}_{\text{feed}}$ is the non-acid dry solids fed, $\text{NADS}_{\text{exit}}$ is the non-acid dry solids removed from the fermentation, $\text{NAVS}_{\text{feed}}$ is the non-acid volatile solids fed, $\text{NAVS}_{\text{exit}}$ is the non-acid volatile solids removed from the fermentation, Ash_{feed} is the inert solids fed in biomass feed and buffer, and Ash_{exit} is the inert solids exiting in all solid and liquid streams. NADS includes the ash and volatile solid component of biomass. Ash is assumed to be conserved in the fermentation (Ash_{feed} equals Ash_{exit}), canceling Ash from Equation 7-7.

Per g NAVS fed, the exit yield (Y_E) represents the sum of acid in the product transfer liquid, waste transfer solids, and liquid samples removed from sampling. The process yield (Y_P) represents all the acid in the product transfer liquid per g of NAVS fed. The feed yield (Y_F) is the total g acid entering with the feed per g NAVS fed, and the culture yield (Y_C) is the exit yield less the feed yield.

7.2.13 Statistical analysis

Statistical analysis was performed using Excel 2007 (Microsoft, USA). The mean and standard deviations of the total acid concentrations, acetic acid equivalent (Aceq), NAVS in and out were determined from steady-state operating data. For all countercurrent trains, the average time required to reach steady state was ~62 d. The

variations between trains with time to reach steady state are caused by slight disturbances in the microorganism community either from fed materials or human error. These averaged values were then used to calculate the acid productivity (P), selectivity (σ), yield (Y), and conversion (x) with a 95% confidence interval (CI). Unless specified otherwise, all comparisons in the Results and Discussion section are statistically significant. The steady-state region was the period during which the product total acid and Aceq concentration, dry solids exiting, liquid volume and solid weight of each fermentor, pH, and mass of acid exiting did not vary by more than 2.2 standard deviations from the average for a period of at least one liquid residence time. For each train, the slope of the summed data was used to calculate the means of the performance variables, which were compared using a Student's two sample t -test (two-tailed, Type 3). The p values had a familywise error rate of 0.05 using the Bonferroni correction. All error bars are reported at 95% CI.

7.3 Results and discussion

Each fermentation train consisted of a four-stage countercurrent semi-continuous submerged fermentation system. Five fermentation trains were operated, each with different residual biomass recycle points: (1) a control train with no recycle (Train C), (2) a train that recycled residual biomass to F1 (Train R1), (3) a train that recycled residual biomass to F2 (Train R2), (4) a train that recycled residual biomass to F3 (Train R3), and (5) a train that recycled residual biomass in parallel to F1, F2, and F3 (Train P).

Each fermentation train was operated at three C-N ratios: low (~ 14 g OC_{NA}/g N), medium (~ 24 g OC_{NA}/g N), and high (~ 74 g OC_{NA}/g N) value. To compare the results of all trains, the LRT and VSLR operating parameters were normalized by explicitly controlling the liquid/solid mass transfer frequency (T), the non-acid volatile solids (NAVS) feed rate, the liquid feed rate, and the amount of solid cake retained in each fermentation reactor per transfer (Tables 7-1 to 7-3). In these residual biomass recycle fermentations, the performance trends that occur with regard to the recycle point could be influenced by any of the multiple components in the residual biomass (e.g., cells, volatile solids, ash, acid, nutrients) that are transported in the solid or liquid streams. For

the fermentations operated at different C-N ratio, the relative performance trends could be the result of the amount of nitrogen or the pH.

For all 15 experimental conditions, the accumulated mass of total carboxylic acids and Aceq exiting, NADS added, and NADS removed from their respective trains were found. The slopes of the quasi-steady-state regression lines provided the daily total acid and Aceq exiting, NADS exiting, and NADS removed on a mass basis (Tables 7-4 to 7-6). Productivity was calculated as the mass rate of acid produced per total fermentor volume.

7.3.1 *Reflux ratio*

Although attempts were made to normalize the residual biomass reflux ratio by recycling a controlled amount of residual biomass (18 g wet) as a proportion of the total mass that exits the train, the biomass waste reflux was higher at the medium C-N ratio (~15 g wet recycled residual biomass/100 g wet residual biomass exiting) than at the low and high C-N ratio (~8 g wet recycled residual biomass/100 g wet residual biomass exiting) (Tables 7-1 to 7-3). The reflux ratio is difficult to normalize because the conversion, and therefore the total solids exiting the fermentation, must be known. Fermentations at the medium C-N ratio had a higher conversion. Because less volatile solids exited, the proportion of biomass that was recycled was higher than for the low and high C-N ratio.

Table 7-1. Operating parameters at C-N ratio ~14 g OC_{NA}/g N. Normalized parameters represent the mean of the steady-state values ± CI (95% CI).

	C	R1	R2	R3	P
Fermentation Train					
Solid and liquid transfer frequency, <i>T</i> (h)	48	48	48	48	48
NAVS feed rate (g NAVS/ <i>T</i>)	24.3	24.3	24.3	24.3	24.3
Dry solids added (g/ <i>T</i>)	32	32	32	32	32
Manure added (g/ <i>T</i>)	7.6	7.6	7.6	7.6	7.6
Urea added (g/ <i>T</i>)	3.0	3.0	3.0	3.0	3.0
Calcium carbonate added (g/ <i>T</i>)	4.0	4.0	4.0	4.0	4.0
Fermentor recycle point	–	F1	F2	F3	F1,2,3
Residual biomass recycled (g)	0	18	18	18	18
Liquid feed rate (mL/ <i>T</i>)	300	300	300	300	300
Solid cake retained in F1 (g, wet)	125	125	125	125	125
Solid cake retained in F2–F4 (g, wet)	225	225	225	225	225
Centrifuged liquid retained in F1–F4 (mL)	0	0	0	0	0.0
Methane inhibitor (μL/(<i>T</i> ·fermentor))	80	80	80	80	80
Fermentor reflux ratio (g recycled biomass/g exiting biomass)	–	0.07 ± 0.00	0.07 ± 0.00	0.08 ± 0.01	0.07 ± 0.03
Volatile solid loading rate, VSLR (g NAVS/(L _{liq} ·d))	7.4 ± 0.14	7.0 ± 0.06	7.4 ± 0.04	7.0 ± 0.07	7.1 ± 0.15
Liquid residence time, LRT (d)	12.9 ± 1.80	11.3 ± 0.94	15.1 ± 0.59	19.5 ± 2.03	15.6 ± 1.1
Total liquid volume, TLV (L)	1.64 ± 0.03	1.73 ± 0.02	1.64 ± 0.01	1.75 ± 0.02	1.71 ± 0.05
Volatile solid, VS, concentration (g NAVS/L _{liq})	62 ± 2.57	62 ± 2.59	72 ± 2.09	55 ± 1.85	59 ± 3
Dry solid, DS, concentration (g NADS/L _{liq})	86 ± 2.78	91 ± 3.01	106 ± 2.33	78 ± 1.90	84 ± 3
Average carbon-nitrogen ratio, C-N ratio (g OC _{NA} /g N)	11.1 ± 3.95	11.3 ± 5.46	13.5 ± 4.97	15.9 ± 8.27	18.2 ± 6.3
Average pH (F1–F4)	8.40 ± 0.15	8.52 ± 0.14	8.26 ± 0.14	8.43 ± 0.11	8.31 ± 0.13
Total urea added (g urea/(L _{liq} ·d))	0.91 ± 0.02	0.86 ± 0.01	0.91 ± 0.01	0.86 ± 0.01	0.88 ± 0.01

NAVS = Non-acid volatile solids

NADS = Non-acid dry solids

Table 7-2. Operating parameters at C-N ratio ~24 g OC_{NA}/g N. Normalized parameters represent the mean of the steady-state values ± CI (95% CI). This data was shown previously in Table 6-1.

Fermentation Train	C	R1	R2	R3	P
Solid and liquid transfer frequency, <i>T</i> (h)	48	48	48	48	48
NAVS feed rate (g NAVS/ <i>T</i>)	24.3	24.3	24.3	24.3	24.3
Dry solids added (g/ <i>T</i>)	32	32	32	32	32
Manure added (g/ <i>T</i>)	7.6	7.6	7.6	7.6	7.6
Urea added (g/ <i>T</i>)	1.0	1.0	1.0	1.0	1.0
Calcium carbonate added (g/ <i>T</i>)	4.0	4.0	4.0	4.0	4.0
Fermentor recycle point	–	F1	F2	F3	F1,2,3
Residual biomass recycled (g)	0	18	18	18	18
Liquid feed rate (mL/ <i>T</i>)	300	300	300	300	300
Solid cake retained in F1 (g, wet)	125	125	125	125	125
Solid cake retained in F2–F4 (g, wet)	225	225	225	225	225
Centrifuged liquid retained in F1–F4 (mL)	0	0	0	0	0.0
Methane inhibitor (μL/(<i>T</i> ·fermentor))	80	80	80	80	80
Fermentor reflux ratio (g recycled biomass/g exiting biomass)	–	0.14 ± 0.02	0.15 ± 0.02	0.12 ± 0.01	0.15 ± 0.03
Volatile solid loading rate, VSLR (g NAVS/(L _{liq} ·d))	6.1 ± 0.06	6.2 ± 0.10	6.4 ± 0.05	6.1 ± 0.07	6.3 ± 0.15
Liquid residence time, LRT (d)	13.6 ± 0.6	13.8 ± 1.3	13.7 ± 0.7	13.6 ± 1.2	13.6 ± 1.1
Total liquid volume, TLV (L)	1.98 ± 0.02	1.95 ± 0.03	1.90 ± 0.02	1.98 ± 0.02	1.92 ± 0.05
Volatile solid, VS, concentration (g NAVS/L _{liq})	55 ± 1	69 ± 2	54 ± 2	58 ± 2	57 ± 3
Dry solid, DS, concentration (g NADS/L _{liq})	91 ± 2	107 ± 3	81 ± 2	94 ± 2	88 ± 3
Average carbon-nitrogen ratio, C-N ratio (g OC _{NA} /g N)	21.4 ± 2.2	21.8 ± 2.3	27.2 ± 6.5	25.5 ± 2.6	26.6 ± 6.3
Average pH (F1–F4)	5.67 ± 0.12	5.47 ± 0.09	5.31 ± 0.13	5.48 ± 0.12	5.51 ± 0.13
Total urea added (g urea/(L _{liq} ·d))	0.25 ± 0.00	0.26 ± 0.00	0.26 ± 0.00	0.25 ± 0.01	0.26 ± 0.00

NAVS = Non-acid volatile solids; NADS = Non-acid dry solids

Table 7-3. Operating parameters at C-N ratio ~74 g OC_{NA}/g N. Normalized parameters represent the mean of the steady-state values ± CI (95% CI).

	C	R1	R2	R3	P
Fermentation Train					
Solid and liquid transfer frequency, <i>T</i> (h)	48	48	48	48	48
NAVS feed rate (g NAVS/ <i>T</i>)	24.3	24.3	24.3	24.3	24.3
Dry solids added (g/ <i>T</i>)	32	32	32	32	32
Manure added (g/ <i>T</i>)	7.6	7.6	7.6	7.6	7.6
Urea added (g/ <i>T</i>)	0.0	0.0	0.0	0.0	0.0
Calcium carbonate added (g/ <i>T</i>)	4.0	4.0	4.0	4.0	4.0
Fermentor recycle point	–	F1	F2	F3	F1,2,3
Residual biomass recycled (g)	0	18	18	18	18
Liquid feed rate (mL/ <i>T</i>)	300	300	300	300	300
Solid cake retained in F1 (g, wet)	125	125	125	125	125
Solid cake retained in F2–F4 (g, wet)	225	225	225	225	225
Centrifuged liquid retained in F1–F4 (mL)	0	0	0	0	0
Methane inhibitor (μL/(<i>T</i> ·fermentor))	80	80	80	80	80
Fermentor reflux ratio (g recycled biomass/g exiting biomass)	–	0.08 ± 0.01	0.08 ± 0.00	0.08 ± 0.00	0.08 ± 0.00
Volatile solid loading rate, VSLR (g NAVS/(L _{liq} ·d))	7.0 ± 0.12	6.8 ± 0.05	6.9 ± 0.05	7.0 ± 0.08	7.0 ± 0.05
Liquid residence time, LRT (d)	14.2 ± 1.48	12.7 ± 1.40	11.5 ± 0.34	12.0 ± 0.74	11.6 ± 0.60
Total liquid volume, TLV (L)	1.74 ± 0.03	1.78 ± 0.01	1.76 ± 0.01	1.74 ± 0.02	1.74 ± 0.01
Volatile solid, VS, concentration (g NAVS/L _{liq})	54 ± 2	55 ± 2	48 ± 1	47 ± 1	48 ± 1
Dry solid, DS, concentration (g NADS/L _{liq})	98 ± 3	85 ± 2	85 ± 2	79 ± 2	83 ± 2
Average carbon-nitrogen ratio, C-N ratio (g OC _{NA} /g N)	75.1 ± 14.5	72.0 ± 13.9	76.3 ± 14.8	78.1 ± 15.1	71.0 ± 13.7
Average pH (F1–F4)	6.04 ± 0.11	6.02 ± 0.09	5.96 ± 0.11	5.98 ± 0.10	5.98 ± 0.09
Total urea added (g urea/(L _{liq} ·d))	0.00 ± 0.12	0.00 ± 0.01	0.00 ± 0.00	0.00 ± 0.00	0.00 ± 0.00

NAVS = Non-acid volatile solids

NADS = Non-acid dry solids

Table 7-4. Performance measures at C-N ratio ~14 g OC_{NA}/g N. Values represent the mean of the steady-state values \pm CI (95% CI).

	C	R1	R2	R3	P
Total carboxylic acid concentration (g/L)	11.90 \pm 0.70	10.82 \pm 0.72	13.53 \pm 0.47	12.55 \pm 0.98	10.49 \pm 0.85
Aceq concentration (g/L)	13.25 \pm 0.79	11.98 \pm 0.82	15.30 \pm 0.53	14.09 \pm 1.12	11.61 \pm 0.93
Total carboxylic acid exiting (g/d)	0.78 \pm 0.00	0.84 \pm 0.01	0.93 \pm 0.00	0.87 \pm 0.01	0.82 \pm 0.01
Aceq exiting (g/d)	0.85 \pm 0.00	0.92 \pm 0.01	1.04 \pm 0.00	0.96 \pm 0.01	0.90 \pm 0.01
Aceq/Acid ratio	1.11 \pm 0.00	1.11 \pm 0.01	1.13 \pm 0.00	1.12 \pm 0.01	1.11 \pm 0.00
Conversion, x (g VS digested/g VS fed)	0.080 \pm 0.000	0.101 \pm 0.001	0.091 \pm 0.001	0.082 \pm 0.000	0.090 \pm 0.000
Selectivity, σ (g acid produced/g NAVS consumed)	0.777 \pm 0.005	0.680 \pm 0.010	0.824 \pm 0.004	0.863 \pm 0.005	0.739 \pm 0.006
Aceq selectivity, σ_a (g Aceq produced/g NAVS consumed)	0.851 \pm 0.005	0.744 \pm 0.011	0.921 \pm 0.004	0.954 \pm 0.007	0.808 \pm 0.007
Exit yield, Y_E (g acid/g NAVS fed)	0.062 \pm 0.000	0.069 \pm 0.001	0.075 \pm 0.000	0.071 \pm 0.000	0.067 \pm 0.001
Exit Aceq yield, Y_{aE} (g Aceq/g NAVS fed)	0.068 \pm 0.000	0.075 \pm 0.001	0.084 \pm 0.000	0.078 \pm 0.001	0.073 \pm 0.001
Culture yield, Y_C (g acid/g NAVS fed)	0.047 \pm 0.000	0.053 \pm 0.001	0.060 \pm 0.000	0.055 \pm 0.000	0.051 \pm 0.001
Process yield, Y_P (g acid/g NAVS fed)	0.038 \pm 0.000	0.044 \pm 0.001	0.046 \pm 0.000	0.050 \pm 0.001	0.042 \pm 0.000
Productivity, P (g total acid/(L _{liq} ·d))	0.357 \pm 0.007	0.376 \pm 0.006	0.453 \pm 0.003	0.389 \pm 0.005	0.370 \pm 0.005
Biogas produced (g/d)	0.53 \pm 0.00	0.53 \pm 0.00	0.62 \pm 0.00	0.39 \pm 0.00	0.43 \pm 0.00
Mass balance closure (g mass in/g mass out)	0.96 \pm 0.00	0.98 \pm 0.00	0.98 \pm 0.00	0.95 \pm 0.00	0.98 \pm 0.00

Table 7-5. Performance measures at C-N ratio ~24 g OC_{NA}/g N. Values represent the mean of the steady-state values \pm CI (95% CI). This data was shown previously in Table 6-3.

	C	R1	R2	R3	P
Total carboxylic acid concentration (g/L)	16.69 \pm 0.52	17.24 \pm 0.65	18.46 \pm 0.75	17.99 \pm 0.56	18.55 \pm 0.89
Aceq concentration (g/L)	26.10 \pm 0.88	27.10 \pm 0.97	29.06 \pm 1.33	28.33 \pm 0.91	29.21 \pm 1.48
Total carboxylic acid exiting (g/d)	2.01 \pm 0.01	2.05 \pm 0.01	2.16 \pm 0.01	2.14 \pm 0.02	2.22 \pm 0.03
Aceq exiting (g/d)	3.15 \pm 0.01	3.24 \pm 0.01	3.52 \pm 0.01	3.40 \pm 0.02	3.52 \pm 0.04
Aceq/Acid ratio	1.57 \pm 0.01	1.57 \pm 0.00	1.57 \pm 0.01	1.57 \pm 0.01	1.57 \pm 0.01
Conversion, x (g VS digested/g VS fed)	0.405 \pm 0.002	0.427 \pm 0.004	0.364 \pm 0.003	0.334 \pm 0.003	0.465 \pm 0.008
Selectivity, σ (g acid produced/g NAVS consumed)	0.403 \pm 0.002	0.388 \pm 0.002	0.482 \pm 0.002	0.522 \pm 0.004	0.387 \pm 0.005
Aceq selectivity, σ_a (g Aceq produced/g NAVS consumed)	0.632 \pm 0.003	0.616 \pm 0.003	0.785 \pm 0.004	0.829 \pm 0.007	0.613 \pm 0.008
Exit yield, Y_E (g acid/g NAVS fed)	0.163 \pm 0.001	0.166 \pm 0.001	0.176 \pm 0.001	0.174 \pm 0.001	0.180 \pm 0.002
Exit Aceq yield, Y_{aE} (g Aceq/g NAVS fed)	0.256 \pm 0.001	0.263 \pm 0.001	0.286 \pm 0.001	0.277 \pm 0.002	0.285 \pm 0.003
Culture yield, Y_C (g acid/g NAVS fed)	0.148 \pm 0.001	0.151 \pm 0.001	0.160 \pm 0.001	0.159 \pm 0.001	0.164 \pm 0.002
Process yield, Y_P (g acid/g NAVS fed)	0.143 \pm 0.001	0.138 \pm 0.001	0.145 \pm 0.001	0.140 \pm 0.001	0.149 \pm 0.003
Productivity, P (g total acid/(L _{liq} ·d))	0.921 \pm 0.010	0.953 \pm 0.015	1.038 \pm 0.009	0.983 \pm 0.012	1.055 \pm 0.027
Biogas produced (g/d)	2.53 \pm 0.01	2.70 \pm 0.01	2.51 \pm 0.01	2.20 \pm 0.01	2.93 \pm 0.02
Mass balance closure (g mass in/g mass out)	0.95 \pm 0.00	0.93 \pm 0.00	0.91 \pm 0.00	0.96 \pm 0.00	0.89 \pm 0.00

Table 7-6. Performance measures at C-N ratio ~ 74 g OC_{NA}/g N. Values represent the mean of the steady-state values \pm CI (95% CI).

	C	R1	R2	R3	P
Total carboxylic acid concentration (g/L)	11.74 \pm 0.49	10.75 \pm 0.38	11.34 \pm 0.29	11.58 \pm 0.33	11.87 \pm 0.27
Aceq concentration (g/L)	15.52 \pm 0.64	14.27 \pm 0.51	15.04 \pm 0.37	15.32 \pm 0.42	15.69 \pm 0.37
Total carboxylic acid exiting (g/d)	0.90 \pm 0.00	0.90 \pm 0.00	1.02 \pm 0.00	0.95 \pm 0.00	1.00 \pm 0.00
Aceq exiting (g/d)	1.19 \pm 0.01	1.20 \pm 0.00	1.36 \pm 0.00	1.25 \pm 0.01	1.32 \pm 0.00
Aceq/Acid ratio	1.33 \pm 0.01	1.33 \pm 0.00	1.33 \pm 0.00	1.32 \pm 0.00	1.32 \pm 0.00
Conversion, x (g VS digested/g VS fed)	0.126 \pm 0.001	0.136 \pm 0.001	0.132 \pm 0.000	0.118 \pm 0.000	0.135 \pm 0.000
Selectivity, σ (g acid produced/g NAVS consumed)	0.584 \pm 0.003	0.537 \pm 0.002	0.629 \pm 0.001	0.653 \pm 0.003	0.598 \pm 0.001
Aceq selectivity, σ_a (g Aceq produced/g NAVS consumed)	0.776 \pm 0.004	0.712 \pm 0.002	0.833 \pm 0.002	0.861 \pm 0.004	0.790 \pm 0.002
Exit yield, Y_E (g acid/g NAVS fed)	0.073 \pm 0.000	0.073 \pm 0.000	0.083 \pm 0.000	0.077 \pm 0.000	0.081 \pm 0.000
Exit Aceq yield, Y_{aE} (g Aceq/g NAVS fed)	0.097 \pm 0.000	0.097 \pm 0.000	0.110 \pm 0.000	0.101 \pm 0.000	0.107 \pm 0.000
Culture yield, Y_C (g acid/g NAVS fed)	0.058 \pm 0.000	0.058 \pm 0.000	0.067 \pm 0.000	0.061 \pm 0.000	0.065 \pm 0.000
Process yield, Y_P (g acid/g NAVS fed)	0.044 \pm 0.000	0.047 \pm 0.000	0.051 \pm 0.000	0.042 \pm 0.000	0.046 \pm 0.000
Productivity, P (g total acid/(L _{liq} ·d))	0.415 \pm 0.009	0.401 \pm 0.003	0.474 \pm 0.003	0.435 \pm 0.005	0.464 \pm 0.003
Biogas produced (g/d)	0.75 \pm 0.00	0.66 \pm 0.00	0.84 \pm 0.00	0.71 \pm 0.00	0.76 \pm 0.00
Mass balance closure (g mass in/g mass out)	0.90 \pm 0.00	0.96 \pm 0.00	0.98 \pm 0.00	0.95 \pm 0.00	0.97 \pm 0.00

Table 7-7. *p* values for performance measures at C-N ratio ~14 g OC_{NA}/g N ($\alpha = 0.05$).

Trains	Conversion	Selectivity	Exit yield	Exit yield Aceq	Culture yield	Process yield	TLV	Productivity	Biogas produced	Total acid conc.	Aceq conc.	Total acid exit	Total Aceq exit	Aceq/ Total acid
C and R1	0.000	0.000	0.000	0.000	0.000	0.000	0.000	0.000	0.540	0.030	0.025	0.000	0.000	0.192
C and R2	0.000	0.000	0.000	0.000	0.000	0.000	0.976	0.000	0.000	0.000	0.000	0.000	0.000	0.000
C and R3	0.000	0.000	0.000	0.000	0.000	0.000	0.000	0.000	0.000	0.272	0.213	0.000	0.000	0.112
C and P	0.000	0.000	0.000	0.000	0.000	0.000	0.000	0.002	0.000	0.011	0.008	0.000	0.000	0.051
R1 and R2	0.000	0.000	0.000	0.000	0.000	0.010	0.000	0.000	0.000	0.000	0.000	0.000	0.000	0.000
R1 and R3	0.000	0.000	0.004	0.000	0.002	0.000	0.265	0.001	0.000	0.005	0.003	0.000	0.000	0.027
R1 and P	0.000	0.000	0.000	0.000	0.001	0.000	0.028	0.104	0.000	0.542	0.535	0.007	0.005	0.963
R2 and R3	0.000	0.000	0.000	0.000	0.000	0.000	0.000	0.000	0.000	0.073	0.052	0.000	0.000	0.028
R2 and P	0.000	0.000	0.000	0.000	0.000	0.000	0.000	0.000	0.000	0.000	0.000	0.000	0.000	0.000
R3 and P	0.000	0.000	0.000	0.000	0.000	0.000	0.003	0.000	0.000	0.002	0.001	0.000	0.000	0.010

p value < 0.005 statistically different, with a familywise error rate of 0.05 using the Bonferroni correction

Table 7-8. *p* values for performance measures at C-N ratio ~24 g OC_{NA}/g N ($\alpha = 0.05$).

Trains	Conversion	Selectivity	Exit yield	Exit yield Aceq	Culture yield	Process yield	TLV	Productivity	Biogas produced	Total acid conc.	Aceq conc.	Total acid exit	Total Aceq exit	Aceq/ Total acid
C and R1	0.000	0.000	0.000	0.000	0.000	0.000	0.068	0.001	0.000	0.187	0.125	0.000	0.000	0.135
C and R2	0.000	0.000	0.000	0.000	0.000	0.004	0.000	0.000	0.027	0.000	0.001	0.000	0.000	0.865
C and R3	0.000	0.000	0.000	0.000	0.000	0.000	0.856	0.000	0.000	0.002	0.001	0.000	0.000	0.598
C and P	0.000	0.000	0.000	0.000	0.000	0.000	0.028	0.000	0.000	0.001	0.001	0.000	0.000	0.255
R1 and R2	0.000	0.000	0.000	0.000	0.000	0.000	0.005	0.000	0.000	0.015	0.019	0.000	0.000	0.370
R1 and R3	0.000	0.000	0.000	0.000	0.000	0.001	0.050	0.003	0.000	0.078	0.066	0.000	0.000	0.606
R1 and P	0.000	0.563	0.000	0.000	0.000	0.000	0.396	0.000	0.000	0.018	0.019	0.000	0.000	0.798
R2 and R3	0.000	0.000	0.131	0.000	0.117	0.000	0.000	0.000	0.000	0.313	0.355	0.025	0.000	0.762
R2 and P	0.000	0.000	0.001	0.000	0.001	0.002	0.250	0.229	0.000	0.872	0.879	0.000	0.885	0.463
R3 and P	0.000	0.000	0.000	0.000	0.000	0.000	0.020	0.000	0.000	0.281	0.299	0.000	0.000	0.717

p value < 0.005 statistically different, with a familywise error rate of 0.05 using the Bonferroni correction

Table 7-9. *p* values for performance measures at C-N ratio ~74 g OC_{NA}/g N ($\alpha = 0.05$).

Trains	Conversion	Selectivity	Exit yield	Exit yield Aceq	Culture yield	Process yield	TLV	Productivity	Biogas produced	Total acid conc.	Aceq conc.	Total acid exit	Total Aceq exit	Aceq/Total acid
C and R1	0.000	0.000	0.503	0.164	0.927	0.000	0.000	0.003	0.000	0.002	0.003	0.038	0.186	0.983
C and R2	0.000	0.000	0.000	0.000	0.000	0.000	0.004	0.000	0.000	0.154	0.197	0.000	0.000	0.785
C and R3	0.000	0.000	0.000	0.000	0.000	0.000	0.066	0.000	0.000	0.575	0.602	0.000	0.000	0.207
C and P	0.000	0.000	0.000	0.000	0.000	0.000	0.063	0.000	0.000	0.644	0.626	0.000	0.000	0.115
R1 and R2	0.000	0.000	0.000	0.000	0.000	0.000	0.017	0.000	0.000	0.015	0.017	0.000	0.000	0.553
R1 and R3	0.000	0.000	0.000	0.000	0.000	0.000	0.002	0.000	0.000	0.001	0.002	0.000	0.000	0.010
R1 and P	0.000	0.000	0.000	0.000	0.000	0.013	0.000	0.000	0.000	0.000	0.000	0.000	0.000	0.001
R2 and R3	0.000	0.000	0.000	0.000	0.000	0.000	0.134	0.000	0.000	0.271	0.322	0.000	0.000	0.057
R2 and P	0.000	0.000	0.000	0.000	0.000	0.000	0.018	0.000	0.000	0.009	0.014	0.000	0.000	0.010
R3 and P	0.000	0.000	0.000	0.000	0.000	0.000	0.819	0.000	0.000	0.171	0.180	0.000	0.000	0.580

p value < 0.005 statistically different, with a familywise error rate of 0.05 using the Bonferroni correction

Table 7-10. *p* values for performance measures to compare fermentations with C-N of 14, 24, and 74 g OC_{NA}/g N ($\alpha = 0.05$).

Trains	Conversion	Selectivity	Exit yield	Exit yield Aceq	Culture yield	Process yield	TLV	Productivity	Biogas produced	Total acid conc.	Aceq conc.	Total acid exit	Total Aceq exit	Aceq/Total acid
C (14) and C (24)	0.000	0.000	0.000	0.000	0.000	0.000	0.000	0.000	0.000	0.000	0.000	0.000	0.000	0.000
C (14) and C (74)	0.000	0.000	0.000	0.000	0.000	0.000	0.008	0.000	0.000	0.698	0.000	0.000	0.000	0.000
C (24) and C (74)	0.000	0.000	0.000	0.000	0.000	0.000	0.000	0.000	0.000	0.000	0.000	0.000	0.000	0.000
R1 (14) and R1 (24)	0.000	0.000	0.000	0.000	0.000	0.000	0.000	0.000	0.000	0.000	0.000	0.000	0.000	0.000
R1 (14) and R1 (74)	0.000	0.000	0.000	0.000	0.000	0.000	0.000	0.000	0.000	0.861	0.000	0.000	0.000	0.000
R1 (24) and R1 (74)	0.000	0.000	0.000	0.000	0.000	0.000	0.000	0.000	0.000	0.000	0.000	0.000	0.000	0.000
R2 (14) and R2 (24)	0.000	0.000	0.000	0.000	0.000	0.000	0.000	0.000	0.000	0.000	0.000	0.000	0.000	0.000
R2 (14) and R2 (74)	0.000	0.000	0.000	0.000	0.000	0.000	0.000	0.000	0.000	0.000	0.415	0.000	0.000	0.000
R2 (24) and R2 (74)	0.000	0.000	0.000	0.000	0.000	0.000	0.000	0.000	0.000	0.000	0.000	0.000	0.000	0.000
R3 (14) and R3 (24)	0.000	0.000	0.000	0.000	0.000	0.000	0.000	0.000	0.000	0.000	0.000	0.000	0.000	0.000
R3 (14) and R3 (74)	0.000	0.000	0.000	0.000	0.000	0.000	0.616	0.000	0.000	0.061	0.043	0.000	0.000	0.000
R3 (24) and R3 (74)	0.000	0.000	0.000	0.000	0.000	0.000	0.000	0.000	0.000	0.000	0.000	0.000	0.000	0.000
P (14) and P (24)	0.000	0.000	0.000	0.000	0.000	0.000	0.000	0.000	0.000	0.000	0.000	0.000	0.000	0.000
P (14) and P (74)	0.000	0.000	0.000	0.000	0.000	0.000	0.007	0.000	0.000	0.004	0.000	0.000	0.000	0.000
P (24) and P (74)	0.000	0.000	0.000	0.000	0.000	0.000	0.000	0.000	0.000	0.000	0.000	0.000	0.000	0.000

p value < 0.003 statistically different, with a familywise error rate of 0.05 using the Bonferroni correction

7.3.2 *Biogas*

When comparing the trains at different C-N ratios, the amount of biogas produced in the trains at a medium C-N ratio were optimal, followed by high C-N ratio, and then low C-N ratio (Tables 7-4 to 7-6, 7-10). At all C-N ratios, there appears to be a loose correlation between conversion and amount of biogas produced (Tables 7-4 to 7-9). Other studies of ethanol and ruminal fermentations show gas production is related to substrate digestibility (Contreras-Govea et al., 2011; Weimer et al., 2005). The average biogas composition was similar to other studies (Ch. 6). No methane was detected in any fermentor.

7.3.3 *Acid concentration*

At a given C-N ratio, the residue recycle point did not influence the total acid or the Aceq concentration, although at medium and low C-N ratios, Train R2 had a higher acid concentrations than Train C (Tables 7-4 to 7-9). However, the C-N ratio did affect the total acid and Aceq concentration. At the low and high C-N ratios, at most recycle points, the total acid and Aceq concentrations were similar, with a $p > 0.003$ and in all cases the concentrations were lower than that observed at the medium C-N ratio (Tables 7-4 to 7-6, 7-10). From this study, the following conclusions can be drawn: (1) the medium C-N ratio is “optimal” for acid concentration, and (2) at medium and low C-N ratios, residual biomass recycle to F2 improved acid concentrations.

7.3.4 *Daily acid production*

In all fermentors of a train, TLV quantifies the total volume of liquid in the solid and liquid phases. When considering the influence of C-N ratio at a respective residual biomass recycle point (e.g., Train C at low, medium, and high C-N ratios), all trains did not have equivalent TLVs, indicating nonuniformity between trains (Tables 7-1 to 7-3, 7-7 to 7-10). To standardize the analyses, the daily amount of acid exiting the fermentors was calculated on a mass basis from the product liquid, waste, and sample streams (Tables 7-4 to 7-6). At low C-N ratio, the total acid exiting and total Aceq exiting (g/d) are ranked as follows: Train R2>R3>R1=P>C (Tables 7-4, 7-7). At the medium C-N

ratio, the total carboxylic acid exiting (g/d) is ranked as follows: Train $P > R2 > R3 > R1 > C$ (Tables 7-4, 7-7). For Aceq exiting (g/d), the corresponding ranks are $P = R2 > R3 > R1 > C$ (Tables 7-5, 7-8). At high C-N ratio, the total carboxylic acid and Aceq exiting (g/d) is ranked as follows: Train $R2 > P > R3 > R1 = C$ (Tables 7-6, 7-9).

When comparing Trains 1, 2, and 3, there is a distinct trend for residual biomass recycle point. Recycling residual biomass to F2 produces the most total and Aceq exiting, then recycling to F3, and then to F1. There is a weaker trend for recycling residue in parallel to F1, F2, and F3. However, a majority of recycle trains produced more acids than the control train with no recycle. These results show that recycling residual biomass can improve the amount of daily total acid exiting the fermentation train, even at C-N ratios that deviate from medium. Therefore, recycling biomass to F2, regardless of C-N ratio, is optimal for production of total acid and Aceq exiting.

However, when comparing C-N ratios, the medium C-N ratio increased the daily total acid and Aceq exiting (g/d) for all trains. Compared to the low C-N ratio, the high C-N ratio increased the acids exiting (g/d) in all trains (Tables 7-4 to 7-9). Therefore, to maximize total acids exiting, medium C-N ratios are preferred, and high C-N ratios are preferred over low C-N ratios.

7.3.5 *Aceq-to-total-acid ratio*

Besides total Aceq concentration and daily Aceq exiting, another measure of the production of more high-molecular-weight carboxylic acids (e.g., valeric, caproic, and heptanoic acid) is the Aceq-to-total-acid ratio. The larger the Aceq-to-total-acid ratio, the more high-molecular-weight acids are present (see Equation 7-5). When comparing fermentation trains at all recycle points and at the respective C-N ratios, a majority of Aceq-to-total-acid ratios were not different; thus, the recycle point did not affect the production of high-molecular-weight carboxylic acids (Tables 7-4 to 7-9). At all residual biomass recycle points, the Aceq-to-total-acid ratio is ranked as follows: C-N ratio $\text{medium} > \text{high} > \text{low}$ (Tables 7-4 to 7-6, 7-10). This suggests that the “medium” C-N ratio in this study is a metabolically optimal substrate-to-nutrient ratio, enabling the bacteria

to increase the proportion of higher-molecular-weight acids, which are more thermodynamically demanding to produce.

7.3.6 *Product spectrum*

The proportion of C2–C7 carboxylic acids (acetic, propionic, butyric, valeric, caproic, heptanoic, respectively), or the *product spectrum*, correlates to variables such as temperature, microorganism community, feedstock, C-N ratio, pH, and oxygen exposure (Chan and Holtzaple, 2003; Golub et al., 2011a; Liu et al., 2008; Smith and Holtzaple, 2011a). In carboxylate fermentation systems, all of the above mentioned variables affect the metabolism of the specific mixed-culture community.

This study highlights the strong effect of C-N ratio and pH on product spectrum. As shown in Figures 7-2 to 7-4, at low C-N ratio fermentations, there is a high concentration of acetic acid (>75%) with less propionic acid (~15%), and the remainder being mostly butyric acid, which agrees with other studies (Rodriguez et al., 2006; Zhang et al., 2009). This large concentration of acetic acid could be an effect of the low C-N ratio or high pH because urea was the nitrogen supplement. At high pH, there are high concentrations of undissociated acid. Because acetic acid has a higher protonating power than the other acids, the bacteria might try to protect themselves from the high pH by producing more acetic acid. Also, considering the fermentation product pathway, other studies have shown that when the production rate of acetate to butyrate increases, the production of H₂ also increases, which is associated with an increase in the enzyme NADH₂-ferredoxin oxidoreductase. This enzyme catalyzes the reaction $\text{NADH}_2 \rightarrow \text{NAD} + \text{H}_2$, which is otherwise thermodynamically unfavored. According to some studies, when this enzyme system is activated, one extra mol of adenosine tri-phosphate (ATP) is produced per mol pyruvate, relative to butyrate (van Andel et al., 1985). This results in a decrease in energy requirements for outwards transport of acetic acid.

The medium C-N ratio fermentations had a more evenly distributed acid profile, with C2, C4, and C6 being the most prominent acids, followed by C3, C5, and C7. Even numbers of carboxylic acids are preferred because the metabolic pathways are based on

acetyl Co-A and only acetyl Co-A can initiate the elongation process (Forrest et al., 2011).

The high C-N ratio fermentations had an almost equivalent amount of C2 and C3 acids (~80%), with a smaller amount of C4 and C5 (~15%), and the remainder being C6 and C7. The acid profile at the high C-N ratio seems to have combined attributes of both the low and medium C-N ratio fermentations, by having a large amount of low-molecular-weight acids like the low C-N ratio, but having a more diverse profile like the medium C-N ratio. For high C-N ratio fermentations, the lack of high-molecular-weight acids can be attributed to not enough nitrogen for energy assimilation. Because the pH of both the high and medium C-N ratio fermentations are somewhat similar, the differences between the profiles of these fermentations are certainly more from the effect of C-N ratio and not pH.

Future studies should include decoupling C-N ratio and pH in continuous countercurrent carboxylate fermentations.

7.3.7 Productivities

At the low C-N ratio, Train R2 had a higher productivity than all other trains at that C-N ratio (Tables 7-4, 7-7). At the medium and high C-N ratios, Train R2 and P had a higher productivity than the control (Train C) run at the respective C-N ratio (Tables 7-5 to 7-9). This result indicates that, compared to the respective control, residual biomass recycle to F2 increased productivities at all C-N ratios, and residual biomass recycle in parallel to F1, F2, and F3 increased productivities in the medium and high C-N ratio.

When comparing the productivities across the C-N ratios (e.g., Train R1 at the low, medium, and high C-N ratio), all fermentations had higher productivities at the medium C-N ratio (Table 7-10). Three of the trains (R1, R3, and P) had their lowest productivities at the low C-N ratio. In general, fermentations with low nitrogen (high C-N ratio) had slightly better productivities than fermentations with excess nitrogen (low C-N ratio). This result indicates that there was a decrease in productivity at low and high C-N ratios that cannot be compensated by residual biomass recycle (Table 7-10).

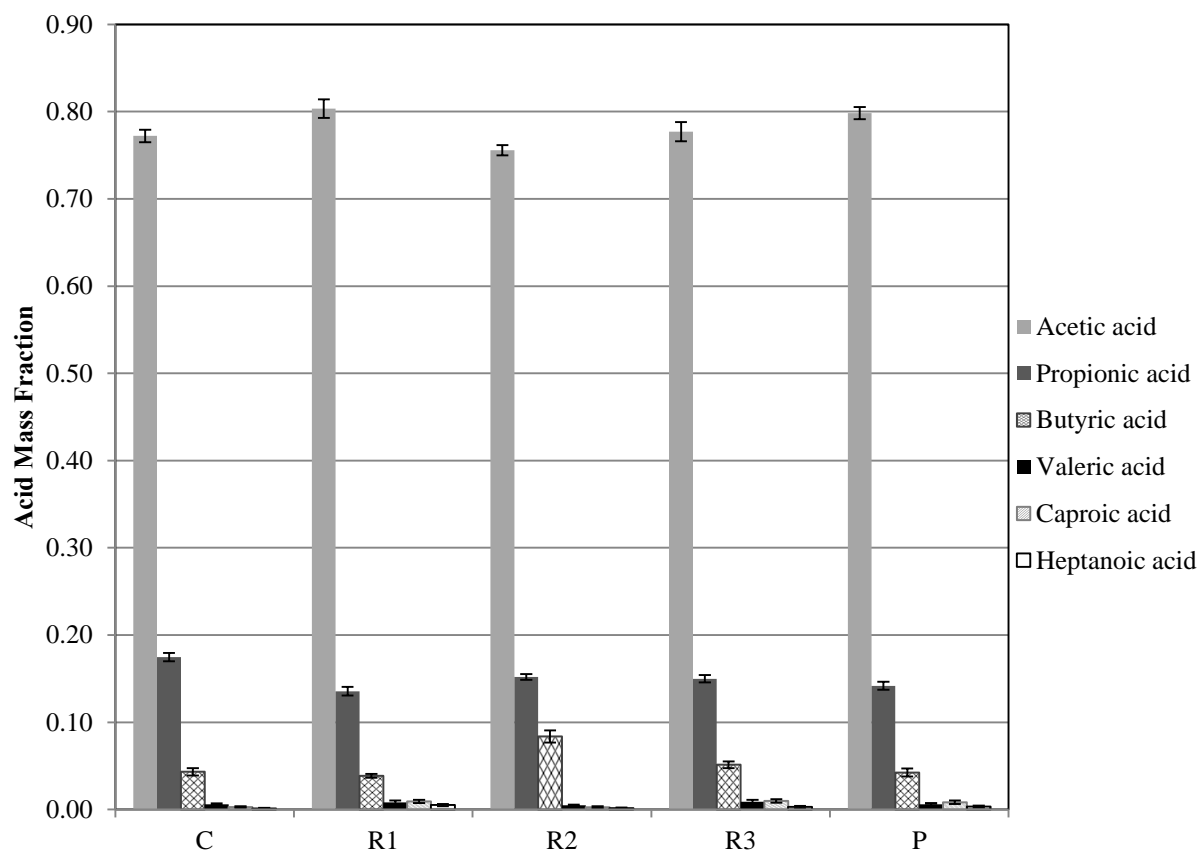


Figure 7-2. Carboxylic acid composition profile at C-N ratio ~ 14 g OC_{NA} /g N. Error bars are the 95% confidence intervals for each carboxylic acid composition during the steady-state period.

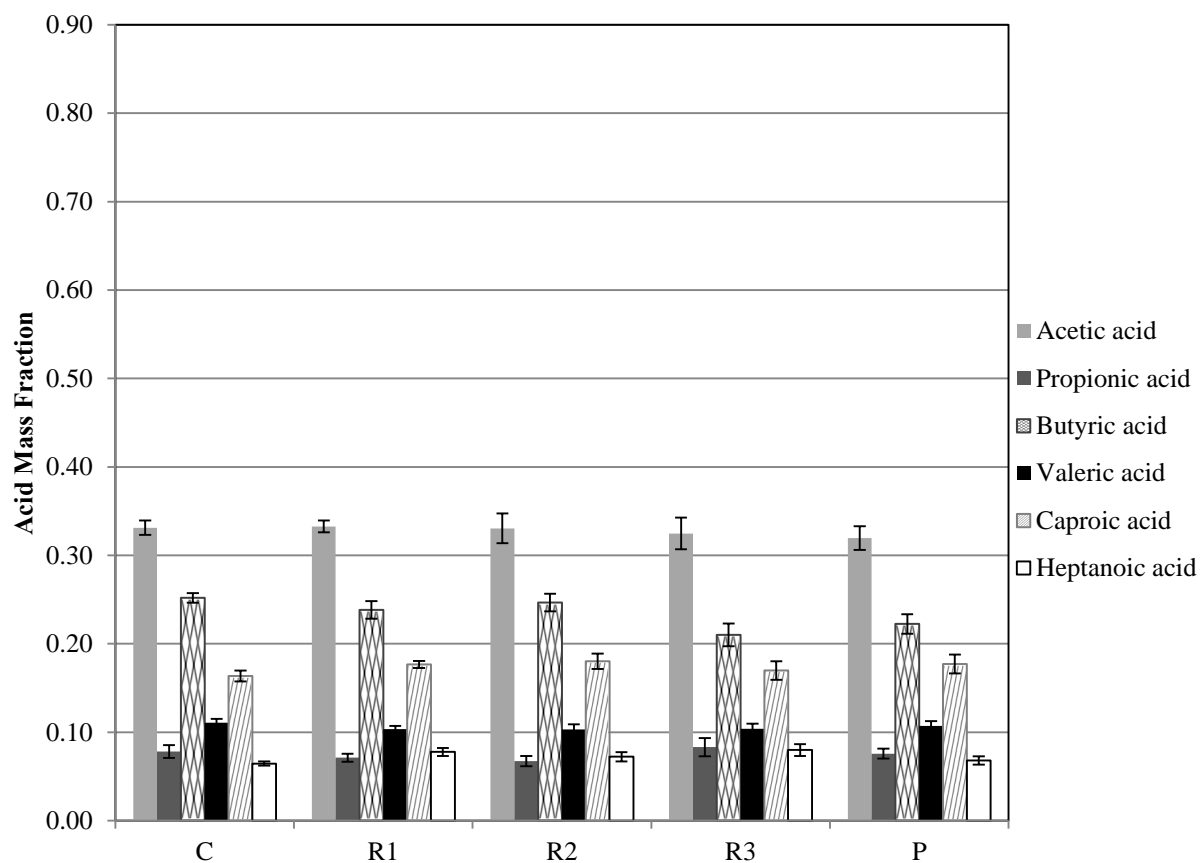


Figure 7-3. Carboxylic acid composition profile at C-N ratio ~ 24 g OC_{NA} /g N. Error bars are the 95% confidence intervals for each carboxylic acid composition during the steady-state period.

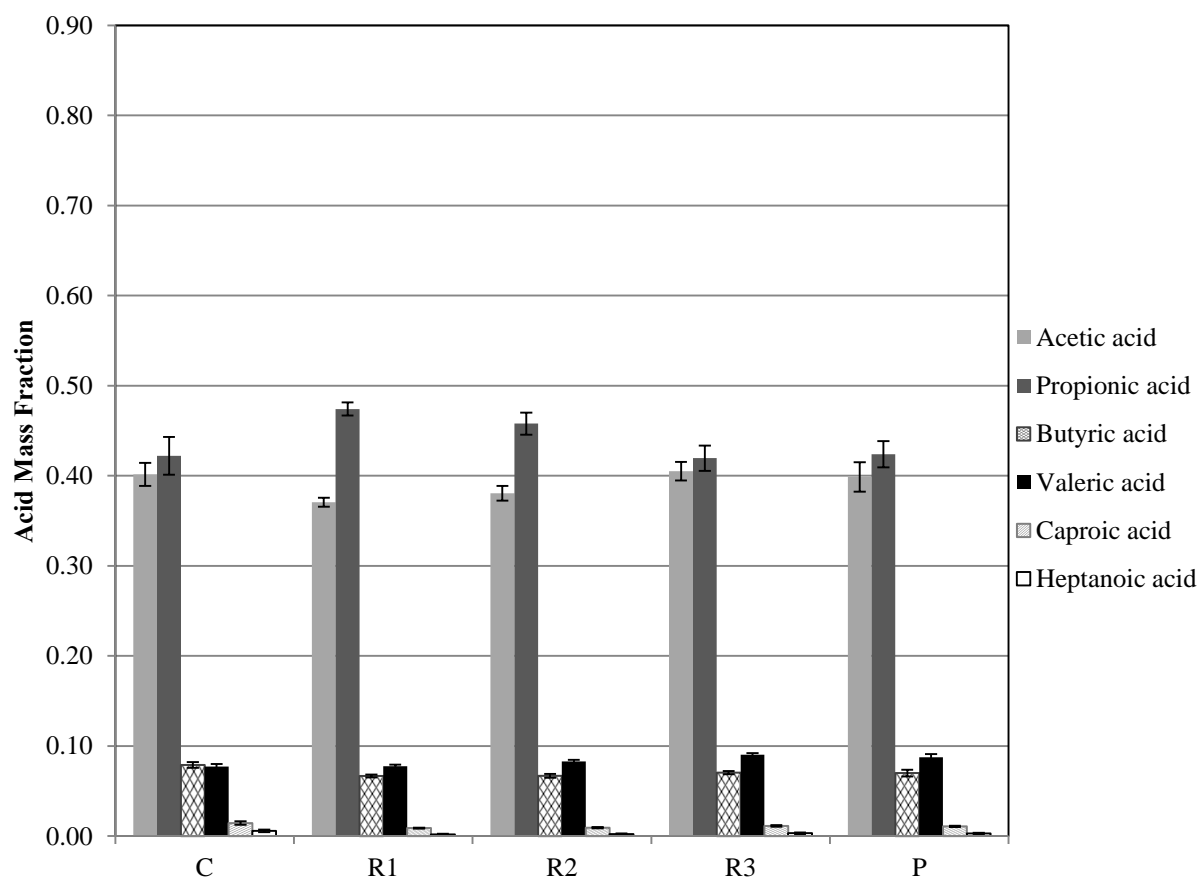


Figure 7-4. Carboxylic acid composition profile at C-N ratio ~ 74 g OC_{NA} /g N. Error bars are the 95% confidence intervals for each carboxylic acid composition during the steady-state period.

7.3.8 Yield

The exit yield Y_E (Equation 7-8) quantifies the sum of acid *exiting* the fermentation in the product transfer liquid, waste transfer solids, and liquid samples per g NAVS feed. The culture yield Y_C (Equation 7-11) represents the acid *produced* by the mixed-culture per g NAVS_{feed} and is equal to the exit yield less the feed yield Y_F (Equation 7-10). At the low C-N ratio, the Y_E and Y_C ranking was as follows: Train R2>R3>R1>P>C (Tables 7-4, 7-7). At the medium C-N ratio, the Y_E and Y_C ranking was as follows: Train P>R2=R3>R1>C (Tables 7-5, 7-8). At the high C-N ratio, the Y_E and Y_C ranking was as follows: Train R2>P>R3>R1=C (Tables 7-6, 7-9). For all C-N ratios, Y_E and Y_C were higher for Trains R2, R3, and P, indicating significant increase in yield from residual biomass recycle to F2, F3, and parallel to F1, F2, and F3. At all residual biomass recycle points, the Y_E and Y_C is ranked as follows: C-N ratio medium>high>low (Tables 7-4 to 7-6, 7-10), suggesting that medium and low amounts of nitrogen increased the Y_E and Y_C .

The exit acetic acid equivalent yield Y_{aE} quantifies the sum of acetic acid equivalents *exiting* the fermentation in the product transfer liquid, waste transfer solids, and liquid samples per g NAVS feed. At all C-N ratios, Y_{aE} was also improved by residual biomass recycle because the recycle trains (Trains R2, R3, P) produced more high-molecular-weight acids (Tables 7-7 to 7-9, Figures 7-2, 7-3) because of the recycling of nutrients or cells. At low C-N ratio, the Y_{aE} ranking was as follows: Train R2>R3=R1=P>C (Tables 7-4, 7-7). At the medium C-N ratio, the Y_{aE} ranking was as follows: Train R2=P>R3>R1=C (Tables 7-5, 7-8). At the high C-N ratio, the Y_{aE} ranking was as follows: Train R2>P>R3>R1=C (Tables 7-6, 7-9). At all residual biomass recycle points, the Y_{aE} is ranked as follows: C-N ratio medium>high>low (Tables 7-4 to 7-6, 7-10), suggesting that medium or low amounts of nitrogen increased the amount of high-molecular-weight acid.

The process yield Y_P (Equation 7-9) quantifies only the acid in the product transfer liquid per g NAVS_{feed}, which is sent downstream to be clarified, concentrated, and processed into chemicals and fuel; thus, Y_P represents the commercially relevant

acid yield. At the low C-N ratio, the Y_P ranking follows: Train $R3=R2>R1>P>C$ (Tables 7-4, 7-7). At the medium C-N ratio, the Y_P ranking follows: Train $P>R2>C>R3>R1$ (Tables 7-5, 7-8). At the high C-N ratio, the Y_P ranking follows: Train $R2>R1=P>C>R3$ (Tables 7-6, 7-9). With regards to the reflux ratios of recycling to F1, F2, or F3, for all three C-N ratios, the general trend is that recycling residual biomass to F2 gives the highest Y_P , followed by recycle to F3, then F1. This trend might exist because recycling residual biomass, which contains nutrients, cells, and substrate, to F2 maximizes the overall nutrient concentrations in F1, F2, F3, and F4. For most residual biomass recycle points, the Y_P is ranked as follows: C-N ratio medium>high>low (Tables 7-4 to 7-6, 7-10), suggesting that medium or low amounts of nitrogen produced more acid in the product liquor.

7.3.9 Conversion and selectivity

At most recycle points, at low, medium, and high C-N ratio, residual biomass recycle improved conversion perhaps because the recycle streams enabled Trains R1, R2, R3, and P to retain additional nutrients and cells. At low C-N ratio, the conversion ranking follows: Train $R1>R2>P>R3>C$ (Tables 7-4, 7-7). At the medium C-N ratio, the conversion ranking follows: Train $P>R1>C>R3>R2$ (Tables 7-5, 7-8). At high C-N ratio, the conversion ranking follows: Train $R1>P>R2>C>R3$ (Tables 7-6, 7-9). For all residual biomass recycle points, the conversion ranking follows: C-N ratio medium>high>low (Tables 7-4 to 7-6, 7-10). By having optimal substrate-to-nutrient ratios, such as the fermentations operating under medium amount of nitrogen, the microorganisms maximize growth by assembling the necessary enzymes to produce energy, and so digest more of the original NAVS.

When analyzing the optimal recycle point by comparing Trains R1, R2, and R3, the following trend is observed for all C-N ratios: as the recycle point is further from residue exit stream (F4), the conversion increases and selectivity decreases. For example, residual biomass recycle to F1 (Train R1) had the lowest selectivity and highest conversion, and residual biomass recycle to F3 (Train R3) had the highest selectivity but lowest conversion (when comparing Trains R1, R2, and R3). At low C-N

ratio, the selectivity ranking follows: Train R3>R2>C>P>R1 (Tables 7-4, 7-7). At the medium C-N ratio, the selectivity ranking follows: Train R3>R2>C>P=R1 (Tables 7-5, 7-8). At high C-N ratio, the selectivity ranking follows: Train R3>R2>P>C>R1 (Tables 7-6, 7-9). Recycling to F2 and F3 gives a higher selectivity than the control regardless of C-N ratio, perhaps because recycling to F2 and F3 maximized adapted cells and/or nutrients, which allowed the cellular metabolism to be more efficient at producing acid.

With the exception of Train C, the trains at the different residual biomass recycle points had a selectivity ranking as follows: C-N ratio low>high>medium (Tables 7-4 to 7-6, 7-10), suggesting that fermentations operating under high amounts of nitrogen tend to be more efficient at producing acids because of selectivity pressures. This also suggests that at medium C-N ratios, the fermentations begin to make alternative products besides acids, such as hydrogen (Lin and Lay, 2004) or are producing more cells.

7.3.10 *Carbon-nitrogen ratio and pH*

Because the carbon-nitrogen (C-N) ratio and pH affect fermentation performance, they must be controlled for accurate analysis. To compare fermentation trains, the C-N ratio was control by adding nitrogen (as urea) to the substrate, and was quantified as previously described (Smith et al., 2011). This study evaluated the low C-N ratio fermentations at 14 ± 3 g organic C_{NA}/g N and pH 8.4 ± 0.1 , the medium C-N ratio fermentations at 24 ± 3 g organic C_{NA}/g N and pH 5.4 ± 0.2 , the high C-N ratio fermentations at 74 ± 3 g organic C_{NA}/g N and pH 6.0 ± 0.03 (Tables 7-1 to 7-3). The performance trends for the C-N ratios could result from the amount of nitrogen or pH. In Tables 7-1 to 7-3, the different urea loading rates correspond to the VSLR and LRT. The pH was controlled with calcium carbonate, an inexpensive and industrially viable buffer. Urea, also inexpensive, was used as the nitrogen source to control C-N ratio. However, urea also affects pH (even with calcium carbonate buffer) by affecting the aqueous nitrogen in the fermentations. Therefore, to imitate industrial effects, pH was not precisely controlled.

In this study, the total ammonia nitrogen for low, medium, and high C-N ratio was typically 2553, 1764, and 776 mg nitrogen (N)/L, respectively. Free ammonia was

not directly measured, but it can be estimated from the total nitrogen and pH. At neutral pH, free ammonia accounts for 0.5% of the total ammonia nitrogen (free ammonia (NH_3) + ammonium ion (NH_4^+)). When the pH reaches 8.0–9.0, toxic amounts of aqueous nitrogen might be present as free ammonia (Ekinici et al., 2000). The medium and high C-N ratios had similar and very small amounts of free ammonia present, whereas the low C-N ratio had a higher amount of free ammonia. At the low C-N ratio, which operated at an average pH of 8.4, the free ammonia was about 12% of total ammonia nitrogen, or 309 mg N/L of free ammonia. At the medium C-N ratio, which operated at an average pH of 5.4, the free ammonia was about 0.02% of total ammonia nitrogen, or 0.28 mg N/L of free ammonia. At the high C-N ratio, which operated at an average pH of 6.0, the free ammonia was about 0.06% of total ammonia nitrogen, or 0.43 mg N/L of free ammonia. Anaerobic microorganisms that perform the acidogenic step resist ammonia nitrogen concentrations up to 16,000 mg N/L at a neutral pH (Lü et al., 2008). However, the microorganism community in these fermentations was not characterized, and therefore, the specific nitrogen tolerance is unknown. With the given information, it is believed that none of the fermentations had excess nitrogen except for fermentations at the low C-N ratio, which were exposed to growth limiting, but not toxic amounts of nitrogen.

Ammonia is a source of nitrogen for the synthesis of amino acids in microbial cells (Hungate, 1966). In this study, fermentations with a low C-N ratio operated with an abundance of nitrogen (C-N ratio < 20 g C/g N). Excess nitrogen is thought to be lost as ammonia gas at C-N ratio < 25 g C/g N (Cheremisinoff and Ouellette, 1985). Trains at the high C-N ratio (~74 g organic C_{NA} /g N) were considered to be nitrogen poor and not nitrogen starved (Smith et al., 2011).

The optimal pH for carboxylate fermentations would optimize the chosen fermentation performance variable and minimize costs. The optimal pH for carboxylate fermentations is controversial and deserves further investigation. For example, calcium carbonate does not buffer to pH 7; however it is inexpensive, is added in excess which potentially reduces fermentation maintenance costs as the pH does not need to be

continuously adjusted, and calcium salts are easier to separate downstream than other salts. Other phosphate or carbonate buffers can better control pH to neutrality, potentially leading to higher fermentation performance with the downside of a more expensive buffer and more pH monitoring costs. For example, ammonium bicarbonate is a superior buffer to calcium carbonate; however, controlling the C-N ratio is more complicated because this buffer requires continuous monitoring (Fu and Holtzapple, 2010a). A study has shown that mixed-acid fermentations are generally conducted at a pH between 5.5 to 6.5, a preferable pH for acidogens (Khanal, 2008). Other studies have shown that mesophilic methane digestors have an optimal pH between 6.7 to 7.4, and do not function well below 6 or above 8 (Frutton and Simmonds, 1959). However, nonmethanogenic organisms are reported to be not as sensitive and are able to function from pH 5 to 8.5 (Cheremisinoff and Ouellette, 1985). Other studies corroborate this result and have shown that marine microorganisms, comparable to the inoculant in this study, can tolerate a high alkalinity (Maeda and Taga, 1980).

The fermentation trains operating at a low C-N ratio had a corresponding high pH of 8.4, which occurred when added urea was hydrolyzed to ammonia and reacted with water to form ammonium hydroxide. All trains at low C-N ratio produced a remarkably high proportion of acetic acid (Figure 7-2). On a mass basis, of all carboxylic acids, acetic acid has the highest number of carboxylic groups (i.e., most protonating power). Therefore, to defend against the high pH (~8), the bacteria might have produced a majority of acetic acid to counteract the high pH. At a more neutral pH (~6), the conversion of acetic acid to high-molecular-weight carboxylic acids reduces acidity and helps mitigate the effect of low pH. If a high selectivity to acetic acid is desired, operating fermentations at a low C-N ratio and high pH could be an option, although at the cost of lower yields and product concentrations. In addition, ammonia inhibits methanogenesis and provides an advantage in the carboxylate fermentation by reducing the need to add methanogen inhibitors (e.g., iodoform). Methanogens, which lack a cell wall, are susceptible to ammonia toxicity because the un-ionized molecule can readily penetrate the cell membrane (Metzler, 2001).

7.3.11 Overview

Using residual biomass recycle, fermentation performance may be improved by retaining cells and nutrients. Five four-stage countercurrent fermentation trains (Figure 7-1) were run: (1) a control train with no recycle (Train C), (2) a train that recycled biomass to F1 (Train R1), (3) a train that recycled biomass to F2 (Train R2), (4) a train that recycled biomass to F3 (Train R3), and (5) a train that recycled biomass in parallel to F1, F2, and F3 (Train P). Each of the five four-stage countercurrent fermentation trains (Figure 7-1) was run at three C-N ratios: ~14 (low), ~24 (medium), and ~74 g C_{NA}/g N (high). Recycling biomass waste at different C-N ratios affects many coupled variables. Uncoupling the variables responsible for the positive or negative effects is difficult. Following are the separate effects of residual biomass recycle point and C-N ratio.

7.3.11.1 Effect of residual biomass recycle point

Trains R1, R2, R3, and P did not have different total acid and Aceq concentrations and Aceq-to-total-acid ratios than Train C. This indicates that, in general, the recycle point did not have an obvious effect on the concentration and proportion of high-molecular-weight carboxylic acids (Tables 7-4 to 7-9).

At all three C-N ratios, almost all recycle trains had higher Y_E , Y_C , and Y_{aE} than the control train. In general, for all C-N ratios, Train R2 had the highest productivity, total carboxylic acid exiting (g/d), Aceq exiting (g/d), Y_E , Y_C , Y_{aE} , and Y_P (Tables 7-7, 7-8). This indicates that residual biomass recycle, specifically to F2, increased microbial performance which improved the yield, production of more acid, and production of more high-molecular-weight acids (Tables 7-4 to 7-9).

At the low, medium, and high C-N ratio, Trains R1 and P consistently had the highest conversions, but lowest selectivities. Train R3 tended to have the highest selectivities but lowest conversions. For all C-N ratios, a trend in recycle point is best illustrated when comparing Trains R1, R2, and R3. Recycling residual biomass solids to F1 (Train 1) allowed for the longest retention of the biomass in the fermentation system, which increased conversion but decreased selectivity. Recycling residual biomass solids

to F3 (Train 3) allowed for the shortest retention of biomass, which increased selectivity but decreased conversion.

When recycling biomass waste to F1 (Train R1), the adapted cells (thought to be mostly in the solid phase, Golub et al. unpublished data), insoluble nutrients, and concentrated recalcitrant solids are retained in the fermentation system for a longer period of time than with Trains R2, R3, and P. This longer residence time allows the microorganisms a maximum amount of time to digest the easily digestible fermentor solids and recalcitrant recycled solids, giving Train R1 the higher conversion, followed by Train 2, and then Train R3. Generally, Train P has an average conversion of those found in Trains 1, 2, and 3.

For all C-N ratios, selectivity increases as the recycle entry point proceeds from F1, F 2, and F3. Nitrogen – a major nutrient source in the fermentation – was supplemented as urea, which is liquid soluble. Therefore, this trend in selectivity might exist because recycling to F1 (Train R1) allows the nitrogen in the waste biomass to quickly exit in the fermentation broth. In contrast, Trains R2, R3, and P might have a longer nitrogen retention time because the nitrogen from the biomass waste is fed to a fermentor farther from the exiting product liquid stream.

7.3.11.2 *Effect of C-N ratio*

Each of the five four-stage countercurrent fermentation trains (Figure 7-1) was run at three C-N ratios: ~14 (low), ~24 (medium), and ~74 g C_{NA}/g N (high). The fermentations adapted to the different nitrogen conditions, revealing that the carboxylate mixed culture can continuously adjust to stressful conditions, perhaps by the microorganisms changing their energy pathways, similar to other reported bacteria (Zhou et al., 2011). Fermentations operating under a medium C-N ratio performed best, followed by low C-N ratio, then by high C-N ratio. The microorganisms at the high C-N ratio might have remained longer in the stationary phase, which lowered performance. But the microorganisms at the low C-N ratio might have been in a more toxic environment, decreasing the cells viability and lowering performance even more than the high C-N ratio.

Compared to the low and high C-N ratios, fermentations run at a medium C-N ratio had higher biogas production, total acid and Aceq concentrations (g/L), daily total acid and Aceq exiting (g/d), Aceq-to-total-acid ratio, productivity, Y_E , Y_C , Y_P , and Y_{aE} , and conversion. Medium C-N ratios increased the overall exiting amount of total acid and Aceq, amount of digested biomass, and increased the proportion of high-molecular-weight acids (Figures 7-2 to 7-4), and therefore may be considered “optimal.”

Compared to the low C-N ratio, fermentations run at a high C-N ratio had higher biogas production, daily total acid and Aceq exiting (g/d), productivity, Aceq-to-total-acid ratio, Y_E , Y_C , Y_P , and Y_{aE} , and conversion, but had similar total acid and Aceq concentrations (g/L). Generally, fermentations run at a low C-N ratio had higher selectivities than the fermentations run at high and medium C-N ratios. This suggests that fermentations operating under high amounts of nitrogen tend to more efficiently produce acids from the recycled solids. Also, at medium C-N ratios, the trains digested more solids but made alternate products besides C2–C7 carboxylic acids, which may include CO₂, H₂, lactic acid, and formic acid. Operating at low C-N ratio and high pH contributed to high selectivity to acetic acid, which might be industrially desirable because acetic acid is preferred to produce electricity from microbial fuel cells (Liu et al., 2005; Min and Angelidaki, 2008), but at the cost of lower yields and product concentrations.

7.4 Conclusions

Recycling residual biomass to Fermentor 2 is the optimal recycle point, which might maximize nutrient and cell concentrations for all respective fermentors, improving most fermentation performance measures. Generally, compared to the low and high carbon-nitrogen (C-N) ratios, fermentations running at medium C-N ratio increased yield, conversion, and amount of high-molecular-weight acids, but decreased selectivity. Fermentations with excess or limited nitrogen were more efficient at producing acids. Because of its simplicity and positive benefit, industrial carboxylate fermentations should employ residual biomass recycle. Based on this study, the recommendation is C-N ratio of ~24 g C/g N and recycle to Fermentor 2.

8. RESIDUAL BIOMASS RECYCLE IN COUNTERCURRENT MIXED-ACID FERMENTATION: DECOUPLING CARBON-NITROGEN RATIO AND PH

To improve the performance of carboxylate fermentations, this study recycled residual biomass. Two four-stage countercurrent fermentations were operated: a control train with no recycle, and a train that recycled residual biomass to Fermentor 2. To decouple the effects of carbon-nitrogen (C-N) ratio and pH, these two trains operated with various combinations of C-N ratio and pH. At low C-N ratios, high concentrations of nitrogen are toxic at high pH, and less toxic near neutrality. In fermentations at low C-N ratios, compared to high pH, neutral pH had dramatically improved yield, conversion, selectivity, productivity, and amounts of high-molecular-weight acid. For fermentations at (1) low C-N ratio at high pH and (2) medium C-N ratio at low pH, recycling residual biomass improved performance. However, at low C-N ratio and near-neutral pH, compared to the no-recycle control, fermentations that recycled residual biomass had decreased performance; one explanation is that inhibiting substances are recycled.

8.1 Introduction

Lignocellulosic biomass demonstrates great potential as a renewable source of liquid transportation fuels (e.g., gasoline, diesel, and aviation fuels). Currently, transportation fuels are predominately supplied by petroleum; however, their combustion causes pollution, acid rain (Alekklett et al., 2010; Demirbas, 2007), and accounts for 57% of global anthropogenic greenhouse gas emissions (WWI, 2009). Converting lignocellulosic biomass into liquid fuels does not cause a net increase in atmospheric carbon dioxide because biomass growth sequesters the same amount of carbon dioxide that was released during combustion (Ragauskas et al., 2006; Sahin, 2011).

Because lignocellulosic biomass is not digestible by humans, its conversion to biofuels does not compete directly with food production. It is inexpensive and abundant,

and is an already important energy source (Zhang, 2008). Biomass has the potential to become one of the primary global energy sources, and modernized bioenergy systems will be an important contributor to establish sustainable development in both developed and developing countries (Demirbas, 2008). One promising technology is the carboxylate platform, which converts biomass into liquid transportation fuels (Agler et al., 2011; Holtzapple and Granda, 2009) and industrial chemicals (Granda and Holtzapple, 2008). The carboxylate platform has attractive economics and is commercially ready (Granda et al., 2009; Pham et al., 2010).

The carboxylate platform is a versatile and continuous biomass-to-energy technology that biologically converts nearly all biomass components (e.g., lignocellulose, fats, proteins, polysaccharides) into carboxylate salts, which can be subsequently chemically converted into chemicals and hydrocarbon fuels (Holtzapple et al., 1999; Holtzapple and Granda, 2009). In the fermentation step, biomass is fermented by a mixed-culture of microorganisms to produce carboxylic acids, which are buffered to form the corresponding carboxylate salts. These salts are precipitated and thermally converted to ketones (e.g., acetone), hydrogenated to mixed alcohols (e.g., isopropanol), and catalytically converted to hydrocarbons (e.g., gasoline, jet fuel). This process uses nearly any biomass feedstock, including waste biomass, which allows farmland and crops to be devoted to food production and not fuel production. The carboxylate platform has low capital and operating costs, does not require sterile operating conditions or added enzymes, and has reached the demonstration level of development.

In multi-staged countercurrent fermentations (Figure 8-1), such as the four-stage train in this study, solids and liquids are transported through a series of fermentors (a *train*) in opposite directions. Because biomass is a heterogeneous mixture, the easily fermentable solids digest first; therefore, as biomass decomposes, it becomes less reactive. The countercurrent flow allows the least-reactive (most-digested) biomass to contact the lowest acid concentration, which minimizes product inhibition (Aiello-Mazzarri et al., 2006). The most-reactive (least-digested) biomass contacts the highest acid concentration, which allows for continued digestion even though the reaction is

highly inhibited. This countercurrent strategy achieves both high product concentration and high conversion (Fu and Holtzapple, 2010b). Fresh biomass is added to Fermentor 1, with the remaining solid residue undergoing conversion in subsequent fermentors to achieve greater substrate conversion. Biomass waste exits Fermentor 4, while product liquid exits Fermentor 1 (Figure 8-1).

Microorganisms (e.g., bacteria, archae, fungi) are the biocatalysts that convert lignocellulose to mixed acids. Recovering and recycling the microorganisms from the waste streams may improve fermentation performance; however, separating microorganisms from biomass may be difficult and costly. Compared to cell recycle, recycling unprocessed residual biomass back into the fermentation system is potentially less expensive and perhaps more commercially viable. In a four-stage countercurrent fermentation system, previous studies have demonstrated that recycling residual biomass enhances fermentation performance, and the optimal recycle point is Fermentor 2 (Ch. 6).

In fermentations, nitrogen is an essential nutrient needed in the largest amount for cell reproduction, maintenance, and metabolism, and therefore has a pronounced impact on fermentation performance. The carbon-nitrogen (C-N) ratio quantifies the relative proportion of non-acid organic carbon (OC_{NA}) to total nitrogen (N). Previous studies have demonstrated that the “medium” C-N ratio in this study (~ 24 g OC_{NA} /g N) is an optimal substrate-to-nutrient ratio, and enables the bacteria to increase the proportion of higher-molecular-weight acids, which are more thermodynamically demanding to produce (Forrest et al., 2011). In continuous fermentations, productivity increases as the C-N ratio approached 30 g OC_{NA} /g N (Smith and Holtzapple, 2010). In batch fermentations, the optimal acid production occurs at 20–40 g OC_{NA} /g N (Smith and Holtzapple, 2011a). In all of the above mentioned studies, urea was used to increase the nitrogen concentration. Nitrogen is essential to cell growth, so a nitrogen-rich environment should provide the microorganisms with a supportive environment for growth. However, urea affects pH, especially at low C-N ratios. These studies have not investigated the separate effects of C-N ratio and pH in continuous fermentations.

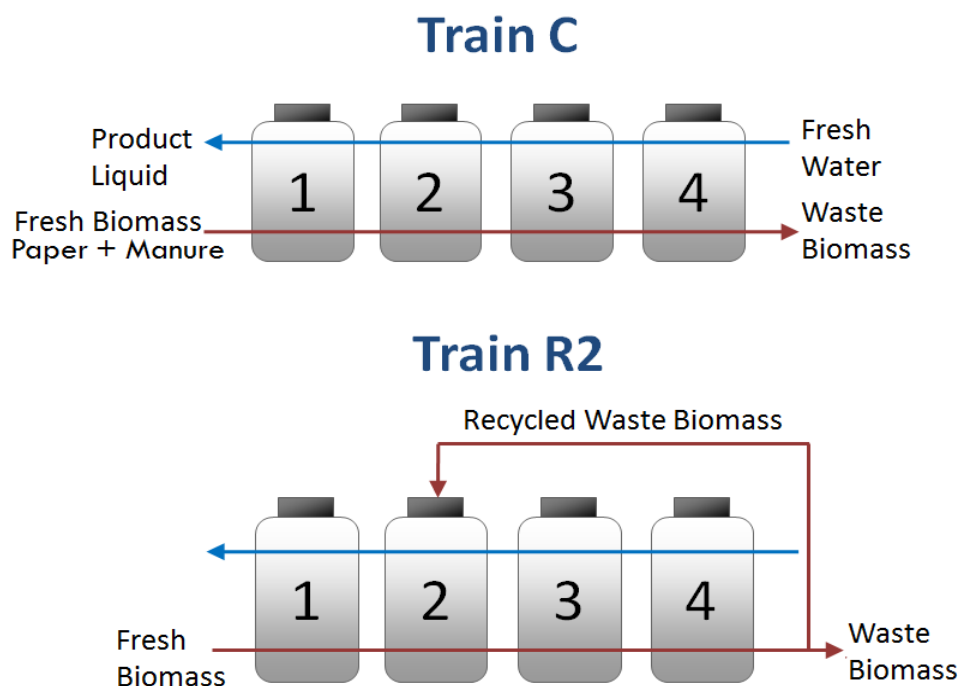


Figure 8-1. Diagram of the residual biomass recycle experiment, depicting the control (Train C) with no recycle and residual biomass recycle to the Fermentor 2 (Train R2).

Conventional carboxylate fermentations employ calcium carbonate, an inexpensive and industrially viable buffer, with small amounts of urea added to supplement nitrogen (Agbogbo, 2005; Aiello-Mazzarri et al., 2006; Domke, 1999; Forrest, 2010; Golub et al., 2011a; Ross, 1998; Smith and Holtzapple, 2011a). In a CO₂-rich atmosphere, the pH is slightly acidic (5.5–6.2). Recently, ammonium bicarbonate has been employed as a buffer, which allows the pH to be nearly neutral (6.7–7.1) (Fu and Holtzapple, 2010a). When ammonium bicarbonate is added as a buffer, the microorganisms grow in a nitrogen-rich environment. Ammonium bicarbonate has been used in carboxylate fermentations, which outperform fermentations buffered with calcium carbonate. However, these studies did not distinguish the separate performance benefits of either the more neutral pH *or* added nitrogen. It is important to understand

the separate effects of C-N ratio and pH. Previous carboxylate fermentation studies with ammonium bicarbonate have not decoupled these variables.

Compared to calcium carbonate, ammonium bicarbonate is inconvenient to use because it buffers alkaline, and therefore must be metered to regulate pH. However, with calcium carbonate, excess calcium carbonate can be added, which solubilizes as needed to regulate the pH. As an alternative to ammonium bicarbonate, this study employed urea as both a source of nitrogen and ammonia ions to buffer acid production. Excess calcium carbonate was added to prevent decreased pH. Because urea hydrolyzes to ammonia, which reacts with water to produce ammonia hydroxide, the pH has the potential to go excessively high. To maintain high amounts of nitrogen at a near-neutral pH, in one set of experiments, the pH was adjusted to near neutrality (6.9 – 7.2) by adding hydrochloric acid.

The purpose of this study is to understand the effects of operating carboxylate fermentations with high concentrations of nitrogen. This was achieved by decoupling the effects of pH and C-N ratio in continuous countercurrent fermentations with and without residual biomass recycle. This can be achieved by evaluating the fermentation performance at (1) low C-N ratio and high pH; (2) low C-N ratio and near-neutral pH; and (3) medium C-N ratio and low pH, which is typical of conventional fermentations buffered with calcium carbonate.

8.2 Materials and methods

8.2.1 Fermentor configuration

The fermentors were 1-L polypropylene centrifuge bottles capped by a rubber stopper inserted with a glass tube (Domke et al., 2004; Thanakoses et al., 2003). Two segments of 1/4-in stainless steel pipe were inserted through the rubber stopper into the vessel to mix the fermentor contents as it rotated in the rolling incubator. A rubber septum sealed the glass tube and allowed for gas sampling and release.

8.2.2 *Fermentation medium*

The deoxygenated medium was prepared by boiling distilled water to liberate dissolved oxygen. After cooling to room temperature in a covered vessel, to further reduce the oxygen content, 0.275 g/L cysteine hydrochloride and 0.275 g/L sodium sulfide were added.

8.2.3 *Inoculum*

The inoculum was an adapted mixed-culture of marine microorganisms from beach sediment collected in Galveston Island, TX. Sediment was removed from the bottom of multiple 0.5-m-deep shoreline pits. Samples were immediately placed in airtight plastic bottles filled with deoxygenated water, capped, and frozen at $-20\text{ }^{\circ}\text{C}$ until use. Before inoculation, samples were thawed, shaken vigorously, and allowed to settle by gravity. Equal parts of the resulting supernatant were homogenized, and aliquots were used to standardize the fermentation inoculum to 12.5% of the initial working volume (Forrest et al., 2010a; Thanakoses, 2002). The composition of the bacterial community in mixed-acid fermentation has been reported elsewhere (Hollister et al., 2010; Hollister et al., 2011).

8.2.4 *Methanogen inhibition*

Iodoform (CHI_3) was used to inhibit methane production. Every 48 h, iodoform solution (80 μL , 20 g CHI_3/L 190-proof ethanol) was added to each fermentor (Domke et al., 2004). Iodoform is sensitive to light, air, and temperature, and so the solution was kept in amber-colored glass bottles wrapped in foil and stored at $-20\text{ }^{\circ}\text{C}$ (Agbogbo and Holtzapple, 2007).

8.2.5 *Carbon-nitrogen ratio*

The C-N ratio is defined as the mass of non-acid organic carbon (g OC_{NA}) per total mass of nitrogen (g N) (Smith et al., 2011). Total C and N contents (g/100 g wet sample) were determined by Texas A&M University Soil, Water, and Forage Testing Laboratory (College Station, TX) using an Elementar Variomax CN. Based on the carbon and nitrogen contents of the paper, chicken manure, and urea (ACS grade), the

amount of each was calculated to achieve the desired C-N ratio and VS concentration (Table 8-1).

8.2.6 *Substrate*

Shredded office paper, which served as the energy source, was obtained from a local recycling center. No pretreatment was required. Chicken manure, which served as an undefined nutrient source, was obtained from Feather Crest Farms, Inc. (Bryan, TX) and was dried at 105 °C for 48 h. Wet chicken manure will degrade over time, so to maintain consistency during the entire experiment, dried and homogenized chicken manure was used. Dried chicken manure had a C-N ratio of 12.9 ± 3.4 g OC_{NA}/g N and an acid concentration of 0.05 ± 0.01 g acid/g dry chicken manure. Previous studies have found the C-N ratio of shredded office paper is 138.3 ± 43 g OC_{NA}/g N (Smith and Holtzapple, 2010). The substrate concentration is expressed as non-acid volatile solids (NAVS), which is the combustible portion of the substrate minus carboxylic acids present in the feed. Urea was used as a supplemental nitrogen source.

8.2.7 *Residual biomass recycle fermentation procedure*

Two four-stage countercurrent fermentation trains (Figure 8-1) were run: (1) a control train with no recycle (Train C), and (2) a train that recycled residual biomass to Fermentor 2 (Train R2). (*Note: Residual biomass* is defined as the centrifuge solids exiting Fermentor 4 (F4), which consisted of ~15% dry mass for the low C-N ratio fermentations and ~25% for the medium C-N ratio fermentations). For Train R2 at all C-N ratios and pH conditions, to normalize the residual biomass recycle ratio, the amount of residual biomass recycled from F4 to F2 during each transfer was controlled (18 g wet, Table 8-1). The residual biomass waste reflux was then calculated as g recycled residual biomass/100 g residual biomass exiting the process from Fermentor 4. (*Note: The moisture content of the recycle stream is the same as the moisture content of the exit stream; therefore, this can be either a wet or dry basis*).

Table 8-1. Operating parameters at (a) low C-N ratio and low pH, (b) low C-N ratio and near-neutral pH, and (c) medium C-N and low pH. Normalized parameters represent the mean of the steady-state values \pm CI (95% CI).

Fermentation Train		C (a)		R2 (a)		C (b)		R2 (b)		C (c)		R2 (c)	
Controlled	Solid and liquid transfer frequency, T (h)	48		48		48		48		48		48	
	NAVS feed rate (g NAVS/ T)	24.3		24.3		24.3		24.3		24.3		24.3	
	Dry solids added (g/ T)	32		32		32		32		32		32	
	Manure added (g/ T)	7.6		7.6		7.6		7.6		7.6		7.6	
	Urea added (g/ T)	3.0		3.0		3.0		3.0		1.0		1.0	
	Calcium carbonate added (g/ T)	4.0		4.0		4.0		4.0		4.0		4.0	
	Fermentor recycle point	–		F2		–		F2		–		F2	
	Residual biomass recycled (g, wet)	–		18		–		18		0		18	
	Liquid feed rate (mL/ T)	300		300		300		300		300		300	
	Solid cake retained in F1 (g, wet)	125		125		125		125		125		125	
	Solid cake retained in F2–F4 (g, wet)	225		225		225		225		225		225	
	Centrifuged liquid retained in F1–F4 (mL)	0		0		0		0		0		0	
	Methane inhibitor (μ L/ T -fermentor)	80		80		80		80		80		80	
	Normalized	Fermentor reflux ratio (g recycled biomass/g exiting biomass)	–		0.07 \pm 0.00		–		0.08 \pm 0.00		–		0.15 \pm 0.02
Volatile solid loading rate, VSLR (g NAVS/ L_{liq} -d)		7.4 \pm 0.14		7.4 \pm 0.04		6.7 \pm 0.12		7.0 \pm 0.08		6.1 \pm 0.06		6.4 \pm 0.05	
Liquid residence time, LRT (d)		12.9 \pm 1.80		15.1 \pm 0.59		12.9 \pm 0.99		18.4 \pm 1.27		13.6 \pm 0.6		13.7 \pm 0.7	
Total liquid volume, TLV (L)		1.64 \pm 0.03		1.64 \pm 0.01		1.82 \pm 0.03		1.75 \pm 0.02		1.98 \pm 0.02		1.90 \pm 0.02	
Volatile solid, VS, concentration (g NAVS/ L_{liq})		62 \pm 3		72 \pm 2		58 \pm 2		58 \pm 2		55 \pm 1		54 \pm 2	
Dry solid, DS, concentration (g NADS/ L_{liq})		86 \pm 3		106 \pm 2		82 \pm 2		87 \pm 2		91 \pm 2		81 \pm 2	
Average carbon-nitrogen ratio, C-N ratio (g OC_{NA} /g N)		11.1 \pm 3.95		13.5 \pm 4.97		9.06 \pm 1.26		9.13 \pm 1.66		21.4 \pm 2.2		27.2 \pm 6.5	
Average pH (F1–F4)		8.40 \pm 0.15		8.26 \pm 0.14		6.92 \pm 0.32		7.22 \pm 0.42		5.67 \pm 0.12		5.31 \pm 0.13	
Total urea added (g urea/ L_{liq} -d)	0.91 \pm 0.02		0.91 \pm 0.01		0.83 \pm 0.00		0.86 \pm 0.00		0.25 \pm 0.00		0.26 \pm 0.00		

NAVS = Non-acid volatile solids; NADS = Non-acid dry solids

The feed consisted of 80% shredded office copier paper and 20% dry homogenized chicken manure on a dry mass basis. Each fermentor was incubated at 40 °C and operated as a submerged fermentation. The fermentation trains were initiated as batch cultures under anaerobic conditions with a concentration of 100 g non-acid dry solids (NADS)/L deoxygenated water, which was achieved by adding substrate, nutrient source (manure and urea), inoculum, buffer (calcium carbonate), and liquid medium to each fermentor.

After the first week of batch growth, solid/liquid transfers began with the objective to reach steady state. Every 48 h, fermentors were removed from the incubator, the gas volume was collected, liquid samples were taken, the pH was measured, fermentors were centrifuged (3300×g, 25 min), and the solid/liquid mass transfers were performed. Fresh deoxygenated water was added to Fermentor 4 (F4), and all of the filtered liquid was transferred from Fermentor 3 (F3) to Fermentor 2 (F2), F2 to Fermentor 1 (F1), and out of F1 as the product liquid. In a countercurrent manner, fresh substrate was fed to F1 and a portion of the homogenized solids was transferred from F1 to F2, F2 to F3, F3 to F4, and exited F4 as residual biomass. During transfers, the solid wet weight retained (including the fed recycled biomass) equaled 225 g in F2, F3, and F4, and 125 g in F1. A preset amount of residual biomass (Table 8-1) was homogenized and recycled back into F2 (Train R2). In each fermentor, the solids were resuspended, iodoform was added, and calcium carbonate was added to neutralize carboxylic acids and buffer the system (Table 8-1). Urea was added to adjust the C-N ratio. During solid and liquid transfers, when the fermentors were open to the atmosphere, anaerobic conditions were maintained by flushing the fermentors with nitrogen gas (Praxair, Bryan, TX). (*Note: Nitrogen flushing was a precautionary step; these anaerobic fermentations have been shown to resist intermittent air exposure (Golub et al., 2011b).*) The fermentors were then resealed and placed back in the incubator.

8.2.8 *Residual biomass recycle mass balance*

All performance variables were calculated based on a mass balance outside of the four fermentations and residual biomass recycle loop system.

8.2.9 *Analytical methods*

8.2.9.1 *Carboxylic acid concentration determination*

Fermentation product liquid was collected every 48 h and analyzed for C2–C7 fatty acids as previously described (Golub et al., 2011a).

8.2.9.2 *Biogas analysis*

For the first week, because of the high initial digestion rate, each fermentor was vented daily; thereafter, it was vented every 48 h. Biogas was removed through the fermentor septum, and the volume was measured by displacing liquid in an inverted graduated glass cylinder filled with a 300 g/L CaCl₂ solution, which prevented microbial growth and carbon dioxide adsorption (Domke, 1999).

Biogas composition (i.e., carbon dioxide, nitrogen, oxygen, and methane) was determined by manually injecting 5-mL gas samples into an Agilent 6890 Series chromatograph with a thermal conductivity detector (TCD). A 4.6-m-long, 2.1-mm-ID stainless steel packed column (60/80 Carboxen 100, Supelco 1-2390) was used. The inlet temperature was 230 °C, the detector temperature was 200 °C, and the oven temperature was 200 °C. The total run time was 10 min and helium was the carrier gas.

8.2.9.3 *Moisture and ash contents*

Moisture and ash contents were determined by drying in a 105 °C forced-convection oven for at least 24 h, and subsequent combustion in a 575 °C furnace for at least 12 h by NREL procedures No. 001 and 005, respectively (NREL, 2004). The ash content was calculated on a dry basis. The consumption of non-acid volatile solids (NAVS) was determined using the inert-ash approach as described previously (Smith et al., 2011).

8.2.10 *Operating parameters*

Previous investigations using continuous countercurrent fermentations have shown that adequate conversion and exit yield were achieved with volatile solid loading rate (VSLR) of ~6.3 g NAVS/L·d and liquid residence time (LRT) of ~13 d (Chan and Holtzapfle, 2003; Ross, 1998; Smith et al., 2011); therefore, this VSLR and LRT were

chosen to investigate the performance of a residual biomass recycle fermentation system. The LRT and VSLR (Table 8-1) were regulated by controlling the liquid and solid transfer frequency (T), the non-acid volatile solids (NAVS) feed rate, and the liquid feed rate per transfer. Volatile solids (VS) are defined as the mass of dry solid material that is combusted at 575 °C after 12 h, and NAVS are defined as VS less the amount of carboxylate salt residue that remains in the ash:

$$\text{NAVS} = (\text{g total biomass})(1 - \text{MC})(1 - \text{AC}) - (\text{g acid in biomass}) \quad (8-1)$$

where MC (g water/g wet biomass) is the fraction of moisture in the biomass, and AC (g ash/g dry biomass) is the fraction of dry ash remaining after 12 h of combustion at 575 °C. In performance calculations, NAVS is preferred because it ensures the product is not quantified with the reactant.

The nutrient source (dried chicken manure) contains carboxylic acids. To more accurately quantify fermentor productivity, the amount of acid entering the system in the manure is subtracted from the amount of acid exiting the system in the product liquid and discarded residual biomass. To determine the amount of acid in the manure, the dry manure was resuspended in distilled water at different concentrations. The acid in the supernatant was analyzed by GC.

The VSLR and the LRT are calculated as follows:

$$\text{VSLR} = \frac{\text{NAVS feed (g)}}{\text{TLV(L)} \cdot \text{time (d)}} \quad (8-2)$$

$$\text{LRT} = \frac{\text{TLV (L)}}{\text{liquid flow rate out of fermentation train (L/d)}} \quad (8-3)$$

The total liquid volume (TLV) includes both free and interstitial liquid. Liquid flow rate out of fermentation train includes product liquid exiting F1 and liquid in residual biomass exiting F4.

8.2.11 Definition of terms

To account for the total mass in the system, a mass balance closure was calculated with Equation 8-4.

$$\text{mass balance closure} = \frac{\text{mass out (g)}}{\text{mass in (g)} + \text{water of hydrolysis (g)}} \quad (8-4)$$

Cellulose is a polysaccharide composed of individual anhydroglucose units (glucan, MW = 162 g/mol). During digestion, cellulose is enzymatically hydrolyzed to glucose by adding a water molecule. The water of hydrolysis was calculated as previously described (Chan and Holtzaple, 2003).

The mixed-acid concentration can be expressed as molar acetic acid equivalents (α), which is the reducing potential of an equivalent amount of acetic acid (Datta, 1981).

$$\begin{aligned} \alpha = & 1.00 \times \text{acetic (mol/L)} + 1.75 \times \text{propionic (mol/L)} \\ & + 2.50 \times \text{butyric (mol/L)} + 3.25 \times \text{valeric (mol/L)} \\ & + 4.00 \times \text{caproic (mol/L)} + 4.75 \times \text{heptanoic (mol/L)} \end{aligned} \quad (8-5)$$

The acetic acid equivalent (Aceq) can be expressed on a mass basis as

$$\text{Aceq (g/L)} = 60.05 \text{ (g/mol)} \times \alpha \text{ (mol/L)} \quad (8-6)$$

Aceq proportionally weighs the higher-chained carboxylic acids (C₃ to C₇); the higher acids have higher Aceq than lower acids.

8.2.12 Measuring performance

The feed and exit rate of acid, ash, NAVS, water, and gas were determined during the steady-state period. The average rate of each component was calculated using the *slope method* (Smith and Holtzapple, 2011b). In this method, the moving cumulative sum of each component is plotted with respect to time. The slope of the steady-state portion of this line is the rate. All performance variables (e.g., conversion, selectivity, and yield) were calculated from the averaged component rates determined by the slope method, as described below:

$$\begin{aligned}
 \text{Conversion } x &\equiv \frac{\text{NADS}_{\text{feed}} \text{ g} - \text{NADS}_{\text{exit}} \text{ (g)}}{\text{NAVS}_{\text{feed}} \text{ (g)}} \\
 &= \frac{\text{NAVS}_{\text{feed}} \text{ g} + \text{Ash}_{\text{feed}} \text{ g} - \text{NAVS}_{\text{exit}} \text{ g} - \text{Ash}_{\text{exit}} \text{ (g)}}{\text{NAVS}_{\text{feed}} \text{ (g)}} \quad (8-7) \\
 &= \frac{\text{NAVS}_{\text{consumed}} \text{ (g)}}{\text{NAVS}_{\text{feed}} \text{ (g)}}
 \end{aligned}$$

Exit yield (Y_E)

$$\equiv \frac{\text{total acid output from solid and liquid streams (g)}}{\text{NAVS}_{\text{feed}} \text{ (g)}} \quad (8-8)$$

$$\text{Process yield } (Y_P) \equiv \frac{\text{total acid output in product liquid stream (g)}}{\text{NAVS}_{\text{feed}} \text{ (g)}} \quad (8-9)$$

$$\text{Culture yield } (Y_C) \equiv \frac{\text{total acid produced (g)}}{\text{NAVS}_{\text{feed}} \text{ (g)}} \equiv Y_E - Y_F \quad (8-10)$$

$$\text{Feed yield } (Y_F) \equiv \frac{\text{total acid entering with feed (g)}}{\text{NAVS}_{\text{feed}} \text{ (g)}} \quad (8-11)$$

$$\begin{aligned} \text{Selectivity } (\sigma) &\equiv \frac{\text{total acid produced (g)}}{\text{NAVS}_{\text{feed}}(\text{g}) - \text{NAVS}_{\text{exit}}(\text{g})} & (8-12) \\ &\equiv \frac{\text{total acid produced (g)}}{\text{NAVS digested (g)}} = \frac{Y_E}{x} \end{aligned}$$

$$\text{Acid productivity } (P) \equiv \frac{\text{total acids produced (g)}}{\text{TLV (L)} \cdot \text{d}} \quad (8-13)$$

where $\text{NADS}_{\text{feed}}$ is the non-acid dry solids fed, $\text{NADS}_{\text{exit}}$ is the non-acid dry solids removed from the fermentation, $\text{NAVS}_{\text{feed}}$ is the non-acid volatile solids fed, $\text{NAVS}_{\text{exit}}$ is the non-acid volatile solids removed from the fermentation, Ash_{feed} is the inert solids fed in biomass feed and buffer, Ash_{exit} is the inert solids exiting in all solid and liquid streams, and TLV is the total liquid volume in the fermentation train including free and interstitial liquid. NADS includes the ash and volatile solid component of biomass. In all liquid and solid streams, ash is accounted for and is assumed to be conserved in the fermentation (Ash_{feed} equals Ash_{exit}), canceling Ash from Equation 8-7.

Per g NAVS fed, the exit yield (Y_E) represents the sum of acid in the product transfer liquid, waste transfer solids, and liquid samples removed from sampling. The process yield (Y_P) represents all the acid in the product transfer liquid per g of NAVS fed. The feed yield (Y_F) is the total g acid entering with the feed per g NAVS fed, and the culture yield (Y_C) is the exit yield less the feed yield.

8.2.13 Statistical analysis

Statistical analysis was performed using Excel 2007 (Microsoft, USA). The mean and standard deviations of the total acid concentrations, acetic acid equivalent (Aceq), NAVS in and out were determined from steady-state operating data. For all countercurrent trains, the average time required to reach steady state was ~67 d. These averaged values were then used to calculate the acid productivity (P), selectivity (σ), yield (Y), and conversion (x) with a 95% confidence interval (CI). Unless specified otherwise, all comparisons in the Results and Discussion section are statistically

significant. The steady-state region was the period during which the product total acid and Aceq concentration, dry solids exiting, liquid volume and solid weight of each fermentor, pH, and mass of acid exiting did not vary by more than 2.2 standard deviations from the average for a period of at least one liquid residence time. For each train, the slope of the summed data was used to calculate the means of the performance variables, which were compared using a Student's two sample *t*-test (two-tailed, Type 3). The *p* values had a familywise error rate of 0.05 using the Bonferroni correction. All error bars are reported at 95% CI.

8.3 Results and discussion

The purpose of this study is to determine the effect of operating fermentors with high nitrogen concentrations (i.e., low C-N ratio), which is achieved by adding urea. Because high urea addition can lead to high pH, in some cases, hydrochloric acid was added to neutralize the pH, which decouples the effect of C-N ratio from pH. Conventionally, fermentors are operated with a medium C-N ratio with calcium carbonate buffer, which is slightly acidic (~5.5). For comparison purposes, these fermentations were included also.

Each fermentation train consisted of a four-stage countercurrent semi-continuous submerged fermentation system. Two fermentation trains were operated, both with different residual biomass recycle points: a control train with no recycle (Train C), a train that recycled residual biomass to Fermentor 2 (Train R2).

Both fermentation trains were operated under three conditions: (1) low C-N ratio and high pH; (2) low C-N ratio and near-neutral pH; and (3) medium C-N ratio and low pH, which is typical of conventional fermentations buffered with calcium carbonate. To compare the results of all trains, the LRT and VSLR operating parameters were normalized by explicitly controlling the liquid/solid mass transfer frequency (*T*), NAVS feed rate, the liquid feed rate, and the amount of cake retained in each fermentation reactor per transfer (Table 8-1). Overall, the performance trends that occurred with residual biomass recycle could be the result of any of the multiple components in the biomass waste (e.g., cells, volatile solids, ash, acid, nutrients) that are transported in the

solid or liquid streams. In previous studies, urea was used to control C-N ratio in fermentations. However, urea affects pH. This study attempts to decouple the effects of C-N ratio and pH; therefore, the relative performance trends affected by the amount of nitrogen versus pH are explored.

For all six experimental conditions, the accumulated mass of total carboxylic acids and Aceq exiting, NADS added, and NADS removed from their respective trains was found. The slopes of the quasi-steady-state regression lines provided the daily total acid and Aceq exiting, NADS exiting, and NADS removed on a mass basis (Table 8-2). Productivity was calculated as the mass rate of acid produced per total liquid volume.

8.3.1 *Reflux ratio*

Attempts were made to normalize the residual biomass reflux ratio by recycling a controlled amount of residual biomass (18 g wet). As a proportion of the total mass that exits the train, the residual biomass waste reflux was higher at the medium C-N ratio (~15 g wet recycled residual biomass/100 g wet residual biomass exiting) than at the low C-N ratio at high and near-neutral pH (~8 g wet recycled residual biomass/100 g wet residual biomass exiting) (Table 8-1). The reflux ratio is difficult to normalize because the conversion, and therefore the total solids exiting the fermentation, are different for each operating condition. Fermentations at the medium C-N ratio had a higher conversion. Because less residual biomass exited, the proportion of biomass that was recycled was higher for the medium C-N ratio than for the low C-N ratio.

Table 8-2. Performance measures at (a) low C-N ratio and low pH, (b) low C-N ratio and near-neutral pH, and (c) medium C-N and low pH. Values represent the mean of the steady-state values \pm CI (95% CI).

	C (a)	R2 (a)	C (b)	R2 (b)	C (c)	R2 (c)
Total carboxylic acid concentration (g/L)	11.90 \pm 0.70	13.53 \pm 0.47	14.32 \pm 0.62	13.62 \pm 0.42	16.69 \pm 0.52	18.46 \pm 0.75
Aceq concentration (g/L)	13.25 \pm 0.79	15.30 \pm 0.53	17.64 \pm 0.79	17.01 \pm 0.58	26.10 \pm 0.88	29.06 \pm 1.33
Total carboxylic acid exiting (g/d)	0.78 \pm 0.00	0.93 \pm 0.00	1.47 \pm 0.01	1.09 \pm 0.00	2.01 \pm 0.01	2.16 \pm 0.01
Aceq exiting (g/d)	0.85 \pm 0.00	1.04 \pm 0.00	1.79 \pm 0.01	1.33 \pm 0.01	3.15 \pm 0.01	3.52 \pm 0.01
Aceq/Acid ratio	1.11 \pm 0.00	1.13 \pm 0.00	1.23 \pm 0.00	1.25 \pm 0.01	1.57 \pm 0.01	1.57 \pm 0.01
Conversion, x (g VS digested/g VS fed)	0.080 \pm 0.000	0.091 \pm 0.001	0.135 \pm 0.000	0.103 \pm 0.000	0.41 \pm 0.00	0.36 \pm 0.00
Selectivity, σ (g acid produced/g NAVS consumed)	0.777 \pm 0.005	0.824 \pm 0.004	0.875 \pm 0.004	0.845 \pm 0.004	0.40 \pm 0.00	0.48 \pm 0.00
Aceq selectivity, σ_a (g Aceq produced/g NAVS consumed)	0.851 \pm 0.005	0.921 \pm 0.004	1.066 \pm 0.005	1.035 \pm 0.005	0.63 \pm 0.00	0.79 \pm 0.00
Exit yield, Y_E (g acid/g NAVS fed)	0.062 \pm 0.000	0.075 \pm 0.000	0.119 \pm 0.001	0.087 \pm 0.000	0.16 \pm 0.00	0.18 \pm 0.00
Exit Aceq yield, Y_{aE} (g Aceq/g NAVS fed)	0.068 \pm 0.000	0.084 \pm 0.000	0.144 \pm 0.001	0.107 \pm 0.001	0.26 \pm 0.00	0.29 \pm 0.00
Culture yield, Y_C (g acid/g NAVS fed)	0.047 \pm 0.000	0.060 \pm 0.000	0.103 \pm 0.001	0.072 \pm 0.000	0.15 \pm 0.00	0.16 \pm 0.00
Process yield, Y_P (g acid/g NAVS fed)	0.038 \pm 0.000	0.046 \pm 0.000	0.097 \pm 0.001	0.063 \pm 0.000	0.14 \pm 0.00	0.14 \pm 0.00
Productivity, P (g total acid/(L _{liq} ·d))	0.357 \pm 0.007	0.453 \pm 0.003	0.706 \pm 0.013	0.513 \pm 0.006	0.92 \pm 0.01	1.04 \pm 0.01
Biogas produced (g/d)	0.53 \pm 0.00	0.62 \pm 0.00	1.24 \pm 0.01	0.71 \pm 0.00	0.71 \pm 0.00	1.24 \pm 0.01
Mass balance closure (g mass in/g mass out)	0.96 \pm 0.00	0.98 \pm 0.00	0.96 \pm 0.00	0.98 \pm 0.00	2.53 \pm 0.01	2.51 \pm 0.01

Table 8-3. *p* values for fermentation performance measures to compare Train C and R2 at (a) low C-N ratio and low pH, (b) low C-N ratio and near-neutral pH, and (c) medium C-N and low pH ($\alpha = 0.05$).

Trains	Conversion	Selectivity	Exit yield	Exit yield Aceq	Culture yield	Process yield	TLV	Productivity	Biogas produced	Total acid conc.	Aceq conc.	Total acid exit	Total Aceq exit	Aceq/Total acid
C (a) and R2 (a)	0.000	0.000	0.000	0.000	0.000	0.000	0.976	0.000	0.000	0.000	0.000	0.000	0.000	0.000
C (b) and R2 (b)	0.000	0.000	0.000	0.000	0.000	0.000	0.000	0.000	0.000	0.064	0.199	0.000	0.000	0.000
C (c) and R2 (c)	0.000	0.000	0.000	0.000	0.000	0.004	0.000	0.000	0.027	0.000	0.001	0.000	0.000	0.865
C (a) and C (b)	0.000	0.000	0.000	0.000	0.000	0.000	0.000	0.000	0.000	0.000	0.000	0.000	0.000	0.000
C (a) and C (c)	0.000	0.000	0.000	0.000	0.000	0.000	0.000	0.000	0.000	0.000	0.000	0.000	0.000	0.000
C (b) and C (c)	0.000	0.000	0.000	0.000	0.000	0.000	0.000	0.000	0.000	0.000	0.000	0.000	0.000	0.000
R2 (a) and R2 (b)	0.000	0.000	0.000	0.000	0.000	0.000	0.000	0.000	0.000	0.769	0.000	0.000	0.000	0.000
R2 (a) and R2 (c)	0.000	0.000	0.000	0.000	0.000	0.000	0.000	0.000	0.000	0.000	0.000	0.000	0.000	0.000
R2 (b) and R2 (c)	0.000	0.000	0.000	0.000	0.000	0.000	0.000	0.000	0.000	0.000	0.000	0.000	0.000	0.000

p value < 0.006 statistically different, with a familywise error rate of 0.05 using the Bonferroni correction

8.3.2 *Carbon-nitrogen ratio and pH*

Ammonia is a source of nitrogen for the synthesis of amino acids in microbial cells (Hungate, 1966). Because the C-N ratio and pH affect fermentation performance, both must be controlled. To compare fermentation trains, the C-N ratio was normalized by controlling the nitrogen (with urea) and substrate and was quantified as previously described (Smith et al., 2011). This study evaluated fermentation performance in the following cases: (1) low C-N ratio (12 ± 2 g OC_{NA}/g N) and high pH (8.3 ± 0.1), (2) low C-N ratio (9 ± 1 g OC_{NA}/g N) and near-neutral pH (7.1 ± 0.1), and (3) medium C-N ratio (24 ± 3 g OC_{NA}/g N) and low pH (5.5 ± 0.2) (Table 8-1).

Microorganisms produce urease, an enzyme that hydrolyzes urea to ammonia, which reacts with water to form ammonium hydroxide, increasing the pH. This study attempts to decouple the effects of nitrogen and pH on fermentation performance. Urea was used as the nitrogen source to control the C-N ratio. In Table 8-1, the different urea loading rates correspond to the VSLR and LRT. In all fermentations, the pH was controlled with calcium carbonate, an inexpensive and industrially viable buffer. However, calcium carbonate buffers at low pH, not high pH (~8.3), which occurs when urea is added to fermentations. Therefore, to obtain a low C-N ratio while maintaining a near-neutral pH, hydrochloric acid was used to control the pH to 6.9–7.2.

In this study, the total ammonia nitrogen for fermentations at low C-N ratio at high pH, low C-N ratio at near-neutral pH, and medium C-N ratio at low pH was typically 2550, 3980, and 1760 mg nitrogen (N)/L, respectively. The free ammonia was not directly measured, but was estimated from the total nitrogen and pH. At neutral pH, equilibrium calculations show that free ammonia accounts for 0.5% of the total ammonia nitrogen (free ammonia (NH₃) + ammonium ion (NH₄⁺)). When the pH reaches 8.0–9.0, toxic amounts of aqueous nitrogen might be present as free ammonia (Ekinici et al., 2000). The fermentations at near-neutral pH had similar and very small amounts of free ammonia present, whereas the fermentations with an uncontrolled high pH had a higher amount of free ammonia.

In this study, fermentations with a low C-N ratio operated with an abundance of nitrogen. At C-N ratio < 25 g C/g N, excess nitrogen is thought to be lost as ammonia gas (Cheremisinoff and Ouellette, 1985). However, at the low C-N ratio and high pH (~8.3), the free ammonia was about 12% of total ammonia nitrogen, or ~310 mg free-ammonia N/L. At the low C-N ratio and near-neutral pH (~7.1), the free ammonia was about 0.7% of total ammonia nitrogen, or ~30 mg free-ammonia N/L. At the medium C-N ratio and acidic pH (~5.5), the free ammonia was about 0.02% of total ammonia nitrogen, or ~0.30 mg free-ammonia N/L. Therefore, the performance of the carboxylate fermentations can be attributed to the total amount of nitrogen and pH, both of which affect the free ammonia concentration. In summary, neutralizing the pH decreased the free ammonia in solution, which improved performance variables.

Anaerobic microorganisms that produce acids resist ammonia nitrogen concentrations up to 16,000 mg N/L at neutral pH (Lü et al., 2008). However, the microbial community in these fermentations was not characterized, and therefore, the specific nitrogen tolerance is unknown. Fermentations at low C-N ratio and high pH were exposed to growth-limiting, but not toxic, concentrations of nitrogen. In addition, ammonia is known to inhibit methanogenesis, which is advantageous in the carboxylate fermentation by making it unnecessary to add methanogen inhibitors (e.g., iodoform). Methanogens, which lack a cell wall, are susceptible to ammonia toxicity because the un-ionized molecule can readily penetrate the cell membrane (Metzler, 2001).

8.3.3 *Biogas*

When comparing Train C and R2 at the low C-N ratio, the amount of biogas produced was highest in the trains at neutral pH (Tables 8-2, 8-3). Train C had greater biogas production than Train R2, perhaps because recycling residual biomass increased the concentration of inhibitory materials. There is a correlation between conversion and amount of biogas produced (Table 8-2). Similarly, studies of ethanol and ruminal fermentation show gas production is related to substrate digestibility (Contreras-Govea et al., 2011; Weimer et al., 2005). The average biogas composition was similar to other studies (Ch. 6, 7). No methane was detected in any fermentor.

8.3.4 *Acid concentration*

For Train C at low C-N ratio, neutralizing the pH increased the total acid and Aceq concentrations in both trains; however, neither were as high as the trains at medium C-N ratio and acidic pH. This suggests that low C-N ratio and high pH both have separate negative effects on acid concentration. However, for Train R2 at low C-N ratio and neutral pH, Aceq concentration increased but not total acid.

For fermentations at low C-N ratio and high pH, and medium C-N ratio and acidic pH, residual biomass recycle improved total acid and Aceq concentration. However, at low C-N ratio and neutral pH, Train C had higher acid concentrations than Train R2 (Tables 8-2, 8-3), perhaps neutralizing the pH produced an inhibiting material (e.g., ammonium chloride) that then was recycled in the interstitial liquid of the residual biomass.

8.3.5 *Daily acid production*

In each fermentor of a train, TLV quantifies the total volume of liquid in the solid and liquid phases. All fermentation trains did not have equivalent TLVs, indicating nonuniformity between trains. To standardize the analyses, the daily amount of acid exiting the fermentors was calculated on a mass basis from the product liquid, residual biomass, and sample streams (Table 8-2).

At low C-N ratio, after neutralizing the pH, the total acid exiting and total Aceq exiting (g/d) increased more than double for Train C and less so for Train R2 (Tables 8-2, 8-3). The trains at low C-N and neutral pH did not have as much acids exiting (g/d) as the medium C-N, suggesting that high amounts of nitrogen have a negative effect on acids exiting separate from the negative effects of high pH (Tables 8-2, 8-3).

At low C-N ratio and high pH, and medium C-N ratio and acidic pH, Train R2 had more total acid exiting and total Aceq exiting (g/d) (Tables 8-2, 8-3). However, this observation was reversed for low C-N ratio and neutral pH; here Train C had more total acid exiting and total Aceq exiting (g/d) than Train R2 (Tables 8-2, 8-3). Therefore, these results show that recycling residual biomass can improve the amount of daily total acid exiting the fermentation train, but not at low C-N ratio and neutral pH.

8.3.6 *Aceq-to-total-acid ratio*

The Aceq-to-total-acid ratio characterizes the production of high-molecular-weight carboxylic acids (e.g., valeric, caproic, and heptanoic acid). The larger the Aceq-to-total-acid ratio, the more high-molecular-weight acids are present (see Equation 8-5). At low C-N ratio, after neutralizing the pH, the Aceq-to-total-acid ratio increased ~11% for Trains C and R2 (Tables 8-2, 8-3). The trains at low C-N and neutral pH did not have as high Aceq-to-total-acid ratio as the medium C-N, suggesting that high amounts of nitrogen have a negative effect separate from a high pH (Tables 8-2, 8-3). Thus, fermentations at low C-N ratio and high pH can have improved performance by neutralizing the pH, but having an optimal C-N ratio is necessary to achieve the best performance.

When comparing fermentation trains at the respective C-N ratio and pH, most Aceq-to-total-acid ratios were higher for Train R2; thus, residual biomass recycle increased the production of high-molecular-weight carboxylic acids (Tables 8-2, 8-3).

8.3.7 *Product spectrum*

The proportion of C2–C7 (acetic, propionic, butyric, valeric, caproic, heptanoic, respectively) carboxylic acids (i.e., *product spectrum*) depends on variables such as temperature, microbial community, feedstock type and concentration, C-N ratio, pH, and oxygen exposure (Chan and Holtzaple, 2003; Golub et al., 2011a; Liu et al., 2008; Smith and Holtzaple, 2011a). In carboxylate fermentation systems, all of the above-mentioned variables affect the metabolism of the mixed-culture community, which some studies assume optimizes the free energy producing and consuming steps and, consequentially, the growth rate (Forrest et al., 2011; Rodriguez et al., 2006).

This study highlights the strong effect of C-N ratio and pH on product spectrum. Figure 8-2 shows that fermentations at low C-N ratio and high pH have a high concentration of acetic acid (C2, >75%) with less propionic acid (C3, ~15%), and the rest being mostly butyric acid (C4), which is similar to other studies (Rodriguez et al., 2006; Zhang et al., 2009).

At the low C-N ratio and neutral pH, more high-molecular-weight acids were formed with an increase in the proportion of C3 and C4, and less C2. The medium C-N ratio fermentations had a more evenly distributed acid profile, with C2, C4, and C6 being the most prominent acids, followed by C3, C5, and C7. The even-numbered acids are preferred.

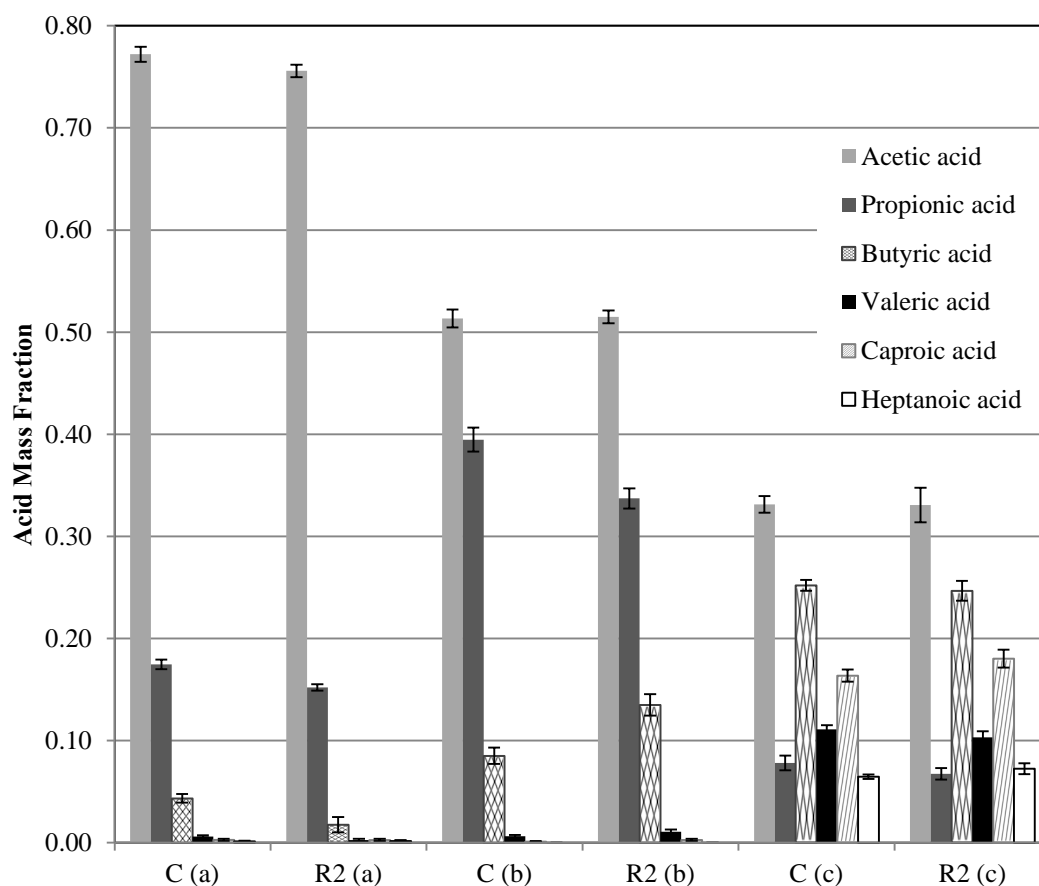


Figure 8-2. Carboxylic acid composition profile at (a) low C-N ratio and high pH, (b) low C-N ratio and near-neutral pH, and (c) medium C-N ratio and low pH. Error bars are the 95% confidence intervals for each carboxylic acid composition during the steady-state period.

For Trains C and R2, at low C-N ratio and high pH, the large concentration of acetic acid appears to be a combined effect from the high pH and low C-N ratio (Figure 8-2). At high pH, there are high concentrations of undissociated acids. Because acetic acid has a higher protonating power than the other acids, the bacteria might be trying to protect themselves from the high pH by producing more acetic acid. Also, at the high pH, there is a high concentration of free ammonia in solution, which is considered a toxic form of nitrogen. In attempts to control the intracellular pH and nitrogen levels, the bacteria may only be able to harvest energy by producing low-molecular-weight acids.

Therefore, it appears that high concentrations of nitrogen are toxic at high pH, but are less toxic at near-neutral pH. The high concentration of nitrogen, even at near-neutral pH, makes high-molecular-weight acids unfavored. However, bacteria can adapt to the high concentrations of nitrogen. Although this factor was not explored in this study, it has been demonstrated in similar studies with methanogens (Debaere et al., 1984).

8.3.8 *Productivities*

At the low C-N ratio, after neutralizing the pH, the productivity increased by double for Train C and to a lesser extent for Train R2 (Tables 8-2, 8-3). However, the productivities for low C-N ratio, even after neutralizing pH, were not as high as for the fermentations at the medium C-N ratio.

For fermentations at the low C-N ratio and high pH, and medium C-N ratio and acidic pH, the productivities for Train R2 were higher than Train C, suggesting that recycling residual biomass boosted productivity. However, the opposite observation was found for fermentations at low C-N ratio at near-neutral pH, where Train C had higher productivities. This suggests that at low C-N ratio and near-neutral pH, residual biomass recycle negatively affects productivity, perhaps from recycling of an inhibitory compound (e.g., ammonium chloride). Ammonium chloride is completely soluble and would be found in the interstitial fluid (75–85 g water/g residual biomass) in the residual biomass.

8.3.9 Yield

The exit yield Y_E (Equation 8-8) quantifies the sum of acid *exiting* the fermentation in the product transfer liquid, exiting residual biomass, and liquid samples per g NAVS feed. The culture yield Y_C (Equation 8-11) represents the acid *produced* by the mixed-culture per g NAVS_{feed} and is equal to the exit yield less the feed yield Y_F (Equation 8-10). The exit acetic acid equivalent yield Y_{aE} quantifies the sum of acetic acid equivalents *exiting* the fermentation in the product transfer liquid, waste transfer solids, and liquid samples per g NAVS feed. The process yield Y_P (Equation 8-9) quantifies only the acid in the product transfer liquid per g NAVS_{feed}, which is sent downstream to be clarified, concentrated, and processed into chemicals and fuel; thus, Y_P represents a commercially relevant acid yield.

At the low C-N ratio, after neutralizing the pH, the yields for Train C almost doubled for all yield values (i.e., Y_E , Y_C , Y_{aE} , and Y_P), and improved the yields for Train R2 to a lesser degree. This suggests that fermentations with high amounts of nitrogen and high pH, neutralizing the pH increases the production of total acid (i.e., Y_E , Y_C), high-molecular-weight acid (i.e., Y_{aE}), acid in the product liquor (i.e., Y_P), relative to the fed NAVS.

At the low C-N ratio and high pH, and medium C-N ratio and low pH, Y_E , Y_C , Y_{aE} , and Y_P were higher for Train R2 than Train C, suggesting that, at those conditions, recycling residual biomass improved yield (Tables 8-2, 8-3). However, at the low C-N ratio and near-neutral pH, Train C had higher yields, indicating that residual biomass recycle is not beneficial in this case, possibly explained by the recycle of an inhibiting compound (e.g., ammonium chloride) not found at high pH.

8.3.10 Conversion and selectivity

At low C-N ratio and high pH, after neutralizing the pH, the conversion and selectivity for Trains C increased by 68% and 14%, respectively; whereas, the conversion and selectivity for Train R2 increased by 13% and 3%, respectively. The fermentations at low C-N ratio at high and near-neutral pH had significantly higher selectivities, but much lower conversions, than the fermentations at medium C-N ratio.

These results suggest that at near-neutral pH, microorganisms are less stressed, can better assemble the enzymes to produce energy, and digest more of the original NAVS. However, fermentations operating with high concentrations of nitrogen tend to be more efficient at producing acids perhaps because osmotic or pH stress induces most cells to be in maintenance mode producing acids as opposed to growth mode. At medium C-N ratios, one explanation is that the fermentations make alternative products besides acids, like hydrogen (Lin and Lay, 2004) or more cells.

At low C-N ratio at high pH, and medium C-N ratio at acidic pH, residual biomass recycle improved selectivity perhaps because the recycle streams enabled Train R2 to retain additional nutrients and cells. However, compared to Train C, after neutralizing the pH at low C-N ratio, residual biomass recycle negatively affected selectivity, perhaps because an inhibiting compound (e.g., ammonium chloride) was being recycled that was not found at the high pH.

8.3.11 Overview

Using residual biomass recycle, fermentation performance may be improved by retaining cells and nutrients. Two four-stage countercurrent fermentation trains (Figure 8-1) were run: (1) a control train with no recycle (Train C), and (2) a train that recycled biomass to Fermentor 2 (Train R2). Both fermentation trains were operated under three conditions: (1) low C-N ratio and high pH; (2) low C-N ratio and near-neutral pH; and (3) medium C-N ratio and acidic pH, which is typical of conventional fermentations buffered by calcium carbonate. By neutralizing the pH in low C-N ratio fermentations, many performance variables are improved. Recycling residual biomass affects many coupled variables (i.e., nutrient concentration, substrate concentration, ash concentration, and cell load). Uncoupling the variables responsible for the positive or negative effects is difficult. From this study, the following conclusions can be drawn: (1) with high nitrogen concentrations, neutralizing the pH is imperative to fermentation performance because it decreases the free ammonia, and (2) recycling residual biomass to F2 improved fermentation performance at medium C-N ratios at acidic pH or low C-N ratios at high pH, but *not* at low C-N ratio and neutral pH. Future carboxylate

fermentation experiments might investigate the effects of urease inhibitors to slow ammonia production and hence control pH. The following text summarizes the separate effects of pH at low C-N ratio and residual biomass recycle.

8.3.11.1 *Effect of pH at low C-N ratio*

The fermentations adapted to the different nitrogen concentrations, revealing that the carboxylate mixed culture can continuously adjust to stressful conditions. One explanation is that the microorganisms shift their energy pathways, which is similar to how other microorganisms deal with stress (Zhou et al., 2011). Fermentations operating under a medium C-N ratio performed best, followed by low C-N ratio at near-neutral pH, and then low C-N ratio at high pH. The microorganisms at the low C-N ratio and high pH were undoubtedly in a more toxic environment, decreasing cell viability and lowering performance.

For Trains C and R2, at a low C-N ratio, neutralizing the pH decreased the amount of free ammonia in solution, which boosted every performance measure. For Train C, neutralizing the pH at low C-N ratio doubled daily biogas production, daily acid production, productivity, yield, and conversion, and increased the Aceq-to-total-acid ratio and selectivity to a lesser degree. Train R2 also improved performance, but not as much as Train C (Tables 8-2, 8-3). The fermentation performance at low C-N ratio and near-neutral pH was not as high as for medium C-N ratio and low pH.

Fermentations at a low C-N ratio and high pH produced mostly low-molecular-weight acids (i.e., C2, C3). In the low C-N ratio fermentations, after the pH was neutralized, proportions of C3 and C4 increased, and C2 decreased, showing that neutralizing the pH increases the amount of high-molecular-weight acids. However, high-molecular-weight acids (i.e., C5–C7) were not produced in the low C-N ratio fermentations as occurred in medium C-N ratio fermentations at acidic pH (Figure 8-2). If a high selectivity to acetic acid is desired, operating fermentations at a low C-N ratio and high pH could be an option, although at the cost of lower yield, productivity, and conversion compared to an optimal C-N ratio.

8.3.11.2 *Effect of residual biomass recycle*

For fermentations at low C-N ratio and high pH, and medium C-N ratio at acidic pH, residual biomass recycle to Fermentor 2 (Train 2) improved total acid concentration, Aceq concentration, daily acid production, Aceq-to-total-acid ratio, productivity, yields, selectivities. However, this observation was reversed for low C-N ratio and neutral pH, where Train C had better performance (Tables 8-2, 8-3).

Nitrogen – a major nutrient in fermentations – was supplemented in the fermentations as urea, which is liquid soluble. Using the enzyme urease, bacteria hydrolyze urea to ammonia. To control the high pH resulting from the ammonium hydroxide, hydrochloric acid was used as a buffer, which produced ammonium chloride. Ammonium chloride is water soluble and is present in the interstitial fluid of the residual biomass in significant amounts (75–85 g water/g residual biomass). This salt could possibly be an inhibiting material that, when recycled back into the system, decreases fermentation performance. Therefore, at low C-N ratio and near-neutral pH, the performance trend between Train C and R2 shows that residual biomass recycle negatively affects performance, which might exist from recycling an inhibiting compound (e.g., ammonium chloride). A different nitrogen supplement and buffer system should be investigated to avoid this problem in the future. Therefore, these results show that recycling residual biomass can improve fermentation performance, but not with the low C-N ratio and neutral pH system studied here.

The high selectivity found in the fermentations with low C-N ratio at both high and neutral pH suggests that fermentations operating under high amounts of nitrogen tend to be more efficient at producing acids from the recycled residual biomass, possibly because the cells are stressed from maintaining intracellular pH and nitrogen levels, and are therefore in maintenance mode rather than growth mode. Operating at low C-N ratio and high pH contributed to high selectivity to acetic acid, which might be industrially desirable because acetic acid is an important commodity chemical and is preferred to produce electricity from microbial fuel cells (Liu et al., 2005; Min and Angelidaki,

2008). However, high acetic acid concentrations come at the cost of lower yields and product concentrations.

8.4 Conclusions

At low C-N ratios, high levels of nitrogen are toxic at high pH, but not as toxic at near-neutral pH. Fermentations at low C-N ratios and near-neutral pH, as compared to a high pH, had dramatically improved yield, conversion, selectivity, productivity, amount of high-molecular-weight acids. Fermentations with excess nitrogen had ~60% higher selectivity. Recycling residual biomass improved performance for low C-N ratio at high pH and medium C-N ratio at low pH. However, at low C-N ratio at near-neutral pH, compared to the no-recycle control, fermentations recycling residual biomass had decreased performance, possibly because inhibiting substances (e.g., ammonium chloride) were recycled.

9. RAPID METHOD TO QUANTIFY TOTAL MICROBIAL ACTIVITY IN BIOMASS, BIOPROCESSES, SOIL, AND SEDIMENT

This study describes a method to quantify microbial activity in liquid and solid samples from bioprocesses and soil sediments. This effective and rapid method measures glucose digestion rates in specified quantities of samples that contain microbial activity. The method is very versatile and can quantify microbial activity in aerobic or anaerobic samples. It is applicable to samples with large quantities of particulates, which would confound many traditional methods (e.g., optical density, flow cytometers), and complex matrices containing undefined mixed cultures, which would be difficult using traditional methods (e.g., cell plating). Since this method relies on glucose metabolism, it quantifies only the living biome, unlike other methods (e.g., real-time PCR). The test sample is added to a dilute solution of glucose, with no nutrient addition to limit microbial growth. During the reaction period, the glucose digestion rate is measured using a glucose oxidase assay. To determine a specific glucose-utilization rate, the effect of sample concentration on glucose digestion rate is measured with several sample dilutions. This method could help quantify microbial activity when screening diverse microbial communities in soils, and help standardize inoculation amounts in bioprocess technologies. Applications of this method include quantifying the microbial activity in marine sediment, anaerobic digestors, sewage treatment plants, and biofuel processes. To optimize performance, commercial-scale technologies could employ this method to better control bioprocesses.

9.1 Introduction

Mixed microbial cultures are widely used in industry and are well suited to a non-sterile, multiple feedstock environment, offering advantages over a pure culture (Angenent et al., 2004; Das and Veziroglu, 2001). The mixed culture establishes a

robust, synergistic community capable of maintaining itself (Rokem et al., 1980). For example, waste water is treated aerobically using the activated sludge process in which a mixed microbial culture consumes the various components in the waste water and converts them to CO_2 and H_2O . In the effluent stream, the cells are settled in a clarifier, a portion of which are recycled to the fermentor, and the remainder are discarded as sewage sludge. In some cities, the sewage sludge is anaerobically digested using a mixed culture that produces CH_4 and CO_2 . The stability of the mixed culture system has been linked to increased diversity of the microbial community and to an increased ability to adapt to changes in the environment of the system (Angenent et al., 2004).

In the above cases, the mixed microbial cultures are used to treat wastes. They can also be used to produce liquid transportation fuels. For example, the carboxylate platform employs a mixed microbial culture that converts biomass into carboxylic acids that are subsequently neutralized to carboxylate salts using a buffer such as CaCO_3 (Chan and Holtzapple, 2003; Holtzapple et al., 1999). The carboxylate salts are recovered and chemically converted to a variety of chemicals (e.g., acetone, isopropanol, acetic acid) and fuels (e.g., gasoline, jet fuel) (Aiello-Mazzarri et al., 2006; Granda et al., 2009). Recent studies have shown that recycling cells to the fermentor increases yield, productivity, and selectivity (Ch. 11).

All of the above examples are inoculated using naturally occurring microorganisms typically derived from terrestrial soil or marine sediment. In all cases, the processes are improved by quantifying the “microbial activity,” a concept analogous to enzyme activity.

For many applied systems, the concentration of enzymes is often not measured directly as mol/L or g/L. In many cases, enzyme preparations are not pure, so the molar or mass concentration is not meaningful. Also, some enzymes (e.g., cellulases) operate as complexes, so it would be very difficult to characterize the concentration of each component. To overcome the problems, enzyme concentration can be characterized by its catalytic activity. The standard unit to measure enzymes is the katal, which is the amount of enzyme that converts one mole of substrate per second. Activity can also be

measured as the reaction rate of a given quantity of enzyme with typical units of g reacted/(g enzyme·min) or g reacted/(mL enzyme·min). Microbial activity has similar units, except the denominator quantifies the amount of microorganisms.

The ability to quantify microbial activity is useful in process development and process control. For example, when developing the carboxylate platform, it is desirable to perform bioprospecting, which involves search for soil samples that have active microbial communities that may harbor microorganisms that are suitable for the process. It would be helpful to have an assay that characterizes the microbial activity in various soil types that may serve as an inoculum. Also, once the process is developed, it will be necessary to control it. For example, in the carboxylate platform, recycling cells to the fermentor improves the process. Ideally, cells would be separated from undigested residue so inert materials are not recycled, which lowers productivity. A high-throughput, inexpensive, simple, and rapid method that quantifies microbial activity will provide necessary feedback to regulate the cell separation and recycle process.

Established microbial quantification techniques include direct methods (e.g., plate counting, fluorescent microscopy) and indirect methods (e.g., DNA-based techniques, immunological assays, turbidometry). Classically, cell concentrations are measured when cells are suspended in liquids that contain only soluble components. In this case, the cell concentration is readily characterized by optical density or in flow cytometers. Also, if the cells are cultureable, it is possible to plate them on a Petri dish containing a nutrient gel. The cell concentration is quantified by appropriately diluting the aqueous suspension of cells so they form independent colony forming units on the plate. However, studies estimate that 99% of microorganisms are not culturable (Schloss and Handelsman, 2005). A direct cell count would measure total cell load, and assumes all cells are metabolically equal. However, bacteria utilize substrates at different rates, and a direct cell count would not capture the metabolic capability. Therefore, capturing the metabolic activity might be a more valuable tool than cell counts.

When microbial communities are attached to solids – which occurs in waste water treatment, anaerobic digestors, and the carboxylate platform – it is impossible to

use traditional cell quantification methods as described above. The solid particles interfere with the optical density and flow cytometer. Because the cells are often attached to the solids, it is difficult to separate them into individual colony forming units. Also, in mixed microbial communities, microorganisms are highly interdependent, making them unculturable when separated.

To overcome the challenges of quantifying the cell density in complex samples (e.g., fermentation biomass or sludge), a number of methods have evolved, such as fluorescent *in situ* hybridization (FISH), real-time polymerase chain reaction (PCR), and metabolic assays. However, FISH and real-time PCR are time-intensive and expensive. Real-time PCR quantifies the number of target DNA sequences in living and dead cell sample, and relates the number of DNA sequences to the number of cells. Unfortunately, the number of DNA strands per cell is an estimate. FISH uses fluorescent probes to bind to specific DNA or RNA sequences, and quantifies a particular microbial group as a percentage of total bacteria in living cells. These are not easily adaptable to on-site testing, require biological expertise to be implemented, and do not distinguish metabolic requirements for a process.

The genetic methods are expensive and time consuming. Although they are suitable for scientific investigations, they are not suitable for routine operations of industrial processes. To overcome these challenges, the sugar assay was developed to quantify microbial activity. In a controlled environment, the rate of sugar consumption is a measure of microbial activity. In principle, any sugar (or other soluble substrate) can be used to quantify microbial activity; here, glucose is employed.

Quantifying bacteria can also be accomplished by monitoring metabolites or metabolic activity. All living organisms utilize available energy sources to produce adenosine 5'-triphosphate (ATP), the universal energy currency of living cells. The production of ATP is a rapid and specific system for mobilization of cellular energy, and so ATP assays have been developed as a reliable approach for determining the presence of microbial contaminants (Chollet et al., 2008), for assessing the viability of microbial biomass (Hammes et al., 2010), and for quantifying biomass (Tseng et al., 1996).

Unfortunately, variability in the physical-chemical and microbiological characteristics of environmental samples precludes the existence and mitigates the usefulness of any "universally" applicable technique for the routine extraction and analysis of ATP, thus limiting the usefulness of the approach. Fewer bacteria are able to use complex carbohydrates like disaccharides (lactose or sucrose) or polysaccharides (starch). Disaccharides and polysaccharides are simple sugars that are linked by glycosidic bonds; bacteria must produce enzymes to cleave these bonds so that the resulting simple sugars can be transported into the cell. If the bacteria cannot produce these enzymes then the complex carbohydrate is not used.

Of similar utility, although much easier to implement, is a simple substrate utilization assay. Heterotrophic bacteria often use carbohydrates as energy sources, and the most common fuel for living cells is the sugar glucose. Many other compounds can serve as food, but almost all of them are converted to glucose, or to intermediates in the glucose metabolic pathway. The energy-extracting processes of cells capture almost half of the energy of glucose in ATP. When O_2 is available, glycolysis is followed by the three pathways of cellular respiration: pyruvate oxidation, citric acid cycle, and the respiratory chain. When O_2 is not available, cellular respiration does not function, and fermentation is added to glycolysis. These characteristics make glucose as close to a universal energy source as may be possible, and so a good reporter for monitoring the metabolic state of a process inoculum or environmental sample.

In cells, glucose oxidase is an enzyme that helps metabolize glucose. Glucose oxidase is an oxidoreductase, where it catalyzes the transfer of electrons. In diagnostics, glucose oxidase is used to determine the amount of glucose in bodily fluids, and commercially in the food industry.

This study uses the glucose oxidase enzyme assay, where glucose oxidase catalyzes the conversion of β -D-glucose, water, and oxygen into D-gluconic acid and hydrogen peroxide. The generation of hydrogen peroxide is indirectly measured by the oxidation of O-dianisidine in the presence of peroxidase. Sulfuric acid stops the reaction progress. The OD can then be measured by spectrophotometry (570 nm), and converted to glucose

concentration with calibration curves and Beer's Law. Similar studies have studied glucose consumption in tissue cultures (Blake and McLean, 1989) with high linearity and reproducibility.

This glucose-utilization assay could be useful for bioprocess techniques aimed at optimizing inoculations, or maintaining or monitoring microorganism activity. Shortcomings of this method include that it measures glucose digestion, which is a metabolic activity, and does not directly measure total cell load. Also, glucose oxidase enzyme is inhibited by metals (e.g., copper, mercury, silver) (Nakamura and Ogura, 1968), which could be present in bioprocesses in concentrations large enough to be inhibitory. Accounting for this inhibition is discussed.

This chapter describes development of a simple, rapid, high-throughput, and cost-effective method to quantify aerobic microbial load from any ecosystem using glucose digestion. Glucose oxidase is used to determine the glucose utilization of pure and complex samples (i.e., soil and fermentation biomass samples). The general performance of this glucose-utilization assay is compared with colony counts on agar plates, an established technique.

9.2 Materials and methods

9.2.1 Inoculum

Pure culture – An *E. coli* (DH5 α) stock was prepared by transfer of a single colony to a culture tube containing 5 mL of TYE (10 g tryptone, 5 g yeast extract, 5 g NaCl, 1 L ddH₂O, autoclaved), followed by incubation overnight in a shaking incubator (>100 rpm, 37°C), and then stored at 4 °C for up to 7 days. Immediately prior to initiation of the assays, 5 mL of TYE media was inoculated from the *E. coli* stock in a ratio of 1:50 (inoculum:media) and incubated as before to an optical density (OD) of ~0.8 at 570 nm. This culture was used to inoculate an autoclaved glucose solution (80 μ g glucose/mL, 50-mM potassium phosphate buffer, 7.5 pH). The culture OD was found with spectrophotometry (570 nm, 250- μ L 96-well plate).

Soil sample – Marine sediment samples were removed from the bottom of 0.5-m-deep shoreline pits in Galveston, TX, which is an inoculum historically used for carboxylate fermentations. Samples were immediately placed in airtight plastic bottles filled with deoxygenated water, capped, and chilled. Samples were frozen at $-20\text{ }^{\circ}\text{C}$ until use and consisted of $80.0 \pm 0.4\%$ dry solids and $21.0 \pm 0.4\%$ volatile solids. When used, the marine sediment was thawed and homogenized.

Fermentation broth – A sample of fermentation broth was taken from a batch carboxylate fermentation that had been incubating 3 weeks. The feed consisted of 80% shredded office copier paper and 20% dry homogenized chicken manure on a dry mass basis. In a roller incubator (~ 6 rpm), the fermentor was incubated at $40\text{ }^{\circ}\text{C}$ and operated as a submerged fermentation under anaerobic conditions with a concentration of 100 g dry solids/L deoxygenated water. This was achieved as previously described by adding substrate, nutrient source (manure and urea), inoculum, buffer (calcium carbonate), and liquid medium to each fermentor (Forrest et al., 2010b). After 3 weeks, the fermentation was sampled after allowing the fermentor contents to settle for 15 min. Using a pipette, a portion of the fermentation broth was collected, refrigerated, and used within 2 h. The inoculum consisted of marine sediment from Galveston, TX, and was identical to the soil sample described above. The bacterial community composition of mixed-acid fermentation has been reported elsewhere (Hollister et al., 2010; Hollister et al., 2011). The fermentation broth consisted of $2.0 \pm 0.0\%$ dry solids of which $63.0 \pm 0.4\%$ were volatile solids.

9.2.2 *Glucose-utilization assay*

The glucose reaction mix was prepared by adding glucose and potassium phosphate (50 mM, pH of 7.5) to ddH₂O, and filter sterilizing (0.2 μm). The glucose reaction mix was aliquoted into capped autoclaved 10-mL glass reaction vessel (Wheaton Science Products, Model# 223686), biomass samples (e.g., fermentation broth and marine sediment) were added, and the vials were incubated in a shaker table incubator at $37\text{ }^{\circ}\text{C}$ and 180 rpm. The 200- μL samples were taken at predetermined time

points and were immediately analyzed for glucose concentration in the glucose oxidase assay.

For *E. coli*, a fresh, mid-log culture was harvested, centrifuged ($4,000\times g$ for 3 min), and washed three times in autoclaved ddH₂O, and resuspended in 0.5-mL autoclaved ddH₂O to 0.6, 0.8, 1.0, 1.2 OD (540 nm). From each sample, 0.5 mL was loaded into a reaction vessel containing 4.5 mL of glucose reaction mix. For fermentation broth, four different volumes of broth (0.20, 0.30, 0.40, and 0.50 mL) were added to the reaction vessel containing the glucose reaction mix, for a total volume of 5.0 mL. The fermentation broth was assumed to have a density of 1 g/mL. For marine sediment, the stock was thawed completely, and mixed well. Four different masses (0.20, 0.30, 0.40, and 0.50 g wet) were removed using a spatula, taking care to take as homogenous a sample as possible, and added to the reaction vessel containing the glucose reaction mix, for a total volume of 5.0 mL. For example, 0.2 g wet marine sediment was added to 4.8 mL glucose reaction mix for a total of 5 mL. The marine sediment was assumed to have a density of 1 g/mL.

9.2.3 *Determining glucose concentration with glucose oxidase*

To determine the glucose concentration in a sample at the specified time points, 200- μ L of the glucose reaction mix and 250- μ L glucose oxidase reaction mix (Sigma Aldrich, GAGO20) (glucose oxidase enzyme, o-dianisidine) was added to a 1.5-mL microcentrifuge tube. After a 10-min incubation for color development at 37 °C without shaking, 250- μ L of 12-M sulfuric acid (99% ACS grade) was added to stop the reaction. (*Note:* To limit potential cell growth, a 10-min incubation was used and found acceptable with linear calibration curves (Figure 9-1) instead of the manufacturer-suggested 30 min (Sigma Aldrich, GAGO20).) For soil and sediment samples that had high quantities of suspended solids, the samples were centrifuged for 3 min, $10,000\times g$. From each sample, 250 μ L was transferred to a 96-well plate, and absorbance at 570 nm was determined. The glucose concentration was determined using a glucose standard curve from 0- to 100- μ g glucose/mL. (*Note:* o-dianisidine is a known human carcinogen. Extreme caution must be used. Use gloves and work in the hood.)

The calibration curve was composed of six glucose concentrations in 50-mM potassium phosphate buffer (0, 20, 40, 60, 80, 100 μg glucose/mL). The standards were treated identically to the experimental samples, with 200- μL transferred to 250- μL of the glucose oxidase reaction mix. After a 10-min incubation for color development at 37 °C without shaking, 250- μL of 12-M sulfuric acid (99% ACS grade) was added to stop the reaction, and 250- μL was analyzed in a 96-well plate at 570 nm.

To control for potential inhibition, glucose calibration curves were made for each biomass concentration. The calibration curves were prepared as seen above, with six glucose concentrations in 50-mM potassium phosphate buffer (0, 20, 40, 60, 80, 100 μg glucose/mL) with biomass addition. The calibration curves had similar biomass concentrations as those in glucose-utilization assay, to calibrate the absorbance to glucose concentration in the presence of biomass.

9.2.4 *Determining CFU*

An *E. coli* stock was prepared by transfer of a single colony to a culture tube containing 5 mL of TYE (10 g tryptone, 5 g yeast extract, 5 g NaCl, 1 L ddH₂O, autoclaved), with overnight incubation in a shaking incubator (>100 rpm, 37 °C). The *E. coli* stock inoculated 5 mL of TYE media in a ratio of 1:50 (inoculum:media) and incubated as before to an optical density (OD) of ~0.8 at 570 nm. After a dilution series, the *E. coli* dilutions were plated on TYE agar (10 g tryptone, 5 g yeast extract, 5 g NaCl, 15 g agar, L ddH₂O, autoclaved). After incubation at 37 °C for 36 h, the colonies plated at the proper dilutions were counted.

9.2.5 *Moisture and ash contents*

Moisture content (MC) and ash content (AC) were determined by drying in a 105 °C forced-convection oven for at least 24 h, and subsequent combustion in a 575 °C furnace for at least 12 h by NREL procedures No. 001 and 005, respectively (NREL, 2004). The ash content was calculated on a dry basis. MC (g water/g wet biomass) is the fraction of moisture in the biomass, and AC (g ash in biomass/g dry biomass) is the fraction of dry ash remaining after 12 h of combustion at 575 °C.

9.3 Results and discussion

Figure 9-1 represents the glucose calibration curves that relate absorbance (570 nm) to the glucose concentration ($\mu\text{g/mL}$). The calibration curves are prepared in the presence of the sample so interferences are considered. The low standard error and R^2 value close to unity (0.998) indicate that the glucose oxidase enzyme assay is a sensitive and repeatable method to quantify small concentrations of glucose (1–100 $\mu\text{g/mL}$).

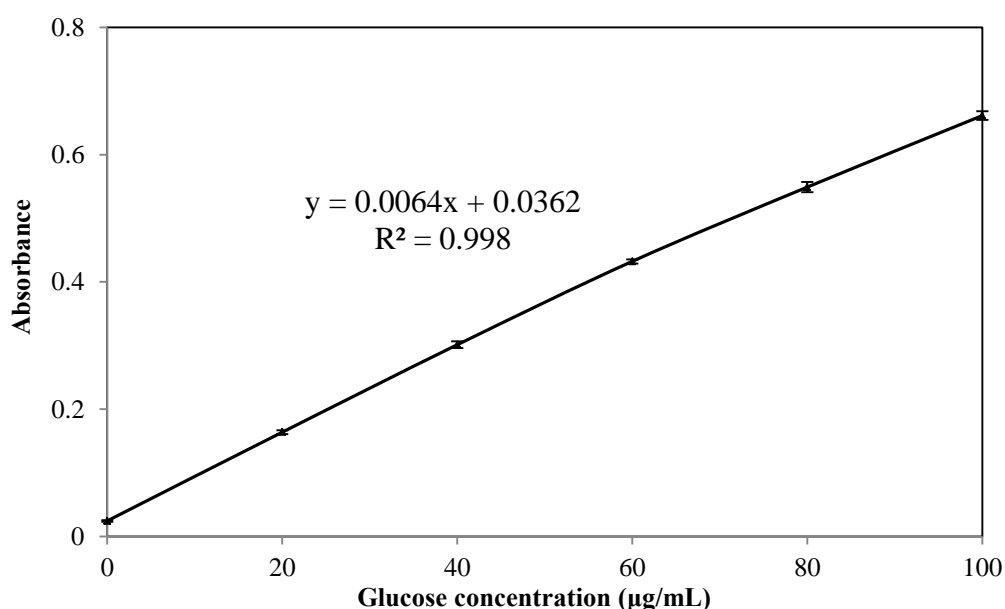


Figure 9-1. Glucose calibration curve without biomass in triplicates. Error bars represent the SE.

E. coli digestion of glucose at an initial cell loading (0.5 mL of cells, 5-mL reaction volume) of 0.6, 0.8, 1.0, and 1.2 OD (570 nm) is shown in Figures 2, which depicts the averaged values of the triplicates with error bars. For all cell loadings, glucose was digested linearly during the reaction period with a minimum of four time points collected. In Figure 2, all R^2 values are close to unity, indicating repeatable digestion, and the slope is the glucose digestion rate for that sample.

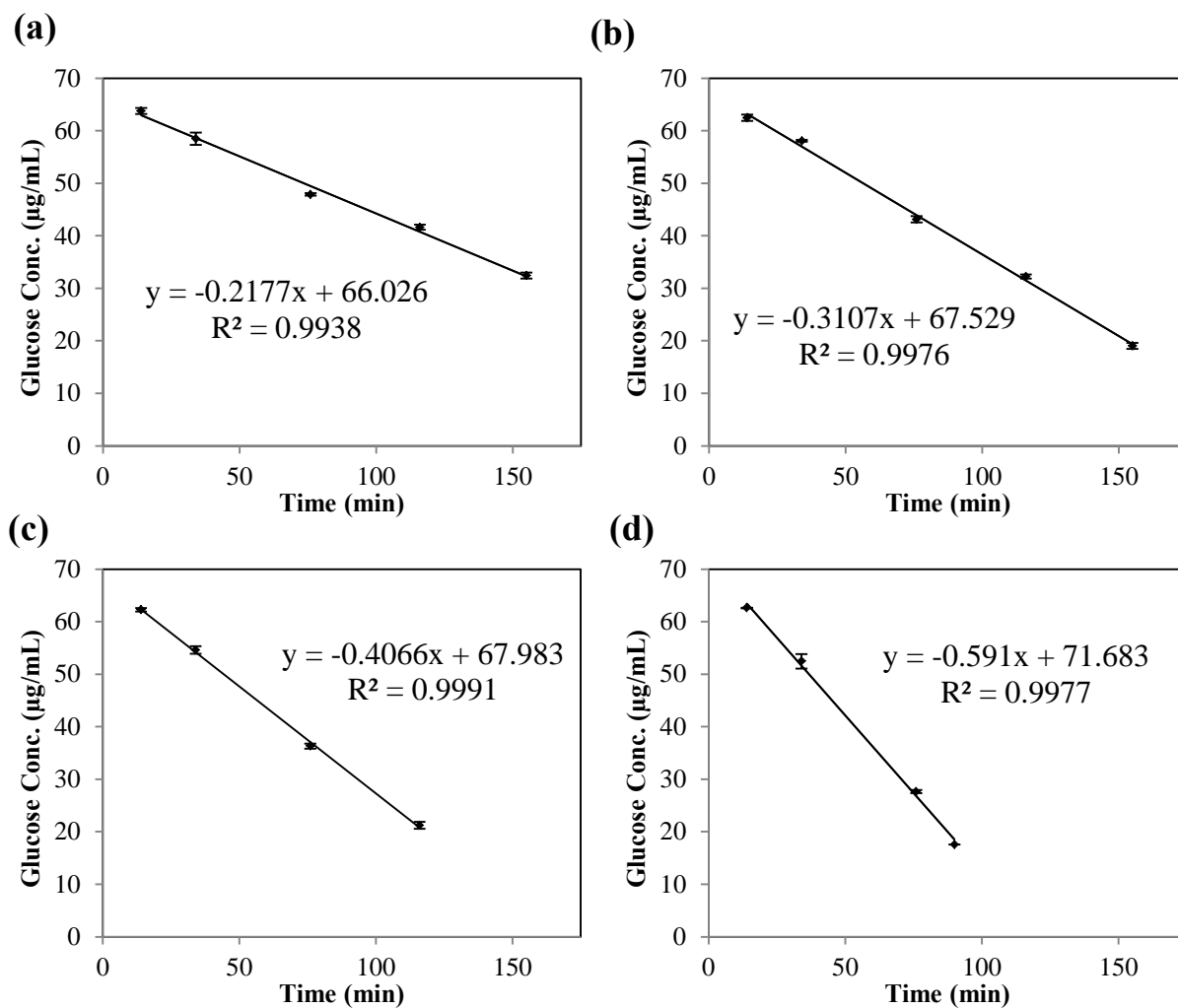


Figure 9-2. Glucose digestion with time inoculated with *E. coli* at an OD of (a) 0.6, (b) 0.8, (c) 1.0, and (d) 1.2. Error bars represent the SE from triplicate experiments.

Cell plating was used to determine the colony forming units (CFU) count associated with each of the *E. coli* test solutions. The CFU per volume were related to the OD of the *E. coli* cells, and gave linear correlation with an R^2 close to unity (0.98). The CFU was then related to the grams of wet *E. coli* (Neidhardt et al., 1990).

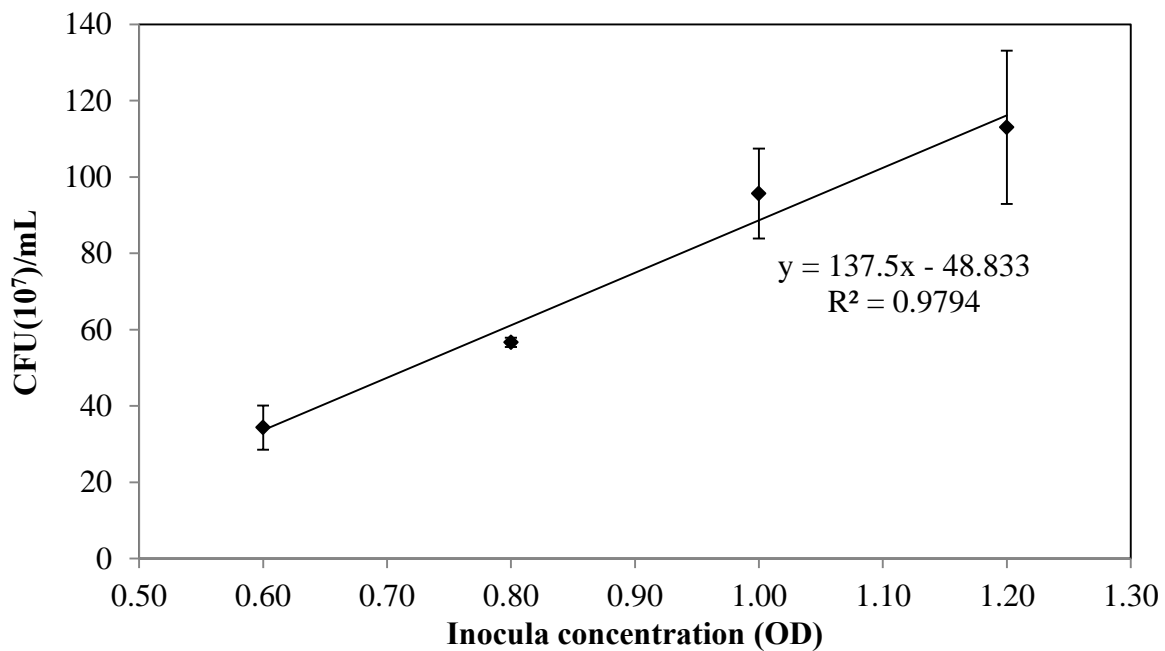


Figure 9-3. Standard curve for CFU corresponding to OD for *E. coli*. Error bars represent the standard error from triplicate plates.

In Figure 9-4, the glucose digestion rate was plotted with respect to the *E. coli* concentration (g/mL), which yielded a linear correlation with an R^2 close to unity (0.999). The slope is the specific digestion rate (3244 μg glucose/(min·g *E. coli*), and is considered to represent the *glucose-utilizing units* of the sample.

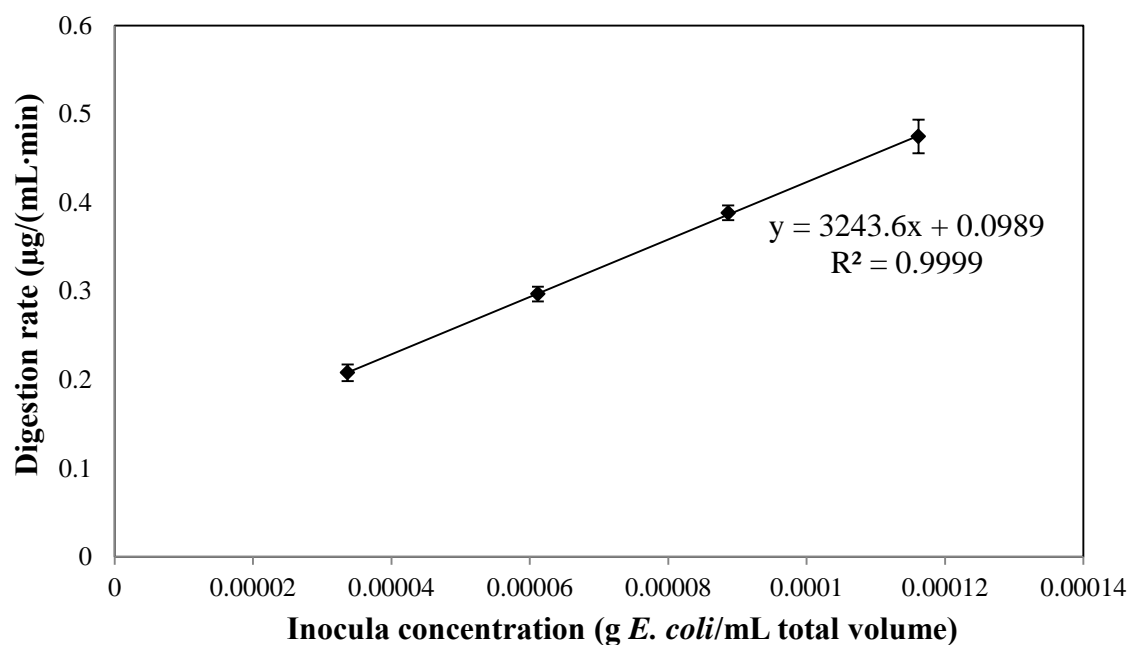


Figure 9-4. Glucose digestion rate inoculated with *E. coli*. Error bars represent the standard error from triplicate experiments. (Note: It is assumed that 1 g *E. coli* = 10^{12} CFU, (Neidhardt et al., 1990))

Similarly, the digestion rates were found for fermentation broth and marine sediment (Figures 9-5 and 9-6). For the fermentation broth and marine sediment, metals and other inhibiting substances might be present. To control for potential inhibition, the glucose samples with the inoculating material (i.e., sediment, broth) could either be (1) immediately filtered and run in the glucose oxidase enzyme assay with a single calibration curve; or (2) run as-is in the GOEA and construct calibration curves for every inoculating material and concentration. This study used the latter of the two choices. For the broth and sediment, instead of using the calibration curve in Figure 9-1 that was used for *E. coli*, calibration curves were made for each inoculating material for each of the four inocula concentrations (not shown). Increased inocula concentration resulted in a calibration curve with a slightly decreased slope, indicating inhibition. More inhibition was present in the fermentation liquid than sand and, *E. coli* was completely uninhibited.

The fermentation broth had more glucose-utilizing units (2.181 μg glucose/(min·g inoculum)), than the marine sediment that served as the inoculum (0.123 μg glucose/(min·g inoculum)). This was expected because the fermentation broth was an active culture with available substrate and nutrients. Further, the community had been adapted to glucose digestion by being fed cellulose in the paper feedstock. The fermentation broth had a mixed-culture of microorganisms, *not* a pure culture, and sufficient quantities of inhibiting substances (e.g., copper from chicken manure nutrient source). Therefore, the R^2 of the fermentation broth (0.94) was less compared to *E. coli* (0.99) and marine sediment (0.98) (Table 9-1). Regardless, all inoculating materials had a sufficiently high linearity (R^2) to be considered valid.

9.4 Conclusion

The glucose-utilization assay is a rapid, high-throughput, and repeatable method for determining the amount of microbial activity in a sample. To approximate the concentration of mixed microorganisms in liquid and solid samples from bioprocesses and soil sediment, the specific glucose digestion rate is an indirect measure of microbial activity. In most assays, there is less than 5% variability with R^2 values near unity, making this suitable for industrial applications.

Table 9-1. Specific digestion rates for *E. coli* in log growth, fermentation broth from carboxylate fermentation, and marine sediment.

Sample	Specific digestion rate (μg glucose/(min·g inoculum))	R^2
<i>E. coli</i>	3244*	0.99
Fermentation broth	2.181	0.96
Marine sediment	0.123	0.97

* Assume 1 g *E. coli* = 10^{12} CFU (Neidhardt et al., 1990).

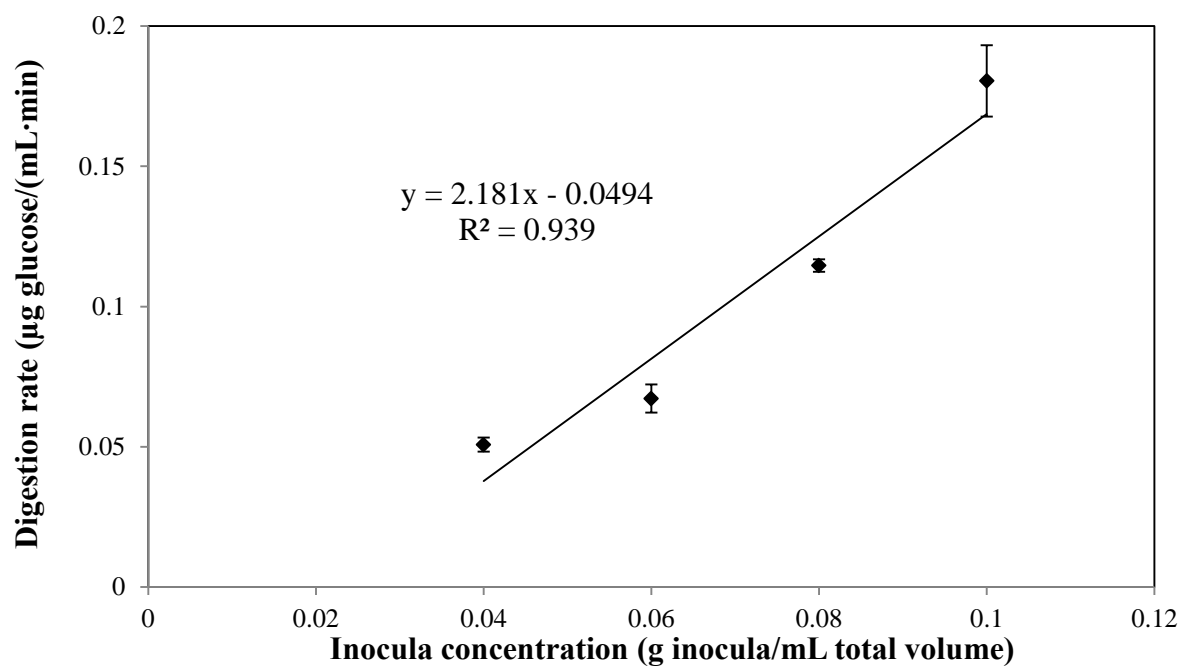


Figure 9-5. Fermentation broth glucose digestion rate. Error bars represent the standard error from triplicate experiments.

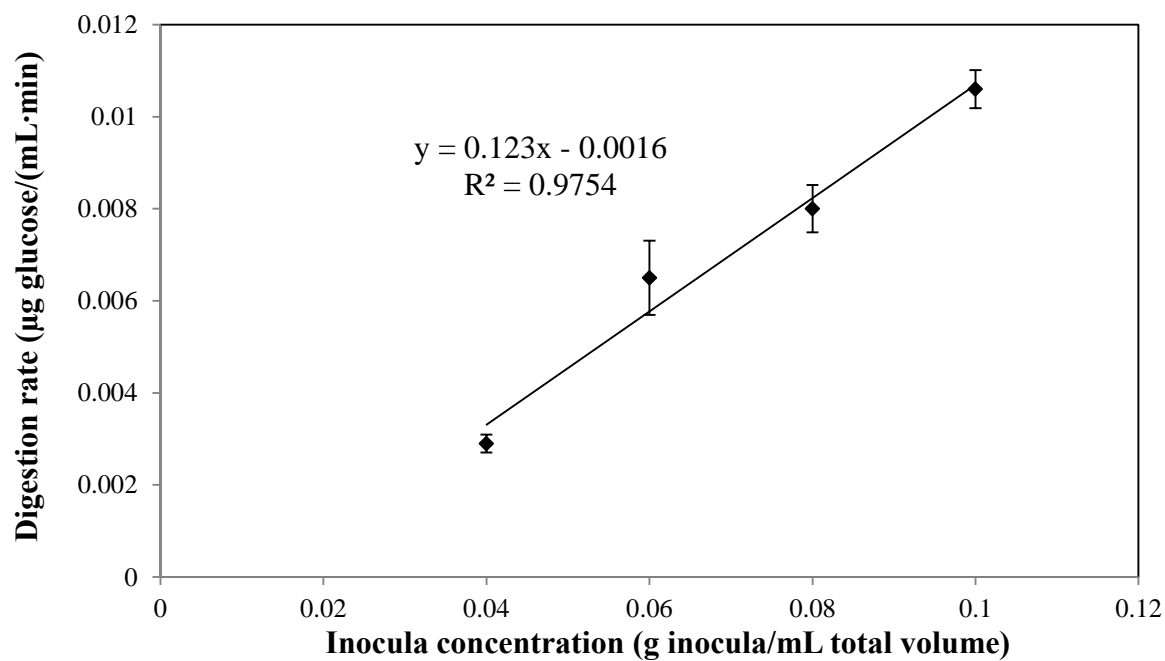


Figure 9-6. Marine sediment glucose digestion rate. Error bars represent the standard error from triplicate experiments.

10. GLUCOSE-UTILIZATION ASSAY ON CELL SEPARATION

PROCEDURE

The purpose of this chapter is to investigate cell separation techniques using the glucose-utilization assay.

10.1 Introduction

Microorganisms (e.g., bacteria, archae, fungi) are the biocatalysts that convert lignocellulose to mixed acids. Recovering and recycling the microorganisms from the waste streams may improve fermentation performance. Previous studies have recycled residual biomass back into the fermentation system because separating microorganisms from residual biomass may be difficult and costly (Ch. 6–8). However, separating microorganisms from the residual biomass might be necessary if there is inhibition from other contents of the recycle stream (i.e., acids, salts, metals, etc.). Further, separating microorganisms from the residual biomass reduces the recycle of inert materials (e.g., lignin) into the fermentor, making better use of its volume.

Established microbial quantification techniques include direct methods (e.g., plate counting, fluorescent microscopy) and indirect methods (e.g., DNA-based techniques, immunological assays, turbidometry). The most common methods to quantify cells in complex samples (e.g., fermentation biomass or sludge) use fluorescent *in situ* hybridization (FISH), real-time polymerase chain reaction (PCR), and metabolic assays. However, FISH and real-time PCR are time-intensive and expensive. Real-time PCR quantifies the number of target DNA sequences in living and dead cell sample, and relates the number of DNA sequences to the number of cells. Unfortunately, the number of DNA strands per cell is an estimate. FISH uses fluorescent probes to bind to specific DNA or RNA sequences, and quantifies a particular microbial group as a percentage of total bacteria in living cells. These are not easily adaptable to on-site testing, require biological expertise to be implemented, and do not distinguish metabolic requirements for a process.

Classically, cells are quantified by plating on a Petri dish. Successful plating of all microbial cells in fermentation broth would be time-consuming, expensive, and perhaps impossible because some studies estimate that 99% of microorganisms are not culturable (Schloss and Handelsman, 2005). A direct cell count would measure total cell load, and assumes all cells are metabolically equal. However, bacteria utilize substrates at different rates, and a direct cell count would not capture the metabolic capability. Therefore, capturing the metabolic activity might be a more valuable tool than cell counts.

Bacteria quantification can also be accomplished by monitoring metabolites that are consumed, released, or accumulated. All living organisms utilize available energy sources in their environment to produce adenosine 5'-triphosphate (ATP), the universal energy currency of living cells. Thus, measurement of ATP is a measure of microbial activity. The production of ATP is a rapid and specific system for mobilization of cellular energy, and so ATP assays have been developed as a reliable approach for determining the presence of microbial contaminants (Chollet et al., 2008), for assessing the viability of microbial biomass (Hammes et al., 2010), and for quantifying biomass (Tseng et al., 1996). Unfortunately, variability in the physical-chemical and microbiological characteristics of environmental samples precludes the existence and mitigates the usefulness of any "universally" applicable technique for the routine extraction and analysis of ATP, thus limiting the usefulness of the approach. Also, it is difficult to extract ATP from complex materials, and requires nonstandard equipment (i.e., luminometer).

Bacteria produce specific enzymes that allow them to utilize specific environmental energy sources. Heterotrophic bacteria often use carbohydrates as energy sources. Fewer bacteria are able to use complex carbohydrates like disaccharides (lactose or sucrose) or polysaccharides (starch). Disaccharides and polysaccharides are simple sugars that are linked by glycosidic bonds; bacteria must produce enzymes to cleave these bonds so that the resulting simple sugars can be transported into the cell. If the bacteria cannot produce these enzymes, then the complex carbohydrate is not used.

Many bacteria use glucose, a simple sugar, because the enzymes required to metabolize it are widely dispersed in nature. Of similar utility, although much easier to implement, is a simple substrate utilization assay. Heterotrophic bacteria often use carbohydrates as energy sources, and glucose is most common fuel for living cells. Many other compounds can serve as food, but almost all of them are converted to glucose, or to intermediates in the glucose metabolic pathway. The energy-extracting processes of cells capture almost half of the energy of glucose in ATP. When oxygen is available, glycolysis is followed by the three pathways of cellular respiration: pyruvate oxidation, citric acid cycle, and the respiratory chain. When oxygen is not available, cellular respiration does not function, and fermentation is added to glycolysis. These characteristics make glucose as close to a universal energy source as may be possible, and so a good reporter for monitoring the metabolic state of a process inoculum or environmental sample.

In the glucose-utilization assay used in this study, glucose digestion is monitored with time using different inoculation concentrations. The glucose concentration is measured with glucose oxidase enzyme. In cells, glucose oxidase is an enzyme that helps metabolize glucose. Glucose oxidase is an oxidoreductase, which catalyzes the transfer of electrons. In diagnostics, glucose oxidase is used to determine the amount of glucose in bodily fluids, and commercially in the food industry.

This study uses the glucose oxidase enzyme assay (GOEA) where glucose oxidase catalyzes the conversion of β -D-glucose, water, and oxygen into D-gluconic acid and hydrogen peroxide. The generation of hydrogen peroxide is indirectly measured by the oxidation of O-dianisidine in the presence of peroxidase. Sulfuric acid stops the reaction progress. The optical density (OD) can then be measured by spectrophotometry (570 nm), and converted to glucose concentration with calibration curves and Beer's Law.

Using the newly developed glucose-utilization assay and well established real-time PCR, this study investigates techniques to separate microorganisms from residual

biomass by measuring the cell distribution between liquid and solid phases in a cell separation process. These studies help answer the questions described in Figure 10-1.

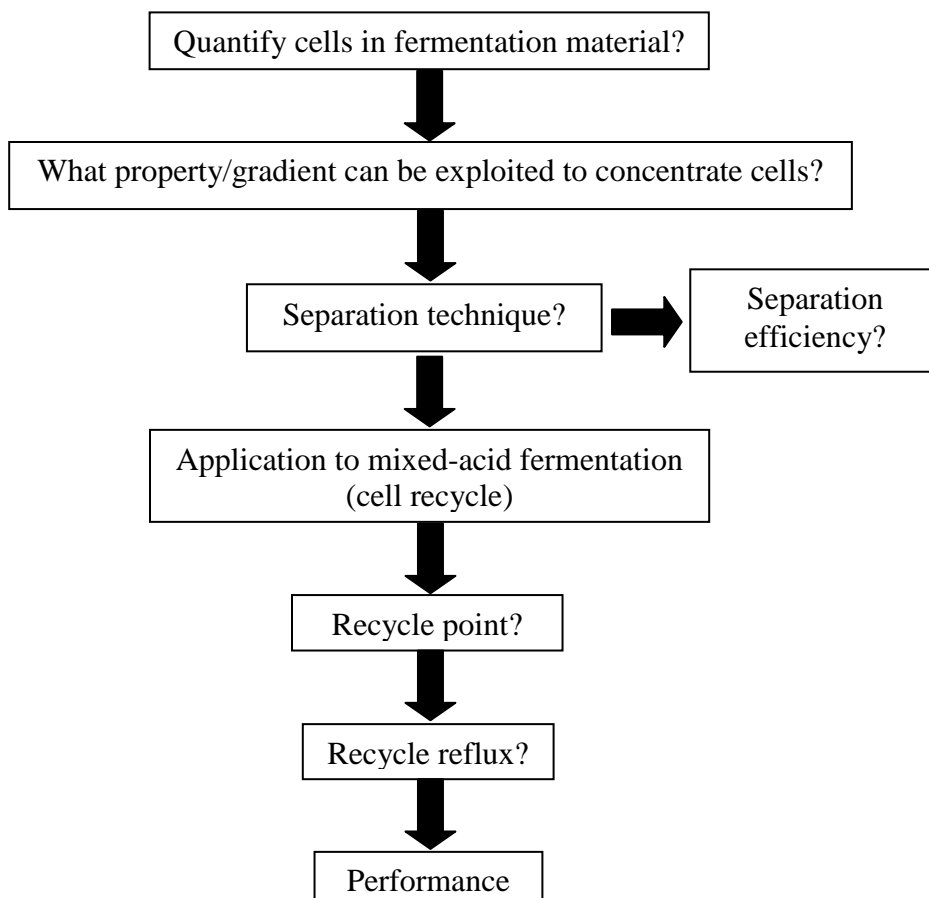


Figure 10-1. Outline of cell-recycle research ideas.

10.2 Materials and methods

10.2.1 *Inoculum*

Fermentation solids were taken from a batch carboxylate fermentation that had been incubating 3 weeks. The feed consisted of 80% shredded office copier paper and 20% dry homogenized chicken manure on a dry mass basis. In a roller incubator (~6 rpm), the fermentor was incubated at 40 °C and operated as a submerged fermentation under anaerobic conditions with an initial substrate concentration of 100 g dry solids/L deoxygenated water. This was achieved as previously described by adding substrate, nutrient source (manure and urea), inoculum, buffer (calcium carbonate), and deoxygenated water to each fermentor (Forrest et al., 2010b). The inoculum for the batch fermentation consisted of marine sediment from Galveston, TX. Every 2 days, the fermentor was vented and iodoform was added to prevent methanogenesis. After 3 weeks, to separate the liquid and solid phases, the fermentation was vented and centrifuged at 3300×g for 25 min. The solid phase was collected and the cell separation procedure was performed. The bacterial community composition of mixed-acid fermentation has been reported elsewhere (Hollister et al., 2010; Hollister et al., 2011). The fermentation solids consisted of 25 ± 0.0% dry material of which 62 ± 0.4% was volatile solids.

10.2.2 *Cell separation procedure*

Fresh residual biomass was diluted, vortexed, gravity settled, filtered, and centrifuged to separate and concentrate cells in the residual biomass waste stream (Figure 10-2). First, the residual biomass solids were collected, and the solids were homogenized by stirring vigorously for 30 s using a beaker and spatula. The homogenate was weighed, diluted four times with deoxygenated water, shaken by hand for 10 s, and then vortexed for 3 min. The homogenate was carefully filtered through a coarse mesh screen (~20 mesh) into a separate container. The debris caught in the filter (cake) was periodically removed and collected to ensure rapid flow. The portion of the homogenate that flowed through the filter (filtrate) was also collected. To remove large particles that

were not caught in the filter, the filtrate was allowed to gravity settle for 10 min. The sediment was collected for analysis. After the liquid phase was decanted, it was centrifuged for 40 min at $5,000\times g$ at room temperature. After centrifuging, the supernatant was decanted, and pellet was resuspended with DI water to make up the “cells.”

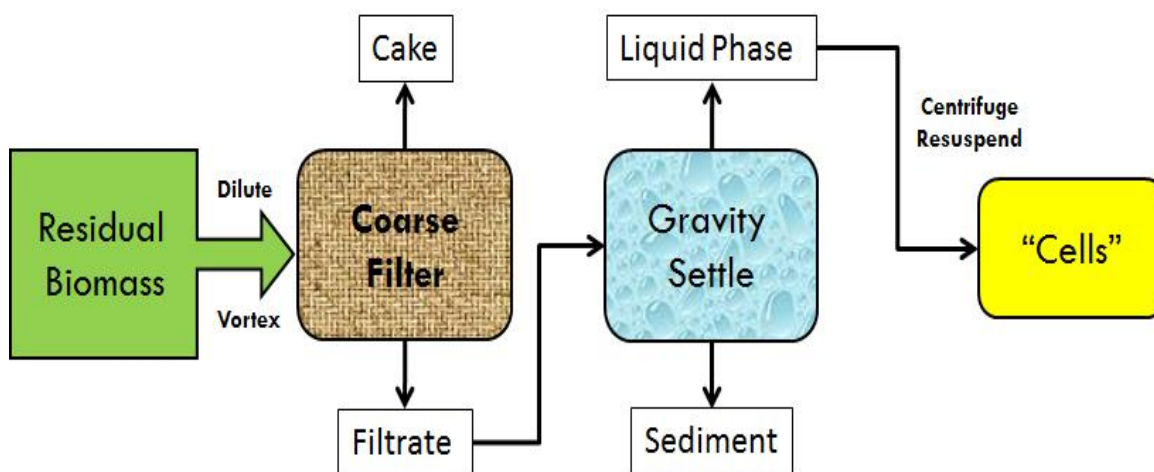


Figure 10-2. Diagram of cell recycle procedure.

10.2.3 Glucose-utilization assay

The glucose reaction mix was prepared by adding glucose deionized and distilled water, buffering with 50-mM potassium phosphate (pH of 7.5), and filter sterilizing (0.2 μm). The glucose reaction mix was aliquoted into capped autoclaved 10-mL glass reaction vessel (Wheaton Science Products, Model# 223686), biomass samples were added, and the vials were incubated in a shaker table incubator at 37 °C and 180 rpm. The 200- μL samples were taken a predetermined time points and were immediately analyzed for glucose concentration in the glucose oxidase enzyme assay (GOEA) using the procedure described in Section 10.2.4. (*Note:* Typically, two samples were taken to

define the reaction rate. The time period between samples was adjusted depending upon the microbial activity; samples were taken more frequently for highly active cultures.)

For liquid samples (i.e., filtrate, liquid phase, sediment, and “cells”), four different volumes of broth (0.20, 0.30, 0.40, and 0.50 mL) were added to the reaction vessel containing the glucose reaction mix (4.8, 4.7, 4.6, 4.6 mL, respectively), for a total volume of 5.0 mL. Liquid samples were assumed to have a density of 1 g/mL.

For solid samples (i.e., residual biomass and cake), four different masses of (0.20, 0.30, 0.40, and 0.50 g wet) were added to the reaction vessel containing the glucose reaction mix (4.8, 4.7, 4.6, 4.6 mL, respectively), for a total volume of 5.0 mL. Solid samples were assumed to have a density of 1 g/mL.

10.2.4 *Glucose concentration determination with glucose oxidase*

Glucose concentrations in samples and calibration standards were calculated as follows. Glucose reaction mix (200 μ L) and glucose oxidase reaction mix (250 μ L, Sigma Aldrich, GAGO20) (glucose oxidase enzyme, O-dianisidine) were added to a 1.5-mL microcentrifuge tube. After a 10-min incubation for color development at 37 °C without shaking, 250 μ L of 12-M sulfuric acid (99% ACS grade) was added to stop the reaction. (*Note:* To limit cell growth, 10-min incubation was used and found acceptable with linear calibration curves instead of the manufacturer-suggested 30 min (Sigma Aldrich, GAGO20).) For soil and sediment samples that had high quantities of suspended solids, the samples were centrifuged for 3 min, 10,000 \times g. From each sample, 250 μ L was transferred to a 96-well plate, and absorbance at 570 nm was determined. Glucose calibration curves were made for each biomass loading. The glucose concentration was determined using a glucose standard curve from 0 to 100 μ g glucose/mL. (*Note:* O-dianisidine is a known human carcinogen. Extreme caution must be used. Use gloves and work in the hood.)

To make calibration curves, six glucose concentrations with 50-mM potassium phosphate buffer (0, 20, 40, 60, 80, 100 μ g glucose/mL) were run in the above glucose oxidase assay. These were analyzed in a 250- μ L 96-well plate (570 nm) (Figure 13-5).

10.2.5 *Moisture and ash contents*

Moisture content (MC) and ash content (AC) were determined by drying in a 105°C forced-convection oven for at least 24 h, and subsequent combustion in a 575 °C furnace for at least 12 h by NREL procedures No. 001 and 005, respectively (NREL, 2004). The ash content was calculated on a dry basis. MC (g water/g wet biomass) is the fraction of moisture in the biomass, and AC (g ash in biomass/g dry biomass) is the fraction of dry ash remaining after 12 h of combustion at 575 °C.

10.2.6 *DNA extraction for real-time PCR*

Fermentation community DNA was extracted using DNeasy Blood and Tissue Kits (Qiagen, Valencia, CA). Prior to extraction, 2.5 mL of fermentation fluid and an equal volume of fermentation solids were placed in a 15-mL centrifuge tube and vortexed at max speed for 5 min. The sample was then centrifuged at 1000×g for 2 min. The resulting supernatant was then centrifuged in a microcentrifuge tube at 5000×g for 10 min until all supernatant was processed. The manufacturer's protocol for Gram-positive bacteria was then followed with the following modification: 200 µL of the elution buffer (10-mM Tris) was added slowly onto the membrane and allowed to incubate at room temperature for 3 min to allow more time for the DNA to bind to the elution buffer. DNA concentration was determined using a ND-1000 spectrophotometer (NanoDrop Technologies, Wilmington, DE) and concentrated to at least 25 ng/µL in an Eppendorf Vacufuge™ (Eppendorf, Hauppauge, NY), and stored at -20 °C until further analysis.

The number of copies was found with real-time PCR by performing 25-µL PCR reactions using the universal bacterial primers 27F (5'-AGA GTT TGA TCC TGG CTC AG-3') and 1492R (5'-CGG TTA CCT TGT TAC GAC TT-3') (Lane, 1991), which amplify the entire 16S rRNA gene region. Each 25-µL reaction contained 100 ng of purified DNA, 1× reaction buffer (10× stock: 500-mM KCl, 300-mM Tris pH 8.3, 15-mM MgCl₂), 2.5 U *Taq* polymerase, forward and reverse primers at a final concentration of 0.4 µM each, 1-µM MgCl₂, 0.1-mM dNTP mix, and 1-mg/mL bovine serum albumin.

Based on methods within Hollister (2008), thermocycling was conducted using a GeneAmp® PCR System 9700 (Applied Biosystems, Foster City, CA) under the following conditions: initial denaturation at 95°C for 1 min; 30 cycles of denaturation at 94°C for 1 min, annealing at 55°C for 1 min, and extension at 72°C for 90 s; and a final extension at 72°C for 10 min (Hollister, 2008).

10.3 Results and discussion

10.3.1 Glucose-utilization assay

In general, from mineral data taken from the biomass recycle trains (Ch. 6–8), potassium, sodium, and nitrogen travel with the liquid phase. Magnesium, calcium, phosphate, copper, iron, zinc, manganese, and carbon travel with solid phases. Therefore, a majority of minerals travel with the solid phase. Copper, which is known in the literature to inhibit GOEA, is present in sufficient quantities to inhibit GOEA in the biomass solids and cells (Table 10-1).

Glucose oxidase enzyme is inhibited by metals (e.g., copper, mercury, silver) (Nakamura and Ogura, 1968). In carboxylate fermentations, small amounts of these metals originate from the chicken manure nutrient source (Table 10-1). The glucose samples with the inoculating material (i.e., biomass, “cells”) could either be (1) immediately filtered and run in GOEA with a single calibration curve, or (2) run as-is in the GOEA and construct calibration curves for every inoculating material and concentration. In this chapter, the latter of the two choices was used because the time to filter the samples would have made the experiment impossible. Instead, calibration tables were constructed at a different time.

Table 10-1. Mineral analysis of dry chicken manure, solid biomass, and cells.

Sample ID	Total Nitrogen (%)	Total Carbon (%)	Organic Carbon (ppm)	P (ppm)	K (ppm)	Ca (ppm)	Mg (ppm)	Na (ppm)	Zn (ppm)	Fe (ppm)	Cu (ppm)	Mn (ppm)
Dry CM	2.19	23.1	–	39860	20215	34855	5277	5763	299	276	146	264
“Solid biomass”	0.47	6.57	3.57	4846	309	21649	366	318	35.28	31.5	3.69	44.18
“Cells”	0.18	2.31	1.19	1567	686	17072	158	63	29.24	5.42	3.74	22.97

For each sample, calibration curves were made for four different inocula concentrations (i.e., 0.10, 0.08, 0.06, and 0.04 g biomass/mL reaction volume). Figure 10-3 shows the glucose calibration curves, relating the absorbance (570 nm) to the glucose concentration ($\mu\text{g/mL}$) of the residual biomass and cells. Increased biomass loadings increased inhibition and decreased the calibration slope. For example, for solid biomass at 0.10 g biomass/mL, the calibration slope is 0.0049 g biomass/(mL·min). Whereas at 0.04 g biomass/mL, the calibration slope is 0.0056 g biomass/(mL·min). Also shown in Figure 10-3, when comparing the biomass solids and resuspended “cells” in a liquid phase, more solid particles in the sample correlates with higher enzyme inhibition. The R^2 values close to unity (~ 0.99), which indicates that GOEA is a sensitive and reproducible method to quantify small concentrations of glucose (1–100 $\mu\text{g/mL}$).

For most biomass loadings, glucose was digested linearly during the short time frame (~ 4 h) with a minimum of four time points collected (0.10 g/mL shown in Figures 10-4 to 10-9). Figures 10-10 to 10-15 plot the glucose digestion (averaged triplicates) of fermentation biomass solids, cake, filtrate, sediment, liquid phase, and “cells” at an initial loading of 0.10, 0.08, 0.06, and 0.04 g biomass/mL (570 nm), with standard error bars. In Figures 10-10 to 10-15, except for the filtrate and liquid-phase cell separation streams, the R^2 values are close to unity, indicating reproducible digestion. For the filtrate and liquid-phase separation streams (Figures 10-12 and 10-14, respectively) the deviations from linearity could result from the difficulty of obtaining homogeneous mixtures of the different carboxylate fermentation cell separation streams.

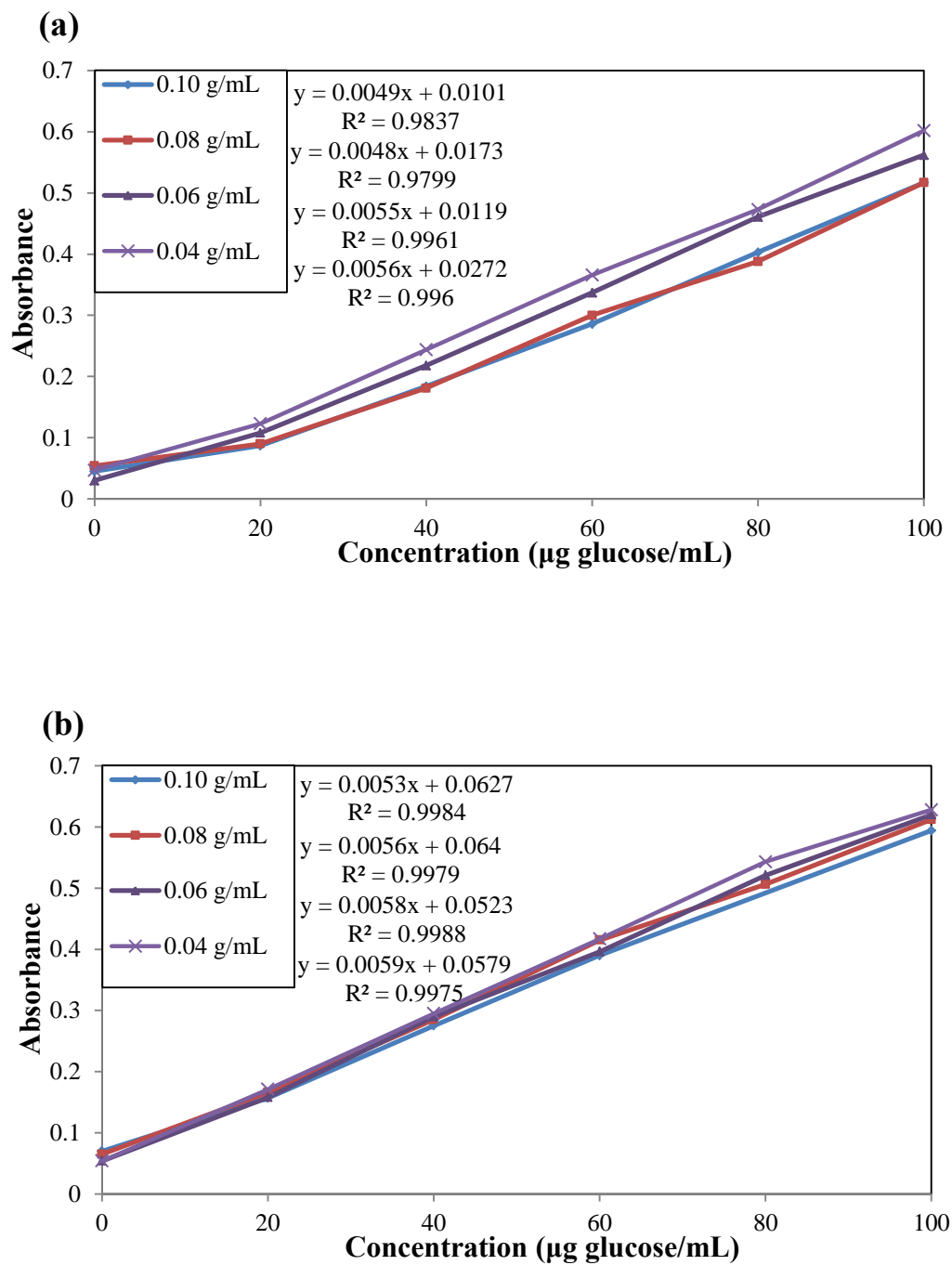


Figure 10-3. Example of glucose calibration curves for (a) biomass solids and (b) “cells” at 0.10, 0.08, 0.06, and 0.04 g biomass/mL.

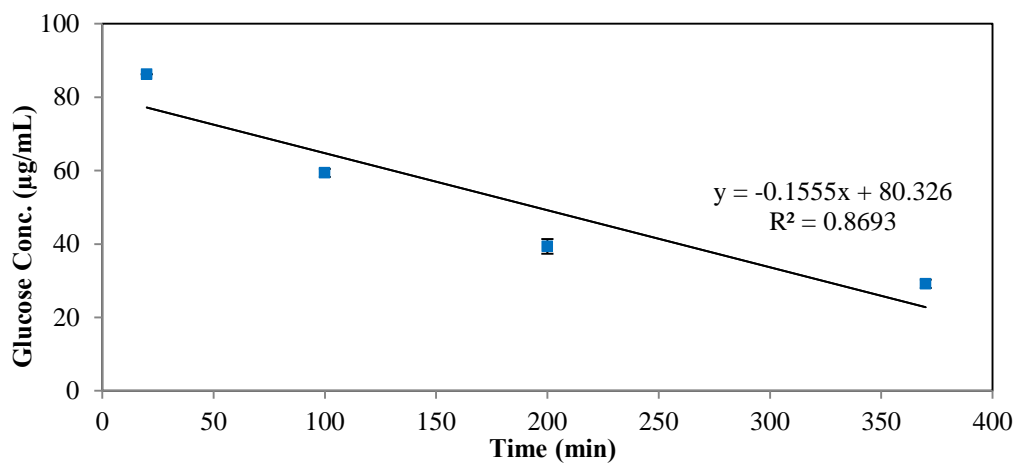


Figure 10-4. Residual biomass glucose digestion with time for 0.10 g biomass/mL loading. Error bars represent the standard error in triplicate experiments.

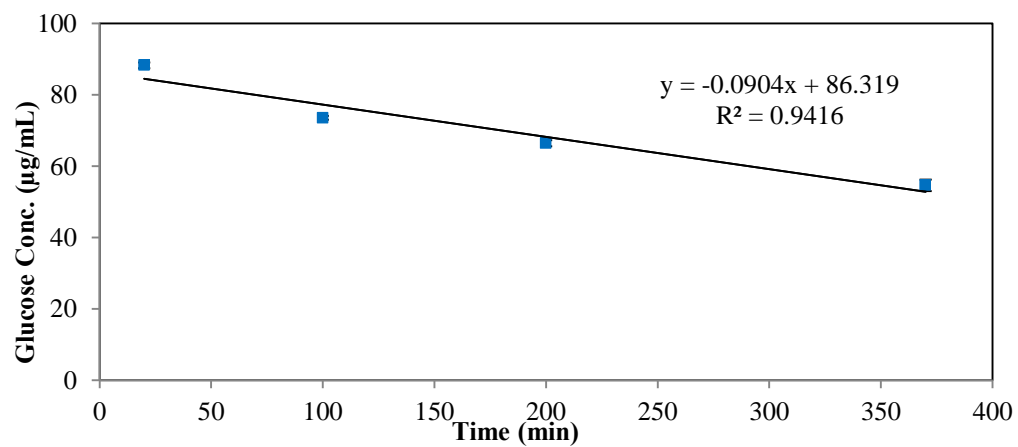


Figure 10-5. Cake glucose digestion with time for 0.10 g biomass/mL loading. Error bars represent the standard error in triplicate experiments.

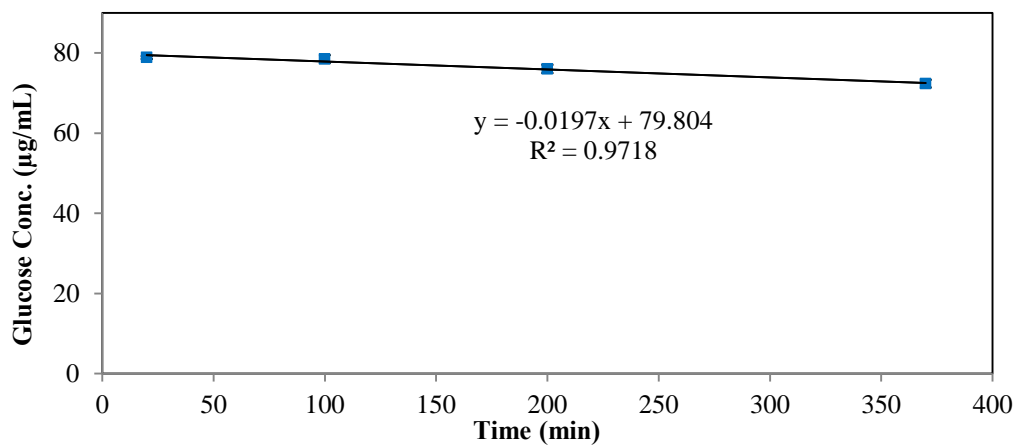


Figure 10-6. Filtrate glucose digestion with time for 0.10 g biomass/mL loading. Error bars represent the standard error in triplicate experiments.

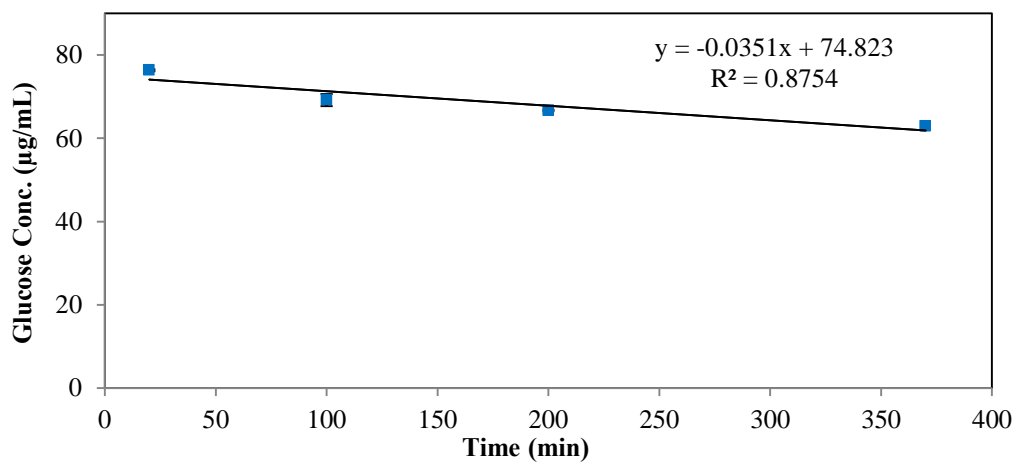


Figure 10-7. Sediment glucose digestion with time for 0.10 g biomass/mL loading. Error bars represent the standard error in triplicate experiments.

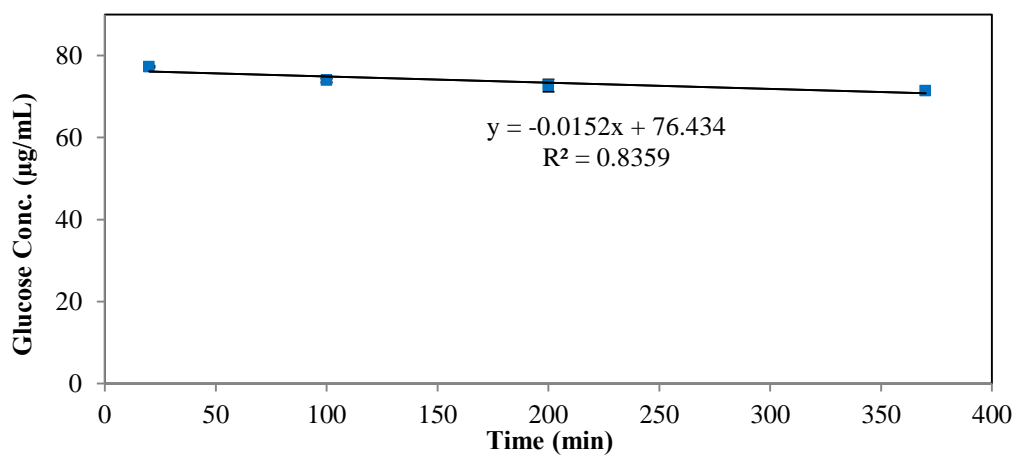


Figure 10-8. Liquid phase glucose digestion with time for 0.10 g biomass/mL loading. Error bars represent the standard error in triplicate experiments.

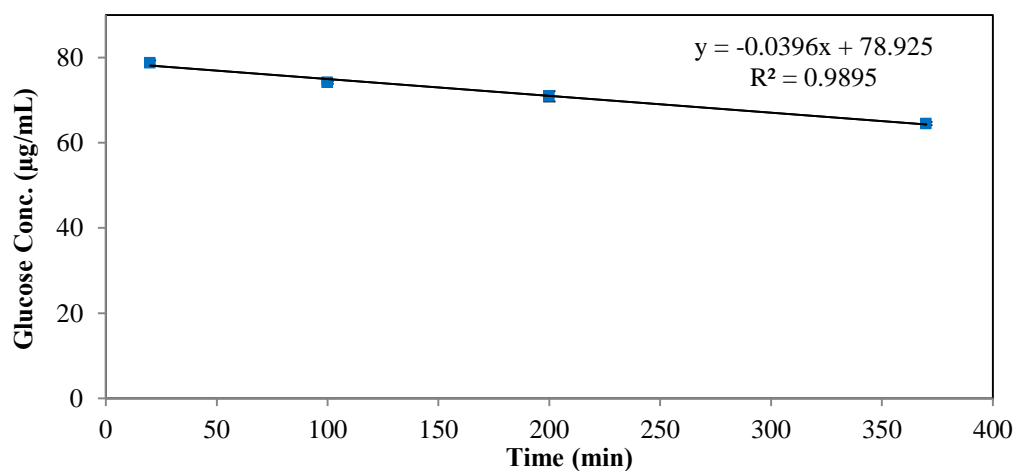


Figure 10-9. "Cells" glucose digestion with time for 0.10 g biomass/mL loading. Error bars represent the standard error in triplicate experiments.

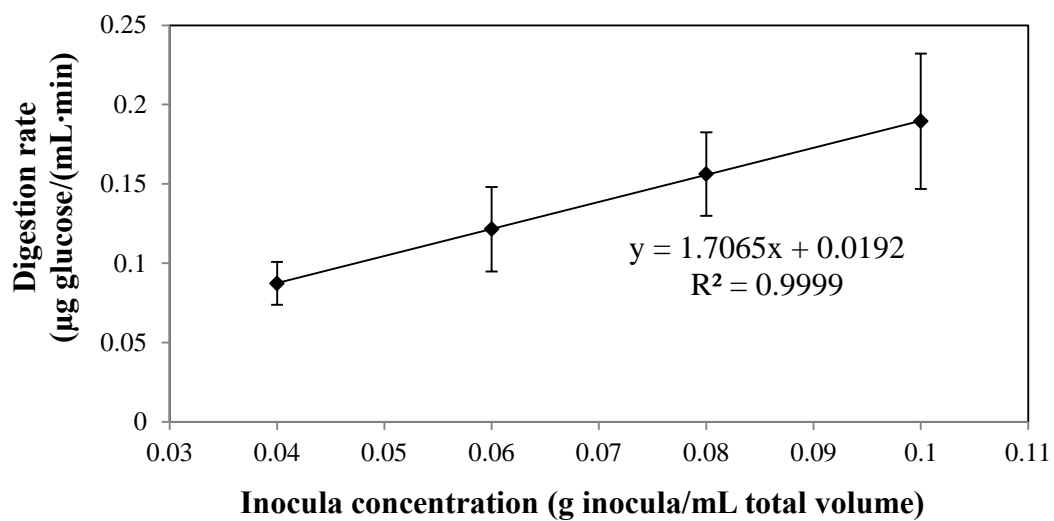


Figure 10-10. Glucose digestion using residual biomass. Error bars represent the standard error in triplicate experiments.

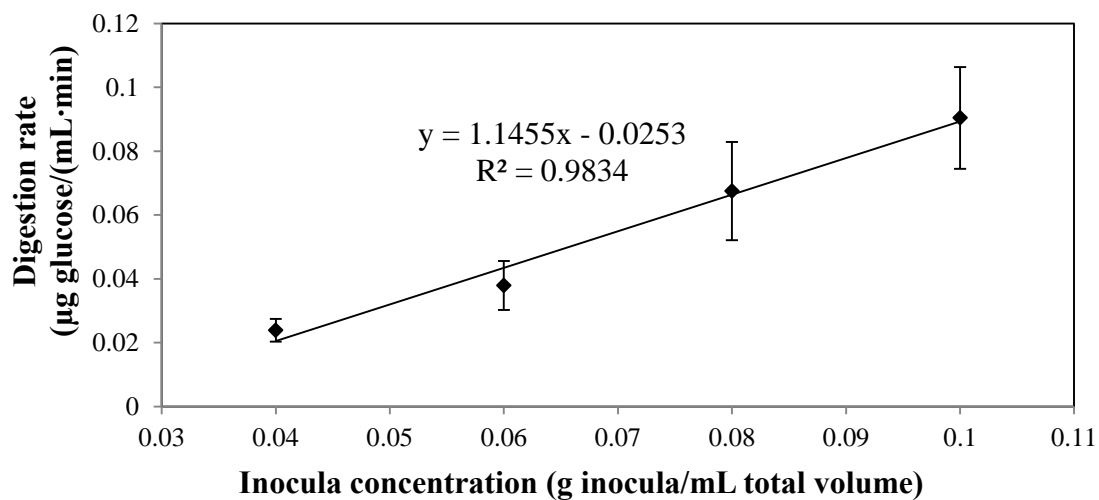


Figure 10-11. Glucose digestion using cake. Error bars represent the standard error in triplicate experiments.

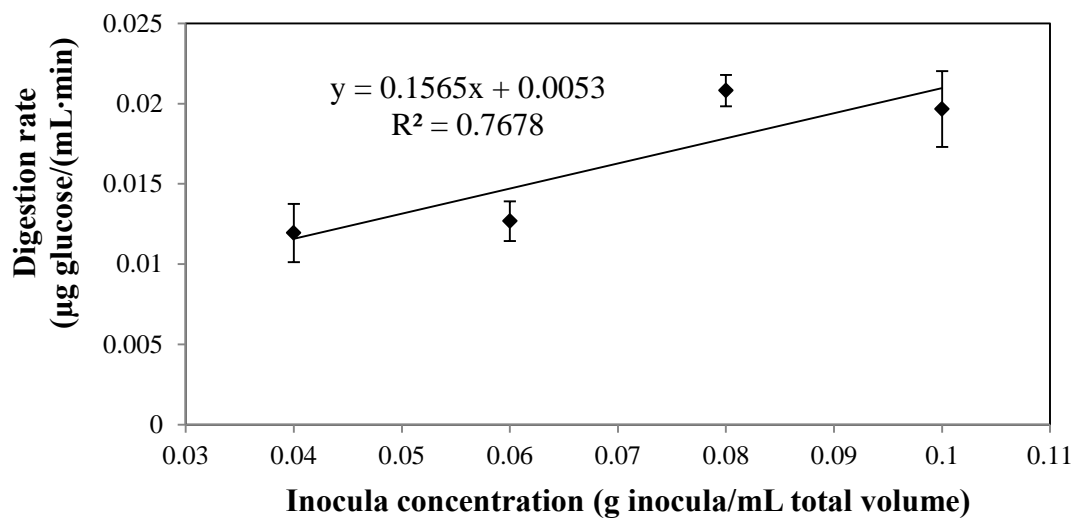


Figure 10-12. Glucose digestion using filtrate. Error bars represent the standard error in triplicate experiments.

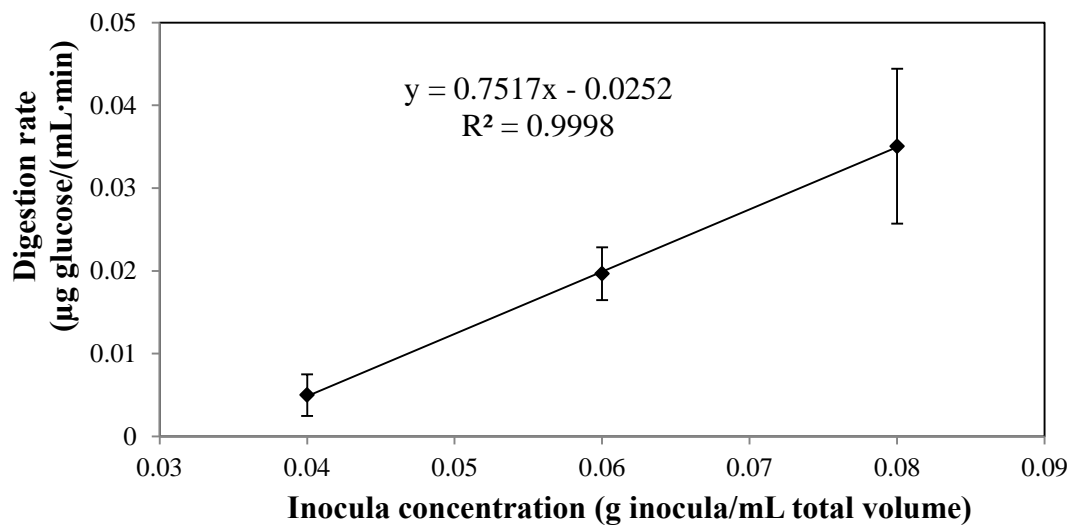


Figure 10-13. Glucose digestion using sediment. Error bars represent the standard error in triplicate experiments.

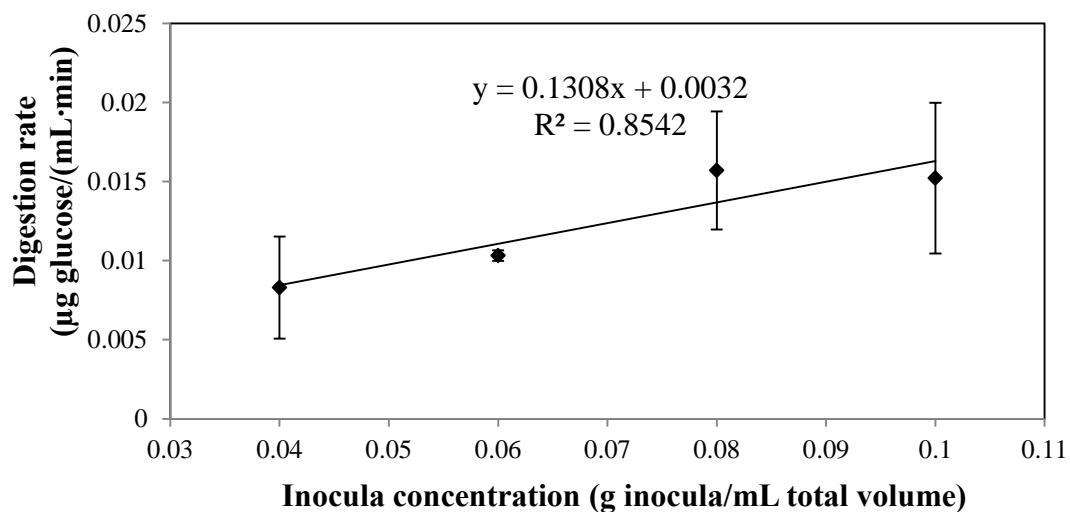


Figure 10-14. Glucose digestion using liquid phase. Error bars represent the standard error in triplicate experiments.

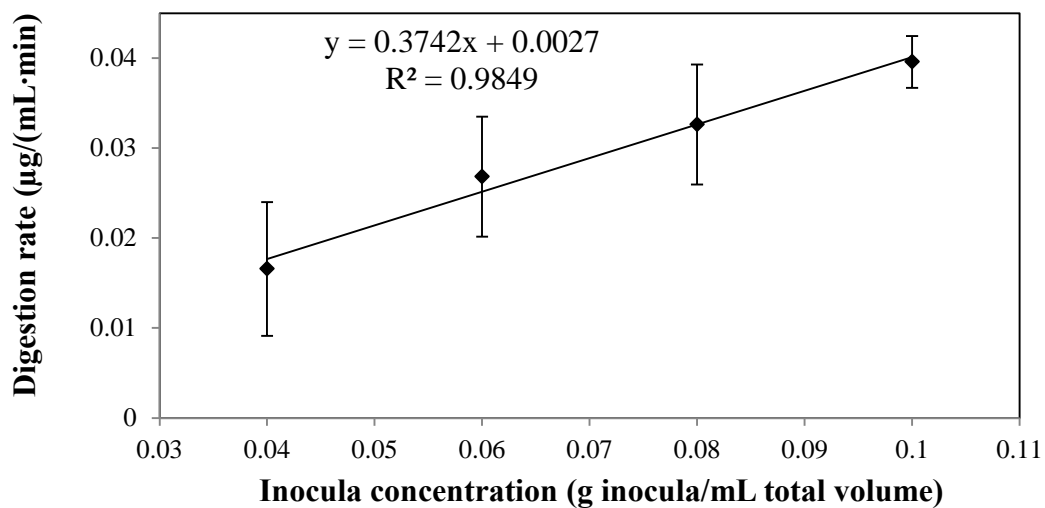


Figure 10-15. Glucose digestion using "cells." Error bars represent the standard error in triplicate experiments.

The fermentation solids had the highest specific digestion rate (1.707 μg glucose/(min·g inoculum), or *glucose-utilization units*, followed by the cake, sediment, filtrate, cells, and liquid phase (Table 10-2). The glucose-utilization assay shows that the coarse filter did not successfully concentrate bacteria in the filtrate, and the gravity settling did not successfully concentrate the bacteria in the liquid phase. Evidently, the streams that had a lower moisture content had higher glucose-utilization units. This might be attributed to the cells attached to solid particles. Perhaps the vortexing was not enough of a physical disruption to detach the cells from the solid particles. However, excessive vortexing may cause cell lysis; further investigation is warranted.

Table 10-2. From the glucose-utilization assay, specific digestion rate of the different separated phases in the cell separation procedure.

Sample	Specific digestion rate (μg glucose/(min·g inoculum))	Mass* (g)	Cell balance	R ²	MC (g water/ g wet biomass)	AC (g ash/ g dry biomass)
Residual biomass	1.707	100.0	100	0.99	0.746 \pm 0.001	0.377 \pm 0.006
Cake	1.146	92.2	63	0.98	0.790 \pm 0.002	0.259 \pm 0.002
Filtrate	0.157	359.3	34	0.77	0.988 \pm 0.000	0.505 \pm 0.003
Sediment	0.752	5.8	3	0.99	0.987 \pm 0.000	0.505 \pm 0.008
Liquid phase	0.131	353.5	28	0.85	0.977 \pm 0.000	0.770 \pm 0.001
“Cells”	0.374	113.7	25	0.98	0.997 \pm 0.000	0.378 \pm 0.024

*Normalized masses obtained for this cell separation collection

To estimate the number of cells in each of the cell separations streams, the glucose-utilization units and overall masses from each stream were multiplied. (*Note:* This assumes there is a direct correlation between glucose digestion and number of cells.) Figure 10-16 shows the cell balance from the sugar-utilization assay, with a 100 cell basis. The coarse filter had excellent closure (97%); however, vortexing does not appear to physically detach a majority of the cells from the solid biomass particles. A majority of the cells (63%) remained in the solid portion of the biomass, and a smaller

portion exit with the filtrate (34%). After inspecting the calibration curves, the amount of inhibitory metals present in the solid biomass and cake are less than in the filtrate. However, this should not affect the results because the calibration curves account for the different inhibitions.

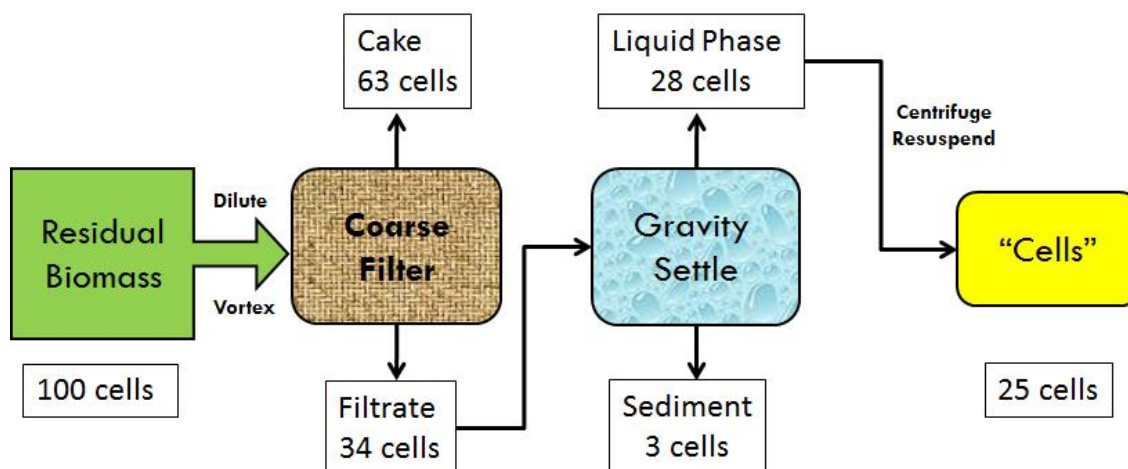


Figure 10-16. Diagram of cell balance on cell recycle procedure using the glucose-utilization assay.

The next separation step used gravity settling, which also had a good closure (91%). Here, more of the solid particles settled out as sediment, which had few cells (3 cells) of the entering 34 cells. The liquid phase, which had a majority of cells after gravity settling, was centrifuged and resuspended in DI water. The separated “cells” had 25% of the initial glucose-utilizing units or cells.

Based on this experiment, gravity settling is unnecessary because an equivalent number of cells can be recovered from the vortexing and coarse filter alone. However, other inexpensive and simple separation processes should be investigated before implementing cell recycle in commercial scale.

10.3.2 Real-time PCR

For a comparison to the sugar-utilization assay, real-time PCR was performed. For real-time PCR, the number of DNA copies (universal bacteria primer) per gram of sample was found. For quality assurance, real-time PCR standard curves were run in triplicates and found to have an R^2 of 0.978. With a rough estimate of 4.4 DNA copies per cell, the total number of bacteria was found per gram. The highest concentration of bacteria was found in the residual biomass. The filtrate, sediment, liquid phase, and cells had similar concentrations of bacteria. The cake had the lowest concentration of bacteria. The coarse filter successfully concentrated the bacteria in the filtrate, and gravity settling successfully concentrated the bacteria in the liquid phase.

Table 10-3. Cell balances using real-time PCR.

Sample	DNA copies/g**	Bacteria/g*	Cell balance
Solid biomass	$6.71 \times 10^9 \pm 9.00 \times 10^5$	1.52×10^9	100
Cake	$3.18 \times 10^7 \pm 2.51 \times 10^4$	7.22×10^6	0
Filtrate	$1.20 \times 10^9 \pm 4.74 \times 10^5$	2.72×10^8	64
Sediment	$7.46 \times 10^8 \pm 1.45 \times 10^5$	1.70×10^8	1
Liquid phase	$1.38 \times 10^9 \pm 1.11 \times 10^5$	3.14×10^8	73
“Cells”	$1.36 \times 10^9 \pm 7.04 \times 10^5$	3.10×10^8	23

*Assuming 1 cell has 4.4 DNA copies

** \pm standard error

Similarly, a cell balance was performed with real-time PCR (Figure 10-17). Real-time PCR had a different cell balance than the glucose-utilization assay, especially for the coarse filter, which had a low closure (64%). However, real-time PCR indicates that 100% of the cells successfully detached from the waste biomass resulting from vortexing and coarse filtration, which is much higher than that predicted by the glucose-utilization

assay (34%). Gravity settling had a closure of 116%, with a majority of the cells in the liquid phase. The separated “cells” had 23% of the initial DNA copy numbers or cells.

From these results, gravity settling is probably unnecessary because an equivalent number of cells can be recovered from the vortexing and coarse filtration alone. However, other inexpensive and simple separation processes should be investigated before implementing cell recycle in commercial scale.

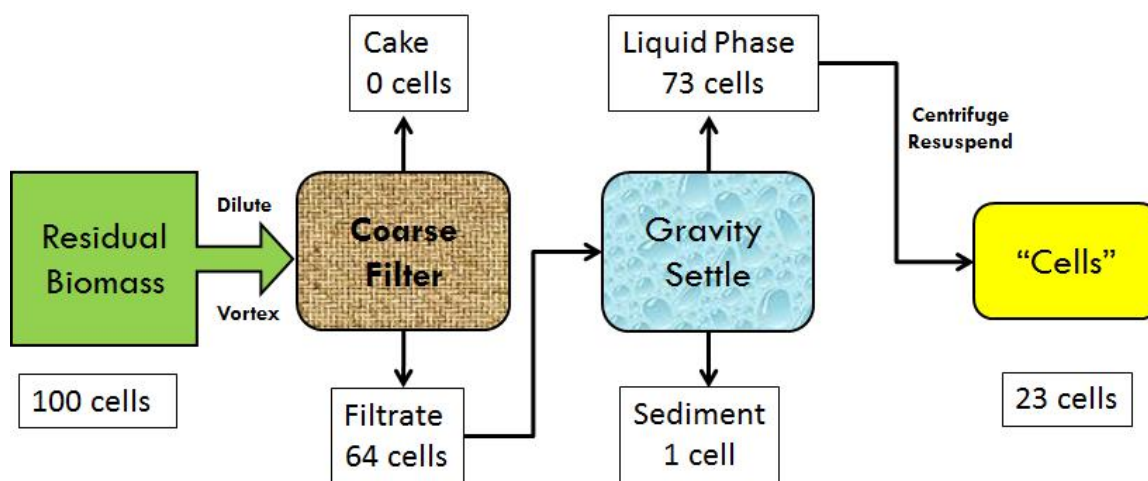


Figure 10-17. Diagram of cell balance on cell recycle procedure using real-time PCR assay.

10.4 Conclusions

To optimize the cell separation technique, both the glucose-utilization assay and real-time PCR were used to measure the bacterial concentrations in each of the six different stages. Neither technique directly quantifies cell load; instead, they measure a metabolite or constituent that indirectly relates to total cell load. The glucose-utilization assay measures the glucose digestion rate of a community of microorganisms, and therefore infers total cell load from metabolic activity. In contrast, real-time PCR

measures the number of copies of a universal bacteria gene in both living and dead bacteria, and therefore infers cell load from a cell constituent.

For both the glucose-utilization assay and real-time PCR, the residual biomass had the highest concentration of bacteria. It was difficult to separate the cells from the initial biomass via vortexing. Perhaps vortexing was not enough of a physical disruption to detach the cells from the solid particles; however, too much vortexing might cause cell lysis. The glucose-utilization assay indicated that separated “cells” were 25% of the “cells” in the initial waste biomass. Similarly, the real-time PCR assay indicated that, the separated “cells” were 23% of the “cells” in the initial waste biomass. Thus, the two assay methods are consistent in their estimate of the final cell recovery from the cell recycle procedure.

Although both the glucose-utilization and real-time PCR assays were consistent in the estimate of the final percentage of cells recovered, they were *not* consistent in their estimated recovery in the intermediate steps. For example, in the coarse-filtration step, the glucose-utilization assay had 100% closure whereas the real-time PCR assay had only 64% closure. This result suggests that the sugar utilization assay is more trustworthy. This conclusion is further reinforced by the observation that real-time PCR estimates that there were no cells in the coarse-filter cake, which would require complete cell separation, which is unreasonable given the difficulty of the task. Further, the real-time PCR results are unreasonable when considering the sugar assay results. How could the coarse-filter cake be cell-free (as suggested by real-time PCR) but also consume glucose (as measured by the glucose-utilization assay)?

In the gravity-settling step, the glucose-utilization assay showed good closure (91%), which was better than the real-time PCR closure (116%). Based upon these results, the glucose-utilization assay is superior to the real-time PCR assay. Further, the glucose-utilization assay measures only live cells (desired) whereas real-time PCR measures both live and dead cells (undesired).

Regarding the efficacy of the cell-recycle procedure, the glucose-utilization assay showed that the coarse filter recovered only about a third of the cells in the initial waste

biomass and gravity settling seemed unnecessary to isolate bacteria. Using simple vortexing, effective separation of bacterial cells from waste biomass exiting the carboxylate fermentation has proved to be difficult. To achieve better cell recovery in the coarse-filtration step, other inexpensive and simple separation processes should be investigated before implementing cell recycle in commercial scale.

Because vortexing had poor cell recovery, the residual biomass had the highest microbial load; recycling the raw residual biomass in the continuous carboxylate fermentations would be useful to retain the microorganisms. Unfortunately, refractory compounds (e.g., lignin) would also be recycled, which occupies fermentor volume unproductively. Using vigorous agitation (vortexing), around 25% of the original cells in the biomass can be recycled with very little recycle of refractory materials. Future research should focus on developing methods that increase cell recovery from the residual biomass.

11. CELLULAR BIOMASS RECYCLE IN COUNTERCURRENT MIXED-ACID FERMENTATION: EFFECT OF TWO REFLUX RATIOS AND THREE CARBON-NITROGEN RATIOS

In carboxylate fermentations, microorganisms are the biocatalysts, but are typically discarded in exit streams. To improve fermentation performance, this study investigated the effect of recycling cells isolated from residual biomass waste. Countercurrent four-stage fermentations were implemented with different reflux ratios. Three carbon-nitrogen (C-N) ratios were employed: 11, 21, and 77 g C/g N. In general, compared to no cell recycle, recycling cellular biomass into Fermentor 1 increased selectivity and yield, but decreased conversion. Compared to lower cell reflux, higher reflux increased productivity, yield, conversion, but decreased selectivity. Generally, compared to previous studies that recycled residual biomass waste, cell recycle had increased selectivity and yield, but decreased conversion. Therefore, continuous fermentation performance can be increased by implementing cell recycle as opposed to residual biomass recycle, although both are beneficial compared to no recycle.

11.1 Introduction

Liquid transportation fuels (e.g., gasoline, diesel, and aviation fuel) are mostly supplied by petroleum. Consumption continues to increase with economic expansion and population growth (Nigam and Singh, 2011); however, petroleum fuels cannot be used indefinitely because their combustion causes global warming, acid rain, and pollution (Armaroli and Balzani, 2011; Demirbas, 2007). Also, petroleum is a finite resource, which inevitably will lead to increasing prices as supplies become more scarce (Alekkett et al., 2010). To supply growing transportation fuel needs and increase national security, developing processes that produce sustainable transportation fuel sources is becoming increasingly important. Currently, biofuels are the only means to displace liquid fossil

fuels, and represent 3.5% vol. of global transportation fuels (IEA, 2011c). Bioethanol and biodiesel are the main biofuel contributors (Demirbas, 2008); however, these fuels are inconvenient to handle and use in the existing petroleum infrastructure (Savage, 2011). One promising alternative is the carboxylate platform, which converts lignocellulose to conventional liquid hydrocarbon fuels (Agler et al., 2011).

The carboxylate platform is a biomass-to-energy technology that biologically converts biomass (e.g., agricultural residues, municipal solid waste, sewage sludge) into carboxylate salts that can be chemically converted into hydrocarbon fuels (Holtzapple et al., 1999; Holtzapple and Granda, 2009) and chemicals (Granda and Holtzapple, 2008). In the fermentation step, biomass is fermented by a mixed-culture of microorganisms to produce carboxylic acids, which are buffered to form carboxylate salts. These salts are precipitated and thermally converted to ketones (e.g., acetone), hydrogenated to mixed alcohols (e.g., isopropanol), and catalytically converted to hydrocarbons (e.g., gasoline, jet fuel).

The carboxylate platform has low capital and operating costs, does not require sterile operating conditions or added enzymes, and has reached the demonstration level of development (Granda et al., 2009; Pham et al., 2010). Converting biomass into liquid fuels does not cause a net increase in atmospheric carbon dioxide because biomass growth sequesters the same amount of carbon dioxide that was released during combustion (Ragauskas et al., 2006; Sahin, 2011).

In multi-staged countercurrent fermentations (Figure 11-1), such as the four-stage train in this study, solids and liquids are transported through a series of fermentors (a *train*) in opposite directions, allowing the least reactive (most digested) biomass to contact the lowest acid concentration, thereby minimizing product inhibition (Aiello-Mazzarri et al., 2006). This countercurrent strategy is designed to achieve both high product concentration and high conversion (Fu and Holtzapple, 2010b). As the biomass decomposes, it becomes less reactive. Because biomass is a heterogeneous mixture, the easily fermentable solids quickly convert into acids in the first fermentor, with the remaining solid residue undergoing conversion in subsequent fermentors to achieve

greater substrate conversion. Residual biomass exits from Fermentor 4, while product liquid exits from Fermentor 1 (Figure 11-1).

Microorganisms (e.g., bacteria, archae, fungi) are the biocatalysts that convert lignocellulose to mixed acids. Recovering and recycling the microorganisms from the waste streams may improve fermentation performance. Previous studies have recycled residual biomass exiting from Fermentor 4 as waste (Ch. 6–8) back into the fermentation system because separating microorganisms from residual biomass may be difficult and costly. However, separating microorganisms from the residual biomass might be necessary if there are negative impacts from other contents of the recycle stream (e.g., acids, ash, recalcitrant volatile solids).

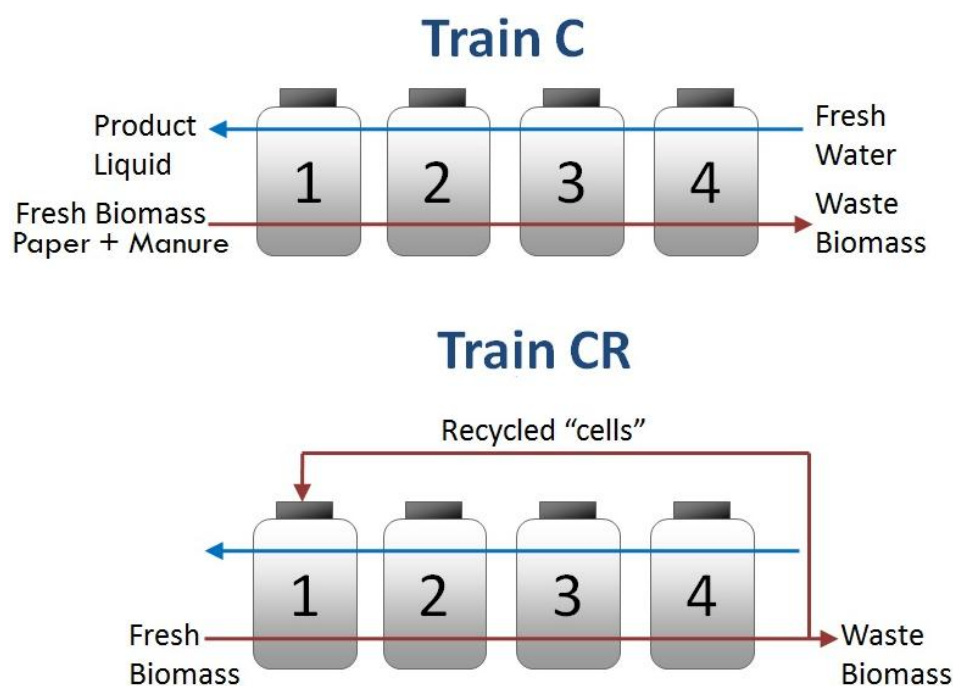


Figure 11-1. Diagram of the cellular recycle experiment, depicting the control (Train C) with no biomass recycle and the cell recycle train (Train CR).

Cell recycle and retention is advantageous when the process microorganisms grow slowly, which is typical in carboxylate fermentations (Hamer, 1982; Karel et al., 1985). Cell recycle has been practiced in industrial fermentations and other bioreactor systems, with performance improvements of up to 12 times the control (Brandberg et al., 2007; Choudhury and Swaminathan, 1998; Cysewski and Wilke, 1977; Palmqvist et al., 1998). Cell recycle is an essential step in the activated sludge process, which is widely used to treat sewage. Many different cell recycle or retention systems have been proposed, including cell filtration, sedimentation, and immobilization. Many cell recycle processes are performed on monoculture bioreactors with low solids concentrations, which allow for easy separation of cells from fermentation broth. In this study, the carboxylate fermentations employ a mixed culture with high solids concentration, which makes it challenging to recycle cells. To recover cells from the residual biomass exiting Fermentor 4, a cellular recycle technique was developed where the residual biomass was diluted, gravity settled, coarsely filtered, microcentrifuged, and recycled into Fermentor 1.

Recycling cells from residual biomass back into the fermentation system might allow adapted microorganisms to be retained for a longer period of time, which could enhance fermentor performance. The purpose of this study is to investigate the effects of cellular recycle on continuous fermentation performance with different cell-recycle reflux ratios and low, medium, and high carbon-nitrogen (C-N) ratios.

11.2 Materials and methods

All materials and methods were previously described (Ch. 6), except for the following.

11.2.1 Countercurrent fermentation procedure

Two four-stage countercurrent fermentation trains (Figure 11-1) were run: a control train with no recycle (Train C), and a train that recycled cellular biomass to Fermentor 1 (Train CR). These two countercurrent trains were run at three carbon-nitrogen ratios (11, 21, 77 g non-acid organic carbon (OC_{NA})/g nitrogen (N)). The cell recycle technique was employed using a preset amount of residual biomass (18 g wet

residual biomass per transfer, Table 11-1) from which the cells were recovered. The conversions for the fermentation trains were affected by the C-N ratio; therefore, for each C-N ratio, the total residual biomass exiting the trains was different. This caused the trains operating at different C-N ratios to have different cellular refluxes ranging from 7 to 15% (i.e., 7 to 15 g wet residual biomass/100 g wet residual biomass exiting the process from Fermentor 4). In one case (C-N = 21 g OC_{NA}/g N), cells were recovered from 35 g wet residual biomass per transfer, which corresponded to a reflux ratio of 48% (Table 11-1).

The feed consisted of 80% shredded office copier paper and 20% dry homogenized chicken manure on a dry mass basis. Each fermentor was inoculated with Galveston inoculum and incubated at 40 °C as a submerged fermentation. The two fermentation trains were initiated as batch cultures under anaerobic conditions with a concentration of 100 g non-acid dry solid (NADS)/L deoxygenated water, which was achieved by adding substrate, nutrient source (manure and urea), inoculum, buffer (calcium carbonate), and liquid medium to each fermentor.

After the first week of batch growth, solid/liquid transfers began and occurred every 48 h to reach steady state. Every 48 h, fermentors were removed from the incubator, the gas volume was collected, liquid samples were taken, the pH was measured, fermentors were centrifuged (3300×g, 25 min), and the solid/liquid mass transfers were performed. Fresh deoxygenated water was added to Fermentor 4 (F4), and all of the filtered liquid was transferred from Fermentor 3 (F3) to Fermentor 2 (F2), F2 to Fermentor 1 (F1), and out of F1 as the product liquid. In a countercurrent manner, fresh substrate was fed to F1 and a portion of the homogenized solids was transferred from F1 to F2, F2 to F3, F3 to F4, and exited F4 as *residual biomass*. During transfers, the solid wet weight retained equaled 225 g in F2, F3, and F4, and 125 g in F1.

Table 11-1. Operating parameters for the control (Train C) and cell recycle train (Train CR) with various C-N ratios and amount of wet biomass used for cell recycle. Normalized values represent the mean of the steady-state values \pm CI (95% CI).

Fermentation train	C		CR		C		CR		C		CR	
	11 (low)		21 (medium)		21 (medium)		77 (high)		77 (high)		77 (high)	
C-N ratio	11 (low)		21 (medium)		21 (medium)		77 (high)		77 (high)		77 (high)	
Amount residual biomass for cell recycle (g wet/ <i>T</i>)	0	18	0	18	35	0	18	35	0	18	35	18
Reflux ratio* (%)	0	7	0	15	48	0	9	9	0	9	9	9
Solid and liquid transfer frequency, <i>T</i> (h)	48	48	48	48	48	48	48	48	48	48	48	48
NAVS feed rate (g NAVS/ <i>T</i>)	24.3	24.3	24.3	24.3	24.3	24.3	24.3	24.3	24.3	24.3	24.3	24.3
Dry solids added (g/ <i>T</i>)	32	32	32	32	32	32	32	32	32	32	32	32
Manure added (g/ <i>T</i>)	7.6	7.6	7.6	7.6	7.6	7.6	7.6	7.6	7.6	7.6	7.6	7.6
Urea added (g/ <i>T</i>)	3.0	3.0	1.0	1.0	1.0	0.0	0.0	0.0	0.0	0.0	0.0	0.0
Calcium carbonate added (g/ <i>T</i>)	4.0	4.0	4.0	4.0	4.0	4.0	4.0	4.0	4.0	4.0	4.0	4.0
Fermentor recycle point	–	F1	–	F1	F1	–	F1	F1	–	F1	F1	F1
Liquid feed rate (mL/ <i>T</i>)	300	300	300	300	300	300	300	300	300	300	300	300
Solid cake retained in F1 (g, wet)	125	125	125	125	125	125	125	125	125	125	125	125
Solid cake retained in F2–F4 (g, wet)	225	225	225	225	225	225	225	225	225	225	225	225
Centrifuged liquid retained in F1–F4 (mL)	0	0	0	0	0	0	0	0	0	0	0	0
Methane inhibitor (μ L/(<i>T</i> ·fermentor))	80	80	80	80	80	80	80	80	80	80	80	80
Reflux ratio* (g recycled biomass/g exiting biomass)	–	0.07 \pm 0.0	–	0.15 \pm 0.02	0.48 \pm 0.12	–	0.09 \pm 0.01	0.09 \pm 0.01	–	0.09 \pm 0.01	0.09 \pm 0.01	0.09 \pm 0.01
Volatile solid loading rate, VSLR (g NAVS/(L _{liq} ·d))	7.4 \pm 0.1	7.2 \pm 0.1	6.1 \pm 0.06	6.3 \pm 0.07	6.2 \pm 0.1	7.0 \pm 0.1	6.9 \pm 0.1	6.9 \pm 0.1	7.0 \pm 0.1	6.9 \pm 0.1	6.9 \pm 0.1	6.9 \pm 0.1
Liquid residence time, LRT (d)	12.9 \pm 1.8	11.6 \pm 0.9	13.6 \pm 0.55	13.9 \pm 0.96	13.0 \pm 0.8	14.1 \pm 1.5	13.2 \pm 1.0	13.2 \pm 1.0	14.1 \pm 1.5	13.2 \pm 1.0	13.2 \pm 1.0	13.2 \pm 1.0
Total liquid volume, TLV (L)	1.6 \pm 0.0	1.7 \pm 0.0	2.0 \pm 0.02	1.9 \pm 0.02	2.0 \pm 0.1	1.7 \pm 0.0	1.8 \pm 0.0	1.8 \pm 0.0	1.7 \pm 0.0	1.8 \pm 0.0	1.8 \pm 0.0	1.8 \pm 0.0
Concentration of volatile solid, VS (g NAVS/L _{liq})	62 \pm 2.6	58 \pm 2	55 \pm 1	56 \pm 1	60 \pm 3	54 \pm 2	54 \pm 1	54 \pm 1	54 \pm 2	54 \pm 1	54 \pm 1	54 \pm 1
Concentration of dry solid, DS (g NADS/L _{liq})	86 \pm 2.8	84 \pm 2	91 \pm 2	86 \pm 2	94 \pm 3	98 \pm 3	89 \pm 2	89 \pm 2	98 \pm 3	89 \pm 2	89 \pm 2	89 \pm 2
Average carbon-nitrogen ratio, C-N (g organic C _{NA} /g N)	11.1 \pm 4.0	11.7 \pm 2.4	21.4 \pm 2.15	21.6 \pm 4.06	20.9 \pm 9.2	75.1 \pm 14.5	80.0 \pm 15.5	80.0 \pm 15.5	75.1 \pm 14.5	80.0 \pm 15.5	80.0 \pm 15.5	80.0 \pm 15.5
Average pH (F1–F4)	8.4 \pm 0.2	8.4 \pm 0.1	5.7 \pm 0.12	5.3 \pm 0.08	5.7 \pm 0.1	6.0 \pm 0.1	6.0 \pm 0.1	6.0 \pm 0.1	6.0 \pm 0.1	6.0 \pm 0.1	6.0 \pm 0.1	6.0 \pm 0.1
Total urea added (g urea/(L _{liq} ·d))	0.91 \pm 0.02	0.89 \pm 0.00	0.25 \pm 0.00	0.26 \pm 0.00	0.25 \pm 0.01	0.00 \pm 0.00	0.00 \pm 0.00	0.00 \pm 0.00	0.00 \pm 0.00	0.00 \pm 0.00	0.00 \pm 0.00	0.00 \pm 0.00

*Reflux ratio: Residual biomass reflux ratio (g wet residual biomass for cell recycle/100 g wet residual biomass exiting)

A preset amount of residual biomass (Table 11-1) was collected, homogenized, and after a series of separation steps (Procedure 2.2), cells were recycled back into F1 (Train R1). In each fermentor, the solids were resuspended, iodoform was added, and calcium carbonate was added to neutralize carboxylic acids and buffer the system (Table 11-1). Urea was added to adjust the C-N ratio. During solid and liquid transfers, when the fermentors were open to the atmosphere, anaerobic conditions were maintained by flushing the fermentors with nitrogen gas (Praxair, Bryan, TX). (*Note:* Nitrogen flushing was a precautionary step; these anaerobic fermentations have been shown to resist intermittent air exposure (Golub et al., 2011b)). The fermentors were then resealed and placed back in the incubator.

11.2.2 *Cellular recycle procedure*

Fresh residual biomass was diluted, vortexed, gravity settled, filtered, and centrifuged to separate and concentrate cells in the residual biomass stream. First, the residual biomass solids were collected, and the solids were homogenized by stirring vigorously for 30 s in a beaker using a spatula. A portion of the homogenate was separated and weighed according to the percent reflux, diluted four times with deoxygenated water, shaken by hand for 10 s, and then vortexed for 3 min. The vortexed homogenate was carefully filtered through a wire mesh filter (~20 mesh) into a separate container. The debris caught in the filter was periodically discarded to ensure flow. To remove large particles that were not caught in the filter, the filtrate was allowed to gravity settle for 10 min. The liquid phase was then decanted and centrifuged for 10 min at $10,000\times g$ at room temperature. The supernatant was decanted, and pellet was resuspended with deoxygenated water. After homogenizing the contents, these were then pipetted back into F1.

11.2.3 *Operating parameters*

Previous investigations using continuous countercurrent fermentations have shown that adequate conversion and exit yield were achieved with a volatile solid loading rate (VSLR) of ~6.3 g NAVS/(L·d) and liquid residence time (LRT) of ~13 d

(Chan and Holtzapple, 2003; Ross, 1998; Smith et al., 2011); therefore, this VSLR and LRT were chosen to investigate the performance of a cell recycle fermentation system. The LRT and VSLR (Table 11-1) were regulated by controlling the liquid and solid transfer frequency (T), the non-acid volatile solids (NAVS) feed rate, and the liquid feed rate per transfer. Volatile solids (VS) are defined as the mass of dry solid material that is combusted at 575 °C after 12 h, and NAVS are defined as VS less the amount of carboxylic acid:

$$\text{NAVS} = (\text{g total wet biomass})(1 - \text{MC})(1 - \text{AC}) - (\text{g acid in biomass}) \quad (11-1)$$

where MC (g water/g wet biomass) is the fraction of moisture in the biomass, and AC (g ash in biomass/g dry biomass) is the fraction of dry ash remaining after 12 h of combustion at 575 °C. In performance calculations, NAVS is preferred because it ensures the product is not quantified with the reactant.

The nutrient source (dried chicken manure) contains carboxylic acids. To more accurately quantify fermentor productivity, the amount of acid entering the system in the manure is subtracted from the amount of acid exiting the system in the product liquid and discarded solids.

The VSLR and LRT are calculated as follows:

$$\text{VSLR} = \frac{\text{NAVS feed (g)}}{\text{TLV(L)} \cdot \text{time (d)}} \quad (11-2)$$

$$\text{LRT} = \frac{\text{TLV (L)}}{\text{liquid flow rate out of fermentation train (L/d)}} \quad (11-3)$$

The total liquid volume (TLV) includes both free and interstitial liquid. Liquid flow rate out of fermentation train includes product liquid exiting and liquid in residual biomass exiting.

11.2.4 Definition of terms

To account for the total mass in the system, a mass balance closure was calculated with Equation 11-4,

$$\text{mass balance closure} = \frac{\text{mass out (g)}}{\text{mass in (g)} + \text{water of hydrolysis (g)}} \quad (11-4)$$

Cellulose is a polysaccharide composed of individual anhydrous glucose units (glucan, MW = 162 g/mol). During digestion, cellulose is enzymatically hydrolyzed to glucose by adding water. The water of hydrolysis was calculated as previously described (Chan and Holtzapfle, 2003).

The mixed-acid concentration can be expressed as molar acetic acid equivalents (α), which is the reducing potential of an equivalent amount of acetic acid (Datta, 1981).

$$\begin{aligned} \alpha = & 1.00 \times \text{acetic (mol/L)} + 1.75 \times \text{propionic (mol/L)} \\ & + 2.50 \times \text{butyric (mol/L)} + 3.25 \times \text{valeric (mol/L)} \\ & + 4.00 \times \text{caproic (mol/L)} + 4.75 \times \text{heptanoic (mol/L)} \end{aligned} \quad (11-5)$$

Acetic acid equivalents (Aceq) can be expressed on a mass basis as

$$\text{Aceq (g/L)} = 60.05 \text{ (g/mol)} \times \alpha \text{ (mol/L)} \quad (11-6)$$

Aceq proportionally weighs the higher-chained carboxylic acids (C₃ to C₇); the higher acids have higher Aceq than lower acids.

11.2.5 Measuring performance

The feed and exit rate of acid, ash, NAVS, water, and gas were determined during the steady-state period. The average rate of each component was calculated using the *slope method* (Smith and Holtzapple, 2011b). In this method, the moving cumulative sum of each component is plotted with respect to time. The slope of the steady-state portion of this line is the rate. All performance variables (e.g., conversion, selectivity, and yield) were calculated from the averaged component rates determined by the slope method, as described below:

$$\begin{aligned}
 \text{Conversion } x &\equiv \frac{\text{NADS}_{\text{feed}} \text{ g} - \text{NADS}_{\text{exit}} \text{ (g)}}{\text{NAVS}_{\text{feed}} \text{ (g)}} \\
 &= \frac{\text{NAVS}_{\text{feed}} \text{ g} + \text{Ash}_{\text{feed}} \text{ g} - \text{NAVS}_{\text{exit}} \text{ g} - \text{Ash}_{\text{exit}} \text{ (g)}}{\text{NAVS}_{\text{feed}} \text{ (g)}} \quad (11-7) \\
 &= \frac{\text{NAVS}_{\text{consumed}} \text{ (g)}}{\text{NAVS}_{\text{feed}} \text{ (g)}}
 \end{aligned}$$

$$\text{Exit yield } (Y_E) \equiv \frac{\text{total acid output from solid and liquid streams (g)}}{\text{NAVS}_{\text{feed}} \text{ (g)}} \quad (11-8)$$

$$\text{Process yield } (Y_P) \equiv \frac{\text{total acid output in product liquid stream (g)}}{\text{NAVS}_{\text{feed}} \text{ (g)}} \quad (11-9)$$

$$\text{Culture yield } (Y_C) \equiv \frac{\text{total acid produced (g)}}{\text{NAVS}_{\text{feed}} \text{ (g)}} \equiv Y_E - Y_F \quad (11-10)$$

$$\text{Feed yield } (Y_F) \equiv \frac{\text{total acid entering with feed (g)}}{\text{NAVS}_{\text{feed}} \text{ (g)}} \quad (11-11)$$

$$\begin{aligned}
 \text{Selectivity } (\sigma) &\equiv \frac{\text{total acid produced (g)}}{\text{NAVS}_{\text{feed}} \text{ (g)} - \text{NAVS}_{\text{exit}} \text{ (g)}} \quad (11-12) \\
 &\equiv \frac{\text{total acid produced (g)}}{\text{NAVS digested (g)}} = \frac{Y_E}{x}
 \end{aligned}$$

$$\text{Acid productivity } (P) \equiv \frac{\text{total acids produced (g)}}{\text{TLV (L)} \cdot \text{d}} \quad (11-13)$$

where $\text{NADS}_{\text{feed}}$ is the non-acid dry solids fed, $\text{NADS}_{\text{exit}}$ is the non-acid dry solids removed from the fermentation, $\text{NAVS}_{\text{feed}}$ is the non-acid volatile solids fed, $\text{NAVS}_{\text{exit}}$ is the non-acid volatile solids removed from the fermentation, Ash_{feed} is the inert solids fed and includes both the ash in the biomass feed and buffer, and Ash_{exit} is the inert solids in all exiting solid and liquid streams. NADS includes the ash and volatile solid component of biomass. Ash is assumed to be conserved in the fermentation (Ash_{feed} equals Ash_{exit}), canceling Ash from Equation 11-7.

Per g NAVS fed, the exit yield (Y_E) represents the sum of acid in the product transfer liquid, waste transfer solids, and liquid samples removed from sampling. The process yield (Y_P) represents all the acid in the product transfer liquid per g of NAVS fed. The feed yield (Y_F) is the total g acid entering with the feed per g NAVS fed, and the culture yield (Y_C) is the exit yield less the feed yield.

11.2.6 Statistical analysis

Statistical analysis was performed using Excel 2007 (Microsoft, USA). The mean and standard deviations of the daily amounts of total acid, acetic acid equivalents (Aceq), non-acid volatile solids (NAVS) in and out were determined from steady-state operating data. For all countercurrent trains, the average time required to reach steady state was ~52 d. The variations between trains with time to reach steady state results from slight disturbances in the microorganism community either from fed materials or human error. These averaged values were then used to calculate the acid productivity (P), selectivity (σ), yield (Y), and conversion (x) with a 95% confidence interval (CI). Unless specified otherwise, all comparisons in the Results and Discussion section are statistically significant. The steady-state region was the period during which the product total acid and Aceq concentration, dry solids exiting, liquid volume and solid weight of each fermentor, pH, and mass of acid exiting did not vary by more than 2.2 standard deviations from the average for a period of at least one liquid residence time. For each

train, the slope of the summed data was used to calculate the means of the performance variables which were compared using a Student's two sample *t*-test (two-tailed, Type 3). The *p* values had a familywise error rate of 0.05 using the Bonferroni correction. All error bars are reported at 95% CI.

11.3 Results and discussion

Each fermentation train consisted of a four-stage countercurrent semi-continuous submerged fermentation system. Two fermentation trains were operated: a control train with no recycle (Train C), and a train that recycled cellular biomass to Fermentor 1 (Train CR). Both fermentation trains operated at three C-N ratios (11, 21, 77 g OC_{NA}/g N).

To compare the results of all trains, the LRT and VSLR operating parameters were normalized by explicitly controlling the liquid/solid mass transfer frequency (*T*), the volatile solids (VS) feed rate, the liquid feed rate, and the amount of cake retained in each fermentation reactor per transfer (Table 11-1). For comparison to residual biomass recycle studies (Ch. 6–8), this cell recycle study helps decouple the effects of cell recycle from the other multiple components in the residual biomass (e.g., volatile solids, ash, acid, nutrients) that are transported in the solid or liquid streams.

For all seven experimental conditions, the accumulated mass of total carboxylic acids and Aceq exiting, NADS added, and NADS removed from their respective trains was found. The slopes of the quasi-steady-state regression lines provided the daily total acid and Aceq exiting, NADS exiting, and NADS removed on a mass basis (Table 11-2). Productivity was calculated as the mass rate of acid produced per TLV.

11.3.1 Carbon-nitrogen ratio

Because the C-N ratio and pH affect fermentation performance, they must be controlled for accurate analysis. To compare fermentation trains, the C-N ratio was used to control the nutrients and substrate and was quantified as previously described (Smith et al., 2011). A computer model developed in Excel 2007 (Microsoft, USA) was used to predict the amount of nitrogen (as urea) that needed to be added to the system (Smith et

al., 2011). The low C-N ratio fermentations were controlled at 11 ± 1 g OC_{NA}/g N and pH 8.4 ± 0.0 , the medium C-N ratio fermentations were controlled at 21 ± 1 g OC_{NA}/g N and pH 5.5 ± 0.1 , and the high C-N ratio fermentations were controlled at 77 ± 3 g OC_{NA}/g N and pH 6.0 ± 0.0 (Table 11-1). (*Note:* The pH in the low C-N ratio was high because large amounts of urea were added, which hydrolyzed to ammonia and raised the pH.)

11.3.2 *Reflux ratio*

For each C-N ratio, cells were recovered from 18 wet g of residual biomass every 48 h. Because the conversions were different for each C-N ratio, the amount of residual biomass exiting Fermentor 4 varied in each case. As a consequence, the *reflux ratio* (g wet residual biomass recycled/100 g wet residual biomass exiting Fermentor 4) was unique for each C-N ratio. For C-N ratios of 11, 21, and 77 g OC_{NA}/g N, the corresponding reflux ratios were 7, 15, and 9% (Table 11-1). To investigate increased cell reflux ratio, for C-N ratios of 24 g OC_{NA}/g N, cells were recovered from 35 wet g of residual biomass every 48 h. In this case, the reflux ratio was 48%.

11.3.3 *Biogas*

When comparing Trains C and CR at different C-N ratios, the amount of biogas produced in the trains at a medium C-N ratio were optimal, followed by high C-N ratio, and then low C-N ratio (Table 11-2). Except at medium C-N ratios (21 g OC_{NA}/g N) at higher reflux (48%), Train C with no cell recycle had slightly higher biogas productions than Train CR. At all C-N ratios, there is a loose correlation between conversion and amount of biogas produced (Table 11-2). Other studies of ethanol and ruminal fermentations show gas production is related to substrate digestibility (Contreras-Govea et al., 2011; Weimer et al., 2005). The average biogas composition was similar to other studies (Ch. 7). No methane was detected in any fermentor.

Table 11-2. Performance measures for control (Train C) and cellular recycle (Train CR) at various C-N ratios and reflux ratios. Values represent the mean of the steady-state values \pm CI (95% CI).

Train	C	CR	C	CR	CR	C	CR
C-N ratio	11 (low)		21 (medium)			77 (high)	
Amount residual biomass for cell recycle (g wet/T)	0	18	0	18	35	0	18
Reflux Ratio* (%)	0	15	0	15	48	0	9
Total carboxylic acid concentration (g/L)	11.90 \pm 0.70	12.70 \pm 0.59	16.69 \pm 0.52	18.66 \pm 0.28	18.00 \pm 0.27	11.74 \pm 0.49	11.14 \pm 0.24
Aceq concentration (g/L)	13.25 \pm 0.79	14.26 \pm 0.67	26.10 \pm 0.88	29.37 \pm 0.49	29.27 \pm 0.44	15.52 \pm 0.64	14.76 \pm 0.32
Total carboxylic acid exiting (g/d)	0.78 \pm 0.00	0.76 \pm 0.00	2.01 \pm 0.01	2.19 \pm 0.01	2.49 \pm 0.01	0.90 \pm 0.00	0.98 \pm 0.00
Aceq exiting (g/d)	0.85 \pm 0.00	0.84 \pm 0.00	3.15 \pm 0.01	3.48 \pm 0.01	4.04 \pm 0.01	1.19 \pm 0.01	1.29 \pm 0.00
Aceq/Acid ratio	1.11 \pm 0.00	1.12 \pm 0.00	1.57 \pm 0.01	1.57 \pm 0.01	1.63 \pm 0.00	1.33 \pm 0.01	1.32 \pm 0.00
Conversion, x (g VS digested/g VS fed)	0.080 \pm 0.000	0.076 \pm 0.000	0.405 \pm 0.002	0.390 \pm 0.002	0.465 \pm 0.006	0.126 \pm 0.001	0.119 \pm 0.000
Selectivity, σ (g acid produced/g NAVS consumed)	0.777 \pm 0.005	0.839 \pm 0.003	0.403 \pm 0.002	0.456 \pm 0.002	0.424 \pm 0.003	0.584 \pm 0.003	0.663 \pm 0.001
Aceq selectivity, σ_a (g Aceq produced/g NAVS consumed)	0.851 \pm 0.005	0.927 \pm 0.004	0.632 \pm 0.003	0.724 \pm 0.003	0.688 \pm 0.004	0.776 \pm 0.004	0.878 \pm 0.001
Exit yield, Y_E (g acid/g NAVS fed)	0.062 \pm 0.000	0.063 \pm 0.000	0.163 \pm 0.001	0.178 \pm 0.001	0.197 \pm 0.001	0.073 \pm 0.000	0.079 \pm 0.000
Exit Aceq yield, Y_{aE} (g Aceq/g NAVS fed)	0.068 \pm 0.000	0.070 \pm 0.000	0.256 \pm 0.001	0.282 \pm 0.001	0.320 \pm 0.001	0.097 \pm 0.000	0.105 \pm 0.000
Culture yield, Y_C (g acid/g NAVS fed)	0.047 \pm 0.000	0.048 \pm 0.000	0.148 \pm 0.001	0.162 \pm 0.001	0.182 \pm 0.001	0.058 \pm 0.000	0.064 \pm 0.000
Process yield, Y_P (g acid/g NAVS fed)	0.038 \pm 0.000	0.036 \pm 0.000	0.143 \pm 0.001	0.145 \pm 0.000	0.178 \pm 0.001	0.044 \pm 0.000	0.051 \pm 0.000
Productivity, P (g total acid/(L _{liq} ·d))	0.357 \pm 0.007	0.341 \pm 0.003	0.921 \pm 0.010	1.033 \pm 0.013	1.170 \pm 0.027	0.415 \pm 0.009	0.445 \pm 0.003
Biogas produced (g/d)	0.53 \pm 0.00	0.39 \pm 0.00	2.53 \pm 0.01	2.49 \pm 0.02	3.13 \pm 0.02	0.75 \pm 0.00	0.73 \pm 0.00
Mass balance closure (g mass in/g mass out)	0.96 \pm 0.00	0.98 \pm 0.00	0.95 \pm 0.00	0.96 \pm 0.00	1.00 \pm 0.00	0.90 \pm 0.00	0.95 \pm 0.00

*Reflux ratio: Residual biomass reflux ratio (g wet residual biomass for cell recycle/100 g wet residual biomass exiting)

Table 11-3. *p* values for performance measures to compare control (Train C) to cellular recycle (Train CR) at various recycle ratios (RR) and C-N ratios ($\alpha = 0.05$).

Trains	Conversion	Selectivity	Exit yield	Exit yield Aceq	Culture yield	Process yield	TLV	Productivity	Biogas produced	Total acid conc.	Aceq conc.	Total acid exit	Total Aceq exit	Aceq/Total acid
C and CR (15 RR, 21 CN)	0.00	0.00	0.00	0.00	0.00	0.00	0.01	0.00	0.00	0.00	0.00	0.00	0.00	0.20
C and CR (48 RR, 21 CN)	0.00	0.00	0.00	0.00	0.00	0.00	0.48	0.00	0.00	0.00	0.00	0.00	0.00	0.00
C and CR (9 RR, 11 CN)	0.00	0.00	0.00	0.00	0.01	0.00	0.02	0.00	0.00	0.08	0.05	0.00	0.09	0.00
C and CR (7 RR, 77 CN)	0.00	0.00	0.00	0.00	0.00	0.00	0.00	0.00	0.00	0.00	0.03	0.00	0.00	0.34

p value < 0.0125 statistically different

11.3.4 *Acid concentration*

Compared to the low and high C-N ratio, at the medium C-N ratio, both Train C and CR had higher total acid and Aceq concentration (Table 11-2). At the medium C-N ratio at both reflux ratios, compared to Train C, Train CR had higher total acid and Aceq concentration (Tables 11-2, 11-3). However, at the medium C-N ratio, increased cell recycle did not significantly increase total acid and Aceq concentration. These results demonstrate that cellular recycle increases acid concentrations at medium, but not at other C-N ratios. Also, higher cellular reflux ratios do not increase acid concentrations.

11.3.5 *Daily acid production*

In each fermentor of a train, TLV quantifies the total volume of liquid, including free liquid and interstitial liquid in the solid phases. Compared to the respective control, Train CR did not always have similar TLVs, indicating slight variation between trains. To further standardize the analyses, the amount of acid exiting the fermentors per day was calculated on a mass basis from the product liquid and waste streams (Table 11-2).

When comparing Trains C and CR at different C-N ratios, the amount of daily acid produced in the trains at medium C-N ratio were optimal, followed by high C-N ratio, and then low C-N ratio (Table 11-2). Compared to the respective control, at medium and high C-N ratios, Train CR had higher total carboxylic acid and Aceq exiting (g/d) (Tables 11-2, 11-3). At medium C-N ratios, compared to the lower cellular reflux of 15%, at the higher cellular recycle of 48%, Train CR produced more total carboxylic acid and Aceq exiting (g/d) (Tables 11-2, 11-3). At a low C-N ratio, compared to Train C, Train CR had a slightly decreased total acid exiting, and no difference in Aceq exiting (g/d) (Tables 11-2, 11-3). At the medium and high C-N ratio, this result shows that recycling cells improves the amount of daily total acid and Aceq exiting the fermentation train. Also, increasing the cellular reflux from 15% to 48% increased the daily total acid and Aceq exiting (g/d).

11.3.6 *Aceq-to-total-acid ratio*

When comparing Trains C and CR at different C-N ratios, the Aceq-to-total-acid ratio in the trains at medium C-N ratio were optimal, followed by high C-N ratio, and then low C-N ratio (Table 11-2). Besides total Aceq concentration and exiting, another measure of the production of higher molecular weight carboxylic acids (e.g., valeric, caproic, and heptanoic acid) is the Aceq-to-total-acid ratio. The larger the Aceq-to-total-acid ratio, the more high-molecular-weight acids are present (see Equation 11-5). When comparing Trains C and CR at high C-N ratio and at the medium C-N ratio with 15% reflux, the Aceq-to-total-acid ratios were not different. However, at low C-N ratio and medium C-N ratio at 48% reflux, Train CR had higher Aceq-to-total-acid ratios than Train C. Thus, cellular recycle increases production of higher-molecular-weight carboxylic acids at low C-N ratios and at medium C-N ratios with higher reflux (Tables 11-2, 11-3).

11.3.7 *Carboxylic acid composition profiles*

The proportion of C2–C7 carboxylic acids, or the *product spectrum*, is affected by variables such as temperature, microorganism community, feedstock, C-N ratio, pH, and oxygen exposure (Chan and Holtzapple, 2003; Golub et al., 2011a; Liu et al., 2008; Smith and Holtzapple, 2011a). In carboxylate fermentation systems, all of the above mentioned variables affect the metabolism of the specific mixed-culture community. Some studies assume that metabolism is optimized by the free energy producing and consuming steps and, consequentially, the growth rate (Forrest et al., 2011).

In this study, the C-N ratio and pH effects are highly similar to those for the residual biomass recycle studies (Ch. 6–8); there are strong effects of cell recycle, C-N ratio, and pH on product spectrum. As shown in Figure 11-2, medium C-N ratio fermentations have an evenly distributed acid profile, with C2, C4, and C6 being the most prominent acids, followed by C3, C5, and C7. The lower cell recycle reflux (15%) does not affect the proportion of carboxylic acids; however, increased cell recycle reflux (48%) increases the proportion of higher-molecular-weight acids.

At low C-N ratio fermentations, there is a high concentration of acetic acid (>75%) with less propionic acid (~15%), and the rest being mostly butyric acid, which agrees with other studies (Rodriguez et al., 2006; Zhang et al., 2009). This large concentration of acetic acid could be an effect of the high pH, which occurred at low C-N ratios. Because urea was the nitrogen supplement, naturally present urease produced ammonia, which raised the pH. Because acetic acid has a higher protonating power than the other acids, the bacteria might be trying to protect themselves from the high pH by producing a higher percentage of acetic acid. Cell recycle again appears to increase the proportion of higher-molecular-weight acids, specifically C3 and C4 (Figure 11-2).

The high C-N ratio fermentations had an almost equivalent amount of C2 and C3 acids (~80%), with a smaller amount of C4 and C5 (~15%), and the remainder being C6 and C7. At the high C-N ratio, the acid profile has combined attributes of both the low and medium C-N ratio fermentations. It has large amount of low-molecular-weight acids like the low C-N ratio, but has a more diverse profile like the medium C-N ratio. For high C-N ratio fermentations, because fixed nitrogen is vital for DNA, RNA, enzymes, and amino acids, the lack of high-molecular-weight acids can possibly be attributed to not enough fixed nitrogen to support cell growth and energy assimilation (Srivastava and Srivastava, 2003). Because the pH of both the high and medium C-N ratio fermentations are somewhat similar, the differences between the profiles of these fermentations are certainly more of the effect of C-N ratio and not pH. Cell recycle does not appear to affect the proportion of acids (Figure 11-2).

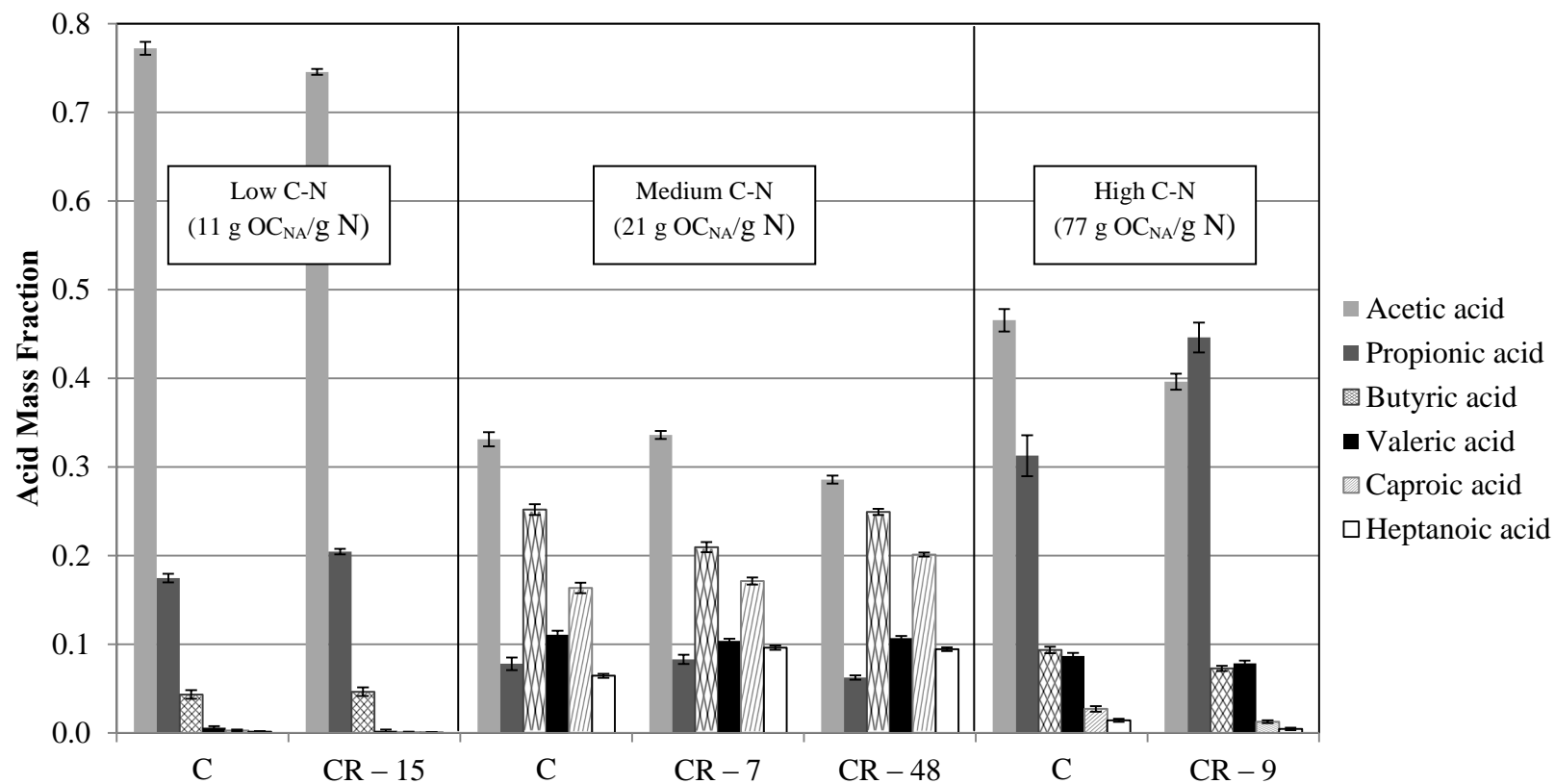


Figure 11-2. Carboxylic acid composition profile for the control (Train C) with no cellular recycle and the cell recycle train (Train CR). For each Train CR, cells were recovered from the recycle stream with the indicated reflux ratio (g wet residual biomass recycled/100 g wet residual biomass exiting Fermentor 4). Error bars are the 95% confidence intervals for each carboxylic acid composition during the steady-state period.

11.3.8 Productivities

When comparing Trains C and CR at different C-N ratios, the productivity in the trains at medium C-N ratio were optimal, followed by high C-N ratio, and then low C-N ratio (Table 11-2). At the medium C-N ratio, at the lower cellular reflux of 15%, Trains CR had 12% higher productivity than the control (Tables 11-2, 11-3). At the higher cellular reflux of 48%, Train CR had 27% higher productivity than the control (Train C) (Tables 11-2, 11-3). This result indicates that there was a significant increase in productivity with higher cellular recycle ratios (Table 11-3). At low C-N ratios, Trains CR had lower productivity than Train C. At high C-N ratios, Train CR had higher productivity than Train C. Compared to the respective control, this result indicates that cellular recycle increased productivities at both high C-N ratios and medium C-N ratios. Also, increasing the cellular recycle reflux ratio increases the productivity, which is similar to the results from other studies with pure cultures (Crespo et al., 1992).

11.3.9 Yield

The exit yield Y_E (Equation 11-8) quantifies the sum of acid exiting the fermentation in the product transfer liquid, residual biomass, and liquid samples per g NAVS feed. The culture yield Y_C (Equation 11-11) represents the acid produced by the mixed culture per g NAVS_{feed} and is equal to the exit yield less the feed yield Y_F (Equation 11-10). The exit acetic acid equivalent yield Y_{aE} quantifies the sum of acetic acid equivalents exiting the fermentation in the product transfer liquid, waste transfer solids, and liquid samples per g NAVS feed. When comparing Trains C and CR at different C-N ratios, all yields in the trains at medium C-N ratio were optimal, followed by high C-N ratio, and then low C-N ratio (Table 11-2). At the low, medium, and high C-N ratios, Y_E , Y_{aE} , and Y_C were improved by cellular recycle indicating significant increase in performance from cellular recycle (Tables 11-2, 11-3). At the medium C-N ratio, compared to the control, the higher cellular reflux of 48% increased Y_E , Y_{aE} , and Y_C by more than 20% (Tables 11-2, 11-3). Therefore, at all C-N ratios, recycling cells back into the fermentation increases yield, and increasing the reflux ratio increases yield.

The process yield Y_P (Equation 11-9) quantifies only the acid in the product transfer liquid per g $NAVS_{feed}$, which is sent downstream to be clarified, concentrated, and processed into chemicals and fuel; thus, Y_P represents a commercially relevant acid yield. At the medium and high C-N ratios, Y_P was improved by cellular recycle, but there was no significant difference in Trains C and CR at the low C-N ratio (Tables 11-2, 11-3). At the medium C-N ratio, compared to the cellular recycle train operating at the low cellular recycle of 15%, the higher cellular reflux of 48% had higher Y_P , and increased Y_P over 20% compared to the control (Tables 11-2, 11-3). Therefore, cellular recycle increased the amount of acid in the product liquor with respect to $NAVS$ fed, and increased Y_P can be achieved with higher reflux ratio.

11.3.10 *Conversion and selectivity*

When comparing Trains C and CR at different C-N ratios, conversion in trains at medium C-N ratio were optimal, followed by high C-N ratio, and then low C-N ratio (Table 11-2). In general, for all C-N ratios and reflux ratios, compared to Train C, Train CR had lower conversion and higher selectivity (Tables 11-2, 11-3). This contrasts with the trend found for biomass recycle (Ch. 6), where with increased reflux, there was an increase in conversion but decrease in selectivity. This suggests the following possibilities: (1) an increase in recycled inhibitors decreased growth rate in the microorganisms, increasing metabolic efficiency; (2) when cells are recycled, the microorganisms sense their increased concentration, allowing them to spend a majority of their life cycle making product as opposed to growing and reproducing, also known as quorum sensing (Miller and Bassler, 2001); (3) when cells are recycled, a maximum cell concentration is reached, and additional cells are used as a substrate that are converted to acids; and/or (4) cell recycle causes the fermentations to make alternative products besides acids. The mixed microorganisms in this study have complex metabolisms, and attributing a single reason for a performance trend is difficult. Most likely, a combination of these explanations is responsible for increased selectivity and decreased conversion.

11.3.11 Overview

Using cellular recycle, many fermentation performance variables are improved. Recycling cells derived from residual biomass helps to decouple the variables affected by recycling residual biomass (Chapters 3–5). The following discussion summarizes the separate effects of cell recycle, cell reflux ratio, pH, and C-N ratio. To investigate how cellular growth affects selectivity, future studies should investigate cellular growth rates with respect to the amount of acid produced.

11.3.11.1 Effect of cell recycle

At all C-N ratios, Train CR had lower conversion and biogas production but higher selectivity, Y_P , Y_E , Y_{aE} , and Y_C (Tables 11-2, 11-3) than Train C. Compared to the respective control, at medium and high C-N ratios, Train CR had higher productivity, total acid and Aceq concentration, total carboxylic acid and Aceq exiting (g/d). The opposite trend is true at low C-N ratios.

At the medium C-N ratio, compared to residual biomass recycle to the same recycle point (F1) with similar reflux ratios, cell recycle increased acid concentration, daily acid produced, selectivity, and Y_E , Y_{aE} , and Y_C . However, recycling residual biomass had higher conversion, biogas production, and Y_P than cell recycle. Therefore, recycling concentrated cells and removing inert and possibly inhibitory materials from the residual biomass improves many performance variables.

11.3.11.2 Effect of cellular reflux ratio

At the medium C-N ratio (21 g OC_{NA}/g N), the cell recycle countercurrent fermentation train (Figure 11-1) was run at 15% and 48% cell reflux. Generally, with increased reflux, some performance variables increased (productivity, Y_P , Y_E , Y_{aE} , Y_C , Aceq-to-total-acid ratios, biogas production), one was not affected (daily acid exiting), and two decreased (selectivity, total acid concentration). Also, increased cell recycle appears to increase the proportion of higher-molecular-weight acids (Figure 11-2).

Compared to the increased reflux with residual biomass recycle (Chapter 3), cell recycle had increased total daily acid exiting, selectivity, Y_P , Y_E , Y_{aE} , Y_C , and productivity, but had decreased conversion and unaffected acid concentrations and

Aceq-to-total-acid ratio. Although similar reflux ratios were sought, higher reflux ratios were obtained with the cell recycle fermentation (48%) compared to residual biomass reflux fermentation (35%) because the reflux setpoint was not adjusted to different exiting moisture contents. Therefore, it is difficult to compare the effect of increased reflux of residual biomass and cell recycle. But, based on the data presented here, at higher reflux, cell recycle is superior to residual biomass recycle.

For the cell recycle fermentations, the conversion and selectivity trend contrasts with the trend found for residual biomass recycle (Ch. 6), where with increased reflux, there was an increase in conversion but decrease in selectivity. Because the mixed microorganisms in this study are complex, it is difficult to attribute a single reason for this trend.

11.3.11.3 Effect of C-N ratio and pH on cell recycle

For both Trains C and CR, besides selectivity, almost all performance variables were highest in medium C-N ratios, followed by high C-N ratio, and then low C-N ratio (Table 11-2). Also, cellular recycle increased production of higher-molecular-weight carboxylic acids at low C-N ratios and at medium C-N ratios with higher reflux (Tables 11-2, 11-3, Figure 11-2). The effects of C-N ratio and pH on cell recycle were similar to those found for residual biomass recycle (Ch. 7).

As shown in Figure 11-2, medium C-N ratio fermentations have an evenly distributed acid profile, with C2, C4, and C6 being the most prominent acids, followed by C3, C5, and C7. At low C-N ratio fermentations, fermentations are dominated by acetic acid (>75%) with less propionic acid (~15%), and the rest being mostly butyric acid, which agrees with other studies (Rodriguez et al., 2006; Zhang et al., 2009). At low C-N ratio fermentations, cell recycle again appears to increase the proportion of higher-molecular-weight acids, specifically C3 and C4 (Figure 11-2). The high C-N ratio fermentations had an almost equivalent amount of C2 and C3 acids (~80%), with a smaller amount of C4 and C5 (~15%), and the remainder being C6 and C7.

11.4 Conclusion

Recycling cells retains microorganisms and boosts selected fermentation performance measures. In general, compared to no cell recycle, recycling cellular biomass into Fermentor 1 increased selectivity and yield, but decreased conversion. Compared to lower cell reflux, higher reflux increased productivity, yield, conversion, but decreased selectivity. Generally, compared to residual biomass recycle, cell recycle had increased selectivity and yield but decreased conversion. Therefore, continuous fermentation performance can be increased by implementing cell recycle as opposed to residual biomass recycle, although both are beneficial. Also, higher cell reflux ratios are more beneficial.

12. COMPARISON OF THREE SCREENING METHODS TO SELECT MIXED-MICROBIAL INOCULUM FOR MIXED- ACID FERMENTATION

Using a mixed culture of microorganisms, the MixAlco™ process converts biomass into hydrocarbons and chemicals. To develop a method that identifies the highest performing inoculum for carboxylate fermentations, five bacterial communities were screened and ranked by three fermentation performance tests: (1) 30-day batch screen, (2) 28-day continuum particle distribution model (CPDM), and (3) 5-month continuous countercurrent fermentation trains. To screen numerous inocula sources, these tests were used sequentially in an aseptic environment. For the batch-fermentation screen, Inoculum 1 achieved the highest conversion. For the CPDM evaluation, the operating map for Inoculum 1 had the highest performance. For the continuous countercurrent fermentation, the train resulting from Inoculum 1 was among the best performers. This study suggests that the three screens are a useful and predictive method for choosing optimal inocula sources. The bacterial community with optimal performance in these three screens could be considered for use in commercial-scale fermentations.

12.1 Introduction

From 2004 to 2009, gross energy production increased 10% and global population increased 5% (IEA, 2011a). To create a sustainable future, a new energy path is necessary. One approach is to convert over a billion tons of agricultural, municipal, and industrial biowastes generated annually in the United States into liquid biofuels (Perlack et al., 2005). Currently, bioethanol and biodiesel production are the primary biomass-to-liquid fuel routes; they provide about 3% of global road transport fuels (REN21, 2011). Unfortunately, these fuels are produced from high-value food crops. An

alternative is the carboxylate platform, which can convert waste lignocellulose into liquid fuels (Agler et al., 2011; Holtzapple et al., 1999).

One approach to the carboxylate platform is the MixAlco™ process, a low-cost, nonsterile, flexible, and continuous technology that does not need added enzymes to convert nearly any biomass feedstock into chemicals and liquid fuels (Forrest et al., 2010b; Granda et al., 2009). The MixAlco™ process employs a mixed culture of naturally occurring microorganisms to ferment biomass into carboxylic salts, which are subsequently converted into a wide array of chemicals (e.g., ketones, alcohols) and hydrocarbons (e.g., jet fuel, gasoline) (Aiello-Mazzarri et al., 2006; Landoll and Holtzapple, 2011). To respond to varying market demands, the acid spectrum in the fermentations can be varied by using temperature as a control variable (Chan and Holtzapple, 2003).

Historically, to convert biomass to mixed volatile carboxylic acids (C₂–C₇), inocula for carboxylate fermentations have been collected from terrestrial environments, such as rumen fluid or compost piles (Aiello-Mazzarri et al., 2006; Ross and Holtzapple, 2001). Recent attempts to improve the fermentation community have greatly increased product yields. For example, a community isolated from a marine ecology (Galveston, TX) replaced the previous terrestrial community (College Station, TX) and doubled acid yields (Thanakoses, 2002). Replacing marine microorganisms with those from the hypersaline Great Salt Lake increased acid concentration by 30% (Fu, 2007). Natural saline environments provide microbial communities better suited to the salty environment in carboxylate fermentations.

Inoculating a biological process with a mixed culture is helpful in nonsterile environments that constantly change due to the nature of the substrates (e.g., agricultural residues) and nutrients (e.g., manure), offering advantages over a monoculture (Angenent et al., 2004; Das and Veziroglu, 2001). At the laboratory scale, it is fairly easy to maintain a monoculture. However, at the industrial scale, maintaining a monoculture is difficult and expensive; it requires specialized fermentors, pipes, pumps, heat exchangers, and filtration equipment. An economic evaluation of a lignocellulose-

to-ethanol process that employs yeast monocultures assumes 7% sugars are lost to contaminants (NREL, 1999).

In carboxylate fermentations, the competitive nature of the mixed culture of microorganisms fosters a strong, synergistic community (Golub et al., 2011b; Hollister et al., 2010). The stability of mixed cultures has been associated with increased community diversity, which increases the ability of mixed cultures to adapt to environmental changes (Hauxhurst et al., 1981; Pynaert et al., 2003).

Previous studies have successfully screened natural inocula sources for improved fermentation production of ethanol and hydrogen, and for biocidal properties against potential pathogens (Casas et al., 2007; Koskinen et al., 2008). Bacterial DNA sequencing of different ecological sites is time intensive, expensive, and might not predict fermentation performance. Instead, screening requires laboratory-scale fermentations that simulate an industrial environment.

This chapter compares three methods to screen microbial communities ecosystems as potential inocula in carboxylate fermentations: (1) a 30-d single-batch screen where the communities were used to inoculate 250-mL fermentors that were spiked with a high initial carboxylate concentration (20 g/L), (2) a 28-d multi-batch screen where five 1-L fermentors with different substrate concentrations were fermented to generate performance maps produced by the continuum particle distribution model (CPDM) (Loescher, 1996), and (3) a continuous countercurrent fermentation where four-stage semi-continuous countercurrent trains were run in 1-L fermentors for several months.

When analyzing hundreds of inocula samples, the single-batch fermentation serves as the initial screen for the highest performing microbial communities. CPDM is the next level of screening used to predict the best performers from those chosen from the initial screen. Then, the continuous countercurrent fermentation is the final screen used to select the inocula that could be useful for industrial carboxylate fermentations. This study establishes the most accurate and efficient inoculum screening method for carboxylate fermentations.

12.2 Materials and methods

12.2.1 Overview of microbial community screening

Four bacterial communities from Brazoria, TX and one from Galveston, TX were collected from their respective soil site and used as inocula in three simultaneous fermentation screens for carboxylate platform fermentations (Table 12-1). The performance variables for the bacterial communities were compared in three simultaneous fermentation performance tests: a 30-day batch screen, continuum particle distribution model, and four-stage countercurrent fermentation trains (Figure 12-1).

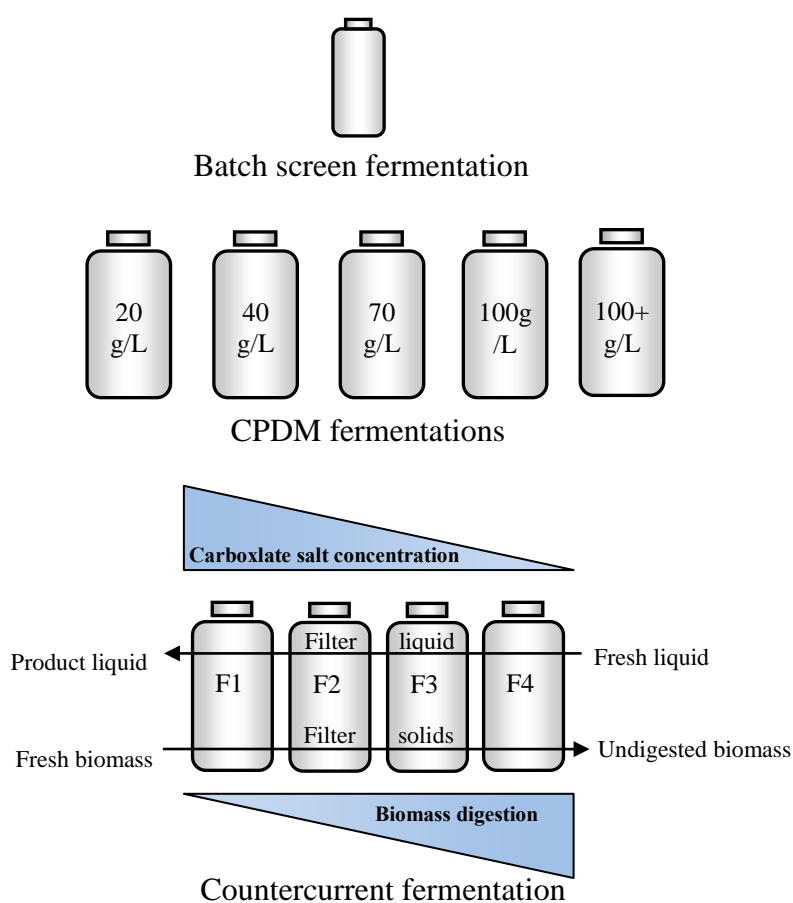


Figure 12-1. Diagram of the batch screen, CPDM, and countercurrent fermentations.

12.2.2 *Inocula*

Five inocula were selected and samples were collected from their respective soil sites (Table 12-1). The four Brazoria inocula were collected with three 20-cm-deep and 7.5-cm-diameter core samples obtained with a soil corer. The control inoculum was aquatic sediment in Galveston, TX, which is the inoculum historically used for MixAlco™ fermentations. This sediment sample was removed from the bottom of 0.5-m-deep shoreline pits. GPS coordinates recorded the exact location of soil collection (Table 12-1). These samples were immediately placed in separate sealed, air-free plastic bags and chilled with dry ice. All inocula were fresh and unfrozen when inoculating the fermentations.

Table 12-1. Soil sample locations for mixed-cultured fermentations.

Inocula nomenclature	Location	Textural class name	pH	EC (S/m)	Temperature (°C ^a)	Latitude (N)	Longitude (W)
1	Salt marsh, Brazoria National Wildlife Refuge near Brazoria, TX	Clay Loam	6.10	3.15	20.80	29.06073	95.26022
2	Salt marsh, Brazoria National Wildlife Refuge near Brazoria, TX	Loam	7.70	5.10	22.30	29.06083	95.24095
3	Salt marsh, Brazoria National Wildlife Refuge near Brazoria, TX	Loam	8.10	5.83	29.00	29.06145	95.23797
4	Salt marsh, Brazoria National Wildlife Refuge near Brazoria, TX	Sandy Clay	6.90	2.98	21.90	29.03787	95.26693
5	Open access beach, 8-Mile Rd, Galveston, TX	Sand	7.92	2.60	27.20	29.23489	94.88268

EC: electrical conductivity

^aSoil temperature at time of collection

12.2.3 *Fermentor configuration*

For the batch screening, the fermentors were 250-mL polypropylene centrifuge bottles capped by a polypropylene cap (Figure 12-1). The fermentors for the CPDM and

countercurrent trains were 1-L polypropylene centrifuge bottles capped by a rubber stopper inserted with a glass tube (Domke et al., 2004; Thanakoses et al., 2003). A rubber septum sealed the glass tube and allowed for gas sampling and release. Two lengths of ¼-in stainless steel pipe were inserted through the rubber stopper into the vessel, which mixed the contents of the fermentor as it rotated in the rolling incubator.

12.2.4 *Substrate*

Shredded recycled office paper was the substrate in all fermentations. Because commercial paper is lignin-free and has a specific composition, it does not need to be pretreated, which removes the variation that would have occurred from pretreating multiple batches of agricultural feedstock.

As a nutrient source, yeast extract was used rather than the more commonly used chicken manure. Chicken manure has been used as the nutrient source in MixAlco™ fermentations because of its economic feasibility for commercial-scale implementation. Yeast extract is an aseptic nutrient, which minimizes the introduction of outside microorganisms from the nutrient source. Paper and yeast extract were fed at a ratio of 90:10 (Forrest, 2010). No other supplementary nutrients were added.

12.2.5 *Methanogen inhibition*

Iodoform (CHI_3) inhibited methane in all fermentors. To ensure no methane was present, for continuous fermentations, the gas phase was monitored with gas chromatography (GC) analysis. Iodoform solution (20 g CHI_3 /L 190-proof ethanol) was added to each fermentor every 48 h throughout the fermentation (Ross, 1998). Because iodoform is light, air, and temperature sensitive, the solution was kept in amber-colored glass bottles and special care was taken to replace the cap immediately after use to prevent degradation.

12.2.6 *Analytical Methods*

12.2.6.1 *Carboxylic acid concentration determination*

Fermentation liquid was centrifuged (4,000 rpm, 3300×g, 25 min) to remove insoluble solids. Then, it was mixed with equal parts of internal standard (1.162 g/L 4-

methyl-*n*-valeric acid) and 3-M phosphoric acid (H_3PO_4), and then ultra-centrifuged (15,000 rpm, $18,360\times g$, 8 min). The carboxylic acid concentration was measured using an Agilent 6890 Series gas chromatograph (GC) system with a flame ionization detector (FID) and an Agilent 7683 automatic liquid sampler. A 30-m fused-silica capillary column (J&W Scientific Model # 123-3232) was used. The column head pressure was maintained at 2 atm abs. After each sample injection, the GC temperature program raised the temperature from 40 to 200 °C at 20 °C/min. The temperature was subsequently held at 200 °C for 2 min. The total run time per sample was 11 min and helium was the carrier gas. The calibration standard was volatile acid mix (Matreya, LLC, Cat No. 1075).

12.2.6.2 *Biogas quantification and composition analysis*

Biogas is a fermentation product that must be quantified for closure calculations and removed from the fermentors to relieve pressure buildup and prevent rupture. In CPDM and countercurrent fermentations, for the first week, each fermentor was vented daily because of the high initial digestion rate, and then each fermentor was vented every other day. The biogas was removed through the fermentor septum and controlled with a valve on the needle. The biogas volume was measured by liquid displacement using a well-sealed inverted graduated glass cylinder. An aqueous solution of 300 g CaCl/L was the liquid used in the glass cylinder to prevent microbial growth and carbon dioxide adsorption.

For the countercurrent fermentations, biogas composition was measured and methane was monitored by manual injection of a 5-mL gas sample into an Agilent 6890 Series chromatograph with a thermal conductivity detector (TCD). A 4.6-m stainless steel packed column with 2.1-mm ID (60/80 Carboxen 100, Supelco 1-2390) was used. The total run time was 10 min and helium was the carrier gas. The inlet temperature was 230 °C, the detector temperature was 200 °C, and the oven temperature was 200 °C.

12.2.6.3 *Moisture and ash contents*

Moisture and ash contents were determined by drying in a 105 °C forced-convection oven for at least 24 h, and subsequent combustion in a 575 °C furnace for at

least 12 h by NREL procedures No. 001 and 005, respectively (NREL, 2004). The ash content was calculated on a dry basis. The consumption of non-acid volatile solids (NAVS) was determined using the inert-ash approach as described previously (Smith et al., 2011).

12.2.7 Definition of terms

To account for the total mass in the system, a mass balance closure was calculated with:

$$\text{mass balance closure} = \frac{\text{mass out (g)}}{\text{mass in (g)} + \text{water of hydrolysis (g)}} \quad (12-1)$$

Cellulose is a polysaccharide composed of individual anhydroglucose units (glucan, MW = 162 g/mol). During digestion, cellulose is enzymatically hydrolyzed to glucose by adding water. The water of hydrolysis was calculated as previously described (Chan and Holtzapfle, 2003).

The mixed-acid concentration can be expressed as molar acetic acid equivalents (α), which is the reducing potential of an equivalent amount of acetic acid (Datta, 1981).

$$\begin{aligned} \alpha = & 1.00 \times \text{acetic (mol/L)} + 1.75 \times \text{propionic (mol/L)} \\ & + 2.50 \times \text{butyric (mol/L)} + 3.25 \times \text{valeric (mol/L)} \\ & + 4.00 \times \text{caproic (mol/L)} + 4.75 \times \text{heptanoic (mol/L)} \end{aligned} \quad (12-2)$$

The acetic acid equivalent (Aceq) can be expressed on a mass basis as

$$\text{Aceq (g/L)} = 60.05 \text{ (g/mol)} \times \alpha \text{ (mol/L)} \quad (12-3)$$

Aceq proportionally weighs the higher-chained carboxylic acids (C₃ to C₇); the higher acids have higher Aceq than lower acids.

Volatile solids (VS) are defined as the mass of dry solid material that is combusted at 575 °C after 12 h, and NAVS are defined as VS less the amount of carboxylic acid:

$$\text{NAVS} = (\text{g total wet biomass})(1 - \text{MC})(1 - \text{AC}) - (\text{g acid in biomass}) \quad (12-4)$$

where MC (g water/g wet biomass) is the fraction of moisture in the biomass, and AC (g ash in biomass/g dry biomass) is the fraction of dry ash remaining after 12 h of combustion at 575 °C. In performance calculations, NAVS is preferred because it ensures the carboxylate product is not quantified with the reactant.

12.2.8 *Measuring performance*

For the batch and CPDM fermentations, all performance variables (e.g., conversion, selectivity, and yield) were calculated from initial and final time points. For the countercurrent fermentations, the feed and exit rate of acid, ash, NAVS, water, and gas were determined during the steady-state period. As previously described (Smith and Holtzapple, 2011b), the average rate of each component was calculated using the *slope method*. In this method, the moving cumulative sum of each component is plotted with respect to time. The slope of the steady-state portion of this line is the rate. For the countercurrent fermentations, all performance variables were calculated from the averaged component rates determined by the slope method, as described below:

$$\begin{aligned}
\text{Conversion } x &\equiv \frac{\text{NADS}_{\text{feed}} \text{ g} - \text{NADS}_{\text{exit}} \text{ (g)}}{\text{NAVS}_{\text{feed}} \text{ (g)}} \\
&= \frac{\text{NAVS}_{\text{feed}} \text{ g} + \text{Ash}_{\text{feed}} \text{ g} - \text{NAVS}_{\text{exit}} \text{ g} - \text{Ash}_{\text{exit}} \text{ (g)}}{\text{NAVS}_{\text{feed}} \text{ (g)}} \quad (12-5) \\
&= \frac{\text{NAVS}_{\text{consumed}} \text{ (g)}}{\text{NAVS}_{\text{feed}} \text{ (g)}}
\end{aligned}$$

$$\text{Exit yield } (Y_E) \equiv \frac{\text{total acid output from solid and liquid streams (g)}}{\text{NAVS}_{\text{feed}} \text{ (g)}} \quad (12-6)$$

$$\text{Process yield } (Y_P) \equiv \frac{\text{total acid output in product liquid stream (g)}}{\text{NAVS}_{\text{feed}} \text{ (g)}} \quad (12-7)$$

$$\begin{aligned}
\text{Selectivity } (\sigma) &\equiv \frac{\text{total acid produced (g)}}{\text{NAVS}_{\text{feed}} \text{ (g)} - \text{NAVS}_{\text{exit}} \text{ (g)}} \quad (12-8) \\
&\equiv \frac{\text{total acid produced (g)}}{\text{NAVS digested (g)}} = \frac{Y_E}{x}
\end{aligned}$$

$$\text{Acid productivity } (P) \equiv \frac{\text{total acids produced (g)}}{\text{TLV (L)·d}} \quad (12-9)$$

where $\text{NADS}_{\text{feed}}$ is the non-acid dry solids fed, $\text{NADS}_{\text{exit}}$ is the non-acid dry solids removed from the fermentation, $\text{NAVS}_{\text{feed}}$ is the non-acid volatile solids fed, $\text{NAVS}_{\text{exit}}$ is the non-acid volatile solids removed from the fermentation, Ash_{feed} is the ash fed in biomass feed and buffer, Ash_{exit} is the ash exiting in all solid and liquid streams, and TLV is the total liquid volume in the fermentation train including free and interstitial liquid. NADS includes the ash, CaCO_3 , and volatile solid component of biomass. Ash is assumed to be unaffected by the fermentation (Ash_{feed} equals Ash_{exit}), canceling Ash from Equation 12-7.

Per g NAVS fed, the exit yield (Y_E) represents the sum of acid in the product transfer liquid, waste transfer solids, and liquid samples removed from sampling. The

process yield (Y_P) represents all the acid in the product transfer liquid per g of NAVS fed.

12.2.9 *Statistical analysis*

Statistical analysis was performed using Excel 2007 (Microsoft, USA). For the countercurrent trains, the mean and standard deviations of the total acid concentrations, acetic acid equivalent (Aceq), non-acid volatile solids (NAVS) in and out were determined from steady-state operating data. For the countercurrent trains, steady state was determined to be Days 120–150 (Train 1), 110–150 (Train 2), 136–156 (Train 3), 112–150 (Train 4), and 134–154 (Train 5). These averaged values were then used to calculate the acid productivity (P), selectivity (σ), yield (Y), and conversion (x) with a 95% confidence interval (CI). Unless specified otherwise, all comparisons in the Results and Discussion section are statistically significant. The steady-state region was the period during which the product total acid and Aceq concentration, dry solids exiting, liquid volume and solid weight of each fermentor, pH, and mass of acid exiting did not vary by more than 2.0 standard deviations from the average for a period of at least one-half liquid residence time. From the slope of the summed data, to compare the means of the groups, a Student's two sample t -test (two-tailed, Type 3) was used to compute the p values between the performance variables of the trains. The p values had a familywise error rate of 0.05 using the Bonferroni correction. All error bars are reported at 95% CI.

12.2.10 *Batch screen*

Each soil sample was incubated in batch mode for 30 d in a 55 °C shaker incubator using a 250-mL centrifuge Nalgene bottle as the fermentor. All collection beakers, screens, and equipment were autoclaved to prevent cross contamination. Each 250-mL bottle was filled with paper, yeast extract, calcium carbonate, calcium salts, distilled water, soil sample, urea, and iodoform (40 μ L of 20 g/L ethanol soln) (Table 12-2). A soil sample was taken to get the amount of moisture and volatile solids for use in calculating performance variables.

The gas was vented and iodoform (40 μL of 20 g/L ethanol soln) was added every other day to inhibit methanogens. Liquid fermentation samples were taken on the first and final day of the experimental run and analyzed for carboxylic acid concentration using gas chromatography (GC). GC samples were not taken in between these days to preserve fermentation integrity.

After fermenting in batch mode for 30 d, the bottles were removed from the shaker incubator and shaken by hand. For 5 min, the solids were allowed to gravity settle, and a liquid sample was removed with a transfer pipette for GC analysis. The liquid phase was separated from the solid phase by centrifugation (4,000 rpm, 3300 $\times g$, 25 min). The mass, moisture content, and ash content of the solid and liquid phase from each fermentor were measured for performance calculations. If necessary, samples were frozen at $-20\text{ }^{\circ}\text{C}$ in a well-sealed 50-mL conical tubes until analysis. A portion of the solid and liquid phase was used for moisture and ash content analysis. The conversion, yield, and selectivity were calculated from the mass of acids exiting and the moisture and ash contents from the resulting solid samples.

Table 12-2. Operating parameters for batch fermentations.

Batch fermentation	1	2	3	4	5
Inoculum added (g)	2.5	2.5	2.5	2.5	2.5
Yeast extract feed (g)	1.0	1.0	1.0	1.0	1.0
Paper feed (g)	9.0	9.0	9.0	9.0	9.0
Total volatile solids feed (g)	9.07	9.01	9.00	9.07	8.97
Deoxy water feed (mL)	150	150	150	150	150
Calcium acetate feed (g)	3.2	3.2	3.2	3.2	3.2
Calcium propionate feed (g)	0.2	0.2	0.2	0.2	0.2
Calcium butyrate feed (g)	0.5	0.5	0.5	0.5	0.5
CaCO ₃ feed (g)	2.2	2.2	2.2	2.2	2.2
Temperature ($^{\circ}\text{C}$)	55	55	55	55	55

12.2.11 Fermentation screening using continuum particle distribution modeling

12.2.11.1 Continuum particle distribution modeling

The continuum particle distribution model (CPDM) is used to quantify the kinetics of a reaction occurring at the interface between solid and fluid phases. This method allows laboratory data to be modeled mechanistically, or to empirically simulate different reactor configurations (Loescher, 1996).

The concept of “continuum particle” – defined as 1 g of volatile solids (VS) entering the fermentor – is used to avoid the difficulties of tracking the geometry of individual discrete particles. Product accumulation in the batch fermentations was used to provide data for the rate equation. The acid generation was modeled using Equation 12-10. Least squares analysis was used to obtain parameters.

$$\text{Aceq} = a + \frac{b t}{1 + c t} \quad (12-10)$$

where a , b , c are empirical constants, t is time, and Aceq is acetic acid equivalents.

The specific rate (Equation 12-13) was determined from Equation 12-12 and this was fit to Equation 12-14. CPDM parameters were obtained using the least squares analysis to minimize the specific rate (r , g of acetic acid equivalent generated/(time·g VS)) using the mass of acetic acid generated.

$$r = \frac{d(\text{Aceq})}{dt} = \frac{b}{(1 + c \cdot t)^2} \quad (12-11)$$

$$r \equiv \frac{r}{S_0} \quad (12-12)$$

$$r = \frac{e(1 - x)^f}{1 + g(\phi \cdot \text{Aceq})^h} \quad (12-13)$$

where e, f, g, h are empirical constants, A_{ceq} is acetic acid equivalents, ϕ is the ratio of total grams of actual acid to grams of A_{ceq} .

$$x(t) = \frac{A_{ceq} - A_{ceq}(t=0)}{S_0 \cdot \sigma} \quad (12-14)$$

The conversion (x) used in the model (Equation 12-14) is defined as the mass of acetic acid equivalent generated (g) per mass of VS fed (g). The selectivity σ of the fermentation (g A_{ceq} /g VS digested) is assumed to be a constant for each system. During the batch mode of operation, the rate equation was integrated using the explicit method of numerical integration. The acetic acid equivalent concentration in the fermentors was determined by dividing the mass of acetic acid equivalents by the volume of liquid in each fermentor. The ratio of total acids to acetic acid equivalents (ϕ) was used to convert the acetic acid equivalent concentrations back to total acid concentrations.

Solver in Microsoft Excel was used to obtain the model parameters in Equations 12-11 and 12-13. The sum of the mean-square error between experimental and predicted values was minimized to obtain the model parameters. Matlab (Appendix N) was used to predict the acetic acid equivalent concentration and conversion for the five fermentations with different mixed cultures at various volatile solids loading rates (VSLR) and liquid residence times (LRT).

12.2.11.2 CPDM fermentation conditions

The rate of reaction for each inocula was found by measuring digestion and acid production in fermentation reactors loaded with five different initial substrate concentrations. The fermentors were loaded with a 20, 40, 70, 100, and 100+ g dry substrate/L fermentation medium with a 90:10 substrate to nutrient ratio, and incubated for 28 d in batch mode in a rolling incubator at 55 °C (Table 12-3). The 100+ g/L substrate concentration had an additional 20 g/L carboxylate salt. Initially, the pH and a 3-mL liquid fermentation sample were taken. Every 48 h, the biogas was vented, the pH

was taken, a 3-mL liquid fermentation sample was taken for GC analysis, and iodoform (120 μ L of 20 g/L ethanol soln) was added. All collection beakers, screens, and equipment were autoclaved between fermentors to prevent cross contamination.

After 28 d, each fermentor was centrifuged (3300 \times g, 25 min) to separate the liquid and solid phases. The mass, moisture content, and ash content of the solid and liquid phases from each fermentor were measured and used to calculate performance. The fermentation liquid was poured through an autoclaved screen to remove any solids. If necessary, samples were temporarily frozen in well-sealed 50-mL conical tubes until analysis. The CPDM coefficients were calculated to prepare a countercurrent train operating map, which plots total acid concentration versus conversion for a VSLR and LRT.

Table 12-3. Operating parameters for CPDM fermentations.

Substrate concentration (g/L)	20	40	70	100	100+
Inoculum added (g)	20	20	20	20	20
Yeast extract feed (g)	0.8	1.6	2.8	4.0	4.0
Urea (g)	1.0	1.0	1.0	1.0	1.0
Paper feed (g)	7.2	14.4	25.2	36	36
Deoxy water feed (mL)	350	350	350	350	350
Calcium acetate feed (g)	0	0	0	0	8.6
Calcium propionate feed (g)	0	0	0	0	0.5
Calcium butyrate feed (g)	0	0	0	0	1.2
CaCO ₃ feed (g)	6.0	6.0	6.0	6.0	6.0
Temperature ($^{\circ}$ C)	55	55	55	55	55

12.2.12 Countercurrent fermentation trains

12.2.12.1 Operating parameters

In the countercurrent fermentation, the LRT and VSLR (Table 12-4) were regulated by controlling the liquid and solid transfer frequency (T), the non-acid volatile solids (NAVS) feed rate, and the liquid feed rate per transfer. The volatile solid loading rate (VSLR) and the liquid residence time (LRT) are calculated as follows:

$$\text{VSLR} = \frac{\text{NAVS feed (g)}}{\text{total liquid volume in all fermentors (L)} \cdot \text{time (d)}} \quad (12-15)$$

$$\text{LRT} = \frac{\text{total liquid volume in all fermentors (L)}}{\text{liquid flow rate out of fermentation train (L/d)}} \quad (12-16)$$

The total liquid volume (TLV) includes both free and interstitial liquid. Liquid flow rate out of fermentation train includes product liquid exiting and liquid in cake exiting.

12.2.12.2 *Countercurrent fermentation conditions*

The four-stage countercurrent fermentation (Figure 12-1) has liquid and solid phases flowing in countercurrent directions in a series of four fermentors. Multi-staged fermentations generate higher conversion and product concentration than batch fermentations, but require more time, space, and effort. As biomass digests, the biomass becomes less reactive and the production of carboxylic acid drops. Acid inhibition is minimized in countercurrent fermentations because the most-digested biomass contacts the lowest product concentration of carboxylate salts and the least-digested biomass contacts the highest product concentration.

The countercurrent fermentation trains began in batch mode with a concentration of 100 g dry solids/L deoxygenated water. Each fermentor was given substrate, nutrient source (yeast extract), inoculum, calcium carbonate (buffer), distilled water, and iodoform (120 μL of 20 g/L ethanol soln) (Table 12-4). Each fermentor was incubated in a roller incubator at thermophilic conditions (55 °C) until steady state was reached.

Steady state

was defined as having a constant acid concentration for a time period of a minimum of two LRT. Each countercurrent fermentation train ran for ~5 months.

Table 12-4. Operating parameters for countercurrent fermentations. Normalized parameters represent the mean of the steady-state values \pm CI (95% CI).

Fermentation Train		1	2	3	4	5
Controlled	Solid and liquid transfer frequency, T (h)	48	48	48	48	48
	NAVS feed rate (g NAVS/ T)	9.0	9.0	9.0	9.0	9.0
	Liquid feed rate (mL/ T)	100	100	100	100	100
	Dry substrate added (g/ T)	11.2	11.2	11.2	11.2	11.2
	Yeast added (g/ T)	0.4	0.4	0.4	0.4	0.4
	Urea added (g/ T)	2.0	2.0	2.0	2.0	2.0
	Solid cake retained in F1–F4 (g)	225	225	225	225	225
	Centrifuged liquid retained in F1–F4 (mL)	0	0	0	0	0
	Calcium carbonate added (g/ T)	4.0	4.0	4.0	4.0	4.0
	Methane inhibitor (μ L/ $(T_L \cdot fermentor)$)	80	80	80	80	80
Normalized	Volatile solid loading rate, VSLR (g NAVS/ $(L_{liq} \cdot d)$)	3.9 \pm 0.0	4.3 \pm 0.0	3.9 \pm 0.0	3.9 \pm 0.0	3.9 \pm 0.0
	Liquid residence time, LRT (d)	37.9 \pm 2.9	34.0 \pm 2.1	40.5 \pm 6.8	40.8 \pm 3.7	45.6 \pm 10.8
	Total liquid volume, TLV (L)	1.17 \pm 0.01	1.05 \pm 0.01	1.15 \pm 0.02	1.15 \pm 0.01	1.16 \pm 0.02
	Volatile solid, VS, concentration (g NAVS/ L_{liq})	136 \pm 7	166 \pm 7	132 \pm 7	128 \pm 5	139 \pm 8
	Dry solid, DS, concentration (g NADS/ L_{liq})	203 \pm 4	261 \pm 5	200 \pm 6	186 \pm 4	212 \pm 6
	Average pH (F1–F4)	6.01 \pm 0.20	5.89 \pm 0.13	6.12 \pm 0.31	6.03 \pm 0.20	6.09 \pm 0.25
	Urea addition rate (g urea/ $(L_{liq} \cdot d)$)	0.86 \pm 0.07	0.96 \pm 0.06	0.87 \pm 0.15	0.87 \pm 0.08	0.86 \pm 0.20

NAVS: Non-acid volatile solids

NADS: Non-acid dry solids

Solid/liquid transfers began after the first week of batch growth and occurred every 48 h. The feed consisted of shredded office copier paper (90%) supplemented with yeast extract (10%). The fermentors were removed from the incubator, the gas volume was collected, liquid samples were taken, the pH was measured, and mass transfers were performed. The fermentors were purged with nitrogen gas when opened to the atmosphere to maintain anaerobic conditions. Iodoform (120 μ L of 20 g/L ethanol soln) was added and the fermentors were returned to the incubator. The fermentations were buffered by adding 1.0 g calcium carbonate to each fermentor every 48 h to neutralize carboxylic acids to control the pH range at 6.0 ± 0.2 (Table 12-4). The pH was monitored during the entire fermentation to ensure adequate buffer addition.

12.3 Results and discussion

The batch screen, CPDM, and continuous countercurrent fermentation were inoculated with Inocula 1, 2, 3, 4, and 5 (Table 12-1, Figure 12-1). The corresponding nomenclature for the batch screen is Fermentation 1, 2, 3, 4, and 5; for the CPDM fermentations is CPDM 1, 2, 3, 4, and 5; and for the countercurrent continuous fermentations is Train 1, 2, 3, 4, and 5.

12.3.1 *Batch screen*

The batch fermentations had virtually identical operating parameters, with the only difference being the total volatile solids feed because of the difference in volatile solids of the actual inoculum sediment (Table 12-2). After the 30-d batch fermentation, the conversion rankings are Fermentations $1 > 3 > 5 > 4 > 2$; selectivity rankings are Fermentations $5 > 3 > 2 = 4 > 1$; total acid produced rankings are Fermentations $5 > 3 > 4 > 2 > 1$; and yield rankings are Fermentations $5 > 3 > 4 > 2 = 1$ (Table 12-5). The fermentation product spectrum was also fairly diverse (Figure 12-2).

This batch screen shows that Inoculum 1 had the highest conversion of volatile solids, but had the lowest production of carboxylic acids. Fermentation 1 could have produced alternative products that were not analyzed, such as lactic acid or hydrogen. Inoculum 5 produced the most amount of acid, but digested only an average amount of

biomass compared to the other four inocula. Of the five inocula samples tested here, based on yield, Inoculum 5 is the optimal microbial community. However, based on conversion, Inoculum 1 is the optimal microbial community.

Table 12-5. Performance for batch fermentations.

Batch fermentation	1	2	3	4	5
Total carboxylic acid produced (g/L)	0.14	0.19	0.95	0.34	2.31
Conversion (g VS digested/g VS fed)	0.13	0.04	0.11	0.07	0.08
Selectivity (g total acid/g VS digested)	0.02	0.08	0.15	0.08	0.46
Yield (g total acid/g VS fed)	0.00	0.00	0.02	0.01	0.04

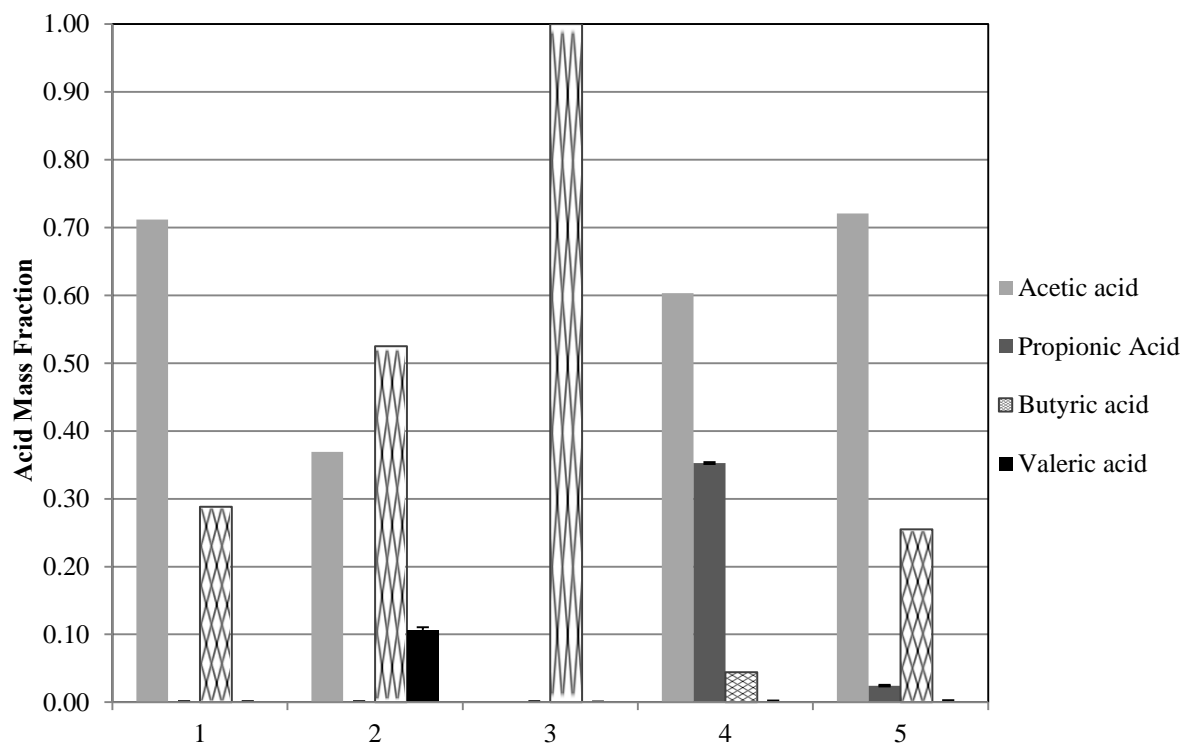


Figure 12-2. Carboxylic acid composition profile for batch Fermentations 1, 2, 3, 4, and 5.

12.3.2 Continuum particle distribution modeling

CPDM modeling was performed on each of the five fermentation inoculum sources (Table 12-1)). Each set of batch fermentation data (20, 40, 70, 100, and 100+ g dry substrate/L medium) for each fermentation (CPDM 1, 2, 3, 4, and 5) was fit to Equation 12-10. Figure 12-3 shows the experimental fits for CPDM 1. Once the a , b , and c parameters were determined, r , r , and $x(t)$ were calculated by Equations 12-11, 12-13, and 12-14 and compiled into a fermentation data matrix (Table 12-6). This matrix was used to fit Equation 12-14 and to determine the values e , f , g , and h (Figure 12-4) for each train. Data for CPDM 1 are shown with a coefficient of determination R^2 of 0.59. These rate parameters were entered into the Matlab simulation; Table 12-7 shows the parameters used in the CPDM simulations for all five inoculum sources. From the simulation, the total carboxylic acid concentrations and conversions were predicted for various LRT and VSLR for each fermentation train. In Figures 12-5(a)–12-5(e), CPDM predictions for conversions and product concentrations for CPDM 1–5 are presented in the “maps.” The overall rankings for the CPDM fermentations are 1>3>5>2>4, which is very similar to the batch screen fermentation rankings (Table 12-7).

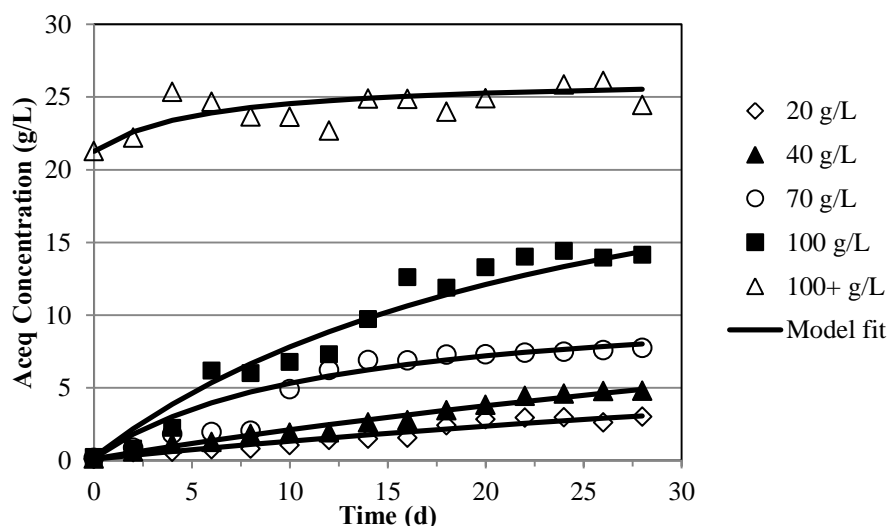


Figure 12-3. Data fit of acetic acid equivalent (Aceq) concentrations to 20, 40, 70, 100 and 100+ g/L batch fermentations for CPDM 1.

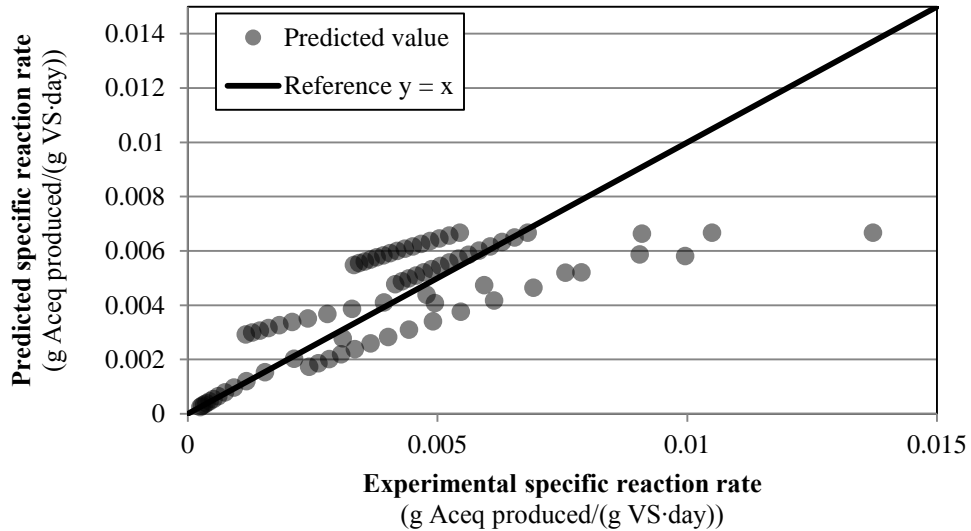


Figure 12-4. The experimental value and the CPDM prediction value for the specific reaction rates in 20, 40, 70, 100 and 100+ g/L batch fermentations for CPDM 1.

Table 12-6. Sample data matrix for the rate equation fit for CPDM 1.

Aceq (g/L)	$x(t)$	r
.	.	.
:	:	:
8.857	0.365	0.00491
9.790	0.404	0.00443
10.633	0.440	0.00401
11.400	0.472	0.00366
12.100	0.502	0.00334
12.742	0.529	0.00307
13.332	0.554	0.00283
13.878	0.577	0.00262
:	:	:
.	.	.

Table 12-7. Constant values used to simulate the fermentations and generate the performance maps in CPDM 1, 2, 3, 4, and 5 and resulting conversion and total acid concentration.

CPDM Fermentation	1	2	3	4	5
Holdup (g liquid/g VS cake)	4.43	3.80	4.81	5.03	4.30
Moisture (g liquid/g solid feed)	0.03	0.03	0.03	0.03	0.03
F1-F4 solid concentration (g VS/L)	136	166	132	128	139
F1-F4 liquid volume (L)	0.29	0.26	0.29	0.29	0.29
Selectivity (g Aceq/g VS digested)	0.449	0.379	0.382	0.479	0.516
ϕ (g total acid/g Aceq)	0.505	0.543	0.507	0.519	0.604
e (g Aceq/(g VSd))	0.007	0.022	0.023	0.024	0.013
f (dimensionless)	1.473	3.890	3.301	1.160	1.00
g (L/g total acid) ^{1/h}	0.001	0.055	0.001	1.332	0.001
h (dimensionless)	1.00	1.00	1.00	1.00	2.847
Conversion x , g VS digested/g VS feed (LRT=30d, VSLR=4 g VS/L·d)	0.57	0.37	0.44	0.30	0.40
Total acid concentration, g/L (LRT=30d, VSLR=4 g VS/L·d)	27	23	30	15	24

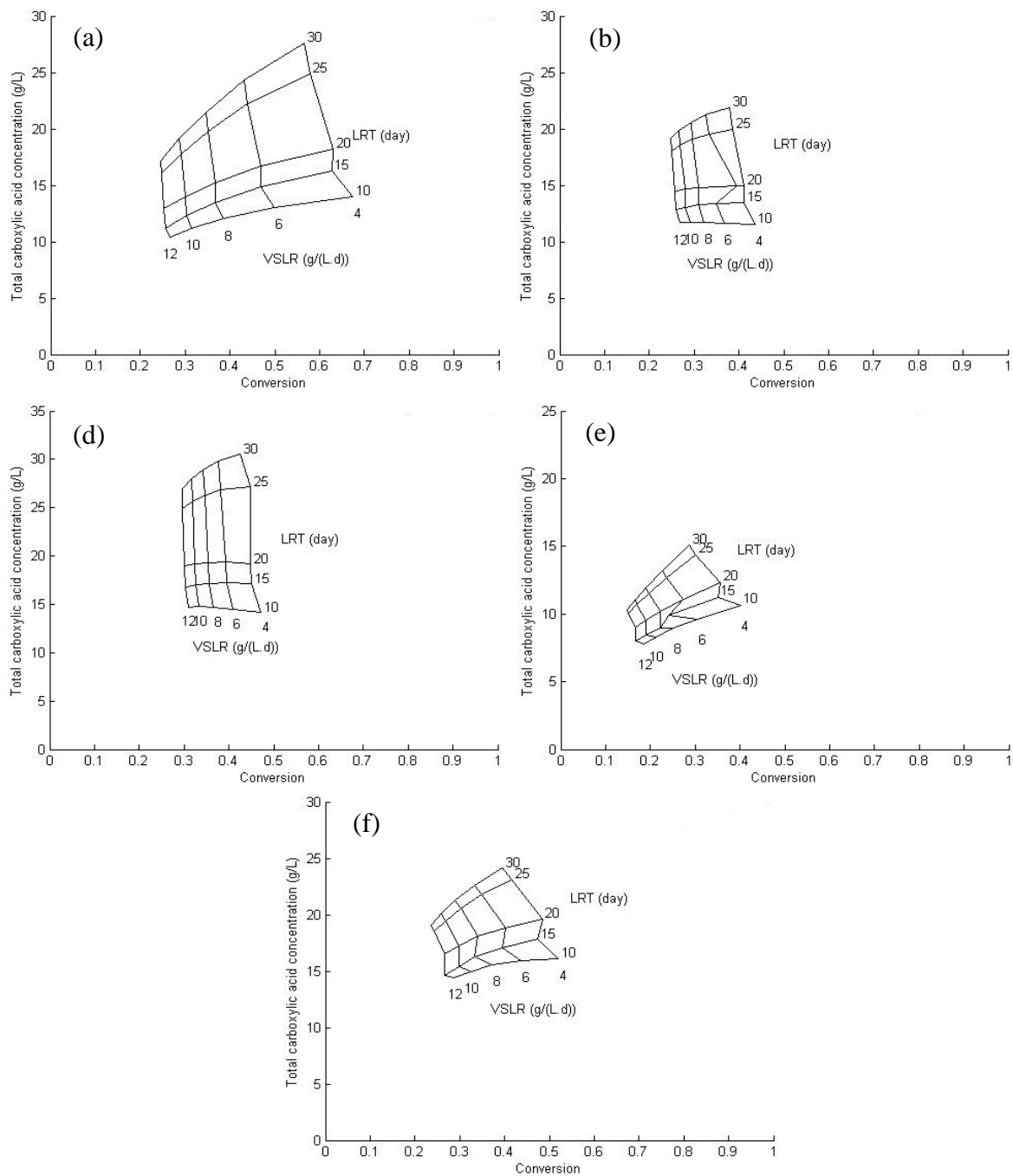


Figure 12-5. Maps for (a) CPDM 1, (b) CPDM 2, (c) CPDM 3, (d) CPDM 4, and (e) CPDM 5.

12.3.3 *Countercurrent continuous fermentation*

Each fermentation train consisted of a four-stage countercurrent semi-continuous submerged-bed fermentation system. To compare the results of all trains, the LRT and VSLR operating parameters were normalized by explicitly controlling the liquid/solid mass transfer frequency (T), the volatile solids (VS) feed rate, the liquid feed rate, and the amount of cake retained in each fermentation reactor per transfer (Table 12-4).

For all five trains, the accumulated amount of total carboxylic acids exiting, NADS added, and NADS removed from their respective trains was found. The slopes of the steady-state regression lines provided the performance data (Table 12-8). A similar analysis was performed with Aceq.

For conversion (g VS digested/g VS fed), the corresponding train ranks are $2 > 1 = 4 = 5 \geq 3$ (Tables 12-8 and 12-9). For selectivity (g acid/g VS digested), the corresponding train ranks are $3 > 1 > 5 > 4 > 2$ (Tables 12-8 and 12-9). Train 2 had the highest conversion (0.44 g VS digested/g VS fed) and productivity (1.07 g/(L-day)), but the lowest selectivity (0.529 g acid/g VS digested). The highest selectivity (0.60 g acid/g VS digested) was obtained from Train 3, which had the lowest conversion. For exit yield (g acid exit/g VS fed), the corresponding train ranks are $1 > 2 > 3 > 4 = 5$ (Tables 12-8 and 12-9). The yields are statistically different at the 95% confidence level, but are fairly similar and do not vary more than 2%.

During the steady-state period, all five trains had similar acid concentrations (Tables 12-8 and 12-9). One measure of the production of higher-molecular-weight carboxylic acids (e.g., valeric, caproic, and heptanoic acid) is the Aceq-to-total-acid ratio. For the Aceq-to-total-acid ratios, the ranks are as follows: Train $1 > 5 > 2 = 3 = 4$. This trend is reflected in Figure 12-6.

In each fermentor of a train, total liquid volume (TLV) quantifies the total volume of liquid in the solid and liquid phases. Most fermentation trains had different TLVs, indicating deviations between trains. To better analyze the data and standardize the analyses, the amount of acid exiting the fermentors per day was calculated on a mass basis from the product liquid and waste streams (Table 12-8). For the total carboxylic

acid exiting (g/d), the ranks are as follows: Train 1>2>3>5=4 (Tables 12-8 and 12-9). For the Aceq exiting (g/d), the ranks are as follows: Train 1>2>3=5>4 (Tables 12-8 and 12-9).

With respect to all the performance variables discussed, Trains 1 and 2 had the best performance, which is similar to the predictions for the batch screen (when the rankings were based on conversion) and the CPDM maps.

12.3.4 *Overview*

To find the highest performing inoculum for carboxylate fermentations, the bacterial communities were screened and ranked by three simultaneous fermentation performance tests: 30-day batch screen, 28-day batch continuum particle distribution model, and 5-month continuous countercurrent fermentation. Aseptic conditions were observed to prevent cross contamination.

For the batch screen, Inoculum 1 achieved the highest conversion, and Inoculum 5 achieved the highest acid concentrations, yields, and selectivities. For the CPDM evaluation, the operating map for Inoculum 1 had the highest performance. For the continuous fermentation, when considering all performance variables, Trains 1 and 2 had the best performance. Of the five inocula sampled, this study predicts that the bacterial community in Inoculum 1 optimizes performance and could be used in commercial-scale fermentations. Also, this study suggests that the three screens (batch, CPDM, continuous countercurrent fermentation) are a useful and predictive method for choosing best-performing inocula sources. However, it does not necessarily predict the rankings of the worst-performing inocula sources.

Table 12-8. Performance measures of countercurrent fermentation Trains 1, 2, 3, 4, and 5. Values represent the mean of the steady-state values \pm CI (95% CI).

Fermentation train	1	2	3	4	5
Total carboxylic acid concentration (g/L)	14.69 \pm 1.43	14.38 \pm 1.21	13.86 \pm 0.97	13.97 \pm 1.38	13.26 \pm 1.94
Total carboxylic acid exiting (g/d)	0.57 \pm 0.00	0.57 \pm 0.00	0.50 \pm 0.00	0.46 \pm 0.00	0.47 \pm 0.00
Aceq concentration (g/L)	21.46 \pm 2.09	20.40 \pm 1.74	19.56 \pm 1.38	19.83 \pm 1.96	19.17 \pm 2.90
Aceq exiting (g/d)	0.84 \pm 0.00	0.81 \pm 0.00	0.68 \pm 0.00	0.66 \pm 0.00	0.67 \pm 0.00
Aceq/Acid ratio	1.46 \pm 0.00	1.42 \pm 0.01	1.41 \pm 0.01	1.42 \pm 0.00	1.44 \pm 0.01
Conversion x (g VS digested/g VS fed)	0.214 \pm 0.011	0.438 \pm 0.008	0.170 \pm 0.023	0.195 \pm 0.013	0.192 \pm 0.032
Selectivity σ (g acid produced/g NAVS consumed)	0.535 \pm 0.003	0.259 \pm 0.001	0.601 \pm 0.007	0.475 \pm 0.003	0.490 \pm 0.009
Aceq selectivity σ_a (g Aceq produced/g NAVS consumed)	0.784 \pm 0.004	0.371 \pm 0.002	0.816 \pm 0.011	0.678 \pm 0.004	0.706 \pm 0.013
Exit yield Y_E (g acid/g NAVS fed)	0.115 \pm 0.000	0.114 \pm 0.000	0.102 \pm 0.001	0.092 \pm 0.000	0.094 \pm 0.001
Exit Aceq yield Y_{aE} (g Aceq/g NAVS fed)	0.168 \pm 0.001	0.162 \pm 0.001	0.138 \pm 0.002	0.132 \pm 0.001	0.135 \pm 0.002
Process yield Y_P (g acid/g NAVS fed)	0.100 \pm 0.001	0.102 \pm 0.000	0.082 \pm 0.001	0.071 \pm 0.000	0.079 \pm 0.002
Productivity P (g total acid/(L _{liq} ·d))	0.972 \pm 0.004	1.070 \pm 0.004	0.871 \pm 0.008	0.799 \pm 0.003	0.798 \pm 0.012
Mass balance closure (g mass in/g mass out)	0.87 \pm 0.00	0.86 \pm 0.00	0.82 \pm 0.01	0.80 \pm 0.00	0.86 \pm 0.01

Table 12-9. *p* values for performance measures for countercurrent fermentation Trains 1, 2, 3, 4, and 5 ($\alpha = 0.05$).

Trains	Conversion	Selectivity	Exit yield	Exit yield Aceq	Process yield	TLV	Productivity	Biogas produced	Total acid conc.	Aceq conc.	Total acid exit	Total Aceq exit	Aceq/ Total acid
1 and 2	0.000	0.000	0.000	0.000	0.000	0.000	0.000	0.000	0.737	0.433	0.000	0.000	0.000
1 and 3	0.001	0.000	0.000	0.000	0.000	0.000	0.000	0.000	0.335	0.138	0.000	0.000	0.000
1 and 4	0.022	0.000	0.000	0.000	0.000	0.000	0.000	0.000	0.463	0.252	0.000	0.000	0.000
1 and 5	0.187	0.000	0.000	0.000	0.000	0.000	0.000	0.000	0.228	0.197	0.000	0.000	0.002
2 and 3	0.000	0.000	0.000	0.000	0.000	0.000	0.000	0.000	0.494	0.444	0.000	0.000	0.282
2 and 4	0.000	0.000	0.000	0.000	0.000	0.000	0.000	0.000	0.653	0.662	0.000	0.000	0.859
2 and 5	0.000	0.000	0.000	0.000	0.000	0.000	0.000	0.000	0.317	0.459	0.000	0.000	0.002
3 and 4	0.056	0.000	0.000	0.000	0.000	0.069	0.000	0.000	0.890	0.820	0.000	0.000	0.173
3 and 5	0.248	0.000	0.000	0.026	0.004	0.000	0.000	0.111	0.569	0.803	0.000	0.360	0.001
4 and 5	0.866	0.002	0.044	0.004	0.000	0.000	0.897	0.000	0.539	0.701	0.053	0.004	0.001

p value < 0.005 statistically different, with a familywise error rate of 0.05 using the Bonferroni correction

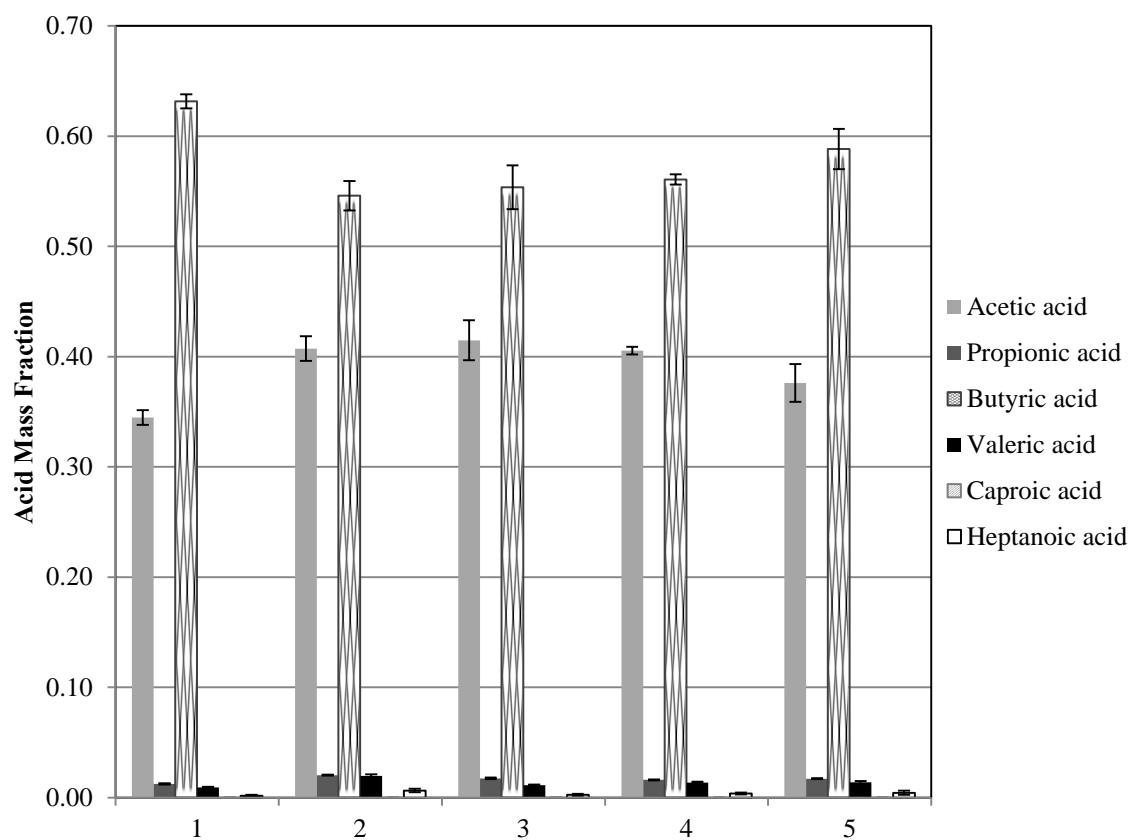


Figure 12-6. Carboxylic acid composition profile for countercurrent Trains 1, 2, 3, 4, and 5. Error bars are the confidence intervals for each carboxylic acid composition during the steady-state period.

12.4 Conclusion

To find the highest performing inoculum for carboxylate fermentations, five bacterial communities were screened and ranked by three fermentation performance tests: (1) batch screen, (2) continuum particle distribution model, and (3) continuous countercurrent fermentation. For screening numerous inocula sources, these tests would be used sequentially. Comparison of the results from the three tests suggests that Inoculum 1 would achieve the best performance. This study suggests that the three screens are a useful and predictive method for choosing optimal inocula sources in an aseptic environment.

13. BIOSCREENING

The goals of the bioscreening project follow: (1) in an initial screen employing batch fermentation, compare different inocula sources to Galveston marine microorganisms to select cultures that have high substrate conversion and product yield; (2) produce CPDM maps from the best inocula sources from the initial screen; (3) run continuous countercurrent fermentations on the inocula with the best CPDM maps.

13.1 Introduction

Fermentation performance and product spectra depend on the types and proportions of microorganisms present in the inoculum. To study the effect of different inocula in the MixAlco™ process, bioprospecting can be used (Leary et al., 2009) to find natural mixed cultures of microorganisms that are well adapted to the unique fermentation environment. Mixed cultures survive and thrive in nature and are far more stable and robust than pure cultures (Hawkes et al., 2007).

A mixed culture is extremely well suited to a non-sterile, dynamic environment with multiple feedstocks, offering advantages over a pure culture (Angenent et al., 2004; Das and Veziroglu, 2001). A pure culture of a single bacterial species might produce significant amounts of a specific desired product, but only in batch mode in a sterile system protected from outside microorganisms. In contrast, a mixed culture can establish a robust, synergistic community that grows faster than a pure culture and can also maintain itself better against microbial contamination (Rokem et al., 1980). The stability of the mixed-culture system has been linked to increased diversity of the microbial community and to an increased ability to adapt to changes in the system environment (Angenent et al., 2004). Additionally, because of their high diversity, these cultures can metabolize mixtures of substrates and the variable composition observed in waste streams (Kleerebezem and van Loosdrecht, 2007; Reis et al., 2003; Rodriguez et al., 2006).

Bioprospecting has two steps: (1) collecting inoculum sources from natural environments, and (2) selecting mixed cultures within the inoculum source that are well adapted to the desired fermentation (Kleerebezem and van Loosdrecht, 2007). Before this project, little research had been done to identify new microbial communities for use in the MixAlco™ process. However, the few attempts to improve the microbial community greatly increased product yields. For example, when a community isolated from a marine ecology (Galveston, TX) replaced the previous terrestrial community (College Station, TX), the acid yields doubled (Thanakoses, 2002). The natural saline environment of the marine ecology had a microbial community better suited to the salty environment of the MixAlco™ process.

Saline and thermal ecosystems are distributed globally and represent a wide range of ecosystem types including salt lakes, hot springs, salt flats, thermal wells, and ancient salt deposits (Oren, 2002). The water, soil, and sediments of these environments harbor active and diverse communities that can survive non-standard and non-conventional environments (Caton et al., 2004; Humayoun et al., 2003; Ley et al., 2006; Mesbah et al., 2007). Microorganisms isolated from these environments have been the subject of several studies that demonstrated their ability to anaerobically digest raw materials, reduce energy consumption, and improve the quality and purity of products (Antranikian et al., 2005; Nicholson and Fathepure, 2005).

The Bioscreening Project is a research effort with collaborations between three Texas A&M Departments: (1) Department of Chemical Engineering, (2) Department of Plant Pathology and Microbiology, and (3) Department of Soil and Crop Sciences. The goals of this project are to collect, screen, and isolate microorganisms that excel at degrading cellulose and hemicellulose for use in the MixAlco™ process.

This research screened over 500 bacterial communities isolated from over 20 different geological sites that were selected to find the highest performing inocula for the MixAlco™ fermentations. Most of the bioscreening efforts, research experiments, and trials are found elsewhere (Forrest, 2010) The bacterial communities were screened, ranked, and selected with a series of three sequential fermentation performance tests: (1)

initial screen, (2) continuum particle distribution model (CPDM), and (3) countercurrent fermentation trains (Figures 13-1 and 13-2). The communities that had the highest conversion from the 28-day initial batch screen and generated the best-performing maps from the 28-day batch CPDM fermentations were then run in four-stage countercurrent trains for over 4.5 months.

Countercurrent fermentations (Figure 13-2(c)) have a liquid and solid phases flowing in countercurrent directions in a series of four fermentors. Multi-staged fermentations generate higher conversions and product concentration than batch fermentations, but require more time, space, and effort. As biomass digests, the biomass becomes less reactive and the production of carboxylic acid decreases. In countercurrent fermentations, acid inhibition is minimized because the most digested biomass contacts the lowest concentration of carboxylate salts and the least digested biomass contacts the highest concentration.

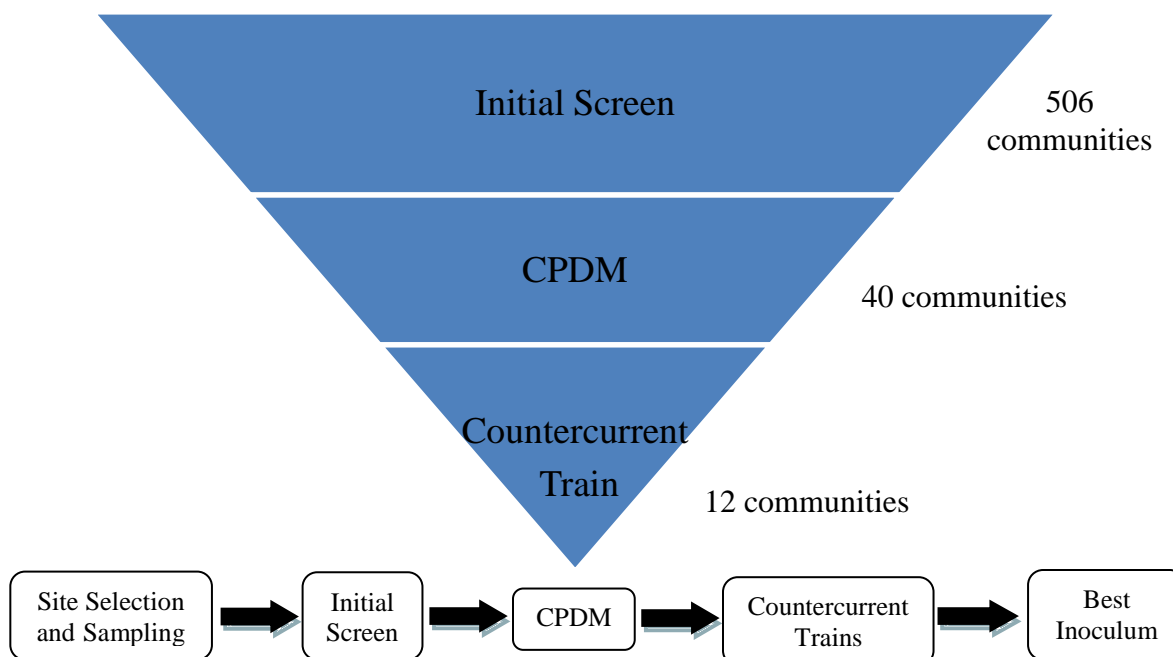


Figure 13-1. Overview of the microbial community screening using carboxylate platform fermentations.

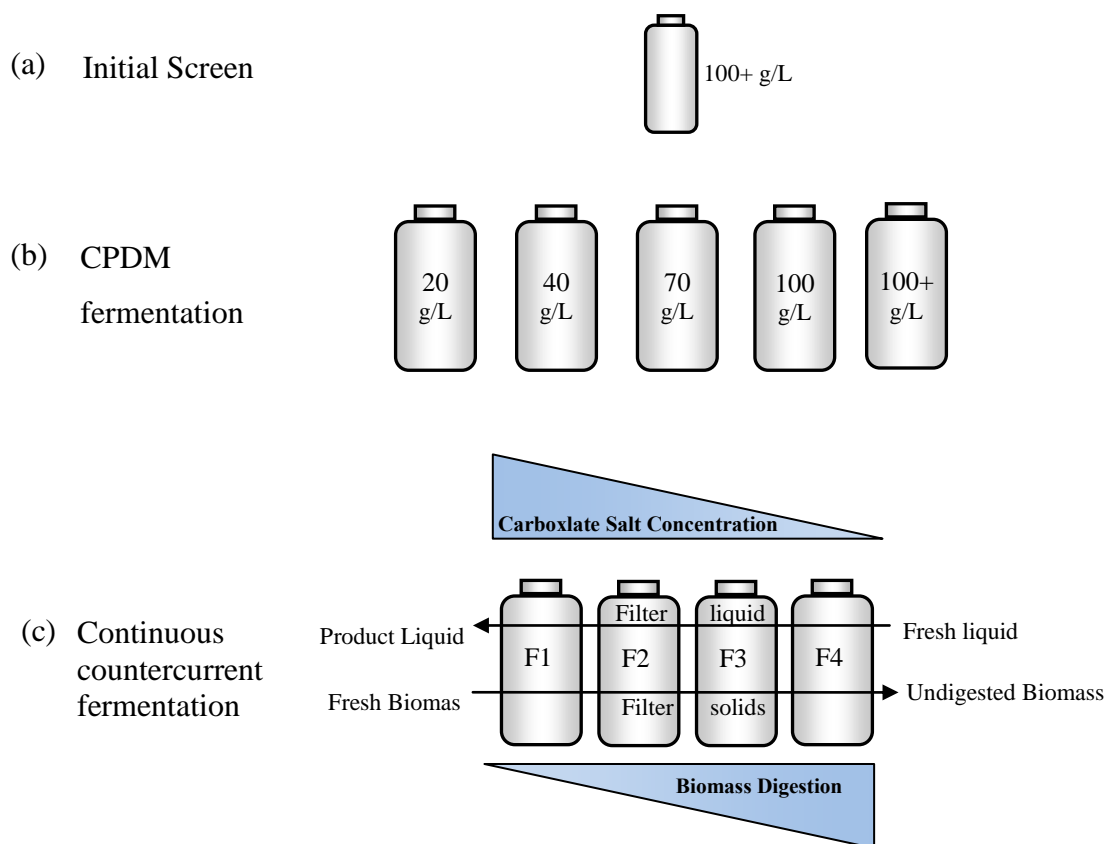


Figure 13-2. Diagram of the (a) initial screen, (b) CPDM, and (c) countercurrent fermentations for the bioscreening experiment.

13.2 Initial site screening

Using a mixed culture of microorganisms, the MixAlco™ process converts substrate into gasoline and jet fuel. To find the highest performing inoculum for carboxylate fermentations, the bacterial communities from saline and thermal ecosystems were inoculated into 30-day batch fermentations.

13.2.1 Site collection

All site sampling was conducted by members of Heather Wilkinson's group in the Department of Plant Pathology and Microbiology. Inocula samples were collected

from multiple sites with a variety of soil types. Three 20-cm-deep and 7.5-cm-diameter core samples were obtained with a soil corer and immediately placed in separate sealed, air-free plastic bags and chilled with dry ice. GPS coordinates recorded the exact location of each soil sample.

The control inoculum was aquatic sediment in Galveston, TX, which is the inoculum historically used for MixAlco™ fermentations. Sediment samples were removed from the bottom of 0.5-m-deep shoreline pits. Samples were immediately placed in airtight plastic bottles filled with deoxygenated water, capped, and chilled. Samples were frozen at $-20\text{ }^{\circ}\text{C}$ until use.

13.2.2 *Fermentation conditions: fermentors, methanogen inhibition, temperature, nutrient source, and substrate to nutrient loading ratio*

The fermentors for the initial screening were 250-mL polypropylene centrifuge bottles (61.8×127.7 mm, Nalgene brand NNI 3120-0250) capped by a polypropylene cap (Figure 14-2(a)).

All fermentations were incubated thermophilically at $55\text{ }^{\circ}\text{C}$, instead of mesophilically at $40\text{ }^{\circ}\text{C}$ because of better conversion and acid concentration (Forrest, 2010). The bottles were placed vertically in a shaker incubator rotating at 100 rpm.

Shredded recycled office paper was the energy source in all fermentations. Because commercial paper is lignin-free, it does not need to be pretreated. It has a constant composition, which removes the variation that would have occurred from pretreating multiple batches of agricultural feedstock.

When inoculating with the soil sample, 2.0 g of soil were added to the fermentor. For Galveston control inoculum, before inoculation, samples were thawed, shaken vigorously, and allowed to settle by gravity. Equal parts of the resulting supernatant were homogenized, and aliquots were used to inoculate each batch fermentor.

Chicken manure has commonly been used as the nutrient source in the MixAlco™ fermentations because it is inexpensive, widely available, and economically feasible for scale-up. Typically it has been added in a ratio of 20 g of dry nutrient to 80 g of dry substrate. Because chicken manure has a high microbial load that could

overwhelm the inoculum source, a nutrient with low microbial load was used. Two nutrient sources were investigated: yeast extract and corn steep liquor. Yeast extract consistently yielded higher fermentation performance than corn steep liquor and was chosen as the nutrient source for these studies (Forrest, 2010). Further testing revealed that the optimum paper to yeast extract ratio was found to be 90 to 10 (Forrest, 2010). Urea was added to supplement the fermentation with nitrogen. Iodoform (CHI_3) inhibited methane in all fermentors. Every 48 hours, iodoform solution (20 g CHI_3/L 190-proof ethanol) was added to each reactor throughout the fermentation (Ross, 1998). Because iodoform is light, air, and temperature sensitive, the solution was kept in amber-colored glass bottles and special care was taken to replace the cap immediately after use to prevent degradation.

13.2.3 *Fermentation performance*

13.2.3.1 *Analytical methods*

13.2.3.1.1 *Carboxylic acid concentration determination*

Fermentation liquid was centrifuged (4,000 rpm, $3300\times g$, 25 min) and mixed with equal parts of internal standard (1.162 g/L 4-methyl-*n*-valeric acid) and 3-M phosphoric acid (H_3PO_4), and then ultra-centrifuged (15,000 rpm, $18,360\times g$, 8 min). The carboxylic acid concentration was measured using an Agilent 6890 Series gas chromatograph (GC) system with a flame ionization detector (FID) and an Agilent 7683 automatic liquid sampler. A 30-m fused-silica capillary column (J&W Scientific Model # 123-3232) was used. The column head pressure was maintained at 2 atm abs. After each sample injection, the GC temperature program raised the temperature from 40 °C to 200 °C at 20 °C per min. The temperature was subsequently held at 200 °C for 2 min. The total run time per sample was 11 min, and helium was the carrier gas. The calibration standard was volatile acid mix (Matreya, LLC, Cat No. 1075).

13.2.3.1.2 *Moisture and ash contents*

Moisture and ash contents were determined by drying the sample in a 105 °C forced-convection oven for over 24 h, and subsequent combustion in a 575 °C furnace

for over 12 h (NREL, 2004). To ensure all volatile acids were in salt form, the fermentations were buffered with calcium carbonate. The ash content was calculated on a dry basis.

13.2.3.2 *Measuring performance definition of terms*

The performance variables were calculated as follows:

$$\text{conversion} = \frac{VS_{\text{in}} - VS_{\text{out}}}{VS_{\text{in}}} = \frac{\text{VS digested}}{\text{VS fed}} \quad (13-1)$$

$$\text{yield} = \frac{\text{total acid output from solid and liquid stream}}{VS_{\text{in}}} \quad (13-2)$$

$$\begin{aligned} \text{selectivity} &= \frac{\text{total acid produced}}{VS_{\text{in}} - VS_{\text{out}}} = \frac{\text{total acids produced}}{\text{VS digested}} \\ &= \frac{\text{yield}}{\text{conversion}} \end{aligned} \quad (13-3)$$

where VS_{in} is the volatile solids fed, and VS_{out} is the volatile solids removed from the solid phase of the fermentation. The VS_{out} does not include the suspended volatile solids in the exiting liquid phase.

$$\text{acid productivity} = \frac{\text{total acids produced}}{\text{total liquid volume} \cdot \text{time}} \quad (13-4)$$

The total mass in the system was accounted for in a mass balance closure,

$$\text{mass balance closure} = \frac{\text{mass out}}{\text{mass in}} \quad (13-5)$$

The carboxylic acid concentrations can be converted to a molar acetic acid equivalent (α).

$$\begin{aligned}
 \alpha &= 1.00 \times \text{acetic (mol/L)} + 1.75 \times \text{propionic (mol/L)} \\
 &+ 2.50 \times \text{butyric (mol/L)} + 3.25 \times \text{valeric (mol/L)} \\
 &+ 4.00 \times \text{caprioc (mol/L)} + 4.75 \times \text{heptanoic (mol/L)}
 \end{aligned}
 \tag{13-6}$$

Acetic acid equivalents (Aceq) can be expressed on a mass basis as

$$\text{Aceq (g/L)} = 60.05 \text{ (g/mol)} \times \alpha \text{ (mol/L)}
 \tag{13-7}$$

13.2.4 *Initial screen procedure*

The initial screen used batch fermentation to find the highest performing inocula. Each soil sample was incubated in batch mode for 30 days in a 55 °C shaker incubator using a 250-mL centrifugal Nalgene bottle (61.8 × 127.7 mm, Nalgene brand NNI 3120-0250) as the fermentor. Each 250-mL bottle was filled with the ingredients in Table 13-1. A soil sample was taken to get the amount of moisture and volatile solids for use in calculating performance variables.

Every other day, the gas was vented and 40 µL of iodoform was added to inhibit methanogens. Liquid fermentation samples were taken on the first and final day of the experimental run and analyzed for carboxylic acid concentration using gas chromatography (GC). To preserve fermentation integrity, GC samples were not taken in between these days.

After fermenting in batch mode for 30 days, the bottles were removed from the shaker incubator and shaken by hand. The solids gravity settled for 2 minutes, and a 3-mL liquid sample was removed with a transfer pipette into a 15-mL conical tube for GC analysis. The liquid phase was separated from the solid phase by centrifuging (4000 rpm, 3300×g, 25 min). The mass, moisture content, and ash content of the solid and liquid phase from each bottle was found for conversion and yield calculations. Because of limited oven and furnace space, samples were temporarily frozen in well-sealed 50-mL conical tubes until analysis. Approximately half of the solid cake was used for

moisture and ash content analysis and half was returned to the bottle with the respective fermentation liquid for bacterial DNA analysis.

The conversion, yield, and selectivity were calculated from the change in acid concentration found from GC and the moisture and ash contents from the resulting solid samples. The bottles were not run in replicate because of the large quantity of sites sampled. The inocula were ranked based on conversion, and one to two samples per site was chosen for further investigation.

Table 13-1. Initial batch fermentation ingredients.

Ingredients
9 g paper
1 g yeast extract
150 mL DO H ₂ O
3.2 g acetate
0.2 g propionate
0.5 g butyrate
2.2 g CaCO ₃
2.5 g wet soil

13.2.5 *Site V - Hawaii*

Site V fermented a total of 28 samples collected from several sites in Hawaii, two Galveston samples, and one control with no inoculum (Table 13-2). Galveston #1 was Galveston inoculum collected from year 2006, and Galveston #2 was Galveston inoculum collected from year 2010. All of the fermentation bottles were autoclaved before loading and inoculation, to prevent cross contamination.

Table 13-2. Initial batch fermentation sample IDs and location.

Sample ID	Sample location ID	Sample Location	Latitude (N)	Longitude (W)	Trip date
V01	HBSP1	Hapuna beach SP, HI	19.9908836	155.824769	5/4/2010
V02	HBSP2		19.9916382	155.82614	5/4/2010
V03	HBSP3		19.994819	155.825956	5/4/2010
V04	APHW1	Alchiline ponds, HI	19.852757	155.9272626	5/4/2010
V05	APHW2		19.8527848	155.92725	5/4/2010
V06	APHW3		19.8948557	155.9018	5/4/2010
V07	APHW4		19.8948466	155.9018	5/4/2010
V08	NELH1	Natural Energy Lab, HI	19.731411	156.0565463	5/4/2010
V09	NELH2		19.731298	156.056777	5/4/2010
V10	NELH3		19.731298	156.056777	5/4/2010
V11	NELH4		19.73127	156.056777	5/4/2010
V12	KKHW1	Kekaha Kai State Park, Hawaii	19.7812468	156.0424609	5/4/2010
V13	KKHW2		19.7810034	156.04193	5/4/2010
V14	KKHW3		19.7810410	156.042026	5/4/2010
V15	KKHW4		19.7811572	156.041957	5/4/2010
V16	KKHW5		19.780491	156.0420647	5/4/2010
V17	GALVESTON #1	Galveston, TX	unknown	unknown	2006
V18	CONTROL - NO INOCULUM	-	-	-	-
V19	ONHW1	Onekahakaha Beach park, HI	19.7372015	155.0375515	5/11/2010
V20	ONHW2		19.7372015	155.0375515	5/11/2010
V21	ONHW3		19.7372015	155.0375515	5/11/2010
V22	ONHW4		19.7372015	155.0375515	5/11/2010
V23	WRHW1	Wailoa River State Park, HI	19.7171918	155.037303	5/11/2010
V24	AFHW1	Akaka Falls State Park, HI	19.855835	155.039079	5/11/2010
V25	AFHW2		19.853698	155.0390523	5/11/2010
V26	AFHW3		19.8537278	155.0390526	5/11/2010
V27	CPHW1	Carlsmith County Park, HI	19.7349488	155.0139037	5/11/2010
V28	CPHW2		19.7360199	155.0134403	5/11/2010
V29	CPHW3		19.7352555	155.0131349	5/11/2010
V30	CPHW4		19.7352278	155.0131918	5/11/2010
V31	GALVESTON #2	Galveston, TX	unknown	unknown	2010

Table 13-3. Initial batch fermentation results at 55 °C for Site V. Yellow highlight indicates highest performers for that variable.

Hawaii – 55 °C													
	Conv. Rank	Ending Total Acid Conc. (g/L)	Change in Acid Conc. (g/L)	Change in Aceq Conc. (g/L)	Acetic (%)	Propionic (%)	Butyric (%)	Valeric (%)	Caproic (%)	Heptanoic (%)	Conversion (g VS digested/g VS fed)	Selectivity (g acid produced/g VS digested)	Yield (g acid produced/g VS fed)
V01	17	18.28	0.55	0.62	79.89	6.07	13.87	0.16	0.00	0.00	0.10	0.09	0.01
V02	27	19.45	0.70	0.84	68.73	4.01	26.82	0.44	0.00	0.00	0.06	0.17	0.01
V03	13	18.55	0.98	1.15	75.46	3.41	21.05	0.07	0.00	0.00	0.11	0.15	0.02
V04	1	17.84	0.96	1.11	76.20	6.44	17.36	0.00	0.00	0.00	0.17	0.09	0.02
V05	21	18.38	0.93	1.08	75.68	3.63	20.61	0.09	0.00	0.00	0.08	0.18	0.02
V06	23	17.48	0.55	0.63	75.96	3.69	20.24	0.10	0.00	0.00	0.08	0.12	0.01
V07	11	21.45	3.17	3.61	77.10	7.33	15.50	0.07	0.00	0.00	0.11	0.46	0.05
V08	15	19.04	1.77	2.05	76.28	4.05	19.67	0.00	0.00	0.00	0.10	0.29	0.03
V09	18	18.70	2.24	2.63	73.25	6.16	20.44	0.15	0.00	0.00	0.09	0.38	0.04
V10	6	19.64	2.18	2.51	76.57	4.81	18.62	0.00	0.00	0.00	0.12	0.28	0.03
V11	12	18.68	0.25	0.29	70.89	9.25	19.79	0.06	0.00	0.00	0.11	0.04	0.00
V12	5	20.09	2.76	3.22	73.14	8.18	18.52	0.16	0.00	0.00	0.15	0.30	0.04
V13	31	18.99	1.31	1.50	77.14	3.80	19.06	0.00	0.00	0.00	0.03	0.81	0.02
V14	16	20.96	3.83	4.38	78.28	3.82	17.86	0.00	0.00	0.04	0.10	0.63	0.06
V15	3	19.99	3.47	3.97	77.65	4.96	17.39	0.00	0.00	0.00	0.16	0.36	0.06
V16	24	19.99	3.71	4.24	78.13	3.73	18.07	0.08	0.00	0.00	0.08	0.80	0.06
V17	26	19.37	2.38	2.79	73.95	5.39	20.51	0.15	0.00	0.00	0.06	0.59	0.04
V18	25	19.73	2.81	3.25	75.31	6.30	18.25	0.15	0.00	0.00	0.07	0.61	0.04
V19	19	19.67	2.90	3.38	73.27	6.75	19.38	0.16	0.06	0.38	0.09	0.48	0.04

Table 13-3 continued

	Conv. Rank	Ending Total Acid Conc. (g/L)	Change in Acid Conc. (g/L)	Change in Aceq Conc. (g/L)	Acetic (%)	Propionic (%)	Butyric (%)	Valeric (%)	Caproic (%)	Heptanoic (%)	Conversion (g VS digested/g VS fed)	Selectivity (g acid produced/g VS digested)	Yield (g acid produced/g VS fed)
V20	7	18.92	6.31	7.11	79.56	5.97	14.38	0.09	0.00	0.00	0.12	0.80	0.10
V21	22	19.72	2.08	2.38	76.76	6.61	16.44	0.18	0.00	0.00	0.08	0.40	0.03
V22	4	20.74	2.69	3.26	67.38	6.14	26.47	0.00	0.00	0.00	0.15	0.28	0.04
V23	2	19.31	2.29	2.56	80.85	4.48	14.66	0.00	0.00	0.00	0.17	0.22	0.04
V24	20	18.63	2.24	2.54	78.13	7.02	14.76	0.10	0.00	0.00	0.09	0.39	0.04
V25	8	19.17	2.41	2.84	71.73	7.72	20.54	0.00	0.00	0.00	0.12	0.31	0.04
V26	9	24.62	1.94	2.46	60.55	4.42	34.92	0.10	0.00	0.00	0.11	0.27	0.03
V27	29	20.81	1.77	2.18	64.99	5.63	29.26	0.12	0.00	0.00	0.05	0.52	0.03
V28	28	20.26	2.43	2.84	72.10	9.29	18.45	0.17	0.00	0.00	0.06	0.64	0.04
V29	14	18.42	2.59	2.96	80.16	0.47	18.30	1.07	0.00	0.00	0.10	0.39	0.04
V30	10	17.68	1.40	1.64	76.23	0.58	21.88	1.30	0.00	0.00	0.11	0.20	0.02
V31	30	17.22	0.36	0.42	74.43	3.25	22.20	0.13	0.00	0.00	0.05	0.12	0.01

Table 13-4. Initial batch fermentation results at 40 °C for Site V. Yellow highlight indicates highest performers for that variable. Red highlight indicates erroneous results*.

Hawaii – 40 °C													
	Conv. Rank	Ending Total Acid Conc. (g/L)	Change in Acid Conc. (g/L)	Change in Aceq Conc. (g/L)	Acetic (%)	Propionic (%)	Butyric (%)	Valeric (%)	Caproic (%)	Heptanoic (%)	Conversion (g VS digested/g VS fed)	Selectivity (g acid produced/g VS digested)	Yield (g acid produced/g VS fed)
V01	3	20.68	2.18	2.46	79.15	5.41	15.31	0.04	0.03	0.06	0.16	0.22	0.04
V02	13	22.03	0.27	0.32	67.07	14.08	18.80	0.04	0.00	0.00	0.09	0.05	0.00
V03	8	18.42	0.52	0.60	74.80	3.55	21.60	0.05	0.00	0.00	0.11	0.08	0.01
V04	25	19.17	2.16	2.50	75.81	4.70	19.39	0.05	0.04	0.00	0.04	0.89	0.04
V05	17	19.81	2.20	2.42	83.40	6.43	10.17	0.00	0.00	0.00	0.08	0.46	0.04
V06	4	19.77	5.39	6.17	78.16	3.33	18.35	0.16	0.00	0.00	0.15	0.56	0.08
V07	1	21.00	1.00	1.13	80.63	2.48	16.84	0.04	0.00	0.00	0.17	0.10	0.02
V08	18	20.31	0.45	0.52	77.35	4.34	18.20	0.11	0.00	0.00	0.07	0.12	0.01
V09	6	17.12	0.24	0.26	79.60	8.66	11.68	0.06	0.00	0.00	0.11	0.03	0.00
V10	21	18.80	0.26	0.30	77.72	8.57	13.66	0.05	0.00	0.00	0.06	0.07	0.00
V11	28	23.68	1.15	1.28	82.38	5.40	12.19	0.03	0.00	0.00	0.04	0.50	0.02
V12	16	17.58	0.22	0.25	79.95	5.66	14.33	0.06	0.00	0.00	0.08	0.05	0.00
V13	2	25.62	0.65	0.73	80.59	5.62	13.76	0.04	0.00	0.00	0.17	0.07	0.01
V14	20	18.76	0.30	0.34	77.06	5.16	17.61	0.17	0.00	0.00	0.06	0.08	0.00
V15	11	19.13	2.48	2.84	77.48	4.54	17.98	0.00	0.00	0.00	0.10	0.40	0.04
V16	29	25.45	1.10	1.25	79.14	3.24	17.61	0.00	0.00	0.00	0.02	0.78	0.02
V17	10	17.75	0.15	0.17	76.37	8.35	15.21	0.07	0.00	0.00	0.11	0.02	0.00
V18	27	17.81	0.31	0.35	79.80	3.63	16.57	0.00	0.00	0.00	0.04	0.13	0.00
V19	23	18.88	1.61	1.76	86.47	0.34	13.19	0.00	0.00	0.00	0.05	0.54	0.03

Table 13-4 continued

	Conv. Rank	Ending Total Acid Conc. (g/L)	Change in Acid Conc. (g/L)	Change in Aceq Conc. (g/L)	Acetic (%)	Propionic (%)	Butyric (%)	Valeric (%)	Caproic (%)	Heptanoic (%)	Conversion (g VS digested/g VS fed)	Selectivity (g acid produced/g VS digested)	Yield (g acid produced/g VS fed)
V20	9	16.69	1.63	1.94	69.90	6.51	23.28	0.30	0.00	0.00	0.11	0.24	0.03
V21	5	18.50	2.70	3.09	76.88	6.52	16.50	0.10	0.00	0.00	0.14	0.32	0.04
V22	15	21.11	0.65	0.75	74.92	8.14	16.90	0.04	0.00	0.00	0.09	0.12	0.01
V23	19	16.90	0.56	0.62	83.11	0.29	16.60	0.00	0.00	0.00	0.06	0.14	0.01
V24	12	19.70	2.87	3.33	74.71	5.69	19.60	0.00	0.00	0.00	0.10	0.47	0.04
V25	14	22.93	0.64	0.77	70.68	4.79	24.52	0.00	0.00	0.00	0.09	0.12	0.01
V26	24	23.96	2.07	2.29	83.40	3.73	12.16	0.07	0.12	0.51	0.04	0.74	0.03
V27	26	32.42	0.64	0.87	47.35	1.20	51.45	0.00	0.00	0.00	0.04	0.27	0.01
V28	30	45.67	2.71	3.89	37.46	1.99	60.45	0.10	0.00	0.00	0.02	2.43	0.04
V29	31	39.15	3.18	4.60	34.21	5.66	60.02	0.11	0.00	0.00	0.00	21.40	0.05
V30	7	20.56	5.15	6.11	70.91	7.13	21.67	0.29	0.00	0.00	0.11	0.74	0.08
V31	22	18.37	1.12	1.28	77.44	6.43	16.13	0.00	0.00	0.00	0.05	0.35	0.02

*Invalid results: These were loaded with too much butyric acid. Butyric acid is used because calcium butyrate salt is very expensive. Butyric acid is in a liquid form and added in small amounts, making measurements difficult. This increase in butyric acid made conversion practically zero, and selectivity too high.

Table 13-5. Initial batch fermentation rankings at 40 °C and 55 °C for Site V.

Rank based on conversion		
	55 °C	40 °C
1	V04	V07
2	V23	V13
3	V15	V01
4	V22	V06
5	V12	V21
6	V10	V09
7	V20	V30
8	V25	V03
9	V26	V20
10	V30	V17
11	V07	V15
12	V11	V24
13	V03	V02
14	V29	V25
15	V08	V22
16	V14	V12
17	V01	V05
18	V09	V08
19	V19	V23
20	V24	V14
21	V05	V10
22	V21	V31
23	V06	V19
24	V16	V26
25	V18	V04
26	V17	V27
27	V02	V18
28	V28	V11
29	V27	V16
30	V31	V28
31	V13	V29

13.2.6 *Conclusion*

The Hawaii sites sampled did not have initial batch fermentation conversions over 0.32 g VS digested/g VS fed. However, the best of sites (V04, V23), based on conversion, should be further investigated. Initial batch fermentations run at 55 °C and 40 °C did not have similar performances, indicating that different microbial communities dominate at different temperatures.

13.3 **CPDM for inoculum selection in carboxylate fermentation**

13.3.1 *Introduction to CPDM*

Long residence times are associated with countercurrent fermentations. Experimentally obtaining a wide range of operating conditions for these 4–8 month continuous fermentations is tremendously time consuming. Mixed-acid fermentation involves many complex reactions between the substrates, products, and the microorganisms. The conventional approach to modeling solid- and fluid-phase reactions is the Residence Time Distribution (RTD) model. One disadvantage of using the RTD model in the MixAlco™ process is that it cannot accurately predict the interfacial reaction rate between the fluid and solid phases because the reactivity and residence time is not unique for all fluid-phase driving forces (Kunii and Levenspiel, 1969; Loescher, 1996).

In contrast to RTD, continuum particle distribution modeling (CPDM) separates fluid and solid dependencies explicitly. CPDM is an empirical approach that accurately models the complex reactions by generalizing the behavior of a specific reaction system (Loescher, 1996; Ross, 1998). CPDM quantifies the kinetics of a reaction occurring at the interface between solid and fluid phases. Examples of such reactions are (1) microbial conversion of lignocelluloses to volatile fatty acids, (2) enzymatic hydrolysis of lignocellulose, (3) microbial coal desulfurization, (4) reactive and non-reactive extraction of soil contaminants, and (5) combustion of high-ash coal. This method allows laboratory data to be modeled mechanistically, or to empirically simulate different reactor configurations (Loescher, 1996).

The concept of “continuum particle” (CP) is used to avoid the difficulties of tracking the geometry of individual discrete particles. A CP has been defined as a collection of biomass particles that equals one gram volatile solids (VS) at time zero and assumes that it is representative of the entire feedstock entering the fermentation (Ross, 1998). Initially in the fermentation, all the CPs are the same. As the reactions occur, the CPs convert at different rates, which are expressed in a distribution function. The CPDM method has been used to successfully predict the product concentration and biomass conversion for several countercurrent fermentations (Agbogbo, 2005; Aiello-Mazzarri, 2002; Forrest, 2010; Fu, 2007; Thanakoses, 2002).

13.3.2 *Batch experiments to obtain CPDM parameters*

To select the highest performing inoculum site, CPDM parameters must be obtained. If there is not enough original sediment sample to inoculate the batch fermentors, which was the case a majority of the time, the specific community of microorganisms must be grown up in the fermentation environment. By allowing the inocula to ferment in batch mode for several weeks, this allowed the community to adapt to digesting the particular feed substrate. The adapted microorganisms were then used to inoculate five batch fermentations containing a range of initial substrate concentration that ran for 28 d. The substrate concentrations used were 20, 40, 70, 100, and 100+ g substrate/L liquid. The 100 and 100+ g substrate/L liquid fermentors had the same initial substrate concentration, but the 100+ fermentor contained medium with a mixture of carboxylate salts in a concentration of 20 g carboxylic acids/L medium. The components and concentrations of the added mixed carboxylic salts in the 100+ batch fermentations are listed in Table 13-6.

Table 13-6. The carboxylate salts used in 100+ fermentations.

Nomenclature	Ratio of acetate salts (mass basis)	Ratio of propionate salts (mass basis)	Ratio of butyrate salts (mass basis)
100+ g/L	80% Ca ²⁺ salts	5% Ca ²⁺ salts	15% Ca ²⁺ salts

The inoculum for the CPDM fermentations was taken from the residue from the initial screen, so that the microorganisms were already adapted to this type of substrate. Because of the small amount of material remaining at the end of the initial screen, the amount of inocula was increased in a batch fermentation containing the same substrate with the same 20 g carboxylic acid/L liquid as both the initial screen and the 100+ fermentors. The resulting broth from this upculture was used to inoculate the CPDM fermentors. The initial carboxylic acid concentration in the batch fermentors results from the acids contained in the inoculum. Calcium carbonate was used as the buffer in these fermentations. The pH, gas production, and gas composition were monitored during the fermentations. Iodoform was added every other day to inhibit methane production. Samples of the liquid were taken from each fermentor and the amount of carboxylic acid was measured by gas chromatography (see Section 13.2.3.1.1).

Because C2–C7 acids are present, the concentration of each type of acid is converted into an acetic acid equivalent (Aceq). Aceq represents the amount of acetic acid that could have been produced in the fermentation if all the carboxylic acids produced were acetic acid (Datta, 1981). The Aceq unit is based on the reducing power of the acids as presented in the following reducing-power-balanced disproportionation reactions (Loescher, 1996). Converting the acids into Aceq allows the CPDM modeling to account for them as one single parameter. Equations 13-8 through 13-12 are used to calculate the Aceq concentration.



Acid concentrations are monitored during the course of the four-week fermentation. Because a spectrum of acids are present, the concentration of each type of acid is converted, based on reducing power, into a single concentration of acetic acid equivalents (Aceq) (Equation 13-13).

$$\begin{aligned} \text{Aceq (g/L)} = & 60.05 \text{ (g/mol)} \times [\text{acetic (mol/L)} \\ & + 1.75 \times \text{propionic (mol/L)} + 2.5 \times \text{butyric (mol/L)} \\ & + 3.25 \times \text{valeric (mol/L)} + 4.0 \times \text{caprioc (mol/L)} \\ & + 4.75 \times \text{heptanoic (mol/L)}] \end{aligned} \quad (13-13)$$

Product accumulation in the batch fermentations was used to provide data for the rate equation. The acid generated was modeled using Equation 13-14. Least squares analysis was used to obtain parameters. For each batch fermentation, the Aceq and time data are fit to Equation 13-14 and a , b , and c are determined.

$$\text{Aceq} = a + \frac{b \cdot t}{1 + c \cdot t} \quad (13-14)$$

where a , b , and c are empirical constants, t is time, and Aceq is acetic acid equivalents. The specific rate (Equation 13-16) was determined from Equation 13-14 and this was fit to Equation 13-17. CPDM parameters were obtained using the least squares analysis to minimize the specific rate (g of Aceq generated/(time·g VS)) using the mass of Aceq generated in the batch fermentor.

$$\text{Rate} = r = \frac{d \text{ Aceq}}{dt} = \frac{b}{1 + c \cdot t^2} \quad (13-15)$$

$$\text{Specific rate} = r = \frac{r}{S_0} \quad (13-16)$$

$$r = \frac{e(1-x)^f}{1 + g(\phi \cdot \text{Aceq})^h} \quad (13-17)$$

where e, f, g, h are empirical constants, Aceq is acetic acid equivalents, ϕ is the ratio of total grams of actual acid to grams of Aceq . S_0 is the initial amount of substrate (g VS/L), and is assumed to be constant throughout each batch fermentation.

$$\text{Conversion} = x_t = \frac{\text{Aceq } t - \text{Aceq } t=0}{S_0 \cdot \sigma} \quad (13-18)$$

The conversion (x) used in the model (Equation 13-18) is defined as the mass of acetic acid equivalent generated (g) per mass of volatile solids (g). The selectivity of the fermentation (g Aceq/g VS digested) σ is assumed to be constant for each system. During the batch mode of operation, the rate equation was integrated using the explicit method of numerical integration. The acetic acid equivalent concentration in the fermentors was determined by dividing the mass of acetic acid equivalents by the volume of liquid in each fermentor. The ratio of total acids to acetic acid equivalents (ϕ) was used to convert the acetic acid equivalent concentrations back to total acid concentrations.

The values of Aceq , the specific reaction rate r , and the conversion x are determined from the experimental data from the batch fermentations (Equations 13-14, 13-16, 13-18, respectively). The parameter values of e, f, g , and h in Equation 13-17 are fit by non-linear regression (*SYSSTAT SIGMAPLOT 12.0*).

Microsoft Excel Solver was used to obtain the model parameters in Equations 13-14 and 13-17. The sum of the mean-square error between experimental and predicted values was minimized to obtain the model parameters. Matlab (program available in

Appendix N) was used to predict the acetic acid equivalent concentration and conversion at various VSLR and LRT.

Once the empirical constants (e , f , g and h) have been determined for a specific reaction system, Equation 13-17 may be used to model and optimize different reactor schemes that will use that system. The other required system parameters for CPDM method are selectivity, holdup (ratio of liquid to solid in wet solids), and moisture (ratio of liquid to solids in feed solids). Based on these parameters of different microorganism communities, the Matlab program for CPDM (Appendix N) can predict the Aceq concentration and conversion for countercurrent fermentations at various VSLRs and LRTs.

CPDM was developed for batch, fed-batch, CSTR, PFR, counter- and co-current CSTR cascades, PFR-CSTR cascades, and CSTR-PFR cascades (Loescher, 1996). It can also be applied to simultaneous saccharification and fermentation (SSF) and mixed-acid fermentations. Because of the diverse nature of this modeling program, the round-robin, biomass and cell recycle, multistage, and bioscreening fermentation experiments could be modeled with the CPDM theory to determine the validity of CPDM on these fermentation modes.

13.3.3 *Fermentation conditions: fermentors, substrate, nutrient source, loading ratio, and temperature*

The fermentors were 1-L polypropylene centrifuge bottles capped by a rubber stopper inserted with a glass tube (Ross, 1998). A rubber septum sealed the glass tube and allowed for gas sampling and release. Two lengths of ¼-in stainless steel pipe, inserted through the rubber stopper into the vessel, mix the contents of the fermentor as it is rotated in the rolling incubator.

Shredded recycled office paper, the substrate material in all fermentations, is lignin free and so it eliminated the need for pretreatment and the associated variability. Yeast extract was the nutrient source used at a ratio of 90 wt% paper and 10 wt% yeast extract in all fermentations. Urea (0.5 g) and calcium carbonate (1.0 g) were used for pH

control. Iodoform solution (20 g CHI₃ /L 190-proof ethanol) was added to each reactor every 48 hours throughout the fermentation to inhibit methane production (Ross, 1998).

All fermentations were incubated thermophilically at 55 °C. Batch experiments were performed to provide the necessary data for continuum particle distribution modeling (CPDM). These data were used to develop a model rate equation for the countercurrent fermentation. The procedure involved operating five different fermentors with different initial substrate concentrations (20, 40, 70, 100 g dry substrate/L liquid). An additional fermentor (100+) had high substrate concentration (100 g dry substrate/ L liquid) and high carboxylic acid concentration (approximately 20 g carboxylic acids/L liquid) to evaluate any inhibition caused by the carboxylic acids. Samples were taken every 48 hours. Total gas volume was measured by liquid displacement and liquid broth samples for pH and carboxylic acid measurements were taken under nitrogen purge. The resulting carboxylic acid concentrations were converted into acetic acid equivalents (as described in Equation 13-13).

The operating parameters and performance variables were calculated as follows:

$$\text{liquid residence time } LRT = \frac{TLV}{Q} \quad (13-19)$$

where Q = flow rate of liquid out of the fermentor set (L/d) and TLV = the total liquid volume

$$TLV = \sum_i (\bar{K}_i \times w + \bar{F}_i) \quad (13-20)$$

where K_i = average wet mass of solid cake in Fermentor i (g), w = average liquid fraction of solid cake in Fermentor i (L liquid/g wet cake), F_i = average volume of free liquid in Fermentor i (L).

$$\text{volatile solids loading rate VSLR} = \frac{\text{VS fed } d}{\text{TLV}} \quad (13-21)$$

$$\text{conversion} = \frac{\text{VS digested}}{\text{VS fed}} \quad (13-22)$$

$$\text{selectivity} = \frac{\text{total acid produced}}{\text{VS digested}} \quad (13-23)$$

where VS fed is the volatile solids fed, and VS digested is the volatile solids digested during the fermentation.

13.3.4 CPDM results and discussion

To predict countercurrent fermentations systems, Continuum Particle Distribution Modeling (CPDM) is a valuable tool that can predict optimum conditions of high conversions and high acid concentrations. Although CPDM modeling is far less time-consuming than traditional laboratory-scale countercurrent fermentations, it is still time and labor intensive. To narrow the number of CPDM fermentations run and select for the best communities, inocula that appeared promising in the initial batch fermentations (conversion of ≥ 0.32 g VS digested/g VS fed, or it was the “best of site”) was chosen for CPDM modeling. Table 13-7 displays the sites chosen for CPDM analysis. All sites were compared to the traditional Galveston inoculum (B01, (Forrest, 2010)). The Bioscreening Group chose to study A21, A23, A25, G21, and G38. A23 was chosen because it was one of the initial screens from Site A that had high acid production. A21 and A25 were studied because of the transect location. G21 was studied because it had a conversion over 32% in the initial screen, and G38 was studied because it was the only fermentation that produced caproic acid.

Table 13-7. Samples selected for CPDM modeling.

Site	Sample	Location	Conversion >0.32	Best of site	Interesting
A	A21	T3-65			√
A	A23	T3-195		√	
A	A25	T3-325			√
G	G21	BL21	√		
G	G38	LP4			√

13.3.5 CPDM parameters and maps

13.3.5.1 Sample A21 from Site A – La Sal del Rey, TX

Batch experiments with 90 wt% paper /10 wt% yeast extract were performed to obtain model parameters for CPDM method, as mentioned in Section 13.3.1. The inocula for these fermentations was taken from the post-reactor material of the initial screening then preserved in a 20% glycerol solution. Calcium carbonate buffered the fermentations. Liquid samples from the fermentations were analyzed for carboxylic acids. The acids were converted to acetic acid equivalents (Aceq) using Equation 13-13. Figure 13-3 shows the Aceq concentrations for the five A21 batch experiments. The smooth lines are the predicted Aceq. Values of the fitted parameters a , b , and c for Equation 13-14 are presented in Table 13-8.

Table 13-8. Values of the parameters a , b , and c fitted by least squares analysis for La Sal del Rey inoculum A21.

Substrate Concentration (g/L)	a (g/L liquid)	b (g/(L liquid·d))	C (d ⁻¹)
20	1.316	0.1946	0.0100
40	1.690	0.3761	0.0281
70	1.834	0.2916	0.0100
100	1.682	0.5997	0.0148
100+	14.88	0.6138	0.0247

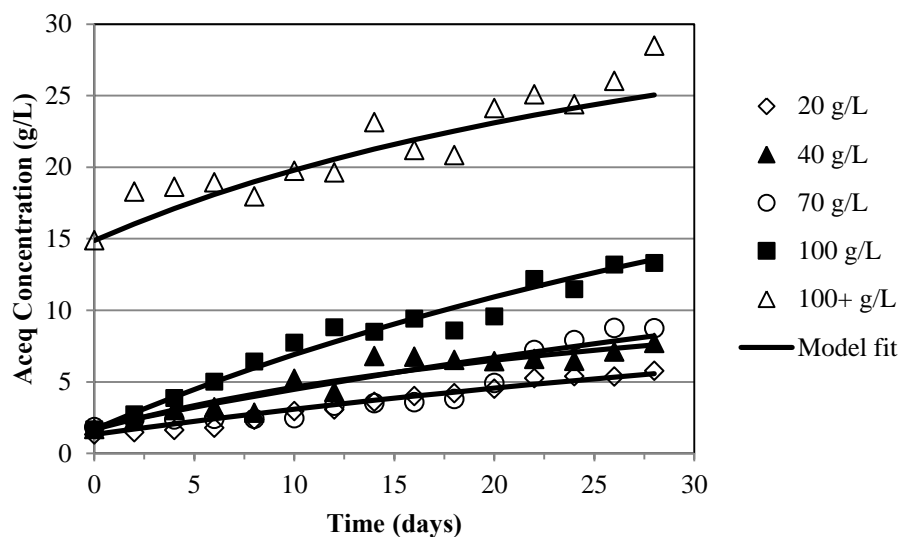


Figure 13-3. Aceq concentrations of A21 inoculated paper/yeast extract fermentation at 20, 40, 70, 100, and 100+ g substrate/L liquid with calcium carbonate buffer.

The reaction rate and the specific reaction rate for the batch fermentations were calculated using Equations 13-15 and 13-16. Conversion was calculated with the experimental acetic acid equivalents using Equation 13-13. Parameters e , f , g , and h presented in the predicted rate equation (Equation 13-17) were calculated by nonlinear regression (*Systat Sigmaplot 12.0*). Figure 13-4 compares the predicted specific rate with the experimental specific rate. The specific rate equation for La Sal del Rey inoculum A21 follows:

$$r_{pred} = \frac{0.0074 (1 - x)^{1.000}}{1 + 0.0010 \phi \cdot Aceq^{2.166}} \quad (13-24)$$

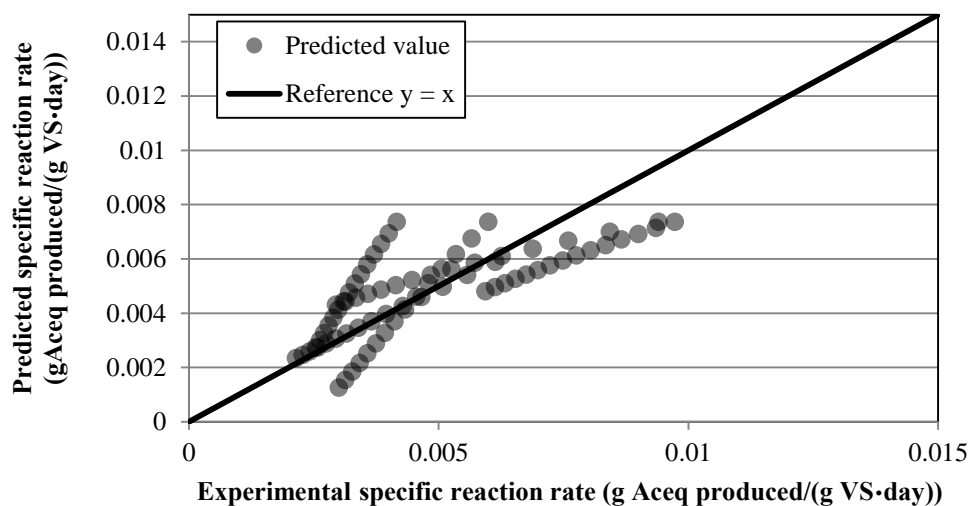


Figure 13-4. The experimental value and the CPDM prediction value for the specific reaction rate in five batch paper/yeast extract fermentation with A21 inoculum.

Table 13-9. Values of the parameters a , b , and c fitted by least squares analysis for La Sal del Rey inoculum A21.

Parameter constant	Value
Holdup (g liquid/g VS cake)	2.0
Moisture (g liquid/ g solid feed)	0.06
Selectivity (g Aceq/g VS digested)	0.31
F1–F4 solid concentration (g VS/L)	169, 214, 214, 214
F1–F4 liquid volume (L)	0.48, 0.28, 0.28, 0.28
ϕ (g total acid/g Aceq)	0.77
e (g Aceq/(g VS·d))	0.0074
f (dimensionless)	1.000
g (L/g total acid) ^{1/h}	0.0010
h (dimensionless)	2.166

Table 13-9 lists the system-specific variables required by the CPDM prediction. Figure 13-5 shows the CPDM “map” for La Sal del Rey inoculum A21 in a 90 wt% paper/10 wt% yeast extract countercurrent fermentation with the single-centrifuge procedure (Thanakoses, 2002) at a fermentation solid concentration of 169 g VS/L liquid. The “map” predicts a total acid concentration of 14.4 g/L and a conversion of

27.2% at an LRT of 30 day and VSLR of 12 g/(L·d). At a VSLR of 4 g/(L·d) and LRT of 10 days, total acid concentration is 13.2 g/L and conversion is 54.1%.

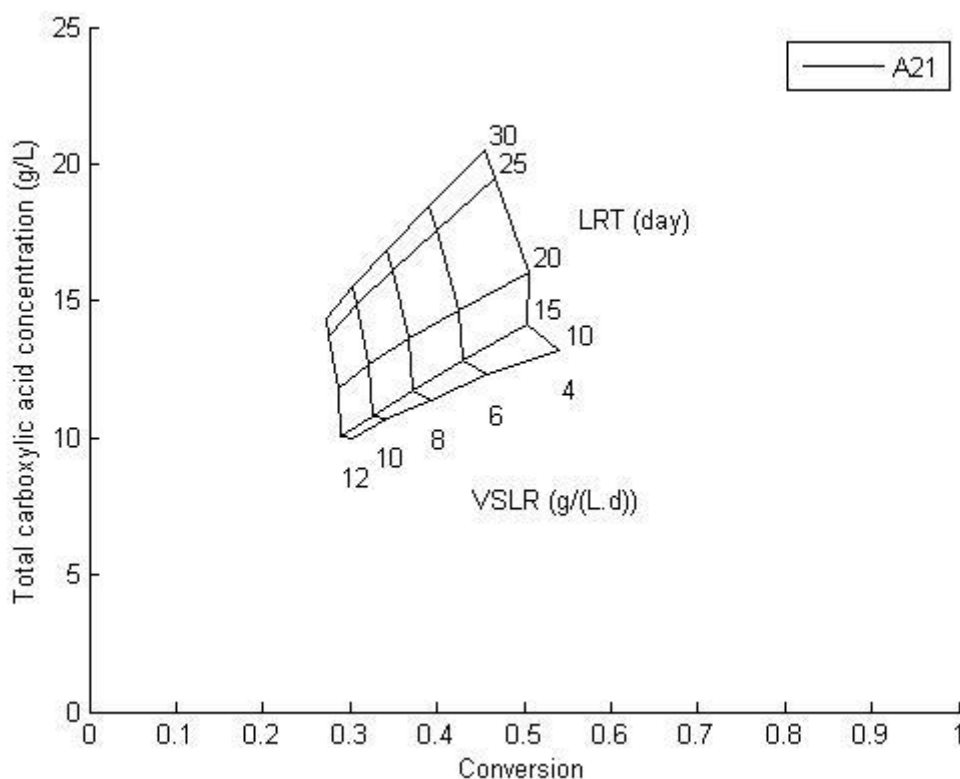


Figure 13-5. The CPDM “map” for 90 wt% paper/10 wt% yeast extract with A21 inoculum.

13.3.5.2 *Sample A23 from Site A – La Sal del Rey, TX*

From the salt lake, La Sal del Rey, in Southern Texas, a total of 26 samples were taken along three transects (T1, T2 and T3) at 20-meter intervals (Trip date: 6/23/2008). These were fermented in an initial screen (Forrest, 2010). Based on acid data, the best-performing bacterial community was A23 found on Transect 3 (T3) at 195 feet along the transect (26.53055 N, 98.06289 W). Batch experiments with 90 wt% paper /10 wt%

yeast extract were performed to obtain model parameters for CPDM method, as mentioned in Section 13.3.1. The inoculum for these fermentations was taken from the post-reactor material of the initial screening then preserved in a 20% glycerol solution. Calcium carbonate buffered the fermentations. Liquid samples from the fermentations were analyzed for carboxylic acids. The acids were converted to acetic acid equivalents (Aceq) using Equation 13-13. Figure 13-6 shows the Aceq concentrations for the five A23 batch experiments. The smooth lines are the predicted Aceq. Values of the fitted parameters a , b , and c for Equation 13-14 are presented in Table 13-10.

Table 13-10. Values of the parameters a , b , and c fitted by least squares analysis for La Sal del Rey inoculum A23.

Substrate Concentration (g/L)	a (g/L liquid)	b (g/(L liquid·d))	c (d ⁻¹)
20	1.710	0.253	0.0256
40	2.786	0.784	0.0426
70	1.488	0.801	0.0100
100	1.583	2.374	0.0488
100+	12.62	1.380	0.1004

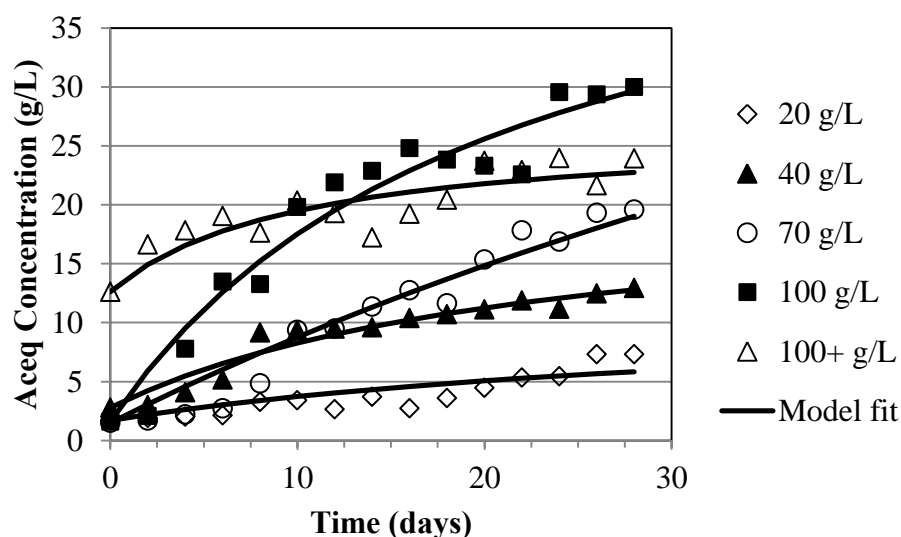


Figure 13-6. Aceq concentrations of A23 inoculated paper/yeast extract fermentation at 20, 40, 70, 100, and 100+ g substrate/L liquid with calcium carbonate buffer.

The reaction rate and the specific reaction rate for the batch fermentations were calculated using Equations 13-15 and 13-16. Conversion was calculated with the experimental acetic acid equivalents using Equation 13-13. Parameters e , f , g , and h presented in the predicted rate equation (Equation 13-17) were calculated by nonlinear regression (*Systat Sigmaplot 12.0*). Figure 13-7 compares the predicted specific rate with the experimental specific rate. The specific rate equation for La Sal del Rey inoculum A23 follows:

$$r_{pred} = \frac{0.0129 (1 - x)^{1.000}}{1 + 0.0010 \phi \cdot \text{Aceq}^{2.214}} \quad (13-25)$$

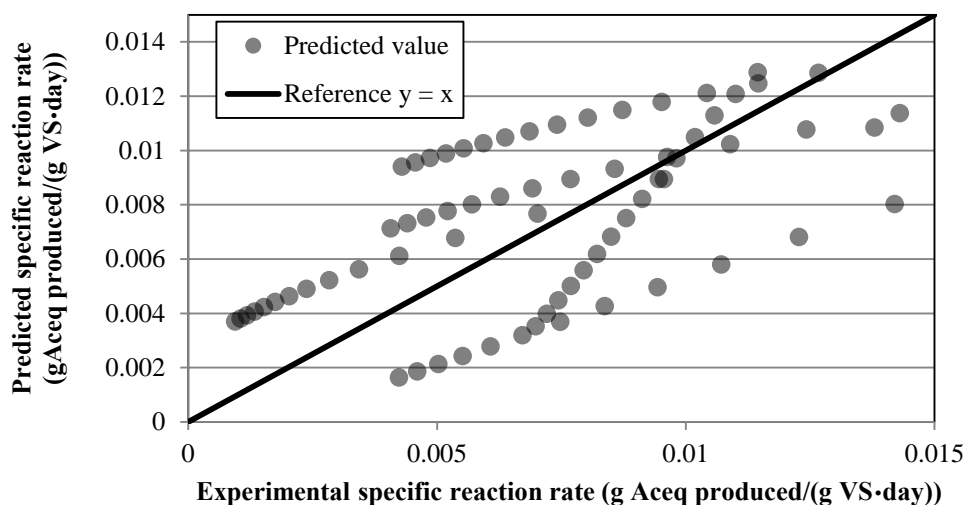


Figure 13-7. The experimental value and the CPDM prediction value for the specific reaction rate in five batch paper/yeast extract fermentation with A23 inoculum.

Table 13-11. Values of the parameters a , b , and c fitted by least squares analysis for La Sal del Rey inoculum A23.

Parameter constant	Value
Holdup (g liquid/g VS cake)	2.0
Moisture (g liquid/ g solid feed)	0.06
Selectivity (g Aceq/g VS digested)	0.50
F1–F4 solid concentration (g VS/L)	169, 214, 214, 214
F1–F4 liquid volume (L)	0.48, 0.28, 0.28, 0.28
ϕ (g total acid/g Aceq)	0.77
e (g Aceq/(g VS·d))	0.0129
f (dimensionless)	1.000
g (L/g total acid) ^{1/h}	0.0010
h (dimensionless)	2.214

Table 13-11 lists the system-specific variables required by the CPDM prediction. Figure 13-8 shows the CPDM “map” for La Sal del Rey inoculum A23 in a 90 wt% paper/10 wt% yeast extract countercurrent fermentation with the single-centrifuge procedure (Thanakoses, 2002) at a fermentation solid concentration of 169 g VS/L liquid. The “map” predicts a total acid concentration of 21.5 g/L and a conversion of 25.2% at an LRT of 30 day and VSLR of 12 g/(L·d). At a VSLR of 4 g/(L·d) and LRT of 10 days, total acid concentration is 17.1 g/L and conversion is 47.7%.

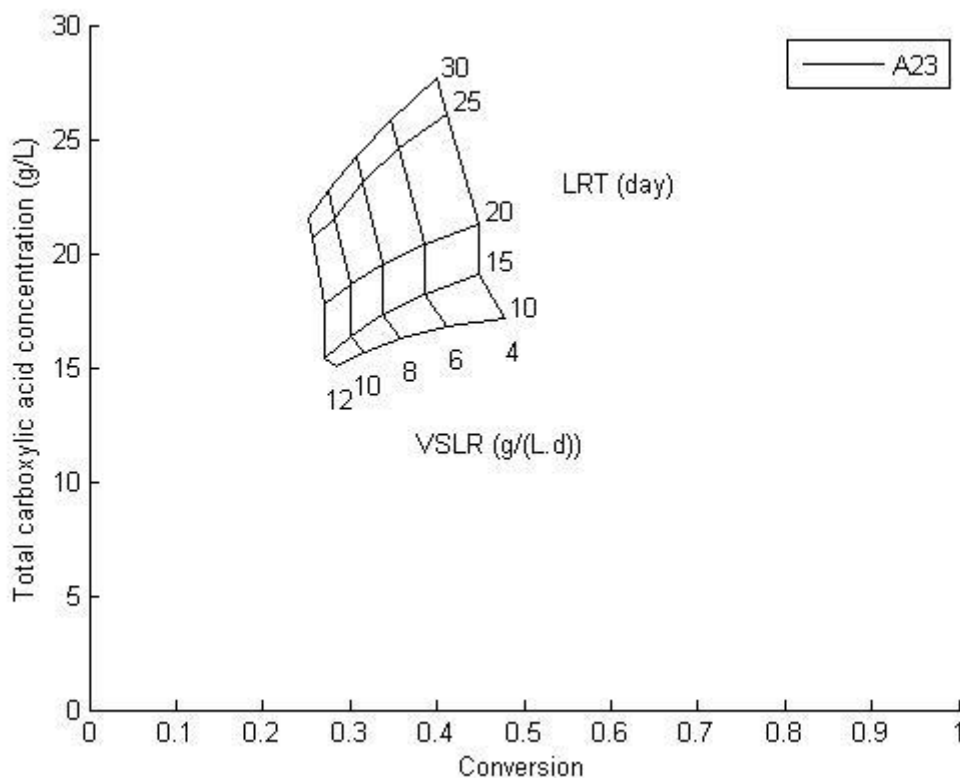


Figure 13-8. The CPDM “map” for 90 wt% paper/10 wt% yeast extract with A23 inoculum.

13.3.5.3 Sample A25 from Site A – La Sal del Rey, TX

Batch experiments with 90 wt% paper /10 wt% yeast extract were performed to obtain model parameters for CPDM method, as mentioned in Section 13.3.1. The inoculum for these fermentations was taken from the post-reactor material of the initial screening then preserved in a 20% glycerol solution. Calcium carbonate buffered the fermentations. Liquid samples from the fermentations were analyzed for carboxylic acids. The acids were converted to acetic acid equivalents (Aceq) using Equation 13-13. Figure 13-9 shows the Aceq concentrations for the five A25 batch experiments. The smooth lines are the predicted Aceq. Values of the fitted parameters a , b , and c for Equation 13-14 are presented in Table 13-12.

Table 13-12. Values of the parameters a , b , and c fitted by least squares analysis for La Sal del Rey inoculum A25.

Substrate Concentration (g/L)	a (g/L liquid)	b (g/(L liquid·d))	c (d ⁻¹)
20	1.468	0.4876	0.05150
40	1.582	0.5917	0.02010
70	0.9215	0.8679	0.04641
100	1.214	0.9707	0.01891
100+	10.73	0.5128	0.01375

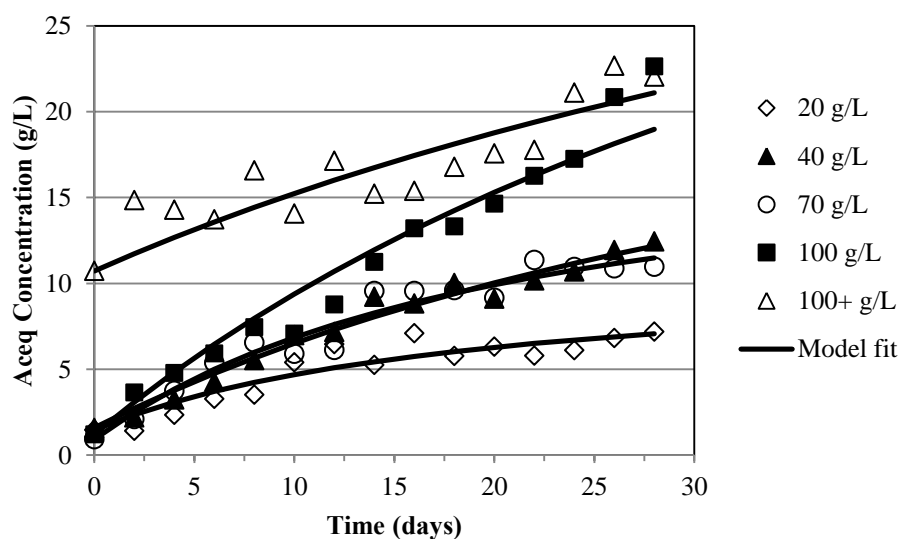


Figure 13-9. Acetate concentrations of A25 inoculated paper/yeast extract fermentation at 20, 40, 70, 100, and 100+ g substrate/L liquid with calcium carbonate buffer.

The reaction rate and the specific reaction rate for the batch fermentations were calculated using Equations 13-15 and 13-16. Conversion was calculated with the experimental acetic acid equivalents using Equation 13-13. Parameters e , f , g , and h presented in the predicted rate equation (Equation 13-17) were calculated by nonlinear regression (*Systat Sigmaplot 12.0*). Figure 13-10 compares the predicted specific rate

with the experimental specific rate. The specific rate equation for La Sal del Rey inoculum A25 follows:

$$r_{pred} = \frac{0.0157 (1 - x)^{1.199}}{1 + 0.0377 \phi \cdot A_{ceq}^{1.432}} \quad (13-26)$$

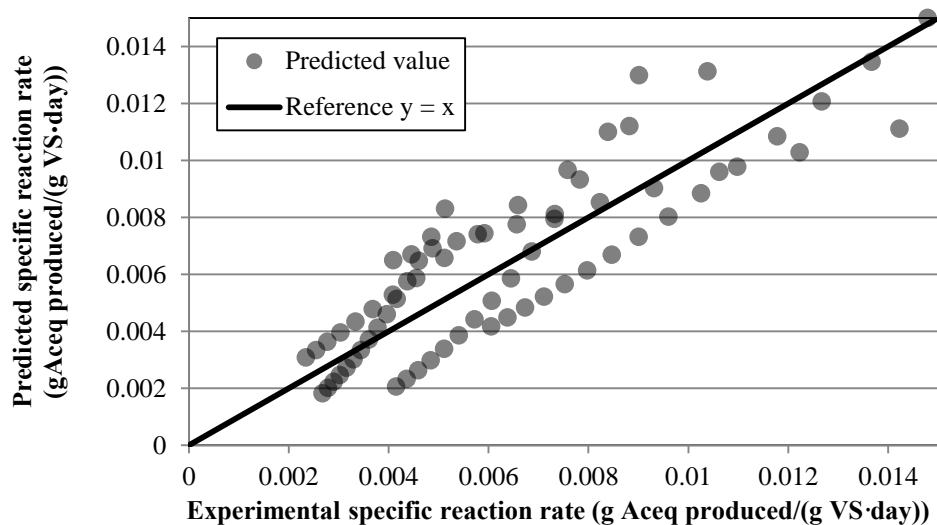


Figure 13-10. The experimental value and the CPDM prediction value for the specific reaction rate in five batch paper/yeast extract fermentation with A25 inoculum.

Table 13-13. Values of the parameters a , b , and c fitted by least squares analysis for La Sal del Rey inoculum A25.

Parameter constant	Value
Holdup (g liquid/g VS cake)	2.0
Moisture (g liquid/ g solid feed)	0.06
Selectivity (g Aceq/g VS digested)	0.42
F1–F4 solid concentration (g VS/L)	169, 214, 214, 214
F1–F4 liquid volume (L)	0.48, 0.28, 0.28, 0.28
ϕ (g total acid/g Aceq)	0.72
e (g Aceq/(g VS·d))	0.016
f (dimensionless)	1.199
g (L/g total acid) ^{1/h}	0.038
h (dimensionless)	1.432

Table 13-14 lists the system-specific variables required by the CPDM prediction. Figure 13-11 shows the CPDM “map” for La Sal del Rey inoculum A25 in a 90 wt% paper/10 wt% yeast extract countercurrent fermentation with the single-centrifuge procedure (Thanakoses, 2002) at a fermentation solid concentration of 169 g VS/L liquid. The “map” predicts a total acid concentration of 18.2 g/L and a conversion of 26.5% at an LRT of 30 day and VSLR of 12 g/(L·d). At a VSLR of 4 g/(L·d) and LRT of 10 days, total acid concentration is 14.3 g/L and conversion is 55.9%.

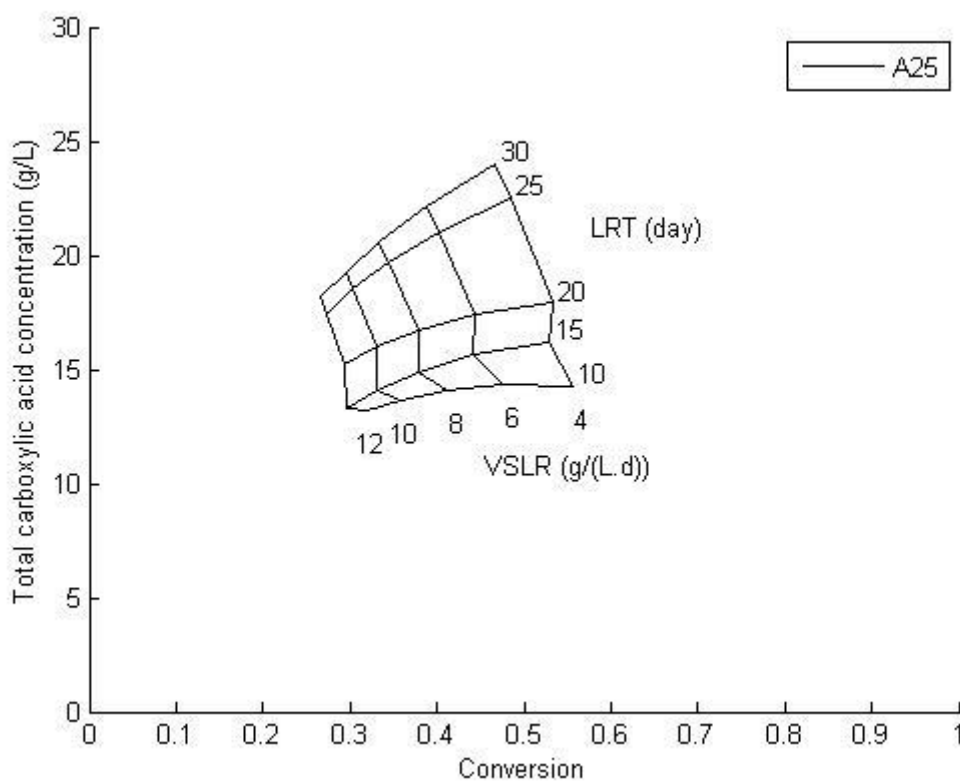


Figure 13-11. The CPDM “map” for 90 wt% paper/10 wt% yeast extract with A25 inoculum.

13.3.5.4 Sample G21 from Site G – Roswell-Carlsbad, NM

Batch experiments with 90 wt% paper /10 wt% yeast extract were performed to obtain model parameters for CPDM method, as mentioned in Section 13.3.1. The inoculum for these fermentations was taken from the post-reactor material of the initial screening then preserved in a 20% glycerol solution. Calcium carbonate buffered the fermentations. Liquid samples from the fermentations were analyzed for carboxylic acids. The acids were converted to acetic acid equivalents (Aceq) using Equation 13-13. Figure 13-12 shows the Aceq concentrations for the five G21 batch experiments. The smooth lines are the predicted Aceq. Values of the fitted parameters a , b , and c for Equation 13-14 are presented in Table 13-14.

Table 13-14. Values of the parameters a , b , and c fitted by least squares analysis for Roswell-Carlsbad, NM inoculum G21.

Substrate Concentration (g/L)	a (g/L liquid)	b (g/(L liquid·d))	C (d ⁻¹)
20	1.461	0.2635	0.0166
40	1.625	0.5422	0.0165
70	0.6419	2.183	0.0503
100	1.466	1.651	0.0500
100+	18.09	0.3629	0.0100

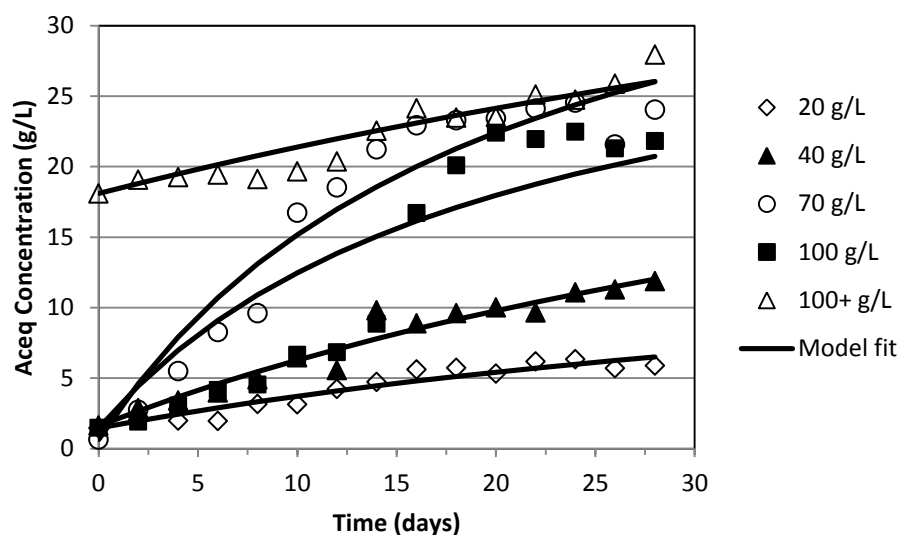


Figure 13-12. Aceq concentrations of G21 inoculated paper/yeast extract fermentation at 20, 40, 70, 100, and 100+ g substrate/L liquid with calcium carbonate buffer.

The reaction rate and the specific reaction rate for the batch fermentations were calculated using Equations 13-15 and 13-16. Conversion was calculated with the experimental acetic acid equivalents using Equation 13-13. Parameters e , f , g , and h presented in the predicted rate equation (Equation 13-17) were calculated by nonlinear regression (*Systat Sigmaplot 12.0*). Figure 13-13 compares the predicted specific rate with the experimental specific rate. The specific rate equation for Roswell-Carlsbad, NM inoculum G21 follows:

$$r_{pred} = \frac{0.0152 (1-x)^{1.000}}{1 + 0.0010 \phi \cdot Aceq^{2.506}} \quad (13-27)$$

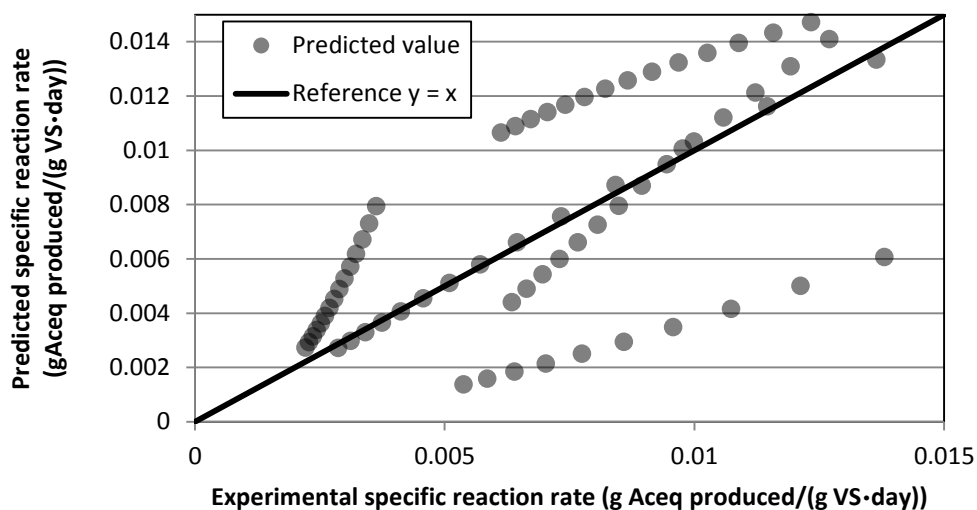


Figure 13-13. The experimental value and the CPDM prediction value for the specific reaction rate in five batch paper/yeast extract fermentation with G21 inoculum.

Table 13-15. Values of the parameters a , b , and c fitted by least squares analysis for Roswell-Carlsbad, NM inoculum G21.

Parameter constant	Value
Holdup (g liquid/g VS cake)	2.0
Moisture (g liquid/ g solid feed)	0.06
Selectivity (g Aceq/g VS digested)	0.47
F1–F4 solid concentration (g VS/L)	169, 214, 214, 214
F1–F4 liquid volume (L)	0.48, 0.28, 0.28, 0.28
ϕ (g total acid/g Aceq)	0.76
e (g Aceq/(g VS·d))	0.0152
f (dimensionless)	1.000
g (L/g total acid) ^{1/h}	0.0010
h (dimensionless)	2.506

Table 13-15 lists the system-specific variables required by the CPDM prediction. Figure 13-14 shows the CPDM “map” for Roswell-Carlsbad, NM inoculum G21 in a 90 wt% paper/10 wt% yeast extract countercurrent fermentation with the single-centrifuge procedure (Thanakoses, 2002) at a fermentation solid concentration of 169 g VS/L liquid. The “map” predicts a total acid concentration of 20.5g/L and a conversion of

25.9% at an LRT of 30 day and VSLR of 12 g/(L·d). At a VSLR of 4 g/(L·d) and LRT of 10 days, total acid concentration is 16.9 g/L and conversion is 49.4%.

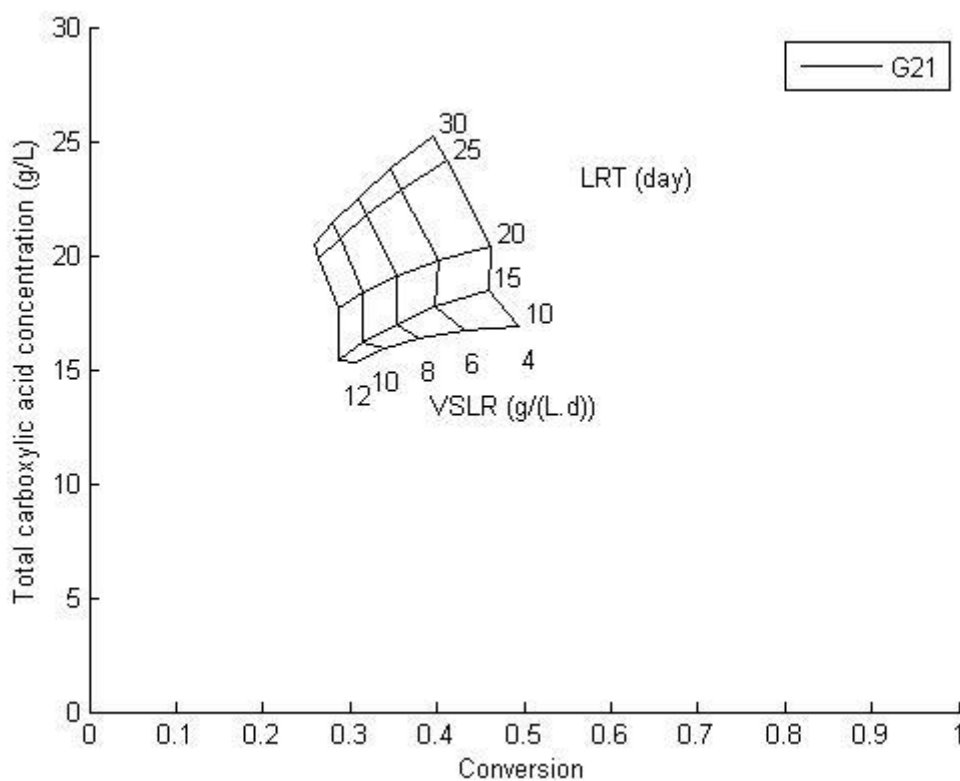


Figure 13-14. The CPDM “map” for 90 wt% paper/10 wt% yeast extract with G21 inoculum.

13.3.5.5 *Sample G38 from Site G – Roswell-Carlsbad, NM*

Batch experiments with 90 wt% paper /10 wt% yeast extract were performed to obtain model parameters for CPDM method, as mentioned in Section 13.3.1. The inoculum for these fermentations was taken from the post-reactor material of the initial screening then preserved in a 20% glycerol solution. Calcium carbonate buffered the fermentations. Liquid samples from the fermentations were analyzed for carboxylic

acids. The acids were converted to acetic acid equivalents (Aceq) using Equation 13-13. Figure 13-15 shows the Aceq concentrations for the five G38 batch experiments. The smooth lines are the predicted Aceq. Values of the fitted parameters a , b , and c for Equation 13-14 are presented in Table 13-16.

Table 13-16. Values of the parameters a , b , and c fitted by least squares analysis for Roswell-Carlsbad, NM inoculum G38.

Substrate Concentration (g/L)	a (g/L liquid)	b (g/(L liquid·d))	C (d ⁻¹)
20	1.639	0.2079	0.0100
40	1.560	0.7524	0.0236
70	1.843	1.514	0.0468
100	1.659	2.173	0.0552
100+	15.31	0.3952	0.0197

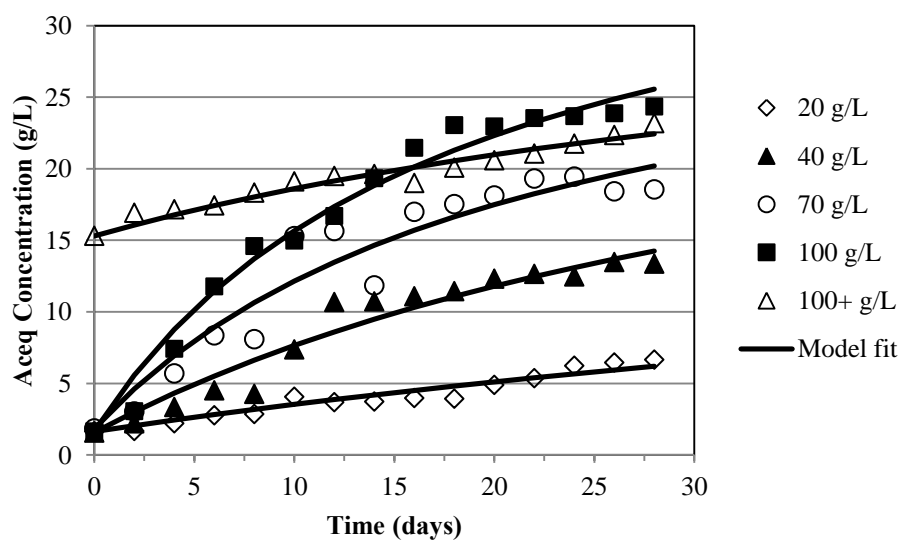


Figure 13-15. Aceq concentrations of G38 inoculated paper/yeast extract fermentation at 20, 40, 70, 100, and 100+ g substrate/L liquid with calcium carbonate buffer.

The reaction rate and the specific reaction rate for the batch fermentations were calculated using Equations 13-15 and 13-16. Conversion was calculated with the experimental acetic acid equivalents using Equation 13-18. Parameters e , f , g , and h presented in the predicted rate equation (Equation 13-17) were calculated by nonlinear regression (*Systat Sigmaplot 12.0*). Figure 13-16 compares the predicted specific rate with the experimental specific rate. The specific rate equation for La Sal del Rey inoculum A23 follows:

$$r_{pred} = \frac{0.0149 (1 - x)^{1.000}}{1 + 0.0029 \phi \cdot A_{ceq}^{2.214}} \quad (13-28)$$

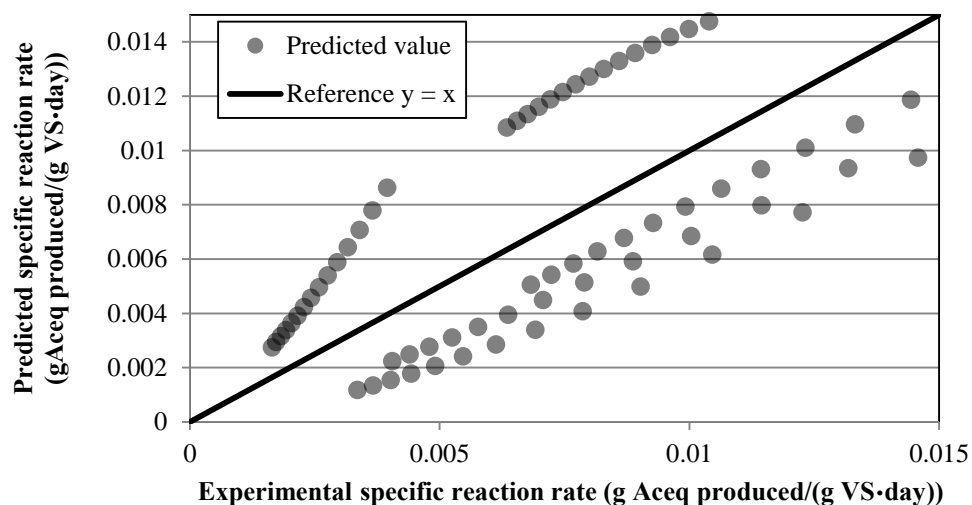


Figure 13-16. The experimental value and the CPDM prediction value for the specific reaction rate in five batch paper/yeast extract fermentation with G38 inoculum.

Table 13-17. Values of the parameters a , b , and c fitted by least squares analysis for Roswell-Carlsbad, NM inoculum G38.

Parameter constant	Value
Holdup (g liquid/g VS cake)	2.0
Moisture (g liquid/ g solid feed)	0.06
Selectivity (g Aceq/g VS digested)	0.57
F1-F4 solid concentration (g VS/L)	169, 214, 214, 214
F1-F4 liquid volume (L)	0.48, 0.28, 0.28, 0.28
ϕ (g total acid/g Aceq)	0.77
e (g Aceq/(g VS·d))	0.0149
f (dimensionless)	1.000
g (L/g total acid) ^{1/h}	0.0029
h (dimensionless)	2.214

Table 13-17 lists the system-specific variables required by the CPDM prediction. Figure 13-17 shows the CPDM “map” for Roswell-Carlsbad, NM inoculum G38 in a 90 wt% paper/10 wt% yeast extract countercurrent fermentation with the single-centrifuge procedure (Thanakoses, 2002) at a fermentation solid concentration of 169 g VS/L liquid. The “map” predicts a total acid concentration of 19.7 g/L and a conversion of 21.7% at an LRT of 30 day and VSLR of 12 g/(L·d). At a VSLR of 4 g/(L·d) and LRT of 10 days, total acid concentration is 16.7 g/L and conversion is 48.4%.

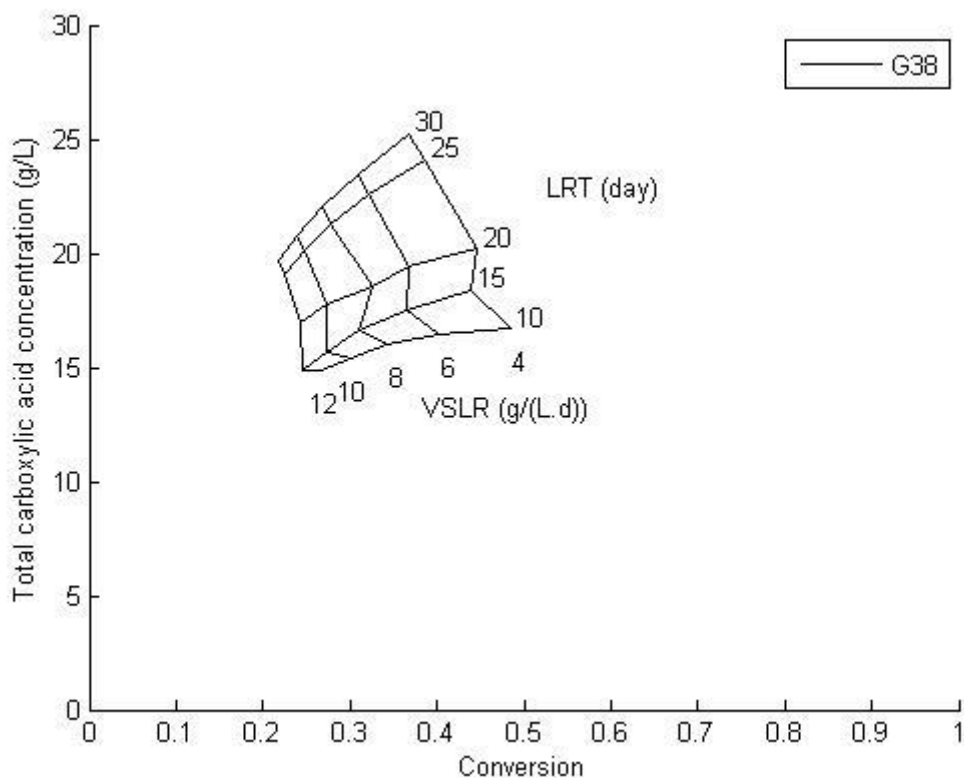


Figure 13-17. The CPDM “map” for 90 wt% paper/10 wt% yeast extract with G38 inoculum.

13.3.6 CPDM conclusions

The following conclusions can be made based on this section:

- 1) The CPDM method is a fast and easy tool to predict product concentrations and biomass conversions for simulated countercurrent trains.
- 2) All inocula (A21, A23, A25, G21, G38) are better at converting biomass and producing carboxylic acids than the traditional comparison Galveston inoculum (B01, (Forrest, 2010)). They show promise for future use in industrial-scale fermentations.

13.4 Continuous fermentations screenings

13.4.1 *Introduction*

The bacterial communities that had the highest conversion from the initial screen and generated the best-performing maps from CPDM fermentations were run in four-fermentor countercurrent fermentations. Countercurrent fermentations are the laboratory procedure that most closely predicts larger-scale fermentations. Four-staged countercurrent fermentation (Figure 13-2(c)) has a liquid and solid phase flowing in countercurrent directions in a series of four fermentation reactors. Multi-staged fermentations generate higher conversion and product concentration than batch fermentations, but require more time, space, and effort. As biomass digests, the biomass becomes less reactive and the production of carboxylic acid decreases. Acid inhibition is minimized in countercurrent fermentations because the most digested biomass contacts the lowest concentration of carboxylic salts and the least digested biomass contacts the highest concentration. See Section 2.1 for more information on continuous countercurrent fermentations.

13.4.2 *Inocula: site selection and sample collection*

Inocula samples were selected and collected from their respective soil sites (see section 13.2.1).

13.4.3 *Countercurrent fermentation conditions and procedures*

The fermentors for the countercurrent trains were 1-L polypropylene centrifuge bottles capped by a rubber stopper inserted with a glass tube (Ross, 1998). A rubber septum sealed the glass tube and allowed for gas sampling and release. Two lengths of ¼-in stainless steel pipe are inserted through the rubber stopper into the vessel which mixed the contents of the fermentor as it rotated in the rolling incubator (see Figure 2-2).

The countercurrent fermentation trains began in batch mode with a concentration of 100 g DS/L distilled water. Each fermentor was given substrate, nutrient source (yeast extract), inoculum, calcium carbonate (buffer), distilled water, and iodoform. Each fermentor was incubated in roller incubator at thermophilic conditions (55 °C) until

steady state was reached. Steady state was first estimated where acid concentrations were within 2 standard deviations and total fermentation mass was within 0.2 standard deviations for a time period of at least one LRT. The steady state was then more rigorously approximated by evaluating the yield, conversion, and selectivity using the *slope method* (Smith and Holtzapple, 2011b).

Solid/liquid transfers began after the first week of batch growth and occurred every 48 h. The feed consisted of shredded office copier paper (90%) supplemented with yeast extract (10%). The fermentors were removed from the incubator, the gas volume was collected, liquid samples were taken, the pH was measured, and mass transfers were performed. The fermentors were purged with nitrogen gas when opened to the atmosphere to maintain anaerobic conditions. Iodoform was added and the fermentors were returned to the incubator. The fermentations were buffered by adding 1.0 g calcium carbonate to each fermentor every 48 h to neutralize carboxylic acids to control the pH range between 5.0 and 7.0. The pH was monitored during the entire fermentation to ensure adequate buffer addition.

13.4.4 *Fermentation performance*

13.4.4.1 *Analytical methods*

Analyzing carboxylic acid concentration, biogas volume and composition, moisture and ash content are previously recorded (see Section 13.2.3).

13.4.4.2 *Measuring performance: definition of terms*

The performance variables were calculated as follows:

$$\begin{aligned}
 \text{Conversion } (x) &\equiv \frac{\text{NADS}_{\text{feed}} - \text{NADS}_{\text{exit}}}{\text{NAVS}_{\text{feed}}} \\
 &= \frac{\text{NAVS}_{\text{feed}} + \text{Ash}_{\text{feed}} - \text{NAVS}_{\text{exit}} - \text{Ash}_{\text{exit}}}{\text{NAVS}_{\text{feed}}} \quad (13-29) \\
 &= \frac{\text{NAVS}_{\text{consumed}}}{\text{NAVS}_{\text{feed}}}
 \end{aligned}$$

$$\text{Exit yield } (Y_E) = \frac{\text{total acid output from solid and liquid stream}}{\text{NAVS}_{\text{feed}}} \quad (13-30)$$

$$\begin{aligned} \text{selectivity } (\sigma) &= \frac{\text{total acid produced}}{\text{NAVS}_{\text{feed}} - \text{NAVS}_{\text{exit}}} \\ &= \frac{\text{total acids produced}}{\text{NAVS digested}} = \frac{Y_E}{x} \end{aligned} \quad (13-31)$$

$$\text{acid productivity} = \frac{\text{total acids produced}}{\text{TLV} \cdot \text{time}} \quad (13-32)$$

where $\text{NADS}_{\text{feed}}$ is the non-acid dry solids fed, $\text{NADS}_{\text{exit}}$ is the non-acid dry solids removed from the fermentation, $\text{NAVS}_{\text{feed}}$ is the non-acid volatile solids fed, $\text{NAVS}_{\text{exit}}$ is the non-acid volatile solids removed from the fermentation, Ash_{feed} is the inert solids fed in biomass feed and buffer, and Ash_{exit} is the inert solids exiting in all solid and liquid streams. NADS includes the ash and volatile solid component of biomass. Ash is assumed to be conserved in the fermentation (Ash_{feed} equals Ash_{exit}), canceling Ash from Equation 13-29.

The total mass in the system was accounted for in a mass balance closure, described previously in Equation 13-5. The carboxylic acid concentrations can be converted to acetic acid equivalent (Aceq) (Equations 13-6, 13-7).

13.4.5 *Operating parameters*

The TLV, VSLR, and LRT are described by Equations 13-18 to 13-20. TLV in the fermentation train including free and interstitial liquid.

13.4.6 *Results and discussion*

Each fermentation train consisted of a four-stage countercurrent semi-continuous submerged-bed fermentation system. To compare the results of all trains, the LRT and VSLR operating parameters were normalized by explicitly controlling the liquid/solid mass transfer frequency (T), the NAVS feed rate, the liquid feed rate, and the amount of

cake retained in each fermentation reactor per transfer (Table 13-18). As shown in Table 13-18, all trains had similar LRT and VSLR, allowing the trains to be comparable.

For all five trains, the total carboxylic acid concentrations were summed to find the accumulated amount of total carboxylic acids exiting, NADS added, and NADS removed from their respective trains. The slopes of the steady-state regression lines provided the performance variables (Table 13-19).

Train H20 had the highest conversion (0.33 g VS digested/g VS fed) and productivity (0.54 g/(L·day)), but the lowest selectivity (0.36 g acid/g VS digested) (Table 13-19, Figure 13-19). The highest selectivity (0.82 g acid/g VS digested) was obtained from Train G08, which had the lowest conversion. The yields are fairly similar and do not vary by more than 2%.

During the steady-state period, all five trains had statistically similar acid concentrations (Figure 13-18, Table 13-19). Not only did the trains produce similar total concentrations of carboxylic acids, they also produced similar ratios of acid product (Table 13-19). Another measure of the production of higher molecular weight carboxylic acids (e.g., valeric, caproic, and heptanoic acid) is the Aceq-to-total-acid ratio. The Aceq-to-total-acid ratios were not statistically different (Table 13-19).

13.4.7 *Countercurrent fermentation conclusions*

The three countercurrent trains studied had similar yields and acid concentrations, but contrary to previous bioscreening trains studied, had different selectivities and conversions (Forrest, 2010). With respect to all the performance variables discussed, Trains G08 and H20 had the best performance.

Table 13-18. Operating parameters for countercurrent continuous Trains G08, H20, and K49.

Fermentation Train		G08	H20	K49
Controlled	Liquid and solid transfer frequency (<i>T</i>)	Every 48 h		
	NAVS feed rate (g NAVS/ <i>T</i>)	8.6	8.6	9.0
	Agitation	Y	Y	Y
	Liquid feed rate (mL/ <i>T</i>)	100	100	100
	Dry solids added (g/ <i>T</i>)	11.2	11	11.2
	Yeast extract added (g/ <i>T</i>)	0.4	0.4	0.4
	Urea added (g/ <i>T</i>)	2	2	2
	Calcium carbonate added (g/ <i>T</i>)	4	4	4
	Methane inhibitor (μ L/ <i>T</i> ·fermentor)	120	120	120
	Normalized	Volatile solid loading rate, VSLR (g NAVS/(L _{liq} ·d))	3.9	4.0
Liquid residence time, LRT (d)		36.9	34.3	33.7
Total liquid volume, TLV (L)		1.09	1.08	1.08
Non-acid volatile solid, NAVS, concentration (g NAVS/L _{liq})		127	140	141
Non-acid dry solid, NADS, concentration (g NADS/L _{liq})		196	222	220
Average pH (F1–F4)	5.8	5.8	5.9	

Table 13-19. Performance measures for fermentation Trains G08, H20, and K49. Values represent the mean of the steady-state values \pm CI (95% CI).

	G08	H20	K49
Total carboxylic acid concentration (g/L)	13.9 \pm 1.0	12.9 \pm 1.2	12.4 \pm 0.8
Acetic acid (wt %)	33.17 \pm 1.73	36.46 \pm 1.3	33.87 \pm 0.91
Propionic acid (wt %)	1.30 \pm 0.05	1.12 \pm 0.1	1.53 \pm 0.15
Butyric acid (wt %)	64.50 \pm 0.92	61.32 \pm 0.6	63.48 \pm 0.52
Valeric acid (wt %)	1.03 \pm 0.07	0.98 \pm 0.0	1.11 \pm 0.06
Caproic acid (wt %)	0.00 \pm 0.00	0.02 \pm 0.0	0.00 \pm 0.00
Heptanoic acid (wt %)	0.00 \pm 0.00	0.10 \pm 0.0	0.01 \pm 0.01
Aceq concentration (g/L)	20.4 \pm 1.5	19.3 \pm 1.7	18.1 \pm 1.6
Aceq/Acid ratio	1.47 \pm 0.01	1.45 \pm 0.01	1.46 \pm 0.01
Conversion, x (g NAVS digested/g NAVS fed)	0.124 \pm 0.011	0.328 \pm 0.014	0.173 \pm 0.009
Selectivity, σ (g acid produced/g NAVS consumed)	0.816 \pm 0.056	0.355 \pm 0.024	0.650 \pm 0.017
Exit yield, Y_E (g acid/g NAVS fed)	0.101 \pm 0.007	0.116 \pm 0.008	0.112 \pm 0.003
Productivity, P (g total acid/(L _{liq} ·d))	0.460 \pm 0.001	0.537 \pm 0.001	0.517 \pm 0.000
Mass balance closure (g mass in/g mass out)	0.934 \pm 0.028	0.941 \pm 0.023	0.983 \pm 0.015

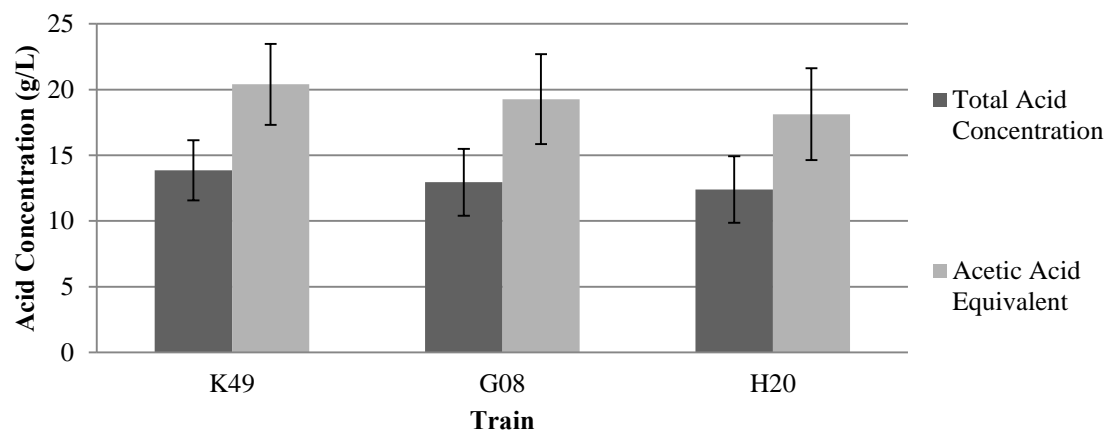


Figure 13-18. Total and Aceq acid concentrations of Trains G08, H20, and K49. Values represent the mean of the steady-state values \pm CI (95% CI).

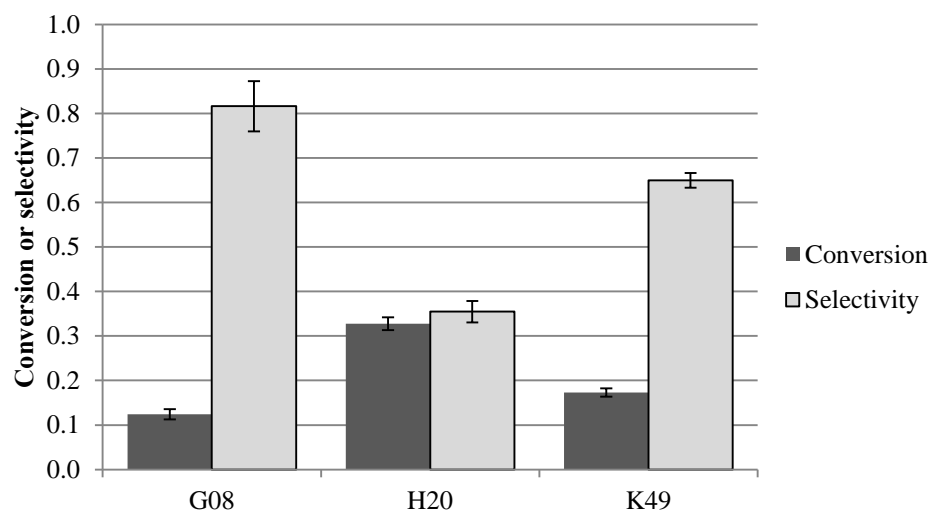


Figure 13-19. Conversion and selectivity comparisons of Trains G08, H20, and K49. Values represent the mean of the steady-state values \pm CI (95% CI).

13.5 Conclusions

The Hawaii sites sampled did not have initial batch fermentation conversions over 0.32 g VS digested/g VS fed. However, the best of sites (V04, V23) should be further investigated. When the initial screen fermentations were run at 55 °C and 40 °C, they had different performances, indicating that different microbial communities dominated at the different temperatures.

The CPDM method is a fast and easy tool to predict product concentrations and biomass conversions for simulated countercurrent trains. In CPDM, all inocula (A21, A23, A25, G21, G38) are better at converting biomass and producing carboxylic acids than the traditional comparison Galveston inoculum (B01, (Forrest, 2010)). They show promise for future use in industrial-scale fermentations.

The three countercurrent trains studied (G08, H20, K49) had similar yields and acid concentrations, but contrary to previous bioscreening trains studied, had different selectivities and conversions (Forrest, 2010). With respect to all the performance variables discussed, Trains G08 and H20 had the best performance.

14. INVESTIGATION OF MULTIPLE SUBSTRATES FOR VIABILITY IN THE MIXALCO™ PROCESS

The goal of this chapter was to run batch fermentations on multiple substrates to determine their potential yield in the MixAlco™ process. Where needed, the substrate was pretreated with hotlime (Appendix L). Where practical, fermentations were run on both pretreated and nonpretreated substrate at two temperatures, 40 °C and 55 °C, and performance was determined.

14.1 Introduction

A growing environmental problem is the accumulation of solid waste biomass. In the United States, approximately 250 million tons of municipal solid waste (MSW) were generated in 2008 (EPA, 2008). This waste contains about 65% biodegradable components, such as paper, food scraps, and yard waste (EPA, 2008). Additionally, the agricultural industry produces tons of agricultural residues each year during harvest. Currently, MSW is disposed in landfills, combusted for energy, or composted. Landfills produce the second largest amount (23% of all methane emissions) of anthropogenic methane in the United States (EPA, 2007).

Combusting MSW in incinerators reduces the volume of MSW while producing electricity; however, pollutants are emitted. The major pollutants of incineration (i.e., dioxins, acid gases, nitrogen oxides, heavy metals, and particulates) have been associated with adverse health effects (i.e., heart, respiratory, thyroid disease, cancer, and congenital abnormalities) (Allsopp et al., 2001). Alternatively, the carboxylate platform provides an environmentally friendly route to decrease MSW while providing a valuable biofuel source. Recycled MSW and biodegradable plastic bags (polylactic acid) will be studied as potential feedstocks in the carboxylate platform.

The carboxylate platform (Figure 1-1) converts waste biomass into usable chemicals and fuels, such as acetic acid and ethanol. It is a continuous process that uses solid biomass feedstocks, does not need sterile conditions, and has already reached the

demonstration level of development. It is considered a 'green' source of fuels because it does not contribute net carbon dioxide to the atmosphere. When burned, biomass-derived fuels release carbon dioxide that is later fixed via photosynthesis; thus, the carbon cycle is balanced.

In the MixAlco™ process, biomass is first pretreated and then fermented to produce carboxylic acids. In one version of the process, the acids are neutralized with a buffer, concentrated, thermally converted into ketones, and finally hydrogenated to mixed secondary alcohols (e.g., isopropanol). Other versions of the process produce mixed primary alcohols (e.g., ethanol), industrial chemicals (e.g., acetic acid, acetone), or fuels (e.g., gasoline, jet fuel).

The biomass is pretreated to make it more digestible by the microorganisms in the fermentation step. Many components of municipal solid waste and food scraps are easily digested and need little to no pretreatment. On the other hand, many agricultural wastes have complex structures that cannot easily be digested and must be pretreated.

In the MixAlco™ process, biomass feedstock is fermented with anaerobic bacteria, in a countercurrent fermentation train where the biomass is converted into carboxylate salts (e.g., calcium acetate). The bacteria are mixed cultures of naturally occurring microorganisms taken directly from terrestrial sources (e.g., compost heaps) or marine sources (e.g., tidal marshes). Because these organisms are found in nature, they are strong and hardy and do not need sterile conditions to thrive. Also, there is no need for genetic engineering, so the microorganisms can be safely released into the environment.

Fermentations can be operated as countercurrent fermentation trains (Figure 1-2), batch reactors, or single-stage CSTR reactors. The liquid extracted from the fermentation train is concentrated to collect the carboxylate salts. These salts may be thermally converted into ketone chemicals (e.g., acetone) and then hydrogenated to produce alcohols (e.g., isopropanol).

Compared to competing processes, the MixAlco™ process has several advantages: (1) it does not require sterile conditions; (2) does not need addition of

expensive enzymes; (3) can easily adapt to a wide variety of feedstock; and (4) has a wide range of products because the process can be modified to produce carboxylic acids, ketones, primary alcohols, secondary alcohols, esters, ethers, and aldehydes.

14.2 Materials and methods

All of the general materials and methods used are presented in this section. Anything not included here can be found in the specific substrate subsection.

14.2.1 *Fermentors*

Figure 2-2 shows the fermentor design. The fermentors are 1-L centrifuge bottle with a rubber stopper with a glass tube inserted into it. A rubber septum seals the glass tube and allows for gas sampling and release. Two lengths of ¼-in stainless steel pipe are inserted through the rubber stopper into the vessel and are used to mix the contents of the fermentor.

14.2.2 *Medium*

The liquid medium was deoxygenated water prepared by boiling distilled water, and after cooling to room temperature, 0.275 g/L cysteine hydrochloride and 0.275 g/L sodium sulfide were added to further reduce the oxygen content.

14.2.3 *Inoculum*

Mixed-microbial inoculum was collected from aquatic sediment in Galveston, TX. Sediment was removed from multiple 1.5-m-deep shoreline pits, and placed in airtight plastic bottles filled with deoxygenated water, 0.275 g/L cysteine hydrochloride and 0.275 g/L sodium sulfide.

14.2.4 *Methanogen inhibition*

Where specified, iodoform (CHI_3) was used as a methanogen inhibitor in the fermentors. An iodoform solution (20 g CHI_3 /L ethanol) was added individually to each fermentor every 48 h. Iodoform is light and air sensitive, so the solution was kept in amber-colored glass bottles wrapped in foil and stored at $-20\text{ }^\circ\text{C}$. Special care was taken to replace the cap immediately after use.

14.2.5 Performance: definition of terms

The performance variables were calculated as follows:

$$\text{Conversion } x \equiv \frac{\text{g NAVS}_{\text{feed}} - \text{g NAVS}_{\text{exit}}}{\text{g NAVS}_{\text{feed}}} \equiv \frac{\text{g NAVS}_{\text{consumed}}}{\text{g NAVS}_{\text{feed}}} \quad (14-1)$$

$$\text{Exit yield } (Y_E) \equiv \frac{\text{g total acid output from solid and liquid streams}}{\text{g NAVS}_{\text{feed}}} \quad (14-2)$$

$$\begin{aligned} \text{Selectivity } (\sigma) &\equiv \frac{\text{g total acid produced}}{\text{g NAVS}_{\text{feed}} - \text{g NAVS}_{\text{exit}}} \quad (14-3) \\ &\equiv \frac{\text{g total acid produced}}{\text{g NAVS digested}} = \frac{Y_E}{x} \end{aligned}$$

$$\text{Acid productivity } (P) \equiv \frac{\text{g total acids produced}}{\text{TLV} \cdot \text{d}} \quad (14-4)$$

where $\text{NAVS}_{\text{feed}}$ is the non-acid volatile solids fed, $\text{NAVS}_{\text{exit}}$ is the non-acid volatile solids removed from the fermentation, and TLV is the total liquid volume in the fermentation train including free and interstitial liquid.

14.3 Batch anaerobic fermentation of municipal solid waste-derived pulp

14.3.1 Objective

To determine the reactivity of pulp derived from municipal solid waste (MSW) in batch anaerobic fermentation.

14.3.2 Substrate

MSW-derived pulp was obtained from Tempico, Inc. (Hammond, LA) and fermented in batch mode without pretreatment. A control material of commercially available shredded copier paper was used. Chicken manure was used as the supplemental nutrient source and was obtained from the Poultry Science Department at Texas A&M University.

14.3.3 Results

Three fermentation sets were performed at 55 °C for 28 days:

- Control – shredded office copier paper (80%) supplemented with chicken manure (20%)
- Supplemented Tempico – MSW-derived pulp (80%) supplemented with chicken manure (20%)
- Tempico – MSW-derived pulp (100%)

In all cases, the biomass had a total concentration of 100 g/L. To determine the reproducibility of the batch experiments, each substrate was fermented in triplicate.

Each fermentor was then purged with nitrogen, capped, and placed into a roller incubator. Every two days, the fermentors were removed from the incubator, the gas volume was collected, the cap was removed, liquid samples were taken, and the pH was measured and adjusted to 7.0 with ammonium bicarbonate. Each fermentor was then purged with nitrogen to maintain anaerobic conditions, iodoform was added, the cap was replaced, and the fermentor was returned to the incubator.

The initial pH for all fermentations was approximately 7.0. During the fermentation, the pH varied from 6.3 to 8.4. The gas produced was analyzed regularly, and no methane was detected in any fermentor.

For all three experimental conditions, Figure 14-1 shows the total carboxylic acid concentrations with respect to time. Table 14-1 shows the results from the fermentations, including the final carboxylic acid concentration, the acid profile, and performance data.

Table 14-2 compares the final acid concentration data of this experiment to previous substrate experiments using the following metric: *substrate-to-control final acid concentration ratio*. Using the final (28-day) acid concentration as a measure of digestibility, this metric is the ratio of the substrate to the control. It allows a meaningful comparison between different substrates by reporting the ratio of each substrate to its respective control, which decreases inherent fluctuations between experiments.

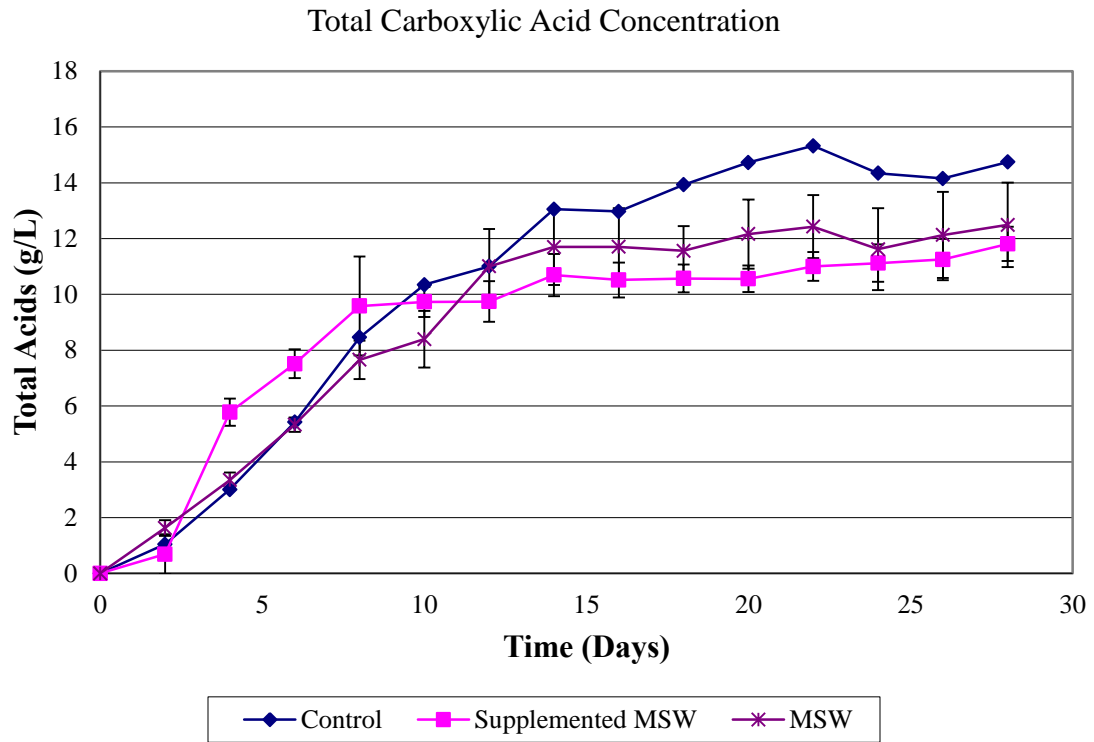


Figure 14-1. Total carboxylic acid concentrations for the MSW-derived pulp and control fermentations. Error bars represent standard errors.

Table 14-1. Performance results for MSW-derived pulp and control fermentations. Values represent averaged values of triplicates \pm standard deviation.

	MSW– Derived Pulp	Supplemented MSW Derived Pulp	Control (Copier Paper)*
Total carboxylic acid conc. (g/L)	13.0 \pm 2.62	12.6 \pm 1.06	15.2
Acetic acid (wt %)	88.2 \pm 0.76	86.9 \pm 0.84	83.3
Propionic acid (wt %)	3.82 \pm 0.38	4.86 \pm 1.10	3.85
Butyric acid (wt %)	5.24 \pm 1.25	5.96 \pm 0.37	14.6
Valeric acid (wt %)	1.99 \pm 0.43	1.76 \pm 0.32	0.41
Caproic acid (wt %)	0	0	0
Heptanoic acid (wt %)	0	0	0.58
Conversion (g VS digested/g VS fed)	0.40 \pm 0.05	0.40 \pm 0.05	0.46
Selectivity (g total acid/g VS digested)	0.33 \pm 0.03	0.36 \pm 0.02	0.36
Yield (g total acid/g VS fed)	0.13 \pm 0.03	0.14 \pm 0.01	0.17
Productivity (g total acid/ L liquid/day)	0.46 \pm 0.94	0.45 \pm 0.04	0.54

*No statistics available because two of the triplicate fermentors burst.

Table 14-2. Substrate-to-control final acid concentration ratio of MSW-derived pulp and other substrates (Forrest et al., 2010b).

Experiment Number	Substrate	Final Acid Conc. (g/L)	Substrate- to- Control Ratio
1	Control	24.02	1.00
	Aloe vera	23.8	0.99
2	Control	16.4	1.00
	Pineapple trash	17.2	1.05
	Water hyacinths	12.03	0.73
3	Control	15.23	1.00
	Tempico	13	0.85
	Supplemented tempico	12.6	0.83

14.3.4 *Conclusions*

The MSW-derived pulp with and without supplementation attained a lower total carboxylic acid concentration than the control. However, the MSW-derived pulp with and without supplementation achieved similar total carboxylic acid concentrations, which indicates that MSW-derived pulp may not need additional nutrients, which could potentially save on feed costs.

With respect to performance data, the MSW-derived pulp with and without supplementation had similar selectivities as the control, but noticeably lower yields, productivities, and conversions. However, the MSW-derived pulp with and without supplementation performed similarly, again leading to the conclusion that MSW-derived pulp may not need additional nutrients.

MSW-derived pulp with and without supplementation has a lower substrate-to-control final acid concentration ratio than occurred with other substrates. Likely, this is caused by the presence of newspaper, which has high lignin content and is not very digestible. Pretreatment can overcome this, but it incurs additional cost.

Overall, MSW-derived pulp has potential to be a substrate for the MixAlco™ process, but more research is needed.

14.4 Batch anaerobic fermentation of SunChips® compostable bag

14.4.1 *Objective*

To determine the reactivity of SunChips® compostable bags in batch anaerobic fermentation.

14.4.2 *Substrates*

SunChips® compostable bags – which are composed primarily of biodegradable polylactic acid – were obtained from Frito Lay, Inc., (Dallas, TX) shredded into 1-cm by 8-cm pieces, and fermented in batch mode with and without pretreatment. The pretreatment method used was 1-h hot-lime pretreatment, where the shredded compostable bags were boiled in a lime solution (~ pH 11) for 1 h. The basic solution was then neutralized to a pH of 7 by bubbling carbon dioxide gas through the broth (see

Appendix L). Dried chicken manure was used as the supplemental nutrient source and obtained from Feather Crest Farms, Inc., (Bryan, TX).

14.4.3 *Fermentation procedure*

Four sets of triplicates were fermented at 55 °C or 40 °C for 28 days:

- **(NP-55)** Non-pretreated SunChips® compostable bags, 55 °C – SunChips® compostable bag (80%) supplemented with chicken manure (20%)
- **(P-55)** Pretreated SunChips® compostable bag, 55 °C – pretreated SunChips® compostable bag (80%) supplemented with chicken manure (20%)
- **(NP-40)** Non-pretreated SunChips® compostable bags, 40 °C – SunChips® compostable bag (80%) supplemented with chicken manure (20%)
- **(P-40)** Pretreated SunChips® compostable bag, 40 °C – pretreated SunChips® compostable bag (80%) supplemented with chicken manure (20%)

In all cases, the biomass had a total concentration of 100 g/L. To determine the reproducibility of the batch experiments, each condition was fermented in triplicate.

Each fermentor was then purged with nitrogen, capped, and placed into a roller incubator. Every two days, the fermentors were removed from the incubator, the gas volume was collected, the cap was removed, liquid samples were taken, and the pH was measured and buffered with calcium carbonate. Each fermentor was then purged with nitrogen to maintain anaerobic conditions, iodoform was added, the cap was replaced, and the fermentor was returned to the incubator.

The initial pH for all fermentations was approximately 7.0. During the fermentation, the pH varied from to 6.3 to 7.9. The product gas was analyzed regularly, and no methane was detected in any fermentor.

14.4.4 *Results*

For all four experimental conditions, Figures 14-2 and 14-3 show the total carboxylic and acetic acid concentrations with respect to time. One interesting result –

which is unique to both non-pretreated and pretreated compostable bags at 55 °C – the acetic acid concentration increased until Day 12, and then decreased as the total acid concentration increased, thus shifting towards high-molecular-weight carboxylic acids. This indicates that independent of pretreatment, at 55 °C the bacteria favor converting SunChips® compostable bag into higher-molecular-weight carboxylic acids. In Figure 14-2, at 40 °C both pretreated and non-pretreated substrates have increasing acid concentrations at Day 28, which indicates the fermentation is not complete and that more acids would be produced if the fermentation had continued.

Tables 14-3 and 14-4 show the results from the fermentations, including final carboxylic acid concentrations, acid profiles, and performance data. In these batch fermentations, the product concentrations and conversions of the compostable bags are significantly less than other substrates (e.g., office paper, *Aloe vera* rinds, pineapple trash, water hyacinths, and municipal solid waste) that have been studied under identical conditions. The final carboxylic acid concentration, conversion, yield, and productivity of the pretreated compostable bags were slightly higher than the non-pretreated compostable bags, at their respective temperatures. However, the selectivities (g acid produced/g biomass digested) of the 40 °C fermentations were much higher than the 55 °C fermentations, because the 40 °C fermentations had higher yield but lower conversion than the 55 °C fermentation for both non-pretreated and pretreated biomass. However, for the pretreated compostable bags, the selectivities were similar to other feedstocks studied in our laboratory.

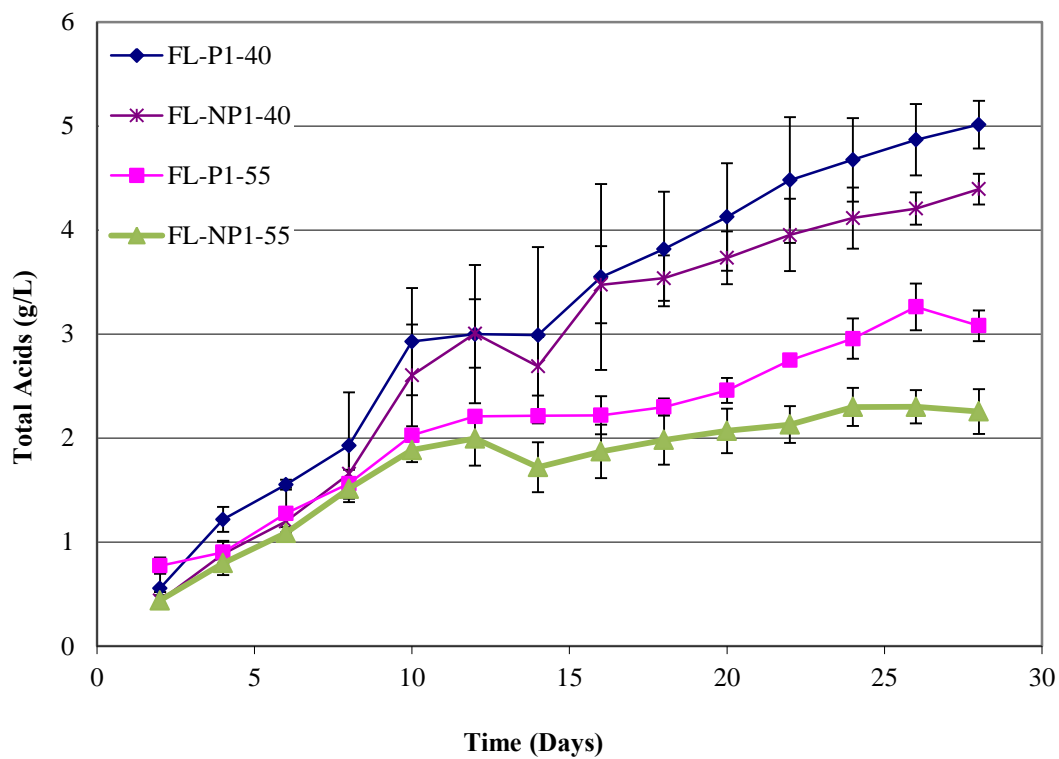


Figure 14-2. Total carboxylic acid concentrations for the SunChips® compostable bag fermentations. Error bars represent standard deviations of triplicate fermentations.

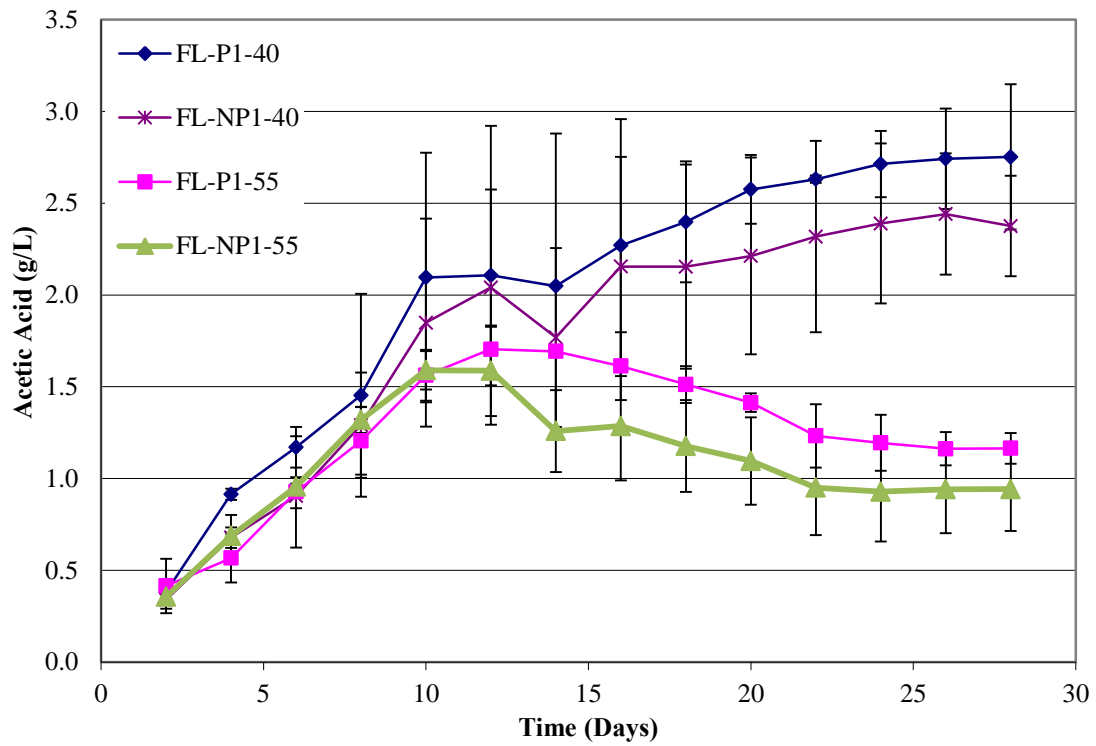


Figure 14-3. Acetic acid concentrations for the SunChips® compostable bag fermentations. Error bars represent the standard deviation of triplicate fermentations.

Table 14-3. Performance results for SunChips® compostable bag fermentations. Values represent averages of triplicate fermentations \pm standard deviation.

	Non-Pretreated SunChips® compostable bag		Pretreated SunChips® compostable bag	
	40° C	55° C	40° C	55° C
Total carboxylic acid conc. (g/L)	4.40 \pm 0.15	2.26 \pm 0.22	5.01 \pm 0.23	3.08 \pm 0.15
Acetic acid (wt %)	54.0 \pm 5.61	41.4 \pm 5.89	55.1 \pm 10.4	38.0 \pm 4.55
Propionic acid (wt %)	5.59 \pm 1.63	0.00 \pm 0.00	7.84 \pm 6.31	0.00 \pm 0.00
Butyric acid (wt %)	33.9 \pm 3.40	57.9 \pm 6.10	17.1 \pm 14.9	59.4 \pm 4.92
Valeric acid (wt %)	1.29 \pm 1.18	1.24 \pm 1.08	2.65 \pm 2.30	2.71 \pm 0.39
Caproic acid (wt %)	5.23 \pm 0.61	0.00 \pm 0.00	8.75 \pm 12.4	0.00 \pm 0.00
Heptanoic acid (wt %)	0.00 \pm 0.00	0.00 \pm 0.00	0.00 \pm 0.00	0.00 \pm 0.00
Conversion (g VS digested/g VS fed)	0.13 \pm 0.07	0.15 \pm 0.02	0.13 \pm 0.05	0.19 \pm 0.04
Selectivity (g total acid/g VS digested)	0.49 \pm 0.40	0.15 \pm 0.03	0.39 \pm 0.15	0.17 \pm 0.03
Yield (g total acid/g VS fed)	0.05 \pm 0.00	0.02 \pm 0.00	0.05 \pm 0.00	0.03 \pm 0.00
Productivity (g total acid/ L liquid/day)	0.16 \pm 0.01	0.08 \pm 0.01	0.18 \pm 0.01	0.11 \pm 0.01

Table 14-4. Performance comparison of SunChips® compostable bag and other substrates.

Substrate	Final Acid Conc. (g/L)	Conversion (g VS digested/g VS fed)	Selectivity (g total acid/g VS digested)	Yield (g total acid/g VS fed)	Productivity (g total acid/ L liquid/day)
Frito Lay-NP-40	4.4	11%	41%	5%	0.16
Frito Lay- NP-55	2.26	15%	15%	2%	0.08
Frito Lay- P-40	5.01	13%	42%	5%	0.18
Frito Lay- P-55	3.08	18%	17%	3%	0.11
Shredded office paper, 40 °C	15.2	58%	36%	17%	0.54
Shredded office paper, 55 °C	24	50%	62%	31%	1.1
<i>Aloe vera</i> rinds, 55 °C	25.5	59%	64%	38%	1.41
Pineapple Trash, 55 °C	17.2	52%	39%	20%	0.71
Water Hyacinths, 55 °C	12	45%	35%	16%	0.62
Recycled Municipal Solid Waste, 40 °C	13.0	40%	33%	13%	0.45

Figures 14-4 to 14-7 show photographs of the compostable bags before and after fermentation. Comparing Figures 14-4 and 14-5 (both 55 °C), it is clear that pretreatment aids the digestion process because the pretreated particles are smaller after fermentation. The difference is even more dramatic when comparing Figures 14-6 and 14-7 (both 40°C) where the non-pretreated compostable bags are barely digested.



Figure 14-4. Picture comparing the pre- and post-reactor fermentation biomass for non-pretreated compostable bags at 55 °C after 28 days.



Figure 14-5. Picture comparing the pre- and post-reactor fermentation biomass for pretreated compostable bags at 55 °C after 28 days.



Figure 14-6. Picture comparing the pre- and post-reactor fermentation biomass for non-pretreated compostable bags at 40 °C after 28 days.



Figure 14-7. Picture comparing the pre- and post-reactor fermentation biomass for pretreated compostable bags at 40 °C after 28 days.

14.4.5 Conclusions

Compared to other substrates studied in our laboratory, the pretreated and non-pretreated SunChips® compostable bags – which were fermented at both 40 °C and 55 °C for 28 days – attained a lower conversion and total carboxylic acid concentration. This could be explained as follows:

- There is a greater presence of undigestible material (e.g., aluminum) in the compostable bags.
- More aggressive pretreatment conditions may be needed.
- The microorganisms may not be adapted to digest polylactic acid, the dominant component of the compostable bags.

At both temperatures, the pretreated compostable bags achieved nearly twice the total carboxylic acid concentrations and slightly higher conversion, yield, and selectivity

compared to the non-pretreated compostable bag, suggesting that pretreatment significantly improves its digestibility.

With respect to performance data, the pretreated and non-pretreated compostable bag fermented at 40 °C had similar selectivities as other substrates, but lower yields, productivities, and conversions. If digestibility can be enhanced even further, it should be possible to achieve product concentrations similar to other feedstocks studied in our laboratory.

Overall, SunChips® compostable bag have the potential to be a substrate for the MixAlco™ process, but more research is needed in the following areas:

- Identify pretreatment conditions that enhance digestibility.
- Determine if other inoculum sources may have enhanced ability to digest polylactic acid.
- Perform fermentations in countercurrent mode.
- Blend the compostable bags with components of municipal solid waste, which is a more realistic industrial feedstock.

14.5 Batch anaerobic fermentation of oregano-supplemented shredded paper

14.5.1 Objective

A series of laboratory experiments and live animal tests using an oregano-based supplement decreased methane emissions in dairy cows by 40% and allowed them to produce more milk (Tekippe et al., 2011). Also, essential oils are recognized as having antimicrobial activity against many different types of microorganisms (Di Pasqua et al., 2006). The original goal for this chapter was to determine if oregano can be substituted as a natural and less toxic methane inhibitor for fermentations. Batch fermentations were run with varying amounts of substrate and oregano at 40 °C and 55 °C to determine if and at what proportion oregano can inhibit methane production in MixAlco™ fermentations at mesophilic and thermophilic conditions. However, for reasons unknown, methane was not produced in the control fermentors despite repeated attempts. Therefore, fermenting oregano-supplemented paper, this section will be comparing the

change of the carboxylic acid profile and fermentation performance as an adaptive mechanism of the cells in response to antimicrobial compounds.

14.5.2 *Substrates*

Oregano was obtained from the Texas A&M Community Garden, the oregano leaves were separated from the stems, and the leaves were homogenized in a blender and refrigerated until used. The oregano was fermented with commercially available shredded copier paper in batch mode without pretreatment. Chicken manure was used as the supplemental nutrient source for the microorganisms and obtained from the Poultry Science Department at Texas A&M University.

14.5.3 *Fermentation procedure*

Eight sets of triplicates were fermented at 55 °C or 40 °C for 28 days:

- **(P80-I-55C)** Shredded office paper (80%), no oregano (0%), supplemented with chicken manure (20%), with iodoform, 55 °C
- **(P80-55C)** Shredded office paper (80%), no oregano (0%), supplemented with chicken manure (20%), *no* iodoform, 55 °C
- **(P75-55C)** Shredded office paper (75%), oregano (5%), supplemented with chicken manure (20%), *no* iodoform, 55 °C
- **(P65-55C)** Shredded office paper (65%), oregano (15%), supplemented with chicken manure (20%), *no* iodoform, 55 °C
- **(P50-55C)** Shredded office paper (50%), oregano (30%), supplemented with chicken manure (20%), *no* iodoform, 55 °C
- **(P80-I-40C)** Shredded office paper (80%), no oregano (0%), supplemented with chicken manure (20%), with iodoform for methane inhibition, 40 °C
- **(P80-40C)** Shredded office paper (80%), no oregano (0%), supplemented with chicken manure (20%), *no* iodoform, 40 °C
- **(P50-40C)** Shredded office paper (50%), oregano (30%), supplemented with chicken manure (20%), *no* iodoform, 40 °C

In all cases, the biomass was loaded on a dry mass basis and had a total concentration of 100 g dry substrate/L liquid. To determine the reproducibility of the batch experiments, each condition was fermented in triplicate. Appendix M details the experimental design.

Each fermentor was purged with nitrogen, capped, and placed into a roller incubator. Every two days, the fermentors were removed from the incubator, the gas volume was collected, the cap was removed, liquid samples were taken, and the pH was measured and buffered with calcium carbonate. Each fermentor was then purged with nitrogen to maintain anaerobic conditions, iodoform was added, the cap was replaced, and the fermentor was returned to the incubator.

The initial pH for all fermentations was approximately 6.3. During the fermentation, the pH varied from 5.5 to 6.7. The product gas was analyzed regularly, and no methane was detected in any fermentor.

14.5.4 *Results*

For all eight experimental conditions, Figures 14-8 and 14-9 show the total carboxylic concentrations and gas production with respect to time. Table 14-5 shows all performance measures. Gas production was not highly correlated to acid concentrations; however, gas productions were slightly correlated with conversion.

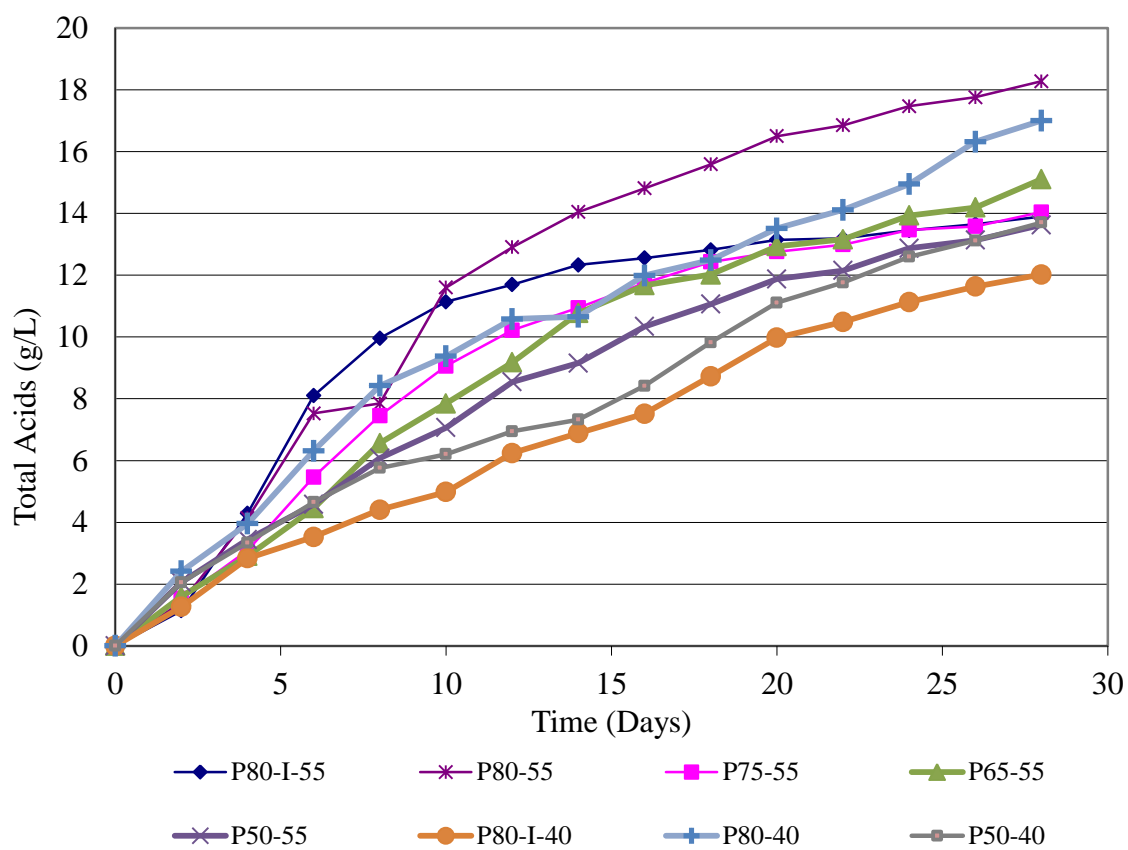


Figure 14-8. Total carboxylic acid concentrations for the oregano supplemented paper fermentations. Error bars were removed for clarity.

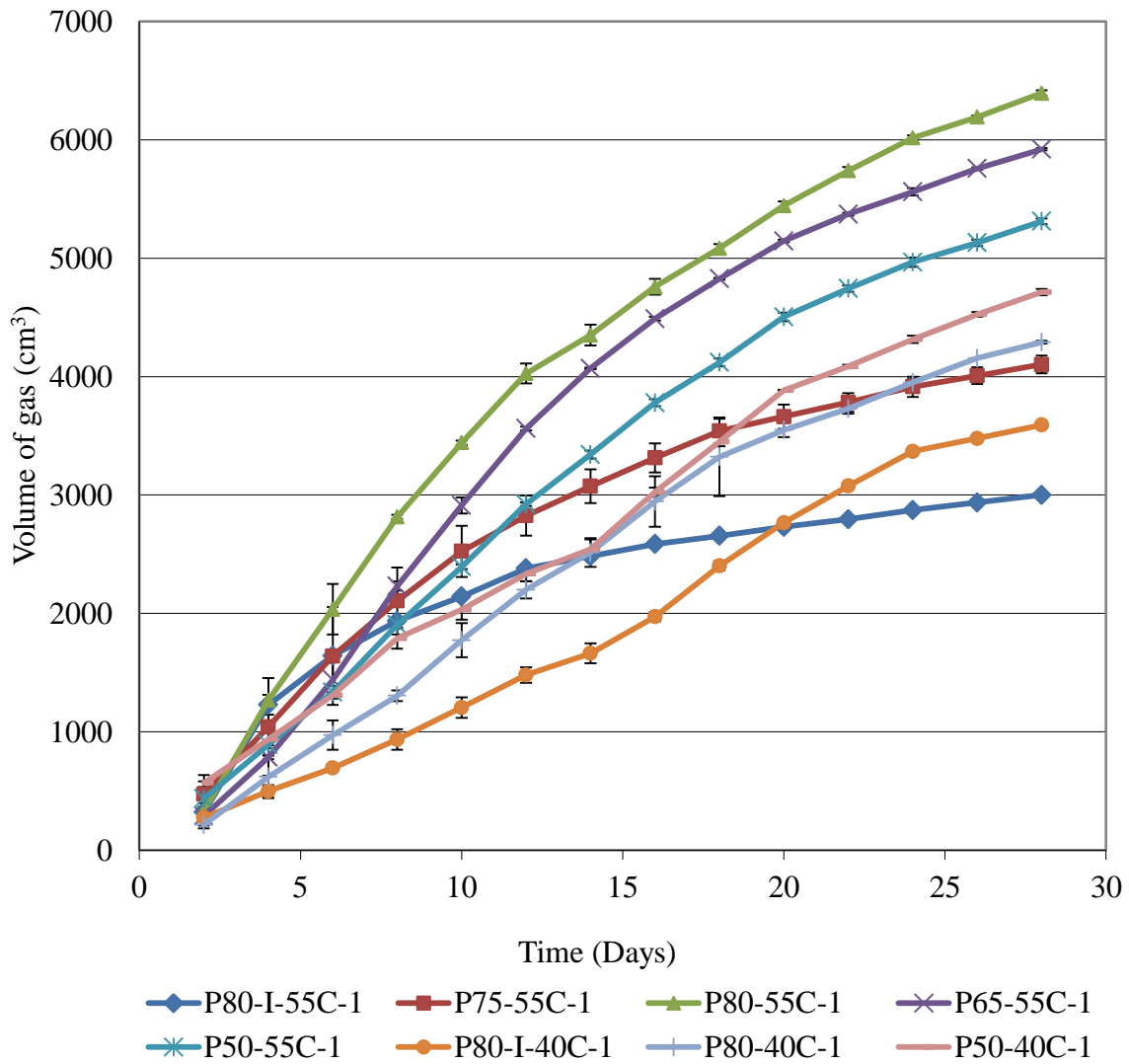


Figure 14-9. Volume of gas produced during the 28-d oregano supplemented paper fermentations. Error bars are standard error.

Table 14-5. Performance results of oregano supplemented paper \pm standard error.

	P80-I-55 *	P80-55	P75-55	P65-55	P50-55	P80-I-40	P80-40	P50-40
Temperature	55 °C	55 °C	55 °C	55 °C	55 °C	40 °C	40 °C	40 °C
Total carboxylic acid conc. (g/L)	13.90	18.27 \pm 2.07	14.04 \pm 1.22	15.10 \pm 0.61	13.63 \pm 0.12	12.02 \pm 2.45	17.00 \pm 2.50	13.70 \pm 1.49
Acetic acid (wt %)	31.6	49.5 \pm 10.2	40.9 \pm 6.8	40.9 \pm 5.7	44.8 \pm 0.21	50.0 \pm 14.1	41.2 \pm 10.5	36.5 \pm 2.7
Propionic acid (wt %)	1.3	2.1 \pm 0.2	2.2 \pm 0.2	2.3 \pm 0.3	2.5 \pm 0.0	15.5 \pm 0.6	12.9 \pm 3.5	7.2 \pm 1.9
Butyric acid (wt %)	67.1	48.2 \pm 10.6	56.9 \pm 7.0	56.8 \pm 5.6	51.3 \pm 0.0	23.6 \pm 4.9	25.7 \pm 12.3	34.0 \pm 6.7
Valeric acid (wt %)	0.0	0.1 \pm 0.2	0.0 \pm 0.0	0.0 \pm 0.0	0.0 \pm 0.0	4.3 \pm 5.2	3.5 \pm 1.8	3.3 \pm 0.6
Caproic acid (wt %)	0.0	0.0 \pm 0.0	0.0 \pm 0.0	0.3 \pm 0.4	1.4 \pm 0.3	6.6 \pm 3.7	12.5 \pm 1.2	18.2 \pm 3.9
Heptanoic acid (wt %)	0.0	0.0 \pm 0.0	0.0 \pm 0.0	0.0 \pm 0.0	0.0 \pm 0.0	0.0 \pm 0.0	4.2 \pm 2.0	0.9 \pm 0.3
Conversion (g VS digested/g VS fed)	0.45	0.53 \pm 0.07	0.35 \pm 0.01	0.30 \pm 0.14	0.34 \pm 0.03	0.26 \pm 0.05	0.31 \pm 0.11	0.25 \pm 0.10
Selectivity (g total acid/g VS digested)	0.29	0.30 \pm 0.10	0.46 \pm 0.05	0.39 \pm 0.06	0.44 \pm 0.06	0.52 \pm 0.04	0.62 \pm 0.11	0.61 \pm 0.17
Yield (g total acid/g VS fed)	0.13	0.16 \pm 0.03	0.16 \pm 0.01	0.16 \pm 0.00	0.15 \pm 0.01	0.13 \pm 0.02	0.18 \pm 0.03	0.15 \pm 0.01
Productivity (g total acid/ L liquid/day)	0.50	0.65 \pm 0.07	0.50 \pm 0.04	0.54 \pm 0.02	0.49 \pm 0.00	0.43 \pm 0.09	0.61 \pm 0.09	0.49 \pm 0.05

* No statistical analysis available because two fermentors of the set of triplicates burst in incubator.

Figure 14-10 graphs the acid concentrations of 28-d batch fermentations loaded with 80% shredded paper and 20% chicken manure on a dry mass, with iodoform (I) and without iodoform, at 40 °C and 55 °C. When comparing fermentations with the same substrate loadings, fermentors with iodoform addition had decreased acid concentration, conversion, selectivity, yield, and productivity (Table 14-5, Figure 14-10). Perhaps iodoform strongly inhibits methanogens and slightly inhibits the mixed culture of microorganisms found in carboxylate fermentations. At 55 °C, fermentations with iodoform addition and without iodoform had a higher rate of acid concentrations and tended to reach steady acid concentrations faster. At 40 °C, fermentations with iodoform addition and without iodoform and at 55 °C without iodoform have increasing acid concentrations at Day 28, which indicates the fermentation is not complete and that more acids would be produced if the fermentation had continued. Therefore, the optimum fermentation conditions are fermentations with no iodoform addition at thermophilic conditions (55 °C).

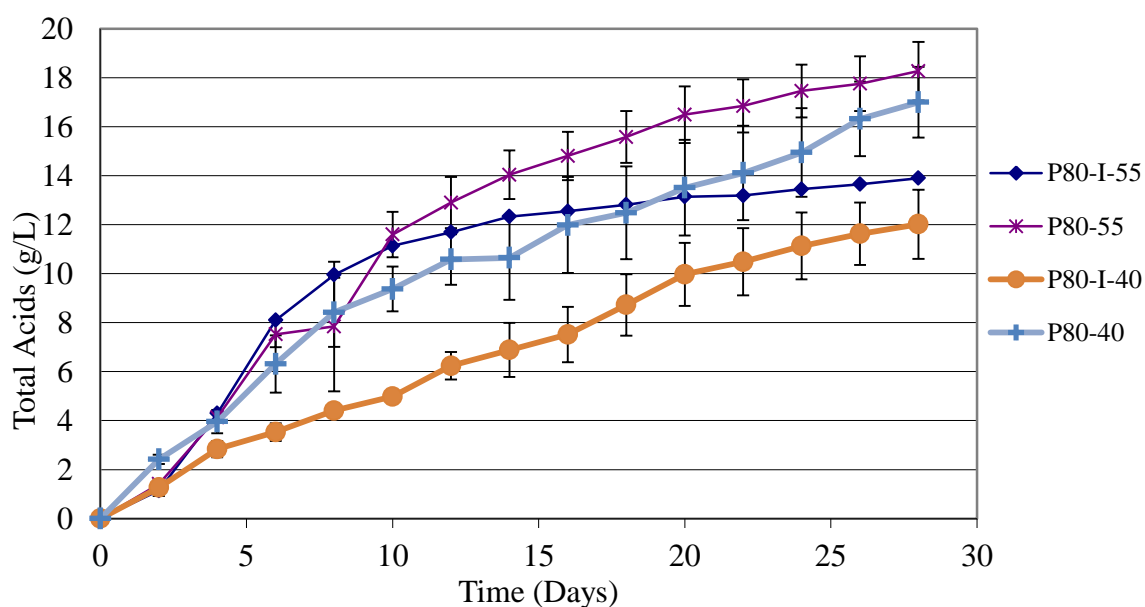


Figure 14-10. Total carboxylic acid concentrations for the paper fermentations without oregano supplementation comparing iodoform addition (I) and without iodoform at 40 and 55 °C. Error bars represent standard error of triplicate fermentations.

Figure 14-11 graphs the acid concentrations of 28-d batch fermentations loaded with 80% shredded paper (P80), 50% paper and 30% oregano (P50), on a dry mass without iodoform addition at 40 °C and 55 °C. Nutrient feed for all fermentations was 20% dry chicken manure. Compared to 40 °C, fermentations at 55 °C with and without oregano supplementation had higher conversion and amounts of butyric acid, similar yield and productivity, but lower selectivity.

At 55 °C, fermentations with oregano supplementation (P50-55) had decreased acid concentration, conversion, and productivity, but similar yield compared to fermentations with no oregano supplementation (P80-55). At 40 °C, fermentations that had a higher percentage of feed supplemented with oregano (P50-40) had lower acid concentrations and conversion, but similar selectivity and yield as fermentations with no oregano supplement (P80-40). Therefore, the optimum fermentation conditions are fermentations with or without oregano supplementation at thermophilic conditions (55 °C).

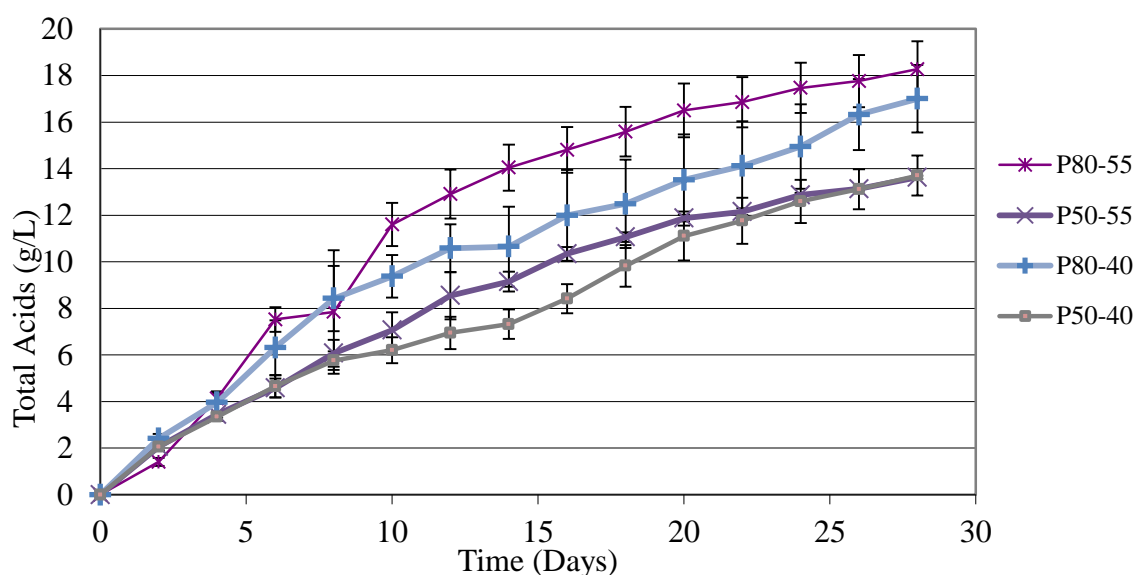


Figure 14-11. Total carboxylic acid concentrations for fermentations without iodoform fed with 80% paper and 0% oregano (P80) and 50% paper and 30% oregano on a dry mass basis, at 40 and 55 °C. Error bars represent the standard error of triplicate fermentations.

Figure 14-12 graphs the acid concentrations of 28-d batch fermentations loaded with 80% shredded paper (P80), 75% paper and 5% oregano (P75), 65% paper and 15% oregano (P65), 50% paper and 30% oregano (P50), on a dry mass without iodoform addition at 55 °C. Nutrient feed for all fermentations was 20% dry chicken manure. Fermentations that had a higher percentage of feed supplemented with oregano had decreased acid concentration, conversion, and productivity compared to fermentations with no oregano supplementation. However, oregano supplementation had similar yield, higher selectivity, and increased production of butyric acid than fermentations with no oregano. Perhaps thymol, the main essential oil in oregano, inhibits the mixed-culture of microorganisms found in carboxylate fermentations. Also, perhaps oregano is harder to digest than paper. Again, the optimum fermentation conditions are fermentations with no oregano supplementation at thermophilic conditions (55 °C).

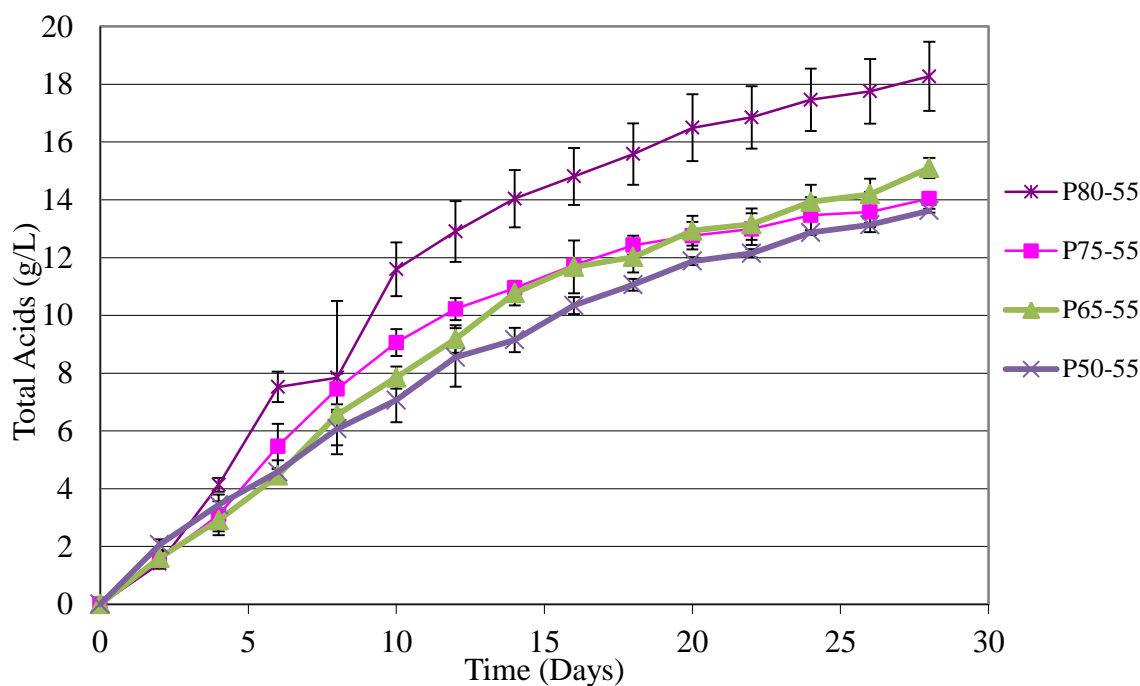


Figure 14-12. Total carboxylic acid concentrations for fermentations without iodoform fed with 80% paper and 0% oregano (P80), 75% paper and 5% oregano (P75), 65% paper and 15% oregano (P65), and 50% paper and 30% oregano on a dry mass basis, at 55 °C. Error bars are standard error.

14.5.5 *Conclusions*

Compared to paper, at both 40 °C and 55 °C, higher amounts of oregano supplementation attained a below-average acid concentration, conversion, and productivity compared to fermentations with no oregano supplementation. However, oregano supplementation had similar yield, higher selectivity, and increased production of butyric acid than fermentations with no oregano. Perhaps thymol, the main essential oil in oregano, inhibits the mixed-culture of microorganisms found in carboxylate fermentations. Also, oregano might not be a high-quality carbon source for carboxylate fermentations.

At both temperatures, the fermentations without iodoform addition achieved over 30% increase in the total carboxylic acid concentrations and higher conversion, yield, and selectivity compared to fermentations with iodoform addition, suggesting that iodoform significantly inhibits the fermentations. Fermentors with iodoform addition had decreased acid concentration, conversion, selectivity, yield, and productivity. Perhaps iodoform strongly inhibits methanogens and slightly inhibits the mixed culture of microorganisms found in carboxylate fermentations. Perhaps other methanogen inhibitors and the lowest effective iodoform dose should be investigated.

Compared to 40 °C, fermentations at 55 °C with and without oregano supplementation had higher conversion and amounts of butyric acid, similar yield and productivity, but lower selectivity. At 55 °C, fermentations with oregano supplementation had decreased acid concentration, conversion, and productivity, but similar yield compared to fermentations with no oregano supplementation. At 40 °C, fermentations that had a higher percentage of feed supplemented with oregano had lower acid concentrations and conversion, but similar selectivity and yield as fermentations with no oregano supplement.

Therefore, the optimum fermentation conditions are fermentations with or without oregano supplementation, without iodoform, at thermophilic conditions (55 °C). Overall, oregano-supplemented paper has the potential to be a substrate for the carboxylate platform, but more research is needed in the following areas:

- Determine if other inoculum sources may have enhanced ability to digest oregano and resist the antimicrobial effects of the essential oils.
- Blend oregano with components of municipal solid waste, which is a more realistic industrial feedstock.

14.6 Batch anaerobic fermentation of raw corn stover

14.6.1 Objective

To determine the reactivity of raw corn stover in batch anaerobic fermentation.

14.6.2 Substrates

Raw corn stover was obtained from Texas A&M AgriLife. It was harvested in 2010, baled, compressed, and wrapped in plastic to maintain constant moisture and to reduce contact with air. For laboratory use, it was milled into 1-cm pieces, and fermented in batch mode without pretreatment. Dried chicken manure was used as the supplemental nutrient source and obtained from Feather Crest Farms, Inc., in Bryan, TX.

14.6.3 Fermentation procedure

Unpretreated, or “raw,” corn was fermented in quadruplets at 40 °C for 28 days. The raw corn stover (80%) was supplemented with chicken manure (20%), on a dry mass basis.

The fermentation had an initial solids concentration of 100 g dry biomass/L and was buffered with calcium carbonate. To determine the reproducibility of the batch experiments, each condition was fermented in quadruplet, although duplicates or triplicates would be sufficient.

Each fermentor was then purged, capped, and placed into a roller incubator. Every two days, the fermentors were removed from the incubator, the gas volume was collected, the cap was removed, liquid samples were taken, and the pH was measured. Each fermentor was then purged with nitrogen to maintain anaerobic conditions, iodoform was added, the cap was replaced, and the fermentor was returned to the incubator.

The initial pH for all fermentations was approximately 6.3. During the fermentation, the pH varied from 6.3 to 5.6. No methane was detected in the product gas.

14.6.4 Results and conclusions

For all four fermentors, Figure 14-13 shows the total carboxylic acid concentrations with respect to time.

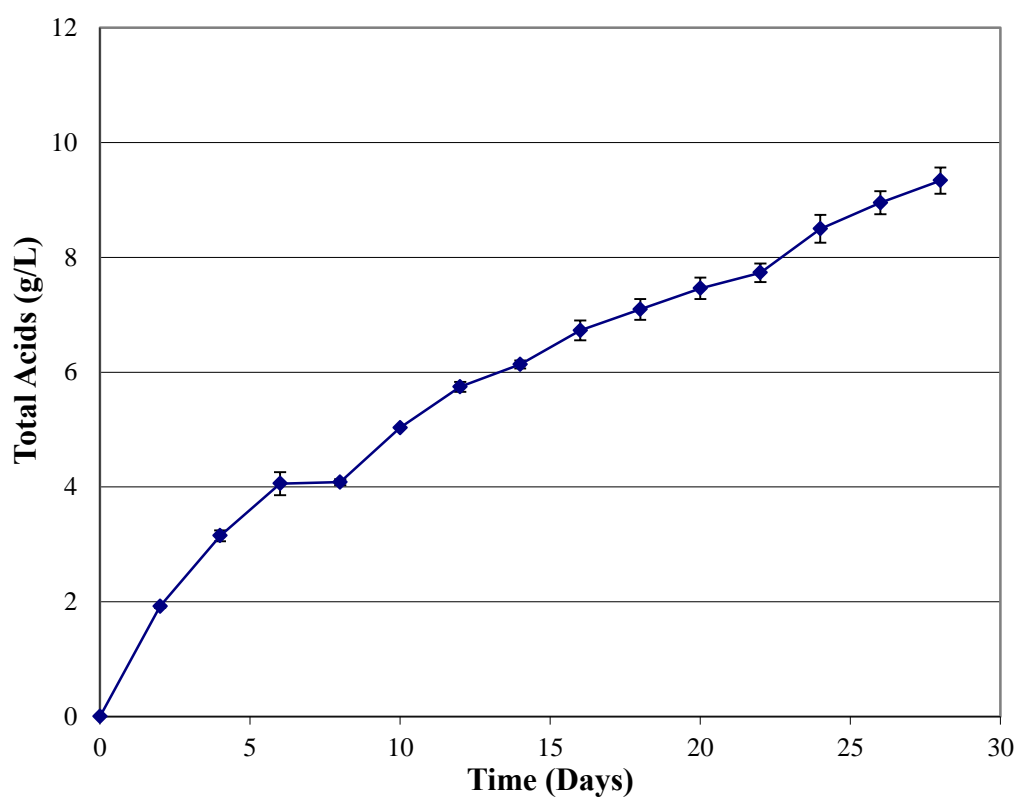


Figure 14-13. Total acid concentration of raw corn stover during a 28-d batch fermentation. Error bars represent the standard error of quadruplet fermentations.

Table 14-6. Performance data of raw corn stover for a 28-d batch fermentation. Values represent the average of quadruplets \pm standard deviation.

Performance	Raw corn stover
Total carboxylic acid conc. (g/L)	9.9 \pm 0.2
Acetic acid (wt %)	51.4 \pm 9.05
Propionic acid (wt %)	5.1 \pm 1.66
Butyric acid (wt %)	30.8 \pm 6.8
Valeric acid (wt %)	0.9 \pm 1.4
Caproic acid (wt %)	8.9 \pm 9.5
Heptanoic acid (wt %)	0
Conversion (g VS digested/g VS fed)	0.14 \pm 0.05
Selectivity (g total acid/g VS digested)	0.77 \pm 0.24
Yield (g total acid/g VS fed)	0.10 \pm 0.02
Productivity (g total acid/ L liquid/day)	0.34 \pm 0.03

Table 14-6 shows the results from the fermentations, including final carboxylic acid concentrations, acid profiles, and performance data. In these batch fermentations, the product concentrations and conversions of the raw corn stover are significantly less than most other substrates (e.g., office paper, *Aloe vera* rinds, pineapple trash, water hyacinths, and municipal solid waste) that have been studied under identical conditions (Table 14-4). Because of the poor performance of raw corn stover in batch fermentations, investigations should be conducted involving pretreatment of raw corn stover.

15. NUTRIENT MICROBIAL LOAD EFFECTS ON BATCH FERMENTATIONS

15.1 Introduction

In carboxylate fermentations, the mixed-microbial community is generally inoculated by sediment from saline, anaerobic environments. These microbial communities have proven to be fairly robust; however, the initial community could be outcompeted with continuous addition of inocula from the substrate or nutrient source. The goal of this study is to investigate how the bacterial community in manure affects carboxylate fermentations by studying the effects of different treatments of chicken manure, which is a nutrient source in batch fermentation. The effects of the microbial load in the nutrient source (chicken manure) were determined by running batch fermentations with dry, wet, sterilized, unsterilized, frozen, and nonfrozen chicken manure.

15.2 Materials and methods

15.2.1 *Fermentors*

The fermentor design was shown previously in Figure 2-2. The fermentor vessel is a 1-L centrifuge bottle with a rubber stopper with a glass tube inserted into it. A rubber septum seals the glass tube and allows for gas sampling and release. Two lengths of ¼-in stainless steel pipe are inserted through the rubber stopper into the vessel and are used to mix the contents of the fermentor.

15.2.2 *Medium*

The liquid medium was deoxygenated water prepared by boiling distilled water, and, after cooling to room temperature, 0.275 g/L cysteine hydrochloride and 0.275 g/L sodium sulfide were added to further reduce the oxygen content.

15.2.3 *Inoculum*

Mixed-microbial inoculum was collected from aquatic sediment in Galveston, TX. Sediment was removed from multiple 1.5-m-deep shoreline pits, and placed in airtight plastic bottles filled with deoxygenated water, 0.275 g/L cysteine hydrochloride, and 0.275 g/L sodium sulfide. This was done to minimize exposure of the microorganisms to oxygen.

15.2.4 *Methanogen inhibition*

Where specified, iodoform (CHI_3) was used as a methanogen inhibitor in the fermentors. An iodoform solution (20 g CHI_3 /L ethanol) was added individually to each fermentor every 48 h. Iodoform is light and air sensitive, so the solution was kept in amber-colored glass bottles wrapped in foil and stored at $-20\text{ }^\circ\text{C}$. Special care was taken to replace the cap immediately after use.

15.2.5 *Substrate*

Shredded recycled office paper was fermented in batch mode without pretreatment. Chicken manure was used as the supplemental nutrient source for the microorganisms and obtained from the Poultry Science Department at Texas A&M University.

15.2.6 *Fermentation procedure*

Eight manure conditions were tested in triplicate.

- **(NWU)** Non-frozen, wet, unsterilized chicken manure
- **(FWU)** Frozen, wet, unsterilized chicken manure
- **(NDU)** Non-frozen, dry, unsterilized chicken manure
- **(FDU)** Frozen, dry, unsterilized chicken manure
- **(NWS)** Non-frozen, wet, sterilized chicken manure
- **(FWS)** Frozen, wet, sterilized chicken manure

- **(NDS)** Non-frozen, dry, sterilized chicken manure
- **(FDS)** Frozen, dry, sterilized chicken manure

Table 15-1. Chicken manure conditions that were used as the nutrient source in batch carboxylate fermentations.

	Wet	Dry
Unsterilized	Non-frozen (NWU) Frozen (FWU)	Non-frozen(NDU) Frozen (FDU)
Sterilized	Non-frozen (NWS) Frozen (FWS)	Non-frozen(NDS) Frozen (FDS)

Table 15-1 summarizes the nomenclature for the chicken manure conditions. The wet chicken manure was fresh and never dried. The dried chicken manure was dried at 105 °C for 48 h in a forced-convection oven. The sterilized chicken manure was autoclaved with an in-house autoclave on wet cycle for 1 h. (*Note:* The sterilized chicken manure is believed to be “pasteurized,” not sterile, because the autoclave, cycle, and time length chosen were not verified to be sufficient to kill the large microbial load. In Section 16.7, autoclaved wet chicken manure was found to have microbial activity as well.) The unsterilized chicken manure was never autoclaved. The non-frozen chicken manure was never previously frozen. The frozen chicken manure, after drying and autoclaving, was previously frozen and thawed before fermenting.

Chicken manure was the nutrient source used at a ratio of 80 wt% paper and 20 wt% chicken manure (dry mass basis) in all fermentations. In all cases, the biomass had a total concentration of 100 g/L, on a dry mass basis. Initially, to each fermentor, 80 µL iodoform solution was added for methane inhibition, and 1.5 g of ammonium bicarbonate was added for pH control. All fermentations were incubated at mesophilic temperatures (40 °C).

Every 48 h, the fermentors were removed from the incubator, the gas volume was collected, the cap was removed, liquid acid samples were taken, and the pH was measured and adjusted to 7.0 with ammonium bicarbonate. Every 48 h, iodoform solution (20 g CHI₃/L 190-proof ethanol) was added to each fermentor throughout the fermentation to inhibit methane production (Ross, 1998). Each fermentor was then purged with nitrogen to maintain anaerobic conditions, the cap was replaced, and the fermentors were returned to the incubator.

Total gas volume was measured by liquid displacement. The pH of liquid broth and carboxylic acid samples were taken under nitrogen purge.

15.2.7 Performance: definition of terms

The performance variables were calculated as follows:

$$\text{Conversion } (x) \equiv \frac{\text{NAVS}_{\text{consumed}}}{\text{NAVS}_{\text{feed}}} \quad (15-1)$$

$$\text{Exit yield } (Y_E) \equiv \frac{\text{g total acid output from solid and liquid streams}}{\text{g NAVS}_{\text{feed}}} \quad (15-2)$$

$$\text{Culture yield } (Y_C) \equiv \frac{\text{g total acid produced in solid and liquid stream.}}{\text{g NAVS}_{\text{feed}}} \quad (15-3)$$

$$\equiv Y_E - Y_F$$

$$\text{Feed yield } (Y_F) \equiv \frac{\text{g total acid entering with feed}}{\text{g NAVS}_{\text{feed}}} \quad (15-4)$$

$$\text{Selectivity } (\sigma) \equiv \frac{\text{g total acid produced}}{\text{g NAVS}_{\text{feed}} - \text{g NAVS}_{\text{exit}}} \equiv \frac{\text{g total acid produced}}{\text{g NAVS digested}} \quad (15-5)$$

$$= \frac{Y_E}{x}$$

$$\text{Acid productivity } (P) \equiv \frac{\text{g total acids produced}}{\text{TLV} \cdot \text{d}} \quad (15-6)$$

where $NAVS_{\text{feed}}$ is the non-acid volatile solids fed, $NAVS_{\text{exit}}$ is the non-acid volatile solids removed from the fermentation, and TLV is the total liquid volume in the fermentation train including free and interstitial liquid.

15.3 Results and discussion

For all fermentations, the initial pH was approximately 7.0. During the fermentation, the pH varied from 6.3 to 8.4. The gas produced was analyzed periodically, and no methane was detected in any fermentor.

For all eight experimental conditions, the total carboxylic acid concentrations and total carboxylic acid concentrations *produced* with respect to time were plotted in Figures 15-1 and 15-2, respectively.

Figure 15-3 shows the cumulative gas produced during the 28-d batch fermentation. The error bars are relatively small, allowing for a more meaningful conclusion. Fermentations fed non-frozen, wet, unsterilized and sterilized chicken manure produced the most gas, whereas the dry, unsterilized (frozen and non-frozen) chicken manure produced the least amount of gas, which is similar to the acid concentration trends. Other studies of ethanol and ruminal fermentations have shown gas production is related to substrate digestibility (Contreras-Govea et al., 2011; Weimer et al., 2005).

Table 15-2 shows the performance variables from the fermentations, including the final carboxylic acid concentration, the acid profile, and performance data.

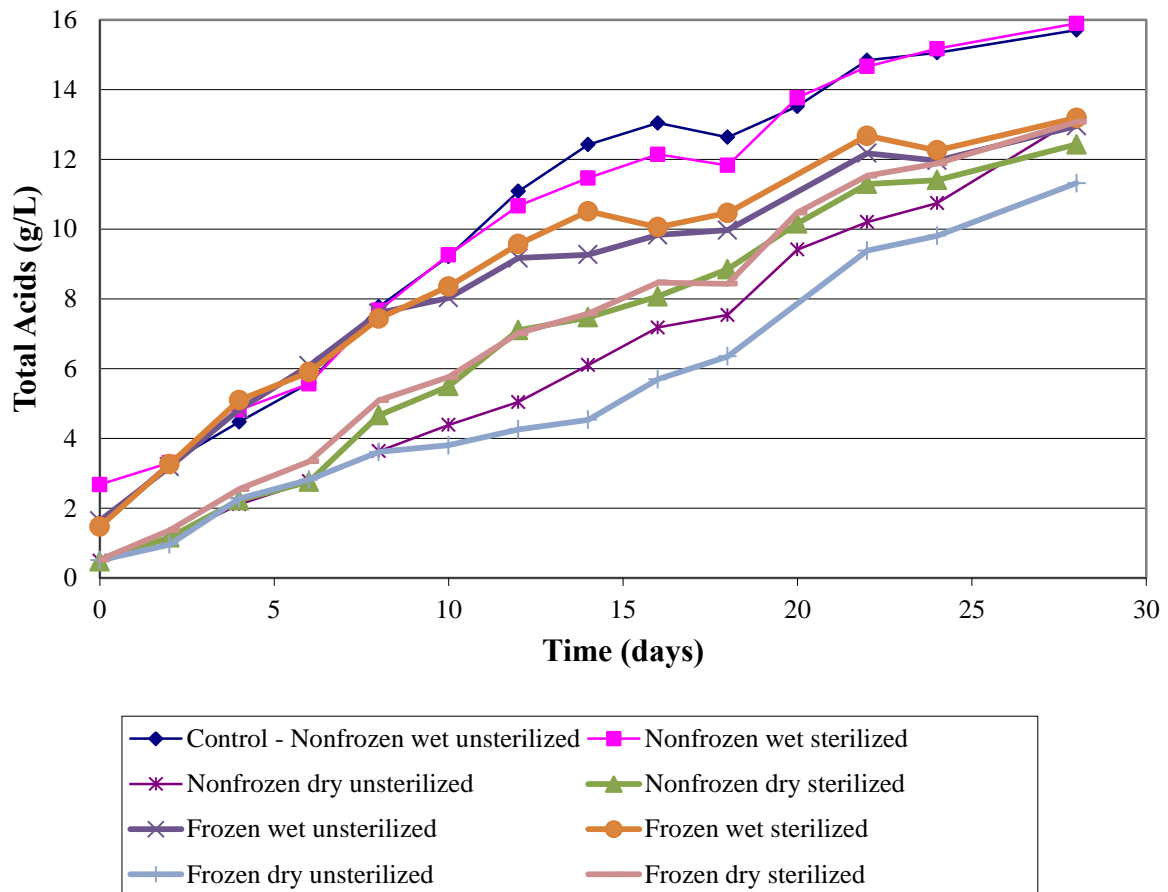


Figure 15-1. Total carboxylic acid concentration during the 28-d batch fermentation for the eight different chicken manure conditions. Error bars were removed for clarity.

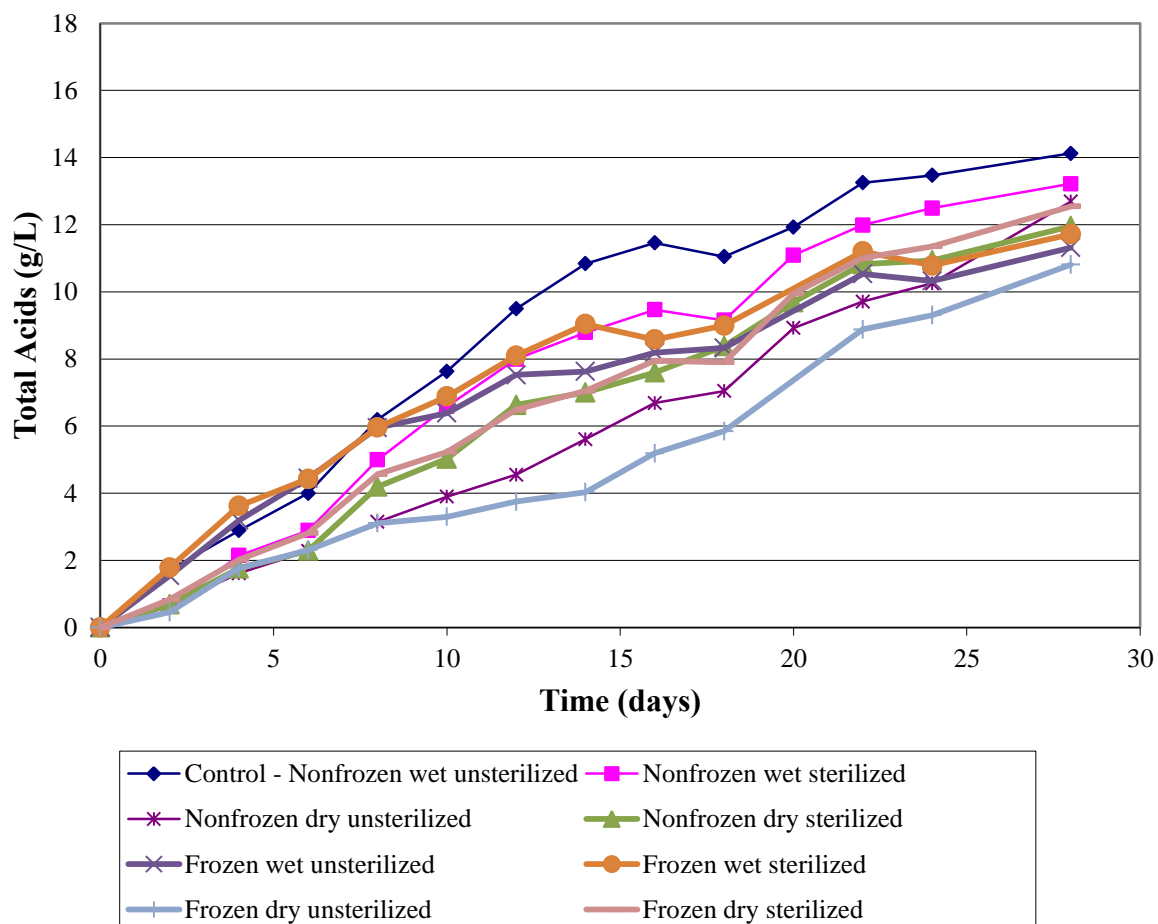


Figure 15-2. Total carboxylic acid concentration produced during the 28-d batch fermentation for the eight different chicken manure conditions. Error bars were removed for clarity.

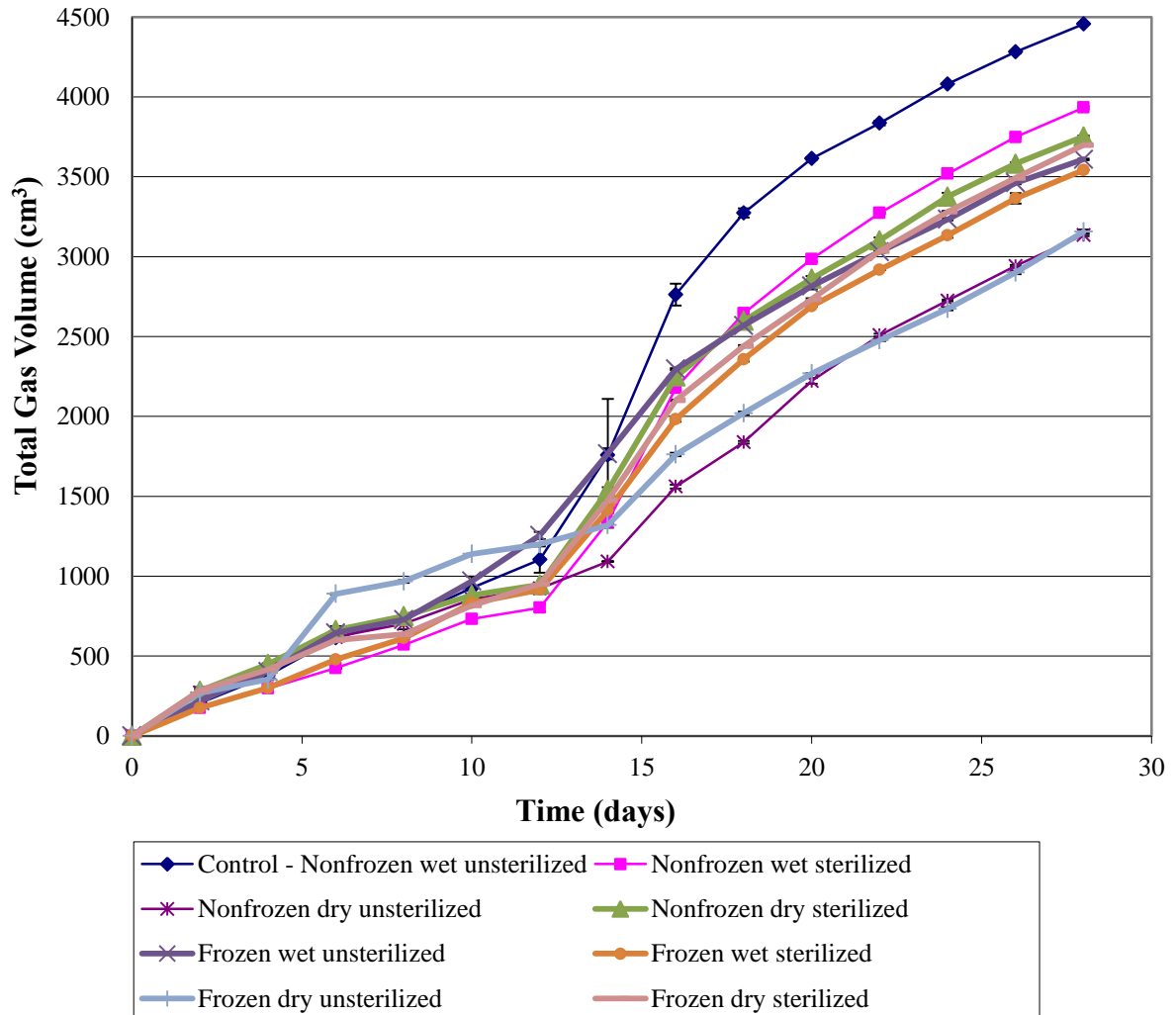


Figure 15-3. Cumulative gas produced during the 28-d batch fermentation for the eight different chicken manure conditions. Error bars are the standard errors of the triplicate fermentations.

Table 15-2. Performance of different conditioned chicken manure batch fermentations. Values represent the mean of the triplicate fermentations \pm standard deviation.

	NWU	FWU	NDU	FDU	NWS	FWS	NDS	FDS
Total carboxylic acid concentration (g/L)	15.71 \pm 0.61	12.96 \pm 3.96	13.18 \pm 1.82	11.32 \pm 2.89	15.90 \pm 2.49	13.19 \pm 6.68	12.43 \pm 3.41	13.08 \pm 4.32
Carboxylic acid concentration produced (g/L)	13.94 \pm 0.46	12.91 \pm 0.44	12.63 \pm 0.14	10.75 \pm 0.26	12.91 \pm 0.16	11.54 \pm 0.62	11.90 \pm 0.28	12.49 \pm 0.33
Total acid produced (g)	4.99 \pm 0.46	3.98 \pm 0.44	4.52 \pm 0.14	3.85 \pm 0.26	4.62 \pm 0.16	4.13 \pm 0.62	4.26 \pm 0.28	4.47 \pm 0.33
Aceq concentration (g/L)	24.9 \pm 0.51	18.5 \pm 6.17	20.0 \pm 2.46	17.5 \pm 3.94	23.0 \pm 2.74	18.6 \pm 9.32	17.4 \pm 3.61	18.8 \pm 4.64
Aceq/Acid ratio	1.59 \pm 0.07	1.43 \pm 0.45	1.52 \pm 0.19	1.55 \pm 0.34	1.45 \pm 0.20	1.41 \pm 0.71	1.40 \pm 0.34	1.44 \pm 0.41
Conversion, x (g VS digested/g VS fed)	0.26 \pm 0.01	0.24 \pm 0.16	0.20 \pm 0.06	0.14 \pm 0.04	0.27 \pm 0.07	0.23 \pm 0.16	0.23 \pm 0.09	0.21 \pm 0.09
Selectivity, σ (g acid produced/g NAVS consumed)	0.67 \pm 0.01	0.69 \pm 0.25	0.74 \pm 0.13	0.86 \pm 0.02	0.63 \pm 0.09	0.69 \pm 0.17	0.60 \pm 0.08	0.71 \pm 0.08
Culture yield, Y_c (g acid/g NAVS fed)	0.16 \pm 0.01	0.13 \pm 0.05	0.14 \pm 0.02	0.12 \pm 0.03	0.14 \pm 0.03	0.13 \pm 0.08	0.13 \pm 0.04	0.14 \pm 0.05
Exit yield, Y_E (g acid/g NAVS fed)	0.17 \pm 0.01	0.14 \pm 0.04	0.14 \pm 0.02	0.12 \pm 0.03	0.17 \pm 0.03	0.14 \pm 0.07	0.14 \pm 0.04	0.15 \pm 0.05
Productivity, P (g total acid/(L _{liq} ·d))	0.56 \pm 0.02	0.46 \pm 0.14	0.47 \pm 0.06	0.40 \pm 0.10	0.57 \pm 0.09	0.47 \pm 0.24	0.44 \pm 0.12	0.47 \pm 0.15

15.3.1 *Effect of drying chicken manure*

As shown in Table 15-2 and Figure 15-3, when comparing the wet and dry chicken manure fermentations, the wet chicken manure had better overall fermentation performance. In Figure 15-2, wet chicken manure has intrinsic carboxylic acid, giving the wet chicken manure fermentation a higher initial acid concentration. When the chicken manure was dried, much of the acid evaporated.

Drying biomass affects microorganism composition and metabolism (Zornoza et al., 2007). Drying also denitrifies the manure. As shown in Section 13.8, drying chicken manure reduces microbial activity, which might have allowed the Galveston inoculum to form the primary microbial community in the fermentation. The microorganisms in the chicken manure appear to be beneficial and supplement the Galveston inoculum. The microorganisms in wet chicken manure produce a high concentration of acids and are adapted to the high-acid environment.

In laboratory-scale fermentations, drying chicken manure provides a consistent nutrient source during the entire course of the experiments; however, drying also decreases fermentation performance. In industrial-scale fermentations, drying chicken manure is economically unfeasible and unnecessary. Because of the negative performance effects in a laboratory setting, drying chicken manure should be avoided if possible.

15.3.2 *Effect of freezing chicken manure*

When comparing the previously frozen and never-frozen chicken manure fermentations, the never-frozen manure had better performance and had significantly increased carboxylic acid production. Freezing the chicken manure decreased microbial activity (Table 15-2, Figure 15-2), which might have allowed the Galveston inoculum to form the primary microbial community in the fermentation. Apparently, the natural microbial community in chicken manure is helpful to the fermentation.

In nature, population dynamics and soil microbial function are influenced by the freeze-thaw cycle by affecting numerous environmental variables (e.g., nutrient cycling,

denitrification, gas fluxes). When microorganisms are frozen, a portion of the microorganisms have decreased metabolic activity with subsequent cell death (Yanai et al., 2004). Also, nutrients (e.g., carbon and nitrogen) are released upon cell lysis (Schimel and Mikan, 2005). Therefore, in carboxylate fermentations, freezing chicken manure should be avoided to preserve the microorganisms present in the manure, which appear to supplement the Galveston inoculum and increase fermentation performance.

15.3.3 Effect of sterilizing chicken manure

When comparing the sterilized and non-sterilized chicken manure fermentations, there was no trend in performance. During the 28-d batch fermentation, sterilization appeared to have little effect on the overall outcome of the carboxylic acid concentration or gas production.

The individual graphs for the fermentations with different chicken manure conditions are shown in Figures 15-4 to 15-11.

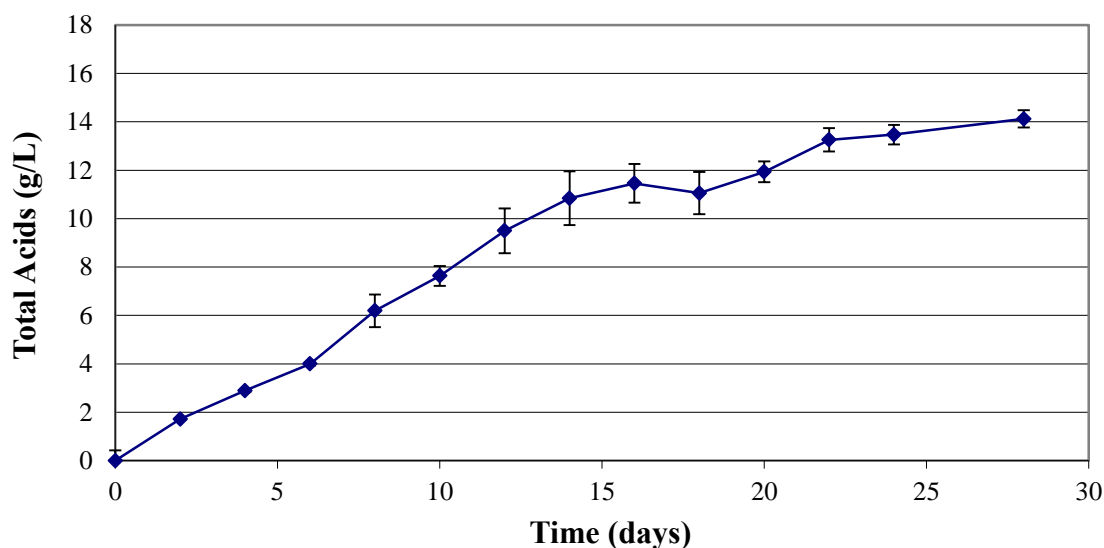


Figure 15-4. Total carboxylic acid produced during the 28-d batch fermentation for the nonfrozen wet unsterilized chicken manure (NWU). Error bars are the standard error of the triplicate fermentations.

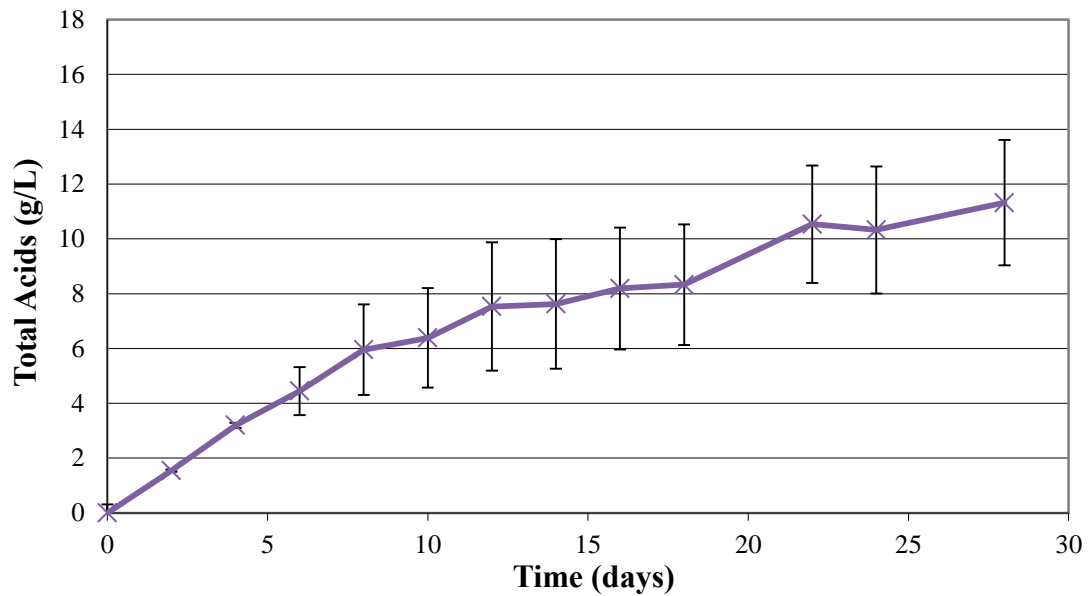


Figure 15-5. Total carboxylic acid produced during the 28-d batch fermentation for the frozen wet unsterilized chicken manure (FWU). Error bars are the standard error of the triplicate fermentations.

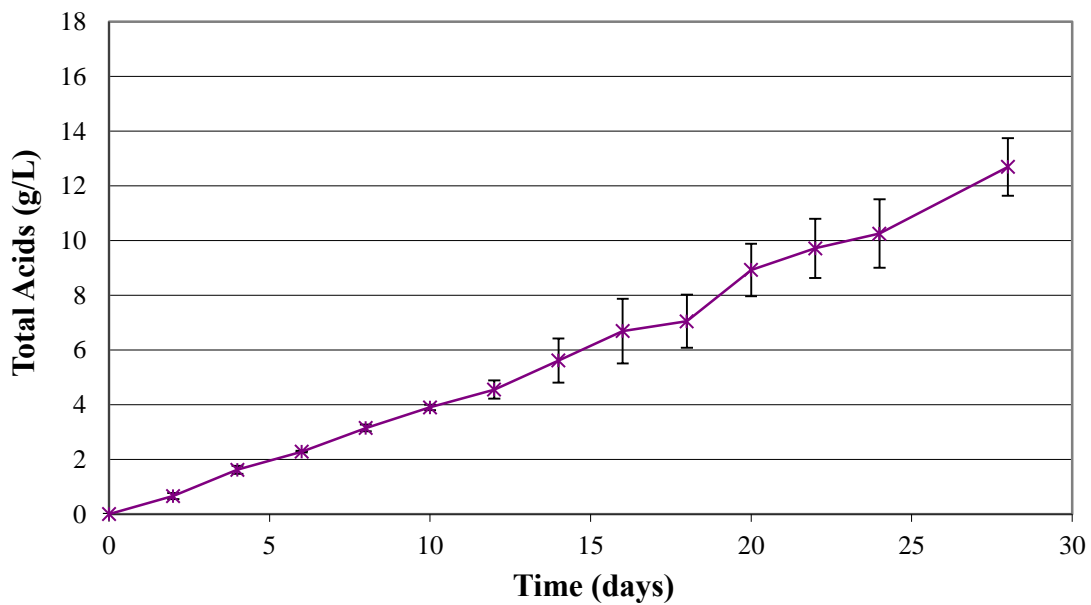


Figure 15-6. Total carboxylic acid produced during the 28-d batch fermentation for the nonfrozen dry unsterilized chicken manure (NDU). Error bars are the standard error of the triplicate fermentations.

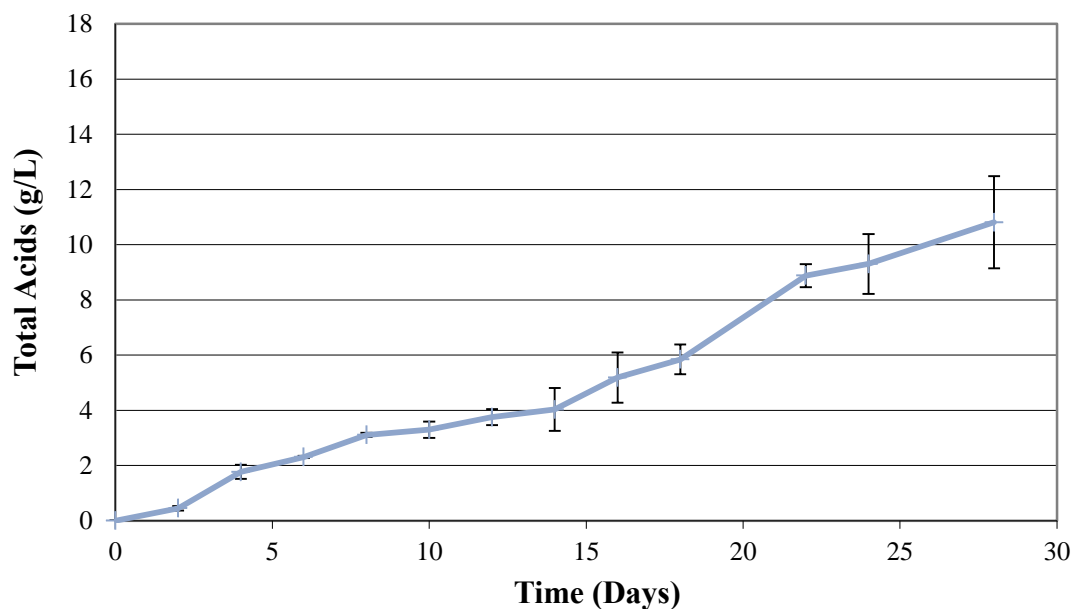


Figure 15-7. Total carboxylic acid produced during the 28-d batch fermentation for the frozen dry unsterilized chicken manure (FDU). Error bars are the standard error of the triplicate fermentations.

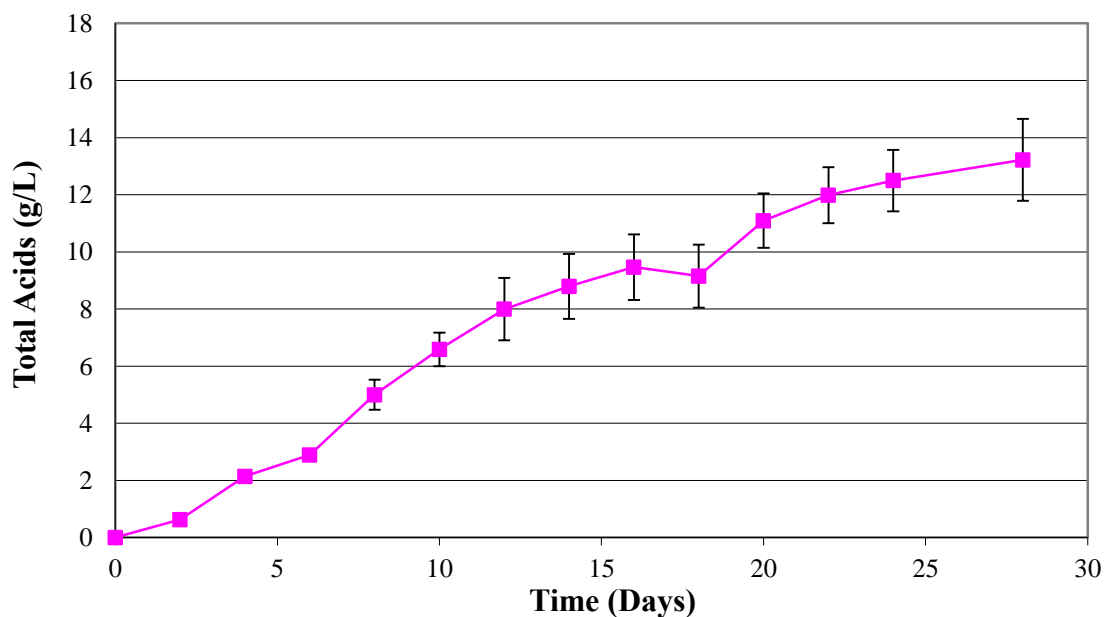


Figure 15-8. Total carboxylic acid produced during the 28-d batch fermentation for the nonfrozen wet sterilized chicken manure (NWS). Error bars are the standard error of the triplicate fermentations.

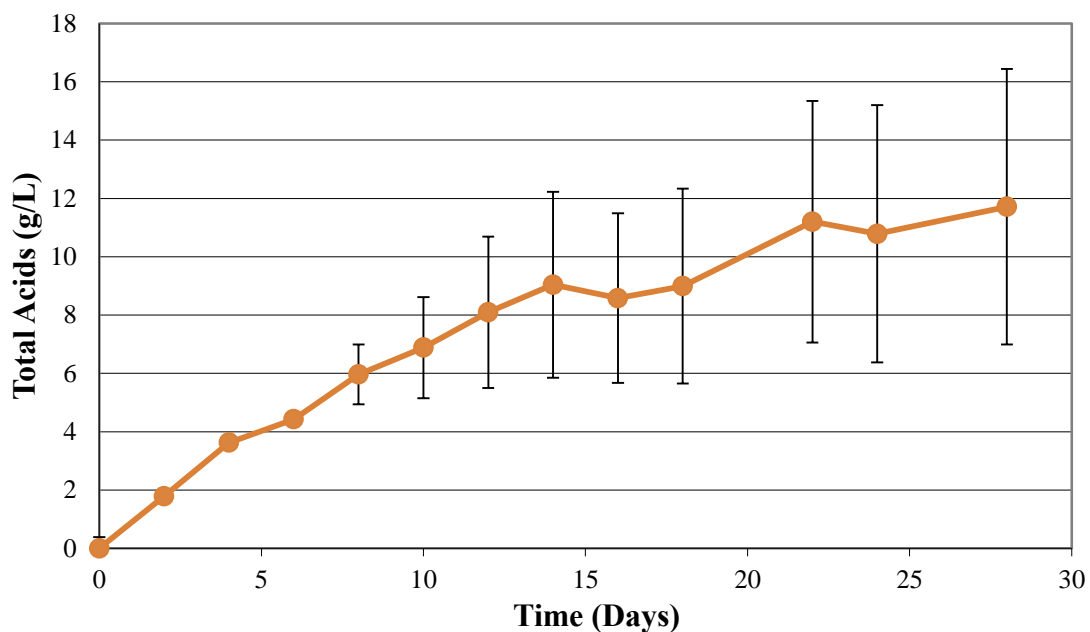


Figure 15-9. Total carboxylic acid produced during the 28-d batch fermentation for the frozen wet sterilized chicken manure (FWS). Error bars are the standard error of the triplicate fermentations.

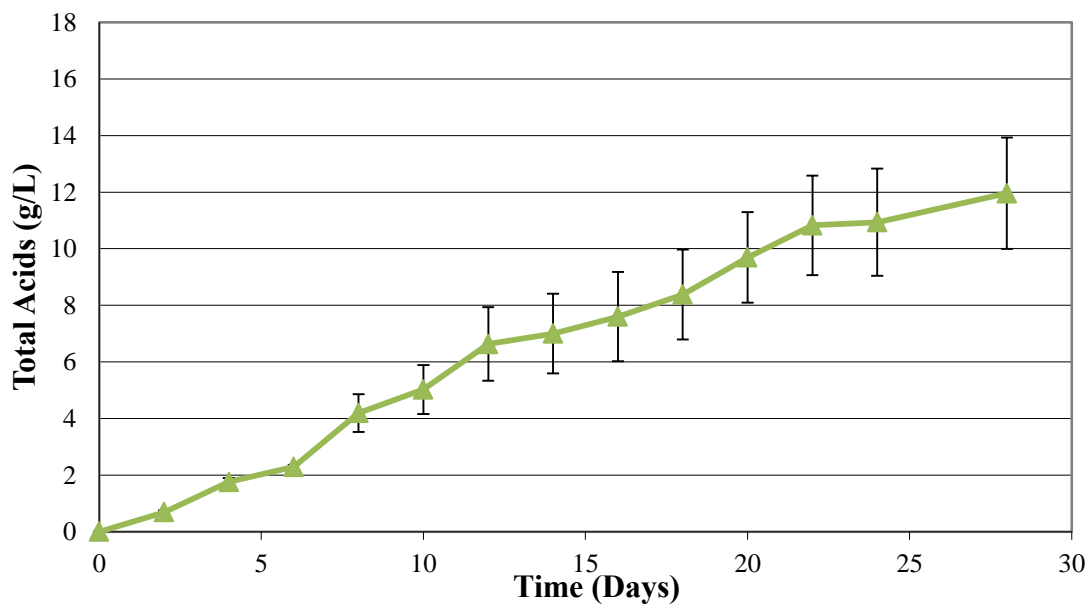


Figure 15-10. Total carboxylic acid produced during the 28-d batch fermentation for the nonfrozen dry sterilized chicken manure (NDS). Error bars are the standard error of the triplicate fermentations.

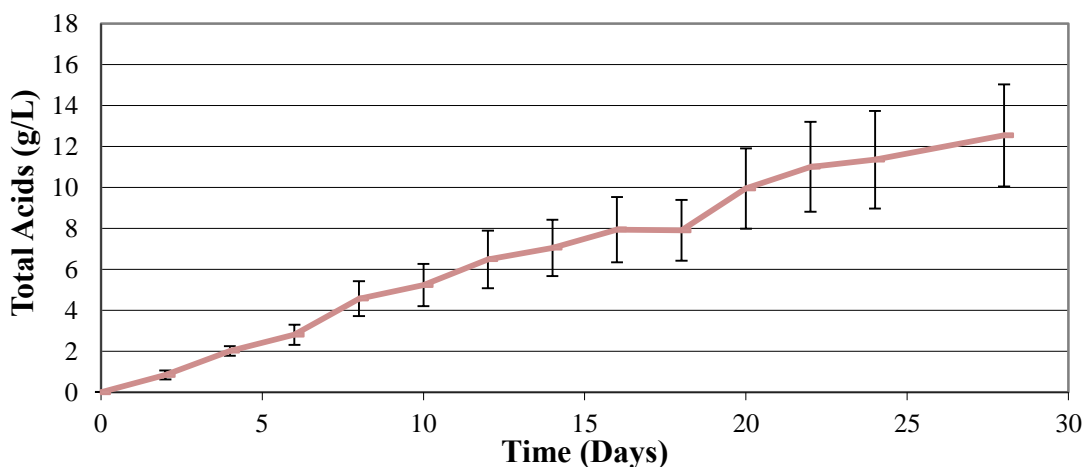


Figure 15-11. Total carboxylic acid produced during the 28-d batch fermentation for the frozen dry sterilized chicken manure (FDS). Error bars are the standard error of the triplicate fermentations.

15.4 Conclusion

This study shows that the bacteria in the chicken manure increase fermentation performance. Because drying and freezing decrease the microbial load in chicken manure, the best-performing fermentations were run with chicken manure as the nutrient source that was wet and never frozen. The fermentation with the worst performance had a chicken manure nutrient source that was dry and previously frozen. Most likely, the freeze-thaw cycle killed a portion of the microorganisms in the chicken manure. Also, drying the chicken manure kills microorganisms and removes nitrogen.

Autoclaving the chicken manure did not affect fermentation performance. Industrially, sterilizing manure by autoclave would not be effective or economically feasible. In the future, the following experiments should be performed: (1) isolate and grow the microorganisms from chicken manure; (2) run fermentations with no Galveston inoculum, using only wet chicken manure as the inoculum and nutrient source; (3) investigate how the wet chicken manure microbial community changes during the fermentation; and (4) extract acid from wet chicken manure before being fed to the fermentation, which would remove any added initial inhibition and allow fermentations to be compared on a common basis.

16. SUGAR-UTILIZATION ASSAY DEVELOPMENT

The goal of this chapter is to develop an accurate and reproducible assay to quantify microbial activity in a biomass sample by measuring sugar (i.e., glucose, xylose, cellobiose) digestion over time. The experiments summarized in this chapter reflect the development process with each subsequent experimental design, the problems encountered, and the assay conditions finally decided upon.

16.1 Introduction

A cell separation technique can be optimized by quantifying the number of cells in each stream, allowing the streams that yield minimal cells to be discarded. Therefore, techniques must be developed that can determine an absolute or relative cell count in the presence of undigested solids. Cell counts would also be useful to determine cell set points and maximum cell concentrations in trains.

Quantifying total cell microbial load in solid biomass is difficult because of the large particles size distribution and different substances present, some of which inhibit certain enzyme assays. Some common ways to quantify the number of cells in a pure culture are turbidity and plating; however, these are not suitable for the mixed-culture community found in carboxylate fermentations. Other methods to quantify cells include: (1) quantitative real-time polymerase chain reaction (real-time PCR), and (2) fluorescent in-situ hybridization (FISH).

Real-time PCR is a technique that amplifies and quantifies a specific DNA molecule in cells. In real time, the amplified DNA is detected throughout the reaction with fluorescent dyes or DNA probes with a fluorescent reporter. The amount of DNA in a sample can be related back to an average number of cells.

FISH is a cytogenic laboratory technique that detects and localizes the presence of specific DNA sequences on chromosomes or mRNA sequences in tissue samples with fluorescent probes. These probes only bind to the segments of chromosome or tissue that are highly similar.

Real-time PCR quantifies both living and dead cells whereas FISH quantifies just living cells. Although real-time PCR and FISH techniques are highly specific to the chosen DNA strands, both are relatively expensive, time-consuming, and require specialized equipment and personnel.

To avoid costly and time-consuming DNA assays, and only quantify living cells, the sugar-utilization assay was developed and explored in this chapter. The sugar-utilization assay is a laboratory technique that quantifies microorganism activity by measuring their sugar (i.e., glucose, xylose, cellobiose) digestion over time. The change in the mass of sugar in the solution per mass of solid biomass added can be used to quantify the relative or absolute number of living microorganisms in the sample. To determine the absolute number of cells in a sample, a cell calibration curve must be developed for each cell type. To quantify the relative number of living microorganisms in a sample, a specific sugar activity unit can be defined and compared to a known pure culture. Equations 16-1 to 16-3 below exemplify the calculations for solid mass, sugar activity, and specific sugar activity. Equation 16-1 shows the amount of solid mass that might be added to the glucose-utilization assay. Conversely, the 1-mL suspension can be used as the biomass added. Equation 16-2 shows the sugar digestion rate, and Equation 16-3 shows the specific sugar activity which divides the amount of sugar digested with time by the mass of inoculum.

$$\text{Solid mass} = \frac{50 \text{ g solids}}{\text{L slurry}} \times 1 \text{ mL suspension} \times \frac{1 \text{ L}}{1000 \text{ mL}} = 0.050 \text{ g solids} \quad (16-1)$$

$$\text{Sugar Activity} = \frac{(30-20) \text{ g sugar}}{\text{L} \cdot 0.5 \text{ h}} \times 10 \text{ mL} \times \frac{1 \text{ L}}{1000 \text{ mL}} = \frac{0.2 \text{ g sugar}}{\text{h}} \quad (16-2)$$

$$\text{Specific Sugar Activity} = \frac{0.2 \text{ g sugar}}{0.050 \text{ g solids} \cdot \text{h}} = 4 \frac{\text{g sugar}}{\text{g solids} \cdot \text{h}} \quad (16-3)$$

Sugar concentration can be measured a variety of ways, two of which were studied in this chapter: (1) high performance liquid chromatography (HPLC), and (2) glucose oxidase enzyme assay (GOEA).

HPLC is a chromatographic technique that uses a liquid mobile phase to separate a mixture of compounds, so that the compounds can be isolated, identified, and quantified. HPLC was used to quantify different sugars in solution.

GOEA is a technique that measures the amount of glucose in solution with glucose oxidase enzyme and color indicator, which is quantified with spectrophotometry. GOEA can measure low concentrations of glucose, allowing for a more rapid assay.

To ensure that the sugar-utilization assay experiment is reproducible, the control bacterial cells must be in a reproducible growth phase and concentration. When bacteria undergo exponential (i.e., balanced) growth, the cell doubling time is the same as the time it takes these cells to double their subcellular contents (e.g., content of DNA, ribosomes, individual enzyme molecules). Working with a culture in balanced growth has several advantages: (1) samples taken over time only vary by the extent of culture growth between these times, otherwise the samples are identical, (2) relative rate of synthesis of all cellular components of the culture becomes known just by measuring the growth rate. Because exponential growth is the most reproducible physiological state of bacterial cultures, experiments done with cultures in balanced growth in different laboratories can usually be directly compared.

When growth becomes unbalanced, bacteria stop growing because syntheses of some cellular components slow down or stop before others. During stationary phase, cells do not have a constant composition and therefore differ chemically with time of sampling. For example, *Escherichia coli* cells in stationary phase continue actively synthesizing DNA after their protein synthesis has decelerated; therefore, their DNA-to-protein ratio will increase with time. Also, cells in stationary phase are smaller than those in exponential phase because cell division continues after the synthesis of most macromolecules have slowed down. If a culture in exponential growth is diluted into

fresh medium, it will continue to grow exponentially. If a culture from stationary phase is diluted, it will have a lag phase, and the lag phase can be variable; therefore, bacterial cultures in stationary phase would not digest sugars reproducibly. All bacterial controls must be in the exponential growth phase.

The effect of pH on cells is also an important variable, and needs to be controlled in the sugar-utilization assay. *Escherichia coli* is a neutrophile, meaning it grows well at pH 6–9, and slower outside this range. Within the cell there is homeostasis, and pH is maintained at ~7.6. When bacteria grow at pH lower than their internal value, their cytoplasm is more alkaline. Similarly, when bacteria grow at a pH higher than their internal pH, their cytoplasm is more acidic. This is caused by proton-motive force, which has two interconvertible components: (1) change in pH, and (2) change in membrane potential, either of which has the capacity to drive protons through the membrane-bound ATPase to generate ATP. The cell must bring protons into the cell and simultaneously create a membrane potential. This task might be accomplished by a proton/K⁺, or a proton/Na⁺ antiport to a lesser degree.

This chapter investigates two sugar-utilization assay methods – Method A and Method B – and summarizes the experiments that were conducted to develop these sugar-utilization assays. Method A analyzed the sugar concentrations with HPLC. Sugar concentration analysis with HPLC required ~30 min/sample and required a larger concentration of sugars in the assay, which increased total sugar digestion time. Method B analyzed the glucose concentration with the glucose oxidase enzyme assay (GOEA) and was quantified with a spectrophotometer, which could measure 96 samples in ~8 s. Because glucose oxidase enzyme assay measures very small concentrations of glucose, the glucose digestion is very rapid, which decreases total assay time. Method B only measured glucose, which allowed for faster analysis, whereas Method A measured glucose, xylose, and cellobiose.

16.2 Materials and methods

16.2.1 *Procedure for Method A: Procedure for quantifying total cell microbial load using a glucose, xylose, and cellobiose digestion assay with HPLC analysis*

Method A was developed to quantify total cell microbial load in solid biomass by measuring glucose, xylose, and cellobiose digestion over time. There are several questions that must be asked about the average sugar activity for a sample, which depends on the amount of each sugar (i.e., glucose, xylose, cellobiose) digested: (1) Are they equally digested, or is one sugar preferred over another? (2) Does this change with time or cell concentration? (3) Does this change when the mixed-microbial community changes?

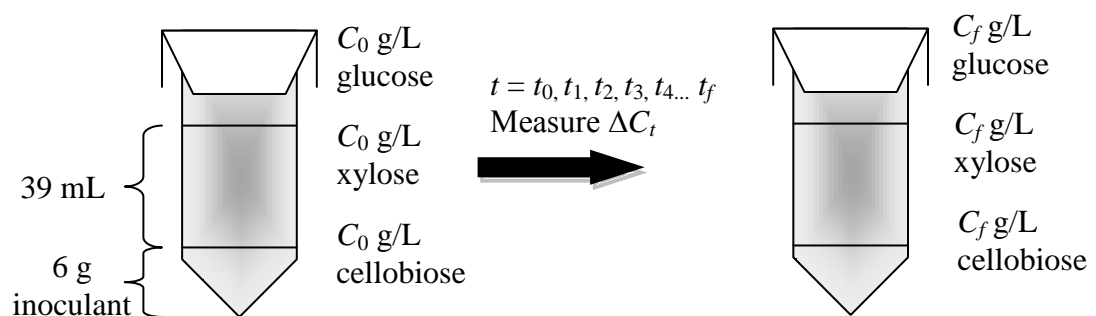
Figure 15-1 shows the overall procedure where the sugar solution was prepared, biomass was added to the autoclaved sugar solution, samples were taken at a predetermined frequency, and the glucose was quantified by HPLC. In the overall setup, the sugar concentration is initially at a predetermined glucose concentration (C_0), which is initially very high (i.e., 5, 10, 20, and 30 g sugar/L). During the incubation and agitation step, the sugar concentration decreased with time as the sugar was digested by the bacteria (C_f).

Overall Procedure



Overall Setup

Fermentor: 50-mL conical tube



Fermentor: 15-mL conical tube

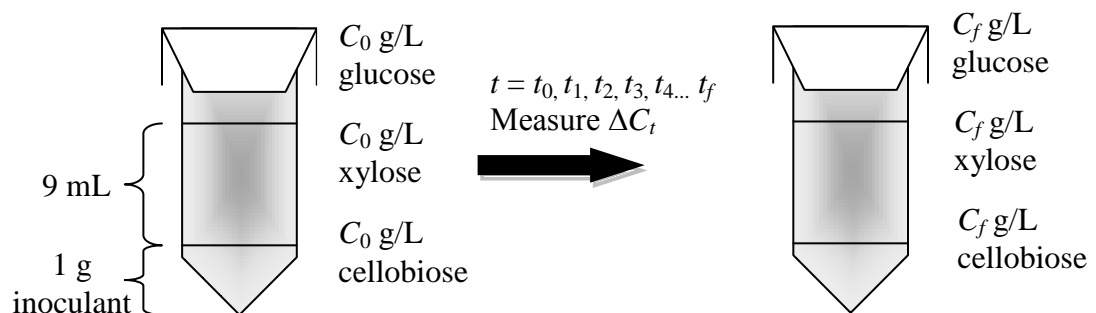


Figure 16-1. Diagram of the overall sugar-utilization assay procedure and experimental setup for Method A.

The equations below exemplify the calculations for solid mass and specific sugar activity.

Example of solid mass calculations:

$$\frac{50 \text{ g solids}}{\text{L slurry}} \times 5 \text{ mL suspension} \times \frac{1 \text{ L}}{1000 \text{ mL}} = 0.250 \text{ g solids}$$

Example of specific sugar activity calculations (15-mL conical tube):

Glucose Activity

$$\frac{(30-20) \text{ g glucose}}{\text{L} \cdot 0.5 \text{ h}} \times 10 \text{ mL} \times \frac{1 \text{ L}}{1000 \text{ mL}} = \frac{0.2 \text{ g glucose}}{\text{h}}$$

$$\text{Glucose Activity} = \frac{0.02 \text{ g glucose}}{0.050 \text{ g solids} \cdot \text{h}} = 4 \frac{\text{g glucose}}{\text{g solids} \cdot \text{h}}$$

Xylose Activity

$$\frac{(30-20) \text{ g xylose}}{\text{L} \cdot 0.5 \text{ h}} \times 10 \text{ mL} \times \frac{1 \text{ L}}{1000 \text{ mL}} = \frac{0.2 \text{ g xylose}}{\text{h}}$$

$$\text{Xylose Activity} = \frac{0.02 \text{ g xylose}}{0.050 \text{ g solids} \cdot \text{h}} = 4 \frac{\text{g xylose}}{\text{g solids} \cdot \text{h}}$$

Cellobiose Activity

$$\frac{(30-20) \text{ g cellobiose}}{\text{L} \cdot 0.5 \text{ h}} \times 10 \text{ mL} \times \frac{1 \text{ L}}{1000 \text{ mL}} = \frac{0.2 \text{ g cellobiose}}{\text{h}}$$

$$\text{Cellobiose Activity} = \frac{0.02 \text{ g cellobiose}}{0.050 \text{ g solids} \cdot \text{h}} = 4 \frac{\text{g cellobiose}}{\text{g solids} \cdot \text{h}}$$

16.2.2 *Procedure for Method B: Procedure for quantifying total cell microbial load using the glucose oxidase enzyme assay (GOEA)*

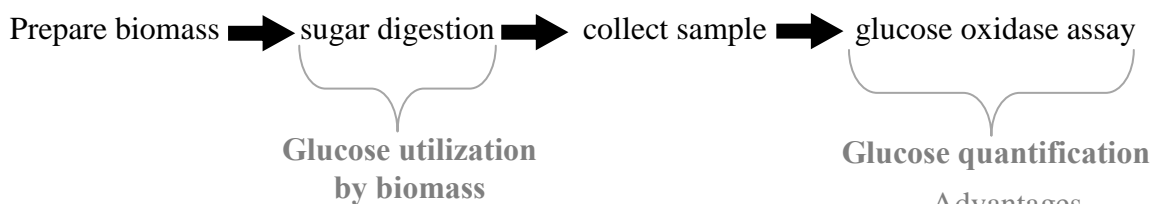
Method B was developed to quantify total cell microbial load in solid or liquid biomass by measuring glucose digestion over time. Measuring only one sugar allows for a more rapid and streamlined analysis. Figure 16-2 shows the overall procedure where the biomass was added to the sterilized sugar solution, samples were taken at a predetermined frequency as the digestion proceeded, and the glucose was quantified by a glucose oxidase enzyme assay. In the overall setup, the sugar concentration is initially at a predetermined glucose concentration (C_0), which was typically very small (~80 μg glucose/mL). During the incubation and agitation step, the sugar concentration decreased with time as the glucose was digested by the bacteria (C_t).

First, the sugar solution was prepared by adding glucose to distilled and deionized water. The solution was buffered with either 30-mM MOPS or 50-mM potassium phosphate (pH 7.5). The sugar solution was sterilized by filter sterilizing (0.2 μm). The glucose solutions were aliquoted into the appropriate vial, and biomass was added. The vials were incubated, and the necessary time points were taken for analysis (Appendix H). Samples were immediately analyzed by the glucose oxidase enzyme assay (Appendix I).

In cells, glucose oxidase is an enzyme that helps metabolize glucose. Glucose oxidase is an oxidoreductase, where it catalyzes the transfer of electrons. In diagnostics, glucose oxidase is used to determine the amount of glucose in bodily fluids, and commercially in the food industry.

As shown in Figure 16-3, in the glucose oxidase enzyme assay, glucose oxidase catalyzes the conversion of β -D-glucose, water, and oxygen into D-gluconic acid and hydrogen peroxide. The generation of hydrogen peroxide is indirectly measured by the oxidation of O-dianisidine in the presence of peroxidase. Sulfuric acid stops the reaction progress, which can then be measured by spectrophotometry (570 nm).

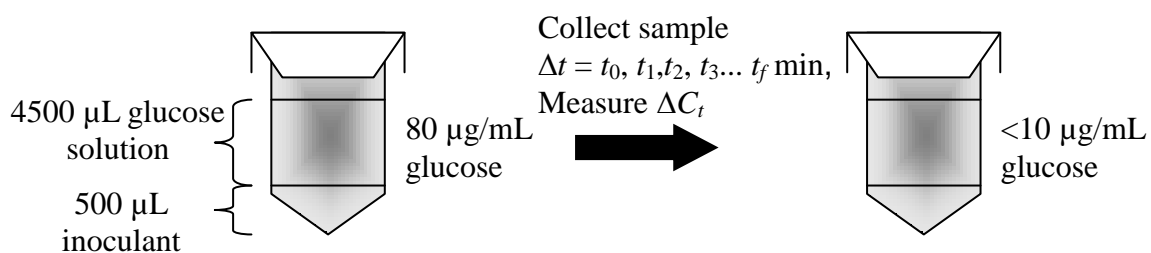
Overall Procedure



Advantages

- Fast incubation (10 min)
- High throughput (96-well plate)
- Good sensitivity and range (0–80 $\mu\text{g/mL}$)
- Reproducible ($R^2 = 0.99$)

Overall Experimental Setup



Time points

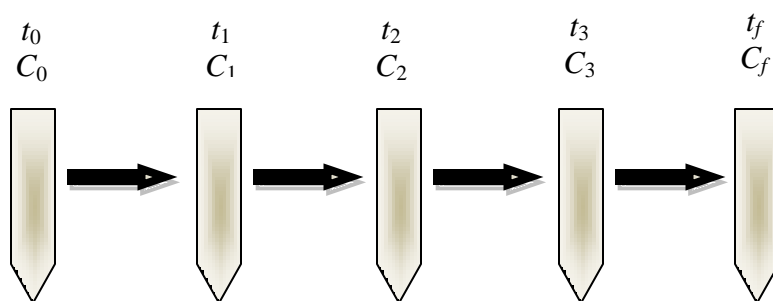


Figure 16-2. Diagram of the overall sugar-utilization assay procedure and general experimental setup for Method B.

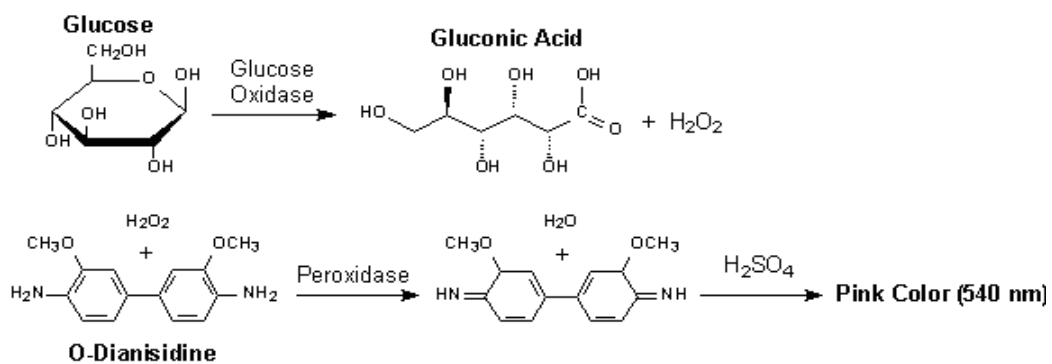


Figure 16-3. Representation of the chemistry of the glucose oxidase enzyme assay.

In a spectrophotometer (Figure 16-4), Beer's Law states the relationship between the light absorbance and concentration of the solution.

$$\text{Absorbance} = \varepsilon \cdot \text{Concentration} \cdot \ell = \log \frac{I_0}{I} \quad (16-4)$$

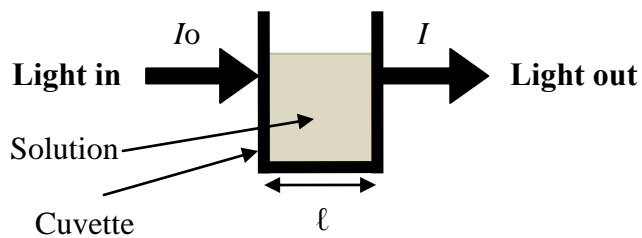


Figure 16-4. Spectrophotometric analysis.

As depicted in Figure 16-5, spectrophotometers can measure 1 to 96 samples at a time. On the left is a spectrophotometer that analyzes the light absorbance of one sample at a time in individual cuvettes. The spectrophotometer on the right analyzes the light absorbance of up to 96 samples in a 96-well plate. The sensitivity of both of these spectrophotometers was analyzed (see Section 16.8).



Figure 16-5. Pictures of spectrophotometers.

16.3 Experiment 1

16.3.1 Objective

Using Method A, the goals of Experiment 1 were to investigate the optimal sampling time and different inocula sources, test overall experimental setup, obtain sugar calibrations from HPLC, investigate HPLC sensitivity to sugar dilutions, and determine if there are free sugars in the fermentation broth and separated “cells.”

16.3.2 Materials and methods

Two time points were sampled (0, 30 min). In this experiment, both time points were collected from a virgin glucose-digestion vial. This was repeated for accuracy. The assay was inoculated with liquid fermentation broth. The vials were agitated in a shaking incubator (40 °C, >100 rpm) in the vertical orientation. For both the sugar-utilization assay and the fermentation broth, the sugar concentration was determined with HPLC.

16.3.3 Results and discussion

Figure 16-6 shows that 30 min was too short of an incubation time to measure cellobiose, glucose, and xylose digestion when inoculated with liquid fermentation broth. This was repeated and verified that a 30-min incubation time was too short to observe digestion.

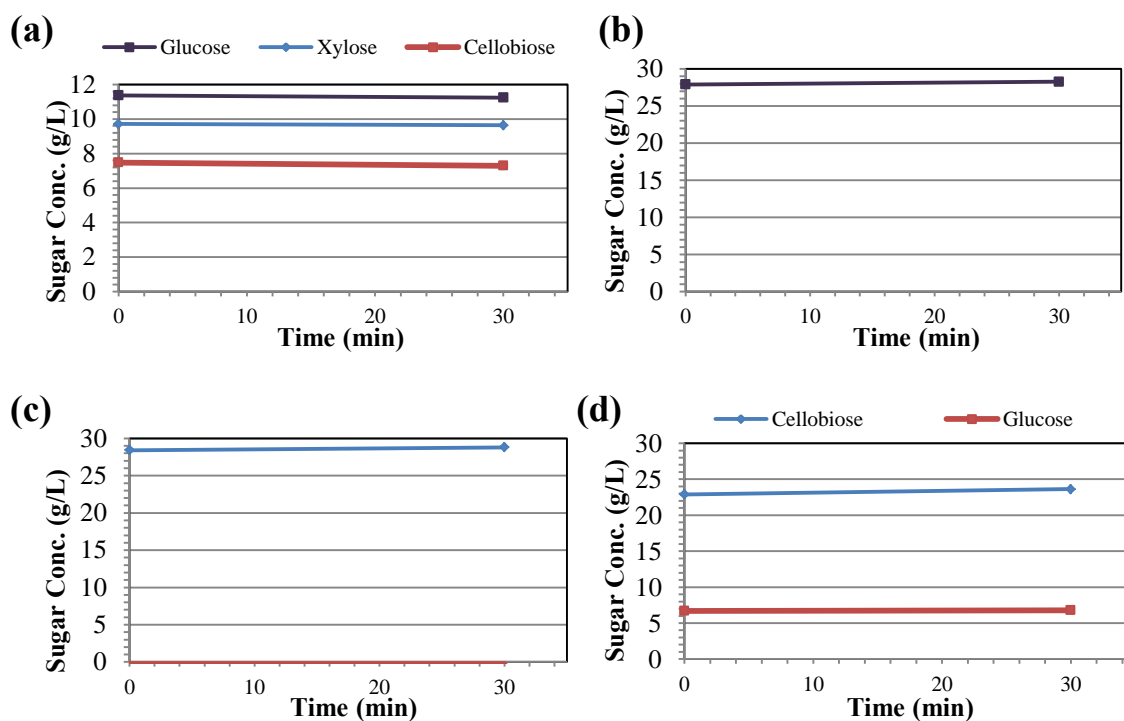


Figure 16-6. Sugar digestion of liquid fermentation broth for (a) cellobiose, glucose, and xylose, (b) glucose, (c) xylose, (d) cellobiose over 30 min in the vertical vial orientation.

Figure 16-7 shows the cellobiose, glucose, and xylose five-point calibration. This was verified to be linear at higher concentrations. Table 16-1 shows that there are no observable free sugars in the fermentation broth nor in the separated “cells.”

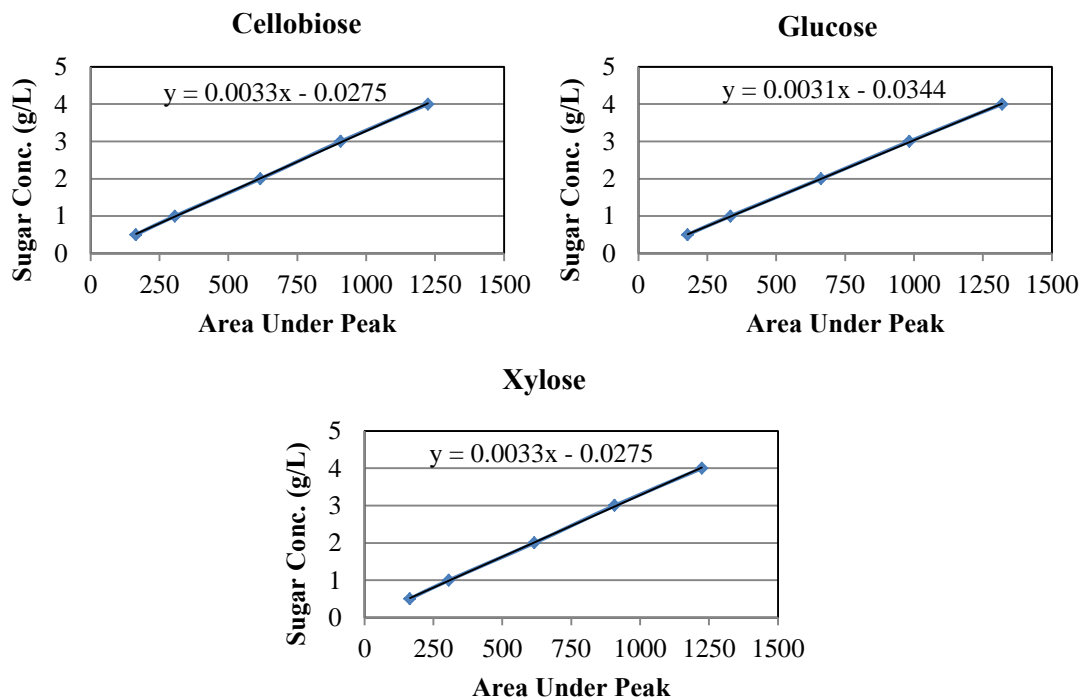


Figure 16-7. HPLC calibrations of cellobiose, glucose, and xylose.

Table 16-1. Original sugar concentration of liquid fermentation broth and “cells” for cellobiose, glucose, and xylose.

Sample	Sugar Concentration (g/L)		
	Cellobiose	Glucose	Xylose
Liquid sample suspension	-0.3	-0.1	-0.1
Cells (3 g/L)	0.1	-0.3	-0.3

16.3.4 *Overview*

When all three were run together during a 30-min digestion, there was no measurable concentration change in glucose, xylose, or cellobiose. This was repeated to verify. The HPLC is calibrated sufficiently and is very sensitive to dilutions. Instead of diluting 10×, calibrating, and multiplying by 10 to get actual concentration (g/L) of the original sugar solution, running undiluted sugar solutions through the HPLC is acceptable, as long as the sugar concentration does not exceed the maximum amount for the column. Also, there are no free sugars in the fermentation broth, nor in the separated “cells” (Appendix G). Future work should include an alternate sugar compositional analysis.

16.4 Experiments 2 and 3

16.4.1 *Objective*

Using Method A, the objective of Experiments 2 and 3 was to further investigate the optimal sugar digestion time by testing longer incubation periods.

16.4.2 *Materials and methods*

Five time points were tested (0, 2, 5.5, 12, and 24 h). In these experiments, every time point was collected from a virgin glucose-utilization vial. The sugar-utilization assay was inoculated from squeezed solid residual biomass samples (equivalent of fermentation broth). The vials were agitated in a spinning incubator (40 °C, >100 rpm) in the vertical orientation. Using Method A, the sugar concentration in the sugar-utilization assay was determined with HPLC. The samples were not diluted when run through the HPLC.

16.4.3 *Results and discussion*

Figure 16-8 shows that 24 h is insufficient to observe a change in sugar digestion. Also, duplicates were run to determine the reproducibility of the data. When performing replicates, there were errors with the assay, either with the HPLC or human error.

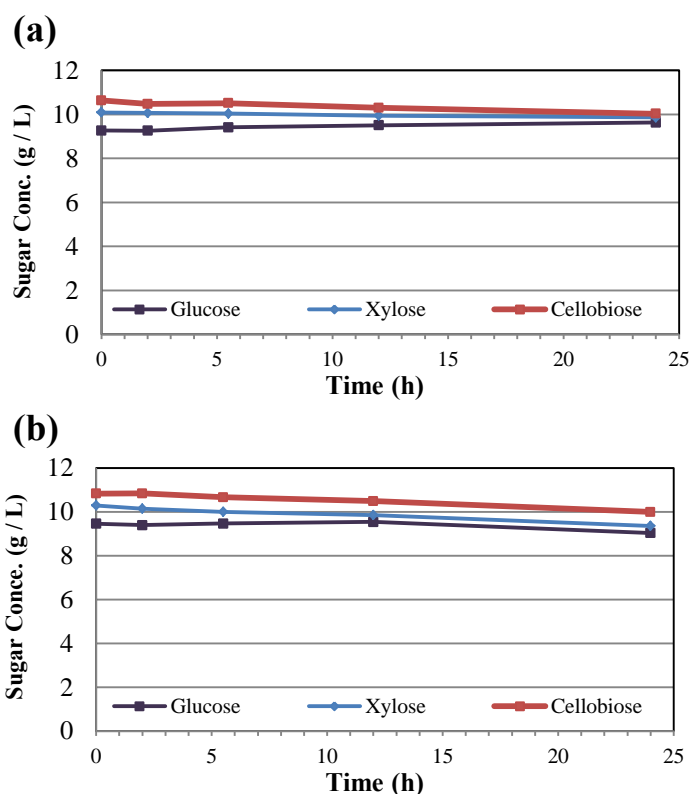


Figure 16-8. Sugar digestion inoculated with (a) liquid broth and (b) solid fermentation waste biomass for cellobiose, glucose, and xylose during 24 h.

16.4.4 Overview

A digestion time period of 24 h was insufficient to observe a change in sugar concentration with time. Also, HPLC machine error was encountered.

16.5 Experiment 4

16.5.1 Objective

Using Method A, the goal of Experiment 4 was to further investigate the optimal sugar digestion time. Also, to verify if a virgin glucose-utilization vial is necessary for every time point, sample collection techniques will be compared (i.e., 1 vial per time interval versus 1 vial per total digestion time).

16.5.2 *Materials and methods*

Six time points were sampled: 0, 1, 2, 3, 4, and 12 d. In this experiment, every time point was collected from a virgin bottle and the vial was “sacrificed.” To determine the need of having a virgin bottle for each time point, data were taken in parallel from the same bottle. The sugar-utilization assay was inoculated with three different inocula: (1) liquid fermentation broth, (2) separated cells (Appendix G), and (3) a pure culture of *Clostridia thermocellum*. The vials were agitated in a spinning incubator (40 °C, >100 rpm) in the vertical orientation. Using Method A, the sugar concentration in the sugar-utilization assay was determined with HPLC. The samples were not diluted when run through the HPLC.

16.5.3 *Results and discussion*

When samples were collected, the vial was opened in the open air, a 1-mL sample was quickly taken, and the vial was immediately shut to prevent contamination from microorganisms from the air. To determine if microorganisms from the environment affected the sugar digestion results, a control was used. The control vial for the glucose utilization was not inoculated, but all other conditions and sampling times were the same. Figure 16-9 shows that the control was acceptable for four days, but by Day 12, the environmental microorganisms degraded the sugars. This means that the current technique of sampling in the open air is sufficient only up to Day 4. (Note: If more samples were taken, perhaps it would have been shown that the assay could be used for more than four days.)

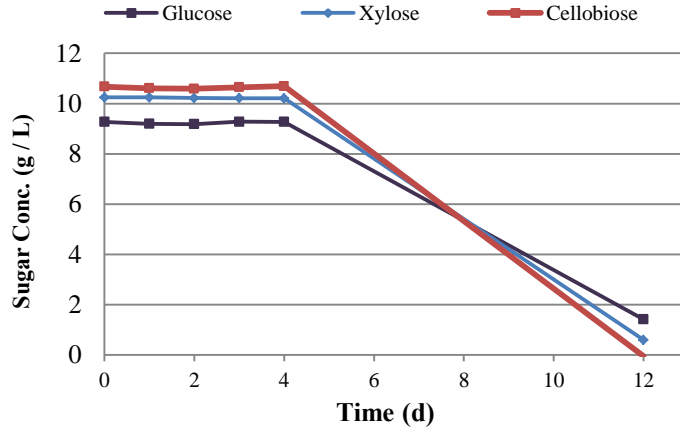


Figure 16-9. Sugar digestion control measuring cellobiose, glucose, and xylose during 12 days.

Figure 16-10 graphs sugar concentration (g/L) with time for two different sample collection techniques: (1) using the same sugar digestion vial during each time sample, and (2) using a different sugar digestion vial during each time sample. The top two graphs represent when each sample and sample time was collected from an individual tube (vial sacrifice). Bottom two graphs were from samples that were collected from the same tube. Similar results were obtained for both collection techniques. The advantages of single-tube collection are that it is easier and cheaper. The disadvantages of single-tube collection are that the sample volume constantly decreases (but concentrations are unchanged between sampling assuming homogenous sampling), and there is possibly more risk for environmental contamination.

Also, cellobiose converted into glucose, making the sugar digestion analysis difficult. For the future, consider analyzing sugar digestion individually.

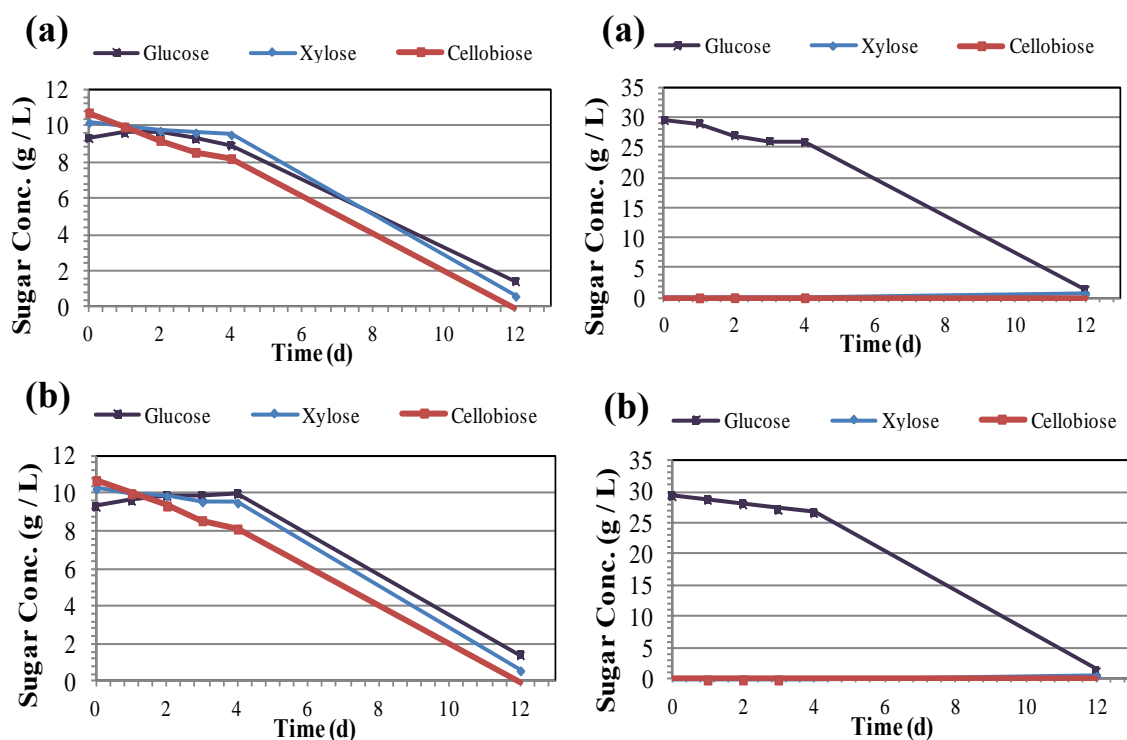


Figure 16-10. Sugar digestion inoculated with liquid broth and solid fermentation waste biomass for cellobiose, glucose, and xylose during 12 h with (a) same tube, and (b) separate tube sampling procedures.

Figure 16-11 shows that the separated cells digested more sugar than the fermentation broth, suggesting that the separation technique yields higher cell concentrations than liquid that was squeezed from the residual biomass. Also, the cells appeared to digest cellobiose faster than glucose, probably because they were adapted to digesting cellobiose from the paper feedstock. Future experiments should consider testing each step of separation technique to determine the necessity of each step.

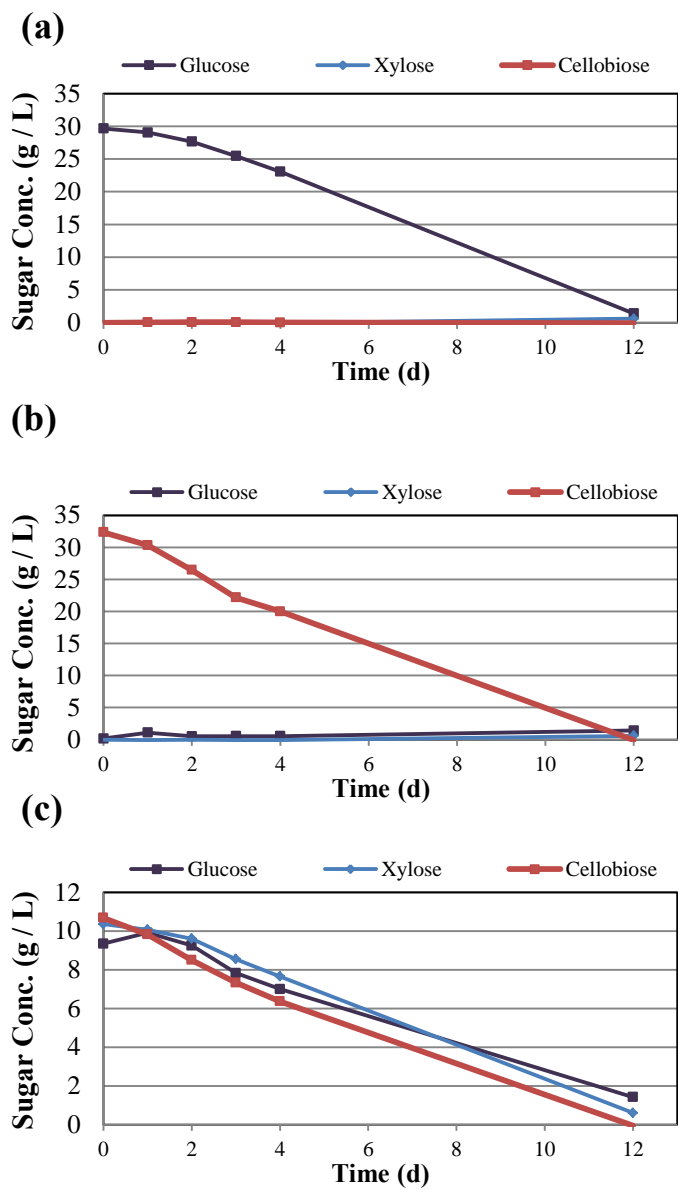


Figure 16-11. Sugar digestion of (a) glucose, (b) cellobiose, and (c) glucose, xylose, and cellobiose inoculated with separated cells (Appendix G) during 12 days.

Figure 16-12 graphs the sugar digestion of a frozen pure *Clostridia* culture. This suggests that frozen *Clostridia* culture is not very robust or viable after it experiences just a single freeze-thaw cycle. However, *Clostridia* is a known anaerobe. Strict anaerobic procedures were not implemented, the effect of which is unknown in this study.

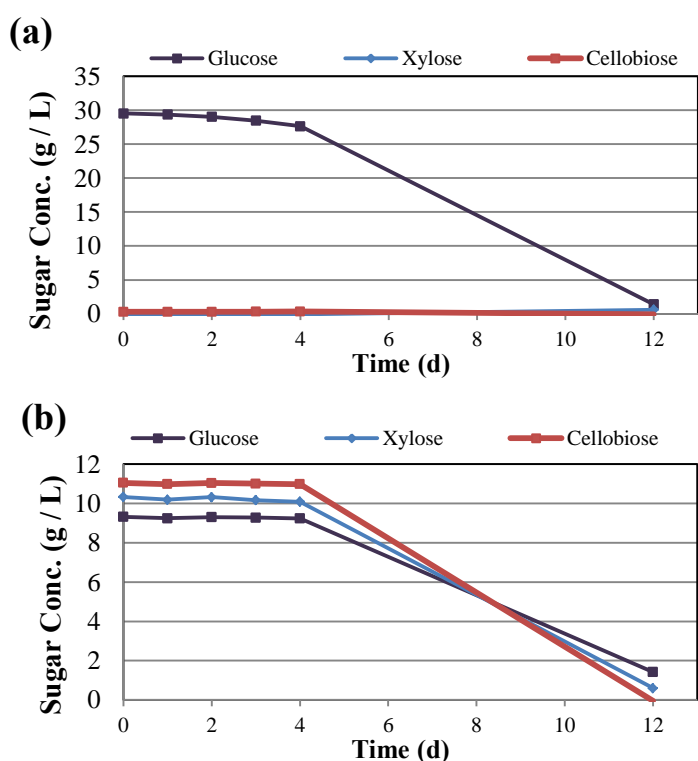


Figure 16-12. Sugar digestion of (a) glucose, and (b) glucose, xylose, and cellobiose inoculated with frozen pure *Clostridia* culture during 12 days.

16.5.4 Overview

After 12 d, all samples (including control) reached 93–94% total sugar conversion. Results suggest that multiple samplings from a single vial have similar results as single samplings from a single vial. Because taking multiple sampling times

from a single glucose-utilization vial is less time consuming and saves resources, this will be used in the future.

16.6 Experiment 5

16.6.1 Objective

Using Method A, the goal of Experiment 5 was to investigate the effects on sugar digestion of vertical and horizontal vial orientation with different inocula.

16.6.2 Materials and methods

Five time points were sampled: 0, 1, 2, 3, and 4 d. Based on the results from Experiment 4, to save time, every time point was collected from the same vial. The sugar-utilization assay was inoculated with three different inocula: (1) soil sediment (College Station, TX), (2) reactor residual biomass, and (3) separated cells (Appendix G). The vials were agitated in a spinning incubator (40 °C, >100 rpm) in the vertical and horizontal orientation. Using Method A, the sugar concentration in the sugar-utilization assay was determined with HPLC. The samples were not diluted when run through the HPLC.

16.6.3 Results and discussion

When samples were collected from the glucose-utilization vial, the vial was opened (not in a hood), a 1-mL sample was quickly taken, and the vial was immediately shut to prevent contamination from microorganisms from the air. To determine if microorganisms from the environment affected the sugar digestion results, a control was used. The control (not shown) had no digestion throughout the 4-day experiment, suggesting that no outside microorganisms were responsible for the digestion over the fairly lengthy digestion time.

Figure 16-13 shows that soil does not have a high total microbial activity. Also, the bacteria in soil digest glucose slightly better than cellobiose and xylose. There are similar results between the horizontal and vertical vial orientations for the soil inoculum.

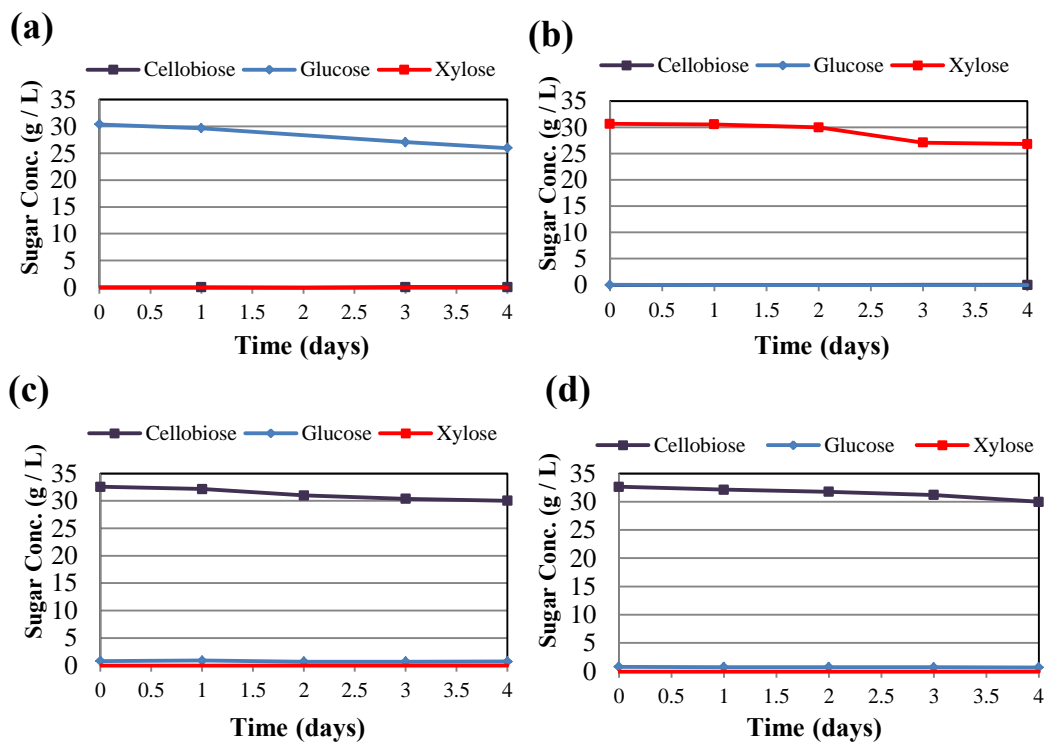


Figure 16-13. Experiment 5 sugar digestion of soil inoculum with vials in (a) horizontal position with glucose, (b) horizontal position with xylose, (c) horizontal position with cellobiose, and (d) vertical position with cellobiose.

Figure 16-14 shows that the solid residual biomass had a high total microbial activity, and it digested cellobiose better than glucose and xylose. For the horizontal orientation, glucose digested linearly whereas cellobiose digested nonlinearly. The cellobiose concentration decreased as it was converted to glucose and then digested. For the horizontal orientation, cellobiose concentration decreased while glucose concentration increased, perhaps because the cellobiose was being hydrolyzed into glucose and not consumed immediately. Error occurred for the vertical vial orientation; therefore, this comparison between vertical and horizontal vial orientation was uncertain. However, the contents of the horizontal vial were visually more agitated than the vertical vial, because of the increased liquid-to-head space area.

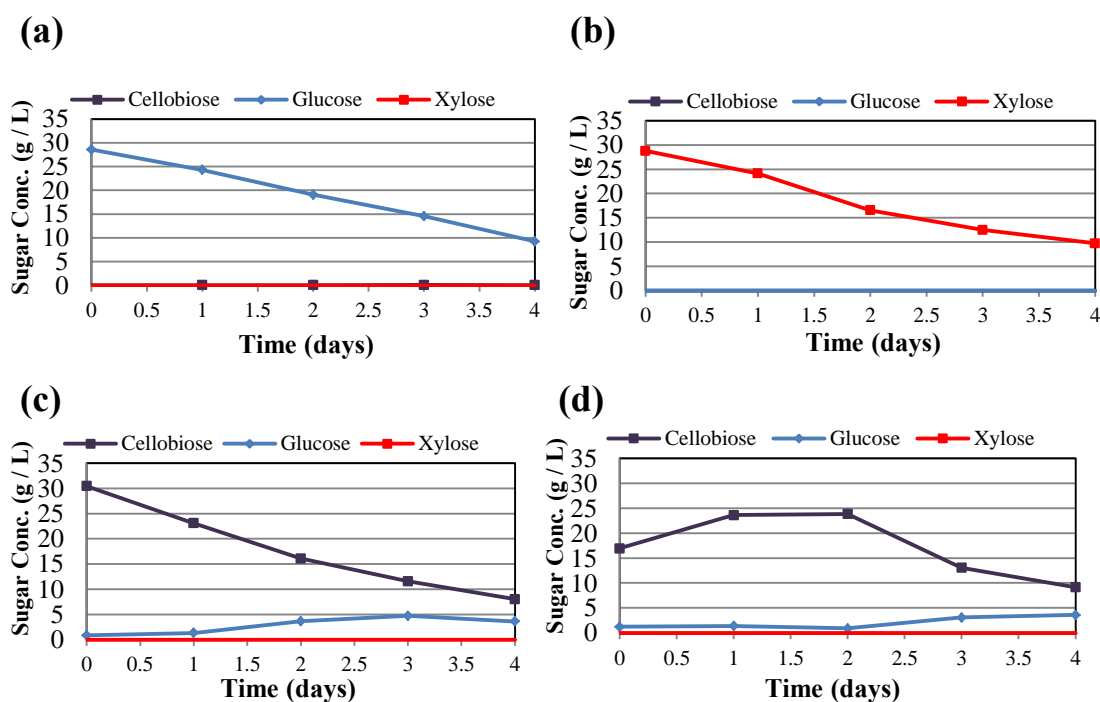


Figure 16-14. Experiment 5 sugar digestion inoculated with fermentation solid waste with vials in (a) horizontal position with glucose, (b) horizontal position with xylose, (c) horizontal position with cellobiose, and (d) vertical position with cellobiose.

Figure 16-15 shows that the separated cells had a high total microbial activity, and they digested cellobiose better than glucose and xylose. The results were ambiguous when comparing vertical and horizontal vial orientation, possibly because of human or machine error.

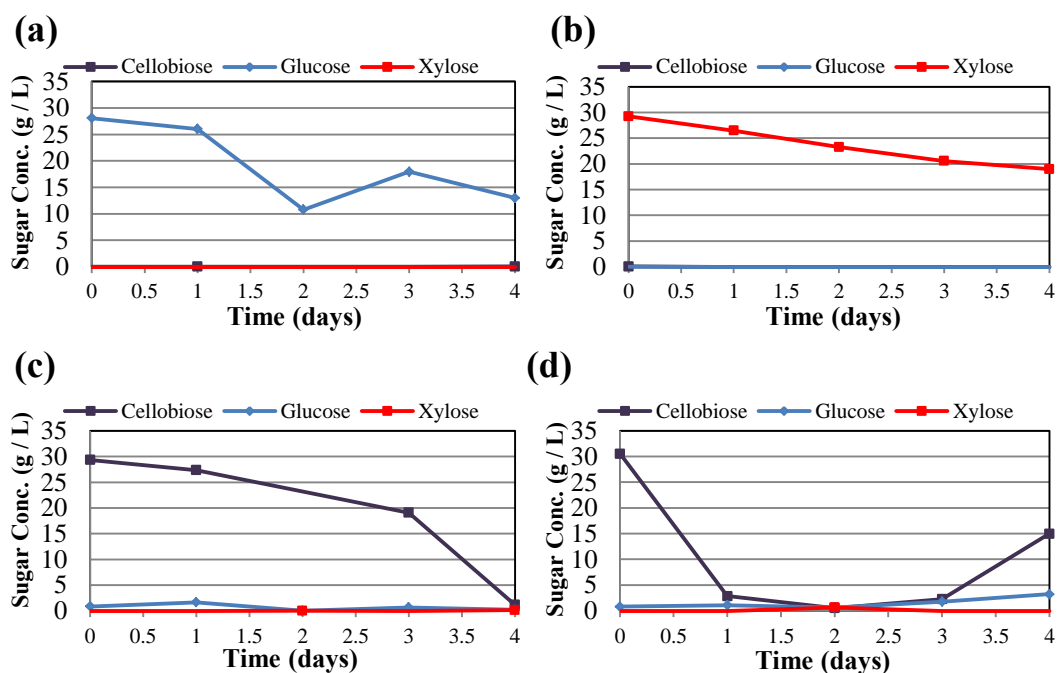


Figure 16-15. Experiment 5 sugar digestion inoculated with cells from bioreactor waste with vials in (a) horizontal position with glucose, (b) horizontal position with xylose, (c) horizontal position with cellobiose, and (d) vertical position with cellobiose.

16.6.4 *Overview*

When visualized, the horizontal vials were better agitated than the vertical vials; therefore, horizontal vial position will be used in future experiments to help obtain better mixing. When comparing vertical and horizontal vial orientation, the results were ambiguous. Error might have occurred because the vertical vials did not digest as well or as homogeneously as the horizontal vials. Because the vertical tubes were not as digested, the sample had more sediment, making it more difficult to filter. An error in filtering might have skewed results; therefore, in the future, sampling vials will be incubated horizontally.

Sugar digestion showed that the reactor waste and cells had a much higher microbial activity than soil samples. However, this definitely depends on the soil sample. This specific soil sample was taken from freshly dug backyard soil with hints of red clay residue (College Station, TX).

16.7 Experiment 6

16.7.1 *Objective*

Using Method A, the goal of Experiment 6 was to investigate the impact of different fermentation ingredients (i.e., paper, yeast extract, nutrient source) on sugar digestion, and the effects of different conditions of the nutrient source (i.e., autoclaved, dry) on sugar digestion.

16.7.2 *Materials and methods*

Five time points were sampled: 0, 1, 2, 3, and 4 d. Based on the results from Experiment 4, to save time, every time point was collected from the same vial. The sugar-utilization assay was inoculated with six different inocula: (1) unsterilized yeast extract, (2) unsterilized shredded office paper, (3) unsterilized wet chicken manure, (4) autoclaved wet chicken manure, (5) unsterilized dry chicken manure, and (6) autoclaved dry chicken manure. The vials were agitated in a spinning incubator (40 °C, >100 rpm) in the horizontal orientation. Only cellobiose and glucose sugar concentrations were run in the sugar-utilization assay, which was analyzed with HPLC (Method A).

16.7.3 Results and discussion

When samples were collected, the vial was opened in the open air, a 1-mL sample was quickly taken, and the vial was immediately shut to prevent contamination from outside microorganisms. To determine if microorganisms from the environment affected the sugar digestion results, a control (not shown) confirmed that the system was unaffected throughout the 4-day experiment.

Figure 16-16 shows that the yeast extract contained cellobiose, which was not readily digested by the bacteria in the yeast extract. The bacteria in the yeast extract appeared to favor glucose.

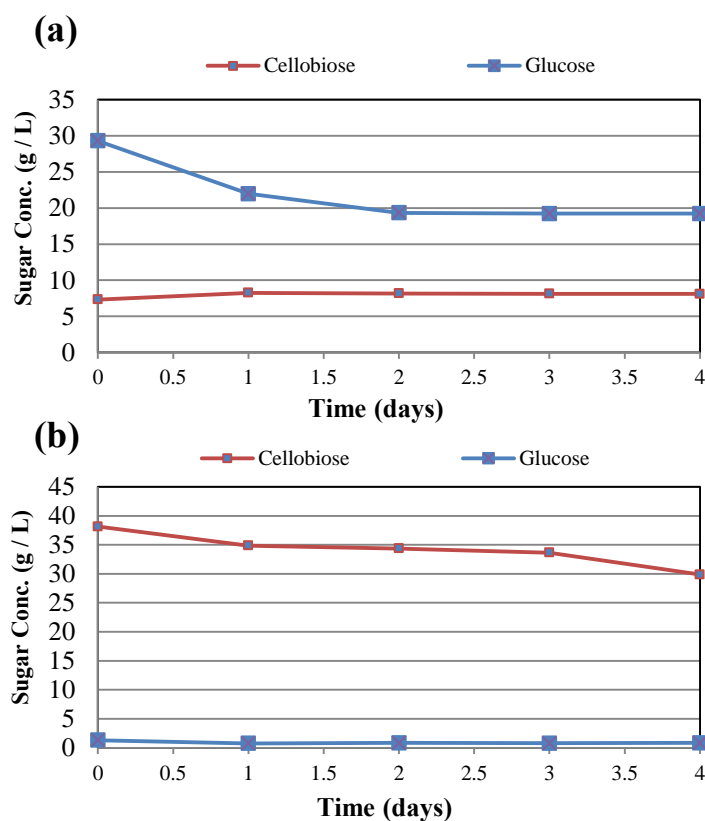


Figure 16-16. Experiment 6 sugar-utilization assay inoculated with unsterilized yeast extract with (a) glucose and (b) cellobiose digestion.

Figure 16-17 shows that the bacteria in paper digested glucose and cellobiose to a small degree. Also, the cellulose in paper appeared to hydrolyze cellobiose.

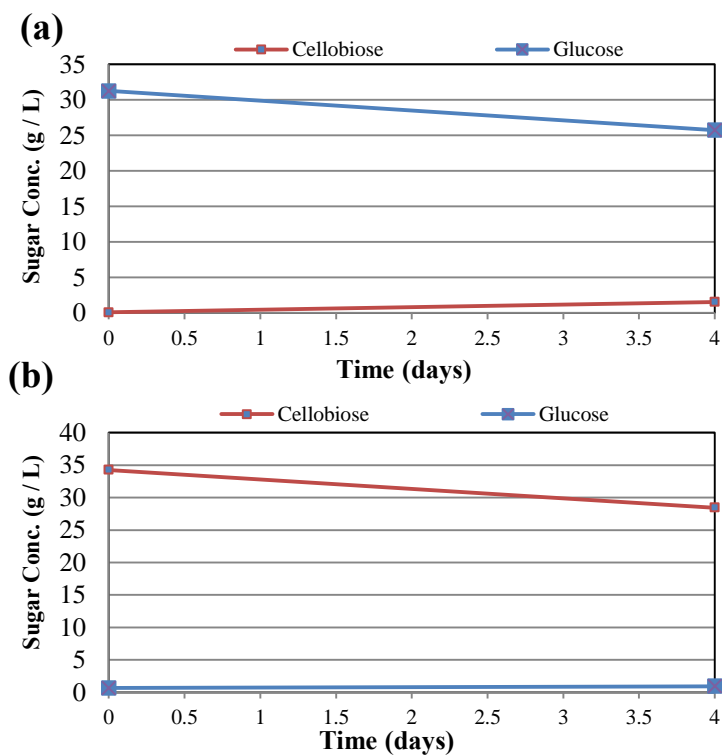


Figure 16-17. Experiment 6 sugar-utilization assay inoculated with unsterilized shredded office paper with (a) glucose and (b) cellobiose digestion.

Figure 16-18 shows the rapid digestion of cellobiose and glucose by unsterilized wet chicken manure. This suggests that unsterilized wet chicken manure has a very high bacterial load, and appears to favor cellobiose over glucose.

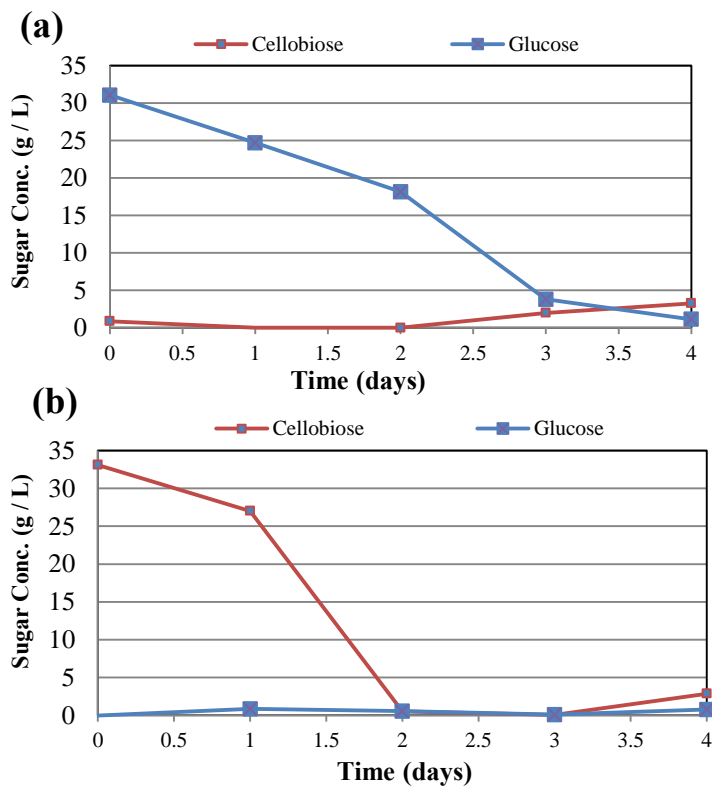


Figure 16-18. Experiment 6 sugar-utilization assay inoculated with unsterilized wet chicken manure with (a) glucose and (b) cellobiose digestion.

Figure 16-19 shows that wet chicken manure was poorly sterilize even when autoclaved, which parallels the results in Ch. 15.

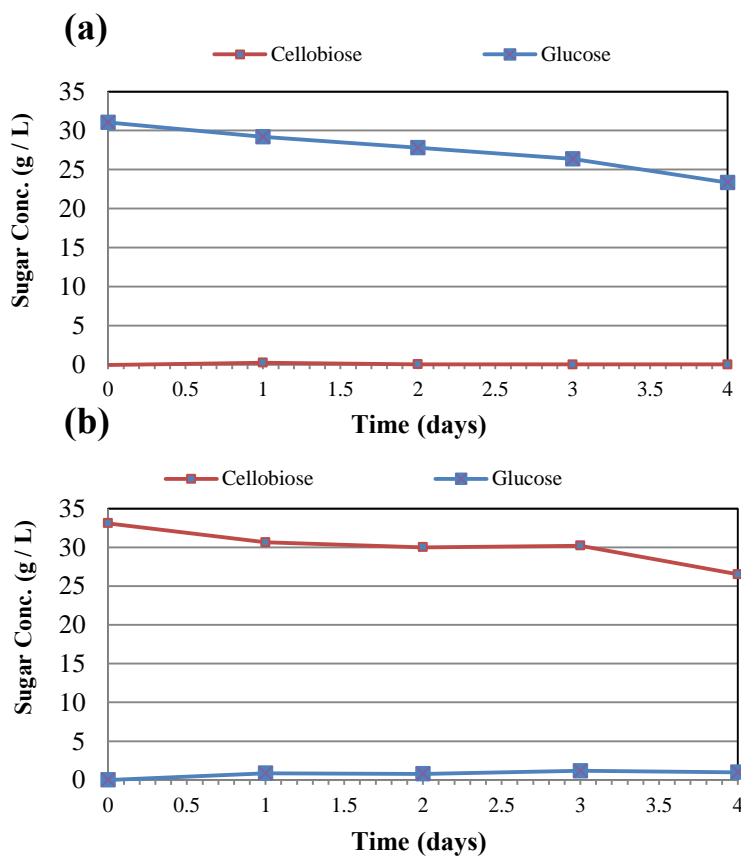


Figure 16-19. Experiment 6 sugar-utilization assay inoculated with autoclaved wet chicken manure with (a) glucose and (b) cellobiose digestion.

Figure 16-20 shows that dry chicken manure was difficult to sterilize even when autoclaved, which parallels the results in Ch. 15.

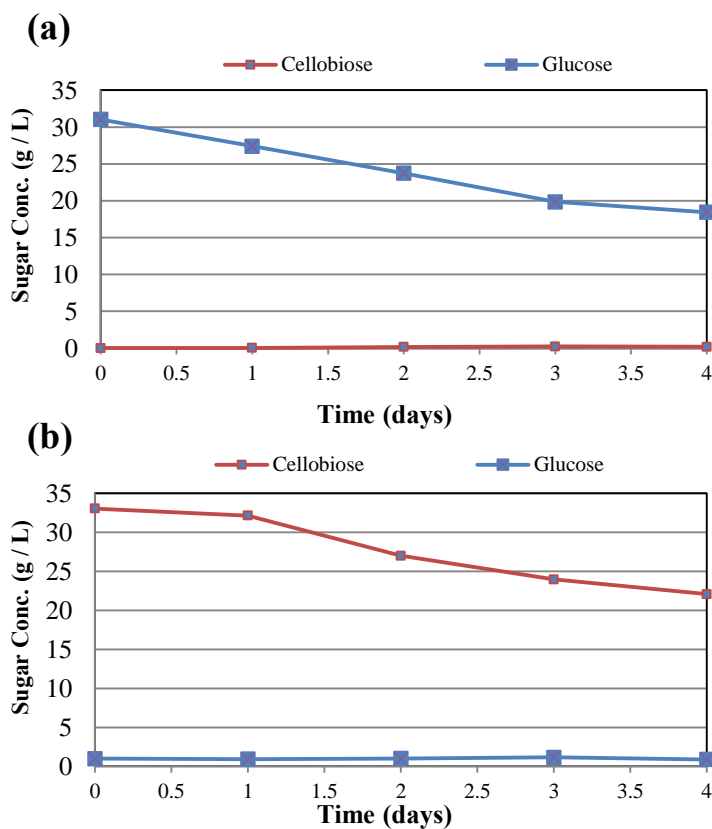


Figure 16-20. Experiment 6 sugar-utilization assay inoculated with unsterilized dry chicken manure with (a) glucose and (b) cellobiose digestion.

Figure 16-21 shows that autoclaved dry chicken manure had much less bacteria than autoclaved wet chicken manure, but volatile nutrients (e.g., nitrogen as ammonia) are lost when chicken manure is dried.

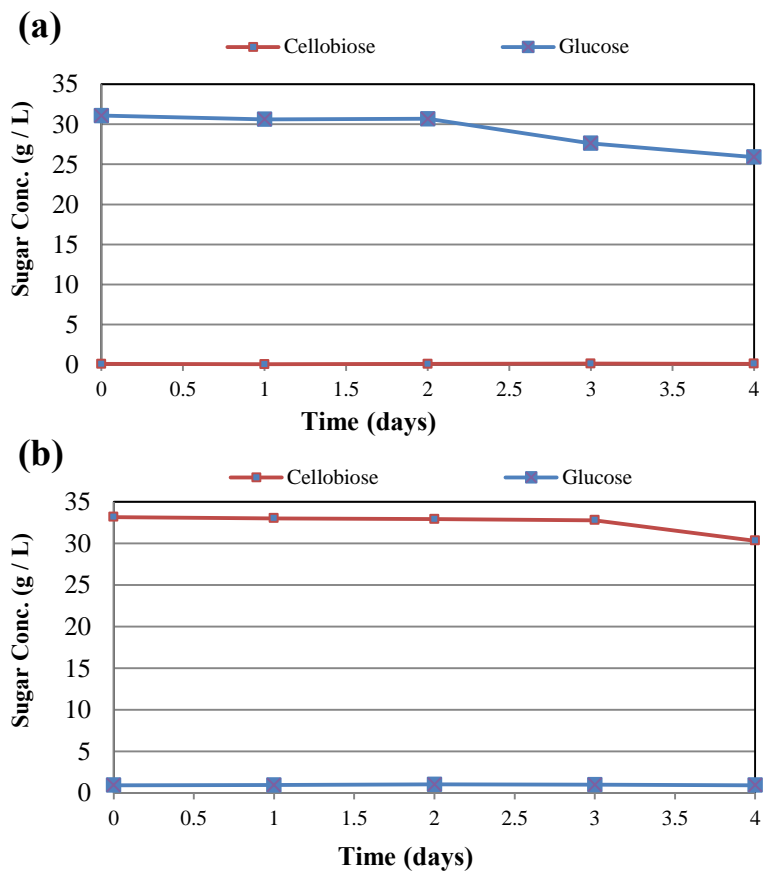


Figure 16-21. Experiment 6 sugar-utilization assay inoculated with autoclaved dry chicken manure with (a) glucose and (b) cellobiose digestion.

16.7.4 *Overview*

Wet chicken manure had a much greater quantity of bacteria, on a wet mass basis, than dry chicken manure. Also, wet chicken manure was harder to sterilize than dry chicken manure, most likely because it had a higher microbial load. Autoclaved dry chicken manure had the least amount of bacterial activity, which is an important consideration when selecting the least-interfering nutrient source for carboxylate fermentations. To maximize total bacterial load, wet chicken manure would be selected as a nutrient source; however, the bacterial community in the wet chicken manure could quite easily outcompete the original inoculum. To minimize the bacterial load from non-inoculating bacteria, autoclaved, dry chicken manure should be selected as a nutrient source; however, there might be loss of nutrient amount/quality (i.e., loss of nitrogen).

16.8 Experiment 7: Glucose oxidase calibration curve (Method B)

16.8.1 *Objective*

The goal of Experiment 7 is to produce calibration curves of absorbance versus glucose concentration in both individual cuvettes (1-mL volume) and 96-well plate (250- μ L volume) for known concentrations of glucose in the glucose oxidase spectrophotometric method (Method B). Also, the goal is to investigate the effect of the MOPS buffer on the calibration curve, to test for interference.

16.8.2 *Materials and methods*

Five glucose concentrations were made (0, 20, 40, 60, and 80 μ g glucose/mL) from three different glucose solutions: (1) a National Institute of Standards and Technology (NIST) glucose standard, (2) a solution prepared with ACS glucose without MOPS (-MOPS), and (3) a solution prepared with ACS glucose with MOPS (+MOPS). These were analyzed in both a 1-mL individual cuvette and a 250- and 100- μ L 96-well plate (570 nm) (Figure 16-5). The glucose concentrations were found with the procedure detailed in Appendices H and I with the glucose oxidase assay kit (Sigma Aldrich, GAGO20).

16.8.3 Results and discussion

Analyzing the glucose concentration in both the 1-mL individual cuvette and 250- μ L 96-well plate gave very similar results. When graphed (Figure 16-22), both yield an R^2 of 0.99, and the same absorbance-glucose concentration equation:

$$\text{Absorbance} = 0.0062 \cdot \text{glucose concentration} + 0.0018 \quad (16-5)$$

Therefore, because the 96-well plate requires less reaction volume, is less costly, and is faster, the 96-well plate can be used in future experiments. The 250- μ L volume well had more linear results and was chosen over the 100- μ L well because of absorbance error at the low volume.

The glucose NIST standard is very similar to the glucose standard prepared in-house with ACS grade glucose, verifying the accuracy of in-house procedures and equipment used to prepare the glucose solution; therefore, glucose standards can be prepared in house with ACS grade glucose for future studies. Also, the glucose solutions with and without MOPS buffer gave very similar results; therefore, MOPS buffer can be added to glucose solutions in the future and will not affect the spectrophotometer readings.

16.8.4 Overview

Glucose solutions were accurately prepared in-house, and MOPS did not affect the absorbance of glucose in the spectrophotometer. For future experiments, instead of a 1-mL cuvette, a 96-well plate can be used for glucose measurements, which is preferable because it is faster, cheaper, and requires less reaction volume. Because of absorbance error at the low volume, the 250- μ L volume was chosen over the 100- μ L volume.

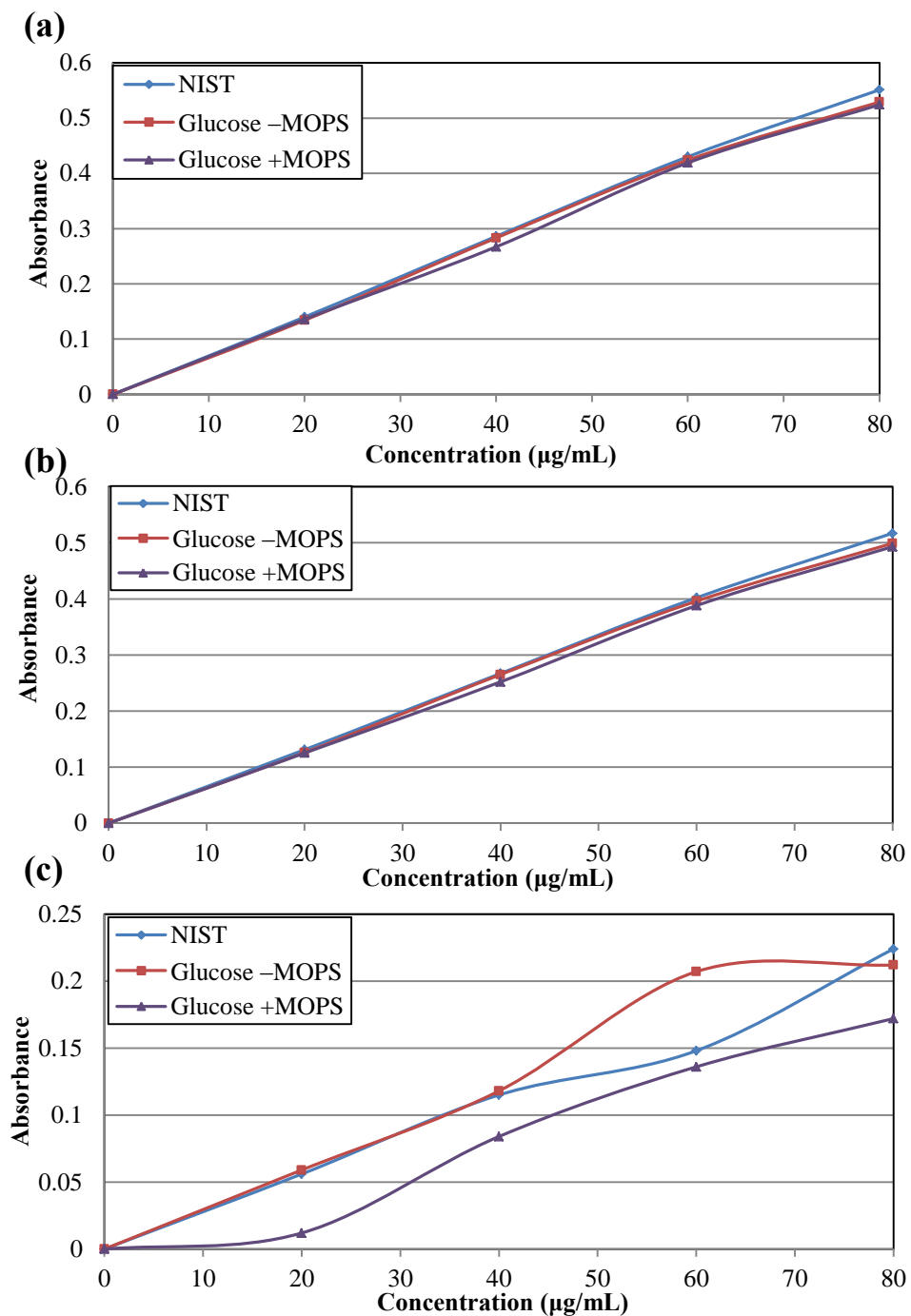


Figure 16-22. Calibration curves for glucose oxidase assay. (a) Glucose concentrations were analyzed with glucose oxidase in 1-mL cuvettes in the spectrophotometer. Glucose concentrations were analyzed with glucose oxidase in a 96-well plate with a volume of (b) 250 μL per well and (c) 100 μL per well in the spectrophotometer.

16.9 Experiment 8: Glucose oxidase calibration curve at different incubation times with potassium phosphate buffer using Method B

16.9.1 Objective

After adding glucose oxidase, the glucose oxidase assay kit (Sigma Aldrich, GAGO20) recommends an incubation time of 30 min. The goal of Experiment 8 is to obtain glucose oxidase calibration curves for different incubation times (Method B) to determine if the incubation time could be decreased to achieve faster results. Also, the interference of potassium phosphate buffer is investigated.

16.9.2 Materials and methods

Five glucose concentrations were made (0, 20, 40, 60, and 80 μg glucose/mL, 50-mM potassium phosphate) and were incubated with glucose oxidase for three separate incubation times: (1) 10 min, (2) 20 min, and (3) 30 min. These were analyzed in a 250- μL 96-well plate (570 nm) (Figure 16-5). The glucose concentrations were found with the procedures detailed in Appendix I.

16.9.3 Results and discussion

Figure 16-23 shows that there is linearity for incubation times of 30, 20, and 10 min. The 10-min incubation achieved an R^2 of 0.99, the 20-min incubation achieved an R^2 of 0.98, and the 30-min incubation achieved an R^2 of 0.99. Therefore, to decrease assay time, an incubation time of 10 min can be used for future experiments.

The 10-min incubation had an absorbance-glucose concentration equation seen below.

$$\text{Absorbance} = 0.0068 \cdot \text{glucose concentration} + 0.0086 \quad (16-6)$$

which was similar to the 20- and 30-min incubation times.

16.9.4 Overview

Based on the R^2 value of 0.99 and the similarity of the absorbance-concentration equation, the 10-min glucose oxidase incubation is sufficient and will allow more rapid processing.

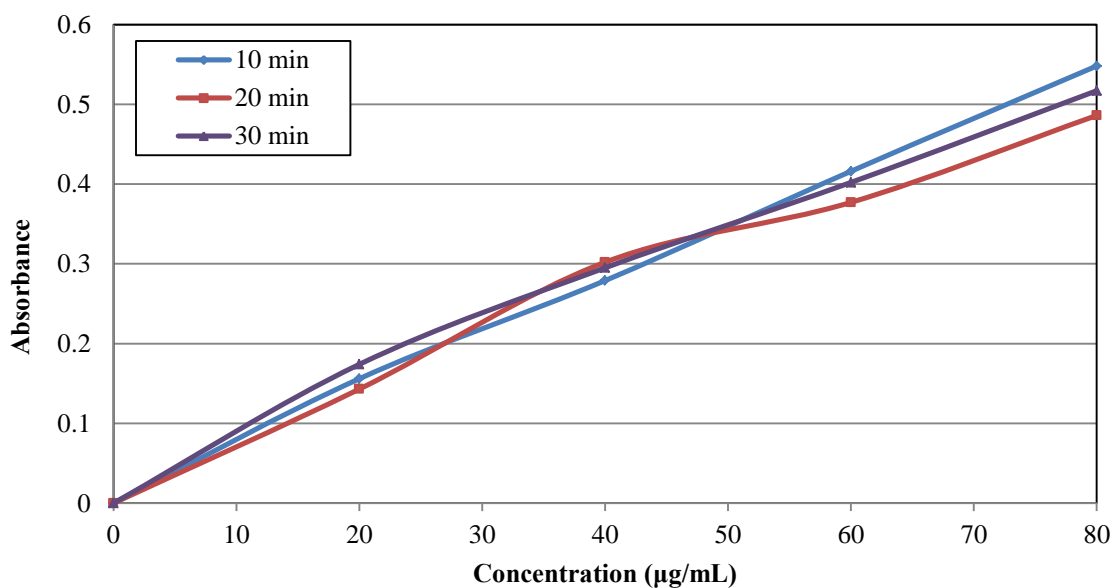


Figure 16-23. Glucose concentration versus absorbance calibration curves for glucose oxidase assay at three different incubation times: 10, 20, and 30 min.

16.10 Experiment 9: The effect of buffer on sugar digestion using Method B

16.10.1 Objective

The goal of Experiment 9 is to determine the effect of buffer on glucose digestion using the glucose oxidase spectrophotometric method (Method B).

16.10.2 Materials and methods

Previously plated *E. coli* (DH5 α) were transferred, by sterilized looping of a colony, to 5 mL of tryptone yeast extract (TYE) media (Appendix J) in round-bottom

tubes. TYE media is a nutrient source that is commonly used to grow bacteria for stocks (Appendix J). The cell stock was grown up for approximately 4–6 h in a shaking incubator (>100 rpm, 37 °C), and then refrigerated. Another round-bottom tube with 5 mL of TYE media was inoculated from the cell stock in a ratio of 1:50 (inoculum:media) for an additional 4–6 h, which was used to inoculate autoclaved glucose solution (80 µg glucose/mL, with and without 0.05-mM potassium phosphate buffer (7.5 pH)).

The glucose-utilization assay was inoculated with *E. coli* and ran for 180 min (procedures are detailed in Appendix H). These were analyzed in a 250-µL 96-well plate (570 nm) (Figure 16-5). The glucose concentrations were found with the procedure detailed in Appendix I.

16.10.3 *Results and discussion*

Figure 16-24 shows the importance of pH when *E. coli* digests glucose. To ensure reproducibility, the pH must be controlled with a buffer in all future sugar digestion assays.

16.10.4 *Overview*

Buffering is crucial for microorganisms to digestion glucose, and all future glucose digestions will be buffered with 50-mM potassium phosphate.

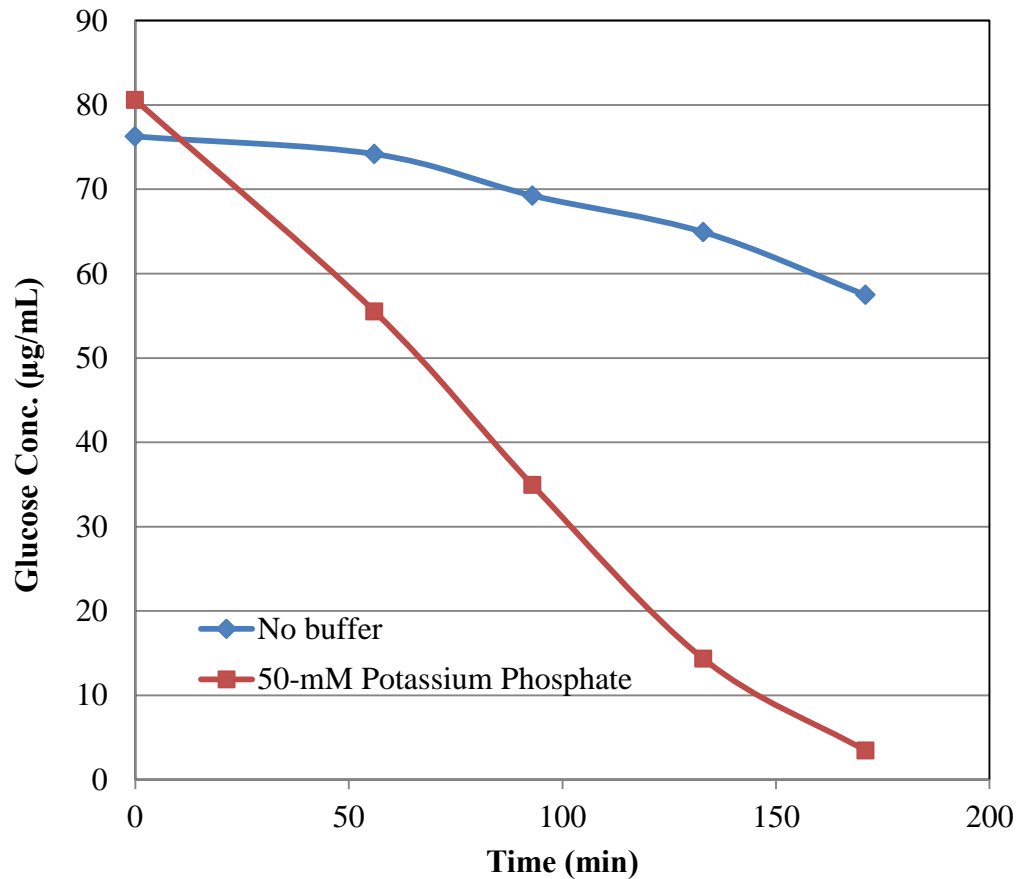


Figure 16-24. Glucose concentration with time for *E. coli* inoculated sugar-utilization assay with and without potassium phosphate buffer.

16.11 Experiment 10: The effect of bacteria type and cell concentration inoculated with cells not at log growth using Method B

16.11.1 Objective

The goal of Experiment 10 is to determine the effect of bacteria type and cell concentration of cells not in the log growth phase using the glucose oxidase spectrophotometric method (Method B).

16.11.2 *Materials and methods*

Previously plated *E. coli* (DH5 α) and *Pseudomonas diminuta* (renamed to *Brevundimonas diminuta*) were transferred, by sterilized looping of a colony, to 5 mL of TYE media (Appendix J) in round bottom tubes. The cell stock was grown up for approximately 4–6 h in a shaking incubator (>100 rpm, 30 °C for *Pseudomonas*, 37 °C *E. coli*), and then refrigerated. Another round-bottom tube with 5 mL of TYE media was inoculated from the cell stock in a ratio of 1:50 (inoculum:media) for an additional 4–6 h, which was used to inoculate autoclaved glucose solution (80 μ g glucose/mL, 50-mM potassium phosphate buffer (7.5 pH)).

The mixed culture originally inoculated the TYE media with fermentation broth in a ratio of 1:5. This cell stock was grown up for approximately 4–6 h, and then refrigerated. Another round-bottom tube with 5 mL of TYE media and 50-mM potassium phosphate buffer (7.5 pH) was inoculated from the stock tube in a ratio of 1:50 (inoculum:media) for an additional 4–6 h, which was used to inoculate autoclaved glucose solution (80 μ g glucose/mL, 50-mM potassium phosphate buffer (7.5 pH)).

All glucose concentrations were analyzed in a 250- μ L 96-well plate (570 nm) (Appendix H). The glucose concentrations were found with the procedure detailed in Appendix I.

16.11.3 *Results and discussion*

E. coli had increased rate of glucose digestion with increasing OD (Figure 16-25); however, *Pseudomonas* and the mixed culture did not digest a significant amount of glucose most likely because they were not in log phase.

16.11.4 *Overview*

The fermentation bacteria and pure *Pseudomonas* were not in the exponential growth phase. Future experiments will include investigating cell growth curves.

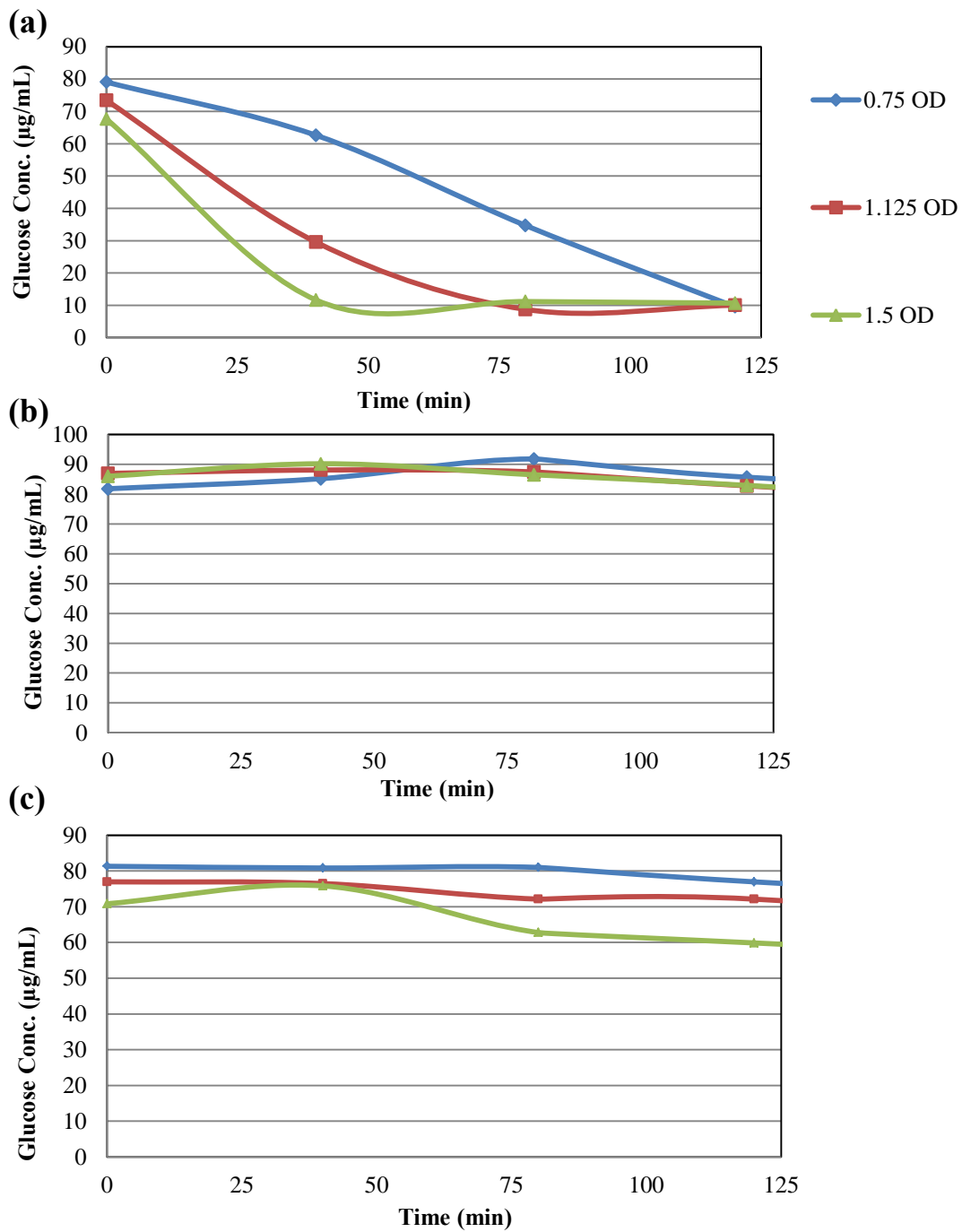


Figure 16-25. Glucose digestion with time inoculated with (a) *E. coli*, (b) *Pseudomonas*, and (c) mixed-culture of bacteria from fermentation solids waste.

16.12 Experiment 11: Sugar-utilization assay inoculated with *E. coli*, *Pseudomonas*, and mixed culture from log growth grown in the presence and absence of glucose using Method B

16.12.1 *Objective*

The goal of Experiment 11 is to determine the growth curves and pH for *E. coli* (DH5 α), *Pseudomonas diminuta*, and fermentation bacteria in the presence and absence of glucose.

16.12.2 *Materials and methods*

Previously plated *E. coli* and *Pseudomonas* were transferred, by sterilized looping of a colony, to 5 mL of TYE media (Appendix J) in round-bottom tubes. The cell stock was grown up for approximately 4–6 h in a shaking incubator (>100 rpm, 30 °C for *Pseudomonas*, 37 °C *E. coli*), and then refrigerated. Another round-bottom tube with 5 mL of TYE media was inoculated from the cell stock in a ratio of 1:50 (inoculum:media), and the OD and pH was recorded in this study.

The mixed culture originally inoculated the TYE media with fermentation broth in a ratio of 1:5. This cell stock was grown up for approximately 4–6 h, and then refrigerated. Another round-bottom tube with 5 mL of TYE media was inoculated from the stock tube in a ratio of 1:50 (inoculum:media), and the OD and pH was recorded in this study. Through spectrophotometry, the OD was recorded (570 nm). The pH was measured with pH strips.

13.1.1 *Results and discussion*

Figure 16-26 displays optical density (OD) of *E. coli* and the mixed culture with time. Also, on the right-hand axis, the pH was recorded. When the cultures that were not preadapted to glucose grew, their OD increased, but their pH remained relatively neutral. However, when the cultures that were preadapted to glucose grew, their OD increased to a lower value, and their pH dropped drastically. The maximum growth rate was proportional to the maximum pH drop. The pH could have dropped because the bacteria began making acids.

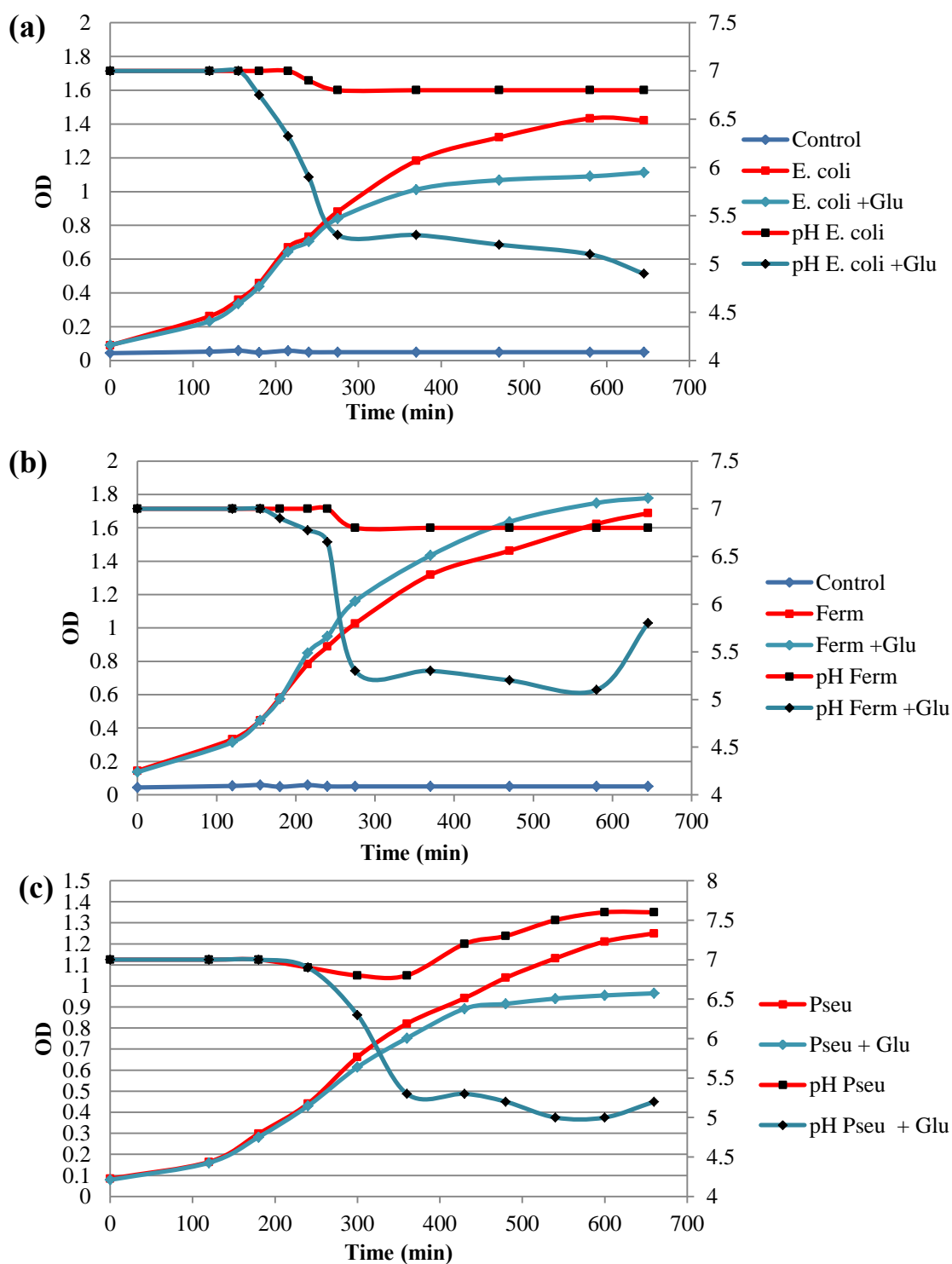


Figure 16-26. Growth curves in the presence and absence of glucose for glucose oxidase assay. The left-hand axis reflects the optical density (OD) of the bacteria with time, and the right-hand axis reflects the pH of the growth media with time for (a) *E. coli*, (b) mixed culture, and (c) *Pseudomonas*.

To determine if the pH drop was caused by acid production, the products were analyzed via HPLC and GC in Table 16-2. The table shows that *E. coli* and mixed culture formed acids, whether they were preadapted to glucose or not. However, the ones that were adapted to glucose made more acids. Therefore, in future studies, all cultures will be grown in the absence of glucose, to prevent pH drop and to ensure reproducibility.

Table 16-2. Acid product concentrations and percent composition of mixed-culture (F) and *E. coli* (E) after incubation in TYE media in the presence (+glu) and absence (–glu) of glucose after a digestion time of 480 min and 1200 min.

Conditions/units	Acid concentration				Composition		
	Lactic acid	Acetic Acid	Propionic Acid	Total	Lactic acid	Acetic Acid	Propionic Acid
	(g/L)	(g/L)	(g/L)	(g/L)	(%)	(%)	(%)
F – 480 min –glu	3.69	0.31	0	4.00	92	8	0
F – 480 min +glu	5.75	0.40	0	6.15	93	7	0
F – 1200 min +glu	0	0.13	0	0.13	0	100	0
E – 480 min –glu	0	0.26	0	0.26	0	100	0
E – 480 min +glu	0	1.68	0.06	1.74	0	97	3

16.12.3 Overview

The maximum cell growth rate for cultures preadapted to glucose in the stock solution was proportional to the maximum pH drop. The pH drop was caused by bacteria producing acids. Therefore, in future studies, all cultures will be grown in TYE in the absence of glucose, to prevent a pH drop and to ensure reproducibility. Also, the middle of log growth phase occurs for *E. coli* at an OD of ~0.8, for *Pseudomonas* at ~0.6, and for the mixed culture at ~1.0. These values can be used in future experiments to ensure that the cell cultures are in log growth before inoculating the sugar-utilization assay.

16.13 Experiment 12: Reproducibility of sugar digestion using Method B

16.13.1 Objective

The goal of Experiment 12 was to determine the reproducibility of the glucose-digestion assay using the glucose oxidase spectrophotometric method (Method B).

16.13.2 Materials and methods

Previously plated *E. coli* (DH5 α) were transferred, by sterilized looping of a colony, to 5 mL of TYE media (Appendix J) in round-bottom tubes. The cell stock was grown up for approximately 4–6 h in a shaking incubator (>100 rpm, 37 °C *E. coli*), and then refrigerated. Another round bottom-tube with 5 mL of TYE media was inoculated from the cell stock in a ratio of 1:50 (inoculum:media) for an additional 2–4 h (until OD was ~0.8 for log growth phase), which was used to inoculate autoclaved glucose solution (80 μ g glucose/mL, 50-mM potassium phosphate buffer (7.5 pH)).

All glucose concentrations were analyzed in a 250- μ L 96-well plate (570 nm) (Appendix H). The glucose concentrations were found with the procedure detailed in Appendix I.

16.13.3 Results and discussion

Figure 16-27 represents three glucose-utilization assays inoculated with *E. coli* from three different cell stock tubes and three different cell growth tubes (E1, E2, E3A). These all grew at similar rates and were inoculated with similar, but not identical, cell ODs.

Figure 16-28 represents three glucose-utilization assays inoculated with *E. coli* from the same cell stock and cell growth tube (E3A, E3B, E3C). These all grew at similar rates and were inoculated with similar cell ODs.

Figures 16-27 and 16-28 show that when cultures are grown and prepared in a standardized condition, the cultures have virtually identical glucose utilization with R^2 of 0.99. These results verify the reproducibility of the glucose-utilization assay.

16.13.4 Overview

The glucose-utilization assay is reproducible when cultures are grown and prepared in standardized conditions because the cultures have virtually identical glucose utilization.

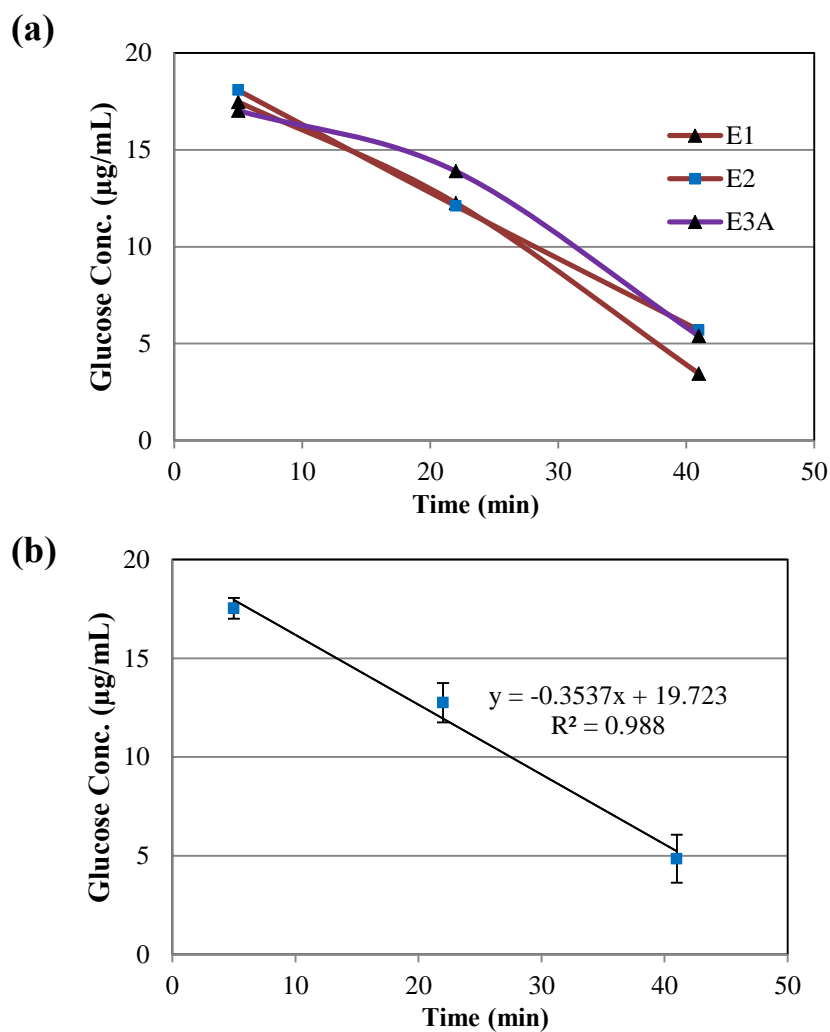


Figure 16-27. Reproducibility of glucose-utilization assay. (a) Three glucose-utilization assays inoculated with *E. coli* from three different cell stock tubes and three different cell growth tubes (E1, E2, E3A), (b) averaged glucose-utilization assay with error bars.

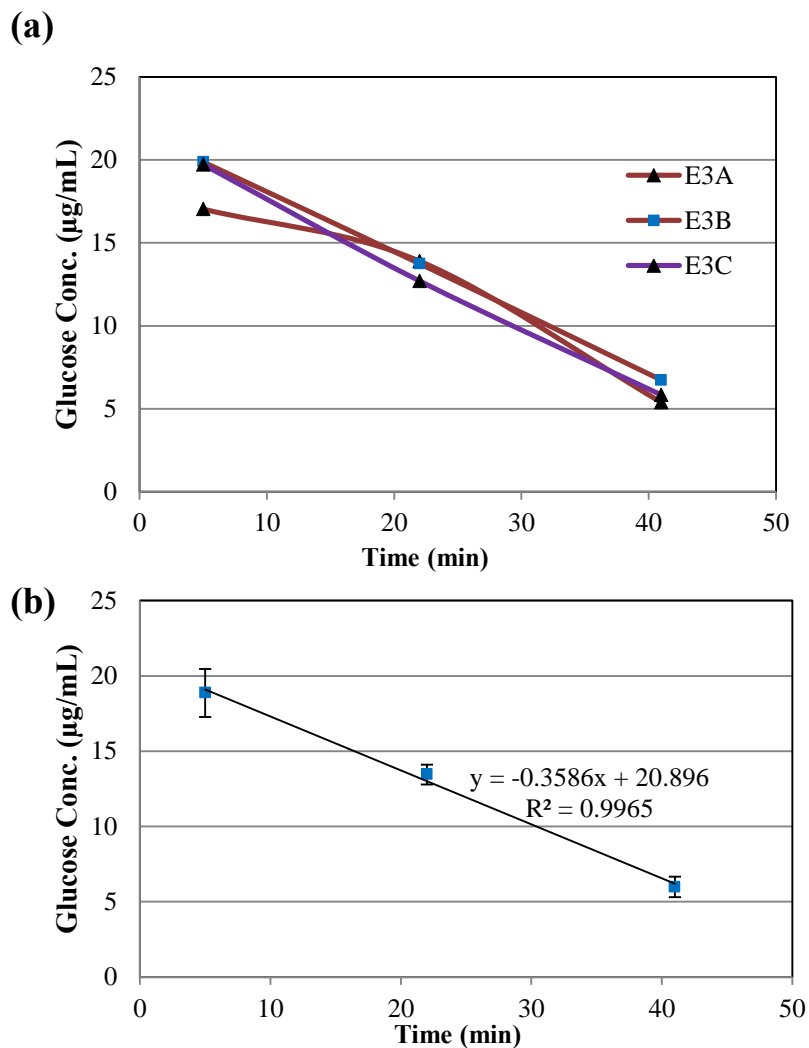


Figure 16-28. Reproducibility of glucose-utilization assay. (a) Three glucose-utilization assays inoculated with *E. coli* from from the same cell stock and cell growth tube (E3A, E3B, E3C), and (b) averaged glucose-utilization assay with error bars.

16.14 Experiment 13: Sugar-utilization assay of *E. coli* and mixed culture from log growth with and without glucose with different inocula-to-media loadings using Method B

16.14.1 Objective

The goal of Experiment 13 is to investigate the effect of glucose addition during the log growth step on glucose digestion using different inocula-to-media loadings using the glucose oxidase spectrophotometric method (Method B).

16.14.2 Materials and methods

Previously plated *E. coli* (DH5 α) were transferred, by sterilized looping of a colony, to 5 mL of TYE media (Appendix J) in round-bottom tubes. The cell stock was grown up for approximately 4–6 h in a shaking incubator (>100 rpm, 37 °C *E. coli*), and then refrigerated. Another round-bottom tube with 5 mL of TYE media was inoculated from the cell stock in a ratio of 1:50, 1:75, 1:100 (inocula:media) for an additional 2–4 h (until OD was ~0.8 for log growth phase), which was used to inoculate autoclaved glucose solution (80 μ g glucose/mL, 50-mM potassium phosphate buffer (7.5 pH)).

The mixed culture originally inoculated the TYE media with fermentation broth in a ratio of 1:5. This cell stock was grown up for approximately 4–6 h, and then refrigerated. Another round-bottom tube with 5 mL of TYE media was inoculated from the stock tube in a ratio of 1:50, 1:75, 1:100 (inocula:media) for an additional 2–4 h (until OD was ~0.8 for log growth phase), which was used to inoculate autoclaved glucose solution (80 μ g glucose/mL, 50-mM potassium phosphate buffer (7.5 pH)).

The culture optical density (OD) was found with spectrophotometry (570 nm). All glucose concentrations were analyzed in a 250- μ L 96-well plate (570 nm) (Appendix H). The glucose concentrations were found with the procedure detailed in Appendix I.

16.14.3 Results and discussion

Figure 16-29 shows the growth curves for *E. coli* and mixed fermentation culture with (+glu) and without glucose adaptation for different loadings of stock cells-to-media ratio (1:50, 1:75, 1:100). The stock cell inoculum was also sampled throughout the run

time, which stayed at the maximum OD in stationary phase. The control was not inoculated and was incubated and sampled throughout.

The cells went through a short lag phase, the log growth phase, and then were beginning the stationary phase of growth. For *E. coli*, the 1:50 inoculum-to-media ratio without glucose appeared to achieve the highest OD of all the inocula loadings. The samples with glucose could have produced acid, which would have inhibited growth. For the fermentation mixed culture, the cultures that were preadapted in glucose-TYE media appeared to reach a slightly higher OD than the cultures that were not preadapted in glucose.

For both *E. coli* and the fermentation mixed culture, for the different inoculum loading conditions, the actual rate of growth appeared to be similar. The *E. coli* without glucose reach the original cell stock OD; however, the fermentation mixed-culture does not.

The glucose-utilization curves (Figure 16-30) display the different glucose digestion curves for *E. coli* and mixed fermentation culture with (+glu) and without glucose adaptation. These cells were harvested from the cultures in the log growth phase for the 1:50 loading of stock cells-to-media ratio, with or without glucose. The cultures were loaded in the glucose-utilization assay (0.5 mL) at concentrations of 0.75 and 1.5 OD.

For *E. coli*, loading with an OD of 1.5 was too concentrated because of the incredibly rapid decrease in glucose concentration. However, the OD of 0.75 appeared to be sufficient. The cultures that were grown in the presence of glucose were more efficient at degrading glucose, which can be seen in the more rapidly decreasing curve for 0.75 OD.

For the mixed fermentation culture, loading with an OD of 1.5 was sufficient for the time period; however, an OD of 0.75 appeared to be too slow for our time period. The cultures that were grown in the presence of glucose were more efficient at degrading glucose.

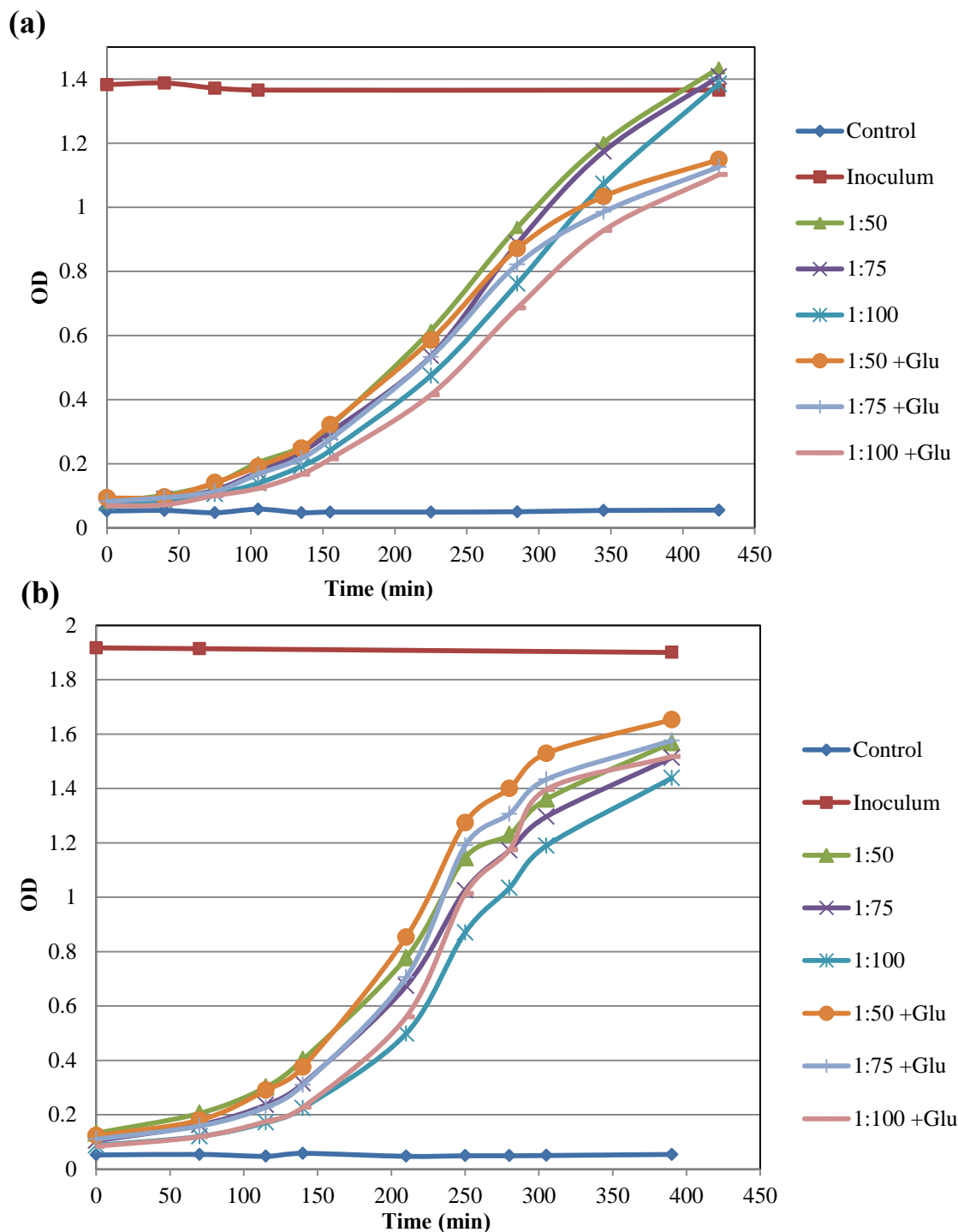


Figure 16-29. Growth curves in the presence and absence of glucose, grown with different ratios of cell stock-to-TYE media. The left hand axis reflects the optical density (OD) of the bacteria with time for (a) *E. coli* and (b) Mixed culture.

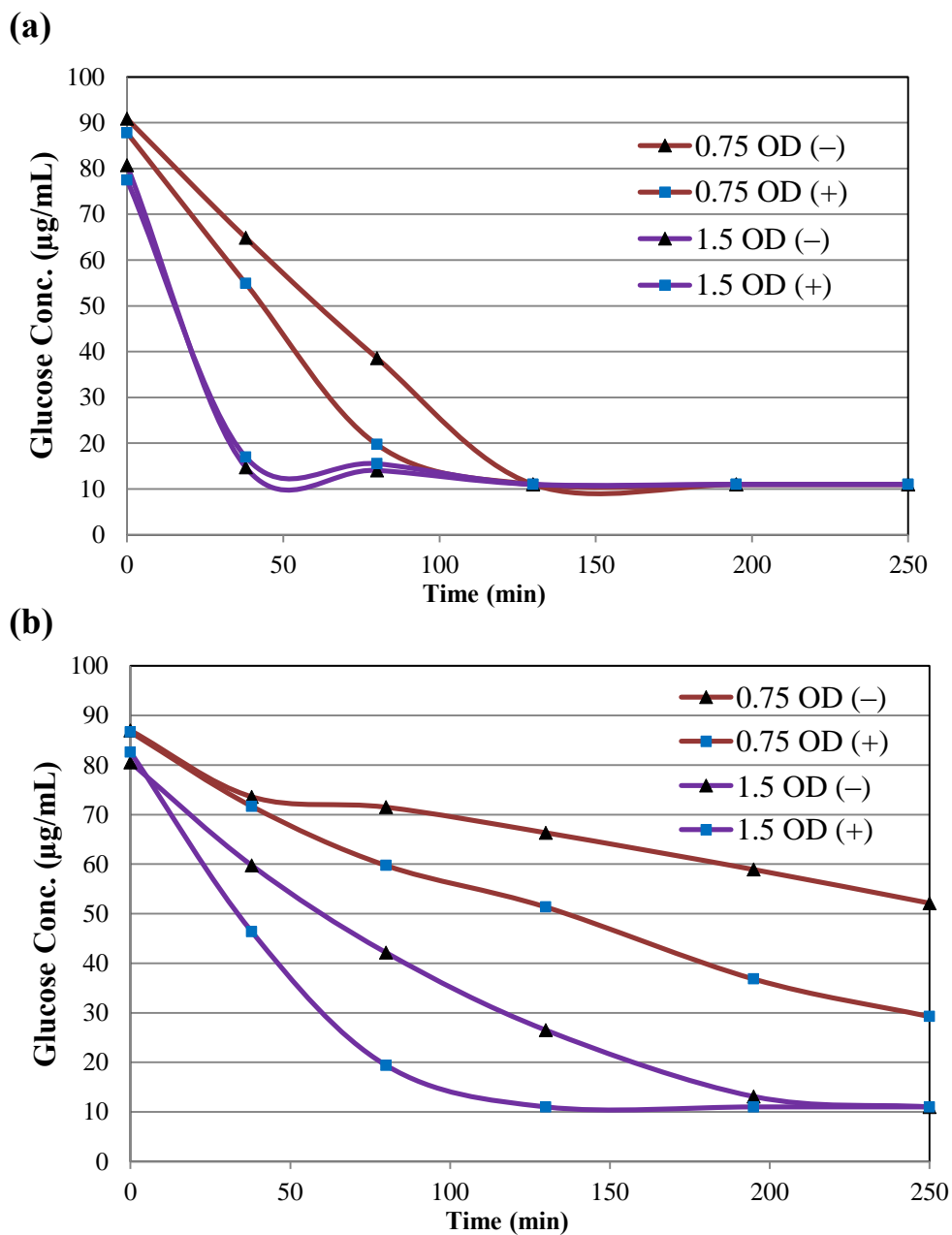


Figure 16-30. Glucose-utilization curves inoculated with cells in the log growth phase grown in the presence (+) and absence (–) of glucose at cell concentrations of 0.75 OD and 1.5 OD. The left hand axis reflects the optical density (OD) of the bacteria with time for (a) *E. coli* and (b) Mixed culture.

16.14.4 *Overview*

The optimal loading of cell culture was from the cultures in the log growth phase for the 1:50 loading of stock cells-to-media ratio without glucose. Although the preadaptation to glucose allowed the culture to digest more glucose, it is unnecessary and could introduce errors and irreproducibility.

16.15 Experiment 15: Sugar-utilization assay of fermentation broth and waste solids using Method B

16.15.1 *Objective*

The goal of Experiment 15 was to investigate the glucose digestion of actual fermentation biomass and liquids using the glucose oxidase spectrophotometric method (Method B).

16.15.2 *Materials and methods*

In the glucose-utilization assay, for better mixing, to prevent contamination from outside microorganisms, and for possible future use of capturing the activity of anaerobes, sealed reaction vessels were used (Figure 16-31). Metal crimps can be used, but for these experiments were not needed.



Figure 16-31. Glass sealed reaction vessels for glucose-utilization assay.

For this glucose-utilization assay, fresh fermentation broth (1 mL) and solid (1 g) portions of a batch fermentation were used to inoculate autoclaved glucose solution (5 mL, 20 μ g glucose/mL, 50-mM potassium phosphate buffer (7.5 pH)) in a capped glass reactor (Figure 16-31) in a water bath (37 °C) and ran for ~160 min (procedures are detailed in Appendix H).

All glucose concentrations were analyzed in a 250- μ L 96-well plate (570 nm). The glucose concentrations were found with the procedure detailed in Appendix I.

16.15.3 *Results and discussion*

As shown in Figure 16-32, the liquid portion of the fermentation inoculum diluted the glucose concentration; however, the glucose digestion can still be captured as the glucose concentration change is more important than the initial value. Both the solid and liquid portions appeared to react at the same rate, signifying that they both have similar microbial activities.

16.15.4 *Overview*

Both the solid and liquid portion of carboxylate fermentations appeared to react at the same rate, signifying that they both have similar microbial activities; more experiments are needed.

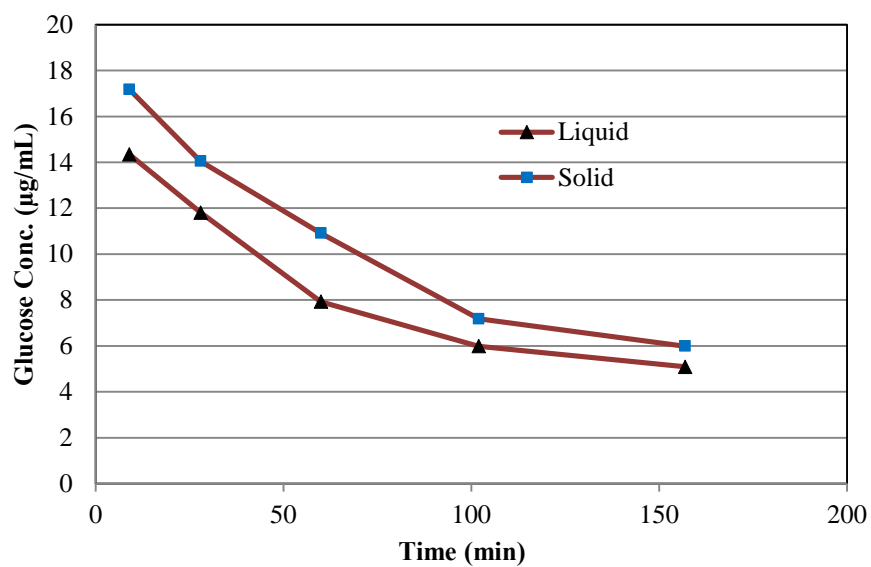


Figure 16-32. Glucose digestion curves inoculated with fermentation mixed-culture cells in the log growth phase grown in the absence of glucose at cell concentrations of 0.75 OD. The left-hand axis reflects the glucose concentration.

16.16 Summary of Experiments 9, 10, 13: Glucose digestion rate with cell concentration

To find the rate of glucose digestion, the change in glucose concentration per time must be found. This is summarized in Table 16-3.

Table 16-3. Glucose-utilization assay summary of experiments for *E. coli* and fermentation mixed culture.

<i>E. coli</i> (DH5 α)							
Experiment	OD	Culture temp. (°C)	Culture dilution	Culture time (min)	Cultured in glu	Rate ($\mu\text{g}/(\text{mL}\cdot\text{min})$)	Time ($C_g = 0$)
9	1	37	1:30	90	–	0.557	171
–	1.5	37	1:20	300	–	1.090	60
	1.125	37	1:20	300	–	0.781	>90
	0.75	37	1:20	300	–	0.367	>90
10	1.5	37	1:10	150	–	1.399	40
	1.125	37	1:10	150	–	1.097	80
	0.75	37	1:10	150	–	0.649	120
13	1.5	37	1:50	240	–	1.736	38
	0.75	37	1:50	240	–	0.613	130
	1.5	37	1:50	240	+	1.592	38
	0.75	37	1:50	240	+	0.851	95

Fermentation Mixed Culture							
Experiment	OD	Culture temp. (°C)	Culture dilution	Culture time (min)	Cultured in glu	Rate ($\mu\text{g}/(\text{mL}\cdot\text{min})$)	Time ($C_g = 0$)
10	1.5	37	1:10	150	–	0.091	>225
	1.125	37	1:10	150	–	0.046	>225
	0.75	37	1:10	150	–	0.036	>225
13	1.5	37	1:50	240	–	0.548	>250
	0.75	37	1:50	240	–	0.114	>250
	1.5	37	1:50	240	+	0.955	120
	0.75	37	1:50	240	+	0.223	195

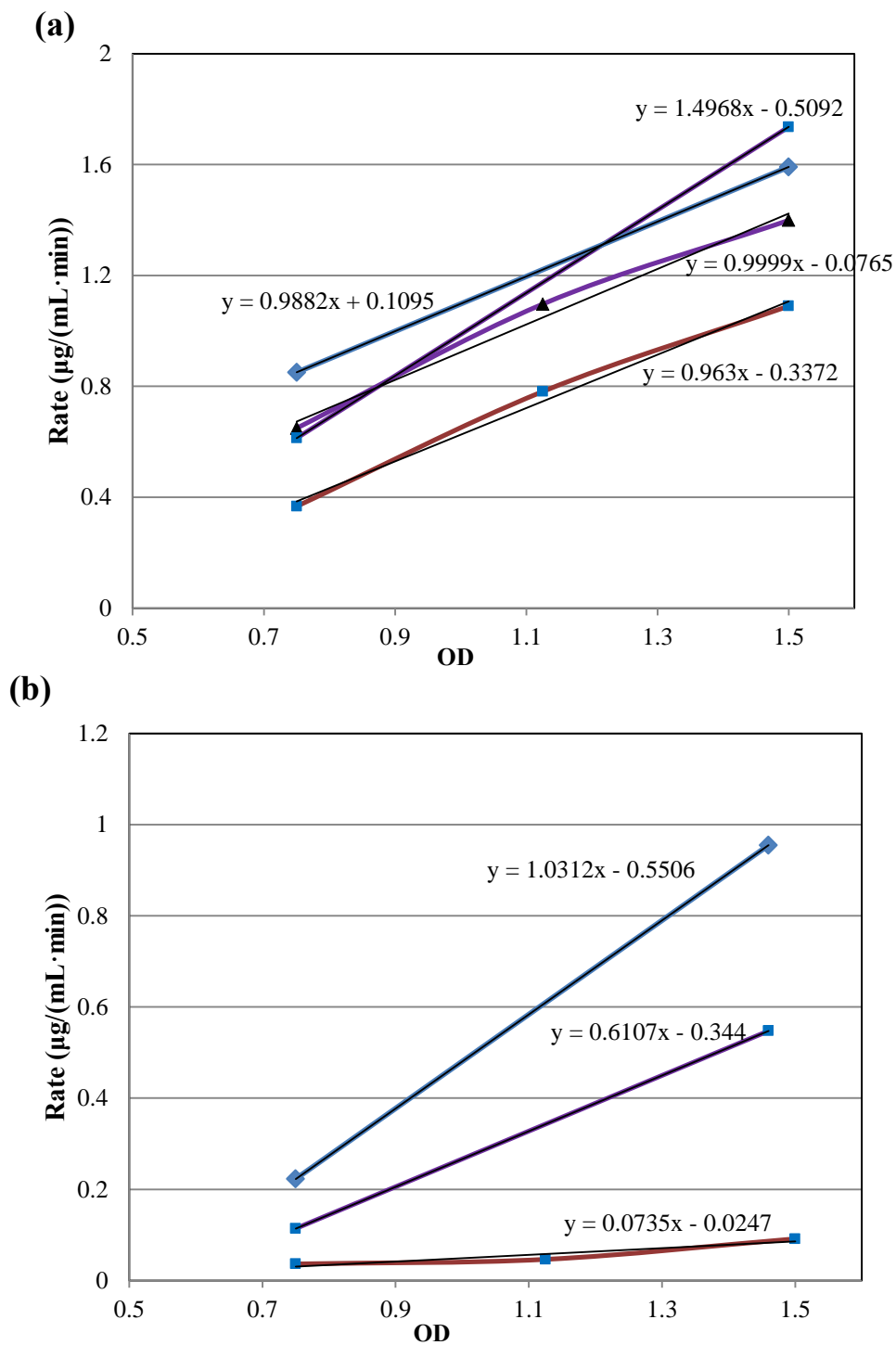


Figure 16-33. Glucose-utilization rate versus optical density (OD) for (a) *E. coli* and (b) fermentation mixed culture.

Based on the results in Figure 16-33 the glucose activities are summarized in Table 16-4.

Table 16-4. Glucose-utilization assay summary of experiments for *E. coli* and fermentation mixed culture.

Experiment	Glucose Activity ($\mu\text{g glucose}/(\text{mL}\cdot\text{min}\cdot\text{OD})$)	
	<i>E. coli</i>	Ferm
(not shown)	0.96	–
10	1.00	0.07
13	1.50	0.61
13 + glu	0.99	1.03

Table 16-4 shows some discrepancy in glucose activity because not all of the cultures were prepared the same way, especially with the fermentation bacteria. For Experiment 10, the fermentation bacteria were not in log growth. Also, when the fermentation bacteria were upcultured, the microbial community changed. Experiment 13 with glucose was different than Experiment 13 (without glucose), because the preadaptation to glucose allowed the microorganisms to become more efficient at digesting glucose. The mixed culture community most likely changed during every upculture, which would make data interpretation futile. However, Table 16-4 helps convey the ultimate goal of the sugar-utilization assay: specific glucose activity.

16.17 Conclusion

Method B of the sugar-utilization assay was much faster and more accurate than Method A. Method B only measured for glucose, which allowed for faster analysis, whereas Method A measure for glucose, xylose, and cellobiose. Also, Method B analyzed the glucose concentration using the glucose oxidase enzyme assay (GOEA), which can use very small concentrations of glucose, allowing the glucose to be measured during a short-duration assay. Method A analyzed the sugar concentrations with HPLC, this required larger concentrations of sugars in the assay, which increased total assay time. Also, Method B analyzed the glucose concentration with a spectrophotometer, which could measure 96 samples in ~8 seconds. Method A analyzed sugar concentration with HPLC, which required ~30 min/sample. In conclusion, Method B is faster, more

accurate, less costly, and more robust than Method A and should be used for future sugar digestion assays.

Measuring only one sugar allows for a more rapid and streamlined analysis. However, measuring the digestion of xylose and cellobiose might allow additional insight into the microbial community. For example, xylose digestion in the presence of glucose could quantify bacteria in the fermentation that prefer five-carbon sugars over six-carbon sugars. Cellobiose digestion in the absence of glucose shows cellulase enzyme efficiency in the fermentation microorganisms.

The glucose-utilization assay is reproducible when cultures are grown and prepared in standardized conditions because the cultures have virtually identical glucose utilization. Based on the R^2 value of 0.99 and the similarity of the absorbance-concentration equation, the 10-min glucose oxidase incubation is sufficient and will allow a more rapid processing than the manufacturer recommended 30-min incubation. Buffering is crucial for reproducible glucose digestion, and all future glucose digestions should be buffered. The optimal loading of cell culture was from the cultures in the log growth phase for the 1:50 loading of stock cells-to-media ratio without glucose. Although the preadaptation to glucose allowed the culture to digest more glucose, it is unnecessary and could introduce errors and irreproducibility.

17. CONCLUSIONS AND RECOMMENDATIONS

17.1 Conclusions

Table 17-1 qualitatively compares the different fermentation configurations and modes of operations.

Table 17-1. Qualitative comparison of performance measures for fermentations operating with different configurations and modes of operation.

	Performance measures					
	Conversion, x (g VS digested/ g VS fed)	Selectivity, σ (g acid produced/ g NAVS consumed)	Exit yield, Y_E (g acid/g NAVS fed)	Productivity, P (g total acid/(L _{liq} ·d))	Total carboxylic acid conc. (g/L)	Aceq-to-total-acid ratio (g/g)
Air Exposure (compared to minimal air exposure)	—	—	—	—	—	↓
Propagated fixed-bed (compared to countercurrent)	↓	—	↓	↓	↓	—
Single stage (compared to four-stage)	↑↑	↓↓	—	—	↓↓	—
Residual biomass recycle (compared to no recycle)	(depends on reflux point)	(depends on reflux point)	↑	↑	—	—
Cell recycle (compared to no recycle)	↓	↑	↑	—	↑	—
Cell recycle (compared to residual biomass recycle)	↓	↑	↑	↑	↑	—

Arrows indicate the qualitative increase or decrease relative to the specified comparison; more arrows indicate a greater change. All comparisons are at optimal C-N ratios. Dashes indicate no difference from the control.

The operating mode that most improved yield over the traditional four-stage countercurrent fermentation was cellular recycle at the higher reflux ratio (~48%). Recycling cells retains microorganisms and boosts selected fermentation performance measures. The cell-separation procedure included diluting and vortexing the biomass to physically dislodge the cells, and separating the solids with a coarse filter and gravity settling. In general, compared to no cell recycle, recycling cellular biomass into Fermentor 1 increased selectivity and yield, but decreased conversion. Compared to lower cell reflux, higher reflux increased productivity, yield, conversion, but decreased selectivity. Generally, compared to residual biomass recycle, cell recycle had increased selectivity and yield but decreased conversion. Therefore, continuous fermentation performance can be increased by implementing cell recycle as opposed to residual biomass recycle, although both are beneficial.

To determine the efficiency of the cell-separation procedure, the glucose-utilization assay was developed, which is a rapid, high-throughput, and repeatable method for determining the amount of microbial activity in a sample. To approximate the concentration of mixed microorganisms in liquid and solid samples from bioprocesses and soil sediment, the specific glucose digestion rate is a measure of microbial activity. Most samples show a variability of less than 5% and R^2 values near unity.

Both the glucose-utilization assay and real-time PCR were used to measure the bacterial concentrations in each of the six different stages. For both the glucose-utilization assay and real-time PCR, the residual biomass had the highest concentration of bacteria. It was difficult to separate the cells from the initial biomass via vortexing. Perhaps vortexing was not enough of a physical disruption to detach the cells from the solid particles; however, too much vortexing might cause cell lysis. The glucose-utilization assay indicated that separated “cells” were 25% of the “cells” in the initial waste biomass. Similarly, the real-time PCR assay indicated that, the separated “cells” were 23% of the “cells” in the initial waste biomass. Thus, the two assay methods are consistent in their estimate of the final cell recovery from the cell recycle procedure.

Because vortexing had poor cell recovery, the residual biomass had the highest microbial load; recycling the raw residual biomass in the continuous carboxylate fermentations would be useful to retain the microorganisms. Unfortunately, refractory compounds (e.g., lignin) would also be recycled, which occupies fermentor volume unproductively. Using vigorous agitation (vortexing), around 25% of the original cells in the biomass can be recycled with very little recycle of refractory materials.

After cellular recycle, the operating mode that next most improved yield was residual biomass recycle at the lower reflux ratio (~14%) to Fermentor 2 and in parallel to Fermentors 1, 2, and 3, which might maximize nutrient and cell concentrations for all respective fermentors, improving most fermentation performance measures. In general, compared to no recycle, recycling residual biomass into Fermentors 1, 2, 3, or in parallel increased yield and productivity. The further the recycle point was from Fermentor 4, where the residual biomass exits, the higher the conversion and lower the selectivity. Relative to lower biomass reflux, higher reflux increased conversion, decreased selectivity, and did not affect acid yield. Because of its simplicity and positive benefit on fermentation performance, industrial carboxylate fermentation systems could employ residual biomass recycle using a 14% reflux ratio. However, if it is desirable to produce other byproducts (e.g., H₂) or reduce solid effluent, then 35% reflux ratio is recommended.

Residual biomass recycle was implemented at different C-N ratios. Generally, compared to the low and high carbon-nitrogen (C-N) ratios, fermentations running at medium C-N ratio increased yield, conversion, and amount of high-molecular-weight acids, but decreased selectivity. Fermentations with excess or limited nitrogen were more efficient at producing acids. The recommended conditions follow: C-N ratio is ~24 g C/g N and recycle to Fermentor 2.

Fermentations with low C-N ratios tended to have high pH. One study involving residual biomass recycle decoupled C-N and pH. At low C-N ratios, high levels of nitrogen are toxic at high pH, but not as toxic at near-neutral pH. Fermentations at low C-N ratios and near-neutral pH, as compared to a high pH, had dramatically improved

yield, conversion, selectivity, productivity, amount of high-molecular-weight acids. Fermentations with excess nitrogen (low C-N ratio) had ~60% higher selectivity. Recycling residual biomass improved performance for low C-N ratio at high pH and medium C-N ratio at low pH. However, at low C-N ratio at near-neutral pH, compared to the no-recycle control, fermentations recycling residual biomass had decreased performance, possibly because inhibiting substances (e.g., ammonium chloride) were recycled.

Propagated fixed-bed fermentations have lower performance than the traditional countercurrent four-stage fermentations. However, propagated fixed-bed fermentations might be more commercially viable because it minimizes solids handling. The propagated fixed-bed fermentation system achieved higher performance at optimal C-N ratios and near-neutral pH. Compared to continuously mixed fermentations, periodic mixing had a similar conversion, but lower yield, selectivity, and acid concentrations. Increasing volatile solid loading rate (VSLR) and increasing liquid residence time (LRT) decreased yield, conversion, selectivity, but increased product concentrations. Compared to countercurrent trains, propagated fixed-bed fermentations have similar selectivities and proportions of acetic acid, but lower yields, conversion, productivities, and acid concentrations.

To investigate the effect of additional fermentors, one- to six-stage countercurrent fermentations were operated with similar LRT and VSLR. Fewer stages increased conversion, whereas more stages increased acid concentration and selectivity. One to four stages achieved similar yields, which were higher than five and six stages. Four to six stages achieved similar maximum acid concentrations (~30 g/L), suggesting that this is the maximum acid concentration that the microorganisms can produce at this LRT and VSLR. Higher acid concentrations that occur with more stages inhibit the microorganisms, which decreases yield and conversion. Carboxylate fermentations achieve maximum conversion with a single stage, but achieve maximum acid concentration with a minimum of four stages.

Mixed-acid fermentations are inoculated with anaerobic bacteria, and therefore, laboratory fermentations are typically operated anaerobically. Industrial fermentations are difficult to maintain anaerobic. To determine the need for industrial fermentations to be operated anaerobically, which would increase costs, fermentations were run with (relaxed) and without (strict) air exposure. Based on total carboxylic acid concentration, strict and relaxed fermentations had similar yields, conversions, and selectivities. However, based on acetic-acid-equivalent concentration, strict trains had significantly higher yields and selectivities than relaxed trains because strict trains produced more high-molecular-weight carboxylic acids. After intermittent oxygen exposure, the microbial flora contained both strict and facultative microbes, and all four fermentor configurations had similar bacterial profiles. Because the quantity and duration of oxygen exposure did not strongly affect fermentor performance or bacterial community composition, an industrial MixAlco™ fermentation could be intermittently exposed to air and maintain efficiency.

The effects of intermittent oxygen exposure on the bacterial profile showed no statistical differences in the bacterial profile of all four fermentor configurations, and that the amount of oxygen transported was sufficiently low to not affect microorganisms. These results suggest the presence of a facultative anaerobic community existing in a biofilm. The facultative anaerobes utilize the majority of oxygen before the oxygen exposure becomes toxic to strict anaerobes; additionally, biofilms may offer strict anaerobes protection from oxygen stresses in the environment.

To find the highest performing inoculum for carboxylate fermentations, five bacterial communities were screened and ranked by three fermentation performance tests: (1) batch screen, (2) continuum particle distribution model, and (3) continuous countercurrent fermentation. For screening numerous inocula sources, these tests would be used sequentially. Comparison of the results from the three tests suggests that Inoculum 1 would achieve the best performance. This study suggests that the three screens are a useful and predictive method for choosing optimal inocula sources in an aseptic environment.

Several substrates were investigated as feedstock in carboxylate fermentations. Pretreated and non-pretreated Sunchips® compostable bags had similar selectivities as other substrates, but lower yields, productivities, and conversions. Higher amounts of oregano supplementation attained a below-average acid concentration, conversion, and productivity compared to fermentations with no oregano supplementation. However, oregano supplementation had similar yield, higher selectivity, and increased production of butyric acid than fermentations with no oregano.

Batch fermentations without iodoform addition achieved over 30% increase in the total carboxylic acid concentrations and higher conversion, yield, and selectivity compared to fermentations with iodoform addition, suggesting that iodoform significantly inhibits the fermentations. Fermentors with iodoform addition had decreased acid concentration, conversion, selectivity, yield, and productivity. Perhaps iodoform strongly inhibits methanogens and slightly inhibits the mixed culture of microorganisms found in carboxylate fermentations.

Bacteria in the chicken manure increase fermentation performance. Because drying and freezing decrease the microbial load in chicken manure, the best-performing fermentations were run with chicken manure as the nutrient source that was wet and never frozen. The fermentation with the worst performance had a chicken manure nutrient source that was dry and previously frozen. Most likely, the freeze-thaw cycle killed a portion of the microorganisms in the chicken manure. Also, drying the chicken manure kills microorganisms and removes nitrogen.

17.2 Future work

Future research should investigate the microorganisms found in carboxylate fermentations, and how the microbial community adjusts to stimuli. If a better understanding of the mixed-culture community is gained, a model could capture this information and allow for more efficient experimental design.

One way to understand the microorganisms is with their substrate digestion rates, which for glucose, can be found with the glucose-utilization assay. For the glucose-utilization assay, future research should include glucose concentration determination

using glucose hexokinase instead of glucose oxidase. This is a safer alternative to the glucose oxidase assay, which requires o-dianisidine (carcinogenic). Also, using the glucose assay, in a batch experiment, the microbial load could be quantified for the duration of the fermentation. For example, the inoculum source can be quantified, and every 7 days, the microbial load can be quantified to determine the rate of microbial growth. If the CPDM method is modified, perhaps these growth rates could be used in model to predict performance.

Similar to the glucose assay, an assay could be developed with xylose or cellobiose as the substrate instead of glucose. This could determine the amount of five-carbon utilizing microorganisms and the microorganisms that can hydrolyze cellobiose, which is necessary for digesting lignocellulose.

Current CPDM models give basic predictions of fermentation performance in carboxylate fermentations, and are accurate within a narrow range. A new model could be developed that include rate equations that incorporate thermodynamics (e.g., Gibbs free energy), which might be dependent on temperature, carbon-nitrogen ratios, and pH. The model could be extended to predict performance with different fermentation mode (e.g., residual biomass recycle, propagated fixed bed, etc.).

Additional investigations could include a model that predicts time to get to steady state. Also, an interesting study would be to incorporate propagated fixed-bed and residual biomass recycle fermentations with different stage numbers, while maintaining constant VSLR, LRT, solids concentrations. Another interesting experiment would be to vary the fresh substrate feed point from Fermentor 1 to another fermentor or a combination of Fermentors 1, 2, and 3. Lastly, investigating methane inhibitors other than iodoform, the lowest effective dose of iodoform, the lifetime of iodoform (i.e., iodoform rate of decomposition), and how much iodoform is absorbed onto the fermentation walls would be helpful to better control and prevent excessive inhibition.

REFERENCES

- Acosta-Martínez, V., Dowd, S., Sun, Y., Allen, V., 2008. Tag-encoded pyrosequencing analysis of bacterial diversity in a single soil type as affected by management and land use. *Soil Biol. Biochem.* 40, 2762–2770.
- Agbogbo, F.K., 2005. Anaerobic fermentation of rice straw and chicken manure to carboxylic acids. Ph.D. Dissertation, Texas A&M University. College Station, TX.
- Agbogbo, F.K., Holtzapple, M.T., 2007. Fixed-bed fermentation of rice straw and chicken manure using a mixed culture of marine mesophilic microorganisms. *Bioresour. Technol.* 98, 1586–1595.
- Agler, M.T., Wrenn, B.A., Zinder, S.H., Angenent, L.T., 2011. Waste to bioproduct conversion with undefined mixed cultures: the carboxylate platform. *Trends Biotechnol.* 29, 70–78.
- Aiello-Mazzarri, C., 2002. Conversion of municipal solid waste to carboxylic acids by anaerobic countercurrent fermentation. Ph.D. Dissertation, Texas A&M University. College Station, TX.
- Aiello-Mazzarri, C., Agbogbo, F.K., Holtzapple, M.T., 2006. Conversion of municipal solid waste to carboxylic acids using a mixed culture of mesophilic microorganisms. *Bioresource Technology* 97, 47–56.
- Aleklett, K., Hook, M., Jakobsson, K., Lardelli, M., Snowden, S., Soderbergh, B., 2010. The Peak of the Oil Age - Analyzing the world oil production Reference Scenario in World Energy Outlook 2008. *Energ. Policy* 38, 1398–1414.
- Allsopp, M., Costner, P., Johnston, P., 2001. Incineration and human health - State of knowledge of the impacts of waste incinerators on human health (Executive summary). *Environmental Science and Pollution Research* 8, 141–145.
- Angenent, L.T., Karim, K., Al-Dahhan, M.H., Wrenn, B.A., Domínguez-Espinosa, R., 2004. Production of bioenergy and biochemicals from industrial and agricultural wastewater. *Trends Biotechnol.* 22, 477–485.
- Antranikian, G., Vorgias, C.E., Bertoldo, C., 2005. Extreme environments as a resource for microorganisms and novel biocatalysts. *Adv. Biochem. Eng. Biotechnol.* 96, 219–262.

- Armaroli, N., Balzani, V., 2011. The Legacy of Fossil Fuels. *Chem.-Asian J.* 6, 768–784.
- Avgustin, G., Wallace, R.J., Flint, H.J., 1997. Phenotypic diversity among ruminal isolates of *Prevotella ruminicola*: Proposal of *Prevotella brevis* sp nov, *Prevotella bryantii* sp nov, and *Prevotella albensis* sp nov and redefinition of *Prevotella ruminicola*. *Int. J. Syst. Bacteriol.* 47, 284–288.
- Blake, D.A., McLean, N.V., 1989. A colorimetric assay for the measurement of d-glucose consumption by cultured cells. *Anal. Biochem.* 177, 156–160.
- Blanch, H.W., Clark, D.C., 1996. *Biochemical Engineering*, Marcel Dekker, Inc. New York.
- Bose, B.K., 2010. Global Warming Energy, Environmental Pollution, and the Impact of Power Electronics. *IEEE Ind. Electron. Mag.* 4, 6–17.
- Bradshaw, D.J., Marsh, P.D., Watson, G.K., Allison, C., 1997. Oral anaerobes cannot survive oxygen stress without interacting with facultative/aerobic species as a microbial community. *Lett. Appl. Microbiol.* 25, 385–387.
- Brandberg, T., Karimi, K., Taherzadeh, M.J., Franzen, C.J., Grustafsson, L., 2007. Continuous fermentation of wheat-supplemented lignocellulose hydrolysate with different types of cell retention. *Biotechnol. Bioeng.* 98, 80–90.
- Brioukhanov, A.L., Netrusov, A.I., 2007. Aerotolerance of strictly anaerobic microorganisms and factors of defense against oxidative stress: A review. *Appl. Biochem. Microbiol.* 43, 567–582.
- Carroll, A., Somerville, C., 2009. Cellulosic biofuels. *Annu. Rev. Plant Biol.* 60, 165–182.
- Casas, E., Martin, J., Tomas-Cobos, L., Garcia-Reverter, J., Villa-Carvajal, M., 2007. Marine natural product bioprospecting: Screening and production bioprocess development of novel bioactive compounds. *J. Biotechnol.* 131, S235–S236.
- Caton, T.M., Witte, L.R., Ngyuen, H.D., Buchheim, J.A., Buchheim, M.A., Schneegurt, M.A., 2004. Halotolerant Aerobic Heterotrophic Bacteria from the Great Salt Plains of Oklahoma. *Microb. Ecol.* 48, 449–462.
- Chan, W.N., Holtzapple, M.T., 2003. Conversion of municipal solid wastes to carboxylic acids by thermophilic fermentation. *Appl. Biochem. Biotechnol.* 111, 93–112.

- Cheremisinoff, P., Ouellette, R., 1985. *Biotechnology Applications and Research*, Technomic Publishing Company, Inc. Lancaster, Pennsylvania.
- Chollet, R., Kukuczka, M., Halter, N., Romieux, M., Marc, F., Meder, H., Beguin, V., Ribault, S., 2008. Rapid detection and enumeration of contaminants by ATP bioluminescence using the Milliflex® Rapid Microbiology Detection and Enumeration System. *Journal of Rapid Methods & Automation in Microbiology* 16, 256–272.
- Choudhury, B., Swaminathan, T., 1998. High cell density lactic acid fermentation with cell recycle bioreactor. *J. Sci. Ind. Res.* 57, 595–599.
- Cole, J.R., Chai, B., Farris, R.J., Wang, Q., Kulam-Syed-Mohideen, A.S., McGarrell, D.M., Bandela, A.M., Cardenas, E., Garrity, G.M., Tiedje, J.M., 2007. The ribosomal database project (RDP-II): introducing myRDP space and quality controlled public data. *Nucleic Acids Res.* 35, D169–D172.
- Cole, J.R., Wang, Q., Cardenas, E., Fish, J., Chai, B., Farris, R.J., Kulam-Syed-Mohideen, A.S., McGarrell, D.M., Marsh, T., Garrity, G.M., Tiedje, J.M., 2009. The Ribosomal Database Project: improved alignments and new tools for rRNA analysis. *Nucleic Acids Res.* 37, D141–D145.
- Contreras-Govea, F.E., Muck, R.E., Mertens, D.R., Weimer, P.J., 2011. Microbial inoculant effects on silage and in vitro ruminal fermentation, and microbial biomass estimation for alfalfa, bmr corn, and corn silages. *Anim. Feed Sci. Technol.* 163, 2–10.
- Crespo, J.P.S.G., Xavier, A.M.R.B., Barreto, M.T.O., Gonçalves, L.M.D., Almeida, J.S., Carrondo, M.J.T., 1992. Tangential flow filtration for continuous cell recycle culture of acidogenic bacteria. *Chem. Eng. Sci.* 47, 205–214.
- Cysewski, G.R., Wilke, C.R., 1977. Rapid ethanol fermentations using vacuum and cell recycle. *Biotechnol. Bioeng.* 19, 1125–1143.
- Das, D., Veziroglu, N., 2001. Hydrogen production by biological processes; a survey of literature. *Int. J. Hydrogen Energy* 26, 13–28.
- Datta, R., 1981. Acidogenic fermentation of corn stover. *Biotechnol. Bioeng.* 23, 61–77.
- Davis, S.J., Peters, G.P., Caldeira, K., 2011. The supply chain of CO₂ emissions. *Proceedings of the National Academy of Sciences*.

- Debaere, L.A., Devocht, M., Vanassche, P., Verstraete, W., 1984. Influence of high NaCl and NH₄Cl salt levels on methanogenic associations. *Water Res.* 18, 543–548.
- Demirbas, A., 2007. Progress and recent trends in biofuels. *Prog. Energy Combust. Sci.* 33, 1–18.
- Demirbas, A., 2008. Biofuels sources, biofuel policy, biofuel economy and global biofuel projections. *Energy Convers. Manage.* 49, 2106–2116.
- DeSantis, T.Z., Hugenholtz, P., Larsen, N., Rojas, M., Brodie, E.L., Keller, K., Huber, T., Dalevi, D., Hu, P., Andersen, G.L., 2006. Greengenes, a chimera-checked 16S rRNA gene database and workbench compatible with ARB. *Appl. Environ. Microbiol.* 72, 5069–5072.
- Di Pasqua, R., Hoskins, N., Betts, G., Mauriello, G., 2006. Changes in membrane fatty acids composition of microbial cells induced by addition of thymol, carvacrol, limonene, cinnamaldehyde, and eugenol in the growing media. *J. Agric. Food Chem.* 54, 2745–2749.
- Domke, S.B., 1999. Fermentation of industrial biosludge, paper fines, bagasse, and chicken manure to carboxylate salts. Ph.D. Dissertation, Texas A&M University. College Station, TX.
- Domke, S.B., Aiello-Mazzarri, C., Holtzapple, M.T., 2004. Mixed acid fermentation of paper fines and industrial biosludge. *Bioresour. Technol.* 91, 41–51.
- Ekinci, K., Keener, H.M., Elwell, D.L., 2000. Composting short paper fiber with broiler litter and additives. *Compost Sci. Util.* 8, 160–172.
- EPA, 2007. Methane: Sources and Emissions, Vol. 2010, U.S. Environmental Protection Agency. Washington, DC.
- EPA, 2008. Municipal Solid Waste Facts, Vol. 2010, U.S. Environmental Protection Agency. Washington, DC.
- Ezzati, M., Kammen, D.M., 2002. The health impacts of exposure to indoor air pollution from solid fuels in developing countries: knowledge, gaps, and data needs. *Environ. Health Perspect.* 110, 1057–1068.
- Felsenstein, J., 2005. PHYLIP (Phylogeny Inference Package) version 3.6, Distributed by author. Department of Genome Sciences, University of Washington, Seattle, WA.

- Forrest, A.K., 2010. Effects of feedstock and inoculum sources on mixed-acid and hydrogen fermentations. Ph.D. Dissertation, Texas A&M University. College Station, TX.
- Forrest, A.K., Hernandez, J., Holtzapple, M.T., 2010a. Effects of temperature and pretreatment conditions on mixed-acid fermentation of water hyacinths using a mixed culture of thermophilic microorganisms. *Bioresour. Technol.* 101, 7510–7515.
- Forrest, A.K., Sierra, R., Holtzapple, M.T., 2010b. Suitability of pineapple, Aloe vera, molasses, glycerol, and office paper as substrates in the MixAlco process(TM). *Biomass Bioenergy* 34, 1195–1200.
- Forrest, A.K., Wales, M.E., Holtzapple, M.T., 2011. Thermodynamic prediction of hydrogen production from mixed-acid fermentations. *Bioresour. Technol.* 102, 9823–9826.
- Fournier, M., Aubert, C., Dermoun, Z., Durand, M.C., Moinier, D., Dolla, A., 2006. Response of the anaerobe *Desulfovibrio vulgaris* Hildenborough to oxidative conditions: proteome and transcript analysis. *Biochimie* 88, 85–94.
- Frutton, J., Simmonds, S., 1959. *General Biochemistry*, John Wiley & Sons, Inc. New York.
- Fu, Z., 2007. Conversion of sugarcane bagasse to carboxylic acids under thermophilic conditions. Ph.D. Dissertation, Texas A&M University. College Station, TX.
- Fu, Z., Holtzapple, M.T., 2010a. Consolidated bioprocessing of sugarcane bagasse and chicken manure to ammonium carboxylates by a mixed culture of marine microorganisms. *Bioresour. Technol.* 101, 2825–2836.
- Fu, Z.H., Holtzapple, M.T., 2010b. Anaerobic mixed-culture fermentation of aqueous ammonia-treated sugarcane bagasse in consolidated bioprocessing. *Biotechnol. Bioeng.* 106, 216–227.
- Golub, K.W., Forrest, A.K., Mercy, K.L., Holtzapple, M.T., 2011a. Propagated fixed-bed mixed-acid fermentation: Part I: Effect of volatile solid loading rate and agitation at high pH. *Bioresour. Technol.* 102, 10592–10601.
- Golub, K.W., Smith, A.D., Hollister, E.B., Gentry, T.J., Holtzapple, M.T., 2011b. Investigation of intermittent air exposure on four-stage and one-stage anaerobic semi-continuous mixed-acid fermentations. *Bioresour. Technol.* 102, 5066–5075.

- Granda, C.B., Holtzapple, M.T., 2008. Biorefineries for solvents: the MixAlco process. in: Bioenergy, (Eds.) J.D. Wall, C.S. Harwood, A. Demain, ASM Press. Washington, DC, pp. 347–360.
- Granda, C.B., Holtzapple, M.T., Luce, G., Searcy, K., Mamrosh, D.L., 2009. Carboxylate platform: The MixAlco process Part 2: Process economics. *Appl. Biochem. Biotechnol.* 156, 537–554.
- Gujer, W., Zehnder, A.J.B., 1983. Conversion Processes in Anaerobic-Digestion. *Water Sci. Technol.* 15, 127–167.
- Hamer, G., 1982. Bioengineering report – recycle in fermentation processes. *Biotechnol. Bioeng.* 24, 511–531.
- Hammes, F., Goldschmidt, F., Vital, M., Wang, Y., Egli, T., 2010. Measurement and interpretation of microbial adenosine tri-phosphate (ATP) in aquatic environments. *Water Res.* 44, 3915–3923.
- Hauxhurst, J.D., Kaneko, T., Atlas, R.M., 1981. Characteristics of bacterial communities in the gulf of Alaska. *Microb. Ecol.* 7, 167–182.
- Hawkes, F.R., Hussy, I., Kyazze, G., Dinsdale, R., Hawkes, D.L., 2007. Continuous dark fermentative hydrogen production by mesophilic microflora: Principles and progress. *Int. J. Hydrogen Energy* 32, 172–184.
- Hileman, B., 1999. Case grows for climate change. *Chemical & Engineering News* 77, 16–23.
- Hollister, E.B., 2008. Land use and land cover change: The effects of woody plant encroachment and prescribed fire on biodiversity and ecosystem carbon dynamics in a Southern Great Plains Mixed Grass Savanna. Ph.D. Dissertation, Texas A&M University. College Station, TX.
- Hollister, E., Forrest, A., Wilkinson, H., Ebbole, D., Malfatti, S., Tringe, S., Holtzapple, M., Gentry, T., 2010. Structure and dynamics of the microbial communities underlying the carboxylate platform for biofuel production. *Appl. Microbiol. Biotechnol.* 88, 389–399.
- Hollister, E.B., Hammett, A.J., Holtzapple, M.T., Gentry, T.J., Wilkinson, H.H., 2011. Microbial community composition and dynamics in a semi-industrial scale facility operating under the MixAlco™ bioconversion platform. *J. Appl. Microbiol.*, 587–596.

- Holtzapple, M.T., Davidson, R.R., Ross, M.K., Aldrett-Lee, S., Nagawani, M., Lee, C.-M., Lee, C., Adelson, S., Karr, W., Gaskin, D., Shiraga, H., Chang, N.-S., Chang, V.S., Loescher, M.E., 1999. Biomass conversion to mixed alcohol fuels using the MixAlco process. *Appl. Biochem. Biotechnol.* 77–79, 609–631.
- Holtzapple, M.T., Granda, C.B., 2009. Carboxylate platform: The MixAlco process Part 1: Comparison of three biomass conversion platforms. *Appl. Biochem. Biotechnol.* 156, 525–536.
- Humayoun, S.B., Bano, N., Hollibaugh, J.T., 2003. Depth Distribution of Microbial Diversity in Mono Lake, a Meromictic Soda Lake in California. *Appl. Environ. Microbiol.* 69, 1030–1042.
- Hungate, R.E., 1966. *The Rumen and Its Microbes*, Academic Press Inc. New York, New York.
- IEA, 2011a. Key world energy statistics. International Energy Agency.
- IEA, 2011b. World energy outlook: Executive summary. International Energy Agency.
- IEA, 2011c. Worldwide production of biofuels in 2008. U.S. Department of Energy.
- Jefferson, M., 2006. Sustainable energy development: performance and prospects. *Renewable Energy* 31, 571–582.
- Karel, S.F., Libicki, S.B., Robertson, C.R., 1985. The immobilization of whole cells – engineering principles. *Chem. Eng. Sci.* 40, 1321–1354.
- Khanal, S.K., 2008. *Anaerobic biotechnology for bioenergy production, principles and applications*, Wiley-Blackwell.
- Kim, M., Gomec, C.Y., Ahn, Y., Speece, R.E., 2003. Hydrolysis and acidogenesis of particulate organic material in mesophilic and thermophilic anaerobic digestion. *Environ. Technol.* 24, 1183–1190.
- Kleerebezem, R., van Loosdrecht, M.C.M., 2007. Mixed culture biotechnology for bioenergy production. *Curr. Opin. Biotechnol.* 18, 207–212.
- Kojima, M., Mitchell, D., Ward, W., 2007. "Considering Trade Policies for Liquid Biofuels," Energy Sector Management Assistance Program Renewable Energy Special Report 004/07, World Bank.
- Koskinen, P.E.P., Lay, C.H., Beck, S.R., Tolvanen, K.E.S., Kaksonen, A.H., Orlygsson, J., Lin, C.Y., Puhakka, J.A., 2008. Bioprospecting thermophilic microorganisms

- from Icelandic hot springs for hydrogen and ethanol production. *Energy & Fuels* 22, 134–140.
- Koster, I.W., 1984. Liquefaction and acidogenesis of tomatoes in an anaerobic 2-phase solid-waste treatment system. *Agr. Wastes* 11, 241–252.
- Kunii, D., Levenspiel, O., 1969. *Fluidization Engineering*. 2, Butterworth-Heinemann. New York.
- Landoll, M.P., Holtzaple, M.T., 2011. Thermal decomposition of mixed calcium carboxylate salts: Effects of lime on ketone yield. *Biomass Bioenerg.* 35, 3592–3603.
- Leary, D., Vierros, M., Hamon, G., Arico, S., Monagle, C., 2009. Marine genetic resources: A review of scientific and commercial interest. *Mar. Policy* 33, 183–194.
- Ley, R.E., Harris, J.K., Wilcox, J., Spear, J.R., Miller, S.R., Bebout, B.M., Maresca, J.A., Bryant, D.A., Sogin, M.L., Pace, N.R., 2006. Unexpected Diversity and Complexity of the Guerrero Negro Hypersaline Microbial Mat. *Appl. Environ. Microbiol.* 72, 3685–3695.
- Lin, C.Y., Lay, C.H., 2004. Carbon/nitrogen-ratio effect on fermentative hydrogen production by mixed microflora. *Int. J. Hydrogen Energy* 29, 41–45.
- Liu, H., Cheng, S.A., Logan, B.E., 2005. Production of electricity from acetate or butyrate using a single-chamber microbial fuel cell. *Environ. Sci. Technol.* 39, 658–662.
- Liu, H., Chen, Y., Dul, G., Chen, J., Liu, X., 2008. Effects of organic matter and initial carbon-nitrogen ratio on the bioconversion of volatile fatty acids from sewage sludge. *J. Chem. Technol. Biotechnol.* 83, 1049–1055.
- Loesche, W.J., 1969. Oxygen Sensitivity of Various Anaerobic Bacteria. *Appl. Microbiol.* 18, 723–727.
- Loescher, M.E., 1996. Volatile Fatty Acid Fermentation of Biomass and Kinetic Modeling Using the CPDM Method. Ph.D. Dissertation, Texas A&M University. College Station, TX.
- Lü, F., Chen, M., He, P.J., Shao, L.M., 2008. Effects of ammonia on acidogenesis of protein-rich organic wastes. *Environ. Eng. Sci.* 25, 114–122.

- Maeda, M., Taga, N., 1980. Alkalotolerant and alkalophilic bacteria in seawater. *Mar. Ecol.-Prog. Ser.* 2, 105–108.
- Mesbah, N.M., Abou-El-Ela, S.H., Wiegel, J., 2007. Novel and Unexpected Prokaryotic Diversity in Water and Sediments of the Alkaline, Hypersaline Lakes of the Wadi An Natrun, Egypt. *Microb. Ecol.* 54, 598–617.
- Metzler, D., 2001. *Biochemistry: The Chemical Reactions of Living Cells*, 2nd edn., Academic Press. San Diego.
- Meysing, D., 2011. Investigations of biomass pretreatment and submerged fixed-bed fermentation. M.S. Thesis, Texas A&M University. College Station, TX.
- Miller, M.B., Bassler, B.L., 2001. Quorum sensing in bacteria. *Annu. Rev. Microbiol.* 55, 165–199.
- Min, B., Angelidaki, I., 2008. Innovative microbial fuel cell for electricity production from anaerobic reactors. *J. Power Sources* 180, 641–647.
- Moody, A.G., 2006. Pilot-scale Fermentation of Office Paper and Chicken Manure to Carboxylic Acids. M.S. Thesis, Texas A&M University. College Station, TX.
- Morris, J.G., 1976. 5th Stenhouse-Williams Memorial Lecture Oxygen and Obligate Anaerobe. *J. Appl. Bacteriol.* 40, 229–244.
- Nakamura, S., Ogura, Y., 1968. Mode of inhibition of glucose oxidase by metal ions. *J. Biochem.* 64, 439–447.
- Nawrocki, E.P., Kolbe, D.L., Eddy, S.R., 2009. Infernal 1.0: Inference of RNA alignments. *Bioinformatics* 25, 1335–1337.
- Neidhardt, F., Ingraham, J., Schaechter, M., 1990. *Physiology of the bacterial cell*, Sinauer Associates, Inc. Sunderland.
- Nicholson, C.A., Fathepure, B.Z., 2005. Aerobic biodegradation of benzene and toluene under hypersaline conditions at the Great Salt Plains, Oklahoma. *FEMS Microbiol. Rev.* 245, 257–262.
- Nigam, P.S., Singh, A., 2011. Production of liquid biofuels from renewable resources. *Prog. Energy Combust. Sci.* 37, 52–68.
- Nishiwaki, A., Dunn, I.J., 1999. Performance of a two-stage fermentor with cell recycle for continuous production of lactic acid. *Bioprocess Biosystems Eng.* 21, 299–305.

- NREL, 1999. Lignocellulosic biomass to ethanol process design and economics utilizing co-current dilute acid prehydrolysis and enzymatic hydrolysis current and futuristic scenarios. Technical report. National Renewable Energy Laboratory, Golden, CO.
- NREL, 2004. Biomass analysis technology team laboratory analytical procedure. Technical report. National Renewable Energy Laboratory, Golden, CO.
- Oren, A., 2002. Halophilic Microorganisms and Their Environment, Kluwer Academic. Boston.
- Palmqvist, E., Galbe, M., Hahn-Hagerdal, B., 1998. Evaluation of cell recycling in continuous fermentation of enzymatic hydrolysates of spruce with *Saccharomyces cerevisiae* and on-line monitoring of glucose and ethanol. *Appl. Microbiol. Biotechnol.* 50, 545–551.
- Perlack, R.D., Wright, L.L., Turhollow, A.F., Graham, R.L., Stokes, B.J., Erbach, D.C., 2005. Biomass as feedstock for a bioenergy and bioproducts industry: The technical feasibility of a billion-ton annual supply. Oak Ridge National Laboratory, Oak Ridge, TN.
- Pham, V., Holtzapfle, M., El-Halwagi, M., 2010. Techno-economic analysis of biomass to fuel conversion via the MixAlco process. *J. Ind. Microbiol. Biotechnol.* 37, 1157–1168.
- Pynaert, K., Smets, B.F., Wyffels, S., Beheydt, D., Siciliano, S.D., Verstraete, W., 2003. Characterization of an autotrophic nitrogen-removing biofilm from a highly loaded lab-scale rotating biological contactor. *Appl. Environ. Microbiol.* 69, 3626–3635.
- Ragauskas, A.J., Williams, C.K., Davison, B.H., Britovsek, G., Cairney, J., Eckert, C.A., Frederick, W.J., Hallett, J.P., Leak, D.J., Liotta, C.L., Mielenz, J.R., Murphy, R., Templer, R., Tschaplinski, T., 2006. The path forward for biofuels and biomaterials. *Science* 311, 484–489.
- Reis, M.A.M., Serafim, L.S., Lemos, P.C., Ramos, A.M., Aguiar, F.R., Van Loosdrecht, M.C.M., 2003. Production of polyhydroxyalkanoates by mixed microbial cultures. *Bioprocess Biosystems Eng.* 25, 377–385.
- REN21, 2011. Renewables 2011 global status report. (Paris: REN21 Secretariat).
- Rodriguez, J., Kleerebezem, R., Lema, J., van Loosdrecht, M., 2006. Modeling product formation in anaerobic mixed culture fermentations. *Biotechnol. Bioeng.* 93, 592–606.

- Rokem, J.S., Goldberg, I., Mateles, R.I., 1980. Growth of Mixed Cultures of Bacteria on Methanol. *J. Gen. Microbiol.* 116, 225–232.
- Rosillo-Calle, F., Hall, D.O., 1992. Biomass energy, forests and global warming. *Energ. Policy* 20, 124–136.
- Ross, M.K., 1998. Production of acetic acid from waste biomass. Ph.D. Dissertation, Texas A&M University. College Station, TX.
- Ross, M.K., Holtzapple, M.T., 2001. Laboratory method for high-solids countercurrent fermentations. *Appl. Biochem. Biotechnol.* 94, 111–126.
- Sahin, Y., 2011. Environmental impacts of biofuels. *Energy Educ. Sci. Technol.-Part A* 26, 129–142.
- Savage, N., 2011. Fuel options: The ideal biofuel. *Nature* 474, S9–S11.
- Schaal, K., Yassin, A., Stackebrandt, E., 2006. The Family Actinomycetaceae: The Genera *Actinomyces*, *Actinobaculum*, *Arcanobacterium*, *Varibaculum*, and *Mobiluncus*. in: *The Prokaryotes*, Springer New York, pp. 430–537.
- Schimel, J.P., Mikan, C., 2005. Changing microbial substrate use in Arctic tundra soils through a freeze-thaw cycle. *Soil Biol. Biochem.* 37, 1411–1418.
- Schloss, P.D., Handelsman, J., 2005. Metagenomics for studying unculturable microorganisms: cutting the Gordian knot. *Genome Biol.* 6.
- Schloss, P.D., Westcott, S.L., Ryabin, T., Hall, J.R., Hartmann, M., Hollister, E.B., Lesniewski, R.A., Oakley, B.B., Parks, D.H., Robinson, C.J., Sahl, J.W., Stres, B., Thallinger, G.G., Van Horn, D.J., Weber, C.F., 2009. Introducing mothur: Open-Source, Platform-Independent, Community-Supported Software for Describing and Comparing Microbial Communities. *Appl. Environ. Microbiol.* 75, 7537–7541.
- Schubert, C., 2006. Can biofuels finally take center stage? *Nat. Biotech.* 24, 777–784.
- Sierra, R., Smith, A., Granda, C., Holtzapple, M.T., 2008. Producing fuels and chemicals from lignocellulosic biomass. *Chem. Eng. Prog.* 104, S10–S18.
- Smith, A.D., 2011. Pilot-scale fermentation and laboratory nutrient studies on mixed-acid fermentation. Ph.D. Dissertation, Texas A&M University. College Station, TX.

- Smith, A.D., Holtzapple, M.T., 2010. Investigation of nutrient feeding strategies in a countercurrent mixed-acid multi-staged fermentation: Development of segregated-nitrogen model. *Bioresour. Technol.* 101, 9700–9709.
- Smith, A.D., Holtzapple, M.T., 2011a. Investigation of the optimal carbon-nitrogen ratio and carbohydrate-nutrient blend for mixed-acid batch fermentations. *Bioresour. Technol.* 102, 5976–5987.
- Smith, A.D., Holtzapple, M.T., 2011b. The slope method: A tool for analyzing semi-continuous data. *Appl. Biochem. Biotechnol.* 163, 826–835.
- Smith, A.D., Lockman, N.A., Holtzapple, M.T., 2011. Investigation of nutrient feeding strategies in a countercurrent mixed-acid multi-staged fermentation: Experimental data. *Appl. Biochem. Biotechnol.* 164, 426–442.
- Srivastava, S., Srivastava, P.S., 2003. *Understanding Bacteria*, Kluwer Academic Pub. Norwell.
- Sterzinger, G., 1995. Making biomass energy a contender. *Technol. Rev.* 98, 34-40.
- Stevenson, D.M., Weimer, P.J., 2007. Dominance of *Prevotella* and low abundance of classical ruminal bacterial species in the bovine rumen revealed by relative quantification real-time PCR. *Appl. Microbiol. Biotechnol.* 75, 165–174.
- Tally, F.P., Stewart, P.R., Sutter, V.L., Rosenblatt, J.E., 1975. Oxygen Tolerance of Fresh Clinical Anaerobic Bacteria. *J. Clin. Microbiol.* 1, 161–164.
- Tekippe, J.A., Hristov, A.N., Heyler, K.S., Cassidy, T.W., Zheljazkov, V.D., Ferreira, J.F.S., Karnati, S.K., Varga, G.A., 2011. Rumen fermentation and production effects of *Origanum vulgare* L. leaves in lactating dairy cows. *J. Dairy Sci.* 94, 5065–5079.
- Thanakoses, P., 2002. Conversion of bagasse and corn stover to mixed carboxylic acids using a mixed culture of mesophilic microorganisms. Ph.D. Dissertation, Texas A&M University. College Station, TX.
- Thanakoses, P., Black, A.S., Holtzapple, M.T., 2003. Fermentation of corn stover to carboxylic acids. *Biotechnol. Bioeng.* 83, 191–200.
- Tseng, D.Y., Chalmers, J.J., Tuovinen, O.H., 1996. ATP measurement in compost. *Compost Science and Utilization* 4, 6–17.
- Ueki, A., Akasaka, H., Satoh, A., Suzuki, D., Ueki, K., 2007. *Prevotella paludivivens* sp nov., a novel strictly anaerobic, Gram-negative, hemicellulose-decomposing

- bacterium isolated from plant residue and rice roots in irrigated rice-field soil. *Int. J. Syst. Evol. Microbiol.* 57, 1803–1809.
- van Andel, J., Zoutberg, G., Crabbendam, P., Breure, A., 1985. Glucose fermentation by *Clostridium butyricum* grown under a self generated gas atmosphere in chemostat culture. *Appl. Microbiol. Biotechnol.* 23, 21–26.
- Ward, A.J., Hobbs, P.J., Holliman, P.J., Jones, D.L., 2008. Optimisation of the anaerobic digestion of agricultural resources. *Bioresour. Technol.* 99, 7928–7940.
- Wee, Y.J., Ryu, H.W., 2009. Lactic acid production by *Lactobacillus* sp RKY2 in a cell-recycle continuous fermentation using lignocellulosic hydrolyzates as inexpensive raw materials. *Bioresour. Technol.* 100, 4262–4270.
- Weimer, P.J., Dien, B.S., Springer, T.L., Vogel, K.P., 2005. In vitro gas production as a surrogate measure of the fermentability of cellulosic biomass to ethanol. *Appl. Microbiol. Biotechnol.* 67, 52–58.
- WHO, 2005. Fact Sheet - Indoor air pollution and household energy, World Health Organization. Geneva.
- WWI, 2009. *State of the world: Into a warming world*. Earthscan Publishers, Washington, DC. 205.
- Yanai, Y., Toyota, K., Okazaki, M., 2004. Effects of successive soil freeze-thaw cycles on soil microbial biomass and organic matter decomposition potential of soils. *Soil Sci. Plant Nutr.* 50, 821–829.
- Zhang, P., Chen, Y.G., Zhou, Q., 2009. Waste activated sludge hydrolysis and short-chain fatty acids accumulation under mesophilic and thermophilic conditions: Effect of pH. *Water Res.* 43, 3735–3742.
- Zhang, Y.H.P., 2008. Reviving the carbohydrate economy via multi-product lignocellulose biorefineries. *J. Ind. Microbiol. Biotechnol.* 35, 367–375.
- Zhou, J.Z., He, Q., Hemme, C.L., Mukhopadhyay, A., Hillesland, K., Zhou, A.F., He, Z.L., Van Nostrand, J.D., Hazen, T.C., Stahl, D.A., Wall, J.D., Arkin, A.P., 2011. How sulphate-reducing microorganisms cope with stress: lessons from systems biology. *Nature Reviews Microbiology* 9, 452–466.
- Zornoza, R., Guerrero, C., Mataix-Solera, J., Arcenegui, V., Garcia-Renes, F., Mataix-Beneyto, J., 2007. Assessing the effects of air-drying and rewetting pre-treatment on soil microbial biomass, basal respiration, metabolic quotient and soluble carbon under Mediterranean conditions. *Eur. J. Soil Biol.* 43, 120–129.

Please note that all data can be found in the supplemental materials.

APPENDIX A. DEOXYDIZED WATER PREPARATION

The liquid medium used in all fermentation experiments was deoxygenated water with cysteine hydrochloride and sodium sulfide.

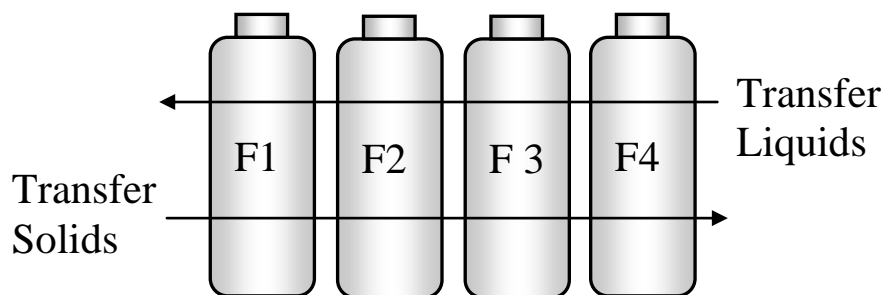
1. Fill a large glass container (≥ 4 L) with distilled water. Place the container over a hot plate to boil.
2. Boil the distilled water for 10 min.
3. Seal the top of the container and cool to room temperature.
4. Add 0.275 g cysteine hydrochloride and 0.275 g sodium sulfide per liter of boiled water.
5. Stir the solution until both chemicals are completely dissolved and pour into storage tank.

APPENDIX B. COUNTERCURRENT TRANSFER PROCEDURE

In countercurrent fermentations, liquid and solid flow in opposite directions. A typical countercurrent train has four fermentors. For a laboratory-scale countercurrent transfer, the transfer of liquid and solids is made every 2 or 3 days, operating in a semi-continuous manner. Countercurrent fermentations are initiated as batch fermentations. The experiments were performed in batch mode until the culture is established in the fermentor (1 to 2 weeks). After the culture developed, the countercurrent operation was started, and the liquid and solids were transferred using the method below. To minimize oxygen exposure in fermentations, solid caps were placed on the bottles at any time solid and liquid was not actively being moved and a nitrogen gas purge was utilized to remove all oxygen from fermentor headspace before the fermentors were returned to the incubator.

1. Remove the fermentors from the incubator and allow to cool for 10 min at room temperature.
2. Release and record the gas production.
3. Remove the fermentor caps and using a nitrogen purge line, remove the residual solids adhered to the stopper and metal bars.
4. Measure and record the pH for each fermentor.
5. Cap the fermentor with a regular solid centrifuge cap.
6. Balance each pair of fermentors using some additional weight supplements. Balance the centrifuge bottles before placing them in the centrifuge.
7. Centrifuge the fermentors to separate the solid and liquid. Centrifuge for 25 min at 4000 rpm and a brake level of 5.
8. After centrifuging, carefully move the bottles to ensure that the solid and liquid do not remix.
9. Place the liquid from Fermentor 1 (F1 in Figure) into a previously weighed plastic graduated cylinder. Record the weight and volume of liquid.
10. Take a 3 mL liquid sample for carboxylic acids analysis. Decant the remaining liquid from F1 into a liquid collection bottle for further VS analysis. Store the sample and collection bottle in a freezer for future analysis.

11. Weigh the fermentor bottle with the remaining solids and compare against the goal weight. Remember that the regular centrifuge cap is not included in this weight. To achieve steady state, a constant wet cake weight must be maintained in each fermentor. If the fermentor weight (wet solids + centrifuge bottle) weighs more than the goal weight, remove the difference and the solids will be added to the next fermentor (F2 in Figure). To simplify the transfer calculation, the goal weight includes the desired wet cake plus the weight of fresh biomass to be added to F1.
12. Add fresh biomass to F1.
13. Pour the liquid from F2 into a preweighed graduated cylinder. Record the weight and volume.
14. Pour the liquid into F1.
15. Weigh F2. Remove the solids resulting of: $\text{Solid removed} = (\text{F2 wet solids} + \text{solids from F1}) - \text{the goal weight}$.
16. Add the solids from F1 to F2.
17. Repeat Steps 13–16 from Fermentors 3 and 4 (F3 and F4 in Figure D-1).
18. Add fresh liquid medium (Appendix C) to F4 according to the predetermined volume.
19. Place the solids removed from F4 in a solid collection bottle and store it in the freezer until the VS analysis is performed.
20. Add buffer, urea (if desired), and methane inhibitor to each fermentor.
21. Mix content well and measure and record the pH.
22. Purge each fermentor with nitrogen and replace fermentor caps.
23. Return fermentors to the incubator.



APPENDIX C. PROPAGATED FIXED-BED TRANSFER PROCEDURE

In propagated fixed-bed fermentations, the liquid phase is transferred but solid phase remains fixed. The propagated fixed-bed fermentations had four fermentors, although more or less can also be used. For a laboratory-scale propagated fixed-bed transfer, every 2 or 3 days, the liquid is transferred operating in a semi-continuous manner. Every 1 to 2 weeks, a fermentor with fresh substrate is brought “on stream” while the most digested fermentor is brought off stream. Propagated fixed-bed fermentations are initiated as batch fermentations. The experiments were performed in batch mode until the culture is established in the fermentor (1 to 2 weeks). After the culture developed, the propagated fixed-bed operation was started, and transfers were performed with the method below. To minimize oxygen exposure in fermentations, solid caps were placed on the bottles at any time solid and liquid was not actively being moved and a nitrogen gas purge was utilized to remove all oxygen from fermentor headspace before the fermentors were returned to the incubator.

I. *Liquid transfer*

Equipment: pH probe, three standards (pH of 4, 7, 10) in 50-mL conical tubes in holder, 500-mL beaker, 300-mL graduated cylinder, spatula, gas volumizer, caps, balance, 15-mL centrifuge tube, deoxygenated water.

1. Remove the fermentors from the incubator and allow to cool for 10 min at room temperature.
2. Release and record the gas production.
3. Remove the fermentor caps and using a nitrogen purge line, remove the residual solids adhered to the stopper and metal bars. Measure and record the pH for each fermentor.
4. Cap the fermentor with a regular solid centrifuge cap. Balance each pair of fermentors using some additional weight supplements. Pay attention to balance the centrifuge bottles before placing them in the centrifuge.
5. Centrifuge the fermentors to separate the solid and liquid. Centrifuge for 25 min at 4000 rpm and a brake level of 5.

6. After centrifuging, carefully move the bottles to ensure that the solid and liquid do not remix.
7. Pour off liquid from the 4th bottle in sequence into a glass beaker.
 - a. Obtain weight and volume
 - b. Obtain 3 mL acid sample in 15-mL centrifuge tube
8. Weigh bottle and solid mass, record.
9. Pour off liquid from 3rd bottle in sequence.
 - a. Obtain weight and volume
10. Pour liquid from 3rd bottle into the 4th bottle in sequence.
11. Weigh bottle and solid weight of 3rd bottle, record.
12. Repeat for 2nd and 1st bottle in sequence.
13. Add 200 mL deoxygenated water to 1st bottle in sequence.
14. Add specified amount of urea to 1st bottle.
15. Add methane inhibitor to each fermentor.
16. Purge each fermentor with nitrogen and replace fermentor caps.
17. Mix all bottles thoroughly, cap, return to incubator.

II. *Fermentor change and liquid transfer*

Equipment: pH probe, three standards (pH of 4, 7, 10) in 50-mL conical tubes in holder, 500-mL beaker, 300-mL graduated cylinder, spatula, gas volumizer, caps, balance, 15-mL centrifuge tube, crucible, 50-mL conical tubes, deoxygenated water, squeeze bottle with distilled water.

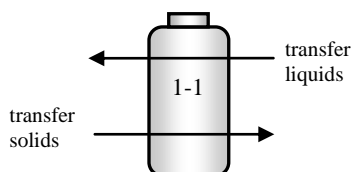
1. Remove the fermentors from the incubator and allow to cool for 10 min at room temperature.
2. Release and record the gas production.
3. Remove the fermentor caps and using a nitrogen purge line, remove the residual solids adhered to the stopper and metal bars. Measure and record the pH for each fermentor.
4. Cap the fermentor with a regular solid centrifuge cap. Balance each pair of fermentors using some additional weight supplements. Pay attention to balance the centrifuge bottles before placing them in the centrifuge.
5. Centrifuge the fermentors to separate the solid and liquid. Centrifuge for 25 min at 4000 rpm and a brake level of 5.
6. After centrifuging, carefully move the bottles to ensure that the solid and liquid do not remix.

7. Setup the new bottle in sequence (can prepare dry materials up to 1 week in advanced).
 - a. Label bottle with correct nomenclature
8. Pour off liquid from the 4th bottle in sequence into glass beaker.
 - a. Obtain weight and volume
 - b. Obtain 3 mL acid sample in 15-mL centrifuge tube
9. Add 100 mL to new bottle in sequence. Dispose of the rest.
10. Weigh bottle and solid mass of old 4th bottle, record.
11. Pour off liquid from old 3rd bottle in sequence.
 - a. Obtain weight and volume
12. Pour liquid from old 3rd bottle into the old 4th bottle in sequence.
13. Weigh bottle and solid weight of old 3rd bottle, record.
14. Repeat steps 11–13 for 2nd and 1st bottle in sequence.
15. Take samples from 1st bottle in sequence for moisture content, ash content, carbon/nitrogen ratio, etc.
16. Add 200 mL fresh deoxygenated water to 1st bottle in sequence.
17. Add specified amount of urea to 1st bottle.
18. Add methane inhibitor to each fermentor.
19. Purge each fermentor with nitrogen and replace fermentor caps.
20. Mix all bottles thoroughly, cap, return to incubator.

APPENDIX D. MULTISTAGE COUNTERCURRENT TRANSFER PROCEDURE

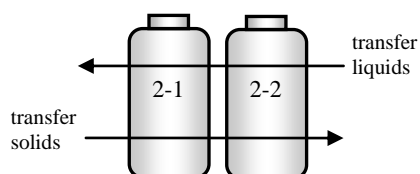
Below are the procedures used to operate the multistage countercurrent trains in Chapter 5.

Train 1 - 1 bottle train, labeled 1-1, 40°C rolling incubator,



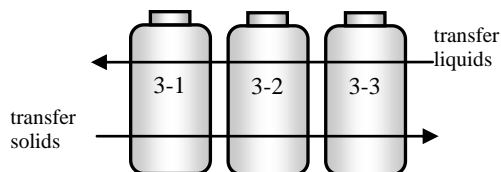
Retain 91 mL
fermentation
liquid in each
bottle

Train 2 - 2 bottle train, labeled 2-1, 2-2, 40°C rolling incubator,



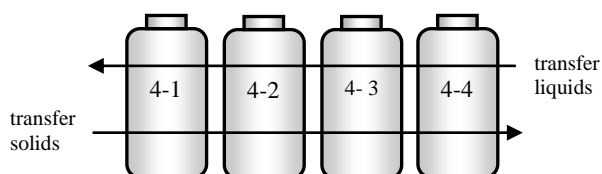
Retain 60 mL
fermentation
liquid in each
bottle

Train 3 - 3 bottle train, labeled 3-1, 3-2, 3-3, 40°C rolling incubator,

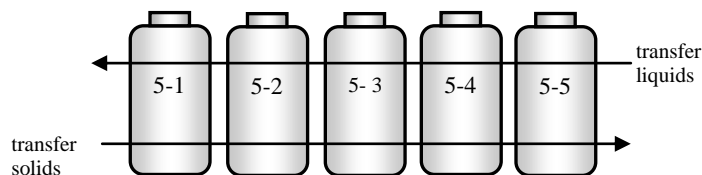


Retain 30 mL
fermentation
liquid in each
bottle

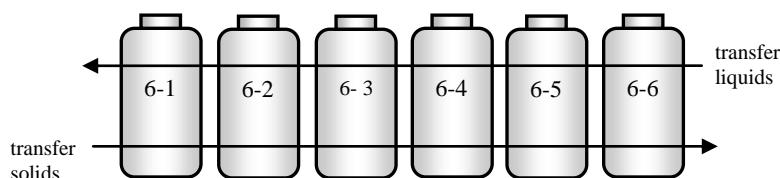
Train 4 - 4 bottle train, labeled 4-1, 4-2, 4-3, 4-4, 40°C rolling incubator,



Train 5 - 5 bottle train, labeled 5-1, 5-2, 5-3, 5-4, 5-5, 40°C rolling incubator,



Train 6 - 6 bottle train, labeled 6-1, 6-2, 6-3, 6-4, 6-5, 6-6, 40°C rolling incubator,



III. Multistage Procedures – *Single-stage train*

Equipment: pH probe, three standards (pH of 4, 7, 10) in 50 mL conical tubes in holder, 500-mL beaker, 300-mL graduated cylinder, spatula, gas volumizer, caps, balance, 15-mL centrifuge tube, deoxygenated water.

1. Remove appropriate bottles from the incubator. Allow to cool to room temperature for 10 min.
2. Vent each bottle, recording starting and finishing height.
3. Open N₂ cylinder in the back corridor.
4. Remove reactor cap.
5. Purge with N₂ and cap.
6. Balance bottles with supplemental weights, centrifuge at 4000 rpm for 25 min.
7. Set up transfer area
 - a. Set up plastic trays for solid transfer
 - b. Label sample tubes with train name and date
 - c. Weigh out fresh paper, manure, calcium carbonate, urea. Get out deoxygenated water.
8. When centrifuge is complete, remove bottles, being careful not to mix the contents.

9. Tare a 250-mL graduated cylinder (or beaker for the weight measurements and then transfer to a 250-mL graduated cylinder for volume measurements) and record weight.
10. Remove the cap from the 1st bottle in the train.
11. Pour the liquid into the graduated cylinder (or beaker). Record weight and volume (with graduated cylinder).
12. Take 3-mL sample in a labeled 15-mL centrifuge tube.
13. Measure and record pH.
14. Weigh out specified amount of “Liquid Weight Retained.” This will be added back to the same bottle it came from once the solid weight has been recorded.
 - a. Keep extra liquid for running MC/AC. Dispose of rest of liquid into biohazard bin.
15. Weigh bottle and cake, record
 - a. If required, take a 5 g MC/AC sample.
16. Remove enough solid to reach the target weight.

$$\text{Solid Removed} = \text{Total Actual Weight} + \text{Solid Weight Added (paper)} + \text{Manure Added} - \text{Target Weight}$$
17. Add specified volume of deoxygenated water to 1st bottle, and specified amount of the fermentation liquid that was previously in the bottle. The bottle should have a total of 121 mL of liquid.
18. Add appropriate amount of fresh paper, urea, calcium carbonate, and dried manure to 1st bottle.
19. Get iodoform from freezer. Add iodoform in the amount specified.
20. Replace iodoform to the freezer.
21. Purge with N₂ and replace each reactor cap tightly.
22. Close N₂ cylinder in the back corridor.
23. Return bottles to incubator.
24. Place samples in freezer.
25. Clean up.

IV. Multistage Procedures – *Two-stage train*

Equipment: pH probe, three standards (pH of 4, 7, 10) in 50 mL conical tubes in holder, 500-mL beaker, 300-mL graduated cylinder, spatula, gas volumizer, caps, balance, 15-mL centrifuge tube, deoxygenated water.

1. Remove appropriate bottles from the incubator. Allow to cool to room temperature for a minimum of 15 min.
2. Vent each bottle, recording starting and finishing height.
3. Open N₂ cylinder in the back corridor.
4. Remove reactor cap.
5. Measure and record pH.
6. Purge with N₂ and cap.
7. Balance bottles with supplemental weights, centrifuge at 4000 rpm for 25 min.

8. Set up transfer area
 - a. Set up plastic trays for solid transfer
 - b. Label sample tubes with train name and date
 - c. Weigh out fresh paper, manure, calcium carbonate, urea. Get out deoxygenated water.
9. When centrifuge is complete, remove bottles, being careful not to mix the contents.
10. Tare a 250-mL graduated cylinder (or beaker for the weight measurements and then transfer to a 250-mL graduated cylinder for volume measurements), and record weight.

1st Bottle

11. Remove the cap from the 1st bottle in the train.
12. Pour the liquid into the graduated cylinder (or beaker). Record weight and volume (with graduated cylinder).
13. Take 3-mL sample in a labeled 15-mL centrifuge tube.
14. Measure and record pH.
15. Weigh out specified amount of fermentation liquid. This will be added back to the same bottle it came from once the solid weight has been recorded.
 - a. Keep extra liquid for running MC/AC. Dispose of rest of liquid into biohazard bin.
16. Weigh bottle and cake, record
 - a. If required, take a 5 g MC/AC sample.
17. Remove enough solid to reach the target weight.

$$\text{Solid Removed} = \text{Total Actual Weight} + \text{Solid Weight Added (paper)} + \text{Manure Added} - \text{Target Weight}$$
18. Place solid weight removed into a weigh boat that will be transferred from 2-1 into 2-2. Record.
19. Add back *specified* amount of “Liquid Weight Retained” that was previously in the bottle. Once the extra amount of liquid from the 2nd bottle is added, the 1st bottle will have a total of 121 mL of liquid.
20. Add appropriate amount of fresh paper, calcium carbonate, and dried manure to 1st bottle.

2nd Bottle

21. Tare graduated cylinder again, and remove cap from the 2nd bottle in the train.
22. Pour liquid into grad cylinder, record weight and volume.
23. Measure and record pH. Take a 3-mL sample once per week.
24. Weigh out specified amount of “Liquid Weight Retained.” This will be added back to the same bottle it came from once the solid weight has been recorded. The extra will be transferred to the 1st bottle in the train.
25. Pour extra liquid from grad cylinder into the 1st bottle. Cap 1st bottle.

26. Weigh bottle and cake, record.
27. Calculate and remove the amount of solid that needed to meet the target weight

$$\text{Solid Removed} = \text{Total Actual Weight} + \text{Solid Weight Added (biomass from previous bottle)} + \text{Manure Added} - \text{Target Weight}$$

28. Place solid from 1st bottle into 2nd bottle.
29. Add specified volume of deoxygenated water to 2nd bottle.
30. Add appropriate amount of fresh paper, urea, calcium carbonate, and dried manure to 2nd bottle.
31. Get iodoform from freezer. Add iodoform in the amount specified.
32. Replace iodoform in the freezer.
33. Purge with N₂ and replace each reactor cap tightly.
34. Close N₂ cylinder in the back corridor.
35. Return bottles to incubator.
36. Place samples in freezer.
37. Clean up.

V. Multistage Procedures – *Three-stage train*

Equipment: pH probe, three standards (pH of 4, 7, 10) in 50 mL conical tubes in holder, 500-mL beaker, 300-mL graduated cylinder, spatula, gas volumizer, caps, balance, 15-mL centrifuge tube, deoxygenated water.

1. Remove appropriate bottles from the incubator. Allow to cool to room temperature for a minimum of 15 min.
2. Vent each bottle, recording starting and finishing height.
3. Open N₂ cylinder in the back corridor.
4. Remove reactor cap.
5. Measure and record pH.
6. Purge with N₂ and cap.
7. Balance bottles with supplemental weights, centrifuge at 4000rpm for 25 min.
8. Set up transfer area
 - a. Set up plastic trays for solid transfer
 - b. Label sample tubes with train name and date
 - c. Weigh out fresh paper, manure, calcium carbonate, and urea. Get out deoxygenated water.
9. When centrifuge is complete, remove bottles, being careful not to mix the contents.
10. Tare a 250-mL graduated cylinder (or beaker for the weight measurements and then transfer to a 250-mL graduated cylinder for volume measurements), and record weight.

1st Bottle

11. Remove the cap from the 1st bottle in the train.
12. Pour the liquid into the graduated cylinder (for weight). Record weight and volume (with graduated cylinder).
13. Take 3-mL sample in a labeled 15-mL centrifuge tube.
14. Measure and record pH.
15. Weigh out specified amount of fermentation liquid. This will be added back to the same bottle it came from once the solid weight has been recorded.
 - a. Keep extra liquid for running MC/AC. Dispose of rest of liquid into biohazard bin.
16. Weigh bottle and cake, record
 - a. If required, take a 5 g MC/AC sample.
17. Remove enough solid to reach the target weight.
 Solid Removed = Total Actual Weight + Solid Weight Added (paper) + Manure Added – Target Weight
18. Place solid weight removed into a weigh boat that will be transferred from 1st into 2nd bottle and set aside. Record.
19. Add specified volume of deoxygenated water to 1st bottle.
20. Add back *specified* amount of “Liquid Weight Retained” that was previously in the bottle. Once the extra amount of liquid from the 2nd bottle is added, the 1st bottle will have a total of 121 mL of liquid.
21. Add appropriate amount of fresh paper, calcium carbonate, and dried manure to 1st bottle.

2nd Bottle

22. Tare graduated cylinder again, and remove cap from the 2nd bottle in the train.
23. Pour liquid into grad cylinder, record weight and volume.
24. Measure and record pH. Take a 3-mL sample once per week.
25. Weigh out specified amount of “Liquid Weight Retained.” This will be added back to the same bottle it came from once the solid weight has been recorded.
 The extra will be transferred to the 1st bottle in the train.
26. Pour extra liquid from grad cylinder into the 1st bottle. Cap 1st bottle.
27. Weigh bottle and cake, record.
28. Calculate and remove the amount of solid that needed to meet the target weight

$$\text{Solid Removed} = \text{Total Actual Weight} + \text{Solid Weight Added (biomass from previous bottle)} + \text{Manure Added} - \text{Target Weight}$$

29. Place solid weight removed into a weigh boat that will be transferred from 2nd into 3rd bottle and set aside. Record.
30. Place solids removed from 1st bottle into 2nd bottle.
31. Add chicken manure, calcium carbonate.

32. Add back *specified* amount of “Liquid Weight Retained” that was previously in the bottle. Once the extra amount of liquid from the 3rd bottle is added, the 2nd bottle will have a total of 121 mL of liquid.
33. Add specified volume of deoxygenated water to 2nd bottle.

3rd Bottle

34. Tare graduated cylinder again, and remove cap from the 3rd bottle in the train.
35. Pour liquid into grad cylinder, record weight and volume.
36. Measure and record pH. Take a 3-mL sample once per week.
37. Weigh out specified amount of “Liquid Weight Retained,” This will be added back to the same bottle it came from once the solid weight has been recorded. The extra will be transferred to the 2nd bottle in the train.
38. Pour extra liquid from grad cylinder into the 2nd bottle. Cap 2nd bottle.
39. Weigh bottle and cake, record.
40. Calculate and remove the amount of solid that needed to meet the target weight

$$\text{Solid Removed} = \text{Total Actual Weight} + \text{Solid Weight Added (biomass from previous bottle)} + \text{Manure Added} - \text{Target Weight}$$

41. Place solid weight removed into a weigh boat that will be transferred out of 3rd bottle. Record.
 - a. Run a MC/AC on the exiting waste. Dispose of the rest in the biohazard bin.
42. Place solids removed from 2nd bottle into 3rd bottle. Add chicken manure, calcium carbonate, urea.
43. Add back *specified* amount of “Liquid Weight Retained” that was previously in the bottle. Once the deoxygenated water is added, the 3rd bottle will have a total of 121 mL of liquid.
44. Add specified volume of deoxygenated water to 3rd bottle.
45. Get iodoform from freezer. Add iodoform in the amount specified.
46. Replace iodoform in the freezer.
47. Purge with N₂ and replace each reactor cap tightly.
48. Close N₂ cylinder in the back corridor.
49. Return bottles to incubator.
50. Place samples in freezer.
51. Clean up.

APPENDIX E. CARBOXYLIC ACID ANALYSIS

For carboxylic acids analysis, at least 3 mL of liquid is sampled from the fermentor, placed in a 15-mL conical centrifuge tube, and stored in the freezer at $-10\text{ }^{\circ}\text{C}$. When analyzed, the samples were defrosted and vortexed. If the acid concentration is high, it may require further dilution before using the method below.

GC LIQUID SAMPLE PREPARATION

1. Centrifuge the liquid sample for 5 min at 4000 rpm.
2. Pipette 0.5 mL of clear liquid broth into a 2.0-mL microcentrifuge tube.
3. Add 0.5 mL of internal standard 4-methyl-valeric acid (1.162 g/L internal standard, ISTD).
4. Add 0.5 mL of 3-M phosphoric acid to convert all salts to acid form.
5. Cap and vortex the tube.
6. Centrifuge the mixture in a microcentrifuge ($8000 \times g$) for 10 min.
7. Remove the tube and decant the mixture into a glass GC vial and cap. The centrifuged sample in the vial is ready to be analyzed now.
8. If the prepared sample will not be analyzed immediately, it can be frozen. Before GC analysis, make sure to thaw and vortex the sample.

GC OPERATION

1. Before starting the GC, check the gas supply cylinders (compressed hydrogen, compressed helium and compressed air from Praxair Co., Bryan, TX) to insure at least 200 psig pressure in each gas cylinder. If there is not enough gas, switch cylinders. Make sure to place an order for new ones.
2. Check the solvent and waste bottles on the injection tower. Fill up solvent vials with methanol. Empty the waste vials in designated waste container.
3. Before starting the GC, replace the septum beneath the injection tower.
4. Up to 150 samples can be loaded in the autosampler tray in one analysis batch. Place the samples in the autosampler racks. Include a vial with the volatile acid standard.

5. Check the setting conditions in the method:
 - a. Inlet Conditions:
 - i. Temperature: 230 °C
 - ii. Pressure: 15 psig
 - iii. Flow rate: 185 mL/min
 - b. Detector conditions:
 - i. Temperature: 230 °C
 - ii. Air flow rate: 400 mL/min
 - iii. H₂ flow rate: 40 mL/min
 - iv. He (makeup) flow rate: 45 mL/min
 - c. Oven conditions:
 - i. Initial temperature: 40 °C
 - ii. Initial hold time: 2 min
 - iii. Ramp rate: 20 °C/min
 - iv. Final temperature: 200 °C
 - v. Final hold time: 1 min
 - d. Total run time per vial: 11 min
6. Start the GC on the computer by selecting the method with the setting conditions mentioned above. Load the sample sequence.
7. For quality control, run the standard mix every 15–25 samples. At the end of the sequence table, set the GC into standby mode to save gas.

APPENDIX F. MOISTURE AND ASH CONTENT ANALYSIS

This procedure was modified from NREL Standard Procedures (2004). If volatile acids are present in sample, lime may be added to retain all acids for more thorough measurement of moisture content (Meysing, 2011). However, when lime is added, the ash content cannot be measured as directed below. In this case, a separate sample must be dried with no lime addition, and subsequently ashed.

1. Record the label and weight of a clean, dry crucible (W1).
2. Place a representative sample of the material (liquid or solid) into the crucible and record the weight (W2).
3. Dry the crucible at 105 °C for 1 day in the drying oven. In a desiccator, allow to cool to room temperature before weighing. Record the dry weight (W3).
4. Ash the crucible at 575 °C for at least 12 h. Remove and allow to cool to room temperature in a desiccator. Record the ash weight (W4).
5. The moisture content (MC) of the sample is calculated as

$$MC = \frac{W2 - W3}{W2 - W1}$$

6. The ash content (AC) of the sample is calculated as

$$AC = \frac{W4 - W1}{W3 - W1}$$

APPENDIX G. CELL SEPARATION PROCEDURE

1. Homogenize solids by stirring vigorously for 30 seconds.
2. Weigh 8.0 g homogenate in a 50-mL conical vial. Repeat once.
3. Dilute 4× by adding 32 mL DI H₂O into both tubes.
4. Shake 10 seconds, vortex 3×1 minute.
5. For both tubes, carefully filter homogenate through metal mesh filter. Do this directly into another clean 50-mL vial. Periodically discard debris caught in filter.
6. Let sit for 10 minutes and decant supernatant into another 50-mL vial.
7. Pour solutions into centrifuge tubes.
8. Turn on ultracentrifuge, open lid, take off top, and put samples in.
9. Replace lid. Centrifuge 10,000×g at RT for 10 min. A lower speed can be used for longer time.
10. Remove and discard supernatant.
11. Pipette 500-μL DI H₂O into each of the 8 tubes. Vortex each for 30 seconds.
12. Pipette 500 μL from each vial into a single vial. Mix all 4 mL.
13. Decant into appropriate location or save for later use.

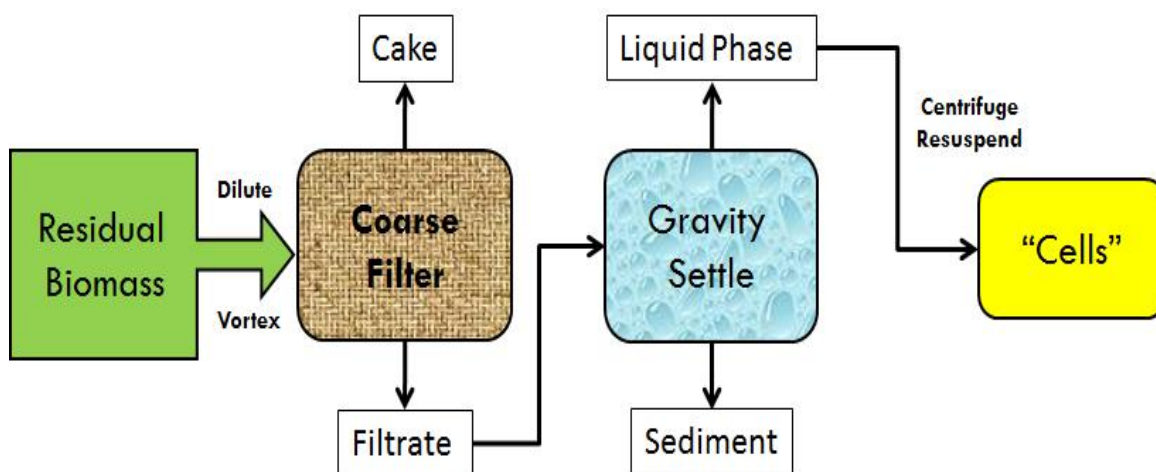


Figure C-1. Diagram of cell recycle procedure.

APPENDIX H. GLUCOSE ASSAY PROCEDURE

1. Preparing Sugar Solution
 - a. Wash out glass containers with soap and warm water 3×. Let air dry.
 - b. Put clean dry stir bar on bottom of container. Put containers on stir plate, turn on to medium stirring and heat.
 - c. With a graduated cylinder, measure out 500 mL of milipore water.
 - d. Pour water into glass container.
 - e. Use an analytical balance, new weigh boat, and clean, dry spatula to measure out the correct mass of sugar.
 - f. Buffer the sugar solution with 50 mM potassium phosphate. If needed, add hydrochloric acid to bring pH to 7.5.
 - g. Filter sterilize

3. Aliquot sugar solution into 10-mL reaction vessel, so that the total volume is 5 mL.

4. Add biomass
 - a. Whenever adding biomass to the sugar solution, make sure biomass is either fresh or, if it is an *E. coli* or *pseudomonas* control, that it is in the exponential phase.
 - b. Using a clean, dry weigh boat and analytical balance, weigh out appropriate mass of solid or liquid biomass and add to appropriate vessel. This solution is now called *glucose reaction mix*.
 - a. Typically, four biomass concentrations are tested: 0.5, 0.4, 0.3, 0.2 g or mL in a total reaction volume of 5 mL.
 - c. Cap and vortex for 20 s.
 - d. Place the reaction vessel in a 37 °C shaking incubator (~180 rpm).

5. Take sample
 - a. For the chosen time points, remove 200 µL sample from glucose reaction mix.
 - b. Place reaction vessel back into incubator.

6. Perform the glucose oxidase enzyme assay to determine the glucose concentration (see Appendix I).

APPENDIX I. GLUCOSE OXIDASE ENZYME ASSAY FOR GLUCOSE DETERMINATION

Procedures

1. In a 1.5-mL microcentrifuge tube, add 200 μL of glucose reaction mix.
2. Add 250 μL of glucose oxidase reaction mix (glucose oxidase enzyme, O-dianisidine, Sigma Aldrich, GAGO20) and let incubate in a 37 °C water bath exactly 10 min.
3. Add 250 μL of 12 M sulfuric acid (99% ACS grade) to stop the reaction.
4. Centrifuge samples for 5 min, 3,000 $\times g$ if necessary.
5. Pipette exactly 250 μL of each sample into one well in a 96-well plate. Make sure there are no bubbles.
6. Use spectrophotometer to analyze glucose concentration (570 nm).
7. Use glucose calibration curves to calculate the glucose concentration from absorbance.

Note: O-dianisidine is a known human carcinogen. Extreme caution must be used. Use gloves and work in the hood.

APPENDIX J. TYE MEDIA PREPARATION

TYE media preparation

1. In a graduated flask, add the following ingredients

	<u>1L</u>	<u>500 mL</u>
Tryptone	10 g	5 g
Yeast Extract	5 g	2.5 g
NaCl	5 g	2.5 g

2. Add to dH₂O, and dilute to final volume with water.
3. Autoclave 20 min on liquid cycle.

TYE plate preparation

1. In a graduated flask, add the following ingredients

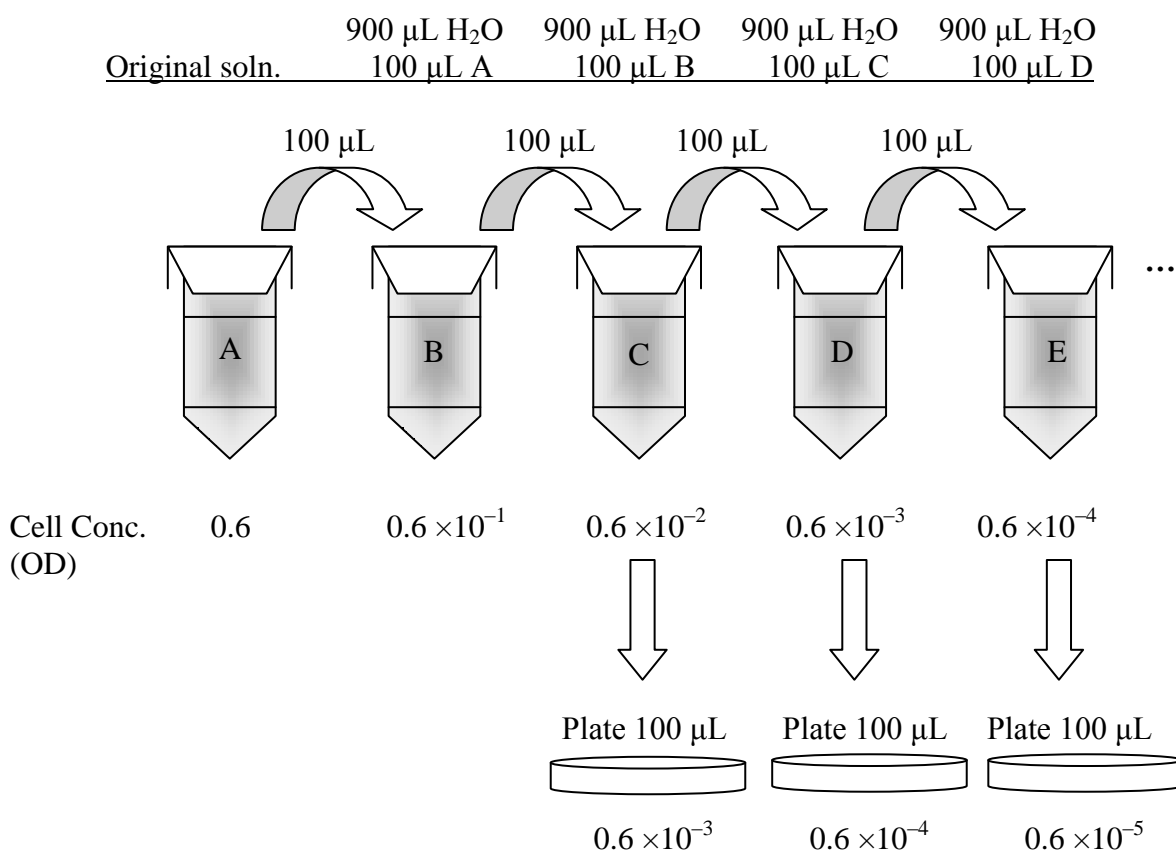
	<u>1L</u>	<u>500 mL</u>
Tryptone	10 g	5 g
Yeast Extract	5 g	2.5 g
NaCl	5 g	2.5 g
Agar	15 g	7.5 g

2. Add to dH₂O, and dilute to final volume with water.
3. Autoclave 20 min on liquid cycle.
4. Cool in a stirring hot plate, with stir bar to stir, until cool enough to touch with thin gloves on. Cooling the media prior to pouring reduces condensation on plates and make it easier to pour.
5. Pour TYE into each plate, until one-half to two-thirds full. To prevent contamination, with a Bunsen burner, flame the graduated flask lid every 10–20 plates.
6. Let plates dry overnight and then refrigerate.

APPENDIX K. BRIEF TUTORIAL ON DIRECT CELL PLATING

Use Appendix J to make TYE agar plates. Because the cell concentration for the sample being plated is generally unknown, a dilution series needs to be used. Too many cells will cause the Petri plate to be so densely populated with colonies, that they are impossible to count. The microbial sample needs to be in a liquid phase with little suspended sediment. For *E. coli* in solution, first find the cell optical density (OD). The OD is an indicator of the range of dilutions that need to be plated.

A dilution series will need to be made. An example follows of cells with an OD of 0.6.



Figures K-1 and K-2 are examples of what Petri plates can look like for a pure culture of *E. coli* (DH5a) and a mixed culture from carboxylate fermentations. In Figure K-1, a pure culture of *E. coli* was used in a dilution series from 10^{-4} to 10^{-8} OD. In Figure K-1, the 10^{-4} and 10^{-5} dilutions could be considered a lawn and too numerous to count (TNTC), while 10^{-8} could be counted but might not have enough colonies to be representative. Usually, 30–300 colonies are preferred. For *E. coli*, all the colonies are around the same size. However, for the mixed culture, there are many different sizes of colonies showing the diversity of microorganisms. This presents a problem in counting because some colonies might be only the size of a pinprick, and therefore difficult to see, while other colonies grow faster and are merging into other colonies, making it difficult to distinguish colonies.

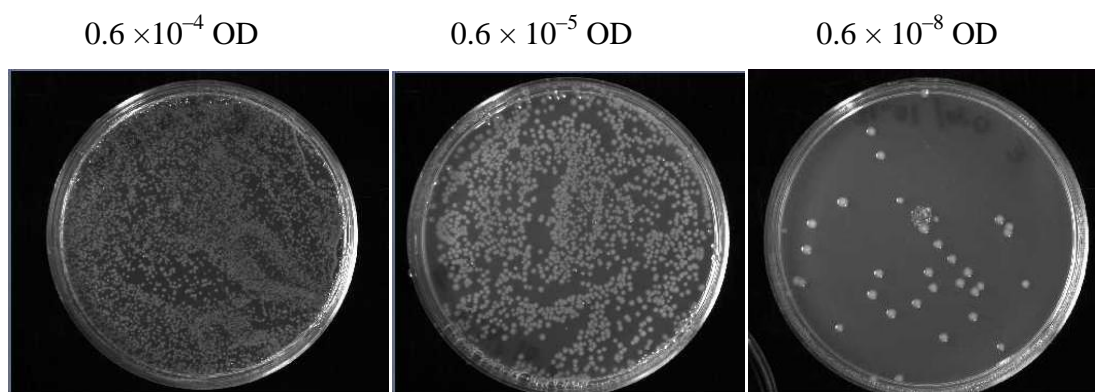


Figure K-1. Pictures of Petri plates inoculated with *E. coli* after 24–36 h incubation at 37 °C.

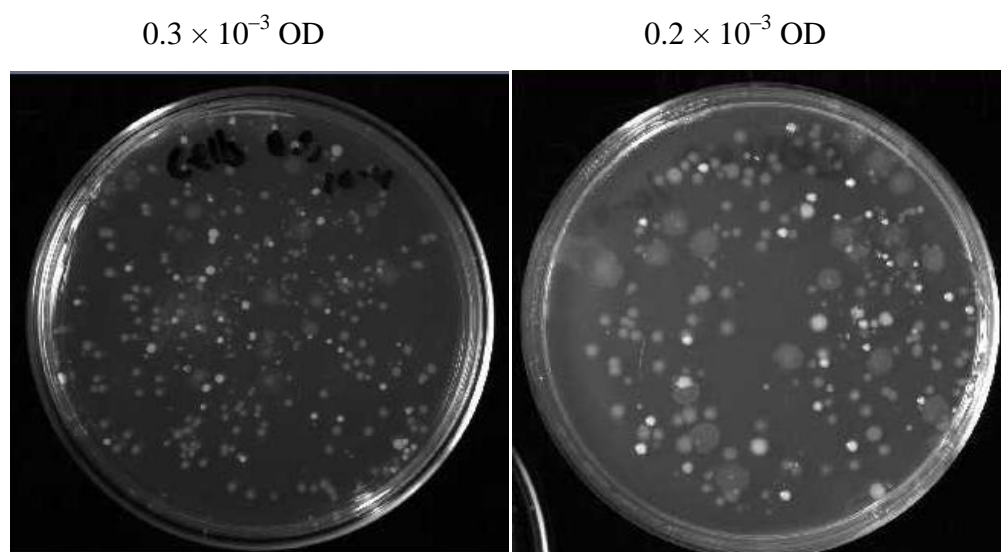


Figure K-2. Pictures of Petri plates inoculated with separated “cells” using the cell separation procedure (Appendix G), after 24–36 h incubation at 37 °C.

APPENDIX L. HOT-LIME-WATER PRETREATMENT PROCEDURE

To increase digestibility, SunChips® compostable bags were treated with calcium hydroxide in the presence of water in a metal tray. The feedstock and calcium hydroxide (0.3 g/g dry biomass) were placed in the metal tray and mixed thoroughly. Enough distilled water was added to cover the material. The tray was then covered with aluminum foil, and the mixture was brought to a boil using Bunsen burners. After the mixture had boiled for an hour, it was allowed to cool to room temperature. It was then neutralized by bubbling gaseous CO₂ through the mixture until the pH was 7.0.

1. In a stainless steel pan, place the preweighed biomass, lime, and distilled water using a loading of 0.3 g Ca(OH)₂/g dry biomass, and mix to ensure even distribution of the lime.
2. Place the pan over Bunsen burners or hot plates and heat to a rolling boil. Boil the mixture for 1 h, stirring occasionally. If water begins to evaporates, add more distilled water
3. Allow the mixture to cool to room temperature, which usually takes several hours. If needed, add more distilled water to the mixture to completely cover the biomass. If foaming occurs, add 2–3 drops of Dow Corning silicone antifoam solution.
4. To neutralize the basic solution, bubble CO₂ through the mixture with diffusing stones until the pH decreases to ~7.0.
5. Wash biomass thoroughly to ensure all lime has been removed.
6. Spread the biomass into thin layers onto trays with aluminum foil. Allow to air dry (5–7 d). Store the dried biomass in a sealed container.

APPENDIX M. EXAMPLE OF EXPERIMENTAL DESIGN FOR THE OREGANO SUPPLEMENTED PAPER BATCH FERMENTATION

1. Substrate pretreatment
 - a. Compositional analysis (before and after pretreatment) lignin inhibits fermentation
 - i. >25% lignin - high pressure pretreatment– quick/very low mass
 - ii. 18-25% - long-term air/lime pretreatment – 4-6 weeks
 - iii. 12-18% - hot lime – 1-2 weeks
 - iv. <12% - no pretreatment needed
 - b. Pretreat with method above, considering time also
2. Fermentation (batch) ~28 days
 - a. Choose buffer
 - i. CaCO₃ pH 6.0
 - ii. NH₄HCO₃ pH 7
 - b. Choose temperature
 - i. 40 or 55 °C
 - c. Load Fermentors 100g/L(ON A DRY SOLIDS BASIS)
 - i. 40 g substrate + nutrients (TriPLICATE)
 1. 80% Substrate
 - a. 80% paper, Iodoform, 55 °C
 - b. 80% paper, no Iodoform, 55 °C
 - c. 75% paper/5% oregano, no Iodoform, 55 °C
 - d. 65% paper/15% oregano, no Iodoform, 55 °C
 - e. 50% paper/30% oregano, no Iodoform, 55 °C
 - f. 80% paper, Iodoform, 40 °C
 - g. 80% paper, No Iodoform, 40 °C
 - h. 50% paper/30% oregano, no Iodoform, 40 °C
 2. 20% Nutrients
 - a. Dry chicken manure
 - ii. 350 mL deoxyH₂O
 - iii. 50 mL Inoculum
 - iv. 6 g CaCO₃
 - v. 1 g Urea
 - d. Start
 - i. Load all ingredients, Shake, pH, GC, cap
 - ii. Put into incubator
 - e. Sample regularly

- i. Every 2 days: vent, take gas sample to measure O₂/N₂, Methane, CO₂, take liquid sample to measure acid concentration with GC, measure pH
3. End Fermentation
 - a. Vent, take samples
 - b. Centrifuge
 - c. Weigh cake and liquid, and bottle. Take cake sample.
 - d. Analyze cake for %MC and %VS

APPENDIX N. CPDM MATLAB PROGRAM FOR SIMULATION OF A FOUR-STAGE COUNTERCURRENT FERMENTATION

```

%MATLAB Code for CPDM Prediction
%This code is for a standard four-stage countercurrent fermentation
%Program predicts acid concentrations and conversion at varying VSLR and LRT.
%Code by Kristina 1/20/2011
%Department of Chemical Engineering, Texas A&M University, College Station, TX

clear all
close all
global so taus a1 b1 e1 f1 g1 h1
global holdup moist ratio stages loading tauoverall
global ratio acid nnot factr1
global x_1 nhat_1 x_2 nhat_2 x_3 nhat_3 x_4 nhat_4

%Start Simulation
disp(['Program starts at: ', datestr(now)]);
tic;

VSLR_data=[4,6,8,10,12]';
LRT_data=[10,15,20,25,30]';
ACID = [];
CONVERSION = [];
VSLR_loop=4; %loop is for varying VSLR.
%To make map, set to lowest VSLR, otherwise, set to specific VSLR
while VSLR_loop<12.1 % if want loop, set to highest VSLR
    LRT_loop=10; %loop is for varying LRT.
    %To make map, set to lowest LRT, otherwise set to specific LRT
    while LRT_loop<30.01 %if want loop, set to highest VSLR

        %%Basic parameters for Fermentation
        stages=4; %Fermentor stages
        so=0.21; %Aceq selectivity (g Aceq/g VS digested)
        holdup =2.0; %ratio of liq to solid in wet cake (g liq/gVS cake)
        %Note: holdup is the liq in the solid cake NOT the lig of the total slurry
        moist =.06; %ratio of liquid to solid in feed (g liq/gVS cake)
        SQ =1.0;
        ratio=0.79; %phi ratio of g total acid to g Aceq
        loading = VSLR_loop;
        tauoverall = LRT_loop;
        vol=[.48,.28,.28,.28]'; %Liquid volime in each fermentor
        totvol=sum(vol);
        liquidfeed = totvol/tauoverall;
        nnotreal = [169,214,214,214]'; %VS concentration (gVS/L) in each fermentor
        solidfeed = loading*totvol; %Solid Feed (g dry weight)
        Convrns = [.1,.2,.3,.4]'; %Initial value for conversion
        nnot = nnotreal./(1-Convrns);
        taus = nnot.*vol/solidfeed;
    end
end

```

```

L = 0.1*ones(stages+1,1); %L initial value for liquid flow rate in every reactor
taul = tauoverall/stages*ones(stages,1);

e1=0.027; f1=5.56; g1=.001; h1=3.36; %CPDM parameters
rmodel = @(x1,acid) e1.*(1-x1).^f1./(1+g1.*(acid.*ratio).^h1);
syms x1 acid
drmodel_1 = diff(e1.*(1-x1).^f1./(1+g1.*(acid.*ratio).^h1),x1);
drmodel = @(x2,acd2) subs(drmodel_1,{x1,acd},{x2,acd2});

done = 0; %The index used to trace whether the condition is satisfied
liqtoler = 0.05; %tolerance for Liquid flowrate
acidtoler = 0.1; %tolerance for acid concentration
nnotoler = 1; %tolerance for nnot

%Initial values for acid, acidold
ans=ones(stages,1);
acid=[30,20,15,5]';
acidold=ones(stages,1);
taulnew = 1000*ones(stages,1); %column vector
nhatzero = 100*ones(stages,1); %CP concentration
creation = ones(stages,1);
destruction = ones(stages,1);
tauoverallnew = 20;

disp('Calculation is in progress.....');

while done < 0.50
    taulnew = 1000*ones(stages,1); %Obtain Flowrate for each fermentor
    tauover_error = 0.001;
    while abs(tauoverall-tauoverallnew) > tauover_error
        liquidfeed = liquidfeed*(1+(tauoverallnew-tauoverall)/tauoverall*0.5);
        L(5) = liquidfeed;
        L(4) = L(5) + solidfeed/1000*holdup*(Convrsn(4)-Convrsn(3));
        L(3) = L(4) + solidfeed/1000*holdup*(Convrsn(3)-Convrsn(2));
        L(2) = L(3) + solidfeed/1000*holdup*(Convrsn(2)-Convrsn(1));
        L(1) = moist*solidfeed/1000 + L(2) - solidfeed/1000*holdup*(1.0-Convrsn(1));
        tauoverallnew = totvol/L(1);
    end

    taul = vol./L(1:stages);
    nnot = nnotreal./(1-Convrsn);
    taus = nnot.*vol/solidfeed;
    scale = ones(stages,1);

    disp([' nnot= ',num2str(nnot),'% 15.5f']);

%parameters for ODE45
options = odeset('RelTol',1e-3,'AbsTol', 1e-3);
x_low=0; x_high=0.99;

```

%Reactor 1

```

i=1;
while abs(taulnew(i) - taul(i))> liqtoler
    nhat0 =nhatzero(i);
    [x,nhat]= ode15s(@Chan1,[x_low,x_high],nhat0,options);
    x_1=x; nhat_1 = nhat;
    F_1 = @(x_1)interp1(x,nhat,x_1);
    factr1 = nnot(i)/quad(F_1,x_low,x_high); %calculate factor
    F_11 = @(x_1) factr1*interp1(x,nhat,x_1).*rmodel(x_1,acid(i));
    robs = quad(F_11,x_low,x_high);
    F_12 = @(x_1) interp1(x,nhat,x_1).*x_1;
    Convrnsn(i) = quad(F_12,x_low,x_high)/nnot(i)*factr1;
    taulnew(i) = (L(i)*acid(i) + solidfeed/1000*(1-Convrnsn(i))*holdup*acid(i)-
L(i+1)*acid(i+1))/(L(i)*robs);
    acid(i) = acid(i) + (taul(i)*robs-(L(i)*acid(i)+solidfeed/1000*(1-Convrnsn(i))*holdup*acid(i)-
L(i+1)*acid(i+1))/L(i)).*0.4;
end
disp([' acid(',num2str(i),')=',num2str(acid(i),'%15.5f'),'
taulnew(',num2str(i),')=',num2str(taulnew(i),'%15.5f'),' robs=', num2str( robs, '%15.5f')]);

```

%Reactor 2

```

i=2;
nnotoler = nnot(i)/500;
while abs(taulnew(i)-taul(i))>liqtoler;
    ndone = 0;
    while ndone <0.50
        nhat0=nhatzero(i);
        options = odeset('RelTol',1e-3,'AbsTol',1e-3);
        [x,nhat] = ode15s(@Chan2,[x_low,x_high],nhat0,options);
        x_2=x; nhat_2=nhat;
        F_2 = @(x_2)interp1(x,nhat,x_2);
        nhattot=quad(F_2,x_low,x_high);
        disp([' nhatzero= ',num2str(nhatzero(i),'%15.5f'),'; nhattot= ',num2str(nhattot,'%15.5f'),';
nnot(',num2str(i),')= ',num2str(nnot(i),'%15.5f')]);
        if abs(nhattot - nnot(i))<nnotoler;
            ndone = 1;
        end
        if (nhatzero(i) + (nnot(i) - nhattot)*1.0)>0
            nhatzero(i)= nhatzero(i) + (nnot(i) - nhattot)*0.7;
        else
            nhatzero(i)= nhatzero(i) + (nnot(i) - nhattot)*0.7;
        end
    end
end

F_22 = @(x_2)interp1(x,nhat,x_2).*x_2;
Convrnsn(i)= quad(F_22,x_low,x_high)/nnot(i);
robs = solidfeed*so/vol(i)*(Convrnsn(i)-Convrnsn(i-1));

    taulnew(i) = (L(i)*acid(i) + solidfeed/1000*(1-Convrnsn(i))*holdup*acid(i)-
L(i+1)*acid(i+1))/(L(i)*robs);

```

```

        acid(i) = acid(i) + (taul(i)*robs-(L(i)*acid(i)+solidfeed/1000*(1-Convrsn(i))*holdup*acid(i)-
L(i+1)*acid(i+1))/L(i))*0.5;
        disp([' taulnew(',num2str(i),')=',num2str(taulnew(i), '%15.5f'),'
taul(',num2str(i),')=',num2str(taul(i),'%15.5f'),,]);
    end
    disp([' acid(',num2str(i),')=',num2str(acid(i),'%15.5f'),'
taulnew(',num2str(i),')=',num2str(taulnew(i),'%15.5f'),' robs=', num2str( robs, '%15.5f')]);

```

%Reactor 3

```

i=3;
nnotoler = nnot(i)/500;
while abs(taulnew(i)-taul(i))>liqtoler;
    ndone = 0;
    while ndone <0.50
        nhat0 =nhatzero(i);
        options = odeset('RelTol',1e-3,'AbsTol',1e-3);
        [x,nhat] = ode15s(@Chan3,[x_low,x_high],nhat0,options); %was chan3
        x_3=x; nhat_3=nhat;
        F_3 = @(x_3)interp1(x,nhat,x_3);
        nhattot=quad(F_3,x_low,x_high);
        disp([' nhatzero= ',num2str(nhatzero(i), '%15.5f'),' nhattot= ',num2str(nhattot, '%15.5f'),'
nnot(',num2str(i),')= ',num2str(nnot(i), '%15.5f')]);
        if abs(nhattot - nnot(i))<nnotoler;
            ndone = 1;
        end
        if (nhatzero(i) + (nnot(i) - nhattot)*1.0)>0
            nhatzero(i)= nhatzero(i) + (nnot(i) - nhattot)*0.7;
        else
            nhatzero(i)= nhatzero(i) + (nnot(i) - nhattot)*0.7;
        end
    end
end

```

```

F_32 = @(x_3)interp1(x,nhat,x_3).*x_3;
Convrsn(i)= quad(F_32,x_low,x_high)/nnot(i);
robs = solidfeed*so/vol(i)*(Convrsn(i)-Convrsn(i-1));
taulnew(i) = (L(i)*acid(i) + solidfeed/1000*(1-Convrsn(i))*holdup*acid(i)-
L(i+1)*acid(i+1))/L(i)*robs);
        acid(i) = acid(i) + (taul(i)*robs-(L(i)*acid(i)+solidfeed/1000*(1-Convrsn(i))*holdup*acid(i)-
L(i+1)*acid(i+1))/L(i))*0.5;
        disp([' taulnew(',num2str(i),')=',num2str(taulnew(i), '%15.5f'),'
taul(',num2str(i),')=',num2str(taul(i),'%15.5f'),,]);
    end
    disp([' acid(',num2str(i),')=',num2str(acid(i),'%15.5f'),'
taulnew(',num2str(i),')=',num2str(taulnew(i),'%15.5f'),' robs=', num2str( robs, '%15.5f')]);

```

%Reactor 4

```

i=4;
nnotoler = nnot(i)/500;
while abs(taulnew(i)-taul(i))>liqtoler;

```

```

ndone = 0;
while ndone < 0.50
    nhat0 = nhatzero(i);
    options = odeset('RelTol',1e-3,'AbsTol',1e-3);
    [x,nhat] = ode15s(@Chan4,[x_low,x_high],nhat0,options);
    x_4=x; nhat_4=nhat;
    F_4 = @(x_4)interp1(x,nhat,x_4);
    nhattot=quad(F_4,x_low,x_high);
    disp([' nhatzero= ',num2str(nhatzero(i), '%15.5f'),'; nhattot= ',num2str(nhattot, '%15.5f'),';
nnot(',num2str(i,')= ',num2str(nnot(i), '%15.5f'))];
    if abs(nhattot - nnot(i))<1;%nnotoler;
        ndone = 1;
    end
    if (nhatzero(i) + (nnot(i) - nhattot)*1.0)>0
        nhatzero(i)= nhatzero(i) + (nnot(i) - nhattot)*0.7; %25/nnot(i);
    else
        nhatzero(i)= nhatzero(i) + (nnot(i) - nhattot)*0.7;
    end
end

F_42 = @(x_4)interp1(x,nhat,x_4).*x_4;
Convrnsn(i)= quad(F_42,x_low,x_high)/nnot(i);
robs = solidfeed*so/vol(i)*(Convrnsn(i)-Convrnsn(i-1));

taulnew(i) = (L(i)*acid(i) + solidfeed/1000*(1-Convrnsn(i))*holdup*acid(i)-solidfeed/1000*(1-
Convrnsn(i-1))*holdup*acid(i-1))/(L(i)*robs);
acid(i) = acid(i) + (taul(i)*robs-(L(i)*acid(i)+solidfeed/1000*(1-Convrnsn(i))*holdup*acid(i)-
solidfeed/1000*(1-Convrnsn(i-1))*holdup*acid(i-1))/L(i))*0.5;
disp([' taulnew(',num2str(i,')= ',num2str(taulnew(i), '%15.5f'),'
taul(',num2str(i,')= ',num2str(taul(i),'%15.5f'),,)];
end
disp([' acid(',num2str(i,')= ',num2str(acid(i),'%15.5f'),'
taulnew(',num2str(i,')= ',num2str(taulnew(i),'%15.5f'),' robs=', num2str( robs, '%15.5f'))];
disp([' Conversion in each stage (from nhat): ',num2str(Convrnsn),'%13.5f'));

if max(abs(acid-acidold))<acidtoler
    done=1;
end
acidold = acid;
end

%Output results section

disp('Congratulations! The simulation is successfully finished!')
toc %toc is used to check the whole time of the process

for i3 = 1:(stages+1);
    disp([' L(',int2str(i3,')= ',num2str(L(i3))]);
end

creation(1) = L(1)*acid(1) + solidfeed/1000*(1-Convrnsn(1))*holdup*acid(2)-L(2)*acid(2);

```

```

    creation(2) = L(2)/acid(2) + solidfeed/1000*(1-Convrsn(2))*holdup*acid(3)-L(3)*acid(3)-
    solidfeed/1000*(1-Convrsn(1))*holdup*acid(2);
    creation(3) = L(3)*acid(3) + solidfeed/1000*(1-Convrsn(3))*holdup*acid(4)-L(4)*acid(4)-
    solidfeed/1000*(1-Convrsn(2))*holdup*acid(3);
    creation(4) = L(4)*acid(4) - solidfeed/1000*(1-Convrsn(3))*holdup*acid(4);

%Calculation of Destruction

destruction(1) = solidfeed/1000*(Convrsn(1)-0);
for i3=2:stages;
    destruction(i3)=solidfeed/1000*(Convrsn(i3)-Convrsn(i3-1));
end
selectivi = creation./destruction;
selec = L(1)*acid(1)/(solidfeed*Convrsn(4));

%output the results
disp([' Selectivity = ',num2str(selectivi,'%15.5f')]);
disp([' Creation = ',num2str(creation,'%15.5f')]);
disp([' Destruction = ',num2str(destruction,'%15.5f')]);
disp([' selectivity = ',num2str(selec,'%15.5f')]);
disp([' tauoverall = ',num2str(tauoverall,'%15.5f')]);
disp([' taus = ',num2str(sum(taus),'%15.5f')]);
disp([' acid levels = ',num2str(acid,'%13.5f')]);

disp([' VSLR_LOOP = ',num2str(VSLR_loop),' LRT_loop = ',num2str(LRT_loop)]);

%Collect data for CPDM map
ACID = [ACID;acid(1)];
CONVERSION = [CONVERSION;Convrsn(4)];
LRT_loop = LRT_loop + 5;
end
VSLR_loop = VSLR_loop + 2;
end

disp([' acid levels = ',num2str(acid,'%13.5f')]); %shows acids levels for the last simulation run
disp([' convrsn levels = ',num2str(Convrsn,'%13.5f')]); %shows conversion levels for the last sim run
disp([' VSLR = ',num2str(VSLR_data,'%13.5f')]);
disp([' LRT = ',num2str(LRT_data,'%13.5f')]);
disp([' Acid levels = ',num2str(ACID,'%13.5f')]); %output final acid conc for each VSLR and LRT loop
disp([' Conversions = ',num2str(CONVERSION,'%13.5f')]); %output final conversion for each VSLR
and LRT

*****End of the MATLAB code**
*****The following are the four function files used in the main source code.

***Chan1.m
function dnhat = nhateq1(x,nhat1)
global so taus a1 b1 e1 f1 g1 h1 i x1
global ratio acid

```



```

rmodel = @(x1,acid)e1.*(1-x1).^f1./(1+g1.*(acid.*ratio).^h1);
drmodel = @(x1,acid)-28341/100000.*(1-
x1)^(101/100)./(1+517/500*3^(273/1000)*5^(727/1000).*acid^(273/1000));

```

```

i=1;
dnhatdt = -nhat1*(drmodel(x,acid(i))+so./taus(i))/rmodel(x,acid(i));
dnhat = [dnhatdt];

```

***Chan2.m

```

function dnhat = nhateq1(x,nhat1)
global so taus a1 b1 e1 f1 g1 h1 i RN x1
global ratio acid nnot factr1
global x_1 nhat_1 x_2 nhat_2 x_3 nhat_3 x_4 nhat_4

```

```

rmodel = @(x1,acid) e1.*(1-x1).^f1./(1+g1.*(acid.*ratio).^h1);
drmodel = @(x1,acid) -28341/100000.*(1-
x1)^(101/100)./(1+517/500*3^(273/1000)*5^(727/1000).*acid^(273/1000));

```

```

F_1m = @(x_m)interp1(x_1,nhat_1,x_m);

```

```

i=2;
dnhatdt = -nhat1*(drmodel(x,acid(i))+so./taus(i))/rmodel(x,acid(i)) + F_1m(x).*nnot(i)./nnot(i-
1)*factr1*so./taus(i)/rmodel(x,acid(i));
dnhat = [dnhatdt];

```

***Chan3.m

```

function dnhat = nhateq1(x,nhat1)
global so taus a1 b1 e1 f1 g1 h1 i RN x1
global ratio acid nnot factr1
global x_1 nhat_1 x_2 nhat_2 x_3 nhat_3 x_4 nhat_4

```

```

rmodel = @(x1,acid) e1.*(1-x1).^f1./(1+g1.*(acid.*ratio).^h1);
drmodel = @(x1,acid) -2247/5000*(1-
x1)^(271/50)/(1+6741/31250*21^(33/100)*25^(67/100)*acid^(133/100));

```

```

F_2m = @(x_m)interp1(x_2,nhat_2,x_m);

```

```

i=3;
dnhatdt = -nhat1*(drmodel(x,acid(i))+so./taus(i))/rmodel(x,acid(i)) + F_2m(x).*nnot(i)./nnot(i-
1)*so./taus(i)/rmodel(x,acid(i));
dnhat = [dnhatdt];

```

***Chan4.m

```

function dnhat = nhateq1(x,nhat1)
global so taus a1 b1 e1 f1 g1 h1 i RN x1
global ratio acid nnot factr1
global x_1 nhat_1 x_2 nhat_2 x_3 nhat_3 x_4 nhat_4

```

```

rmodel = @(x1,acid) e1.*(1-x1).^f1./(1+g1.*(acid.*ratio).^h1);

```

```

drmodel = @(x1,acid) -28341/100000.*(1-
x1)^(101/100)./(1+517/500*3^(273/1000)*5^(727/1000).*acid^(273/1000));

F_3m = @(x_m)interp1(x_3,nhat_3,x_m);

i=4;
dnhatdt = -nhat1*(drmodel(x,acid(i))+so./taus(i))/rmodel(x,acid(i)) + F_3m(x).*nnot(i)./nnot(i-
1)*so./taus(i)/rmodel(x,acid(i));
dnhat = [dnhatdt];

```

MATLAB CODE FOR CPDM PREDICTION MAP

```

VSLR=[12;12;12;12;12;10;10;10;10;10;8;8;8;8;6;6;6;6;4;4;4;4];
LRT=[10;15;20;25;30;10;15;20;25;30;10;15;20;25;30;10;15;20;25;30;10;15;20;25;30];
CONVERSION=[0.14;0.135;0.134;0.13;0.127;0.16;0.15;0.149;0.143;0.14;0.184;0.18;0.17;0.163;0.16;0.2
4;0.22;0.218;0.2;0.19;0.45;0.4;0.39;0.32;0.3];
ACID=[9.1;10.8;11.9;15.4;16.5;9.2;10.9;11.9;15.5;16.8;9.4;10.9;12;15.7;17;9.5;10.9;12.1;15.7;17.2;10.9;
12.3;13.3;16.6;17.9];
%Enter collected Conversion and Acid data into the two above matrices that correspond to the VSLR and
LRT
mapdata=[VSLR,LRT,CONVERSION,ACID];
VSLR_sorted=sortrows(mapdata,1);
LRT_sorted=sortrows(mapdata,2); %sort
[map_num,map_1]=size(mapdata);
VSLR_sort = sort(mapdata(:,1));
uniqueM = [diff(VSLR_sort);1] > 0;
VSLR_sort1 = VSLR_sort(uniqueM);
VSLR_number = diff(find([1;uniqueM]));
LRT_sort = sort(mapdata(:,2));
uniqueM = [diff(LRT_sort);1] > 0;
LRT_sort1 = LRT_sort(uniqueM); %Unique LRT
LRT_number = diff(find([1;uniqueM]));
%plot for VSLR part
temp1=zeros(length(VSLR_sort1)+1,1);
for j1=1:length(VSLR_sort1)
temp1(j1+1)=temp1(j1)+VSLR_number(j1);
mapdata_1=VSLR_sorted(temp1(j1)+1:temp1(j1+1),:);

%for VSLR(j1)
F = @(x)interp1(mapdata_1(:,3),mapdata_1(:,4),x,'spline');
hold on;
plot(mapdata_1(:,3),F(mapdata_1(:,3)), 'k');
%notes of formatting the plots:
%default is a solid line '-'
%a dashed line is '--'
%a dotted line is '.'
%a dash and dotted line is '-.'
% colors are r = red, g = green, b = blue, c = cyan
% m = magenta, y = yellow, k = black, w = white
%note remember to do both the VSLR lines and the LRT lines
if j1==1

```

```

for j3=1:length(mapdata_1(:,3))
text(mapdata_1(j3,3)-0.01,mapdata_1(j3,4)+0.5, [' ', num2str(mapdata_1(j3,2))]
,'HorizontalAlignment','left');
end
text(mapdata_1(1,3)-0.3,mapdata_1(1,4)-5.5, 'VSLR (g/(L.d))','HorizontalAlignment','left');
end
end

%plot for LRT part
temp1=zeros(length(LRT_sort1)+1,1);
for j1=1:length(LRT_sort1)
temp1(j1+1)=temp1(j1)+LRT_number(j1);
mapdata_2=LRT_sorted(temp1(j1)+1:temp1(j1+1),:);
%for LRT(j1)
F2 = @(x)interp1(mapdata_2(:,3),mapdata_2(:,4),x,'spline');
hold on;
plot(mapdata_2(:,3),F2(mapdata_2(:,3)), 'k');
if j1==1
for j3=1:length(mapdata_2(:,3))
text(mapdata_2(j3,3)+0.02,mapdata_2(j3,4)-1.5, [' ', num2str(mapdata_2(j3,1))] ,
'HorizontalAlignment','right');
end
text(mapdata_2(1,3)+0.31,mapdata_2(1,4)+5, ' LRT (day) ','HorizontalAlignment','left');
end
end
legend('Galveston',1) %adjust as necessary, number is the legend position
hold off;
xlabel('Conversion');
ylabel('Total carboxylic acid concentration (g/L)');
axis([0 1 0 25]); %adjust as necessary for size of map

```

VITA

Name: Kristina Warnock Golub

Address: Care of: Dr. Mark T. Holtzapple
Texas A&M University
Dept. of Chemical Engineering
232 Jack E. Brown Building (MS 3122)
College Station, TX 77843

Email Address: golubkw@gmail.com

Education: B.S., Chemical and Biomolecular Engineering, Georgia Institute of Technology, 2007
Ph.D., Chemical Engineering, Texas A&M University, 2012

Publications: Golub, K.W., Forrest, A.K., Mercy, K.L., Holtzapple, M.T., 2011. Propagated fixed-bed mixed-acid fermentation: Part I: Effect of volatile solid loading rate and agitation at high pH. *Bioresour. Technol.* 102, 10592–10601.

Golub, K.W., Smith, A.D., Hollister, E.B., Gentry, T.J., Holtzapple, M.T., 2011. Investigation of intermittent air exposure on four-stage and one-stage anaerobic semi-continuous mixed-acid fermentations. *Bioresour. Technol.* 102, 5066–5075.